Université de Liège

Faculté de Médecine

Mémoire présenté en vue de l'obtention du grade d'Agrégé de l'Enseignement Supérieur

Untangling regulatory cues that control cell cycle progression and fate specification in the oligodendroglial lineage

Centre de Recherches en Neurobiologie Cellulaire et Moléculaire (C.N.C.M.)

Service de Neurologie

(Professeur G. Moonen)

Shibeshih Belachew

Chercheur qualifié du F.N.R.S.

Docteur en Médecine

Docteur en Sciences Biomédicales

2005

Université de Liège

Faculté de Médecine

Le présent mémoire peut être livré à l'impression.

Liège, le 15 mars 2005.

Le Secrétaire de la Faculté.

(S) Ph. BOXHO.

Le Doyen de la Faculté.

(S) G. MOONEN.

La Secrétaire du Jury.

(S) A. NOËL.

« Article 6 de l'Arrêté Royal du 10 mai 1931 appliquant la loi du 21 mai 1929 sur la collation des grades académiques et le programme des examens universitaires :
En aucun cas, les opinions de l'auteur ne peuvent être considérées, par le fait de l'autorisation d'impression de la dissertation, comme étant celles du Jury ou de l'Université ».

Remerciements

A l'aube des dernières lignes de ce travail, qu'il m'est agréable de pouvoir remercier ceux qui ont permis que tout ceci voit le jour.

C'est bien sûr avant tout à Gustave Moonen que je pense en me remémorant les étapes du parcours qui m'a mené jusqu'ici. Je l'ai rencontré quand je n'étais qu'un adolescent attardé il y a maintenant quinze ans. Il fut l'instigateur de mon éveil à la science et l'inspirateur de chaque minute de ce travail. Ma gratitude et mon affection à son égard n'ont d'égales que la puissance de ses infinis talents, les lumières de sa clairvoyance et la confiance qu'il ne cesse de me témoigner.

Ce travail n'aurait pas pu naître sans avoir croisé la route de Vittorio Gallo. C'est une fois encore à Gustave Moonen que je dois cette rencontre cruciale. Vittorio Gallo, Adan Aguirre et Ramesh Chittajallu furent mon rêve américain, successivement au *National Institutes of Health* (Bethesda, Maryland) puis au *Children's National Medical Center* (Washington DC). Contrairement à ce qui pourrait abusivement transparaître dans certains de mes propos ci-après, j'ai adoré vivre aux Etats-Unis. Merci à Vittorio, Adan et Ramesh. Je ne pourrais plus me passer de la richesse des gens qu'il me fut donné de rencontrer au pays de l'oncle Sam. Dans ces contrées lointaines, j'ai une pensée particulière pour François Vautier et Xiaoqing Yuan.

J'ai aussi eu le privilège de faire mes premiers pas dans la Neurologie sous l'aile protectrice du Professeur Georges Franck. Je me suis délecté trois années durant au contact de l'acuité insondable de sa maîtrise de la Neurologie sous toutes ses formes.

Depuis des années et j'espère pour longtemps encore, j'ai pu travailler à l'unisson avec les Dr Brigitte Malgrange et Laurent Nguyen. Dans des styles bien différents mais complémentaires, il me plaît de leur avouer qu'ils sont tous deux indispensables à l'équilibre de mon quotidien scientifique. Je leur suis redevable à l'infini et, bien au-delà de nos collaborations, je les remercie surtout pour leur indéfectible amitié. De même, je ne peux passer sous silence tout ce que je dois au Prof. Jean-Michel Rigo qui fut la pierre angulaire de mon doctorat et avec qui je continue d'entretenir des liens étroits et une collaboration désormais trans-frontalière.

Merci à Patricia Ernst qui sut me témoigner bien plus que son inégalable compétence dans la gestion des cultures cellulaires.

Je voudrais aussi remercier les collaborateurs plus récents avec lesquels je prends aujourd'hui un immense plaisir à travailler dans un superbe esprit d'enthousiasme et d'émulation. Merci à Pierre Beukelaers, Laurence Borgs, Ingrid Breuskin, Jean-Marie Mangin et Renaud Vandenbosch.

Au cours de ces années de travail, j'ai pu apprécier les qualités et compétences de nombreuses personnalités côtoyées au sein du Centre de Recherches en Neurobiologie Cellulaire et Moléculaire (C.N.C.M.). Merci au Prof. Philippe Lefebvre pour ses avis et ses encouragements toujours judicieux et éclairés. Merci aux Dr Bernard Rogister et Pierre Leprince pour leurs précieux conseils depuis la première heure. Merci à Arlette Brose pour son aide technique. Je remercie également, pour leurs apports respectifs, le Prof. Didier Martin, les Dr Pierre Robe, Paul Delrée, Rachelle Franzen, Sabine Wislet-Gendebien ainsi que François Lallemend, Murielle Wouters, Patricia Piscicelli et Jacqueline Randaxhe.

Je voudrais aussi exprimer ma profonde reconnaissance au Fonds National de la Recherche Scientifique et en particulier à sa secrétaire générale, Madame Marie-Josée Simoen, pour m'avoir toujours accordé sa confiance.

Je remercie chaleureusement tous mes collègues du Service de Neurologie dont certains se montrèrent très conciliants à divers moments afin de permettre à ce travail de voir le jour. Merci aux secrétaires du Service de Neurologie et en particulier à Lucienne Arena pour son assistance dévouée.

Je remercie également les membres du Jury - les professeurs Bernard Zalc, Serge Schiffmann, Vincent Seutin, Agnès Noël, Jean Schoenen, Vincent Geenen et Marie-Paule Defresne – d'avoir accepté d'évaluer mon travail.

Merci à tous mes amis, dont principalement Patrizio, Frédéric, Michel et Michele, Thomas et Xavier, Youri et Christian, Dani et Sylvanos, Christos et Georges, Frédérique et les autres filles de la Famille…

Merci à Guy et Christine pour leur accueil et leur générosité.

Merci à mes parents avec qui j'ai vécu 22 années d'un bonheur indélébile. Je voudrais leur dire que ce qui nous a rassemblé est bien plus fort que ce qui nous sépare.

Enfin, je dédie ce mémoire aux trois phares qui illuminent ma vie :

Si je suis allé au bout de ce parcours, c'est avant tout pour partager avec toi, mon frère, la conviction que tout cela n'est qu'une gentille mascarade. Je devine ton sourire. Tu me manques aujourd'hui comme jamais.

A Ulysse, à la magie de son enfance, à la magie de ce qu'il fait vibrer en moi, à nos voyages futurs.

A Catherine sans laquelle j'aurais peut-être la faiblesse de penser que cet ouvrage signifie quelque chose. Merci d'être si belle. Merci pour ton amour. Merci de m'avoir appris la vie.

A l'Art, le vrai, celui des Artistes et de leurs créations.

Préambule

Mes travaux de recherches m'ont conduit à vivre à Washington DC au moment des attentats du 11 septembre 2001. Deux jours après le drame, je recevais, au même titre que tous les employés du gouvernement américain, un courriel dont je vous retranscris certains passages ci-après : *« On Tuesday morning, September 11, 2001, terrorists attacked America in a series of despicable acts of war. […] Civilized people around the world denounce the evildoers who devised and executed these terrible attacks. Justice demands that those who helped or harbored the terrorists be punished -- and punished severely. The enormity of their evil demands it. We will use all the resources of the United States and our cooperating friends and allies to pursue those responsible for this evil, until justice is done. […] Scripture says: "Blessed are those who mourn for they shall be comforted. […] We will persevere through this national tragedy and personal loss. In time, we will find healing and recovery; and, in the face of all this evil, we remain strong and united, one Nation under God." […] GEORGE W. BUSH »* Oui, mais quel Dieu ? Les Etats-Unis d'Amérique, les compagnies pétrolières et les industries d'armement continueront de diriger le monde en utilisant la science comme fidèle serviteur du Dieu de la religion marchande. La semaine suivante (20 avril 2001), le bureau éditorial du célèbre magazine *Nature* titrait **:** *« Fighting against terrorism, engaging with Islamic science. Last week's attacks in New York and Washington were an offence against fundamental values that merits a well-targeted response, helped by science. But enhanced contacts with Islamic colleagues should also be pursued. »* Ces propos eurent de pénibles lendemains. Où en sommes-nous aujourd'hui? A une époque où l'on voit émerger des traitements anti-rétroviraux formidablement efficaces dans la lutte contre le SIDA qui sont inaccessibles pour un continent comme l'Afrique qui compte 60 millions de patients, à une époque où les pays du Nord multiplient les pressions bilatérales sur les pays du Sud pour qu'ils restreignent ou retardent la production locale ou l'importation de médicaments génériques essentiels, n'est-il pas triste de constater que la communauté scientifique ne puisse pas se targuer d'exercer une influence instrumentale favorable sur l'évolution de la société vers un monde meilleur. Le plus grand défi pour la science de demain sera donc de se tourner vers les hommes qu'elle ignore et non de servir les seuls intérêts de ceux qui peuvent investir dans ses valeurs ? Qu'il est bon de rêver encore…

« I have a dream… »
(Martin Luther King., sur les marches du Lincoln Memorial, Washington DC, 28 août 1963)

Table of contents

1 Introduction et synthèse en français 5

2 Intrinsic features defining oligodendrocyte progenitor cells: identification of a driver for proliferation and of alternative routes of differentiation 8

2.1 The CNP-EGFP transgenic mouse: an animal model for developmental and physiological studies in oligodendroglial lineage cells 9

2.2 The *Yin* and *Yang* of cell cycle decisions in oligodendrocyte progenitor cells: balancing on the verge of cdk2 10

2.2.1 Ubiquitous molecular mechanisms that control cell cycle progression 10

2.2.2 Essential cell-cycle related genes that control oligodendroglial proliferation 13

2.2.2.1 The cdk2 switch: turning on and off OPC proliferation without affecting differentiation 14

2.2.2.2 Broad-scale effects of chemical inhibitors of cdks on oligodendroglial development 16

2.2.2.3 There is a life without cyclin E and cdk2 with mere collateral damage 17

2.2.3 Molecular control of the onset of oligodendroglial differentiation . . 18

2.2.3.1 At the beginning, there was Martin C. Raff and the quest for a cell-intrinsic timer that operates during oligodendrocyte development 19

2.2.3.2 Which and how time really matters: who's the tick of the clock? 19

2.2.3.2.1 The role of $p27^{Kip1}$ 20

2.2.3.2.2 The role of p18Ink4c 21

2.2.3.2.3 The role of p53 21

2.2.3.2.4 The role of basic helix-loop-helix (bHLH) proteins 22

2.2.3.2.4.1 Mash1 23

2.2.3.2.4.2 Olig genes 23

2.2.3.2.4.3 Id2 and Id4 24

2.2.3.2.4.4 Hes 5 25

2.2.3.2.5 Extrinsic cues 25

2.2.4 Teasing apart two models of relationships between proliferation and differentiation in the oligodendroglial lineage. G0 versus G1 cell cycle arrest 28

2.3 Revisiting lineage fate potential of previously so-called "oligodendrocyte" progenitor cells in the postnatal brain: on the trail of a serial progenitor . . . 29

2.3.1 Principal features of the postnatal OPC as an established oligodendrocyte progenitor expressing the NG2 proteoglycan surface marker 29

2.3.2 NG2-expressing cells actually represent a bi-potential oligodendrocyte/interneuron (OIN) precursor cell type in the

postnatal brain 30
2.3.2.1 Neurogenesis in numbers in the adult brain 31
2.3.2.2 Current nomenclature for “glial” neural stem cells in the adult CNS 32
2.3.2.3 Postnatal $NG2^+$ progenitor cells expressing the CNP gene are intrinsically multipotent and generate functional neurons 33
2.3.2.4 $NG2^+$ progenitors are type C-like cells in the subventricular zone and may be a possible source of interneuron renewal in the adult hippocampus 34
2.3.2.5 Finding a spot for $NG2^+$ OIN precursors in or out of the A,B,C... neural stem cell nomenclature 35
2.3.3 What would a real OPC now be ? 37
2.3.3.1 Proposed recommendations for redefining an OPC 37
2.3.3.1.1 Marker-based definition 38
2.3.3.1.2 Integration of region-based and contextual parameters 39
2.4 Summary conclusions 39
2.4.1 Nascent perspectives for novel strategies aimed at improving OPC recruitment after demyelination 39
2.4.1.1 Transplantation of allogenic progenitors 40
2.4.1.2 Counteracting the recruitment failure of endogenous progenitors 40
2.4.1.3 Counteracting the differentiation failure of endogenous progenitors 41
2.4.2 There is a need to redefine remyelinating cells to circumvent the ”specification failure” of formerly termed OPCs 42

3 Extrasynaptic and synaptic neurotransmitter receptors in glial precursors’ quest for identity 44
3.1 Expression of neurotransmitter receptors in CNS precursor cells of the postnatal brain 44
3.1.1 A focus on a newcomer: glycine receptors in perinatal CNS precursor cells 48
3.1.2 Not only neurotransmitter receptors, but also voltage-gated potassium channels in OPCs 49
3.2 Established functional involvement of neurotransmitter receptors in postnatal CNS precursor cell biology 50
3.2.1.1 AMPA/kaïnate receptors: a matter of cell cycle or cell death 50
3.2.1.2 $GABA_A$ receptors 53
3.3 Discussion point: neuron-glia versus neuron-neuroblast signaling? 54
3.3.1 The $NG2^+$ progenitor 54
3.3.2 Astrocytes 56

4 Conclusions and perspectives 57

4.1 The good: NG2$^+$ OINPCs, a dual source of repair that may serve for interneuron renewal in the postnatal hippocampus and for remyelination elsewhere 57
4.2 The bad: new neurons in the postnatal/adult brain: what for? 59
4.3 The (not so) ugly: is there a glimpse of hope in the fuzzy near future of stem/progenitor cell-based therapy in humans ? 62

5 References 64

6 List of abbreviations 79

7 Appendix - Publications 80
7.1 Publication #1: Belachew,S., Yuan,X., and Gallo,V. (2001). Unraveling oligodendrocyte origin and function by cell-specific transgenesis. *Dev. Neurosci.* 23:287-298. 81
7.2 Publication #2: Yuan,X., Chittajallu,R., Belachew,S., Anderson,S., McBain,C.J., and Gallo,V. (2002). Expression of the green fluorescent protein in the oligodendrocyte lineage: a transgenic mouse for developmental and physiological studies. *J. Neurosci. Res.* 70:529-545. 94
7.3 Publication #3: Belachew,S., Aguirre,A.A., Wang,H., Vautier,F., Yuan,X., Anderson,S., Kirby,M., and Gallo,V. (2002). Cyclin-dependent kinase-2 controls oligodendrocyte progenitor cell cycle progression and is downregulated in adult oligodendrocyte progenitors. *J. Neurosci.* 22:8553-8562. 112
7.4 Publication #4: Nguyen,L., Malgrange,B., Rocher,V., Hans,G., Moonen,G., Rigo,J.M., and Belachew,S. (2003). Chemical inhibitors of cyclin-dependent kinases control proliferation, apoptosis and differentiation of oligodendroglial cells. *Int. J. Dev. Neurosci.* 21:321-326. 123
7.5 Publication #5: Belachew,S., Chittajallu,R., Aguirre,A.A., Yuan,X., Kirby,M., Anderson,S., and Gallo,V. (2003). Postnatal NG2 proteoglycan-expressing progenitor cells are intrinsically multipotent and generate functional neurons. *J. Cell Biol.* 161:169-186. 130
7.6 Publication #6: Aguirre,A.A., Chittajallu,R., Belachew,S., and Gallo,V. (2004). NG2-expressing type C multipotent progenitor cells of the subventricular zone: a possible source of interneuron renewal the adult hippocampus. *J. Cell Biol.* 165:575-589. 154
7.7 Publication #7: Nguyen, L., Rigo, J.-M., Rocher, V., Belachew, S., Malgrange, B., Rogister, B., Leprince, P., and Moonen, G. (2001) Neurotransmitters as early signals for central nervous system development. *Cell Tissue Res.* 305:187-202. 175
7.8 Publication #8: Nguyen, L., Rigo. J.-M., Malgrange, B., Moonen, G., and Belachew, S. (2003). Untangling the functional potential of PSA-NCAM-expressing cells in CNS development and brain repair strategies. *Curr. Med. Chem.* 10:2185-2196. 192
7.9 Publication #9 (was part of our *PhD* thesis): Belachew, S., Malgrange, B., Rigo, J.-M., Rogister, B., Coucke, P., Mazy-Servais, C., and Moonen, G. (1998). Developmental regulation of neuroligand-induced responses in cultured

oligodendroglia. *Neuroreport* 9:973-980. 205
7.10 Publication #10 (was part of our *PhD* thesis): Belachew, S., Rogister, B., Rigo, J.-M., Malgrange, B., Mazy-Servais, C., Xhauflaire, G., Coucke, P., and Moonen, G. (1998). Cultured oligodendrocyte progenitors derived from cerebral cortex express a glycine receptor which is pharmacologically distinct from the neuronal isoform. *Eur. J. Neurosci.* 10:3556-3564. 214
7.11 Publication #11 (was part of our *PhD* thesis): Belachew, S., Malgrange, B., Rigo, J.-M., Rogister, B., Leprince, P., Hans, G., Nguyen, L., and Moonen G. (2000). Glycine triggers an intracellular calcium influx in oligodendrocyte progenitor cells which is mediated by the activation of both the ionotropic glycine receptor and Na^+- dependent transporters. *Eur. J. Neurosci.* 12:1924-1930. 224
7.12 Publication #12: Nguyen, L., Malgrange, L., Breuskin, I., Lallemend, F., Hans, G., Moonen, G., Belachew, S., and Rigo, J.-M. (2004) Striatal PSA-$NCAM^+$ precursor cells from the newborn rat express functional glycine receptors. *Neuroreport* 15:583-587. 232
7.13 Publication #13: Nguyen, L., Malgrange, B., Belachew, S., Rogister, B., Rocher, V., Moonen, G., and Rigo J.-M. (2002). Functional glycine receptors are expressed by postnatal nestin-positive neural stem/progenitor cells. *Eur. J. Neurosci.* 15:1299-1305. 238
7.14 Publication #14: Vautier, F., Belachew, S., Chittajallu, R., and Gallo, V. (2004). *Shaker*-type potassium channel subunits Kv1.3-1.4 and Kv1.6 differentially control oligodendrocyte progenitor cell cycle progression. *Glia* 48:337-345. 246
7.15 Publication #15: Nguyen, L., Malgrange, B., Breuskin, I., Bettendorff, L., Moonen, G., Belachew, S., and Rigo, J.-M. (2003). Autocrine/paracrine activation of the $GABA_A$ receptor inhibits the proliferation of neurogenic polysialylated neural cell adhesion molecule-positive (PSA-$NCAM^+$) precursor cells from postnatal striatum. *J. Neurosci.* 23:3278-3294. 256

1 Introduction et synthèse en français

Il est désormais bien établi qu'une ébauche de remyélinisation demeurant incomplète apparaît spontanément dans les lésions démyélinisantes du système nerveux central (SNC) (Ludwin, 1987;Prineas et al., 1993;Raine, 1997). L'identité des cellules potentiellement remyélinisantes du SNC reste débattue actuellement mais l'hypothèse la plus raisonnable consiste à considérer que ce ne sont pas les oligodendrocytes matures résiduels mais plutôt les progéniteurs oligodendrocytaires (OPCs), exprimant le protéoglycan membranaire NG2, qui remplissent cette fonction au niveau des sites lésionnels. La réparation spontanée de la myéline dans une affection démyélinisante telle que la sclérose en plaques demeure cependant quantitativement et qualitativement insatisfaisante car dépourvue de bénéfice fonctionnel réel. Aucune thérapeutique n'est actuellement disponible pour agir sur les OPCs dans l'optique de stimuler leur propension à proliférer et à se différencier en oligodendrocytes capables de régénérer la myéline. Il est néanmoins communément admis que l'échec spontané de la remyélinisation est principalement le résultat d'un échec du recrutement des OPCs quiescents qui ne parviennent pas à quitter la phase G0 du cycle cellulaire pour réintégrer une phase de prolifération en réponse à la démyélinisation (Wolswijk, 1997;Wolswijk, 1998).

Dans la première partie de notre travail, nous avons développé une souris transgénique exprimant sélectivement la *green fluorescent protein* (EGFP) dans la lignée oligodendrocytaire sous la dépendance du double promoteur oligodendroglial-spécifique (CNP1-2, 3.7 kb) du gène de la 2', 3'-cyclic nucleotide 3'-phosphodiesterase (CNPase). Ce modèle transgénique murin consitue la pierre angulaire de cet ouvrage et nous a permis de traquer plus facilement les propriétés phénotypiques des OPCs $NG2^+$ in vivo.

De manière à disséquer les mécanismes moléculaires régissant les "décisions" intervenant au fil de la progression du cycle cellulaire dans les OPCs, nous avons étudié le rôle de différentes kinases nucléaires cycline-dépendantes, à savoir cdk2, cdk4 et cdk6. Nous savons en effet que ces enzymes sont essentielles pour l'intégrité de la transition entre les phases G1 et S du cycle cellulaire au niveau de laquelle convergent la plupart des régulations critiques de la prolifération des OPCs. Par des expériences de gain et de perte de fonction, nous avons démontré dans le présent travail que cdk2 régulait le niveau de prolifération des OPCs $NG2^+$ en culture. Nos manipulations de l'expression de cdk2 aboutissant à stimuler ou à bloquer le cycle cellulaire des OPCs, n'eurent aucune conséquence sur la cinétique de différenciation oligodendrogliale. Ceci démontra que le mécanisme inconnu du timing intracellulaire déclenchant la sortie du cycle cellulaire associée à l'initiation de la différenciation oligodendrocytaire agit vraisemblablement en aval du *checkpoint* G1/S contrôlé par le couple cyclineE/cdk2 et apparaît indépendant du nombre de cycles accomplis par ces progéniteurs.

Nous avons aussi constaté que les niveaux d'expression protéique de la cycline E et de cdk2 ainsi que l'activité enzymatique du couple cycline E/cdk2 étaient nettement plus faibles dans les OPCs de cerveau adulte en comparaison des OPCs de la période néonatale. Au vu du rôle de ce complexe enzymatique dans la progression du cycle cellulaire des OPCs au niveau de la transition G1/S in vitro, nous pensons que les faibles capacités de prolifération des OPCs adultes en conditions normale comme pathologique (par exemple dans la sclérose en plaques) pourraient être la conséquence directe d'un déficit fonctionnel d'activité cdk2. Si nous confirmons cette hypothèse par de prochains travaux utilisant des animaux invalidés pour cdk2, cela nous permettra de définir une première cible moléculaire spécifique dans l'optique de concevoir des stratégies de thérapie visant à recruter les OPCs "quiescents" dans les maladies démyélinisantes.

En outre, les OPCs $NG2^+$ représentent le plus important groupe de progéniteurs postnataux/adultes proliférant dans le SNC (Dawson et al., 2000;Dawson et al., 2003). Ces

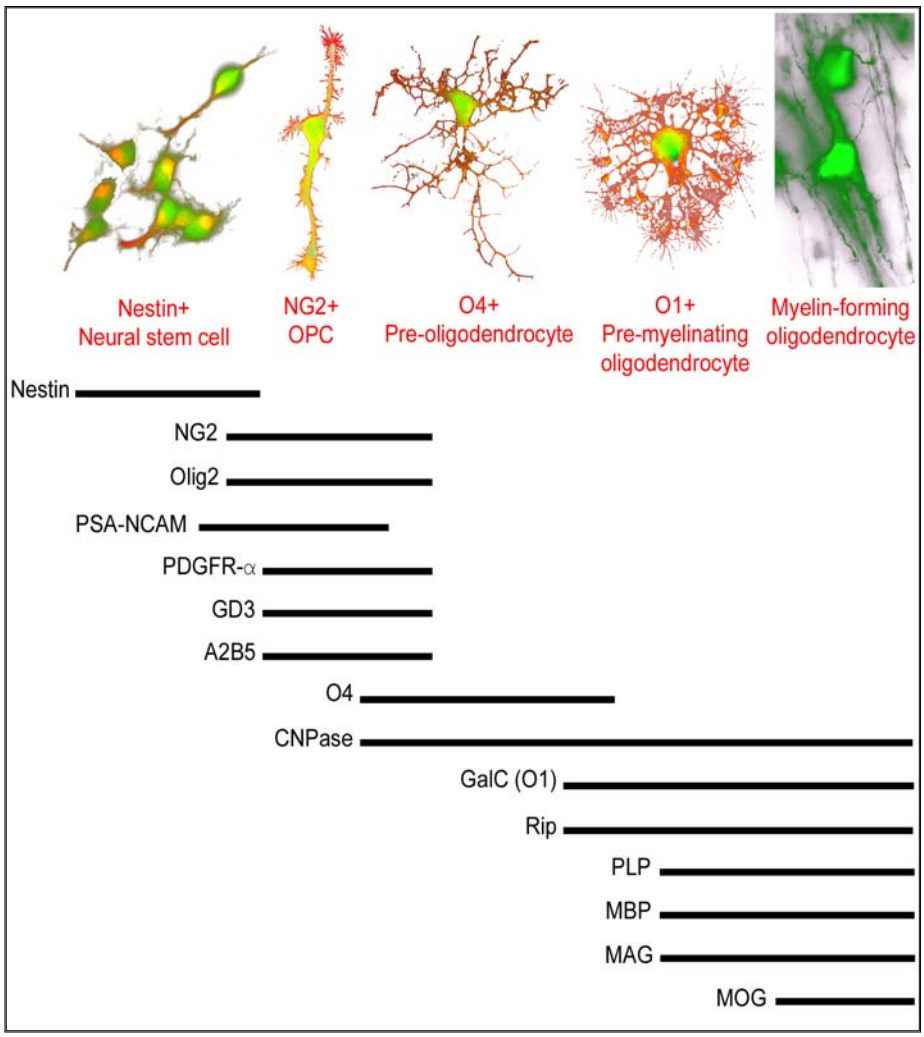

Figure 1: *Sequential expression of commonly used antigenic markers of oligodendrocyte lineage development*
Nestin is an intermediate filament protein expressed by neural stem cells (NSCs) (Lendahl et al., 1990). Antibodies against the NG2 chondroitin sulfate proteoglycan have been a valuable tool, both in vivo and in vitro, and NG2-expressing immature glial precursor cells are now generally termed oligodendrocyte precursor cells or OPCs, due to their proliferative potential and to their ability to differentiate into oligodendrocytes (Dawson et al., 2003). A2B5 antibody stains OPCs at the same stages than NG2 whereas O4 immunoreactivity appears a little later than NG2 in lineage progression and is the principal feature of pre-oligodendrocytes that already represent post-mitotic cells. PSA-NCAM is the polysialylated form of neural cell adhesion molecule which is expressed once NSCs have become pre-OPCs that are already committed to the oligodendrocyte lineage (Ben Hur et al., 1998). PDGFR-α, the platelet-derived growth factor (PDGF) receptor-alpha is responsible for the transduction of the mitogenic effect of PDGF on OPCs. CNPase is the 2'-3'-cyclic nucleotide 3'-phosphodiesterase. Even though its function remains relatively elusive, the CNPase gene is one of the earliest known myelin-specific proteins which is abundantly expressed in developing oligodendrocytes (Scherer et al., 1994). Two CNP isoforms, CNP1 (46 kD) and CNP2 (48 kD) are both encoded by a single gene. Although CNP1 is the most prominent mRNA and protein found postnatally in mature oligodendrocytes, CNP2 mRNA and protein are also expressed by differentiated cells (Scherer et al., 1994). CNP2 mRNA is to date the only isoform synthesized at low levels in early embryonic life in OPCs (Scherer et al., 1994). GalC, the galactocerebroside (recognized by O1 antibodies) is a galactolipidic component of myelin. The proteolipid protein (PLP), the myelin basic protein (MBP), the myelin-associated glycoprotein (MAG) and the myelin oligodendrocytic glycoprotein (MOG) represent four constitutive proteins of the myelin (Baumann and Pham-Dinh, 2001).

progéniteurs ont longtemps été considérés comme des progéniteurs exclusivement oligodendrogliaux malgré le paradoxe de leur présence inexpliquée dans des régions

essentiellement neurogènes du cerveau postnatal. Dans une seconde étape de notre travail, nous avons pu démontrer que les OPCs $NG2^+$ issus de la zone sous-ventriculaire (ZSV), sont également capables de générer des interneurones GABAergiques fonctionnels in vitro. Nous avons ensuite montré que cette différenciation des progéniteurs $NG2^+$ de la ZSV en interneurones GABAergiques hippocampiques pouvait également se produire in vivo pendant les premières semaines de vie postnatale. Enfin, nous avons observé que ces progéniteurs $NG2^+$ de la ZSV possèdaient toutes les caractéristiques phénotypiques des progéniteurs multipotents dits *transit-amplifying*, soit selon la nomenclature en vigueur les «cellules C» qui sont la descendance directe des cellules souches neurales ou «cellules B» (Doetsch et al., 1999;Doetsch et al., 2002a;Doetsch, 2003).

Nos travaux montrent qu'une sous-population d'interneurones de l'hippocampe est effectivement issue de progéniteurs $NG2^+$, ce qui signifie que ceux-ci ne sont pas exclusivement restreints à un destin oligodendroglial. Les OPCs $NG2^+$ doivent donc désormais être perçus comme un réservoir de progéniteurs bipotentiels du SNC postnatal, particulièrement intéressant en raison de sa taille et de sa capacité à fournir à la fois des cellules oligodendrogliales et des neurones GABAergiques.

Dans la dernière partie de ce travail, nous avons remis en perspective l'ensemble de nos données objectivant la présence de récepteurs aux neurotransmetteurs à la fois dans les cellules souches neurales, dans les progéniteurs restreints à un destin neuronal et dans les progéniteurs $NG2^+$ dont nous savons désormais qu'ils peuvent emprunter deux types de voies de différenciation phénotypique. Nous avons discuté les différentes hypothèses rendant compte de la fonction et de la signification développementale de ces stigmates "d'excitabilité" neurone-*like* dans ces cellules immatures et plus particulièrement dans les cellules $NG2^+$. Le plus grand défi des années à venir sera d'élucider le rôle instructeur potentiel de ces connections synaptiques et extra-synaptiques entre des neurones matures et des progéniteurs aux destins multiples.

En conclusion, ce travail jette les base d'une réflexion plus générale sur l'identité et le rôle fonctionnel d'une population de progéniteurs d'oligodendrocytes dont l'insuffisance de réactivité après démyélinisation pourrait s'expliquer par une déficience intrinsèque de la machinerie moléculaire de prolifération et par l'ambivalence d'un destin phénotypique dont l'hétérogénéité était sans doute sous-évaluée. Ces travaux soulignent l'immensité de notre méconnaissance des propriétés biologiques précises de la plus importante population de progéniteurs du cerveau adulte. L'avenir devrait permettre d'en déchiffrer progressivement l'infinie complexité à condition d'accorder une attention prioritaire à l'intégration des paramètres variables dépendant de facteurs spatio-temporels et contextuels qui furent trop souvent négligés par le passé. Ce n'est qu'à ce prix que nous comprendrons un jour pourquoi le SNC adulte ne remyélinise pas. C'est aussi par ce type d'approche que nous appréhenderons un jour toute l'étendue du registre phénotypique, la dynamique et la nature de la signification fonctionnelle de la production de nouveaux neurones dans l'hippocampe adulte tout au long de la vie.

2 Intrinsic features defining oligodendrocyte progenitor cells: identification of a driver for proliferation and of alternative routes of differentiation

Oligodendrocytes are the myelin-forming cells of the central nervous system (CNS). They derive from progenitor cells that undergo a series of developmental stages to reach the mature myelinating phenotype (Pfeiffer et al., 1993). The progression from progenitor to myelinating oligodendrocyte entails a sequence of events, including cell cycle withdrawal, onset and progression of a differentiation program in which cytoskeletal changes and synthesis of myelin components occur. The end-point of differentiation is the formation of myelin sheaths around multiple axons that facilitates saltatory nerve conduction (Franklin, 2002). Although the majority of oligodendrocyte progenitor cells (OPCs) develop into oligodendrocytes, some persist in the adult CNS as a population of slowly dividing precursor cells (Ffrench-Constant and Raff, 1986;Wolswijk and Noble, 1989;Reynolds and Hardy, 1997) that are thought to be the major cellular reservoir responsible for remyelination after injury (Gensert and Goldman, 1997;Blakemore and Keirstead, 1999;Chang et al., 2000;Franklin, 2002;Chang et al., 2002).

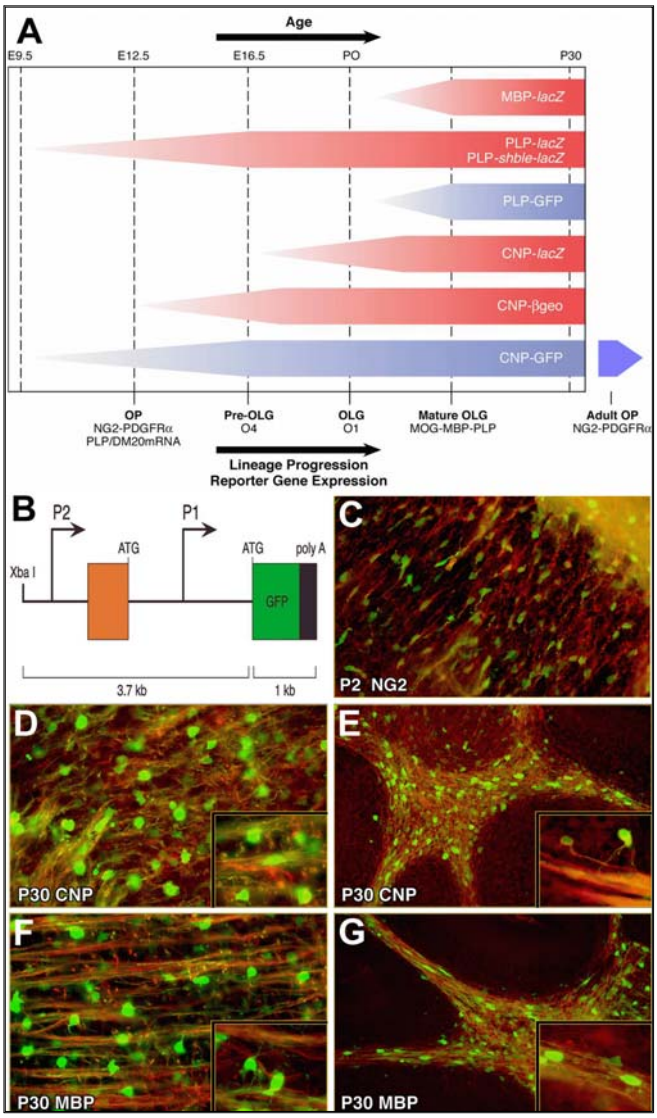

Figure 2: *The CNP-EGFP transgenic mouse*
(A) Developmental regulation of reporter gene expression in distinct transgenic mice aimed at assessing oligodendrogliogenesis (see Publication #1). (B) The CNP promoters that specifically direct oligodendroglial expression are indicated as P1 (for CNP1) and P2 (for CNP2), and the EGFP sequence is shown in green. The orange box denotes exon 0 of the CNP gene. The black box indicates the polyadenylation sequence from bovine growth hormone. The relative size of the individual sequences and the total size of the construct are also indicated. (C-G) Microtome frozen sagittal sections (50 µm) were obtained from P2 (C) and P30 (D-G) CNP-EGFP transgenic mice. Immunostaining with anti-NG2 antibody (C; red fluorescence) in the SVZ showed that the vast majority of EGFP-expressing cells (green fluorescence) is also $NG2^+$ at the P2 perinatal stage. By P30, in corpus callosum (D, F) and cerebellar white matter (E, G), most EGFP-expressing cells (green fluorescence) are immunoreactive for mature oligodendroglial antigens (D-G; red fluorescence) such as CNPase (D, E) and MBP (F, G) which are constitutive myelin proteins.

Remyelination by OPCs requires the recapitulation of a similar sequence of events occurring during development: progenitors proliferate, migrate to the site of lesion, contact the axon, and differentiate into myelin-forming cells (Franklin, 2002). Before OPCs can differentiate into (re)-myelinating oligodendrocytes, the initial step in remyelination is to populate an area of demyelination with sufficient OPCs. These might come from cells that are already present within the lesion, or be

recruited from surrounding intact white matter (Carroll and Jennings, 1994;Franklin et al., 1997;Sim et al., 2002). In experimental models, remyelination generally occurs with such efficiency that it can be difficult to create situations in which it fails. One might therefore expect demyelinating diseases to carry a favorable prognosis. Yet in multiple sclerosis (MS), this is evidently not the case.

Multiple mechanisms underlie the eventual progressive deterioration that typifies MS natural history, but there is no doubt that the inefficiency of the remyelination process, resulting in lesions that remain largely or entirely demyelinated, is a significant contributor (Compston and Coles, 2002). Likewise insufficient remyelination in animal models (Sim et al., 2002), remyelination might fail in MS because of an inadequate provision of OPCs (recruitment failure) and/or because of a failure of recruited OPCs to differentiate into remyelinating oligodendrocytes (differentiation failure). One needs to emphasize that it is a widely held assumption that the initial recruitment phase obviously necessitate OPC proliferation.

In the first part of this work, we will describe a transgenic mouse model that we generated in order to facilitate the study of oligodendroglial lineage cells in vivo. This model has stemmed the research tracks that are developped in the second and third parts, allowing us to get more insights into why remyelination fails.

Given the importance of initial proliferative events for myelination during normal development and for remyelination after myelin damage, the second part will then turn to an in-depth review of the progress achieved in unraveling intrinsic regulatory signals that control the kinetics of cell division in OPCs. We will notably discuss putative and compelling relationships between neat intrinsic cues and possible links between proliferation and differentiation during oligodendrocyte lineage progression.

The third part of this chapter will be devoted to addressing the need for redefining what an oligodendrocyte progenitor is in the sense of a committed cell restricted to a glial fate. Remyelination strategies so far may have mistaken the ideally suited target since so-called OPCs do share a previously unexpected oligodendroglial/neuronal potential in the postnatal brain.

2.1 The CNP-EGFP transgenic mouse: an animal model for developmental and physiological studies in oligodendroglial lineage cells

Publication #1: Belachew,S., Yuan,X., and Gallo,V. (2001). Unraveling oligodendrocyte origin and function by cell-specific transgenesis. *Dev. Neurosci.* 23:287-298.
Publication #2: Yuan,X., Chittajallu,R., Belachew,S., Anderson,S., McBain,C.J., and Gallo,V. (2002). Expression of the green fluorescent protein in the oligodendrocyte lineage: a transgenic mouse for developmental and physiological studies. *J. Neurosci. Res.* 70:529-545.

The oligodendroglial lineage is one of the best characterized of the CNS (Raff, 1989) thanks to the presence of antigens (Figure 1) on the surface of OPCs that has allowed cell purification, clonal analysis and determination of their growth and differentiation properties in vitro (Pfeiffer et al., 1993;Baumann and Pham-Dinh, 2001). Cell-specific promoters driving the expression of reporter genes are well-established tools to trace development in transgenic mice. In the present work, we generated a transgenic mouse that allows direct identification of oligodendrocytes in live tissue through the expression of a fluorescent protein. To generate such a mouse, we took advantage of a gene promoter that comprises DNA elements that direct tissue- and cell-specific gene expression in oligodendrocytes and Schwann cells. The 3.7 kb promoter region of the 2'-3'-cyclic nucleotide 3'-phosphodiesterase (CNP) gene contains the two promoters for this gene, CNP1 and CNP2 (Figure 2) (Gravel et al., 1998). These promoters

are active at distinct developmental stages, because CNP2 mRNA transcripts are detected in embryonic brain, whereas CNP1 mRNA is found only after birth (Scherer et al., 1994). It has been previously shown that the combination of CNP1 and CNP2: i) restricts reporter gene expression to the oligodendrocyte and Schwann cell lineages and ii) confers a gene expression pattern during development that recapitulates the complex spatiotemporal expression profile of the endogenous CNP gene in the oligodendroglial lineage (Figure 2) (Gravel et al., 1998;Chandross et al., 1999). Importantly, and in contrast to the case for most myelin genes, the onset of CNP gene transcription occurs at early embryonic developmental stages and is maintained in adulthood (Scherer et al., 1994). This property makes the CNP promoter an ideal molecular tool with which to direct cell-specific heterologous gene expression in myelinating cells during the entire development of the mammalian nervous system.

We thus generated a transgenic mouse (CNP-EGFP) expressing the enhanced form of the green fluorescent protein (EGFP), specifically in the oligodendroglial lineage under the dependence of the CNP1-2 gene promoter (Figure 2) (Publication #1 - Belachew et al., 2001;Publication #2 - Yuan et al., 2002). In such a CNP-EGFP transgenic mouse, EGFP expression could be readily detected from embryonic day 10 to adulthood and was restricted to cells of the oligodendrocyte and Schwann cell lineages (Publication #1 - Belachew et al., 2001;Publication #2 - Yuan et al., 2002). Importantly, cells with a phenotype of adult OPCs and gray matter oligodendroglial cells could be identified in mature transgenic mouse brains. These classes of cells were not identified by reporter gene expression in previous transgenic mice (Chandross et al., 1999). Visualization of EGFP-expressing cells in situ allowed direct electrophysiological recordings in acutely isolated brain slices, and notably a study of the role of K^+ channels in the regulation of OPC proliferation (Publication #2 - Yuan et al., 2002). Finally, the CNP-EGFP mouse described here allowed rapid isolation by fluorescence-activated cell sorting (FACS®) of pure and viable oligodendrocyte-lineage cells (Publication #2 - Yuan et al., 2002). Importantly, the antigenic properties of these cellular fractions were identical to their counterpart before FACS® isolation, indicating that the purified EGFP-expressing cells were representative of the EGFP-expressing cells in situ (Publication #2 - Yuan et al., 2002).

2.2 The *Yin* and *Yang* of cell cycle decisions in oligodendrocyte progenitor cells: balancing on the verge of cdk2

2.2.1 Ubiquitous molecular mechanisms that control cell cycle progression

Consistently matching old universal claims from thinkers of the Han Chinese dynasty, cell cycle progression is ruled by two opposite principles, or two principles that oppose one another in their actions, yin and yang. All the opposite cues one perceives that regulate cell proliferation can be reduced to one of these opposite forces, which either promotes or slows down cell cycle progression. On each side of this dualistic view, one has to distinguish between intrinsic/intracellular and extrinsic/extracellular levels of regulation. Until recently, it was stunning how poor was our understanding of intrinsic signals that are essential for cell cycle decisions, particularly in OPCs, while a more and more extensive list of extrinsic cues was proved to be involved. Since intrinsic molecular actors of a cell division scene represent a final common pathway for whatever extrinsic influences, one first needs to gain a compelling knowledge of the complex interwoven networks of intrinsic interactions in order to next be able to investigate their interplay with extrinsic factors.

In response to extrinsic mitogenic stimulations, dividing cells of the CNS, like other

cycling cells outside of neural tissues, move through four phases of the cell cycle: G1, S, G2 and M (Figure 3). Each of these phases can be translated into molecular terms and appears to be regulated by the coordinated action of kinases and proteases (Sherr and Roberts, 1995;King et al., 1996). In vitro, when deprived of mitogen supply, dividing cells continue to cycle until they complete mitosis, whereupon they exit into the G0 state (Pardee, 1974;Pardee, 1989). These cells can be reintroduced into the cell cycle by the re-addition of their mitogen. During G1 progression, the presence of the mitogen is necessary until R restriction point (Figure 3), which occurs several hours prior to the transition between G1 and S (Pardee, 1989;Zetterberg et al., 1995;Planas-Silva and Weinberg, 1997). In mitogen-deprived cells, all the growth factor-stimulated events that are necessary for completion of one round of the cell cycle occur before the R point. Furthermore, mitogens are not needed later to complete the other stages of the cell cycle.

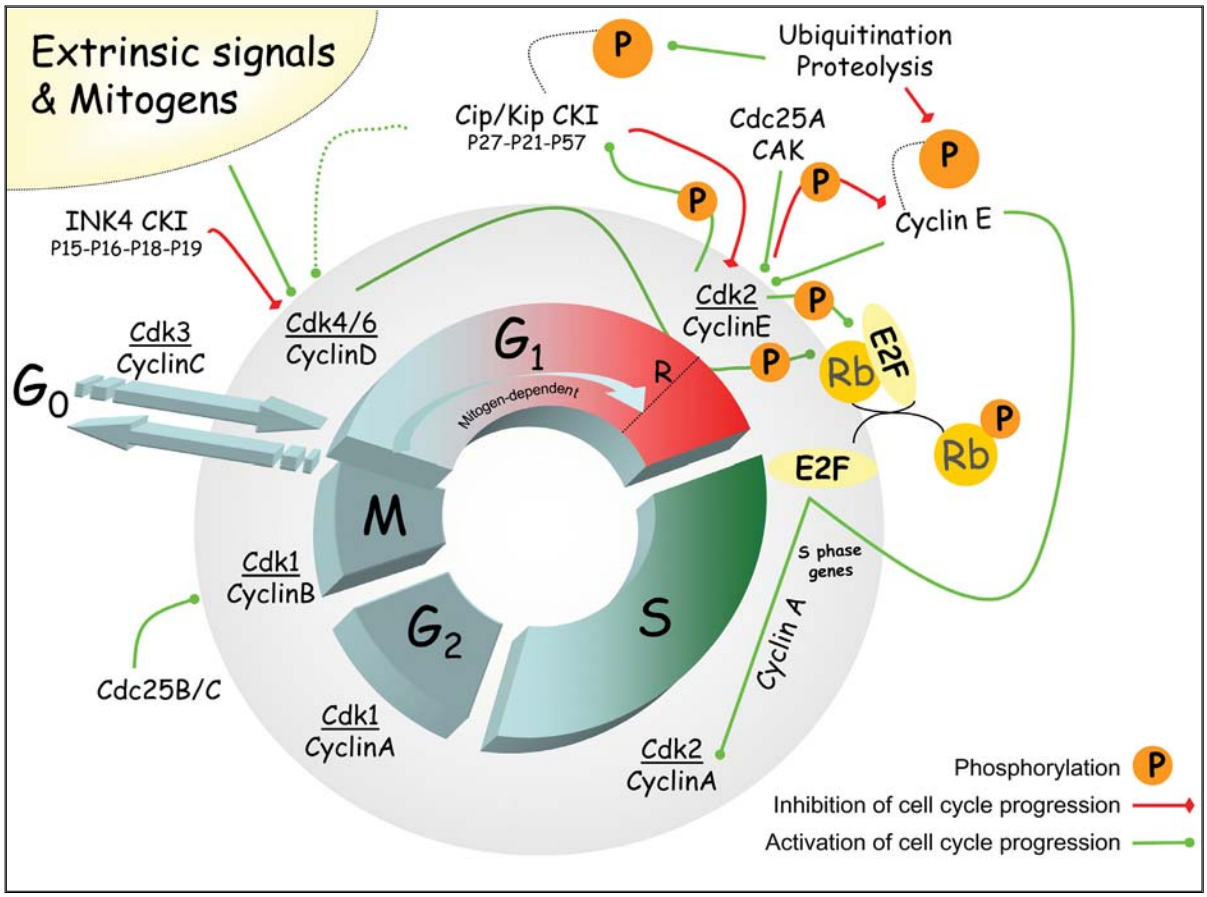

Figure 3: *Integrated view of interwoven interactions between cell cycle-related proteins that govern cell cycle progression and particularly the critical G1-S transition checkpoint.*

Mammalian G1 cyclins and their associated kinases are regulators of the cell division cycle that integrate information flow from outside the cell to drive G1-phase progression and initiate DNA replication in response to mitogenic signals. The relevant proteins include three D-type cyclins (D1, D2, and D3) that, in different combinations, bind to, and allosterically regulate, one of two Cdk subunits, Cdk4 and Cdk6, as well as the E-type cyclins (E1 and E2), which, in analogous fashion, govern the activity of a single catalytic subunit, Cdk2 (Morgan, 1995;Morgan, 1997;Sherr and Roberts, 2004). Various combinations of D-type cyclins are expressed in different cell types, whereas cyclin E/Cdk2 complexes are expressed ubiquitously. Mitogenic signals promote the assembly of active cyclin D-dependent kinases containing either CDK4 (or CDK6) and a Cip/Kip protein. Sequestration of Cip/Kip proteins lowers the inhibitory threshold and facilitates activation of the cyclin E/CDK2 complex. The cyclin D- and E-dependent kinases contribute sequentially to Rb phosphorylation, canceling its ability to repress E2F family members and activating genes required for entry into S phase. The latter include cyclins E and A, as well as a bank of gene products that regulate nucleotide metabolism and DNA synthesis per se (Dyson, 1998;Stevaux and Dyson, 2002). CyclinE/CDK2 antagonizes p27 by phosphorylating it and triggering its proteolysis. The degradation of Cip/Kip proteins and the induction of cyclins by E2F contribute to mitogen independence and to the irreversibility of the transition (for review see current text and Sherr & Roberts, 2004).

G0 exit and G1 entry (Ren and Rollins, 2004) and the completion of G1 cell cycle program necessitates the phosphorylation of the retinoblastoma tumor-suppressor protein (Rb), which is the basis of the current molecular definition of the R point (Pardee, 1989). At least three classes of G1 cyclin-dependent kinases (cdks) (Morgan, 1997;Ren and Rollins, 2004) collaborate to fully phosphorylate Rb (Sherr, 1996;Stevaux and Dyson, 2002). In their unphosphorylated state, members of Rb family (Rb, p107 and p130 in mammals) have been found to inhibit progression through the post-R point late G1 phase (Sherr, 1996). This negative-regulatory function of the Rb protein is constrained by phosphorylation at multiple cdk phosphorylation sites. Sequential phosphorylations disrupt the repressive binding between Rb and transcription factors such as E2F (Sherr, 1996;Stevaux and Dyson, 2002), thereby allowing these transcription factors to activate genes required for S-phase entry and DNA synthesis (Dyson, 1998). One of the critical target genes of E2F transcription factors is cyclin E (Dyson, 1998), which together with its partner cdk2, is required for the initiation of DNA replication (Tsai et al., 1993;van den Heuvel S. and Harlow, 1993;Ohtsubo et al., 1995). Hence, the potential effect of a mitogen on dividing cells is intrinsic to its ability to eventually promote phosphorylation of Rb.

Cdks represent essential components operating at crucial checkpoints between successive phases of the cycle, and particularly the critical late G1 progression and S phase entry transition (Morgan, 1997). Cdks are subject to multi-level positive and negative regulations (Morgan, 1995;Sherr and Roberts, 1999). Their activation requires, on distinct residues, a dephosphorylation by cdc25 phosphatases and a phosphorylation by cdk-activating kinase (CAK) (Morgan, 1997;Sherr and Roberts, 1999), as well as the binding of specific cyclin proteins (Sherr, 1995;Roberts, 1999). Among the regulatory cyclins active during G1 phase, cyclin C is specific for cdk3 (Ren and Rollins, 2004), D-type cyclins are specific for binding cdk4/6 and E-type cyclins for cdk2 (Sherr, 1994a;Sherr, 1995;Sherr and Roberts, 1999). It is now actually acknowledged that activated cyclin C-cdk3 initiates Rb phosphorylation at G1 entry (Ren and Rollins, 2004), then cyclin D-cdk4/6 complexes rapidly take over subsequent phosphorylation of Rb in early G1 (Sherr, 1994b;Weinberg, 1995), whereas cyclin E-cdk2 complexes are responsible for the additional phosphorylation of Rb and other substrates during late G1 (Ohtsubo et al., 1995). The early effect of cyclin D-cdk4/6 complexes on Rb triggers E2F release-dependent activation of cyclin E gene in mid-G1. This will allow Rb to be subsequently phosphorylated mostly by active cyclin E-cdk2 complexes during late G1 progression, thus creating a sort of cyclin E-mediated auto-activated loop (Figure 3).

Superimposed upon this core unit, cyclin-cdk complexes have their endogenous inhibitors (cdki) acting at G1-S transition that can be divided into two families: the INK4 (i.e., p15Ink4b, p16Ink4a, p18Ink4c and p19Ink4d) and the Cip/Kip (i.e., $p21^{Cip1}$, $p27^{Kip1}$, $p57^{Kip2}$) (Sherr and Roberts, 1995;Sherr and Roberts, 1999). The inhibition of cdk2 activity by members of the Cip/Kip family has been well documented by crystallographic studies elucidating the structure of tripartite cyclin/cdk2/p27 complexes (Russo et al., 1996). Clearly, the role of $p21^{Cip1}$ and $p27^{Kip1}$ on the kinase activity appears to occur at a 1:1 stoichiometry (Hengst et al., 1998) and they bind cyclin-cdk2 complexes as extended structures that interact with both cyclins and cdk2 (Russo et al., 1996). $p27^{Kip1}$ has been shown to bind conserved cyclin-box residues of cyclin proteins (Russo et al., 1996). On cdk2, $p27^{Kip1}$ binds and rearranges the amino-terminal lobe and inserts into the catalytic cleft, mimicking ATP (Russo et al., 1996).

Interestingly, besides their canonical role as cell cycle inhibitors, Cip/Kip family members also have the ability to act as "paradoxical positive regulators" of cdk4/6 (LaBaer et al., 1997;Cheng et al., 1999). In the absence of INK4 family members, $p21^{Cip1}$ and $p27^{Kip1}$ favors the assembly of cyclinD-cdk4 complexes. In the presence of the INK4 factors, they act preferentially

as cdk2 inhibitors, because they are displaced by the INK4 family members, binding preferentially to cdk4/6 (Figure 3).

Revealing another level of regulation, recent and ongoing works have indicated that many important regulators of G1 and S phase progression and G1/S transition are targeted for ubiquitination and subsequent degradation by the 26S proteasome (Tyers and Jorgensen, 2000;Yew, 2001). The ubiquitin system drives the cell division cycle by orchestrating the timely proteolytic destruction of numerous key regulatory proteins during G1 and S phases (Figure 3). In particular, the abundance of cyclin E, $p21^{Cip1}$ and $p27^{Kip1}$ is controlled by proteolysis mediated through the ubiquitin-proteasome pathway (Wang et al., 1999;Nakayama et al., 2000;Malek et al., 2001;Nakayama et al., 2001;Bornstein et al., 2003). Interestingly, the ubiquitin-proteasome-mediated degradation of cyclin E and $p27^{Kip1}$ necessitate their phosphorylation by cdk2 (Sheaff et al., 1997;Vlach et al., 1997;Welcker et al., 2003). Thus cdk2-associated kinase activity regulates the proteolysis of both its activator cyclin E and its inhibitor $p27^{Kip1}$.

The fine-tuning of such multi-level yin and yang processes appears to be central for proper custodial regulation of DNA replication but also for the maintenance of cellular homeostasis in general. Altogether, the role of individual cell cycle molecules during development is not equivalent and their expression pattern is not overlapping. Therefore, different combinations of positive and negative regulators may control proliferation and induce differentiation into distinct cell types (Cunningham and Roussel, 2001).

2.2.2 Essential cell-cycle related genes that control oligodendroglial proliferation

Previous studies in cultured cells and in mutant mice have analyzed some of the cell cycle regulatory mechanisms in OPCs, with a focus on proteins involved in G1/S progression (Durand et al., 1997;Casaccia-Bonnefil et al., 1997;Durand et al., 1998;Tang et al., 1998;Casaccia-Bonnefil et al., 1999;Ghiani et al., 1999a;Ghiani et al., 1999b). One of the mechanisms that has received much attention involves the endogenous cdkis $p21^{Cip1}$ and $p27^{Kip1}$ and their binding to the cyclin E-cdk2 complex. The levels of these cdkis increase in OPCs, either during permanent cell cycle withdrawal associated with differentiation (Durand et al., 1997;Casaccia-Bonnefil et al., 1997;Durand et al., 1998;Casaccia-Bonnefil et al., 1999;Ghiani et al., 1999a;Ghiani et al., 1999b), or during reversible cell cycle arrest in G1 caused by extracellular signals, such as β2-adrenergic (Ghiani et al., 1999a) and AMPA/kaïnate receptor stimulation (Gallo and Ghiani, 2000) or K^+ channel blockade (Ghiani et al., 1999b) that inhibit cell cycle progression driven by the mitogen platelet-derived growth factor (PDGF). $p27^{Kip1}$ is also involved in cAMP-induced cell cycle withdrawal and differentiation of a glial cell line after cAMP treatment (Friessen et al., 1997). The increase in $p27^{Kip1}$ protein levels observed during OPC differentiation results in an enhancement of its binding to the cyclin E-cdk2 complex and inhibition of cdk2 activity (Tikoo et al., 1997;Tang et al., 1998). Ectopic expression of $p27^{Kip1}$ in OPCs causes a significant reduction in cyclin E-cdk2 activity and cell cycle arrest (Tikoo et al., 1998;Tang et al., 1999).

Cristina Ghiani and Vittorio Gallo have demonstrated that PDGF-stimulated dividing OPCs display higher protein levels of cyclin E and D and cdk2, 4, and 6 than cells that had permanently withdrawn from the cycle (Ghiani and Gallo, 2001). The kinase activities of both cyclin D-cdk4/6 and cyclin E-cdk2 were also higher in dividing OPCs (Ghiani and Gallo, 2001). This was associated with a decrease in the formation of the cyclin E-cdk2 and cyclin D-cdk4/cyclin D-cdk6 complexes in differentiated oligodendrocytes that had permanently withdrawn from the cell cycle (Ghiani and Gallo, 2001). In contrast, reversible cell cycle arrest in G1 induced by glutamatergic and β2-adrenergic receptor activation or cell depolarization did

not modify cyclin E and cdk2 protein expression compared with proliferating OPCs (Ghiani and Gallo, 2001). Instead, these agents caused a selective decrease in cdk2 activity and an impairment of cyclin E-cdk2 complex formation, whereas cyclin D-associated kinase activity was not modified in G1-arrested OPCs (Ghiani and Gallo, 2001).

The regulation of cyclin E-cdk2 activity, however, cannot be seen as an event completely separate from cyclin D-cdk4 regulation. As previously discussed, the activity of cyclin E-cdk2 complexes is dependent on the bioavailability of Cip/Kip inhibitors, but is also affected by INK4 protein levels. High levels of INK4 inhibitors render Cip/Kip proteins more available to act on their cyclin E-cdk2 target, thus favoring growth arrest. Consistent with this model, the p18Ink4c family member has been found to accumulate in OPCs before growth arrest and its overexpression is able to stop proliferation of OPCs, even in the presence of mitogens (Tokumoto et al., 2002)

2.2.2.1 The cdk2 switch: turning on and off OPC proliferation without affecting differentiation

Publication #3: Belachew,S., Aguirre,A.A., Wang,H., Vautier,F., Yuan,X., Anderson,S., Kirby,M., and Gallo,V. (2002). Cyclin-dependent kinase-2 controls oligodendrocyte progenitor cell cycle progression and is downregulated in adult oligodendrocyte progenitors. *J. Neurosci.* 22:8553-8562.

In order to demonstrate the causal link between cyclin E-cdk2 activity and OPC proliferation, we used a transfection procedure to modify cdk2 activity in cultured perinatal OPCs (Publication #3 - Belachew et al., 2002). We have overexpressed wild-type (wt) or dominant-negative (dn) mutants of different cdk genes (van den Heuvel S. and Harlow, 1993) in primary cultures of OPCs and in the CG-4 oligodendrocyte progenitor cell line (Louis et al., 1992). We observed that dn-cdk2 overexpression inhibited PDGF-driven proliferation of OPCs, whereas wt-cdk2 overexpression prevented G1 cell cycle arrest induced by anti-mitotic extrinsic signals that block G1/S transition (Publication #3 - Belachew et al., 2002). Importantly, dn-cdk2 and wt-cdk2-mediated regulation of G1/S transition, per se, did not influence the initiation of OPC differentiation triggered by thyroid hormone treatment and mitogen withdrawal (Publication #3 - Belachew et al., 2002). Altogether, we provided evidence that cyclin E-cdk2 activity plays a pivotal function in OP cell cycle decisions occurring at G1/S restriction point and that initiation of OPC differentiation is independent from cyclin E/cdk2 dependent checkpoint.

To gain some insights on the function of cyclin E-cdk2 in oligodendroglial cells in vivo, we purified OPCs from CNP-EGFP mice by using FACS® (Figure 4) (Publication #2 - Yuan et al., 2002). By kinase assays and Western blot analysis, we were able to demonstrate a developmental down-regulation of cyclin E-cdk2 activity and cyclin E and cdk2 protein expression between the perinatal (postnatal day 6, P6) and adult stages (P30) (Figure 4) (Publication #3 - Belachew et al., 2002). We also performed an immunohistochemical characterization of proliferation markers, i.e. proliferating cell nuclear antigen (PCNA) (Bolton et al., 1994;Hyde-Dunn and Jones, 1997) and cdk2 expression in postnatal OPCs that were recognized by an antibody staining the OPC-specific hallmark NG2 chondroïtin sulfate proteoglycan (Dawson et al., 2000;Levine et al., 2001). After assessment of the subventricular zone (SVZ), subcortical and cerebellar white matter, we detected in all regions a drastic parallel decrease of the percentage of proliferating and cdk2-expressing $NG2^+$ OPCs between the perinatal period and adulthood (Publication #3 - Belachew et al., 2002). Furthermore, we showed that nearly all the few (~5-10 % at P30 versus ~80 % at P6) OPCs that remain proliferative ($PCNA^+$) in the adult brain sustained a high level of cdk2 expression, whereas about

half of total CDK2$^+$ OPCs of the adult brain were non-proliferative (PCNA-negative) (Publication #3 - Belachew et al., 2002).

These data indicate that high levels of cdk2 expression represent a necessary but insufficient condition to maintain OPCs in a proliferative state, which is consistent with the established essential role of cyclin E and likely other key cell cycle-related proteins acting

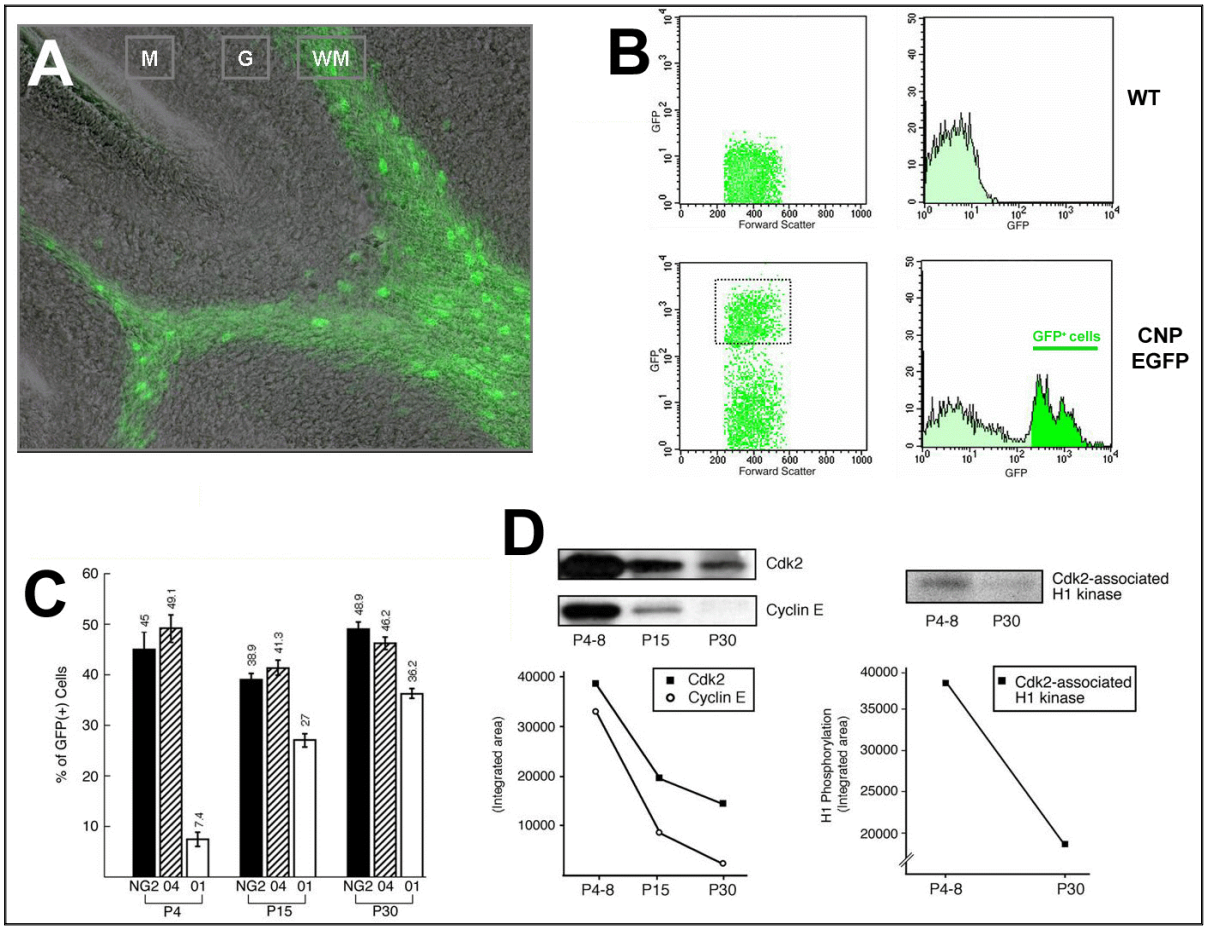

Figure 4: *Developmental down-regulation of cyclin E/cdk2 protein levels and activity during postnatal maturation of the oligodendroglial lineage in vivo* (A) EGFP fluorescence in P30 cerebellar white matter tracts. FACS® analysis of acutely dissociated cell suspensions of whole brain from wild-type and CNP-EGFP littermates displayed identical light forward and side scatter distributions (data not shown). (B) To eliminate erythrocytes and cell debris, forward scatter gating parameters were chosen for further GFP fluorescence analysis. Cells from CNP-EGFP suspensions that were considered GFP$^+$ (bar and boxed area in lower panels) and FACS®-selected, were in a range of fluorescence far above (ratio > 5X) maximal background intensity yielded by the wild-type cell suspension (upper panels). (C) Immunophenotype of acutely-isolated CNP-EGFP$^+$ oligodendroglial cells after FACS-purification. We previously demonstrated that EGFP expression in CNP-EGFP transgenic mice was restricted to oligodendrocyte lineage cells (Belachew et al., 2001; Yuan et al., 2002), and that the FACS procedure resulted in a 100% pure population of EGFP$^+$ cells whose antigenic properties were identical to those in vivo (Yuan et al., 2002). Values represent the percentage (mean ± SEM) of NG2$^+$, O4$^+$ and O1$^+$ cells in FACS-sorted cell suspensions derived from P4, P15 and P30 CNP-EGFP transgenic mice. Total cells counted ranged from 652 to 2185 for each condition. (D) Western blot analysis of cdk2 and cyclin E expression was performed with samples containing pure oligodendroglial cells freshly isolated from postnatal P4-8, P15 and P30 brains. Samples were obtained by FACS-sorting of EGFP$^+$ cells from CNP-EGFP transgenic mice. Cdk2-associated histone H1-kinase activity was also measured in FACS-purified CNP-EGFP$^+$ cells at P4-8 and P30, as previously described (Ghiani and Gallo, 2000).

upstream or downstream of the cdk2-associated checkpoint. Altogether, our data strongly suggest that regulation of cyclin E and cdk2 expression and cyclin E-cdk2 activity within the oligodendroglial lineage in vivo causally underlies the progressive breakdown of the intrinsic proliferative potential of OPCs that occurs during postnatal maturation. One now has to consider that besides extrinsic environmental differences at the level of mitogen supply and response (Chan et al., 1990;Wolswijk and Noble, 1992;Engel and Wolswijk, 1996;van Heyningen

et al., 2001), another major reason for the slower rate of proliferation of adult OPCs relies on intrinsic developmental regulation of the molecular machinery that controls G1/S cell cycle checkpoint. These findings shed a new light on our understanding of the so-called "quiescent" state of adult OPCs in human normal adult white matter and in MS lesions (Wolswijk, 1998;Chang et al., 2000;Maeda et al., 2001), thus unraveling novel neat targets for strategies aimed at preventing the recruitment failure in remyelination.

2.2.2.2 Broad-scale effects of chemical inhibitors of cdks on oligodendroglial development

Publication #4: Nguyen,L., Malgrange,B., Rocher,V., Hans,G., Moonen,G., Rigo,J.M., and Belachew,S. (2003). Chemical inhibitors of cyclin-dependent kinases control proliferation, apoptosis and differentiation of oligodendroglial cells. *Int. J. Dev. Neurosci.* 21:321-326.

Based upon the established function of cdks in cell cycle regulation, and given that approximately 90% of all neoplasias are associated with cdk hyperactivation (Hartwell and Kastan, 1994), several strategies have recently been designed to develop pharmacological compounds that are capable of inhibiting the catalytic cdk subunit, i.e. its ATP-binding site. Such chemical cdk inhibitors (CKIs) are extensively evaluated in cancer chemotherapy as well as in other indications, including neurodegenerative disorders, since these agents also inhibit apoptosis in post-mitotic neuronal cells (Sausville et al., 1999). In the present work, considering the prominent role of cdk regulation in OPC cell cycle arrest and withdrawal (Publication #3 - Belachew et al., 2002), we assessed the effect of synthetic exogenous CKIs on proliferation, differentiation and cell death within the oligodendroglial lineage in vitro (Publication #4 - Nguyen et al., 2003). More specifically, we used small molecular weight purine derivatives (roscovitine, RP107 and aminopurvalanol) and paullones (alsterpaullone) that are relatively selective for Cdk2.

Roscovitine, which is the most potent inhibitor of cdk2 among the tested CKIs, had the most effective anti-mitotic activity on cultured OPCs with an IC50 value (concentration giving rise to a half-maximal anti-mitotic effect) in the micromolar range (Publication #4 - Nguyen et al., 2003).We also demonstrated that roscovitine alone had no effect on oligodendrocyte maturation but potentiated thyroid hormone-induced differentiation in the presence of PDGF (Publication #4 - Nguyen et al., 2003). These results are consistent with the increasing evidence that Cip/Kip endogenous cdkis acting on cdk2 may play a major role in OPC cell cycle withdrawal and differentiation (Durand et al., 1997;Casaccia-Bonnefil et al., 1997;Durand et al., 1998;Casaccia-Bonnefil et al., 1999).

Our data are also in accordance with the key role of cyclin E-cdk2 complex, the main biochemical target of roscovitine during oligodendroglial development (Ghiani and Gallo, 2001;Publication #3 - Belachew et al., 2002). Thus, roscovitine appears to be sufficient to induce OPC cell cycle arrest by mimicking the effect of endogenous cdkis such as p27 acting on the cdk2-dependent G1/S checkpoint. In contrast, the effect of roscovitine on oligodendroglial differentiation, is likely to be cyclin E-cdk2 independent and thereby somehow mimics the effect of another endogenous cdki p21 that can also be pro-differentiating besides its action at the G1/S transition (Zezula et al., 2001). As a matter of facts, since cdk2-dependent G1/S cell cycle arrest is known to be a necessary but insufficient condition to trigger differentiation in the oligodendroglial lineage (Publication #3 - Belachew et al., 2002), we have to assume that roscovitine increases OPC differentiation by interacting with other intracellular kinases, perhaps at the cytoplasmic level. In addition, we observed that low concentrations of roscovitine prevented OPC apoptosis induced by growth factor deprivation (Publication #4 - Nguyen et al.,

2003), which is thought to be independent from the cyclin E-cdk2-controlled cell cycle machinery (Casaccia-Bonnefil, 2000). Altogether, our findings suggest that roscovitine, which is also known to regulate non cell cycle-related cdks, such as cdk5, cdk7, and to a lesser extent extracellular signal-regulated kinases ERK1/ERK2 (Meijer et al., 1997;Knockaert et al., 2002), may thus regulate other molecular targets than cyclin E-cdk2 in olgodendroglial cells. Such cyclin E-cdk2-independent pathways could be crucial to the yet unknown thyroid hormone-induced intracellular cascade. Furthermore, it is of interest to emphasize that recent works have shown that Cip/Kip endogenous cdkis might also have new activities that are unrelated to their function as cyclin E-cdk2 inhibitors and cell cycle regulators (Coqueret, 2003;Besson et al., 2004;Assoian, 2004). The identification of new targets of Cip/Kip proteins as well as evidence of Cip/Kip cytoplasmic relocalization have revealed unexpected functions for these proteins in the control of cdk activation, in the regulation of migration, apoptosis, and in transcriptional activation (Coqueret, 2003;Besson et al., 2004;Assoian, 2004).

2.2.2.3 There is a life without cyclin E and cdk2 with mere collateral damage

For the mammalian somatic cell cycle, the current thinking is that cyclins E and A, in combination with cdk2, initiate chromosome and centrosome duplication, whereas subsequent activation of cyclin A- and cyclin B-driven cdk1 complexes governs later events that terminate with mitosis (Figure 3). Activation of this intrinsic cell cycle program is linked to extracellular proliferative cues through D-type cyclins and their kinase partners cdk4/6 (Figure 3). In the absence of INK4, their mitogen-dependent assembly and activation sequesters the Cip/Kip cdk2 inhibitor p27 and inactivates the repressive effects of Rb family proteins, thereby promoting synthesis of cyclin E and A and activation of cdk2 allowing G1-S transition (Figure 3) (Sherr and Roberts, 1999).

New works addressing the functions of cdk2 (Ortega et al., 2003;Berthet et al., 2003) and cyclin E (Geng et al., 2003;Parisi et al., 2003) have now recently called key features of this model into question, since disabling these critical genes in the mouse has fewer effects than anticipated. It actually turned out that mouse cells might survive and proliferate with a couple of "broken lights". As a matter of facts, $cdk2^{-/-}$ mice are viable and do not display gross anatomical (except for size and weight) and behavioral (except for severe gonad atrophy) abnormalities (Ortega et al., 2003;Berthet et al., 2003). $Cdk2^{-/-}$ embryonic fibroblasts were shown to be capable to proliferate in culture but enter delayed into S phase (Ortega et al., 2003;Berthet et al., 2003). On the other hand, cyclin E-deficient embryos survived until the 10^{th} gestational day. Prenatal death was caused by the mutant placenta, but some cyclin $E^{-/-}$ embryos successfully completed gestation when they developed in a wild-type placenta (Geng et al., 2003;Parisi et al., 2003). In culture, cyclin $E^{-/-}$ embryonic fibroblasts were able to undergo several rounds of division before becoming senescent earlier than wild-type cells (Geng et al., 2003). Interestingly, the only critical requirement for cyclin E genes was for cell cycle reentry, since cyclin $E^{-/-}$ cells were unable to reenter a proliferation phase from the G0 quiescent state (Geng et al., 2003).

In the case of $cdk2^{-/-}$ cells, viability is likely due to surrogate kinases associating with cyclin A, since it is known that cyclin A can associate with cdk1 that can supply for cdk2 kinase activity. In contrast, as far as we know, E-type cyclins associate exclusively with cdk2 in vivo and, indeed, seem to lack any associated kinase activity in $cdk2^{-/-}$ cells (Ortega et al., 2003). Hence, although other explanations are likely conceivable, it now seems possible that essential functions of cyclin E such as G0 to G1 transition are not cdk-dependent. This hypothesis was recently confirmed

by the demonstration that cyclin E contains a 20 amino acids centrosomal localization signal, which is essential for both centrosomal targeting and for promoting S phase entry in a cdk2-independent manner (Matsumoto and Maller, 2004).

Given the conclusions drawn from these recent provocative works, we face the unbearable question of whether cdk2 ordinarily has an essential ubiquitous function (Aleem et al., 2004) that can be compensated by other cdks or whether cdk2 is simply dispensable for typical mitotic cell cycles. The fact that many regulatory signaling pathways, which are thought to couple cell cycle progression to extrinsic anti-mitogenic signals (Cunningham and Roussel, 2001), target cdk2 for inhibition supports the idea that cdk2 normally has an essential function. This interpretation requires inhibition of cdk2 (as occurs in anti-mitogenic signaling) to be different from loss of cdk2 (as in knock-out mouse), because the former causes the cell cycle to arrest, but the latter does not. Perhaps cdk2 impedes the ability of other cdks to substitute for it. It will now be of crucial importance to determine whether extrinsic regulatory pathways controlling cell cycle progression operate correctly in the absence of cdk2.

Besides knock-out animals for cdk2 and E-type cyclins, recent studies from the Barbacid and Sicinski groups have also reported the effects of deleting both cdk4 and cdk6 genes (Malumbres et al., 2004) or all three D-type cyclins (Kozar et al., 2004) in the mouse. In both cases, lethality was observed at around embryonic day 16, accompanied by a major failure in hematopoesis including erythropoesis, which is the likely cause of death. Thus, apart from hematopoesis, it seems that the majority of embryonic tissues can undergo cyclin D-independent cell cycles. In summary, the functions of G1 cell cycle regulatory genes are often essential only in specific cell types and/or at specific temporal stages (Jirawatnotai et al., 2004), pointing to our limited understanding of tissue-specific expression, redundancy and compensating mechanisms in the cdk network.

It is important to emphasize that $cdk2^{-/-}$ mice have not been assessed to date at the level of their CNS integrity and particularly regarding cell cycle kinetics in postnatal progenitor cells, such as NG2-expressing OPCs. One may assume that cdk2 functions obviously need to be efficiently compensated possibly by cyclin A-cdk1 complexes in $cdk2^{-/-}$ mice to allow CNS development to evolve without yielding easily detectable defects particularly at the level of locomotion. In contrast, we would not expect the lack of cdk2 to spontaneously trigger any major phenotype in the non-injured postnatal brain, since cdk2-expressing $NG2^{+}$ OPCs, which represent the largest pool of $cdk2^{+}$ cells are largely "quiescent" in the adult brain. In order to address such issues and to ascertain the functional significance of cdk2 expression in adult OPCs in vivo, we are currently collaborating with the lab of Philipp Kaldis (Berthet et al., 2003), to cross-breed our CNP-EGFP mice (Publication #1 - Belachew et al., 2001;Publication #2 - Yuan et al., 2002) with cdk2-null mutants. Using such double transgenic animals, in a second phase, we will also assess how cdk2-deficient adult OPCs will react following a demyelinating insult that stimulates a proliferation-dependent recruitment of OPCs. That will help us get more insights into the potential role of cdk2 in remyelination.

2.2.3 Molecular control of the onset of oligodendroglial differentiation

In contrast with proliferation, specific molecular targets involved in OPC differentiation remain elusive, and little is known about the relationship between cell cycle-related pathways and oligodendroglial differentiation (Tokumoto et al., 1999;Tokumoto et al., 2001;Zezula et al., 2001;Tokumoto et al., 2002;Huang et al., 2002).

2.2.3.1 *At the beginning, there was Martin C. Raff and the quest for a cell-intrinsic timer that operates during oligodendrocyte development*

Martin C. Raff has conducted over the last two decades a pioneering work effort to identify integrated sequential signals that control oligodendrocyte differentiation. Raff's contribution is based on a model system in which the normal timing of oligodendrocyte development can be reconstituted in cultures of dissociated embryonic and perinatal optic nerve (Raff et al., 1985), as long as OPCs are stimulated to divide by PDGF (Raff et al., 1988).

When individual or purified OPCs isolated from postnatal day 7 (P7) rat optic nerve were stimulated to proliferate in culture by either the presence of astrocytes or saturating amounts of PDGF, the cells divided up to eight times before they stopped and differentiated (Temple and Raff, 1986;Barres et al., 1994a). The progeny of a single precursor cell stopped dividing and differentiated at about the same time (Temple and Raff, 1985;Temple and Raff, 1986). Raff and Temple have elegantly shown that if the two daughter cells of a single OPC were separated and cultured on astrocyte monolayers in separate microwells, they divided the same number of times before they differentiated, indicating that an intrinsic mechanism operates in the precursor cells to limit the number of times, or the period of time, that the cell normally divides (Temple and Raff, 1985;Temple and Raff, 1986). The next issue was whether the counting mechanism counts cell divisions, or measures time in some other way. It was actually demonstrated that OPCs cultured at 33˚C divided more slowly, but stopped dividing and differentiated after fewer divisions, compared to cells cultured at 37˚C (Gao et al., 1997). Furthermore, our findings that cdk2-dependent cell cycle arrest did not retain a more immature oligodendroglial phenotype, nor did a faster cdk2-dependent cell cycle kinetics accelerate differentiation, emphasize that OPCs do not count the number of cell cycles before they start to differentiate (Publication #3 - Belachew et al., 2002). These two different sets of data provide evidence that the cell-intrinsic mechanism that regulates the onset of oligodendroglial differentiation program does not operate by counting cell divisions but, instead, measures elapsed time in some other way. Therefore, one now has to refer to it as a timer.

2.2.3.2 *Which and how time really matters: who's the tick of the clock?*

The view of Raff and colleagues was that the timer consisted of at least two components: a timing component that measures elapsed time and an effector component that stops cell proliferation and initiates differentiation when time is up (Bogler and Noble, 1994;Barres et al., 1994a). Although the timer is cell intrinsic, it is not cell autonomous since its normal function depends on extracellular signals (Figure 5A): PDGF is required for the timing component to operate (Raff et al., 1988;Noble et al., 1988), while thyroid hormone (TH) acting through α1 TH receptor subtype (Billon et al., 2001;Billon et al., 2002) regulates the effector component (Barres et al., 1994a). In the absence of PDGF, OPCs immediately stop dividing and prematurely differentiate into oligodendrocytes (Noble and Murray, 1984;Temple and Raff, 1985) (Figure 5A). In the presence of PDGF and the absence of TH, most cultured OPCs do not differentiate and tend to keep dividing endlessly with a lack of replicative senescence (Barres et al., 1994a;Ahlgren et al., 1997;Gao et al., 1998;Tang et al., 2000;Tang et al., 2001) (Figure 5A). If TH is added to such a culture after 8 days, when most OPCs would have differentiated, had TH been present, then OPCs soon massively stop dividing and differentiate (Barres et al., 1994a) (Figure 5A). This indicates that in the presence of mitogens and in the absence of TH, OPCs can still keep track of time, but seem unable to stop dividing and differentiate when the appropriate

time has come. Even in the absence of TH, however, a minor sub-population of OPCs cultured in PDGF spontaneously stop dividing and differentiate (Barres et al., 1994a;Ahlgren et al., 1997;Tang et al., 2001) (Figure 5A). Thus, whereas TH is required for the normal timing of OPC differentiation, it is not required for oligodendrocyte development per se.

It is yet unknown whether the timer in OPCs primarily controls the onset of differentiation, the cessation of proliferation, or both. Because the precursor cells stop dividing immediately and differentiate when deprived of PDGF (Raff et al., 1988), it is suspected that the timer primarily controls the irreversible cell cycle withdrawal that occurs in the differentiation pathway. If this is the case, the timer must, at some point, interact with the regulatory mechanisms that drive progress through the cell division cycle. We have outlined hereafter candidate factors that are likely to be part of the molecular structure of this cell-intrinsic timer (Figure 5B), but this will still not answer the fascinating question of how the timer works.

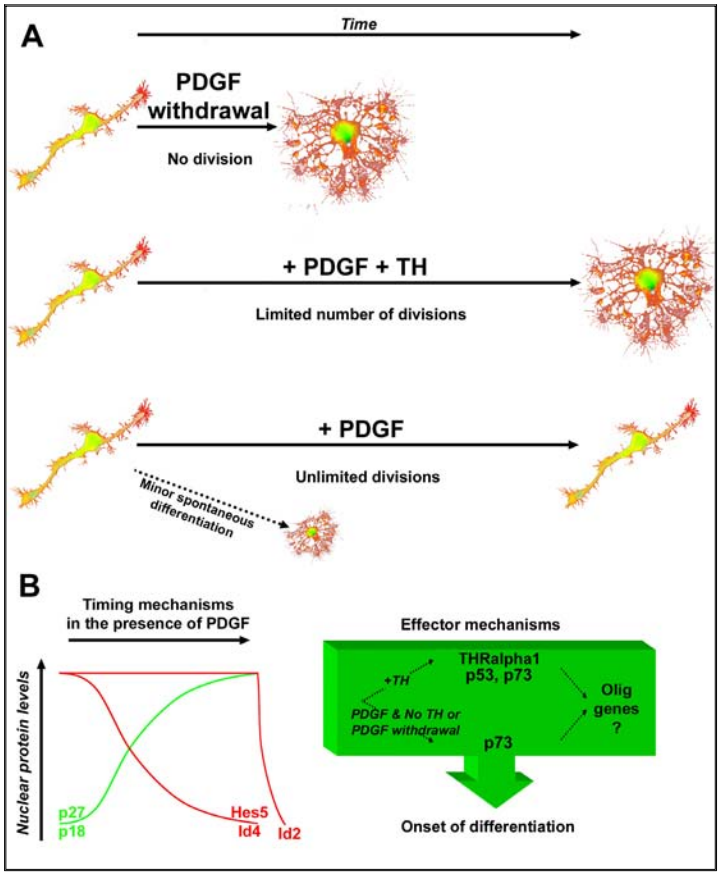

Figure 5: *A cell-intrinsic timer regulates the onset of oligodendroglial differentiation*
(A) Usual experimental paradigms used to study factors that regulate the different components of this timer. (B) Molecular cues known to be involved in the timing and effector components of the timer.

2.2.3.2.1 The role of $p27^{Kip1}$

There are now strong evidences supporting that $p27^{Kip1}$ is one element of this TH-regulated timer. First, $p27^{Kip1}$ levels are high in mature oligodendrocytes , both in vivo and in vitro, whereas they are variable in OPCs (Durand et al., 1997). Second, $p27^{Kip1}$ levels increase rapidly when precursor cells in culture are deprived of PDGF and the rate of increase is similar to the rate at which the precursor cells commit to cell-cycle withdrawal and differentiation, suggesting that $p27^{Kip1}$ is part of the effector mechanism (Durand et al., 1997). Third, $p27^{Kip1}$ levels progressively increase when OPCs are cultured in the presence of PDGF, but in the absence of TH (Durand et al., 1997), conditions where the timing component continues to operate, but the effector component is defective (Barres et al., 1994a). $p27^{Kip1}$ levels plateau after about 8 days in such cultures, when most of the cells would have differentiated had TH been present (Durand et al., 1997). In the absence of TH, however, despite high levels of $p27^{Kip1}$, OPCs continue to divide, indicating that high levels of $p27^{Kip1}$ alone are insufficient to stop the cell cycle. Fourth, $p27^{Kip1}$ levels in OPCs rise faster at 33˚C than at 37˚C, as would be expected if $p27^{Kip1}$ is part of the timer, since the timer runs faster at the lower temperature (Gao et al., 1997). Fifth, and most importantly, OPCs isolated from $p27^{Kip1}$-deficient mice divide with a normal cell cycle time, but

many of them go through one or two more divisions, compared to wild-type cells, before they differentiate (Durand et al., 1998). Detailed analysis of p27-deficient cells suggests that they are defective in both the timing (Durand et al., 1998) and the TH-dependent effector (Casaccia-Bonnefil et al., 1997;Durand et al., 1998) components of the timer. Experiments in which $p27^{Kip1}$ is overexpressed in OPCs have shown an acceleration of oligodendrocyte differentiation, but only in the presence of TH (Tokumoto et al., 2002), consistent with a prominent role in the timing component of the timer. In contrast, in the absence of TH, the overexpression of $p27^{Kip1}$ stopped the proliferation but fails to stimulate the differentiation, thereby confirming as previously discussed that G1 cell cycle arrest is not causally coupled to the onset of the differentiation (Tokumoto et al., 2002). Hence, we can also conclude that: i) the function of $p27^{Kip1}$ in the effector component of the timer interacts with TH-mediated signaling to operate, and ii) the low rate of differentiation that occurs in the presence of mitogens, but in the absence of TH, involves a different intracellular mechanism from that of TH-dependent differentiation. The identification of $p27^{Kip1}$ as a component of the timer however does not indicate how $p27^{Kip1}$ works in this regard. It is still likely that this complex role may be due to the involvement of this protein, not only in the fine tuning of cyclin E-cdk2 inhibition, but in much broader cdk-independent functions, as suggested by its possible cytoplasmic localization (Coqueret, 2003).

2.2.3.2.2 The role of p18Ink4c

Three lines of evidence suggest that p18Ink4c may be part of the TH-regulated timer in developing OPCs. First, it was found that p18Ink4c protein levels, like $p27^{Kip1}$ (Durand et al., 1997), increased as OPCs proliferated in culture (Tokumoto et al., 2002). Second, it was shown, like $p27^{Kip1}$, that overexpression of p18Ink4c in OPCs accelerated the timer, causing the cells to differentiate prematurely when cultured in the presence of PDGF and TH (Tokumoto et al., 2002). Similarly to $p27^{Kip1}$, overexpression of p18Ink4c also stops cell cycle progression but fails to accelerate the spontaneous differentiation of OPCs cultured in PDGF without TH (Tokumoto et al., 2002). Third, $p18Ink4c^{-/-}$ mice have a phenotype that closely resembles that of $p27^{Kip1}$-deficient mice (Franklin et al., 1998), and there is compelling evidence that $p27^{Kip1}$ is a component of the timer in OPCs (Durand et al., 1997;Casaccia-Bonnefil et al., 1997;Durand et al., 1998). As both p18Ink4c- and $p27^{Kip1}$-deficient mice have increased numbers of cells in all organs examined (Fero et al., 1996;Kiyokawa et al., 1996;Nakayama et al., 1996), it seems likely that both cdkis help cells in many lineages withdraw from the cell cycle at the appropriate time.

2.2.3.2.3 The role of p53

The p53 tumor suppressor gene represents a nodal point of convergence of several signal transduction pathways. The response of individual cells to p53 activation is dependent upon several factors, including the nature of the activating stimulus, secondary modifications of the protein (i.e., ubiquitination, phosphorylation, or acetylation) and the specific cell type (Giaccia and Kastan, 1998). Depending on the levels and modality of activation, p53 can act as transcriptional activator or repressor of many genes, causing apoptosis, cell cycle arrest in G1 or G2/M, or differentiation, depending on the cell type (Giaccia and Kastan, 1998). In proliferating OPCs, p53 protein levels are low and the protein is likely not functional, due to its cytoplasmic localization (Eizenberg et al., 1996). Upon removal of mitogens, however, p53 is transiently translocated to the nucleus and may be involved in both growth arrest and the onset of differentiation (Eizenberg et al., 1996).

It was demonstrated that overexpression of a p53 dominant-negative (Dn) molecule containing a point mutation in the C-terminal transactivation domain, affected proliferation and differentiation of OPCs cultured in the presence of PDGF and TH although it had no effect on the differentiation process induced by mitogen withdrawal (Tokumoto et al., 2001). OPCs infected with retroviral vector encoding Dn-p53 failed to stop dividing and to differentiate in response to TH, but stopped dividing and differentiate normally in response to PDGF withdrawal (Tokumoto et al., 2001). They also displayed a normal rate of spontaneous differentiation in the presence of PDGF and in the absence of TH (Tokumoto et al., 2001). These findings suggested that TH-induced OPC differentiation depends on p53 or one of its relatives (Yang and McKeon, 2000;Levrero et al., 2000;Yang et al., 2002), whereas both spontaneous and PDGF-withdrawal-induced differentiation do not. More importantly, they suggest that a p53 family protein is an essential part of the effector component of the intrinsic timer that helps control OPC differentiation in the presence of PDGF and TH (Figure 5B).

More recently, it was shown that among p53 family proteins, both p53 and p73, but not p63, are involved in TH-induced OPC differentiation (Billon et al., 2004). Furthermore, p73 was also observed to normally play a crucial part in PDGF-withdrawal-induced OPC differentiation, which is the first demonstration of a role for p73 in the differentiation of a normal mammalian cell type (Billon et al., 2004).

Such findings, together with data from $p27^{Kip1}$ overexpression (Tokumoto et al., 2002) strengthen the evidence that TH-induced and spontaneous or PDGF-withdrawal-induced differentiation are mediated by distinct intracellular molecular pathways, which still commonly include p73-dependent processes (Billon et al., 2004) (Figure 5B). To what extent these signaling pathways might possibly coexist in vivo remains to be established.

2.2.3.2.4 The role of basic helix-loop-helix (bHLH) proteins

The basic HLH transcription factor family regulates the development of many cells by orchestrating cell-type-specific gene expression (Guillemot, 1999;Schuurmans and Guillemot, 2002;Ross et al., 2003). Genes of the bHLH class, such as the *Achaete-Scute* (AS-C) complex in *Drosophila* and its mammalian homologue Mash1 control the determination and differentiation of neurons (Johnson et al., 1990;Bertrand et al., 2002;Parras et al., 2002;Ross et al., 2003). Until two oligodendrocyte lineage-specific bHLH proteins (Olig1 and Olig2) were recently identified, it was not yet known whether there were bHLH proteins required for glial specification and differentiation (Lu et al., 2000;Zhou et al., 2000;Zhou et al., 2001).

Tissue-specific class B bHLH proteins control cell type specification and differentiation by dimerizing with more ubiquitously expressed E2A-type class A bHLH proteins such as E12 and E47. The function of tissue-specific B-type bHLH proteins is blocked by Id (inhibitor of DNA binding) proteins that are HLH proteins lacking the DNA binding domain of bHLH proteins (Benezra et al., 1990;Norton et al., 1998;Norton, 2000). Ids block differentiation in diverse cell types, including neural cells, by acting as dominant-negative blockers of the function of bHLH proteins. Id proteins bind to class A bHLH proteins (also named E proteins), preventing their dimerization with class B bHLH proteins and activation of gene transcription (Norton, 2000;Zebedee and Hara, 2001). Besides Ids, Hes5, a mammalian homologue of the "antineural" Drosophila bHLH genes Hairy and Enhancer-of-split (Akazawa et al., 1992), can bind to and antagonize the action of proneural bHLH proteins such as Mash1 (Akazawa et al., 1992;Sasai et al., 1992). Hes proteins can also bind to N-box elements in DNA and recruit co-repressor proteins to inhibit proneural gene transcription (Grbavec and Stifani, 1996;Fisher et al., 1996).

2.2.3.2.4.1 Mash1

Although Mash1 mRNA and protein were found to be expressed in OPCs and down-regulated during differentiation (Kondo and Raff, 2000a;Wang et al., 2001), the overexpression of Mash1, however, did not detectably interact with oligodendrocyte differentiation when the precursor cells were cultured in PDGF and TH (Kondo and Raff, 2000a). In the absence of Mash1, it was also shown that OPCs were able to differentiate normally and that the timing of their differentiation in response to TH was normal (Wang et al., 2001).

What function might Mash1 have in oligodendrocyte lineage cells if it does not control oligodendrocyte differentiation? Recently, others and we discovered that so-called OPCs cultured under certain conditions have the ability to generate neurons as well as glial cells (see part 3 of the present manuscript) (Kondo and Raff, 2000b;Publication #5 - Belachew et al., 2003;Nunes et al., 2003;Publication #6 - Aguirre et al., 2004). The finding that TH rapidly down-regulates Mash1 in cultured OPCs (Wang et al., 2001) raises the interesting possibility that the presence of Mash1 in OPCs might correlate with, or be necessary for, their ability to undergo neurogenesis (Parras et al., 2004). If so, the TH-mediated downregulation of Mash1 might explain why multipotential neural stem cells that persist within the adult mammalian brain appear unable to generate many neurons in vivo, while they can in vitro.

2.2.3.2.4.2 Olig genes

Several laboratories have recently identified a novel family of genes named Olig, encoding bHLH transcription factors (Lu et al., 2000;Zhou et al., 2000;Takebayashi et al., 2000). We will focus here on Olig1 and Olig2, although a third family member, Olig3, is known to be expressed in a non-overlapping pattern (Takebayashi et al., 2000), and reports of additional homologues are emerging. Loss-of-function studies comparing single Olig1 or Olig2 (Lu et al., 2002) and double Olig1-Olig2 (Zhou and Anderson, 2002) deficiencies have indicated overlapping functions for Olig proteins in OPC specification with functional redundancy between the two genes in certain region of the CNS, although the activities of Olig1 and Olig2 appear to be highly context-dependent (Rowitch et al., 2002). Importantly, no OPCs were observed anywhere in the entire CNS of Olig1-Olig2 double mutant mice (Zhou and Anderson, 2002). We will not describe here the complex functions of Olig genes in the control of the timing of OPC specification (Rowitch et al., 2002) together with other transcription factors such as Sox 9 (Stolt et al., 2003) or the homeodomain transcription factor Nkx6.1 (Liu et al., 2003a).

Besides their crucial role in oligodendrocyte lineage determination it appears that Olig proteins may also regulate the timing of oligodendrocyte differentiation, as suggested by their persistent expression throughout the whole oligodendroglial lineage until mature stages. Whereas Olig2, the primordial Olig gene, plays especially prominent roles in the developing spinal cord where it is essential for oligodendrocyte and motor neuron specification (Lu et al., 2002), Olig1 is not required for motor neuron development but promotes formation and maturation of oligodendrocytes, especially within the brain (Lu et al., 2001). The fact that Olig1$^{-/-}$ mice display a delayed oligodendrocyte maturation also supports this notion (Lu et al., 2002). In the brain of Olig1$^{-/-}$ mice, multilamellar wrapping of myelin membranes around axons does not occur, despite recognition and contact of axons by oligodendrocytes, thus showing that axonal recognition and myelination are separable processes (Xin et al., 2005). Hence, Olig1-null mice develop widespread progressive axonal degeneration and gliosis (Xin et al., 2005). In contrast, myelin sheaths are formed in the spinal cord of Olig1$^{-/-}$ mice, although the extent of myelination

is severely reduced (Xin et al., 2005).

Recent studies indicated that signals regulating the subcellular localization and/or activity of Olig1 during development may play an additional and critical role in activating OPCs in the adult CNS, since remyelination completely fails in adult Olig1$^{-/-}$ mice (Arnett et al., 2004). However, Arnett et al. used a different transgenic line from that of Xin and colleagues (Xin et al., 2005), in which developmental myelination of the brain is grossly normal (Arnett et al., 2004) because the molecular construction allows compensatory mechanisms by Olig2 (a gene encoding a protein with 80% homology to Olig1, and located just 40kb away from the Olig1 locus) or other unidentified genes in the region of the *PGK* sequences inserted into Olig1 locus (Balabanov and Popko, 2005).

Interestingly, the accumulation of Olig2 in the nucleus was shown to repress astrocytic differentiation of neural stem cells (Setoguchi and Kondo, 2004). It has also been suggested that Olig2 interacts with the homeodomain transcription factor Nkx2.2, not only at the level of OPC specification (Zhou et al., 2001;Sun et al., 2001), but also forms a cooperative complex that promotes oligodendrocyte differentiation during later embryonic development (Qi et al., 2001;Fu et al., 2002;Sun et al., 2003). Altogether, these results strongly indicate that Olig genes and their interaction with homeodomain transcription factor Nkx2.2 might be relevant components of the intrinsic timer of oligodendrocyte differentiation, but only detailed kinetic in vitro analyses will accurately explain their actual involvement in this regard.

2.2.3.2.4.3 Id2 and Id4

Id proteins are ideal candidates to help couple proliferation to differentiation, as in many cell types they are upregulated by mitogens and help to promote proliferation (Zebedee and Hara, 2001) as well as to inhibit differentiation by interacting with Rb and other bHLH proteins responsible for differentiation. It was found that: i) overexpression of Id2 powerfully inhibited oligodendrocyte differentiation, ii) Id2 normally translocated out of the nucleus at the onset of differentiation, and iii) the absence of Id2 induced premature oligodendrocyte differentiation in vitro (Wang et al., 2001).

The expression of another Id family member Id4 in OPCs decreased in vivo and in vitro with a time course expected if Id4 was part of the timer (Kondo and Raff, 2000c). It was also shown that Id4 expression decreased prematurely when the OPCs were induced to differentiate by PDGF withdrawal (Kondo and Raff, 2000c). Finally, enforced expression of Id4 stimulated OPC proliferation and blocked differentiation induced either by TH treatment or PDGF withdrawal (Kondo and Raff, 2000c). Unfortunately, it is not established so far whether Id4$^{-/-}$ OPCs would prematurely differentiate as occurs when Id2 is absent (Wang et al., 2001).

Such findings indicate that a progressive fall of Id4 expression and a final cytoplasmic translocation of Id2 are part of the intracellular timer that helps determine when OPCs withdraw from the cell cycle and differentiate. In the presence of mitogens, Id proteins may thus dimerize in OPCs with a class A bHLH, thereby sequestering it and preventing its binding to an as yet unidentified class B bHLH protein necessary for oligodendrocyte differentiation. This latter might belong to the Olig gene family (Figure 5B) as suggested by recent bacterial two-hybrid and co-immunoprecipitation studies, which demonstrated that Id4, and to a lesser extent Id2, complexed with Olig1 and Olig2 (Samanta and Kessler, 2004). In addition, the Olig and Id proteins both interacted with the E2A proteins E12 and E47 (Samanta and Kessler, 2004). These observations suggests that the nuclear induction of Id4 and Id2 inhibits oligodendroglial lineage commitment by sequestrating both Olig proteins and E2A proteins.

2.2.3.2.4.4 Hes 5

Notch-mediated signaling which has been shown to inhibit the differentiation of OPCs induced the expression of Hes5 (Wang et al., 1998). Hence it was not surprising that the overexpression of Hes5 led on its own to inhibiting oligodendrocyte differentiation induced by either mitogen withdrawal or TH addition (Kondo and Raff, 2000a). This at least suggests that Hes5 protein is an important effector of the Notch-mediated signaling in the oligodendrocyte lineage. Furthermore, Hes5 mRNA progressively decreases as developing OPCs proliferate in vivo and in vitro and is no longer detectable when the precursors differentiate into oligodendrocytes (Kondo and Raff, 2000a). This down-regulation of Hes5 expression occurs even in the absence of a significant change in Notch-mediated signaling (Kondo and Raff, 2000a). It seems likely that the progressive decrease in Hes5 protein plays a part in regulating when the precursors start to differentiate but further experiments are needed to ascertain this possible contribution to the intrinsic timing mechanism.

2.2.3.2.5 Extrinsic cues

We want to emphasize here that it is outside the scope of the present manuscript to exhaustively describe the relationships between the vast intricate networks of extrinsic regulatory factors that do exert an integrated control over previously discussed intrinsic mechanisms. We will just summarize in table 1 the most relevant actors of this play and their established effects on proliferation and differentiation of OPCs.

Table 1: *Extrinsic regulation of oligodendrocyte development, downstream of OPC determination (i.e. regardless of cues that control OPC specification)*

Factors	Receptors	Effect	Selected References
		Growth factors	
PDGF (platelet-derived growth factor)	PDGFRα	-↑ proliferation -↓ onset of differentiation -↑ migration -chemoattraction -↑ survival	(Raff et al., 1988) (Noble et al., 1988) (Richardson et al., 1988) (Fruttiger et al., 1999) (Calver et al., 1998) (Baron et al., 2002) (Armstrong et al., 1990) (Milner et al., 1997) (Barres et al., 1992)
FGF2 (type 2 fibroblast growth factor)	FGFR1, FGFR2, FGFR3	-↑ proliferation -↓ terminal differentiation -↑ migration	(McKinnon et al., 1990) (Wolswijk and Noble, 1992) (Bansal et al., 1996) (Osterhout et al., 1997) (Goddard et al., 2001)
Neuregulins (NRG-1)	erbB2, erbB3, erbB4	-↑ proliferation -↑ differentiation -↑ survival	(Canoll et al., 1996) (Vartanian et al., 1999) (Park et al., 2001) (Calaora et al., 2001) (Kim et al., 2003)
BMPs (Bone morphogenetic proteins)	type-1 and type-2 BMP receptors	-↓ initial specification and favors astrocyte commitment	(Gross et al., 1996) (Mabie et al., 1997) (Mekki-Dauriac et al., 2002) (Gomes et al., 2003) (Kondo and Raff, 2004) (Samanta and Kessler, 2004) (See et al., 2004)
NT3 (neurotrophin-3)	TrkC	-↑ proliferation -↑ survival	(Barres et al., 1994b) (Cohen et al., 1996a)
IGF-1 (insulin-like growth factor 1)	IGF1R	-synergizes with PDGF and FGF2 to increase proliferation -↑ survival -↑ remyelination	(McMorris et al., 1986) (Barres et al., 1993) (Mason et al., 2000) (Mason et al., 2003) (Mason and Goldman, 2002) (Jiang et al., 2001)
TGFβ1		-↓ proliferation	(McKinnon et al., 1993)
		Chemokines-Cytokines	
CXCL1	CXCR2	↓ migration	(Tsai et al., 2002)
CNTF/LIF/IL-6 (ciliary neurotrophic factor - leukemia inhibitory factor - interleukin-6)	gp130	-↑differentiation -↑ myelination -↑ survival -↑ remyelination	(Louis et al., 1993) (Mayer et al., 1994) (Barres et al., 1996) (Marmur et al., 1998) (Stankoff et al., 2002) (Valerio et al., 2002) (Linker et al., 2002) (Butzkueven et al., 2002)
GROα (growth-related oncogene-α)	CXCR2	-↑proliferation	(Robinson et al., 1998) (Wu et al., 2000) (Filipovic et al., 2003)
IL-1β (interleukin-1β)	IL-1R	-↓ proliferation	(Vela et al., 2002)

Factors	Receptors	Effect	Selected References
IFNγ	IFNγR	-↑oligodendrocyte death and myelin loss	(Vartanian et al., 1995) (Corbin et al., 1996) (Horwitz et al., 1997)
TNFα	TNFR1, TNFR2	-↑oligodendrocyte death and myelin loss (TNFR1) -↑proliferation (TNFR2) -↓ oligodendrocyte death and myelin loss (TNFR2)	(Selmaj and Raine, 1988) (Akassoglou et al., 1998) (Liu et al., 1998a) (Arnett et al., 2001)
Extracellular matrix molecules			
Tenascin-C,vitronectin	αv integrins	-↑proliferation and ↓ differentiation (αvβ3) -↑differentiation (αvβ5) -↑migration (αvβ1)	(Milner and Ffrench-Constant, 1994) (Milner et al., 1996) (Blaschuk et al., 2000) (Garcion et al., 2001) (Baron et al., 2002)
Laminin	α6β1 integrin	-↑myelination and survival	(Malek-Hedayat and Rome, 1994) (Buttery and Ffrench-Constant, 1999) (Frost et al., 1999) (Colognato et al., 2002) (Baron et al., 2003)
Neurotransmitters			
Glutamate	AMPA/kaïnate receptors	-↓ proliferation -↑oligodendrocyte excitotoxic death	(Oka et al., 1993) (Patneau et al., 1994) (Gallo et al., 1996) (Matute et al., 1997) (McDonald et al., 1998) (Ghiani et al., 1999a) (Gallo and Ghiani, 2000) (Pitt et al., 2000;Smith et al., 2000)
Acetylcholine	M1 and M2 muscarinic receptors + nicotinic	-↑proliferation	(Cohen and Almazan, 1994) (Cohen et al., 1996b) (Publication #9 - Belachew et al., 1998) (Rogers et al., 2001)
Norepinephrine	α1A and β2	-↓ proliferation	(Cohen and Almazan, 1993) (Ghiani et al., 1999a) (Khorchid et al., 1999) (Ghiani and Gallo, 2001) (Khorchid et al., 2002)
Adenosine	A1, A2, and A3	-↓ proliferation -↑differentiation -↑migration	(Stevens et al., 2002) (Othman et al., 2003)
Neuropeptides			
PACAP (pituitary adenylyl cyclase-activating peptide)	PAC1	-↑proliferation -↓differentiation	(Lee et al., 2001)
Opioids	σ, μ and κ	-↑survival -↑myelination	(Hauser et al., 1993) (Knapp et al., 1998) (Demerens et al., 1999) (Knapp et al., 2001)
Others			

Factors	Receptors	Effect	Selected References
Jagged1	Notch1	-↓differentiation	(Wang et al., 1998) (Givogri et al., 2002)
Contactin	Notch1, (Notch2?)	-↑differentiation	(Hu et al., 2003)
PSA-NCAM (polysialylated form of neural cell adhesion molecule)	?	-↓myelination	(Charles et al., 2000) (Charles et al., 2002)
Axonal electrical activity	?	-↑proliferation -↑myelination	(Barres and Raff, 1993) (Demerens et al., 1996) (Barres and Raff, 1999)
Thyroid hormone	THRα1	-↑differentiation	(Barres et al., 1994a;Billon et al., 2002)
Cannabinoids	CB1	-↑survival	(Molina-Holgado et al., 2002)
IgGs	γ chain of immunoglobulin Fc receptors (FcR γ)	-↑differentiation	(Nakahara et al., 2003)
Netrin-1	DCC	chemorepellent (embryonic chick spinal cord) or chemoattractant (embryonic mouse optic nerve) ?	(Jarjour et al., 2003) (Spassky et al., 2002) (Sugimoto et al., 2001) (Tsai et al., 2003)
Class 3 semaphorin	Neuropilin 1 and 2	chemorepellent	(Sugimoto et al., 2001) (Spassky et al., 2002) (Cohen et al., 2003)

2.2.4 Teasing apart two models of relationships between proliferation and differentiation in the oligodendroglial lineage. G0 versus G1 cell cycle arrest

G1 cell cycle arrest induced by $p27^{Kip1}$ (Tikoo et al., 1998;Tang et al., 1999;Tokumoto et al., 2002), p18Ink4c (Tokumoto et al., 2002) or Dn-cdk2 (Publication #3 - Belachew et al., 2002) overexpression, or by extracellular signals that block cyclin E-cdk2 (Ghiani et al., 1999a;Ghiani et al., 1999b;Ghiani and Gallo, 2001), such as glutamate receptor agonists (i.e., AMPA/kainate), Na^+ channel openers (i.e., veratridine) or K^+ channel blockers (i.e., tetraethylammonium), can prevent entry into S-phase, but is not sufficient per se to start a differentiation program if mitogens are present in the medium. This may be presumably due to the existence of an inhibitory component (possibly cyclin D) induced by the mitogens (Huang et al., 2002). At a molecular level, this uncoupled state with G1 arrest and no differentiation is characterized by high levels of $p21^{Cip1}$, $p27^{Kip1}$, Rb, cyclin D1 and E (likely due to the presence of PDGF) (Huang et al., 2002). Taken together, the results of all these experiments argue against the validity of the simplistic linear model in which mitogens would activate transduction pathways that converge on a single signal responsible for promoting cell division while inhibiting differentiation, although they also provide correlative evidence linking high cyclin D1 and E levels to inhibition of differentiation.

In contrast to reversible G1-arresting conditions, one has to distinguish PDGF-withdrawal-induced G0 arrest, which is irreversible and characterized by low levels of G1 cyclins. Unlike the G1 arrest, which appears to be necessary but insufficient for differentiation, a G0 arrest is necessary and sufficient to trigger the differentiation program. One possible explanation for the "sufficiency" of G0 arrest is that cell cycle regulatory molecules, and particularly Rb (that is unphosphorylated in G0), may affect the sequestration of differentiation inhibitors (i.e. Id2, Id4) (Kondo and Raff, 2000a;Kondo and Raff, 2000c;Wang et al., 2001) that

normally keep OPCs in an undifferentiated state (Wang et al., 2001). Because unphosphorylated Rb has the ability to bind and sequester Id2 (Iavarone et al., 1994;Norton et al., 1998), it is conceivable that differentiation in G0 arrested cells may occur by de-repression due to sequestration of the Ids by Rb. Alternatively, cell cycle exit toward G0 state may directly result in histone deacetylase activation leading to a massive rearrangement of the chromatin conformation in the promoter region of the Ids, so that their levels may be decreased, thus allowing the differentiation to occur (Marin-Husstege et al., 2002).

2.3 Revisiting lineage fate potential of previously so-called "oligodendrocyte" progenitor cells in the postnatal brain: on the trail of a serial progenitor

After addressing the role of cell cycle regulation in OPCs, we wanted here in this next part of the manuscript to question the real identity of OPCs with respect to their fate potential. We will recapitulate recent data challenging that OPCs may not represent the best guys to be ready for action on the battlefield of remyelination.

2.3.1 Principal features of the postnatal OPC as an established oligodendrocyte progenitor expressing the NG2 proteoglycan surface marker

Although the glial complement of the adult CNS is generally thought to consist of astrocytes, oligodendrocytes and microglia, numerous reports in the last 30-40 years have identified populations of glial cells within adult animals that do not easily fall into these three basic cell groups. For example, in 1968, Vaughn and Peters identified cells in adult, embryonic and perinatal rat optic nerves with small irregularly shaped cell bodies and stout protrusions that contained neither the dense bundles of filaments associated with astrocytes nor the abundant microtubules characteristic of oligodendrocytes (Vaughn and Peters, 1968). They further showed that these unusual cells, which comprise 5% of all glia in the optic nerve, increased in number during Wallerian degeneration and that this increase in cell number was probably caused by cell division (Vaughn et al., 1970;Skoff and Vaughn, 1971). Cells with a similar appearance were then identified in rat cerebral cortex and termed β-astrocytes (Reyners et al., 1982;Reyners et al., 1986). This cell was both mitotically active and radiosensitive. In both of these studies, the authors had already suggested that these novel glial cells might be multipotent but glia-committed precursor cells.

Much of what we know about the multipotentiality of glial development comes from tissue culture studies initiated by Martin Raff and his colleagues in the early 1980s (Raff et al., 1983). Using antibody markers to identify all the cell types present in low-density cultures of perinatal rat optic nerve, they were able to identify a cell, termed an O-2A progenitor cell, that could develop into either an oligodendrocyte or a type II astrocyte, depending on tissue culture conditions (Raff et al., 1983). Subsequent work by a number of groups has established NG2 chondroïtin sulfate proteoglycan as an excellent marker of O-2As in vivo (Levine et al., 1993;Nishiyama et al., 1996;Reynolds and Hardy, 1997;Trapp et al., 1997;Keirstead et al., 1998;Nishiyama et al., 1999;Chang et al., 2000;Chang et al., 2002). Postnatal $NG2^+$ O-2As can also alternatively be visualized by their expression of PDGFRα (Nishiyama et al., 1996;Redwine and Armstrong, 1998) or by their tendency to take up cobalt when stimulated with quisqualate (Fulton et al., 1992). What was not completely resolved was the question of whether the O-2A lineage operated in vivo in the same manner seen in cell cultures. While it seemed clear that $NG2^+$ O-2As give rise to oligodendrocytes in vivo, evidence for the derivation of astrocytes from

this same lineage is by far less abundant (Levine et al., 1993;Luskin et al., 1993;Grove et al., 1993;Levison and Goldman, 1993;Nishiyama et al., 1996;Trapp et al., 1997;Levison et al., 1999;Marshall and Goldman, 2002). The fashion has thus rapidly changed to refer to these cells as oligodendrocyte progenitor cells.

In this part of our work, we will reappraise the current status in terms of fate potential of this unusual cell type, which has become known as OPC (i.e. oligodendrocyte progenitor cell) (Levine et al., 2001).

Although adult OPCs divide slowly in situ (the labeling index for cells within the adult cerebellar cortex is 0.2-0.3%), they are the principal dividing cell population within the adult brain parenchyma (Levine et al., 1993;Horner et al., 2000). When adult rats are pulse-labeled with bromodeoxyuridine (BrdU), as many as 70% of the BrdU-labeled cells in the spinal cord (Horner et al., 2000) and 75% of those in the cortex express NG2 (Levine et al., 2001;Dawson et al., 2003). In these same short-term survival experiments, no BrdU-positive oligodendrocytes were observed. Six days after a BrdU pulse, however, there are some BrdU-positive oligodendrocytes in the cortex, suggesting that at least some of these are the progeny of dividing OPCs (Dawson et al., 2000;Levine et al., 2001). Studies using injections of retroviruses to mark and follow dividing cells in the adult rat neocortex showed that OPCs, identified by NG2 expression, comprised 35% of all infected cells (Levison et al., 1999). Some of the clusters of retrovirally-marked cells that develop within adult animals contained both $NG2^+$ OPCs and oligodendrocytes. This supports the notion that adult OPCs are a dividing population of precursor cells that can develop into oligodendrocytes, although there has not yet been a direct demonstration that a single OPC can differentiate into a myelin-forming cell within normal adult animals. There is thus a paradoxical lack of data that would determine how homogeneous or heterogeneous the $NG2^+$ OPCs are with regard to their real ability to differentiate into oligodendrocytes in the postnatal/adult brain.

2.3.2 NG2-expressing cells actually represent a bi-potential oligodendrocyte/interneuron (OIN) precursor cell type in the postnatal brain

Publication #5: Belachew,S., Chittajallu,R., Aguirre,A.A., Yuan,X., Kirby,M., Anderson,S., and Gallo,V. (2003). Postnatal NG2 proteoglycan-expressing progenitor cells are intrinsically multipotent and generate functional neurons. *J. Cell Biol.* 161:169-186.
Publication #6: Aguirre,A.A., Chittajallu,R., Belachew,S., and Gallo,V. (2004). NG2-expressing type C multipotent progenitor cells of the subventricular zone: a possible source of interneuron renewal the adult hippocampus. *J. Cell Biol.* 165:575-589.

During CNS development, the well-characterized anatomical distribution of $NG2^+$ progenitors (Spassky et al., 1998) overlaps with areas where multipotent NSCs reside and ongoing neurogenesis occurs (Alvarez-Buylla and Temple, 1998;Temple and Alvarez-Buylla, 1999). It is also clear that numerous $NG2^+$ cells are located in gray matter areas of the brain, including the cerebral cortex (Reynolds and Hardy, 1997;Publication #2 - Yuan et al., 2002;Mallon et al., 2002), i.e. regions that display relatively less myelination, as compared to white matter areas. Furthermore, $NG2^+$ cells persist in the gray matter of the adult CNS long after myelination has terminated (Nishiyama et al., 1996;Reynolds and Hardy, 1997). Cells that express the NG2 proteoglycan represent the largest pool of postnatal proliferative progenitors scattered throughout neurogenic as well as non-neurogenic areas of the CNS (Dawson et al., 2000;Dawson et al., 2003). Such evidences have raised intriguing questions regarding the lineage specificity and physiological role of these $NG2^+$ OPCs. Although one cannot contest that these

cells are capable of differentiating into myelinating oligodendrocytes, it is debatable whether this developmental program occurs for all CNS cells that express the NG2 proteoglycan.

Even if first described as multipotent, OPCs were never thought until recently to be capable of generating non-glial cells. The initial breakthrough to jeopardize this tenacious tenet came from the demonstration that OPCs from neonatal optic nerve, normally restricted to giving rise to oligodendrocytes and type II astrocytes in vitro (Raff, 1989), reverted via an astrocytic state to multipotent neural stem cells (NSCs) that were able to self-renew and generate neurons, when cultured in serum- and then FGF2-containing medium successively (Kondo and Raff, 2000b). These findings could still be viewed as the result of irrelevant epigenetic reprogramming of cells occurring only in long-term culture experiments that lack essential contextual cues.

Likewise, other glial cells that are now known to serve as CNS stem cells in the adult brain (Goldman, 2003;Doetsch, 2003), our recent works have ascertained that $NG2^+$ cells represent a new class of CNS multipotent cells in vitro and in vivo (Publication #5 - Belachew et al., 2003;Publication #6 - Aguirre et al., 2004). In this chapter, we will sum up current opinions about adult neurogenesis and address how and to what extent $NG2^+$ cells may be related or not to other phenotypes in the novel emerging nomenclature of glial precursors of neurons.

2.3.2.1 Neurogenesis in numbers in the adult brain

Neurogenesis, i.e. the generation of newly born neurons, has been shown to persist in two areas of the adult mammalian CNS: the olfactory bulb and the dentate gyrus (DG) region of the hippocampus (Taupin and Gage, 2002). The first evidence of continuous neurogenesis in certain regions of the adult mammalian CNS came from [^{3}H]-thymidine labeling studies conducted by in the 1960s (Altman and Das, 1965). In the 1990s, new methods for labeling dividing cells such as using BrdU (marker of the S-phase of the cell cycle) or retroviruses, helped to unravel the ins and outs of neurogenesis in the adult CNS. Neurogenesis is now known to occur in adult DG areas during the entire lifespan of mammals (Gould and Gross, 2002) from rodents (Altman and Das, 1965;Kaplan and Hinds, 1977;Bayer et al., 1982;Kaplan and Bell, 1983;Kaplan and Bell, 1984;Kuhn et al., 1996;Kempermann et al., 1997a) to human (Eriksson et al., 1998) and non-human primates (Kornack and Rakic, 1999;Gould et al., 2001).

A common dogma was still recently to consider that only excitatory granule cells (GCs) constituted the several thousand new neurons that are produced each day in the adult mammalian hippocampus (Cameron and McKay, 2001). However, it has now been established that the phenotype of adult-born hippocampal neurons is heterogeneous since approximately 14% of newly generated neurons in the DG of adult rodents were found to be inhibitory basket cells (BCs) (Liu et al., 2003b).

As many as 9000 new cells per day and more that 250 000 cells per month are produced in the DG areas of a young adult rat (Cameron and McKay, 2001). This number of new DG neurons represents a renewal of about 3 to 6 % of the total size of the granule cell population of a young adult per month, or about 0.1 % per day (Kempermann et al., 1997b;Cameron and McKay, 2001). Many of the newly generated neuronal progenitor cells in the adult rat DG die between the first and second week after they were born (Cameron et al., 1993;Gould et al., 1999a). The new DG neurons that survive were detected up to 11 months post-BrdU injections in rodents (Kempermann et al., 2003), up to 781 days post-BrdU injections in adult humans (Eriksson et al., 1998) and up to 12 weeks after injections in adult macaque monkeys (Gould et

al., 2001). Furthermore, recent works assessing short-term and long-term survival of new neurons in rat DG have suggested that granule cells born during adulthood that become integrated into circuits and survive to maturity are very stable and may permanently replace granule cells born during development (Dayer et al., 2003). However, due to uncertainties in labeling efficiencies, due to the occurrence of cell death and possible dilution of labeling agents with continued division, the accurate magnitude of adult DG neurogenesis remains elusive and is likely to be underestimated by current available assessment techniques.

2.3.2.2 Current nomenclature for "glial" neural stem cells in the adult CNS

The nomenclature of neuronal progenitors in the postnatal and adult brain has been recently redefined with more accuracy and identifies precursor cells that were previously thought to be restricted to a glial fate (Goldman, 2003;Doetsch, 2003).

Two major multipotent NSC phenotypes have been described principally in the

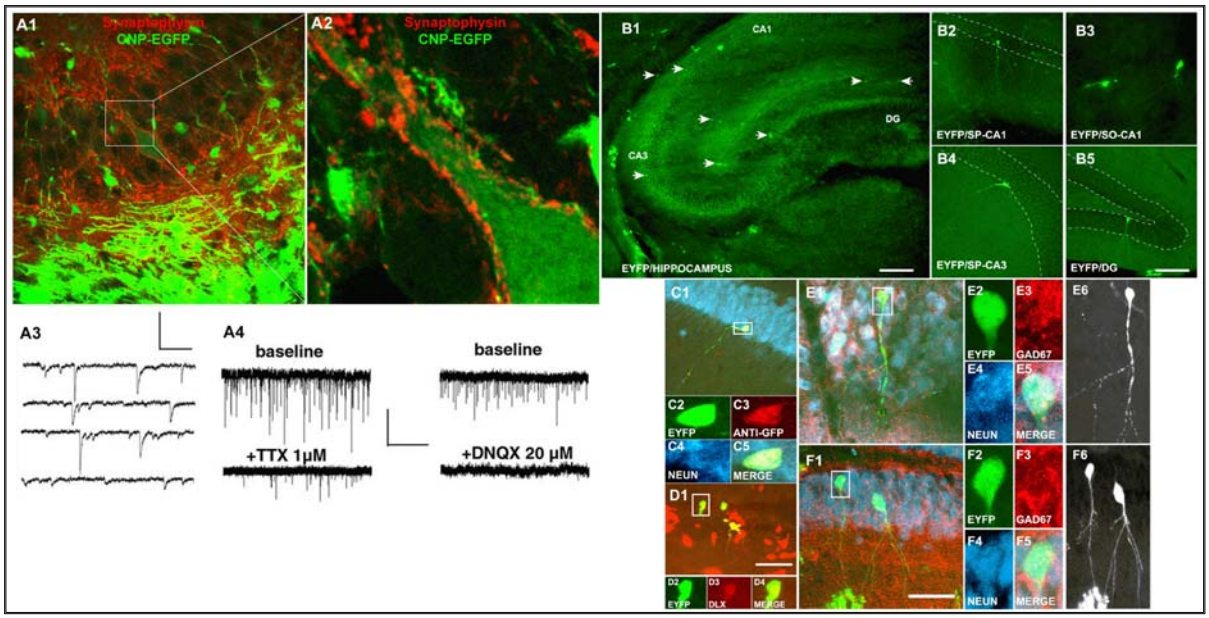

Figure 6: *NG2 proteoglycan-expressing progenitor cells generate functionally-integrated GABAergic interneurons in the postnatal hippocampus*
(A) Endogenous CNP-EGFP$^+$ hippocampal neurons express the presynaptic marker synaptophysin. A2 highlights at higher magnification the boxed area of A1 where one can observe synaptophysin$^+$ puncta bordering the soma and the apical dendrite of a CNP-EGFP$^+$ neurons from CA3. (A3) Continuous recording (total = 2.4 s) of spontaneous post-synaptic currents under voltage-clamp (-60mV) in a CNP-EGFP$^+$ neuron of the hilar dentate gyrus area (scale = 0.5s, 50pA). (A4) Synaptic activity of dentate gyrus CNP-EGFP$^+$ neurons was blocked by application of 1µM tetrodotoxin (TTX) and 20 µM of DNQX (antagonist of AMPA/kaïnate subtypes of glutamate receptors). Spontaneous synaptic currents recorded in baseline conditions were compared with those of the same cell (bottom traces) 2 min after drug application (scale = 30s; 50pA). (B) One week after grafting, NG2$^+$/EGFP$^+$ cells (green) were found in the hippocampus (arrows) displaying a typical neuronal morphology in the stratum oriens of the CA1 (B3) and CA3 (not depicted), in the stratum pyramidale of the CA1 and CA3 (B2 and B4, respectively), and in the DG (B5). The tissue was also stained with anti-GFP antibodies (C, red), confirming that these neurons are derived from the transplanted NG2$^+$/EGFP$^+$ fraction. Migratory EGFP$^+$ cells acquired immature neuronal markers one week after grafting, as shown by Dlx (D, red) and TUJ1 (not depicted) immunostainings. (E and F) 3 week after transplantation, all the grafted EGFP$^+$ cells (green) found in the hippocampus were labeled with anti-NeuN antibodies (blue). EGFP$^+$/NeuN$^+$ cells (green/blue) were found in the pyramidal layer of CA1 (not depicted) and CA3 (E) and in the subgranular layer of the DG (F). EGFP$^+$ cells were also labeled with anti–GAD-67 (red) antibodies in the CA3 area (E) and DG (F), confirming their GABAergic fate. In E6 and F6, EGFP was converted to grayscale. Anti-GFP antibodies recognize all the GFP variants, including EGFP, EYFP, and ECFP. EGFP$^+$ cells are shown at higher magnification in boxed areas. Bars: (A, C, E, and F) 50 µm; (B1) 300 µm; (B2–B5) 100 µm.

subventricular zone (SVZ), but also in the hippocampus, based on the expression of the intermediate filament protein glial fibrillary acidic protein (GFAP) (Doetsch et al., 1999;Seri et al., 2001;Capela and Temple, 2002;Doetsch et al., 2002a) (see Figure 7). Type B cells in the SVZ

express the astrocytic marker GFAP and display ultrastructural characteristics of astrocytes (Doetsch et al., 1999;Laywell et al., 2000). SVZ type B cells give rise to the rapidly dividing, transit-amplifying Type C cells, which are not immunopositive for GFAP. It has been demonstrated that SVZ Type C cells: i) are able to generate neurospheres in the presence of epidermal growth factor (EGF); ii) express the distal-less homeobox transcription factor dlx2 and the EGF receptor (EGFR), and iii) give rise to chains of neuroblasts (termed type A cells) that migrate tangentially through the rostral migratory stream (RMS) where they are the direct precursors of granule neurons generated in the adult olfactory bulb (Doetsch et al., 1999;Doetsch et al., 2002a).

Adult NSCs were also shown to express the Lewis X (LeX) carbohydrate antigen, which is detected in GFAP$^+$ type B NSCs, but also in GFAP-negative cells of the SVZ (Capela and Temple, 2002), indicating that this brain region contains a LeX$^+$/GFAP-negative cell population with neurogenic potential. Since Type C cells are a GFAP-negative and highly proliferative cell population, it is likely that the LeX$^+$/GFAP-negative stem cells are in fact Type C progenitors (Capela and Temple, 2002;Doetsch et al., 2002a) (see Figure 7).

GFAP and LeX expression in NSCs however mostly applies to adult SVZ-derived neurogenesis in the olfactory bulb (Doetsch et al., 1997;Doetsch et al., 1999) and to a lesser extent to the generation of new excitatory granule cells in DG sub-granular layer of the adult hippocampus (Palmer et al., 1997;Seri et al., 2001). Therefore, it does not account for neurogenesis of hippocampal inhibitory interneurons (Liu et al., 2003b) or for neurogenesis occurring in early postnatal development or outside anatomically identified neurogenic areas (Palmer et al., 1995;Weiss et al., 1996;Shihabuddin et al., 2000). In the absence of suitable specific markers to visualize postnatal NSCs in situ, their phenotype(s) and possible existence outside of neurogenic regions of the CNS (Palmer et al., 1995;Weiss et al., 1996;Gould et al., 1999b;Shihabuddin et al., 2000;Magavi et al., 2000) have remained elusive questions (Gage, 2000;Alvarez-Buylla et al., 2001;Kornack and Rakic, 2001).

We propose hereafter that NG2$^+$ cells may underlie a significant part of most unresolved features of adult neurogenesis, since they are present throughout the brain and represent a source of adult-born GABAergic interneurons in the hippocampus (Publication #5 - Belachew et al., 2003;Publication #6 - Aguirre et al., 2004).

2.3.2.3 *Postnatal NG2$^+$ progenitor cells expressing the CNP gene are intrinsically multipotent and generate functional neurons*

Publication #5: Belachew,S., Chittajallu,R., Aguirre,A.A., Yuan,X., Kirby,M., Anderson,S., and Gallo,V. (2003). Postnatal NG2 proteoglycan-expressing progenitor cells are intrinsically multipotent and generate functional neurons. *J. Cell Biol.* 161:169-186.

Using the CNP-EGFP transgenic mouse, we demonstrated that postnatal NG2$^+$ progenitor cells expressing the CNP gene display antigenic and developmental features of multipotent CNS progenitor cells in vitro, including: i) a nestin$^+$ immunophenotype (Reynolds and Weiss, 1992;Johe et al., 1996), ii) the capacity to form neurospheres when cultured in uncoated conditions in EGF- and FGF2-containing medium (Reynolds and Weiss, 1992;Johe et al., 1996), and iii) the typical trilineage differentiation potential of a single cell able to give rise to electrically excitable neurons, to astrocytes and oligodendrocytes (Publication #5 - Belachew et al., 2003).

We could also consistently find postnatal hippocampal CNP-EGFP$^+$ cells located in the dentate gyrus, expressing both the neuronal marker NeuN and glutamate decarboxylase 67 kD

(GAD-67) (Publication #5 - Belachew et al., 2003). Such CNP-EGFP$^+$ hippocampal neurons elicited spontaneous tetrodotoxin-sensitive post-synaptic currents that were blocked by AMPA/kainate receptor antagonists, thus confirming that they receive functional neurotransmitter-mediated synaptic inputs (Figure 6A) (Publication #5 - Belachew et al., 2003). Therefore, we suggested that a sizeable pool of NG2$^+$/CNP-EGFP$^+$ cells represent progenitor cells that generate new functional GABAergic neurons in the adult murine hippocampus.

Similarly, in human, another group observed at the same time that progenitor cells expressing the CNP gene and derived from normal adult white matter could be passaged as neurospheres and displayed a multipotent phenotype in vitro (Nunes et al., 2003). They also provided evidence that such CNP gene-expressing progenitor cells from human white matter generated functionally competent GABAergic neurons after xenograft into the fetal rat brain (Nunes et al., 2003). Two independent works thus simultaneously raised the issue that GABAergic neurons and oligodendrocytes may share a common progenitor cell at least in certain locations of the postnatal brain, and likewise during embryonic development (He et al., 2001;Yung et al., 2002;Chojnacki and Weiss, 2004).

2.3.2.4 *NG2$^+$ progenitors are type C-like cells in the subventricular zone and may be a possible source of interneuron renewal in the adult hippocampus*

Publication #6: Aguirre,A.A., Chittajallu,R., Belachew,S., and Gallo,V. (2004). NG2-expressing type C multipotent progenitor cells of the subventricular zone: a possible source of interneuron renewal the adult hippocampus. *J. Cell Biol.* 165:575-589.

At this stage, it was still unclear how the cellular and developmental properties of NG2$^+$ progenitors related to those of other multipotent cell types identified in the postnatal/adult CNS, and what types of neurons were generated from NG2$^+$ cells in vivo. To address such issues, we decided first to study NG2$^+$/CNP-EGFP$^+$ progenitor cells in the SVZ, i.e. in a location where stem cell phenotypes (A,B,C) (Doetsch, 2003) were initially described and where their relationships have been the most highly characterized. We provided direct evidence that NG2$^+$/CNP-EGFP$^+$ cells are transit-amplifying Type C-like cells of the SVZ (Figure 6 and 7) and may be a source of GABAergic interneurons in the hippocampus.

These conclusions were based on the following findings (Publication #6 - Aguirre et al., 2004): i) SVZ NG2$^+$/EGFP$^+$ cells are mitotically active; ii) the majority of SVZ NG2$^+$/EGFP$^+$ cells expressed the EGF receptor, and a large percentage were immunopositive for dlx transcription factors; iii) SVZ NG2$^+$/EGFP$^+$ cells expressed the LeX antigen, and were negative for the astroglial markers GFAP and GLAST; iv) LeX$^+$/dlx$^+$/NG2$^+$/EGFP$^+$ cells gave rise to multipotent self-renewing neurospheres in vitro; v) FACS-purified NG2$^+$/EGFP$^+$ cells transplanted into the postnatal lateral ventricle generated functionally integrated GABAergic interneurons in the hippocampus (Figure 6B-E); and vi) endogenous hippocampal GAD-67$^+$/CNP-EGFP$^+$ interneurons displayed the same cellular phenotype as neurons generated from transplanted NG2$^+$/CNP-EGFP$^+$ progenitors in vivo or from NG2$^+$/CNP-EGFP$^+$ neurospheres in vitro (Publication #6 - Aguirre et al., 2004).

It remains to be determined to what extent our data suggest that endogenous newborn adult interneurons (Liu et al., 2003b) in the hippocampus may derive from SVZ progenitor cells, likely located in the posterior SVZ. It would raise the possibility that a sub-population of type C-like progenitor cells from the SVZ would be able to migrate backward and radially (Marshall et al., 2003;Suzuki and Goldman, 2003) instead of their classical route of tangential forward migration through the rostral migratory stream towards the olfactory bulb.

This type of backward migration of SVZ cells occurs during embryonic development when progenitor cells from the caudal ganglionic eminence populate the hippocampus (Wichterle et al., 2001;Nery et al., 2002;Brazel et al., 2003). In contrast, in the postnatal brain, none of the studies that have examined ventricular cell migration with retroviral labeling assays (Luskin, 1993;Morshead et al., 1994;Doetsch and Alvarez-Buylla, 1996;Morshead et al., 1998;Suzuki and Goldman, 2003) have ever brought any obvious demonstration that endogenous SVZ cells, no matter how rostral or caudal, could migrate backward and radially to integrate the hippocampus. However, postnatal migration routes skirting the dorsal hippocampus have been described (Marshall et al., 2003;Suzuki and Goldman, 2003).

Hence, we would be inclined to stick to the widely held assumption that there may not be a significant amount of endogenous SVZ $NG2^+/EGFP^+$ cells migrating towards the hippocampus in the adult, at least in the conditions of an intact brain. This would imply the following consequences:

i) If they are restricted to forward migration through the RMS, similar to typical SVZ type C cells that generate OB granule neurons, endogenous SVZ $NG2^+/EGFP^+$ cells with a type C-like phenotype may be a source of tangentially migrating neuroblast, which could become olfactory bulb interneurons (Aguirre and Gallo, 2004), since interneurons are also adult-generated in this location (Lois and Alvarez-Buylla, 1994;Carleton et al., 2003).

ii) The endogenous $NG2^+/EGFP^+$ cells that reside in the hippocampus may underlie the generation of newborn hippocampal interneurons (Liu et al., 2003b). We now have to assess whether $NG2^+/EGFP^+$ cells residing in the hippocampus also display a transit-amplifying phenotype and correspond to so-called hippocampal type D-like cells (Doetsch, 2003) that would represent a subset of DG-located type D population giving rise specifically to interneurons, and not to granule neurons as typical type D cells do.

iii) Even if not occurring in the intact brain, we provide evidence that the migration route from the SVZ (likely posterior and dorsolateral parts) to the hippocampus does exist, but local positional cues possibly prevent endogenous progenitors from using it effectively. Interestingly, after ischemia, it has been shown that periventricular progenitor cells, likely originating from the caudal SVZ, can invade the hippocampus though the anterior part of CA1 and regenerate functional neurons secondarily (Nakatomi et al., 2002). We showed that a subset of exogenous $NG2^+/EGFP^+$ cells FACS-purified from the perinatal whole brain however retain the intrinsic molecular machinery that is necessary for patterning this unusual route of migration and for the cellular and regional determination of interneuron identity within the hippocampus.

2.3.2.5 Finding a spot for $NG2^+$ OIN precursors in or out of the A,B,C... neural stem cell nomenclature

It is yet to be investigated whether there may be a link between B-type $LeX^+/GFAP^+$ neural stem cells generating newborn granule neurons in the olfactory bulb and hippocampus (Doetsch et al., 1999;Alvarez-Buylla et al., 2001;Seri et al., 2001;Doetsch et al., 2002a), and $LeX^+/NG2^+/CNP\text{-}EGFP^+$ cells generating hippocampal interneurons in the postnatal/adult murine brain both in the hippocampus and in the olfactory bulb (Publication #5 - Belachew et al., 2003;Publication #6 - Aguirre et al., 2004;Aguirre and Gallo, 2004). The sole experimental data in favor of such a link relies on the detection of NG2 proteoglycan in some hippocampal cells expressing EGFP under the control of the GFAP gene promoter (Matthias et al., 2003). We illustrated in Figure 7 that SVZ $NG2^+$ multipotent progenitor cells correspond to transit-amplifying multipotent cells (Doetsch et al., 2002a), i.e. so-called type C-like cells with respect

to the nomenclature established by Arturo Alvarez-Buylla, Jose M. Garcia-Verdugo and Fiona Doetsch (Doetsch et al., 1999;Alvarez-Buylla and Garcia-Verdugo, 2002;Doetsch et al., 2002a;Doetsch, 2003). We and others have also observed that a subset of $NG2^+$ cell-derived $O4^+$ progenitor cells (or $NG2^+$ cells co-expressing O4), previously so-called pre-oligodendrocytes, also retain a residual neuronal fate potential (Publication #5 - Belachew et al., 2003) (J.L. Mason, G. Lin, J.-E. Goldman, personal communication and Abstract # 421.3, *Society for Neuroscience* Annual Meeting, 2002). So far we have no evidence indicating astrocyte generation from $NG2^+$ cells in neurogenic regions in vivo (in contrast to white matter areas) (Aguirre and Gallo, 2004), at least under physiological conditions of an uninjured brain. We propose at this stage that type C-like $NG2^+$ cells represent precursor cells with a restricted oligodendrocyte/interneuron fate, hence termed postnatal OIN precursor cells (Figure 8). However, the accurate time-course of postnatal interneuronogenesis from type C-like $NG2^+$ OIN precursor cells remains to be fully investigated by birthdating experiments.

At this stage, a simple hypothesis would be to consider that a subset of early postnatal and maybe adult $NG2^+$ cells indeed have a type C-like phenotype unrelated to B cells, but likely to be ontogenically linked to the Dlx^+ basal forebrain multipotent stem cells that are known to generate both GABAergic interneurons and oligodendrocytes during embryonic CNS development (Figure 7) (He et al., 2001;Yung et al., 2002;Chojnacki and Weiss, 2004). Recent data have consistently provided evidence that transgenically targeted ablation of dividing GFAP-

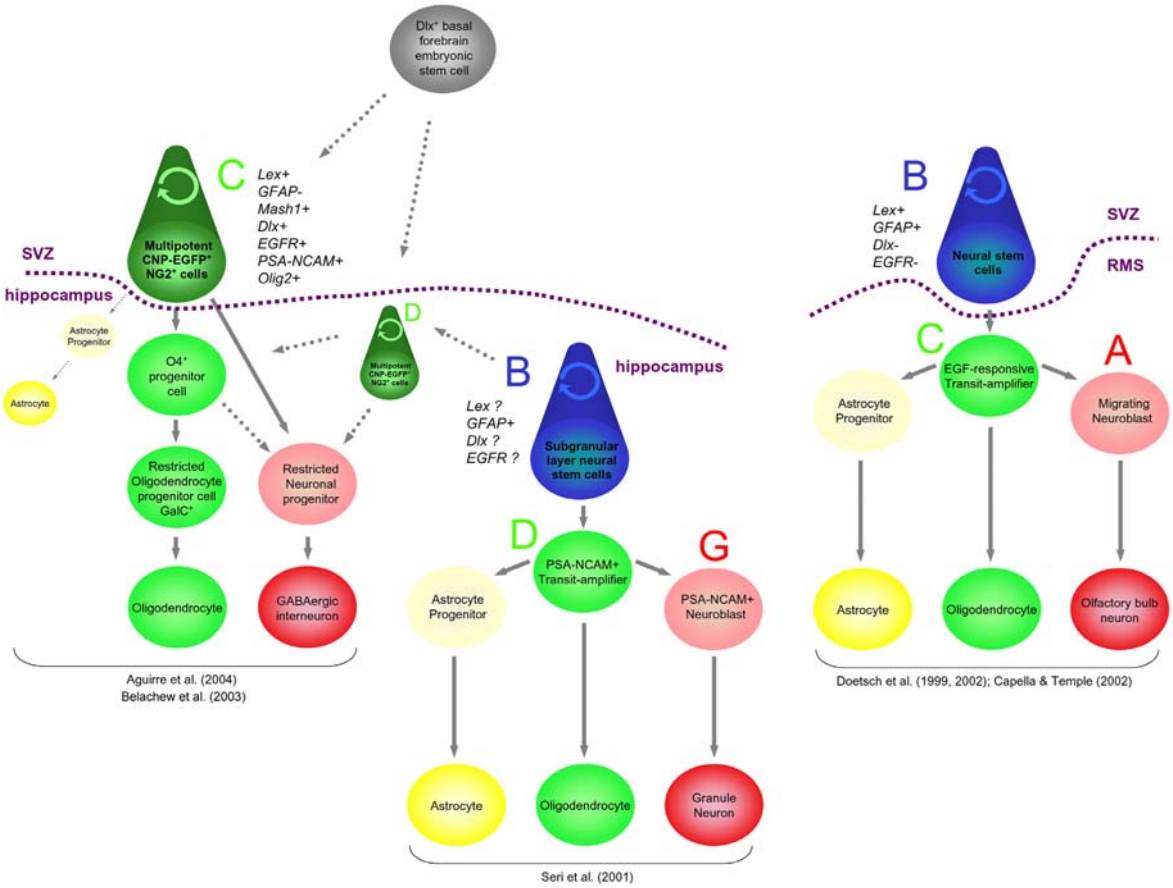

Figure 7: *Schematic representation of major multipotent phenotypes described in the SVZ and hippocampal areas of the postnatal/adult murine brain.*
Established lineage continua are shown with dashed arrows whereas hypothetical relationships are displayed with dotted arrows. $Lex^+/CNP\text{-}EGFP^+/NG2^+$ cells represent a subpopulation of type C-like multipotent cells that can generate oligodendrocytes and GABAergic interneurons in the hippocampus (see text for details).

expressing cells in the adult mouse totally stopped the generation of new neurons in the olfactory bulb and drastically abolished (1.8 % of control) hippocampal neurogenesis (Imura et al., 2003;Morshead et al., 2003;Garcia et al., 2004).This recent work has strengthened the assumption that type C-like NG2$^+$ OIN precursor cells may be generating newborn hippocampal interneurons mostly if not exclusively during the first two or three postnatal weeks.

Interestingly, the discrepancy between lineage properties of NG2$^+$ cells in vitro (tri-potential) and in vivo (bi-potential) indicates that a large reservoir, if not all multipotent progenitor cells in the adult brain may be bi-potential instead of tri-potential in vivo, as recently observed during embryonic CNS development (Stiles, 2003;Gabay et al., 2003). Furthermore, it emphasizes that the real fate potential of an apparently homogenous cell phenotype can only be reliably assessed in vivo and varies with region-specific positional cues.

2.3.3 What would a real OPC now be ?

2.3.3.1 Proposed recommendations for redefining an OPC

Altogether, the data presented here also highlight that we can no longer rely on a single

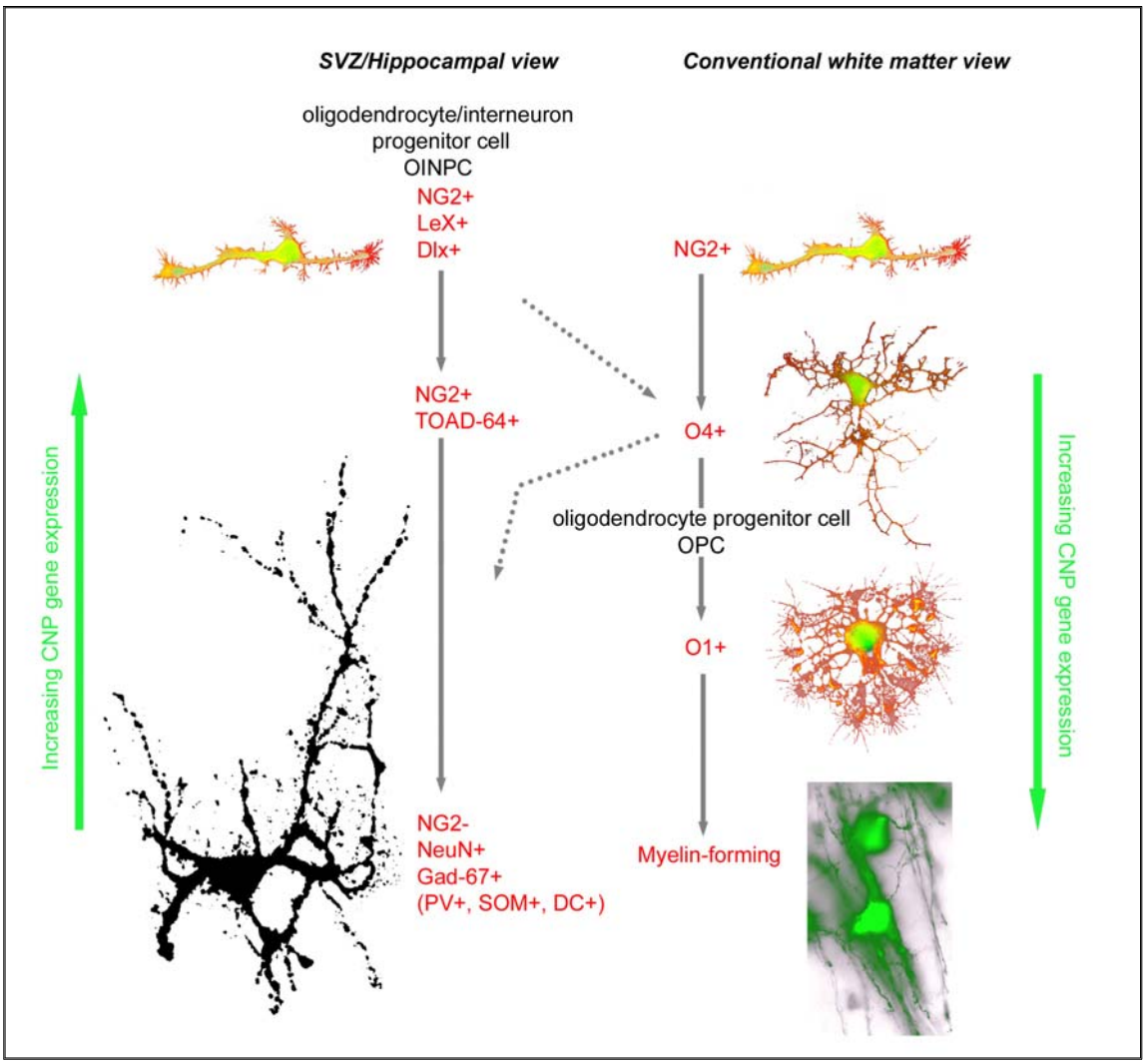

Figure 8: *Revisiting the definition of an oligodendrocyte-committed NG2$^+$ OPCs in regard of NG2$^+$ OIN precursors of oligodendrocytes and GABAergic interneurons expressing parvalbumin (PV), doublecortin (DC) or somatostatin (SOM)*
We propose that dlx-negative/LeX-negative/NG2$^+$ cells may represent the real OPCs within the total NG2$^+$ cell population.

antigenic marker to identify a specific cell phenotype. In particular, the fact that NG2 proteoglycan expression was seen in functionally distinct cell populations outlined that NG2 cannot be further considered as tightly linked to OPC identity in a broad general sense. There is now a crucial need for (re)defining region- and context-specific functional and antigenic criteria that underlie the accurate definition of an OPC (Figure 8) with respect to meaning a cell that would be restricted to a glial fate.

2.3.3.1.1 Marker-based definition

We first have to revisit the way we refer to conventional antigenic markers that have been extensively used until now as hallmarks of oligodendroglial lineage development, i.e. NG2 for the OPC stage, O4 for the late proliferative and early post-mitotic pre-oligodendrocyte, and O1 for the pre-myelinating oligodendrocyte (Figure 1) (Baumann and Pham-Dinh, 2001). Taking into account that $NG2^+$ and to a lesser extent $O4^+$ stages retain a neurogenic potential (Publication #5 - Belachew et al., 2003;Publication #6 - Aguirre et al., 2004) (J.L. Mason, G. Lin, J.-E. Goldman, personal communication and Abstract # 421.3, *Society for Neuroscience* Annual Meeting, 2002), $O1^+$ pre-myelinating oligodendrocytes would now become the first real oligodendrocyte-committed stage (Figure 8). However, it stands to reason that one cannot identify $O1^+$ cells as progenitor cells since they represent a strictly post-mitotic stage. Hence, seeking a more adequate OPC definition will necessitate classifying specific subsets of $NG2^+$ cells in regard to their differentiation potential.

The initial step in this direction has stemmed from our demonstration that only LeX^+ cells among total $NG2^+$ cells have the capacity to form neurospheres in culture (Publication #6 - Aguirre et al., 2004) and displayed bi-potential OIN progenitor cell phenotype in vivo after transplantation (unpublished data). FACS®-purified LeX-negative/$NG2^+$ cells were unable to generate neurospheres and could represent a phenotype restricted to becoming oligodendroglial lineage cells exclusively (Publication #6 - Aguirre et al., 2004). One would now have to perform an in-depth investigation of the differentiation potential of LeX-negative/$NG2^+$ cells to ascertain whether they retain the capacity to undergo non-oligodendroglial differentiation.

Furthermore, dlx expression in $NG2^+$ cells may also be a discriminative criterion. Using the pan anti-dlx antibody, recognizing both the early (dlx1/2) and the late (dlx5/6) members of the dlx homeobox gene family (Panganiban et al., 1997;Panganiban and Rubenstein, 2002), we found that 40% of the $NG2^+$/CNP-$EGFP^+$ cells were also dlx^+ in the postnatal/adult SVZ, respectively (Publication #6 - Aguirre et al., 2004). Dlx was also expressed in LeX^+/CNP-$EGFP^+$ cells. Since it has been demonstrated that dlx proteins are expressed in bipotential oligodendrocyte/GABAergic interneuron progenitors and their neuronal progeny during development (He et al., 2001;Yung et al., 2002;Panganiban and Rubenstein, 2002;Chojnacki and Weiss, 2004), we wanted to determine whether dlx was also expressed in postnatal NG2-negative/CNP-$EGFP^+$ cells that displayed more mature oligodendrocyte markers, such as myelin basic protein (MBP) (Publication #2 - Yuan et al., 2002). We were unable to find a single example of cells co-expressing dlx and mature oligodendrocyte markers (Publication #6 - Aguirre et al., 2004). Thus, we can hypothesize that dlx expression: i) characterizes the OINPC stage, ii) is likely to be an instructive signal in the specification/differentiation of adult-born GABAergic interneurons derived from OINPCs, and iii) may allow to distinguish between OINPCs and real OPCs among the total $NG2^+$ cell population, at least in the SVZ.

We could logically speculate here that dlx-negative/LeX-negative/$NG2^+$ cells have the ideal profile to be proliferative oligodendrocyte-committed OPCs in a meaningful sense. There

is currently a great deal of interest in this hypothesis and this will rapidly trigger all necessary neat experiments to test its validity.

2.3.3.1.2 Integration of region-based and contextual parameters

Besides antigenic markers, the definition of a specific phenotype as is right and proper must integrate positional and context-dependent influences. It is perfectly obvious that $NG2^+$ cell population may differ between subcortical white matter, corpus callosum, hippocampus, basal ganglia, SVZ, RMS, olfactory bulb, or distinct cortical areas. This functional heterogeneity between cells sharing a common antigenic profile in different anatomical locations may vary in a stage-dependent manner during postnatal development and could differ if comparing a normal brain with specific pathological conditions. At present, except for describing morphological differences (Dawson et al., 2003), there is a total lack of data that integrate region- and context-based regulations to add another level of complexity to the full picture of the functional diversity within the $NG2^+$ cell phenotype.

One way to untangle the heterogeneous functional potential of these cells would be to develop transgenic knock-in strategies targeting the locus of the NG2 gene with Cre-recombinase, avian leukose virus receptor or EGFP reporter sequences. This will facilitate region- and context-specific studies allowing us to understand the function of NG2 proteoglycan in CNS cells, to track the fate of $NG2^+$ cells, and to study and manipulate their gene expression, about which we know so little (Ye et al., 2003;Stegmuller et al., 2003). These approaches are now close to giving rise to the first reports in several labs.

2.4 Summary conclusions

2.4.1 Nascent perspectives for novel strategies aimed at improving OPC recruitment after demyelination

In summary, we have highlighted in the first part of this work that multiple proteins contribute to the regulation of cell cycle kinetics and to the timing mechanism of oligodendrocyte differentiation, some increasing and others decreasing over time as OPCs proliferate. One advantage of such a multi-component timing mechanism is that it is robust: inactivation of individual components does not inactivate the timing of normal development, but instead causes it to function inaccurately. The challenge at this stage is now two-fold: i) to go on identifying all of these components and determine how their levels are controlled, such that they change in a time- and context-dependent manner, but also ii) to address how these crucial developmental genes are regulated and how their protein products interact in pathological conditions such as demyelination.

Demyelination occurs in a variety of adult diseases, including MS, the leukodystrophies and some aspects of spinal cord injuries. Myelin is destroyed, as are oligodendrocytes and nerve fibers. Some remyelination has been documented, although in most chronic lesions remyelination fails to initiate or remains incomplete. Due to the nature of MS, and the extended period before clinical diagnosis is made, extensive demyelination has usually occurred before commencement of treatment. For this reason, replacement or repair of lost myelin by endogenous or transplanted progenitor cells would provide an attractive alternative to preventive immunotherapy, aimed at limiting demyelination.

2.4.1.1 *Transplantation of allogenic progenitors*

As for gene therapy strategy, the choice of the accurate cell phenotype to target is of paramount importance for any transplantation experiment. Multipotent stem cells have been considered, but since the rate of differentiation from stem cell to myelinating oligodendrocytes is limited both in vitro and in vivo (Svendsen and Smith, 1999), committed oligodendrocyte progenitors may be more suited to be the cells of choice as long as we agree on their definition. Furthermore, studies comparing oligodendroglial populations at different developmental stages have shown that OPCs also tend to survive and migrate better, therefore being more useful than fully differentiated oligodendrocytes (Warrington et al., 1993). Studies of oligodendrocyte development have shown that purified perinatal OPCs, which have an excellent ability for self-renewal, can remyelinate axons when transplanted into a demyelinated brain (Groves et al., 1993;Franklin and Blakemore, 1997).

Unfortunately, embryonic or perinatal OPCs do not form a useful source of remyelinating cells, because of graft rejection problems and availability issues pertaining to fetal human material. Instead, adult OPCs could be purified from the patient's own white matter, expanded in vitro with growth factors, and transplanted into a demyelinated lesion. Although this constitutes a potentially viable therapeutic strategy, it is not clear whether and to what extent adult human OPCs can be expanded in vitro and would actively undergo a controlled proliferation, migrate and myelinate chronic lesions after allogenic transplantation. One could speculate that more pragmatic expectations may arise from the alternative struggle to improve our strategies to overcome the recruitment and differentiation failure of endogenous OPCs.

2.4.1.2 *Counteracting the recruitment failure of endogenous progenitors*

While OPCs in the adult make up almost 8% of the glial cell population in the central nervous system, their function in the healthy brain and behavior in disease is still not well understood. Tissue culture studies have shown that adult OPCs generally divide, migrate and differentiate at very slow rates (Wolswijk and Noble, 1989;Wolswijk et al., 1991;Wren et al., 1992;Engel and Wolswijk, 1996). Indeed, it was recently found in an ethidium bromide-induced demyelination model that slower remyelination in older rats was associated with impaired recruitment and differentiation of OPCs (Sim et al., 2002). Although little is known about the factors that signal OPC recruitment in vivo, growth factors are known to stimulate OPC proliferation and motility in vitro. Additional evidence supporting a role for proliferation in recruitment is provided by observations in cases of chronic stage MS, where lesions were found to contain a relatively quiescent population of OPCs that did not express the nuclear proliferation antigen recognized by the Ki-67 antibody (Wolswijk, 1997;Wolswijk, 1998;Wolswijk, 2000). Some partially remyelinated lesions in MS were also observed to be associated with at least a transient increase in the number of OPCs (Keirstead et al., 1998), indicating a tentative but limited proliferative response to injury. There is compelling evidence that exposure of normal adult OPCs to both PDGF and type 2 fibroblast growth factor (FGF2) causes a marked increase in their rates of division and migration (Wolswijk and Noble, 1992;Engel and Wolswijk, 1996). Both of these factors are elevated after injury to the adult CNS (Logan et al., 1992;Lotan and Schwartz, 1992;Gehrmann et al., 1996). This may represent part of the yet insufficient mechanism by which adult OPCs are stimulated to generate remyelinating oligodendrocytes after damage. However, besides a lack of efficient extrinsic stimulation, it appears likely that remyelination ultimately fails because of an intrinsic impairment of

proliferative potential of adult OPCs and/or due to an increased sensitivity to anti-mitotic agents in these cells (Blakemore and Keirstead, 1999). The observation of depletion of adult OPCs in the vicinity of the lesion indeed suggests a deficiency in the ability of adult OPCs to proliferate (Keirstead et al., 1998).

Our data here suggest that a lack of cdk2-associated kinase activity in adult OPCs may be responsible for the quiescent status of these cells in or near MS lesions, thus underlying the failure of recruitment that undermines remyelination efficiency. Our next first plan will be to determine whether proliferation is disrupted in adult cdk2-deficient OPCs from cdk2$^{-/-}$/CNP-EGFP mice in normal conditions or following experimental demyelination. In more of a long-term perspective, as demonstrated in previous studies (Publication #1 - Belachew et al., 2001;Publication #2 - Yuan et al., 2002;Mallon et al., 2002), the use of CNP or proteolipid protein (PLP) promoter-driven coding sequences appears to be best suited for loss/gain-of-function genetic engineering strategies to selectively target adult expression of many other genes of interest (see part 2) that may help in fighting the recruitment failure of endogenous OPCs.

2.4.1.3 Counteracting the differentiation failure of endogenous progenitors

Less is known in vivo about the mechanisms by which OPCs differentiate into myelin sheath-forming oligodendrocytes than about their proliferation and migration. In the context of MS, this is an area of oligodendrocyte biology that has acquired particular significance with the realization that failure of differentiation might be a significant contributor to remyelination failure (Franklin, 2002). It is worth bearing in mind however that inhibitors of differentiation might contribute to the recruitment phase by keeping OPCs in a state in which they are still responsive to recruitment signals .Thus, the identification of differentiation inhibitors in tissue from MS patients does not necessarily imply that remyelination has failed.

A major breakthrough has been recently made that provides the first demonstration that the re-activation of a repressive pathway known to control oligodendrocyte maturation during development may play a role in MS remyelination failure. As previously discussed, the Jagged-Notch-Hes pathway has been implicated in cell fate determination affecting many aspects of the development and function of the CNS, including myelination (Wang et al., 1998;Ohtsuka et al., 1999;Kondo and Raff, 2000a;Givogri et al., 2002). OPCs and O4^{+} pre-myelinating oligodendrocytes express Notch1 receptors, while neurons/axons express the ligand Jagged1 (Wang et al., 1998). Contact-mediated activation of Notch1 by Jagged1 induces expression of the inhibitory Hes5, which blocks the maturation of Notch1-expressing OPCs, a response that is thought to facilitate migration of precursor cells to white-matter tracts of the CNS (Wang et al., 1998;Ohtsuka et al., 1999;Kondo and Raff, 2000a). As development proceeds, expression of Jagged1 is downregulated, OPCs mature and myelination commences (Wang et al., 1998). Thus, re-expression of components of this pathway in the MS lesions could function to arrest oligodendrocyte maturation. Consistent with this hypothesis, it was shown that in active MS lesions, Jagged1 was expressed by reactive astrocytes, and Notch1 and Hes5 were expressed by oligodendrocytes, whereas transforming growth factor-β1 (TGF-β1) localized to perivascular extracellular matrix (John et al., 2002). In contrast, astrocytes in remyelinated areas did not show Jagged1 immunoreactivity (John et al., 2002). Taken together, these data have first suggested that astrocytic expression Jagged1 induced by TGF-β1 and acting on oligodendroglial Notch1 receptor may be causally related to the limited remyelination observed in MS by blocking the differentiation of recruited OPCs. However, it appears that the re-expression of Notch1 and Jagged1 after CNS demyelination might not be a major rate-determining factor for remyelination

(Stidworthy et al., 2004).

Following this pioneering track, further works are soon expected to assess in MS the possible re-enactment of other acknowledged intrinsic and extrinsic pathways that play out during oligendrocyte development (see part 2b and 2c). Though, one has to be cautious since the re-expression of genes, which are essential for developmental myelination, following demyelination in the adult does not per se imply similar function. In this regard, it was recently shown that requirements for Olig1 function are subtle during development, yet striking during the repair of a demyelinating lesion (Arnett et al., 2004). This would suggest that cell-intrinsic activity of Olig1 can be compensated for during myelination but not remyelination. Such data also imply that molecular pathways controling the differentiation of adult OPCs into myelinating oligodendrocytes display intrinsic differences to that of perinatal OPCs.

With respect to our work, one may also hypothesize here that anti-apoptotic and pro-differentiating properties of synthetic chemical CKIs in the oligodendroglial lineage may allow these drugs to be of interest with respect to stimulating the myelinating potential of "quiescent" OPCs known to persist both in adult normal white matter and in MS lesions. Considering that synthetic CKIs such as roscovitine and others are already used in clinical trials as chemotherapeutic agents and seem well tolerated (Senderowicz and Sausville, 2000), the question of the potential pro-differentiating and anti-apoptotic actions of these drugs on oligodendroglial lineage cells in vivo should now rapidly be addressed using experimental autoimmune encephalomyelitis as an animal model of immune-mediated demyelination.

2.4.2 There is a need to redefine remyelinating cells to circumvent the "specification failure" of formerly termed OPCs

Although we cannot rule out that a significant proportion of $NG2^+$ cells of the white matter in the adult CNS will undergo limited divisions in response to demyelination, this proportion remains minor however (Keirstead et al., 1998;Blakemore and Keirstead, 1999). Besides previously described extrinsic and intrinsic hurdles to the recruitment phase of remyelination in MS plaques (Franklin, 2002), we should now also consider that part of OPCs defined by NG2 labeling may not be sufficiently committed to become oligodendrocytes in the adult white matter. A "specification failure" may thus definitely be a newly identified causal factor that partially underlies the differentiation failure.

Actually, we now have some clues indicating that $NG2^+$ cells may retain a neuronal potential outside SVZ/hippocampal germinatives regions of the adult brain. In particular, a striking observation was recently made (Chittajallu et al., 2004) that a subpopulation of $NG2^+$ cells located in the cortex displayed cellular and physiological properties of immature neurons, i.e. expression of class III β-tubulin and tetrodotoxin-sensitive spikes upon depolarizing current pulses. This latter phenomenon is most likely due to the presence of a significantly higher density of voltage-activated Na^+-channels coupled with a lower density of the delayed outward rectifying K^+-channels than that seen in non-spiking cortical $NG2^+$ and white matter $NG2^+$ cells. Furthermore, cortical $NG2^+$ cells FACS®-purified from postnatal cortices generated a significant percentage of $Tuj1^+$ and $NeuN^+$ neurons in culture, thus indicating their potential to give rise to a neuronal population (personal communication and *Society for Neuroscience Abstract #* 455.1, New Orleans 2003). Furthermore, another group reached the same conclusions by injecting adult rats (8-9 weeks) with BrdU and examining the fate of migrating cells in the cortex. They showed that BrdU-labeled cells can co-express NeuN and NG2 with varying staining intensities, suggesting that $NG2^+$ cells in the rat cortex are not all OPCs, but may actually be a

heterogeneous population, some of which divide and produce new neurons in the normal adult rat cortex (Dayer et al., 2005).

These data demonstrated that cortical $NG2^+$ cells display properties that are distinct from those expected in OPCs and therefore raises questions as to the role and identity of a subpopulation of gray matter cells expressing the NG2 proteoglycan that may be adult bi-potential OINPCs as are SVZ/hippocampal $NG2^+$ cells (Publication #5 - Belachew et al., 2003;Publication #6 - Aguirre et al., 2004). One could speculate that white matter $NG2^+$ cells that are also actively dividing adult progenitors also retain the intrinsic ability to generate GABAergic neurons, since adult human $A2B5^+$ (another marker of the $NG2^+$ stage) cells expressing the CNP gene can do so (Nunes et al., 2003). Despite the fact that we are all aware that no neurogenesis occurs in MS plaques, the fact that a significant percentage of white matter $NG2^+$ cells may represent OINPCs instead of committed OPCs could explain why the environmental context of demyelination fails to trigger a satisfactory boost for regeneration of mature oligodendrocytes. There is now an urgent need to shed a new light on the functional heterogeneity of the distinct subsets of white matter $NG2^+$ cells in order to unravel their respective lineage potential and the molecular mechanisms that control decisions of fate specification and differentiation in vivo. It will help us to identify who's the best-suited cell phenotype in the total $NG2^+$ cell population to be targeted as an effective remyelinating cell. It is a necessary condition before we are able to design appropriate strategies that would efficiently stimulate remyelination by the endogenous pool of postnatal progenitor cells. At some point hopefully one will finally break down the frustration of having cells out there that cannot get the job done.

3 Extrasynaptic and synaptic neurotransmitter receptors in glial precursors' quest for identity

There has been already a long history of works indicating that interaction between neurotransmitters and their receptors could play essential roles during CNS development, far before they become directly involved in synaptic transmission (Barker et al., 1998;Cameron et al., 1998a;Publication #7 - Nguyen et al., 2001). It is established that neurotransmitters are present and surround neural cells during the CNS maturation period (Miranda-Contreras et al., 1998;Miranda-Contreras et al., 1999;Miranda-Contreras et al., 2000) and functional ligand-gated ion channel (i.e. ionotropic) receptors have been described in neuronal precursor cells before the establishment of cortical and subcortical synapses (Serafini et al., 1995;Ma and Barker, 1995;LoTurco et al., 1995;Flint et al., 1998;Haydar et al., 2000). Furthermore, neurotransmitters and activation of their ionotropic receptors have been shown to regulate functional developmental processes at specific stages of neuronal maturation (LoTurco et al., 1995;Haydar et al., 2000;Ben Ari, 2002;Publication #15 - Nguyen et al., 2003). The accurate role of neurotransmitter receptor-mediated signaling during neural differentiation in vivo remains however largely unknown and most loss-of-function studies have failed to disclose obvious developmental defects. Hence, there might be large redundancies between respective functions of distinct neurotransmitter receptor subunits, since surrogate mechanisms efficiently compensate specific ionotropic receptor deficiencies during neural development.

We and others have recently demonstrated that glycine, type A γ-aminobutyric acid ($GABA_A$), AMPA/kaïnate and nicotinic acetylcholine ionotropic receptors are also expressed in "non-neuronal" progenitor cells, and particularly in OPCs (Patneau et al., 1994;Publication #9 - Belachew et al., 1998;Publication #10 - Belachew et al., 1998;Gallo and Ghiani, 2000;Publication #11 - Belachew et al., 2000;Rogers et al., 2001;Publication #7 - Nguyen et al., 2001;Atluri et al., 2001;Publication #13 - Nguyen et al., 2002;Publication #15 - Nguyen et al., 2003). Until recently, extrasynaptic neurotransmitter receptors expressed in immature "non-neuronal" cells were considered to be transducers of putative neurotransmitter-mediated neuron-glia interactions (Fields and Stevens-Graham, 2002). However, we have now demonstrated that previously so-called OPCs represent a subset of bipotential neuron-oligodendrocyte progenitor cells in specific locations of the postnatal brain (Publication #5 - Belachew et al., 2003;Nunes et al., 2003;Publication #6 - Aguirre et al., 2004). We here want to address a provocative but legitimate thesis consisting of wondering to what extent, in neurogenic regions, neurotransmitter receptor expression by postnatal "OPCs" could reflect their neuronal potential and represent instructive signaling pathways that may be involved at specific stages of neuronal differentiation. In other words, could it be that neurotransmitter receptors in postnatal neurogenic regions are expressed preferentially in "OPCs" that retain the ability to potentially give rise to neurons in an appropriate extrinsic environment? We will recapitulate here the ins and outs of neurotransmitter receptor expression in OPCs addressing whether this might represent developmental factors that regulate oligodendrocyte lineage progression and/or that instruct terminal neuronal maturation?

3.1 Expression of neurotransmitter receptors in CNS precursor cells of the postnatal brain

Publication #7: Nguyen, L., Rigo, J.-M., Rocher, V., Belachew, S., Malgrange, B., Rogister, B., Leprince, P., and Moonen, G. (2001) Neurotransmitters as early signals for central nervous system development. *Cell Tissue Res.* 305:187-202.

Publication #8: Nguyen, L., Rigo. J.-M., Malgrange, B., Moonen, G., and Belachew, S. (2003). Untangling the functional potential of PSA-NCAM-expressing cells in CNS development and brain repair strategies. *Curr. Med. Chem.* 10:2185-2196.

We will first summarize current experimental evidences showing that neurotransmitter receptors are expressed in neuron-committed (Table 2) and multipotent or glia-oriented (Table 3) progenitor cells (for reviews, see also *Publications #7 and #8*). We will restrict our in-depth listing by focusing our summary tables on ionotropic receptors that were studied using postnatal tissues.

We will detail thereafter our contribution to the understanding of the developmental profile of ionotropic glycine receptor (GlyR) expression in CNS precursor cells at the perinatal period. To be exhaustive in depicting how excitable a non-neuronal precursor cell can be, we will finally say a few words about the functional meaning of voltage-gated ion channel expression in these cells.

Table 2: *Ionotropic neurotransmitter receptors expressed in neuron-committed precursor cells*

Age	Receptor	Progenitor cell phenotype	Model	Species	Results & Effects of NT	References
			GABA			
P6-P8	$GABA_A$	Cerebellar granule cell progenitors	in vitro Cell culture	Rat	MAPK-dependent ↑ proliferation	(Fiszman et al., 1999)
P6-P8	$GABA_A$	Immature cerebellar granule cells	in vitro Cell culture	Rat	Ca^{2+}-dependent ↓ of neurite outgrowth	(Borodinsky et al., 2003)
P0-P3	$GABA_A$	Striatal PSA-$NCAM^+$ precursors	in vitro Cell culture & slices	Rat	MAPK- and Ca^{2+}-dependent ↓ of proliferation	(Publication #15 - Nguyen et al., 2003)
P13-P70	$GABA_A$	anterior SVZ-RMS-olfactory bulb neuronal precursors	ex vivo Tissue slices	Mice	Neuronal progenitors of the SVZ/RMS/OB contain GABA and are depolarized by GABA-mediated activation of first extrasynaptic and then later synaptic $GABA_A$ receptors	(Carleton et al., 2003;Wang et al., 2003;Gallo and Haydar, 2003;Belluzzi et al., 2003)
P0-P1	$GABA_A$	Anterior SVZ neuronal precursors	in vitro Cell culture	Rat	SVZa neuronal precursor cells are GABAergic and express functional $GABA_A$ receptors	(Stewart et al., 2002)
			GLUTAMATE			
P0-P3	N.D.	Striatal PSA-$NCAM^+$ precursors	in vitro Cell culture	Rat	Glutamate induces inward currents	(Publication #8 - Nguyen et al., 2003)
P0-adult	NMDA	Dentate gyrus progenitor cells	in vivo	Rat	Blockade of NMDA receptor increase cell death and [^{3}H]-thymidine incorporation particularly in granule cells	(Gould et al., 1994;Cameron et al., 1995;Cameron et al., 1998b)
P7-P11	NMDA	Immature cerebellar granule cells	in vitro & in vivo	Rat	Activation of NMDA receptor ↑ survival	(Balazs et al., 1988a;Balazs et al., 1988b;Monti and Contestabile, 2000;Monti et al., 2002)

Age	Receptor	Progenitor cell phenotype	Model	Species	Results & Effects of NT	References
P70	AMPA	Tangentially migrating olfactory bulb neuroblasts	ex vivo Tissue slices	Mice	Expression of first extrasynaptic and later synaptic AMPA receptors	(Carleton et al., 2003)
P70	NMDA	Radially migrating olfactory bulb neuroblasts	ex vivo Tissue slices	Mice	Expression of extraynaptic functional NMDAR	(Carleton et al., 2003)
			GLYCINE			
P0-P3	GlyR	Striatal PSA-NCAM$^+$ precursors	in vitro Cell culture	Rat	Functional GlyR expressed in these neonatal neuronal precursor cells	(Publication #12 - Nguyen et al., 2004)
			ACETYLCHOLINE			
P0-P3	N.D.	Striatal PSA-NCAM$^+$ precursors	in vitro Cell culture	Rat	Acetylcholine induces inward currents	(Publication #8 - Nguyen et al., 2003)
P1-P3	Nicotinic (α7) AChR	Olfactory bulb neuronal precursors	in vitro Cell culture	Rat	Activation of nAChR ↑ neurite outgrowth	(Coronas et al., 2000)
P5	Nicotinic (α3) AChR	Cerebellar external granule layer (EGL) neuronal precursors	in vitro Cell culture	Mouse	Activation of nAChR ↑ proliferation and survival in EGL neuroblasts	(Opanashuk et al., 2001)

Table 3: *Ionotropic neurotransmitter receptors expressed in multipotent and glia-oriented precursor cells*

Age	Receptor	Progenitor cell phenotype	Model	Species	Results & Effects of NT	References
			GABA			
Adult	$GABA_A$	Astrocytes and astrocyte precursors from and hippocampus	in vitro Tissue slices	Rat	GABA induces depolarizing chloride-mediated inward currents	(MacVicar et al., 1989)
P0-P3	$GABA_A$	Spinal cord and cerebral OPCs	in vitro Cell Culture & slices	Rat & mouse	GABA induces depolarizing chloride-mediated inward currents and ↑ $[Ca^{2+}]_i$	(Gilbert et al., 1984;Kettenmann et al., 1984b;Kirchhoff and Kettenmann, 1992;Pastor et al., 1995;Publication #9 - Belachew et al., 1998)
			GLUTAMATE			
P1	AMPA and kaïnate	Whole brain and hippocampus	in vitro Cell culture & slices	Rat	Ca^{2+}-permeable functional AMPA/kainate receptor expression, the activation of which induces depolarization	(Bowman and Kimelberg, 1984;Kettenmann et al., 1984a;Sontheimer et al., 1988;Jabs et al., 1994;Steinhauser et al., 1994;Porter and McCarthy, 1995)

Age	Receptor	Progenitor cell phenotype	Model	Species	Results & Effects of NT	References
Juvenile adult	AMPA and kaïnate	Hippocampus	in vitro Tissue slices	Mouse	Glial inwardly rectifying K^+ channels (Kir) are rapidly inhibited upon activation of AMPA/kaïnate-type glutamate receptors, most probably due a receptor-mediated influx of Na^+, which plugs the channels from the intracellular side	(Jabs et al., 1994;Robert and Magistretti, 1997;Schroder et al., 2002)
P1	AMPA and kaïnate	Cortical astrocytes and mixed glial cells from optic nerve	in vitro Cell culture & Slices	Rat	Glutamate receptor-mediated regulation of immediate early gene expression (c-fos, c-jun, jun-B, ...)	(McNaughton and Hunt, 1992;Mack et al., 1994)
P1	AMPA and kaïnate	Cortical and optic nerve OPCs	in vitro Cell culture	Rat	Functional AMPA and kaïnate specific subtypes of glutamate receptors are expressed by OPCs	(Barres et al., 1990;Jensen and Chiu, 1993;Patneau et al., 1994;Gallo et al., 1994a;Gallo et al., 1994b)
P1	AMPA and kaïnate	Cortical OPCs	in vitro Cell culture & Slices	Rat	AMPA/kaïnate receptor activation: i) triggers Ca^{2+}-dependent early gene expression, ii) induces a blockade of voltage-dependent K^+ channels (Kv1) that is mediated by depolarization and Na^+ entry, iii) inhibits proliferation at G1/S transition by regulation of cyclinE/cdk2 complex activity	(Pende et al., 1994;Liu and Almazan, 1995;Gallo et al., 1996;Knutson et al., 1997;Pende et al., 1997;Ghiani et al., 1999a;Ghiani et al., 1999b;Gallo and Ghiani, 2000;Ghiani and Gallo, 2001;Publication #3 - Belachew et al., 2002;Chittajallu et al., 2002)
P1	AMPA	Cortical OPCs	in vitro Cell culture	Rat	Overactivation of AMPA receptors causes apoptosis in oligodendrocyte progenitors through mechanisms involving Ca^{2+} influx, depletion of glutathione, and activation of JNK, calpain, and caspase-3	(Liu et al., 2002)
			GLYCINE			
P0-P3	GlyR	Nestin-expressing striatal stem cells	in vitro Cell culture	Rat	Functional GlyR expressed in these stem cells	(Publication #13 - Nguyen et al., 2002)
P0-P3	GlyR	Cortical OPCs	in vitro Cell culture	Rat	Activation of functional GlyR induces depolarizing chloride-mediated inward currents and ↑ $[Ca^{2+}]_i$	(Publication #10 - Belachew et al., 1998;Publication #11 - Belachew et al., 2000)
			ACETYLCHOLINE			
P1	Nicotinic (α7) AChR	Hippocampal astrocytes	in vitro Cell culture	Rat	Activation of nAChR ↑ intracellular calcium concentration	(Sharma and Vijayaraghavan, 2001)
P0-P3	Nicotinic AChR	Cortical OPCs	In vitro Cell culture	Rat	Functional nAChR expressed by cultured OPCs	(Publication #9 - Belachew et al., 1998)

Age	Receptor	Progenitor cell phenotype	Model	Species	Results & Effects of NT	References
P1	Nicotinic AChR	OPCs from corpus callosum	ex vivo & in vitro Cell culture	Rat	Activation of nAChR ↑ intracellular calcium concentration. Expression of α3, α4, α5, α7, β2 and β4 subunits.	(Rogers et al., 2001)

3.1.1 A focus on a newcomer: glycine receptors in perinatal CNS precursor cells

Publication #9 (was part of our *PhD* thesis): Belachew, S., Malgrange, B., Rigo, J.-M., Rogister, B., Coucke, P., Mazy-Servais, C., and Moonen, G. (1998). Developmental regulation of neuroligand-induced responses in cultured oligodendroglia. *Neuroreport* 9:973-980.
Publication #10 (was part of our *PhD* thesis): Belachew, S., Rogister, B., Rigo, J.-M., Malgrange, B., Mazy-Servais, C., Xhauflaire, G., Coucke, P., and Moonen, G. (1998). Cultured oligodendrocyte progenitors derived from cerebral cortex express a glycine receptor which is pharmacologically distinct from the neuronal isoform. *Eur. J. Neurosci.* 10:3556-3564.
Publication #11 (was part of our *PhD* thesis): Belachew, S., Malgrange, B., Rigo, J.-M., Rogister, B., Leprince, P., Hans, G., Nguyen, L., and Moonen G. (2000). Glycine triggers an intracellular calcium influx in oligodendrocyte progenitor cells which is mediated by the activation of both the ionotropic glycine receptor and Na^+- dependent transporters. *Eur. J. Neurosci.* 12:1924-1930.
Publication #12: Nguyen, L., Malgrange, L., Breuskin, I., Lallemend, F., Hans, G., Moonen, G., Belachew, S., and Rigo, J.-M. (2004) Striatal PSA-$NCAM^+$ precursor cells from the newborn rat express functional glycine receptors. *Neuroreport* 15:583-587.
Publication #13: Nguyen, L., Malgrange, B., Belachew, S., Rogister, B., Rocher, V., Moonen, G., and Rigo J.-M. (2002). Functional glycine receptors are expressed by postnatal nestin-positive neural stem/progenitor cells. *Eur. J. Neurosci.* 15:1299-1305.

Strychnine-sensitive glycine receptor chloride channels (GlyRs) are members of the nicotinic ligand-gated ion channel family (Le Novere and Changeux, 2001). They mediate postsynaptic inhibition by increasing the chloride permeability of the postsynaptic cell membrane in adult spinal cord, brainstem and some higher brain regions (Betz, 1991;Kuhse et al., 1995;Schofield et al., 1996). GlyR is a pentameric transmembrane protein composed of glycosylated integral transmembrane α- (48 kDa) and β-subunits (58 kDa) (Schofield et al., 1996). Four α- (α1, α2, α3 and α4) (Kuhse et al., 1990;Matzenbach et al., 1994) and one β-subunit variant (Schofield et al., 1996) have been described so far. In newborn rats, the GlyR is α2-homomeric and differs from the adult stoechiometry, which is classically made of three α1- and two β-subunits (Langosch et al., 1988). In contrast to the adult brain, the activation of GlyR has an excitatory action in immature neural cells resulting from a depolarized chloride equilibrium potential in these cells during the developmental period (LoTurco et al., 1995). GlyR-mediated depolarization of immature neurons induces a calcium entry through voltage-gated calcium channels (VGCC) (Reichling et al., 1994;Flint et al., 1998), which may modulate cell proliferation, migration and differentiation in neural precursors (Publication #7 - Nguyen et al., 2001;Ben Ari, 2001;Ben Ari, 2002) and, later, maturation of fully differentiated neurons bearing inhibitory synapses (Moss and Smart, 2001;Legendre, 2001). In that respect, we recently demonstrated that GlyRs can be expressed in three distinct types of early postnatal neural precursor cells in vitro.

Functional GlyRs have been described in newborn rat astrocytes, oligodendrocytes and OPCs in spinal cord slices (Pastor et al., 1995;Kirchhoff et al., 1996;Publication #9 - Belachew et al., 1998). During oligodendroglial lineage progression GlyR expression (α2 and β subunits) culminates at the OPC stage and decreases thereafter (Publication #10 - Belachew et al., 1998).

We demonstrated that glycine-induced chloride currents recorded from newborn rat cortical oligosphere-derived OPCs, were mediated by GlyRs that seem to be not only pharmacologically, but also structurally distinct from the homologous neuronal receptor (Publication #10 - Belachew et al., 1998). Furthermore, glycine application on cultured OPCs induced a rise of $[Ca^{2+}]_i$ via the opening of VGCC. This effect was mediated by a depolarization related to the concurrent activation of GlyR and Na^+-dependent glycine transporters GLYT1 and/or GLYT2 (Publication #11 - Belachew et al., 2000).

Using the classical neurosphere culture model from early postnatal striatum (Reynolds et al., 1992;Reynolds and Weiss, 1992), we also demonstrated the expression of GlyR α1-, α2- and β genes and could detect GlyRα subunit proteins in multipotent nestin-expressing stem/progenitor cells (Publication #13 - Nguyen et al., 2002). We consistently observed in these multipotent progenitor cells that GlyR subunits formed functional chloride channels gated by glycine and sensitive to inhibition by strychnine and picrotoxin which are GlyR antagonists (Publication #13 - Nguyen et al., 2002).

Similarly, immunocytochemical analysis showed that GlyRs were expressed in PSA-$NCAM^+$ neurogenic progenitors from the early postnatal rat striatum both in vitro and in situ (Publication #12 - Nguyen et al., 2004). Glycine thus triggered inward strychnine-sensitive currents in most of these neurogenic striatal precursors (Publication #12 - Nguyen et al., 2004). Finally, neurogenic PSA-$NCAM^+$ progenitors expressed GlyRs that displayed intermediate electrophysiological characteristics with respect to those of nestin-expressing neural stem cells (Publication #13 - Nguyen et al., 2002) and mature interneurons (Sergeeva, 1998;Sergeeva and Haas, 2001) from the early postnatal striatum.

Such results raised the yet unresolved issue that glycine and GlyRs, together with other neurotransmitters and voltage-gated ion channels, may also control the development of postnatal neural precursors, i.e. i) cell fate choice and the progression of distinct differentiation pathways from nestin-expressing stem cells, ii) neurogenesis derived from PSA-$NCAM^+$ neuronal precursors, iii) the maturation of OPCs into myelinating cells, and iv) cell cycle kinetics in all of these immature phenotypes.

3.1.2 Not only neurotransmitter receptors, but also voltage-gated potassium channels in OPCs

Publication #14: Vautier, F., Belachew, S., Chittajallu, R., and Gallo, V. (2004). *Shaker*-type potassium channel subunits Kv1.3-1.4 and Kv1.6 differentially control oligodendrocyte progenitor cell cycle progression. *Glia* 48:337-345.

Similar to the above-described widespread array of neurotransmitter receptors that are displayed in CNS precursor cells, voltage-gated ion channels, and in particular voltage-dependent K^+ (Kv) channels are expressed not only in neuron-committed, but also in multipotent and glia-oriented precursor cells. The prototypical Kv channels have been divided into four families (Kv1-Kv4) based on sequence homology and on their sequence similarity to single gene orthologues in *Drosophila* (name given in italics): Kv1 (*Shaker*), Kv2 (*Shab*), Kv3 (*Shaw*), and Kv4 (*Shal*) (Trimmer and Rhodes, 2004). There is a correlation between the expression of large delayed outward-rectifying voltage-gated K^+-currents (I_k) and the proliferative state of different types of cells, and pharmacological block of such potassium channels can interfere with cell proliferation (DeCoursey et al., 1984;Sontheimer et al., 1989;Barres et al., 1990;Berger et al., 1991;Kettenmann et al., 1991;Dubois and Rouzaire-Dubois, 1993;Wonderlin and Strobl, 1996;Knutson et al., 1997;MacFarlane and Sontheimer, 1997;Sobko et al., 1998). Proliferative OPCs express large I_k, whereas non-dividing and mature oligodendrocytes display much smaller

outward currents (Knutson et al., 1997). These large I_k currents occur in G1 phase of OPC cell cycle and have been related to a RNA synthesis-dependent selective increase of expression of K^+ channel subunit proteins Kv1.3 and Kv1.5 (Gallo et al., 1996;Knutson et al., 1997;Ghiani et al., 1999b;Chittajallu et al., 2002). The inhibition of outward K^+ channels by blocker tetraethylammonium or by cell membrane depolarization through Na^+ channel opener veratridine inhibits OPC proliferation (Knutson et al., 1997;Ghiani et al., 1999b). The use of subunit-specific pharmological blockers first suggested that outward K^+ channels containing the Kv1.3 subunit played a critical role in cell cycle progression in proliferating OPCs (Chittajallu et al., 2002). Next, we recently performed gain-of-function experiments, providing evidence that overexpression of Kv1.3-1.4 increases OPC proliferation in the absence of mitogen, whereas Kv1.6 overexpression inhibits mitogen-induced OPC cell cycle progression (Publication #14 - Vautier et al., 2004). In contrast, Kv1.3-1.6 subunit overexpression does not interfere with the kinetics of oligodendrocyte differentiation (Publication #14 - Vautier et al., 2004). This study represents the first demonstration that the activity of potassium channels containing distinct Kv1 subunit proteins not only correlates with specific stages of oligodendrocyte lineage progression, but directly controls oligodendroglial proliferation in mitogenic as well as in growth factor-free conditions (Figure 9).

3.2 Established functional involvement of neurotransmitter receptors in postnatal CNS precursor cell biology

3.2.1.1 AMPA/kaïnate receptors: a matter of cell cycle or cell death

Publication #3: Belachew,S., Aguirre,A.A., Wang,H., Vautier,F., Yuan,X., Anderson,S., Kirby,M., and Gallo,V. (2002). Cyclin-dependent kinase-2 controls oligodendrocyte progenitor cell cycle progression and is downregulated in adult oligodendrocyte progenitors. *J. Neurosci.* 22:8553-8562.

In the adult/postnatal brain, glutamate is released from neurons (either synaptically or axonally) and reaches effective concentrations that can activate glutamate receptors on mature glia to cause: i) modulation of transmitter uptake into glial cells, thereby affecting termination of synaptic transmission (Chiu and Kriegler, 1994;Vernadakis, 1996;Bergles and Jahr, 1997); ii) modulation of K^+ conductances within glial cells, with consequences on the extracellular ionic environment (Muller et al., 1992;Vernadakis, 1996); and iii) release of neuroactive substances from glia that can feedback and modulate synaptic transmission (Araque et al., 1999).

In parallel with glutamate receptor functions in mature glial cells, during late embryonic and early postnatal development, astrocytes and oligodendrocytes arise from CNS precursor cells of the subventricular zone that also express glutamate-activated channels (LoTurco et al., 1995;Yuan et al., 1998). Excitatory transmitter glutamate that activates glutamate receptors (GluRs) inhibits OPC proliferation and prevents their differentiation in vitro and in tissue culture

slices (Gallo et al., 1996;Yuan et al., 1998). These antiproliferative effects of glutamate receptor activation are Ca^{2+}-independent and arise from an increase in intracellular Na^{+} and the subsequent block of outward K^{+} currents (Gallo et al., 1996;Knutson et al., 1997). AMPA/kaïnate glutamate receptor agonist or the direct blockade of outward K^{+} conductances caused a reversible G1 arrest in OPCs that correlate with an accumulation of the cyclin-dependent kinase inhibitors $p27^{Kip1}$ and $p21^{CIP1}$, with a selective decrease in cdk2 activity and with an impairment of cyclin E-cdk2 complex formation (Figure 10) (Ghiani et al., 1999a;Ghiani et al., 1999b;Ghiani and Gallo, 2001). Furthermore, we recently showed that the overexpression of cdk2 reverted AMPA/kaïnate- or K^{+} blockade-induced G1 arrest in OPCs (Publication #3 - Belachew et al., 2002), thus demonstrating that the regulation of cdk2 activity causally underlies cell cycle exit triggered by GluR-dependent or pharmacological inhibition of K^{+} channels.

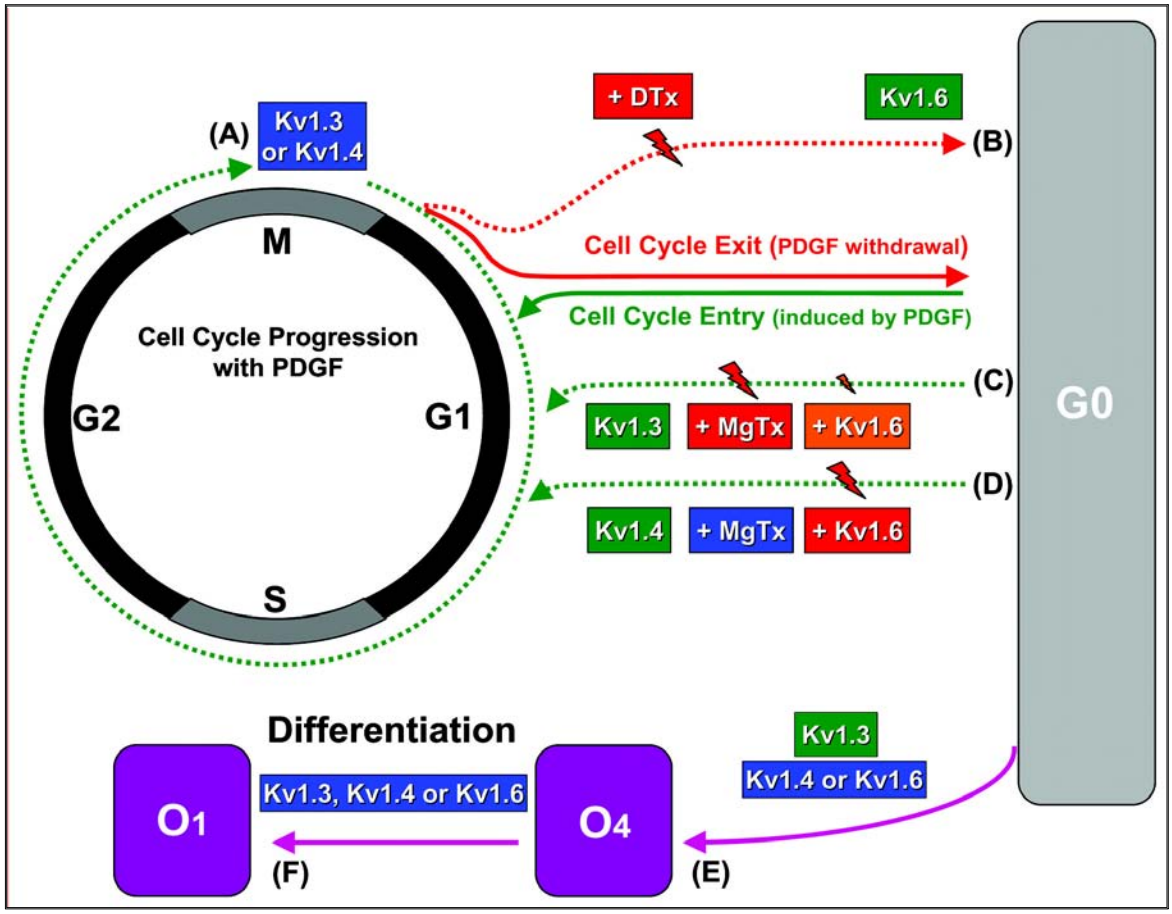

Figure 9: *Schematic illustrating the effects of Kv1 subunit over-expression on OPC proliferation and differentiation*
The schematic summarizes the major findings of our recent studies. Green boxes denote a significant effect on OP cell cycle following the over-expression of the corresponding Kv1 subunits. Red and orange boxes denote antagonism of these effects. Blue boxes denote no effect following over-expression of Kv1 subunits. Note, experiments in which Kv1.5 was over-expressed consistently resulted in no effect on cell cycle and so are omitted from the schematic for clarity. (A) Over-expression of Kv1.3 and 1.4 had no effect on OPCs that were already within PDGF-induced cell cycle. (B) In contrast, over-expression of Kv1.6 causes withdrawal from the cell cycle in a manner similar to that seen following PDGF removal. This effect was completely antagonized by Dtx. (C) and (D) Kv1.3 and 1.4 over-expression in cell cycle arrested OPCs led to the induction of proliferation in a manner similar to PDGF. MgTx inhibited this cell cycle entry only in response to Kv1.3 over-expression. Co-expression of Kv1.6 partially inhibited the Kv1.3-induced cell cycle entry and completely abolished the Kv1.4 effect. (E) and (F) Prolonged withdrawal of PDGF leads to differentiation of OPCs through O4 and O1 lineage stages. Kv1.4 and 1.6 over-expression does not affect this process. However, a small increase in $O4^{+}$ cell number (but not $O1^{+}$) is noted with Kv1.3 over-expression.

It still needs to be determined whether AMPA/kaïnate receptor activation may also interacts with cell cycle progression in CNS precursor cells from adult tissue and whether, hippocampal, versus white matter or cortical $NG2^+$ cells, could display distinct receptor subtypes with area-specific functions.

Several groups have also demonstrated that AMPA/kaïnate receptor activation can trigger excitotoxic cell death in the oligodendroglial lineage, but most of these works were performed using cultures of $O4^+/GalC^+$ post-mitotic pre-oligodendrocytes (Oka et al., 1993;Yoshioka et al., 1995;Matute et al., 1997;Sanchez-Gomez and Matute, 1999;Alberdi et al., 2002;Sanchez-Gomez et al., 2003). In contrast, no convincing evidence has ever been produced showing that cultured proliferating OPCs or mature myelinating oligodendrocytes were directly sensitive to excitotoxic insults (Gallo et al., 1996;Rosenberg et al., 2003), especially in human tissues (Wosik et al., 2004). In vivo, the mechanistic interpretation of AMPA/kaïnate receptor-mediated excitotoxic lesions in white matter oligodendroglial cells (McDonald et al., 1998;Matute, 1998;Pitt et al., 2000;Smith et al., 2000;Follett et al., 2000;Li and Stys, 2000;Matute et al., 2001;Tekkok and Goldberg, 2001) is subject to intense controversy since surrounding microglia (Noda et al., 2000) and astrocytes (Jabs et al., 1994;Verkhratsky and Steinhauser, 2000;Schroder et al., 2002;Matthias et al., 2003) also express such receptors and therefore may be intermediate actors of the toxic cascade. It is actually astounding to recall that the unique electrophysiological demonstration of functional AMPA/kaïnate receptor expression in adult so-called "OPCs" in vivo was not performed in the white matter, but in the hippocampus (Bergles et al., 2000). It is of

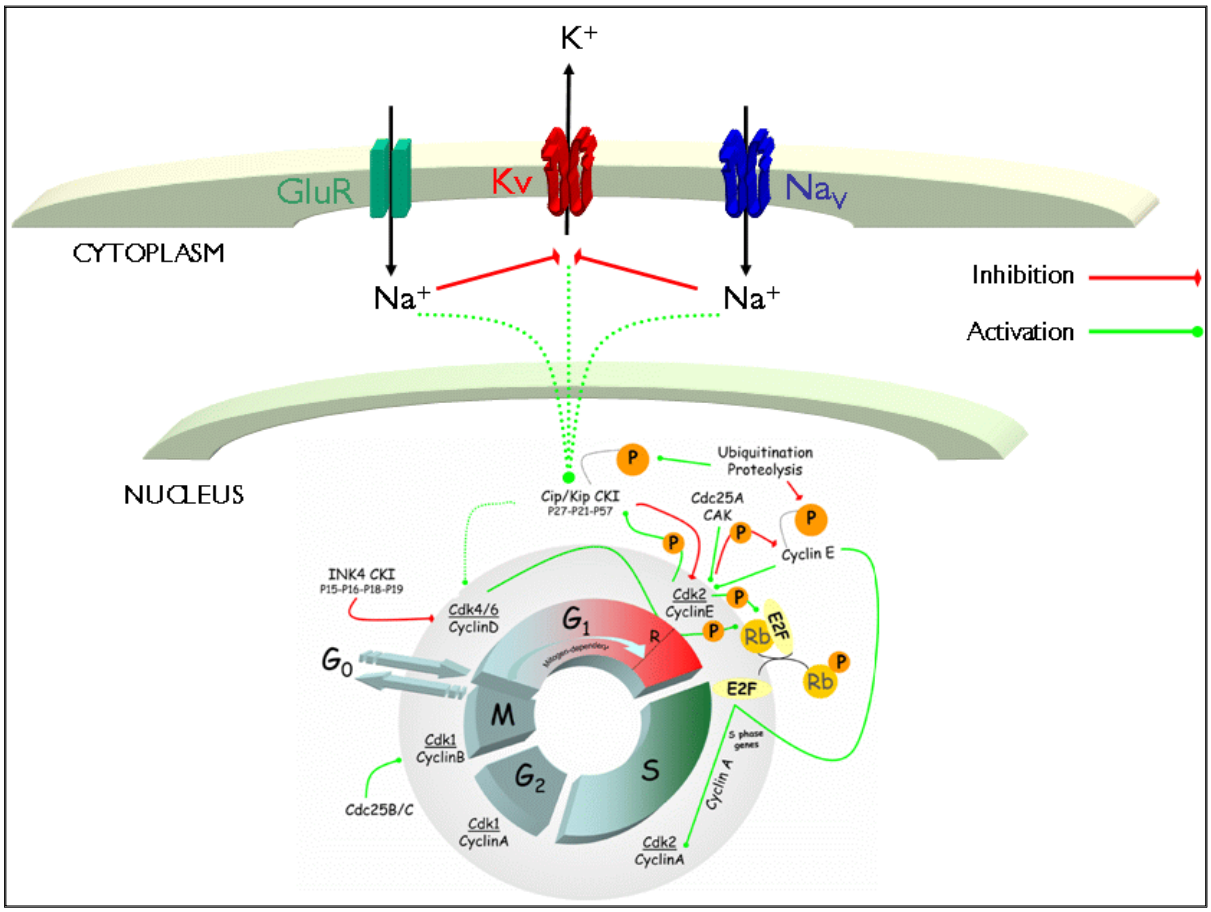

Figure 10: *Schematic diagram of the intracellular signal transduction pathways that couple glutamate receptors and voltage-gated ion channels to cell-cycle arrest in OPCs.*
Activation of glutamate receptors, opening of Na^+ channels or closure of K^+ channels stimulates accumulation of $p27^{Kip1}$ and $p21^{Cip1}$. An increase in intracellular Na^+ concentration, as a result of transmembrane influx through glutamate-activated or voltage-dependent channels, blocks K^+ channel activity. Broken lines indicate as yet unidentified signal transduction pathways.

interest to emphasize that, no matter what triggers it, the demonstration of excitotoxicity in adult white matter oligodendroglial cells cannot be taken per se as a straightforward piece of evidence of the presence of AMPA/kaïnate receptors onto these cells. It will be crucial in the near future to address this thorny issue by recording astrocytes and oligodendroglial cells from the adult white matter by taking advantage of cell-specific reporting transgenic mice that are now available (Zhuo et al., 1997;Publication #1 - Belachew et al., 2001;Nolte et al., 2001;Publication #2 - Yuan et al., 2002;Mallon et al., 2002). In the particular case of demyelinating disorders, this should rapidly tell us whether excitotoxic GluRs overactivation, which occurs primarily or secondarily to auto-immune activation, triggers direct oligodendroglial and axonal damages and/or modulate astroglial/microglial components of the inflammatory reaction that would then operate the final toxic effect (Pitt et al., 2000;Smith et al., 2000;Matute et al., 2001;Wosik et al., 2004).

3.2.1.2 $GABA_A$ receptors

Publication #15: Nguyen, L., Malgrange, B., Breuskin, I., Bettendorff, L., Moonen, G., Belachew, S., and Rigo, J.-M. (2003). Autocrine/paracrine activation of the $GABA_A$ receptor inhibits the proliferation of neurogenic polysialylated neural cell adhesion molecule-positive ($PSA\text{-}NCAM^+$) precursor cells from postnatal striatum. *J. Neurosci.* 23:3278-3294.

In the embryonic cerebrum, the neurotransmitter GABA reportedly partially blocks the bFGF-induced increase in proliferation in cortical progenitor cells (Antonopoulos et al., 1997) and reduces the number of proliferating cells and cell cycle kinetics in dissociated or organotypic cultures from the neocortex (LoTurco et al., 1995) or SVZ areas (Haydar et al., 2000). During early postnatal CNS development, we recently assessed the expression and function of $GABA_A$ receptors in SVZ/striatal neural precursor cells. On the basis of their isopycnic properties in a buoyant density gradient, we developed an isolation procedure that enable us to purify proliferative neural precursor cells from early postnatal rat striatum and adjacent SVZ, which expressed the polysialylated form of the neural cell adhesion molecule (PSA-NCAM) (Publication #15 - Nguyen et al., 2003). We investigated whether GABA may control the proliferation of these postnatal $PSA\text{-}NCAM^+$ precursors from newborn rat striata and reported that: i) epidermal growth factor (EGF)-responsive proliferative $PSA\text{-}NCAM^+$ precursors generate neurospheres committed mostly to a neuronal fate; ii) postnatal striatal/SVZ $PSA\text{-}NCAM^+$ precursors express functional $GABA_A$ receptors ($GABA_ARs$) and GABA-synthesizing enzymes glutamate decarboxylase (GAD) 65 and GAD 67 in vitro and in situ ; iii) proliferation of $PSA\text{-}NCAM^+$ precursors is inhibited by an EGF-controlled endogenous production of GABA that activates $GABA_AR$ in these cells; and iv) $GABA_AR$-dependent inhibition of $PSA\text{-}NCAM^+$ cell proliferation is mediated by a complex intracellular signaling notably involving the inhibition of the mitogen-activated protein kinase (MAPK) pathway and an increase of intracellular calcium concentration by opening of voltage-gated calcium channels (Publication #15 - Nguyen et al., 2003). This demonstration that early postnatal $PSA\text{-}NCAM^+$ striatal/SVZ neuronal precursors synthesized and released GABA suggested that an autocrine/paracrine GABA/$GABA_AR$-triggered mechanism may regulate their endogenous EGF-driven proliferation.

Similarly, $GABA_A$ receptor activation by exogenous application of $GABA_A$ agonist in early postnatal OPCs from cultured organotypic cerebellar slices also inhibited proliferation in these precursor cells (Yuan et al., 1998). However, treatment of the slices with the $GABA_A$ receptor antagonist bicuculline did not modify proliferation of cerebellar OPCs (Yuan et al., 1998), suggesting that endogenous activation of $GABA_A$ receptors is not a major mechanism of control

of cell cycle progression in postnatal OPCs in vivo, at least at the level of the cerebellum.

Altogether these works strongly indicate that $GABA_A$ receptors may be directly involved in the regulation of the maturation of early postnatal precursor cells in the process of becoming neurons. Like perinatal cells, adult (P13-P70) neuronal progenitors of the SVZ/RMS/OB pathway contain GABA, and are depolarized by GABA-mediated activation of first extrasynaptic and then later synaptic $GABA_A$ receptors (Carleton et al., 2003;Wang et al., 2003;Gallo and Haydar, 2003). Thus, $GABA_A$ receptor-mediated signaling may be part of the complex extrinsic influences that regulate adult neurogenesis.

3.3 Discussion point: neuron-glia versus neuron-neuroblast signaling?

3.3.1 The $NG2^+$ progenitor

In recent papers, Bergles and colleagues (Bergles et al., 2000;Lin and Bergles, 2004) have suggested that OPCs receive glutamatergic and GABAergic synaptic inputs from interneuronal collaterals in CA1 area of postnatal/adult hippocampus. The sole criterion used for identifying recorded cells as OPCs was immunohistochemical detection of the expression of NG2 chondroitin sulphate proteoglycan. It is obvious that NG2 has been widely used as an excellent marker of OPCs in vivo by a large number of groups (Levine et al., 2001). Although one cannot contest that $NG2^+$ cells are capable of differentiating into myelinating oligodendrocytes in white matter areas, it is debatable whether this developmental program occurs for all CNS cells that express NG2, especially in regions that display relatively less ongoing oligodendrogenesis, but more neurogenesis in adulthood. As a matter of fact, we and others have now demonstrated that precursor cells which were thought to be restricted to an oligodendroglial fate, i.e. so-called OPCs, were able to generate neurons in certain conditions in vitro and in vivo (Kondo and Raff, 2000b;Publication #5 - Belachew et al., 2003;Nunes et al., 2003). Furthermore, although neural stem cells per se are thought to have an undifferentiated phenotype, cells with glial features of the astroglial lineage, from radial glia to astrocytes, act as neural stem cells in the embryo and in adulthood across metazoan taxa (Doetsch et al., 1999;Malatesta et al., 2000;Noctor et al., 2001;Doetsch, 2003;Merkle et al., 2004).

Importantly, these studies have also led to redefining the neural stem cell nomenclature, to include glial progenitors as stem cells capable of generating neurons (Goldman, 2003). Based on these recent findings, it is still premature to define functional synaptic connections onto all NG2-expressing cells in the hippocampus as directly involved in neuron-oligodendroglial signaling, until it is proven that all $NG2^+$ cells that receive excitatory and inhibitory synapses are restricted to becoming oligodendrocytes in this particular region. The synapses analyzed and characterized by Bergles and colleagues might be in fact synaptic contacts between mature resident interneurons and early post-mitotic progenitors of adult GABAergic neurons. As previously described in the olfactory bulb (Carleton et al., 2003), this would also imply that the establishment of synaptic inputs occurs before GABAergic neuronal progenitors are able to propagate action potential spikes during the course of interneuron renewal in the hippocampus (Liu et al., 2003b). Unlike in the developing brain, where neurogenesis usually precedes the maturation of neural circuits, in the adult, newborn neurons have to integrate into a preexisting neuronal network. During SVZ-RMS-OB neurogenesis, it was shown that tangentially migrating neuroblasts in the RMS first expressed extrasynaptic $GABA_A$ receptors, and then secondarily AMPARs (Carleton et al., 2003). Again, this differs from the developing mammalian brain, where most often, NMDARs are first detected and functional AMPAR recruitment is induced by

NMDAR activation (Durand et al., 1996). Adult-generated OB granule neurons actually receive synaptic inputs shortly after completing their radial migration as they begin developing their dendritic arbor, and GABAergic synaptic events appear first, before AMPAR-mediated glutamatergic ones (Carleton et al., 2003). In sharp contrast with prenatal development, maturing adult OB granule neurons receive both $GABA_A$-mediated events and excitatory synaptic inputs before being able to propagate action potentials (Carleton et al., 2003). Unlike in newborn OB granule neurons, however, in adult-generated OB periglomerular neurons, the maturation of voltage-dependent sodium currents, and consequently the capacity of newly-formed cells to fire action potentials, seems to precede the appearance of synaptic contacts (Belluzzi et al., 2003). Thus, the sequential pattern of functional integration of newborn adult neurons appears to be cell-specific. At present, it remains to be elucidated whether activation of extrasynaptic and then synaptic $GABA_A$ and AMPA receptors represent instructive signals required for subsequent neuronal maturation, including the appearance of voltage-gated channels.

In contrast to SVZ-RMS-OB neurogenesis, there are currently no studies that have addressed the precise spatial migration and temporal course of electrophysiological maturation of adult-born hippocampal neurons. Since it is widely accepted that neurogenesis in the adult intact brain is restricted to SVZ and dentate gyrus areas, it is not without caveats to speculate that cells recorded by Bergles and colleagues in adult CA1 region may be immature neuronal precursors, potentially able to become GABAergic interneurons (Gage, 2000;Lie et al., 2004). Bergles and colleagues performed their recordings exclusively in the stratum radiatum region of CA1 in hippocampi taken from young (P6-16) and adult (> P33) rats (Bergles et al., 2000;Lin and Bergles, 2004). To our knowledge, there is no evidence that neurogenesis occurs in this region of the normal intact hippocampus, a fact confirmed in a recent report (Liu et al., 2003b). Furthermore, it is difficult to assume that immature neuronal precursor cells that are already synaptically-integrated could retain significant migrating properties. Thus, if CA1 $NG2^+$ cells indeed represent neuronal precursor cells, one would have to consider them as stuck in their neuronal differentiation, but potentially ready to be recruited to finally differentiate into mature newborn CA1 neurons, as observed in pathological conditions such as after ischemia (Nakatomi et al., 2002).

In conclusion, although it still needs to be established what percentage of $NG2^+$ cells in the hippocampus give rise to neurons and oligodendrocytes, respectively, a more detailed cellular and developmental characterization of the cell population studied is necessary to unequivocally conclude that they represent OPCs. Recent data also emphasize that we cannot rely any longer on a single antigenic marker to identify a specific cell phenotype. In particular, there is now a crucial need for revisiting with region- and context-specific functional and antigenic criteria the accurate definition of an OPC, as a cell that would be restricted to a glial vs. a neuronal fate. The precise characterization of the developmental potential of $NG2^+$ cells in distinct brain regions will go beyond issues of mere nomenclature, to define whether glutamate- and GABA-mediated signaling on these progenitors is an exclusive form of neuron-oligodendroglia communication, or if a proportion is in fact representative of neuron to neuroblast signaling. Besides white matter, where one cannot contest that $NG2^+$ cells do express AMPA/kaïnate receptors (Publication #2 - Yuan et al., 2002) that are likely involved in strict neuron-oligodendroglial interactions, the situation is thus by far more elusive and necessitates further studies to elucidate the meaning of extrasynaptic and possibly synaptic neurotransmitter receptors in $NG2^+$ cells located in the olfactory bulb, hippocampal, striatal and cortical areas.

3.3.2 Astrocytes

The term neuroglia, or "nerve glue", was coined in 1859 by Rudolph Virchow, who conceived of it as an inactive connective tissue in the CNS. We now all acknowledge its various active roles in brain function, metabolism and development. In the glial kingdom, astrocytes are characterized by sheet-like or lamellate processes enwrapping the brain surface, capillaries, neuronal cell bodies, dendrites and synapses. The astrocytic processes also express a broad range of ion channels and neurotransmitter receptors that can trigger $[Ca^{2+}]_i$ elevation in response to synaptic activity (Haydon, 2001;Araque et al., 2001). Calcium signaling in astrocytes is thought to influence glial morphology, function and gene expression, and in turn, to feed back onto neurons (Verkhratsky and Kettenmann, 1996). In particular, extensive attention has been paid to glutamate receptors (GluRs) on astrocytes as possible mediators of activity-dependent neuron-glia interplay (Steinhauser and Gallo, 1996), in the sense of both neuron-to-glia and glia-to-neuron signaling (Gallo and Ghiani, 2000). However, there was little experimental evidence until recently that supported this idea or elaborated upon possible mechanisms involved.

Bergmann glia in the cerebellum ensheathe Purkinje cell dendrites and synapses, and express high levels of Ca^{2+}-permeable glutamate receptors (GluRs) (Muller et al., 1992;Burnashev et al., 1992). Suppression of Ca^{2+} permeability by virus-mediated GluR2 transfer has revealed that GluR-mediated Ca^{2+} signaling is essential to maintain both anatomical and functional connections between Bergmann glial cell and the glutamatergic synapses (Iino et al., 2001). The finding that structural affinity of Bergmann glial processes for wrapping Purkinje cell synapses is thus mediated by the glial Ca^{2+}-permeable GluRs further suggests that under physiological conditions, glia-synapse interaction could undergo structural modifications in response to synaptic activities (Gallo and Chittajallu, 2001;Watanabe, 2002). Astrocytes also express high-affinity glutamate transporters, and particularly GLAST and GLT-1, that play a major role in controlling the rapid clearance from the synaptic cleft of glutamate that has been released from neurons (Chaudhry et al., 1995;Rothstein et al., 1996;Tanaka et al., 1997;Oliet et al., 2001). Such a process appears to be central in terminating the effects of released neurotransmitters and ensures the fine-tuning of excitatory synaptic transmission in the adult brain.

In contrast with synaptic events observed in $NG2^+$ cells (Bergles et al., 2000;Lin and Bergles, 2004), we want to emphasize that astrocytic glutamate uptake mechanisms washing out the synaptic cleft, or GluR2-containing AMPA receptor-dependent homeostasis of appropriate connections between Bergmann glia and Purkinje cell synapses, represent true unambiguous examples of neuron-glia interaction. In future studies, however, it would be intriguing to assess such intimate functional and structural relationships of astrocytes with closely neighboring neurons or neuronal precursors in locations such as the hippocampus, where so-called astrocytes or GFAP-expressing cells have been suggested to give rise to neurons (Seri et al., 2001;Doetsch, 2003). It is striking that together with recent studies reporting that astrocytes can regulate synapse formation and synaptic transmission (Ullian et al., 2001;Mauch et al., 2001;Nagler et al., 2001), other works have demonstrated that hippocampal astrocytes can instruct neurogenesis from neural stem cells and/or from committed neuronal precursor cells in the adult brain (Song et al., 2002a;Song et al., 2002b). It remains to be established whether and to what extent "glial" neurotransmitter-mediated signaling may be involved in these specific developmental properties of astrocytes in neurogenic regions.

4 Conclusions and perspectives

4.1 The good: NG2$^+$ OINPCs, a dual source of repair that may serve for interneuron renewal in the postnatal hippocampus and for remyelination elsewhere

In the present work, we have developed a transgenic mouse model that allows us to track more easily the biological properties of NG2-expressing oligodendrocyte progenitor cells in vivo. We have provided evidence that: i) cdk2 is a master controller of cell cycle decisions in the oligodendroglial lineage in vitro and, ii) that its down-regulation in adult OPCs may underlie the progressive decline of proliferative capacities during postnatal maturation of oligodendroglial cells, thus underlying the so-called quiescent state that characterizes adult OPCs, which fail to remyelinate demyelinated areas of the CNS. However, it was an amazing surprise for the entire "cell cycle" community to recently note that two groups independently reported that cdk2-null mice were viable and, apart from male and female sterility due to meiotic defects, were ostensibly free of other gross pathology and survived for up to two years (Ortega et al., 2003;Berthet et al., 2003). In fact, other experiments in which the genes encoding all three D-type cyclins, the two E-type cyclins or cyclin D-dependent cdk4 and cdk6 have been disrupted in the mouse germ line have revealed that much of fetal development occurs normally in their absence (Sherr and Roberts, 2004).

As recently shown for cdk4, surrogate compensatory mechanisms that allow mitotic cell cycles to occur in the absence of cdks during embryonic development may fail to fully compensate cdk loss in specific postnatal/adult progenitor cells (Jirawatnotai et al., 2004). Hence, in order to ascertain how masterful cdk2 may really be for OPC proliferation in vivo, we plan to elucidate the functional role of cdk2 during postnatal white matter development in the normal uninjured brain and in models of genetic dysmyelination (leukodystrophies) or acquired demyelination. In this regard, we will first characterize oligodendroglial lineage development in double transgenic mice resulting from the cross-breeding of cdk2-deficient (Berthet et al., 2003) with CNP-EGFP reporter mice. We will then assess the role of cdk2 in the established increase of OPC proliferation that occurs in a murine model of Pelizaeus-Merzbacher disease (Jimpy mutant) (Wu et al., 2000). Cdk2$^{-/-}$ CNP-EGFP mice will allow us: i) to assess the involvement of cdk2 in the recruitment of OPC proliferation that occurs after acquired demyelination, and ii) to address to what extent remyelination efficiency correlates with OPC proliferation in vivo. On the other hand, we also have in mind to analyze the role of cdk2 in proliferative events occurring in the neurogenic SVZ area where p27^{kip1} (an endogenous cyclin E/cdk2 inhibitor) appears to be a key regulator of cell division for type C transit-amplifier multipotent progenitors that underlie adult neurogenesis (Doetsch et al., 2002b). Finally, cultured NG2-expressing cells derived from cdk2$^{-/-}$ animals will represent a crucial material to stretch conceptual boundaries and to evaluate the accurate molecular consequences of cdk2 deficiency, possibly identifying new essential cell cycle regulatory genes that can fill in for cdk2 loss.

In the second and third part of this work, we have demonstrated that NG2 proteoglycan-expressing progenitor cells — i.e. previously so-called OPCs — that were considered to be tightly committed to become myelinating oligodendrocytes are indeed more diverse and more plastic than previously thought. Early postnatal hippocampal and SVZ-located NG2$^+$ progenitor cells co-expressing the dlx homeobox transcription factor and the Lewis X antigen (LeX) represent bipotential cells that actually give rise to GABAergic interneurons both in the dentate gyrus (Publication #5 - Belachew et al., 2003;Publication #6 - Aguirre et al., 2004) and in the olfactory bulb (Aguirre and Gallo, 2004). Interestingly, as highlighted in the third part of the

present work, like nestin$^+$ neural stem cells or PSA-NCAM$^+$ neuronal precursor cells, NG2$^+$ progenitor cells also express voltage-dependent ion channels and a broad array of neurotransmitter receptors that control their physiological properties (Belachew and Gallo, 2004). NG2$^+$ progenitor cells also receive GABAergic and AMPA/Kaïnate-mediated glutamatergic synaptic inputs in CA1 region of the adult hippocampus (Bergles et al., 2000;Lin and Bergles, 2004). A recent striking observation was that a subpopulation of cortical, but not white matter NG2$^+$ cells, elicit depolarization-induced spikes that are akin to immature action potentials (Chittajallu et al., 2004). Furthermore, Dwight Bergles' group has now reported that quantal release of glutamate occurring along axons triggers rapid AMPA receptor currents in NG2$^+$ progenitor cells from the corpus callosum (personal communication and Ziskin JL, Nishiyama A, Bergles DE, Society for Neuroscience Abstract #494.16, 2004).

Altogether, these data have widely questioned — to say the least — the dogmatic view of NG2$^+$ cells being seen as OPCs in a strict sense. There is now a need for consensus meeting and discussion to redefine real oligodendrocyte-committed OPCs. As mentioned before, we proposed here that LeX-negative/NG2$^+$ progenitor cells could be appropriate to represent this phenotype. However, we are far from approaching the full picture of what heterogeneity means in the NG2 lineage. It will take tremendous endeavor to further assess context- and area-dependent specific properties and fate potential of NG2$^+$ cells throughout the postnatal/adult brain. The question remains for instance whether a lineage relationship between NG2$^+$ cells and neurons is also found outside the hippocampus and olfactory bulb areas, such as in the cortex. The presence of postnatal cortical neurogenesis under physiological conditions remains a highly controversial issue, due to conflicting reports in the literature (Gould et al., 1999b;Gould et al., 2001;Kornack and Rakic, 2001;Letinic et al., 2002;Rakic, 2002a;Rakic, 2002b;Rakic, 2002c). However, it has been demonstrated that neurogenesis in the cortex occurs following various experimentally-induced CNS injuries (Magavi et al., 2000). The developmental origin of these newly born neurons remains unknown. Since it is well accepted that NG2$^+$ cells are the largest population of postnatal progenitors in the CNS and persist into adulthood (Dawson et al., 2000;Levine et al., 2001;Dawson et al., 2003), it is possible that spiking cortical NG2$^+$ cells (Chittajallu et al., 2004) under certain pathophysiological conditions could be triggered into neuronal maturation.

Why certain subtypes of NG2$^+$ cells display neuron-like properties (spikes and synaptic contacts) while devoid of antigenic features of committed immature neurons is also a fascinating issue. Such synaptically-connected and/or spiking NG2$^+$ cells may alternatively be seen as i) a newly identified excitable glial phenotype that would play complex adapter functions at the interface of neuron-glia communication, or ii) intrinsically multipotent but regionally-specified transit-amplifying progenitor cells (quiescent or not ?) receiving rapid neuron-derived signaling through chemical and perhaps electrical synapses that may influence their interneuronal or oligodendroglial fate determination and maturation in the postnatal/adult CNS.

Besides the understanding of the fine-tuning of adult "glial" stem cell-derived neurogenesis that has become increasingly controversial between distinct models explaining how a GFAP-expressing cell give rise to newborn granule neurons (Doetsch, 2003;Kempermann et al., 2004;Garcia et al., 2004), the quest for determining the full identity of NG2$^+$/GFAP-negative progenitor cells appears to be equally challenging.

4.2 The bad: new neurons in the postnatal/adult brain: what for?

In most studies, only few parameters have been assessed to characterize the regulation of adult neurogenesis. The most widely used parameters are cell proliferation in the subgranular zone, cell survival, and neuronal differentiation. Consequently, the patterns of regulation appeared relatively uniform since systemic unspecific stimuli (e.g. hormonal changes or physical activity) (Gould et al., 1992;van Praag et al., 1999a;van Praag et al., 1999b), functionally specific stimuli (e.g. learning and the experience of complexity) (Kempermann et al., 1997b;Gould et al., 1999a) and pathological stimuli (e.g. ischemia, trauma or seizures) (Bengzon et al., 1997;Gould and Tanapat, 1997;Parent et al., 1997;Liu et al., 1998b) all have "identical" effects on adult neurogenesis, ending up inducing proliferation of a precursor cell or increasing their survival? If adult hippocampal neurogenesis is functionally relevant and represents an evolutionary benefit, it does not make sense to react with such sensitivity and without specificity to every kind of stimulus, even if the net result of more new neurons might look very similar. The impression of a standardized neurogenic response is likely to be due to a still relatively simplistic view of what actually constitutes adult neurogenesis. We also have to cope with the crucial lack of studies that actually have helped filling the gap that still separates the level of global extrinsic stimuli from effector molecular cues that regulate neurogenesis (Table 4).

Table 4: *Essential intrinsic cues that regulate adult stem cell-derived neurogenesis in vivo*

Neurogenic areas	Essential intrinsic signals	Effects	References
Dentate gyrus & SVZ	TLX	TLX, an orphan nuclear receptor, maintains adult neural stem cells in an undifferentiated, self-renewing, proliferative state.	(Shi et al., 2004)
Dentate gyrus & SVZ	Shh	Sonic hedgehog signaling is required to maintain proliferation of neural progenitor cells in postnatal germinative areas. Shh is required for cell proliferation in the mouse forebrain's SVZ stem cell niche and for the production of new olfactory interneurons in vivo.	(Lai et al., 2003) (Machold et al., 2003) (Palma et al., 2005)
Dentate gyrus & SVZ	VEGF	Intracerebroventricular administration of vascular endothelial growth factor (VEGF) into rat brain was shown to increase proliferation of neurogenic progenitor cells in the SVZ and in the subgranular zone of the dentate gyrus, where VEGFR2/Flk-1 was colocalized with the immature neuronal marker, doublecortin. VEGF, acting through kinase insert domain receptor (KDR), actually mediates the effect of the environment on neurogenesis and cognition.	(Jin et al., 2002) (Cao et al., 2004)
Dentate gyrus & SVZ	Cyclin D2	Adult mice mutated in the cell cycle regulatory gene *Ccnd2*, encoding cyclin D2, lack newly born neurons in the olfactory bulb and dentated gyrus areas. In contrast, genetic ablation of cyclin D1 does not affect adult neurogenesis.	(Kowalczyk et al., 2004)
SVZ	Bmi-1	The polycomb family transcriptional repressor Bmi-1 is required for the self-renewal of adult neural stem cells but not for their survival and differentiation. In contrast, restricted neural progenitors from the adult forebrain proliferate normally in the absence of Bmi-1.	(Molofsky et al., 2003)
Dentate gyrus	MBD1	Methyl-CpG binding protein 1 (MBD1) is a member of the methylated DNA-binding protein family. Adult MBD1$^{-/-}$ mice had decreased neurogenesis, impaired spatial learning, and a significant reduction in long-term potentiation in the dentate gyrus of the hippocampus.	(Zhao et al., 2003)
Dentate gyrus	NRSE/RE1	The small, noncoding double-stranded (ds) RNA NRSE/RE1(neuron restricted silencing element) can trigger gene expression of neuron-specific genes through interaction with NRSF/REST (neuronal restricted silencing factor/RE-1 silencing transcription factor) transcriptional machinery, resulting in the transition from neural stem cells with neuron-specific genes silenced by NRSF/REST into cells with neuronal identity that can express neuronal genes.	(Kuwabara et al., 2004)

Neurogenic areas	Essential intrinsic signals	Effects	References
SVZ	BMPs/Noggin	The bone morphogenetic protein (BMP) antagonist Noggin is expressed by ependymal cells adjacent to the SVZ. SVZ cells were found to express BMPs as well as their cognate receptors. BMPs potently inhibited neurogenesis both in vitro and in vivo whereas ectopically expressed noggin promoted neuronal differentiation in vivo.	(Lim et al., 2000) (Chmielnicki et al., 2004)

Adult neurogenesis and its regulation can be understood only if quantitative considerations such as cell counts are combined with a qualitative assessment of neuronal development. How a stimulus influences the quality of neuronal development might be as meaningful as the numbers of newly generated neurons. This will be of particular importance for contexts in which normal adult neurogenesis apparently fails, such as in temporal lobe epilepsy (Parent and Lowenstein, 2002), or where its failure has been discussed as a possible factor, such as in major depression (Jacobs et al., 2000;Santarelli et al., 2003;Kempermann and Kronenberg, 2003). However, the prerequisite for understanding the altered function is to enhance the quality of our characterization of normal neuronal development in the adult dentate gyrus. In general, the mere existence of adult hippocampal neurogenesis is undisputed today but its accurate time-course and the reasons underlying its progressive breakdown with postnatal/adult maturation (Kuhn et al., 1996;Kempermann et al., 2003) remain to be elucidated, in particular during the perinatal to juvenile period when most of the collapse occurs. It is also true that many individual results are controversial because of the methodological limitations of birth-marking dividing cells with bromodeoxyuridine (BrdU) and the problem of deciding on sufficient criteria to identify a cell as a neuron or a neuron-committed cell.

Although we already knew that human neural stem cells behave differently from their rodent equivalents in culture (Ostenfeld et al., 2000;Arsenijevic et al., 2001;Jakel et al., 2004), the direct study of human brain tissue has recently shown additional significant and clinically relevant species-specific differences (Sanai et al., 2004). In adult humans, "glial progenitor cells" form a prominent layer, or ribbon, that is restricted to a specific region in the brain that lines the lateral cerebral ventricle (Sanai et al., 2004). This region is also present in non-human primates, but it is thinner and less well delineated than in humans (Kornack and Rakic, 2001;Rakic, 2002b;Koketsu et al., 2003). Furthermore, the pathway known as the rostral migratory stream in rodents and primates — which contains neuroblasts that migrate from the SVZ to the olfactory bulb to give rise to adult-born neurons — is absent in humans (Sanai et al., 2004). Such findings add to the evidence that, with the exception of newborn granule cells in the dentate gyrus (Eriksson et al., 1998), the human brain shows no signs of spontaneous neuronal turnover. Back to the potential of glial progenitors in the adult brain, it means that their function in humans given that they do not give rise to neurons (apart from the DG region) might be to serve as i) a major source for the turnover of astrocytes and oligodendrocytes (possibly after demyelination), ii) to be a reservoir for a certain type of astrocytes that migrates to sites of traumatic, infectious, inflammatory or degenerative brain lesions, and iii) to represent a dormant cause of certain types of invasive glial tumors (Oliver and Wechsler-Reya, 2004;Yuan et al., 2004;Berger et al., 2004;Singh et al., 2004a;Singh et al., 2004b), but never of malignant tumors of any neuronal cell type — thereby confirming that there must be amazing suppressors that block the production of neuronal cells in the adult human non-hippocampal brain regions (Rakic, 2002b).

In conclusion, the inability of adult human brain to replace lost neurons outside the dentate gyrus might be because it is reluctant to accept newcomers into an established neural

network, rather than because potential progenitors are absent. One could further speculate that the systematic decrease in the extent of adult neurogenesis during vertebrate evolution, culminating in primates, may be the result of an evolutionary gain that represents an adaptation to keep neuronal networks with a constantly accumulating experience over an entire life span (Rakic, 2002b).

The situation in the hippocampus however is obviously different, as functional neurogenesis is possible there even though, ironically, we are still far from truly understanding what this function means (Doetsch and Hen, 2005). The function of neurons is extremely complex to say the least and is revealed on distinct conceptual levels — cellular, network and system being the minimal number of distinct levels — thus hindering simple interpretations. Adult-generated dentate gyrus neurons become electrophysiologically functional in vivo, extend axons along the mossy fiber tract to CA3 and are integrated as granule cells (Markakis and Gage, 1999;Hastings and Gould, 1999;van Praag et al., 2002). Nevertheless, this does not tell us a word about the functional relevance of adult DG neurogenesis at the system level. The elimination of proliferative cells in the dentate gyrus affects performance on some but not other hippocampus-dependent learning tasks (Shors et al., 2001;Shors et al., 2002;Shors, 2004) and such studies were using cytostatic agents that can be questioned for their multi-parametric side-effects besides modulating progenitor cell cycle. One would now need to assess cognitive functions after inducing a selective impairment of neurogenesis using transgenically-targeted techniques of ablation of the progenitor pool (Imura et al., 2003;Morshead et al., 2003;Garcia et al., 2004). Furthermore, the time-scale of such experiments should ideally take into consideration the logical assumption that effects of disrupted neurogenesis should show up weeks after the defect, not immediately. Similarly, experience of environmental complexity as well as more specific learning stimuli lead to an increase of adult dentate gyrus neurogenesis (Kempermann et al., 1997b;Gould et al., 1999a) but the time it takes neurons to mature and become integrated on the network level (N. Toni, E.A. Bushong, E.M. Teng, Y. Jones, H. Van Praag, M.E. Martone, M.H. Ellisman, F.H. Gage: Synaptogenesis of new neurons in the adult hipocampus. Abstract N° 833.18., *Society for Neuroscience Meeting*, 2004) argues against the idea that they could be of any use for the process that might have triggered their generation. Manipulations of adult neurogenesis and of a potential functional outcome occur on different time-scales, making it likely that the function of new neurons is part of long-term adaptive processes rather than acute benefits. In contrast, at present, adult neurogenesis could even be seen as functionally deleterious since new results suggested the existence of a critical period for new neuron maturation, during which synaptic competition for release sites may occur between newborn neurons and adult neurons, thereby influencing the development, connectivity and possibly also survival of adult-born but also resident neurons (N. Toni, E.A. Bushong, E.M. Teng, Y. Jones, H. Van Praag, M.E. Martone, M.H. Ellisman, F.H. Gage: Synaptogenesis of new neurons in the adult hipocampus. Abstract N° 833.18., *Society for Neuroscience Meeting*, 2004).

Altogether, one has to confess at this stage that we still do not know enough to recognize adult hippocampal neurogenesis as a realistic contributor to cognitive function, be it under physiological or pathological conditions.

4.3 The (not so) ugly: is there a glimpse of hope in the fuzzy near future of stem/progenitor cell-based therapy in humans ?

We developed in our lab strategies aimed at understanding why neuronal or oligodendroglial cell replacement is so limited in the normal uninjured adult brain. A distinct, related but equally complex issue is the reason why endogenous progenitor cells of any kind fail to regenerate lost cells at some point in basically all degenerative disorders of the CNS. While we struggle for answering why endogenous hurdles represent unbearable caveats to CNS regeneration, we may actually just prepare the niche to make it more accessible for transplanted exogenous guests. As a matter of fact, the problems associated with transplantation of neural and other tissue-specific stem cells, including isolation difficulties, limited available quantities, tumorigenicity concerns, and the questionable existence of a full range of easily controllable differentiating potential (towards various neuronal subtypes in particular), may be circumvented by the future use of embryonic stem (ES) cells.

By recapitulating development, ES cells have the potential to be driven down specific lineage and in particular neural pathways (Tropepe et al., 2001;Plachta et al., 2004;Bibel et al., 2004) to replenish damaged tissues and, as with adult somatic stem cells, to be used for cell replacement therapy of monocellular degenerative diseases. There is now evidence that ES cells can be coaxed down certain specific glial or neuronal phenotypes in vitro (Zhang et al., 2001;Ding et al., 2003;Plachta et al., 2004;Bibel et al., 2004;Perrier et al., 2004;Glaser et al., 2004) that could serve for further in vivo transplantation (Brustle et al., 1999;Kim et al., 2002). These processes now start to be modeled with human ES cells (Perrier et al., 2004) but before lineage cell pathways can be safely manipulated and better understood through ES cell technologies, a more diverse repertoire of ES cells is required. Unfortunately, restrictions imposed by US President G.W. Bush in August of 2001 (Cimons, 2001a;Cimons, 2001b) limited federal funding to research done on the 70 ES cell lines derived prior to his announcement, 22 of which are currently useable. These boundaries limit the genetic diversity of human ES cells available and will inevitably impede therapeutic developments. Recently, 17 new ES cell lines derived from embryos produced from in vitro fertilization clinics were described and offered to the public, yet research involving these new lines must be privately funded, at least for the four years to come (Macilwain et al., 2004;Bush and Kerry, 2004).

Combined with ES cell potential, nuclear transfer (NT) techniques have also brought stunning perspectives into the limelight. NT entails the transfer of a post-mitotic somatic cell nucleus into an enucleated oocyte, creating a cloned organism whose genetic information comes solely from the original donor nucleus. The "to clone or not to clone" debate has been further stimulated by the possibility of using NT to isolate ES cells from the inner cell mass of a NT-derived blastocyst, thereby generating a potentially limitless source of pluripotent cells that would have innumerable therapeutic applications (Wakayama et al., 2001;Barberi et al., 2003). This technology offers the potential to genetically customize ES cells for individual patients, thereby erasing the need for lifelong immunosuppression after transplantation as well as making ES cell therapies available to a more diverse population. However, despite the promises such a system even in humans (Hwang et al., 2004), the lack of a reliable and efficient way to produce NT-derived ES cell lines remains a considerable hurdle. The cause of the inefficiency to develop NT-derived ES cell lines from the inner cell mass of a blastocyst (Hwang et al., 2004) has yet to be determined. Other unexpected molecular hitches have also been reported with NT-derived ES cell lines, including alterations of gene expression patterns and mitotic spindle malfunctions in somatic clones (Bortvin et al., 2003;Simerly et al., 2003). Finally, one has to keep in mind that

there is still a great deal of concerns about the long-term stability of specific mature neuronal or glial phenotypes that could be induced from NT-derived ES cell lines.

Further research on NT and ES cell technologies as well as a better knowledge of the basic biology of ES and tissue-specific (in particular neural) stem cells will still be needed obviously for a long time. Hopefully these findings will pave the way to a new paradigm that will move one day cellular therapy to the clinic.

5 References

Aguirre AA, Gallo V (2004) Postnatal neurogenesis and gliogenesis in the olfactory bulb from NG2-expressing progenitors of the subventricular zone. J Neurosci 24: 10530-10541.

Ahlgren SC, Wallace H, Bishop J, Neophytou C, Raff MC (1997) Effects of thyroid hormone on embryonic oligodendrocyte precursor cell development in vivo and in vitro. Mol Cell Neurosci 9: 420-432.

Akassoglou K, Bauer J, Kassiotis G, Pasparakis M, Lassmann H, Kollias G, Probert L (1998) Oligodendrocyte apoptosis and primary demyelination induced by local TNF/p55TNF receptor signaling in the central nervous system of transgenic mice: models for multiple sclerosis with primary oligodendrogliopathy. Am J Pathol 153: 801-813.

Akazawa C, Sasai Y, Nakanishi S, Kageyama R (1992) Molecular characterization of a rat negative regulator with a basic helix-loop-helix structure predominantly expressed in the developing nervous system. J Biol Chem 267: 21879-21885.

Alberdi E, Sanchez-Gomez MV, Marino A, Matute C (2002) Ca(2+) influx through AMPA or kainate receptors alone is sufficient to initiate excitotoxicity in cultured oligodendrocytes. Neurobiol Dis 9: 234-243.

Aleem E, Berthet C, Kaldis P (2004) Cdk2 as a master of s phase entry: fact or fake? Cell Cycle 3: 35-37.

Altman J, Das GD (1965) Autoradiographic and histological evidence of postnatal hippocampal neurogenesis in rats. J Comp Neurol 124: 319-335.

Alvarez-Buylla A, Garcia-Verdugo JM (2002) Neurogenesis in adult subventricular zone. J Neurosci 22: 629-634.

Alvarez-Buylla A, Garcia-Verdugo JM, Tramontin AD (2001) A unified hypothesis on the lineage of neural stem cells. Nat Rev Neurosci 2: 287-293.

Alvarez-Buylla A, Temple S (1998) Stem cells in the developing and adult nervous system. J Neurobiol 36: 105-110.

Antonopoulos J, Pappas IS, Parnavelas JG (1997) Activation of the GABAA receptor inhibits the proliferative effects of bFGF in cortical progenitor cells. Eur J Neurosci 9: 291-298.

Araque A, Carmignoto G, Haydon PG (2001) Dynamic signaling between astrocytes and neurons. Annu Rev Physiol 63: 795-813.

Araque A, Parpura V, Sanzgiri RP, Haydon PG (1999) Tripartite synapses: glia, the unacknowledged partner. Trends Neurosci 22: 208-215.

Armstrong RC, Harvath L, Dubois-Dalcq ME (1990) Type 1 astrocytes and oligodendrocyte-type 2 astrocyte glial progenitors migrate toward distinct molecules. J Neurosci Res 27: 400-407.

Arnett HA, Fancy SP, Alberta JA, Zhao C, Plant SR, Kaing S, Raine CS, Rowitch DH, Franklin RJ, Stiles CD (2004) bHLH Transcription Factor Olig1 Is Required to Repair Demyelinated Lesions in the CNS. Science 306: 2111-2115.

Arnett HA, Mason J, Marino M, Suzuki K, Matsushima GK, Ting JP (2001) TNF alpha promotes proliferation of oligodendrocyte progenitors and remyelination. Nat Neurosci 4: 1116-1122.

Arsenijevic Y, Villemure JG, Brunet JF, Bloch JJ, Deglon N, Kostic C, Zurn A, Aebischer P (2001) Isolation of multipotent neural precursors residing in the cortex of the adult human brain. Exp Neurol 170: 48-62.

Assoian RK (2004) Stopping and Going with p27(kip1). Dev Cell 6: 458-459.

Atluri P, Fleck MW, Shen Q, Mah SJ, Stadfelt D, Barnes W, Goderie SK, Temple S, Schneider AS (2001) Functional nicotinic acetylcholine receptor expression in stem and progenitor cells of the early embryonic mouse cerebral cortex. Dev Biol 240: 143-156.

Balabanov R, Popko B (2005) Myelin repair: developmental myelination redux? Nat Neurosci 8: 262-264.

Balazs R, Hack N, Jorgensen OS (1988a) Stimulation of the N-methyl-D-aspartate receptor has a trophic effect on differentiating cerebellar granule cells. Neurosci Lett 87: 80-86.

Balazs R, Jorgensen OS, Hack N (1988b) N-methyl-D-aspartate promotes the survival of cerebellar granule cells in culture. Neuroscience 27: 437-451.

Bansal R, Kumar M, Murray K, Morrison RS, Pfeiffer SE (1996) Regulation of FGF receptors in the oligodendrocyte lineage. Mol Cell Neurosci 7: 263-275.

Barberi T, Klivenyi P, Calingasan NY, Lee H, Kawamata H, Loonam K, Perrier AL, Bruses J, Rubio ME, Topf N, Tabar V, Harrison NL, Beal MF, Moore MA, Studer L (2003) Neural subtype specification of fertilization and nuclear transfer embryonic stem cells and application in parkinsonian mice. Nat Biotechnol 21: 1200-1207.

Barker JL, Behar T, Li YX, Liu QY, Ma W, Maric D, Maric I, Schaffner AE, Serafini R, Smith SV, Somogyi R, Vautrin JY, Wen XL, Xian H (1998) GABAergic cells and signals in CNS development. Perspect Dev Neurobiol 5: 305-322.

Baron W, Decker L, Colognato H, Ffrench-Constant C (2003) Regulation of integrin growth factor interactions in oligodendrocytes by lipid raft microdomains. Curr Biol 13: 151-155.

Baron W, Shattil SJ, Ffrench-Constant C (2002) The oligodendrocyte precursor mitogen PDGF stimulates proliferation by activation of alpha(v)beta3 integrins. EMBO J 21: 1957-1966.

Barres BA, Burne JF, Holtmann B, Thoenen H, Sendtner M, Raff MC (1996) Ciliary neurotrophic factor enhances the rate of oligodendrocyte generation. Mol Cell Neurosci 8: 146-156.

Barres BA, Hart IK, Coles HS, Burne JF, Voyvodic JT, Richardson WD, Raff MC (1992) Cell death and control of cell survival in the oligodendrocyte lineage. Cell 70: 31-46.

Barres BA, Koroshetz WJ, Swartz KJ, Chun LL, Corey DP (1990) Ion channel expression by white matter glia: the O-2A glial progenitor cell. Neuron 4: 507-524.

Barres BA, Lazar MA, Raff MC (1994a) A novel role for thyroid hormone, glucocorticoids and retinoic acid in timing oligodendrocyte development. Development 120: 1097-1108.

Barres BA, Raff MC (1993) Proliferation of oligodendrocyte precursor cells depends on electrical activity in axons. Nature 361: 258-260.

Barres BA, Raff MC (1999) Axonal control of oligodendrocyte development. J Cell Biol 147: 1123-1128.

Barres BA, Raff MC, Gaese F, Bartke I, Dechant G, Barde YA (1994b) A crucial role for neurotrophin-3 in oligodendrocyte development. Nature 367: 371-375.

Barres BA, Schmid R, Sendnter M, Raff MC (1993) Multiple extracellular signals are required for long-term oligodendrocyte survival. Development 118: 283-295.

Baumann N, Pham-Dinh D (2001) Biology of oligodendrocyte and myelin in the mammalian central nervous system. Physiol Rev 81: 871-927.

Bayer SA, Yackel JW, Puri PS (1982) Neurons in the rat dentate gyrus granular layer substantially increase during juvenile and adult life. Science 216: 890-892.

Belachew S, Gallo V (2004) Synaptic and extrasynaptic neurotransmitter receptors in glial precursors' quest for identity. Glia 48: 185-196.

Belluzzi O, Benedusi M, Ackman J, LoTurco JJ (2003) Electrophysiological differentiation of new neurons in the olfactory bulb. J Neurosci 23:

10411-10418.
Ben Ari Y (2001) Developing networks play a similar melody. Trends Neurosci 24: 353-360.
Ben Ari Y (2002) Excitatory actions of gaba during development: the nature of the nurture. Nat Rev Neurosci 3: 728-739.
Ben Hur T, Rogister B, Murray K, Rougon G, Dubois-Dalcq M (1998) Growth and fate of PSA-NCAM+ precursors of the postnatal brain. J Neurosci 18: 5777-5788.
Benezra R, Davis RL, Lockshon D, Turner DL, Weintraub H (1990) The protein Id: a negative regulator of helix-loop-helix DNA binding proteins. Cell 61: 49-59.
Bengzon J, Kokaia Z, Elmer E, Nanobashvili A, Kokaia M, Lindvall O (1997) Apoptosis and proliferation of dentate gyrus neurons after single and intermittent limbic seizures. Proc Natl Acad Sci U S A 94: 10432-10437.
Berger F, Gay E, Pelletier L, Tropel P, Wion D (2004) Development of gliomas: potential role of asymmetrical cell division of neural stem cells. Lancet Oncol 5: 511-514.
Berger T, Schnitzer J, Kettenmann H (1991) Developmental changes in the membrane current pattern, K+ buffer capacity, and morphology of glial cells in the corpus callosum slice. J Neurosci 11: 3008-3024.
Bergles DE, Jahr CE (1997) Synaptic activation of glutamate transporters in hippocampal astrocytes. Neuron 19: 1297-1308.
Bergles DE, Roberts JD, Somogyi P, Jahr CE (2000) Glutamatergic synapses on oligodendrocyte precursor cells in the hippocampus. Nature 405: 187-191.
Berthet C, Aleem E, Coppola V, Tessarollo L, Kaldis P (2003) Cdk2 knockout mice are viable. Curr Biol 13: 1775-1785.
Bertrand N, Castro DS, Guillemot F (2002) Proneural genes and the specification of neural cell types. Nat Rev Neurosci 3: 517-530.
Besson A, Gurian-West M, Schmidt A, Hall A, Roberts JM (2004) p27Kip1 modulates cell migration through the regulation of RhoA activation. Genes Dev.
Betz H (1991) Glycine receptors: heterogeneous and widespread in the mammalian brain. Trends Neurosci 14: 458-461.
Bibel M, Richter J, Schrenk K, Tucker KL, Staiger V, Korte M, Goetz M, Barde YA (2004) Differentiation of mouse embryonic stem cells into a defined neuronal lineage. Nat Neurosci 7: 1003-1009.
Billon N, Jolicoeur C, Tokumoto Y, Vennstrom B, Raff M (2002) Normal timing of oligodendrocyte development depends on thyroid hormone receptor alpha 1 (TRalpha1). EMBO J 21: 6452-6460.
Billon N, Terrinoni A, Jolicoeur C, McCarthy A, Richardson WD, Melino G, Raff M (2004) Roles for p53 and p73 during oligodendrocyte development. Development.
Billon N, Tokumoto Y, Forrest D, Raff M (2001) Role of thyroid hormone receptors in timing oligodendrocyte differentiation. Dev Biol 235: 110-120.
Blakemore WF, Keirstead HS (1999) The origin of remyelinating cells in the central nervous system. J Neuroimmunol 98: 69-76.
Blaschuk KL, Frost EE, Ffrench-Constant C (2000) The regulation of proliferation and differentiation in oligodendrocyte progenitor cells by alphaV integrins. Development 127: 1961-1969.
Bogler O, Noble M (1994) Measurement of time in oligodendrocyte-type-2 astrocyte (O-2A) progenitors is a cellular process distinct from differentiation or division. Dev Biol 162: 525-538.
Bolton WE, Freeman JW, Mikulka WR, Healy CG, Schmittling RJ, Kenyon NS (1994) Expression of proliferation-associated antigens (PCNA, p120, p145) during the reentry of G0 cells into the cell cycle. Cytometry 17: 66-74.
Bornstein G, Bloom J, Sitry-Shevah D, Nakayama K, Pagano M, Hershko A (2003) Role of the SCFSkp2 ubiquitin ligase in the degradation of p21Cip1 in S phase. J Biol Chem 278: 25752-25757.
Borodinsky LN, O'Leary D, Neale JH, Vicini S, Coso OA, Fiszman ML (2003) GABA-induced neurite outgrowth of cerebellar granule cells is mediated by GABA(A) receptor activation, calcium influx and CaMKII and erk1/2 pathways. J Neurochem 84: 1411-1420.
Bortvin A, Eggan K, Skaletsky H, Akutsu H, Berry DL, Yanagimachi R, Page DC, Jaenisch R (2003) Incomplete reactivation of Oct4-related genes in mouse embryos cloned from somatic nuclei. Development 130: 1673-1680.
Bowman CL, Kimelberg HK (1984) Excitatory amino acids directly depolarize rat brain astrocytes in primary culture. Nature 311: 656-659.
Brazel CY, Romanko MJ, Rothstein RP, Levison SW (2003) Roles of the mammalian subventricular zone in brain development. Prog Neurobiol 69: 49-69.
Brustle O, Jones KN, Learish RD, Karram K, Choudhary K, Wiestler OD, Duncan ID, McKay RD (1999) Embryonic stem cell-derived glial precursors: a source of myelinating transplants. Science 285: 754-756.
Burnashev N, Khodorova A, Jonas P, Helm PJ, Wisden W, Monyer H, Seeburg PH, Sakmann B (1992) Calcium-permeable AMPA-kainate receptors in fusiform cerebellar glial cells. Science 256: 1566-1570.
Bush GW, Kerry J (2004) Bush and Kerry Offer Their Views on Science. Science.
Buttery PC, Ffrench-Constant C (1999) Laminin-2/integrin interactions enhance myelin membrane formation by oligodendrocytes. Mol Cell Neurosci 14: 199-212.
Butzkueven H, Zhang JG, Soilu-Hanninen M, Hochrein H, Chionh F, Shipham KA, Emery B, Turnley AM, Petratos S, Ernst M, Bartlett PF, Kilpatrick TJ (2002) LIF receptor signaling limits immune-mediated demyelination by enhancing oligodendrocyte survival. Nat Med 8: 613-619.
Calaora V, Rogister B, Bismuth K, Murray K, Brandt H, Leprince P, Marchionni M, Dubois-Dalcq M (2001) Neuregulin signaling regulates neural precursor growth and the generation of oligodendrocytes in vitro. J Neurosci 21: 4740-4751.
Calver AR, Hall AC, Yu WP, Walsh FS, Heath JK, Betsholtz C, Richardson WD (1998) Oligodendrocyte population dynamics and the role of PDGF in vivo. Neuron 20: 869-882.
Cameron HA, Hazel TG, McKay RD (1998a) Regulation of neurogenesis by growth factors and neurotransmitters. J Neurobiol 36: 287-306.
Cameron HA, McEwen BS, Gould E (1995) Regulation of adult neurogenesis by excitatory input and NMDA receptor activation in the dentate gyrus. J Neurosci 15: 4687-4692.
Cameron HA, McKay RD (2001) Adult neurogenesis produces a large pool of new granule cells in the dentate gyrus. J Comp Neurol 435: 406-417.
Cameron HA, Tanapat P, Gould E (1998b) Adrenal steroids and N-methyl-D-aspartate receptor activation regulate neurogenesis in the dentate gyrus of adult rats through a common pathway. Neuroscience 82: 349-354.
Cameron HA, Woolley CS, McEwen BS, Gould E (1993) Differentiation of newly born neurons and glia in the dentate gyrus of the adult rat. Neuroscience 56: 337-344.
Canoll PD, Musacchio JM, Hardy R, Reynolds R, Marchionni MA, Salzer JL (1996) GGF/neuregulin is a neuronal signal that promotes the proliferation and survival and inhibits the differentiation of oligodendrocyte progenitors. Neuron 17: 229-243.
Cao L, Jiao X, Zuzga DS, Liu Y, Fong DM, Young D, During MJ (2004) VEGF links hippocampal activity with neurogenesis, learning and

memory. Nat Genet 36: 827-835.
Capela A, Temple S (2002) LeX/ssea-1 is expressed by adult mouse CNS stem cells, identifying them as nonependymal. Neuron 35: 865-875.
Carleton A, Petreanu LT, Lansford R, Alvarez-Buylla A, Lledo PM (2003) Becoming a new neuron in the adult olfactory bulb. Nat Neurosci 6: 507-518.
Carroll WM, Jennings AR (1994) Early recruitment of oligodendrocyte precursors in CNS demyelination. Brain 117 (Pt 3): 563-578.
Casaccia-Bonnefil P (2000) Cell death in the oligodendrocyte lineage: a molecular perspective of life/death decisions in development and disease. Glia 29: 124-135.
Casaccia-Bonnefil P, Hardy RJ, Teng KK, Levine JM, Koff A, Chao MV (1999) Loss of p27Kip1 function results in increased proliferative capacity of oligodendrocyte progenitors but unaltered timing of differentiation. Development 126: 4027-4037.
Casaccia-Bonnefil P, Tikoo R, Kiyokawa H, Friedrich V, Jr., Chao MV, Koff A (1997) Oligodendrocyte precursor differentiation is perturbed in the absence of the cyclin-dependent kinase inhibitor p27Kip1. Genes Dev 11: 2335-2346.
Chan CL, Wigley CB, Berry M (1990) Oligodendrocyte-type 2 astrocyte (O-2A) progenitor cells from neonatal and adult rat optic nerve differ in their responsiveness to platelet-derived growth factor. Brain Res Dev Brain Res 55: 275-282.
Chandross KJ, Cohen RI, Paras P, Jr., Gravel M, Braun PE, Hudson LD (1999) Identification and characterization of early glial progenitors using a transgenic selection strategy. J Neurosci 19: 759-774.
Chang A, Nishiyama A, Peterson J, Prineas J, Trapp BD (2000) NG2-positive oligodendrocyte progenitor cells in adult human brain and multiple sclerosis lesions. J Neurosci 20: 6404-6412.
Chang A, Tourtellotte WW, Rudick R, Trapp BD (2002) Premyelinating oligodendrocytes in chronic lesions of multiple sclerosis. N Engl J Med 346: 165-173.
Charles P, Hernandez MP, Stankoff B, Aigrot MS, Colin C, Rougon G, Zalc B, Lubetzki C (2000) Negative regulation of central nervous system myelination by polysialylated-neural cell adhesion molecule. Proc Natl Acad Sci U S A 97: 7585-7590.
Charles P, Reynolds R, Seilhean D, Rougon G, Aigrot MS, Niezgoda A, Zalc B, Lubetzki C (2002) Re-expression of PSA-NCAM by demyelinated axons: an inhibitor of remyelination in multiple sclerosis? Brain 125: 1972-1979.
Chaudhry FA, Lehre KP, van Lookeren CM, Ottersen OP, Danbolt NC, Storm-Mathisen J (1995) Glutamate transporters in glial plasma membranes: highly differentiated localizations revealed by quantitative ultrastructural immunocytochemistry. Neuron 15: 711-720.
Cheng M, Olivier P, Diehl JA, Fero M, Roussel MF, Roberts JM, Sherr CJ (1999) The p21(Cip1) and p27(Kip1) CDK 'inhibitors' are essential activators of cyclin D-dependent kinases in murine fibroblasts. EMBO J 18: 1571-1583.
Chittajallu R, Aguirre AA, Gallo V (2004) NG2-positive cells in the white and grey matter display distinct physiological properties. J Physiol 561: 109-122.
Chittajallu R, Chen Y, Wang H, Yuan X, Ghiani CA, Heckman T, McBain CJ, Gallo V (2002) Regulation of Kv1 subunit expression in oligodendrocyte progenitor cells and their role in G(1)/S phase progression of the cell cycle. Proceedings of the National Academy of Sciences of the United States of America 99: 2350-2355.
Chiu SY, Kriegler S (1994) Neurotransmitter-mediated signaling between axons and glial cells. Glia 11: 191-200.
Chmielnicki E, Benraiss A, Economides AN, Goldman SA (2004) Adenovirally expressed noggin and brain-derived neurotrophic factor cooperate to induce new medium spiny neurons from resident progenitor cells in the adult striatal ventricular zone. J Neurosci 24: 2133-2142.
Chojnacki A, Weiss S (2004) Isolation of a Novel Platelet-Derived Growth Factor-Responsive Precursor from the Embryonic Ventral Forebrain. J Neurosci 25: 10888-10899.
Cimons M (2001a) Bush is a threat to US stem-cell research. Nat Med 7: 263.
Cimons M (2001b) Bush policy: attention turns to existing human ES cells. Nat Med 7: 981-982.
Cohen RI, Almazan G (1993) Norepinephrine-stimulated PI hydrolysis in oligodendrocytes is mediated by alpha 1A-adrenoceptors. Neuroreport 4: 1115-1118.
Cohen RI, Almazan G (1994) Rat oligodendrocytes express muscarinic receptors coupled to phosphoinositide hydrolysis and adenylyl cyclase. Eur J Neurosci 6: 1213-1224.
Cohen RI, Marmur R, Norton WT, Mehler MF, Kessler JA (1996a) Nerve growth factor and neurotrophin-3 differentially regulate the proliferation and survival of developing rat brain oligodendrocytes. J Neurosci 16: 6433-6442.
Cohen RI, Molina-Holgado E, Almazan G (1996b) Carbachol stimulates c-fos expression and proliferation in oligodendrocyte progenitors. Brain Res Mol Brain Res 43: 193-201.
Cohen RI, Rottkamp DM, Maric D, Barker JL, Hudson LD (2003) A role for semaphorins and neuropilins in oligodendrocyte guidance. J Neurochem 85: 1262-1278.
Colognato H, Baron W, Avellana-Adalid V, Relvas JB, Baron-Van Evercooren A, Georges-Labouesse E, Ffrench-Constant C (2002) CNS integrins switch growth factor signalling to promote target-dependent survival. Nat Cell Biol 4: 833-841.
Compston A, Coles A (2002) Multiple sclerosis. Lancet 359: 1221-1231.
Coqueret O (2003) New roles for p21 and p27 cell-cycle inhibitors: a function for each cell compartment? Trends Cell Biol 13: 65-70.
Corbin JG, Kelly D, Rath EM, Baerwald KD, Suzuki K, Popko B (1996) Targeted CNS expression of interferon-gamma in transgenic mice leads to hypomyelination, reactive gliosis, and abnormal cerebellar development. Mol Cell Neurosci 7: 354-370.
Coronas V, Durand M, Chabot JG, Jourdan F, Quirion R (2000) Acetylcholine induces neuritic outgrowth in rat primary olfactory bulb cultures. Neuroscience 98: 213-219.
Cunningham JJ, Roussel MF (2001) Cyclin-dependent kinase inhibitors in the development of the central nervous system. Cell Growth Differ 12: 387-396.
Dawson MR, Levine JM, Reynolds R (2000) NG2-expressing cells in the central nervous system: are they oligodendroglial progenitors? J Neurosci Res 61: 471-479.
Dawson MR, Polito A, Levine JM, Reynolds R (2003) NG2-expressing glial progenitor cells: an abundant and widespread population of cycling cells in the adult rat CNS. Mol Cell Neurosci 24: 476-488.
Dayer AG, Cleaver KM, Abouantoun T, Cameron HA (2005) New GABAergic interneurons in the adult neocortex and striatum are generated from different precursors. J Cell Biol 168: 415-427.
Dayer AG, Ford AA, Cleaver KM, Yassaee M, Cameron HA (2003) Short-term and long-term survival of new neurons in the rat dentate gyrus. J Comp Neurol 460: 563-572.
DeCoursey TE, Chandy KG, Gupta S, Cahalan MD (1984) Voltage-gated K+ channels in human T lymphocytes: a role in mitogenesis? Nature 307: 465-468.
Demerens C, Stankoff B, Logak M, Anglade P, Allinquant B, Couraud F, Zalc B, Lubetzki C (1996) Induction of myelination in the central

nervous system by electrical activity. Proc Natl Acad Sci U S A 93: 9887-9892.
Demerens C, Stankoff B, Zalc B, Lubetzki C (1999) Eliprodil stimulates CNS myelination: new prospects for multiple sclerosis? Neurology 52: 346-350.
Ding S, Wu TY, Brinker A, Peters EC, Hur W, Gray NS, Schultz PG (2003) Synthetic small molecules that control stem cell fate. Proc Natl Acad Sci U S A 100: 7632-7637.
Doetsch F (2003) The glial identity of neural stem cells. Nat Neurosci 6: 1127-1134.
Doetsch F, Alvarez-Buylla A (1996) Network of tangential pathways for neuronal migration in adult mammalian brain. Proc Natl Acad Sci U S A 93: 14895-14900.
Doetsch F, Caille I, Lim DA, Garcia-Verdugo JM, Alvarez-Buylla A (1999) Subventricular zone astrocytes are neural stem cells in the adult mammalian brain. Cell 97: 703-716.
Doetsch F, Garcia-Verdugo JM, Alvarez-Buylla A (1997) Cellular composition and three-dimensional organization of the subventricular germinal zone in the adult mammalian brain. J Neurosci 17: 5046-5061.
Doetsch F, Hen R (2005) Young and excitable: the function of new neurons in the adult mammalian brain. Curr Opin Neurobiol 15: 121-128.
Doetsch F, Petreanu L, Caille I, Garcia-Verdugo JM, Alvarez-Buylla A (2002a) EGF converts transit-amplifying neurogenic precursors in the adult brain into multipotent stem cells. Neuron 36: 1021-1034.
Doetsch F, Verdugo JM, Caille I, Alvarez-Buylla A, Chao MV, Casaccia-Bonnefil P (2002b) Lack of the cell-cycle inhibitor p27Kip1 results in selective increase of transit-amplifying cells for adult neurogenesis. J Neurosci 22: 2255-2264.
Dubois JM, Rouzaire-Dubois B (1993) Role of potassium channels in mitogenesis. Prog Biophys Mol Biol 59: 1-21.
Durand B, Fero ML, Roberts JM, Raff MC (1998) p27Kip1 alters the response of cells to mitogen and is part of a cell-intrinsic timer that arrests the cell cycle and initiates differentiation. Curr Biol 8: 431-440.
Durand B, Gao FB, Raff M (1997) Accumulation of the cyclin-dependent kinase inhibitor p27/Kip1 and the timing of oligodendrocyte differentiation. EMBO J 16: 306-317.
Durand GM, Kovalchuk Y, Konnerth A (1996) Long-term potentiation and functional synapse induction in developing hippocampus. Nature 381: 71-75.
Dyson N (1998) The regulation of E2F by pRB-family proteins. Genes Dev 12: 2245-2262.
Eizenberg O, Faber-Elman A, Gottlieb E, Oren M, Rotter V, Schwartz M (1996) p53 plays a regulatory role in differentiation and apoptosis of central nervous system-associated cells. Mol Cell Biol 16: 5178-5185.
Engel U, Wolswijk G (1996) Oligodendrocyte-type-2 astrocyte (O-2A) progenitor cells derived from adult rat spinal cord: in vitro characteristics and response to PDGF, bFGF and NT-3. Glia 16: 16-26.
Eriksson PS, Perfilieva E, Bjork-Eriksson T, Alborn AM, Nordborg C, Peterson DA, Gage FH (1998) Neurogenesis in the adult human hippocampus. Nat Med 4: 1313-1317.
Fero ML, Rivkin M, Tasch M, Porter P, Carow CE, Firpo E, Polyak K, Tsai LH, Broudy V, Perlmutter RM, Kaushansky K, Roberts JM (1996) A syndrome of multiorgan hyperplasia with features of gigantism, tumorigenesis, and female sterility in p27(Kip1)-deficient mice. Cell 85: 733-744.
Ffrench-Constant C, Raff MC (1986) Proliferating bipotential glial progenitor cells in adult rat optic nerve. Nature 319: 499-502.
Fields RD, Stevens-Graham B (2002) New insights into neuron-glia communication. Science 298: 556-562.
Filipovic R, Jakovcevski I, Zecevic N (2003) GRO-alpha and CXCR2 in the human fetal brain and multiple sclerosis lesions. Dev Neurosci 25: 279-290.
Fisher AL, Ohsako S, Caudy M (1996) The WRPW motif of the hairy-related basic helix-loop-helix repressor proteins acts as a 4-amino-acid transcription repression and protein-protein interaction domain. Mol Cell Biol 16: 2670-2677.
Fiszman ML, Borodinsky LN, Neale JH (1999) GABA induces proliferation of immature cerebellar granule cells grown in vitro. Brain Res Dev Brain Res 115: 1-8.
Flint AC, Liu X, Kriegstein AR (1998) Nonsynaptic glycine receptor activation during early neocortical development. Neuron 20: 43-53.
Follett PL, Rosenberg PA, Volpe JJ, Jensen FE (2000) NBQX attenuates excitotoxic injury in developing white matter. J Neurosci 20: 9235-9241.
Franklin DS, Godfrey VL, Lee H, Kovalev GI, Schoonhoven R, Chen-Kiang S, Su L, Xiong Y (1998) CDK inhibitors p18(INK4c) and p27(Kip1) mediate two separate pathways to collaboratively suppress pituitary tumorigenesis. Genes Dev 12: 2899-2911.
Franklin RJ (2002) Why does remyelination fail in multiple sclerosis? Nat Rev Neurosci 3: 705-714.
Franklin RJ, Blakemore WF (1997) Transplanting oligodendrocyte progenitors into the adult CNS. J Anat 190 (Pt 1): 23-33.
Franklin RJ, Gilson JM, Blakemore WF (1997) Local recruitment of remyelinating cells in the repair of demyelination in the central nervous system. J Neurosci Res 50: 337-344.
Friessen AJ, Miskimins WK, Miskimins R (1997) Cyclin-dependent kinase inhibitor p27kip1 is expressed at high levels in cells that express a myelinating phenotype. J Neurosci Res 50: 373-382.
Frost EE, Buttery PC, Milner R, Ffrench-Constant C (1999) Integrins mediate a neuronal survival signal for oligodendrocytes. Curr Biol 9: 1251-1254.
Fruttiger M, Karlsson L, Hall AC, Abramsson A, Calver AR, Bostrom H, Willetts K, Bertold CH, Heath JK, Betsholtz C, Richardson WD (1999) Defective oligodendrocyte development and severe hypomyelination in PDGF-A knockout mice. Development 126: 457-467.
Fu H, Qi Y, Tan M, Cai J, Takebayashi H, Nakafuku M, Richardson W, Qiu M (2002) Dual origin of spinal oligodendrocyte progenitors and evidence for the cooperative role of Olig2 and Nkx2.2 in the control of oligodendrocyte differentiation. Development 129: 681-693.
Fulton BP, Burne JF, Raff MC (1992) Visualization of O-2A progenitor cells in developing and adult rat optic nerve by quisqualate-stimulated cobalt uptake. J Neurosci 12: 4816-4833.
Gabay L, Lowell S, Rubin LL, Anderson DJ (2003) Deregulation of dorsoventral patterning by FGF confers trilineage differentiation capacity on CNS stem cells in vitro. Neuron 40: 485-499.
Gage FH (2000) Mammalian neural stem cells. Science 287: 1433-1438.
Gallo V, Chittajallu R (2001) Unwrapping glial cells from the synapse: what lies inside? Science 292: 872-873.
Gallo V, Ghiani CA (2000) Glutamate receptors in glia: new cells, new inputs and new functions. Trends in Pharmacological Sciences 21: 252-258.
Gallo V, Haydar T (2003) GABA: exciting again in its own right. J Physiol 550: 665.
Gallo V, Patneau DK, Mayer ML, Vaccarino FM (1994a) Excitatory amino acid receptors in glial progenitor cells: molecular and functional properties. Glia 11: 94-101.
Gallo V, Wright P, McKinnon RD (1994b) Expression and regulation of a glutamate receptor subunit by bFGF in oligodendrocyte progenitors.

Glia 10: 149-153.
Gallo V, Zhou JM, McBain CJ, Wright P, Knutson PL, Armstrong RC (1996) Oligodendrocyte progenitor cell proliferation and lineage progression are regulated by glutamate receptor-mediated K+ channel block. Journal of Neuroscience 16: 2659-2670.
Gao FB, Apperly J, Raff M (1998) Cell-intrinsic timers and thyroid hormone regulate the probability of cell-cycle withdrawal and differentiation of oligodendrocyte precursor cells. Dev Biol 197: 54-66.
Gao FB, Durand B, Raff M (1997) Oligodendrocyte precursor cells count time but not cell divisions before differentiation. Curr Biol 7: 152-155.
Garcia AD, Doan NB, Imura T, Bush TG, Sofroniew MV (2004) GFAP-expressing progenitors are the principal source of constitutive neurogenesis in adult mouse forebrain. Nat Neurosci 7: 1233-1241.
Garcion E, Faissner A, Ffrench-Constant C (2001) Knockout mice reveal a contribution of the extracellular matrix molecule tenascin-C to neural precursor proliferation and migration. Development 128: 2485-2496.
Gehrmann J, Lannes-Vieira J, Wekerle H (1996) Differential expression of fibroblast growth factor-2 and receptor by glial cells in experimental autoimmune encephalomyelitis (EAE). Glia 16: 93-100.
Geng Y, Yu Q, Sicinska E, Das M, Schneider JE, Bhattacharya S, Rideout WM, Bronson RT, Gardner H, Sicinski P (2003) Cyclin E ablation in the mouse. Cell 114: 431-443.
Gensert JM, Goldman JE (1997) Endogenous progenitors remyelinate demyelinated axons in the adult CNS. Neuron 19: 197-203.
Ghiani CA, Eisen AM, Yuan XQ, DePinho RA, McBain CJ, Gallo V (1999a) Neurotransmitter receptor activation triggers p27(Kip1) and p21(CIP1) accumulation and G(1) cell cycle arrest in oligodendrocyte progenitors. Development 126: 1077-1090.
Ghiani CA, Gallo V (2001) Inhibition of cyclin E-cyclin-dependent kinase 2 complex formation and activity is associated with cell cycle arrest and withdrawal in oligodendrocyte progenitor cells. Journal of Neuroscience 21: 1274-1282.
Ghiani CA, Yuan XQ, Eisen AM, Knutson PL, DePinho RA, McBain CJ, Gallo V (1999b) Voltage-activated K+ channels and membrane depolarization regulate accumulation of the cyclin-dependent kinase inhibitors p277(Kip1) and p21(CIP1) in glial progenitor cells. Journal of Neuroscience 19: 5380-5392.
Giaccia AJ, Kastan MB (1998) The complexity of p53 modulation: emerging patterns from divergent signals. Genes Dev 12: 2973-2983.
Gilbert P, Kettenmann H, Schachner M (1984) gamma-Aminobutyric acid directly depolarizes cultured oligodendrocytes. J Neurosci 4: 561-569.
Givogri MI, Costa RM, Schonmann V, Silva AJ, Campagnoni AT, Bongarzone ER (2002) Central nervous system myelination in mice with deficient expression of Notch1 receptor. J Neurosci Res 67: 309-320.
Glaser T, Perez-Bouza A, Klein K, Brustle O (2004) Generation of purified oligodendrocyte progenitors from embryonic stem cells. FASEB J.
Goddard DR, Berry M, Kirvell SL, Butt AM (2001) Fibroblast growth factor-2 inhibits myelin production by oligodendrocytes in vivo. Mol Cell Neurosci 18: 557-569.
Goldman S (2003) Glia as neural progenitor cells. Trends Neurosci 26: 590-596.
Gomes WA, Mehler MF, Kessler JA (2003) Transgenic overexpression of BMP4 increases astroglial and decreases oligodendroglial lineage commitment. Dev Biol 255: 164-177.
Gould E, Beylin A, Tanapat P, Reeves A, Shors TJ (1999a) Learning enhances adult neurogenesis in the hippocampal formation. Nat Neurosci 2: 260-265.
Gould E, Cameron HA, Daniels DC, Woolley CS, McEwen BS (1992) Adrenal hormones suppress cell division in the adult rat dentate gyrus. J Neurosci 12: 3642-3650.
Gould E, Cameron HA, McEwen BS (1994) Blockade of NMDA receptors increases cell death and birth in the developing rat dentate gyrus. J Comp Neurol 340: 551-565.
Gould E, Gross CG (2002) Neurogenesis in adult mammals: some progress and problems. J Neurosci 22: 619-623.
Gould E, Reeves AJ, Graziano MS, Gross CG (1999b) Neurogenesis in the neocortex of adult primates. Science 286: 548-552.
Gould E, Tanapat P (1997) Lesion-induced proliferation of neuronal progenitors in the dentate gyrus of the adult rat. Neuroscience 80: 427-436.
Gould E, Vail N, Wagers M, Gross CG (2001) Adult-generated hippocampal and neocortical neurons in macaques have a transient existence. Proc Natl Acad Sci U S A 98: 10910-10917.
Gravel M, Di Polo A, Valera PB, Braun PE (1998) Four-kilobase sequence of the mouse CNP gene directs spatial and temporal expression of lacZ in transgenic mice. J Neurosci Res 53: 393-404.
Grbavec D, Stifani S (1996) Molecular interaction between TLE1 and the carboxyl-terminal domain of HES-1 containing the WRPW motif. Biochem Biophys Res Commun 223: 701-705.
Gross RE, Mehler MF, Mabie PC, Zang Z, Santschi L, Kessler JA (1996) Bone morphogenetic proteins promote astroglial lineage commitment by mammalian subventricular zone progenitor cells. Neuron 17: 595-606.
Grove EA, Williams BP, Li DQ, Hajihosseini M, Friedrich A, Price J (1993) Multiple restricted lineages in the embryonic rat cerebral cortex. Development 117: 553-561.
Groves AK, Barnett SC, Franklin RJ, Crang AJ, Mayer M, Blakemore WF, Noble M (1993) Repair of demyelinated lesions by transplantation of purified O-2A progenitor cells. Nature 362: 453-455.
Guillemot F (1999) Vertebrate bHLH genes and the determination of neuronal fates. Exp Cell Res 253: 357-364.
Hartwell LH, Kastan MB (1994) Cell cycle control and cancer. Science 266: 1821-1828.
Hastings NB, Gould E (1999) Rapid extension of axons into the CA3 region by adult-generated granule cells. J Comp Neurol 413: 146-154.
Hauser KF, Gurwell JA, Bhat NR (1993) Endogenous opioid systems and the growth of oligodendrocyte progenitors: paradoxical increases in oligodendrogenesis as an indirect mechanism of opioid action. Glia 9: 157-162.
Haydar TF, Wang F, Schwartz ML, Rakic P (2000) Differential modulation of proliferation in the neocortical ventricular and subventricular zones. J Neurosci 20: 5764-5774.
Haydon PG (2001) GLIA: listening and talking to the synapse. Nat Rev Neurosci 2: 185-193.
He W, Ingraham C, Rising L, Goderie S, Temple S (2001) Multipotent stem cells from the mouse basal forebrain contribute GABAergic neurons and oligodendrocytes to the cerebral cortex during embryogenesis. J Neurosci 21: 8854-8862.
Hengst L, Gopfert U, Lashuel HA, Reed SI (1998) Complete inhibition of Cdk/cyclin by one molecule of p21(Cip1). Genes Dev 12: 3882-3888.
Horner PJ, Power AE, Kempermann G, Kuhn HG, Palmer TD, Winkler J, Thal LJ, Gage FH (2000) Proliferation and differentiation of progenitor cells throughout the intact adult rat spinal cord. J Neurosci 20: 2218-2228.
Horwitz MS, Evans CF, McGavern DB, Rodriguez M, Oldstone MB (1997) Primary demyelination in transgenic mice expressing interferon-

gamma. Nat Med 3: 1037-1041.
Hu QD, Ang BT, Karsak M, Hu WP, Cui XY, Duka T, Takeda Y, Chia W, Sankar N, Ng YK, Ling EA, Maciag T, Small D, Trifonova R, Kopan R, Okano H, Nakafuku M, Chiba S, Hirai H, Aster JC, Schachner M, Pallen CJ, Watanabe K, Xiao ZC (2003) F3/contactin acts as a functional ligand for Notch during oligodendrocyte maturation. Cell 115: 163-175.
Huang Z, Tang XM, Cambi F (2002) Down-regulation of the retinoblastoma protein (rb) is associated with rat oligodendrocyte differentiation. Mol Cell Neurosci 19: 250-262.
Hwang WS, Ryu YJ, Park JH, Park ES, Lee EG, Koo JM, Jeon HY, Lee BC, Kang SK, Kim SJ, Ahn C, Hwang JH, Park KY, Cibelli JB, Moon SY (2004) Evidence of a pluripotent human embryonic stem cell line derived from a cloned blastocyst. Science 303: 1669-1674.
Hyde-Dunn J, Jones GE (1997) Visualization of cell replication using antibody to proliferating cell nuclear antigen. Methods Mol Biol 75: 341-347.
Iavarone A, Garg P, Lasorella A, Hsu J, Israel MA (1994) The helix-loop-helix protein Id-2 enhances cell proliferation and binds to the retinoblastoma protein. Genes Dev 8: 1270-1284.
Iino M, Goto K, Kakegawa W, Okado H, Sudo M, Ishiuchi S, Miwa A, Takayasu Y, Saito I, Tsuzuki K, Ozawa S (2001) Glia-synapse interaction through Ca2+-permeable AMPA receptors in Bergmann glia. Science 292: 926-929.
Imura T, Kornblum HI, Sofroniew MV (2003) The predominant neural stem cell isolated from postnatal and adult forebrain but not early embryonic forebrain expresses GFAP. J Neurosci 23: 2824-2832.
Jabs R, Kirchhoff F, Kettenmann H, Steinhauser C (1994) Kainate activates Ca(2+)-permeable glutamate receptors and blocks voltage-gated K+ currents in glial cells of mouse hippocampal slices. Pflugers Arch 426: 310-319.
Jacobs BL, van Praag H, Gage FH (2000) Adult brain neurogenesis and psychiatry: a novel theory of depression. Mol Psychiatry 5: 262-269.
Jakel RJ, Schneider BL, Svendsen CN (2004) Using human neural stem cells to model neurological disease. Nat Rev Genet 5: 136-144.
Jarjour AA, Manitt C, Moore SW, Thompson KM, Yuh SJ, Kennedy TE (2003) Netrin-1 is a chemorepellent for oligodendrocyte precursor cells in the embryonic spinal cord. J Neurosci 23: 3735-3744.
Jensen AM, Chiu SY (1993) Expression of glutamate receptor genes in white matter: developing and adult rat optic nerve. J Neurosci 13: 1664-1675.
Jiang F, Frederick TJ, Wood TL (2001) IGF-I synergizes with FGF-2 to stimulate oligodendrocyte progenitor entry into the cell cycle. Dev Biol 232: 414-423.
Jin K, Zhu Y, Sun Y, Mao XO, Xie L, Greenberg DA (2002) Vascular endothelial growth factor (VEGF) stimulates neurogenesis in vitro and in vivo. Proc Natl Acad Sci U S A 99: 11946-11950.
Jirawatnotai S, Aziyu A, Osmundson EO, Moons DS, Kineman RD, Kiyokawa H (2004) Cdk4 is indispensable for postnatal proliferation of the anterior pituitary. J Biol Chem.
Johe KK, Hazel TG, Muller T, Dugich-Djordjevic MM, McKay RD (1996) Single factors direct the differentiation of stem cells from the fetal and adult central nervous system. Genes Dev 10: 3129-3140.
John GR, Shankar SL, Shafit-Zagardo B, Massimi A, Lee SC, Raine CS, Brosnan CF (2002) Multiple sclerosis: re-expression of a developmental pathway that restricts oligodendrocyte maturation. Nat Med 8: 1115-1121.
Johnson JE, Birren SJ, Anderson DJ (1990) Two rat homologues of Drosophila achaete-scute specifically expressed in neuronal precursors. Nature 346: 858-861.
Kaplan MS, Bell DH (1983) Neuronal proliferation in the 9-month-old rodent-radioautographic study of granule cells in the hippocampus. Exp Brain Res 52: 1-5.
Kaplan MS, Bell DH (1984) Mitotic neuroblasts in the 9-day-old and 11-month-old rodent hippocampus. J Neurosci 4: 1429-1441.
Kaplan MS, Hinds JW (1977) Neurogenesis in the adult rat: electron microscopic analysis of light radioautographs. Science 197: 1092-1094.
Keirstead HS, Levine JM, Blakemore WF (1998) Response of the oligodendrocyte progenitor cell population (defined by NG2 labelling) to demyelination of the adult spinal cord. Glia 22: 161-170.
Kempermann G, Gast D, Kronenberg G, Yamaguchi M, Gage FH (2003) Early determination and long-term persistence of adult-generated new neurons in the hippocampus of mice. Development 130: 391-399.
Kempermann G, Jessberger S, Steiner B, Kronenberg G (2004) Milestones of neuronal development in the adult hippocampus. Trends Neurosci 27: 447-452.
Kempermann G, Kronenberg G (2003) Depressed new neurons--adult hippocampal neurogenesis and a cellular plasticity hypothesis of major depression. Biol Psychiatry 54: 499-503.
Kempermann G, Kuhn HG, Gage FH (1997a) Genetic influence on neurogenesis in the dentate gyrus of adult mice. Proc Natl Acad Sci U S A 94: 10409-10414.
Kempermann G, Kuhn HG, Gage FH (1997b) More hippocampal neurons in adult mice living in an enriched environment. Nature 386: 493-495.
Kettenmann H, Backus KH, Schachner M (1984a) Aspartate, glutamate and gamma-aminobutyric acid depolarize cultured astrocytes. Neurosci Lett 52: 25-29.
Kettenmann H, Blankenfeld GV, Trotter J (1991) Physiological properties of oligodendrocytes during development. Ann N Y Acad Sci 633: 64-77.
Kettenmann H, Gilbert P, Schachner M (1984b) Depolarization of cultured oligodendrocytes by glutamate and GABA. Neurosci Lett 47: 271-276.
Khorchid A, Cui Q, Molina-Holgado E, Almazan G (2002) Developmental regulation of alpha 1A-adrenoceptor function in rat brain oligodendrocyte cultures. Neuropharmacology 42: 685-696.
Khorchid A, Larocca JN, Almazan G (1999) Characterization of the signal transduction pathways mediating noradrenaline-stimulated MAPK activation and c-fos expression in oligodendrocyte progenitors. J Neurosci Res 58: 765-778.
Kim JH, Auerbach JM, Rodriguez-Gomez JA, Velasco I, Gavin D, Lumelsky N, Lee SH, Nguyen J, Sanchez-Pernaute R, Bankiewicz K, McKay R (2002) Dopamine neurons derived from embryonic stem cells function in an animal model of Parkinson's disease. Nature 418: 50-56.
Kim JY, Sun Q, Oglesbee M, Yoon SO (2003) The role of ErbB2 signaling in the onset of terminal differentiation of oligodendrocytes in vivo. J Neurosci 23: 5561-5571.
King RW, Deshaies RJ, Peters JM, Kirschner MW (1996) How proteolysis drives the cell cycle. Science 274: 1652-1659.
Kirchhoff F, Kettenmann H (1992) GABA Triggers a [Ca2+]i Increase in Murine Precursor Cells of the Oligodendrocyte Lineage. Eur J Neurosci 4: 1049-1058.
Kirchhoff F, Mulhardt C, Pastor A, Becker CM, Kettenmann H (1996) Expression of glycine receptor subunits in glial cells of the rat spinal cord. J Neurochem 66: 1383-1390.

Kiyokawa H, Kineman RD, Manova-Todorova KO, Soares VC, Hoffman ES, Ono M, Khanam D, Hayday AC, Frohman LA, Koff A (1996) Enhanced growth of mice lacking the cyclin-dependent kinase inhibitor function of p27(Kip1). Cell 85: 721-732.
Knapp PE, Itkis OS, Zhang L, Spruce BA, Bakalkin G, Hauser KF (2001) Endogenous opioids and oligodendroglial function: possible autocrine/paracrine effects on cell survival and development. Glia 35: 156-165.
Knapp PE, Maderspach K, Hauser KF (1998) Endogenous opioid system in developing normal and jimpy oligodendrocytes: mu and kappa opioid receptors mediate differential mitogenic and growth responses. Glia 22: 189-201.
Knockaert M, Greengard P, Meijer L (2002) Pharmacological inhibitors of cyclin-dependent kinases. Trends Pharmacol Sci 23: 417-425.
Knutson P, Ghiani CA, Zhou JM, Gallo V, McBain CJ (1997) K+ channel expression and cell proliferation are regulated by intracellular sodium and membrane depolarization in oligodendrocyte progenitor cells. J Neurosci 17: 2669-2682.
Koketsu D, Mikami A, Miyamoto Y, Hisatsune T (2003) Nonrenewal of neurons in the cerebral neocortex of adult macaque monkeys. J Neurosci 23: 937-942.
Kondo T, Raff M (2000a) Basic helix-loop-helix proteins and the timing of oligodendrocyte differentiation. Development 127: 2989-2998.
Kondo T, Raff M (2000b) Oligodendrocyte precursor cells reprogrammed to become multipotential CNS stem cells. Science 289: 1754-1757.
Kondo T, Raff M (2000c) The Id4 HLH protein and the timing of oligodendrocyte differentiation. EMBO J 19: 1998-2007.
Kondo T, Raff MC (2004) A role for Noggin in the development of oligodendrocyte precursor cells. Dev Biol 267: 242-251.
Kornack DR, Rakic P (1999) Continuation of neurogenesis in the hippocampus of the adult macaque monkey. Proc Natl Acad Sci U S A 96: 5768-5773.
Kornack DR, Rakic P (2001) Cell proliferation without neurogenesis in adult primate neocortex. Science 294: 2127-2130.
Kowalczyk A, Filipkowski RK, Rylski M, Wilczynski GM, Konopacki FA, Jaworski J, Ciemerych MA, Sicinski P, Kaczmarek L (2004) The critical role of cyclin D2 in adult neurogenesis. J Cell Biol 167: 209-213.
Kozar K, Ciemerych MA, Rebel VI, Shigematsu H, Zagozdzon A, Sicinska E, Geng Y, Yu Q, Bhattacharya S, Bronson RT, Akashi K, Sicinski P (2004) Mouse development and cell proliferation in the absence of d-cyclins. Cell 118: 477-491.
Kuhn HG, Dickinson-Anson H, Gage FH (1996) Neurogenesis in the dentate gyrus of the adult rat: age-related decrease of neuronal progenitor proliferation. J Neurosci 16: 2027-2033.
Kuhse J, Betz H, Kirsch J (1995) The inhibitory glycine receptor: architecture, synaptic localization and molecular pathology of a postsynaptic ion-channel complex. Curr Opin Neurobiol 5: 318-323.
Kuhse J, Schmieden V, Betz H (1990) Identification and functional expression of a novel ligand binding subunit of the inhibitory glycine receptor. J Biol Chem 265: 22317-22320.
Kuwabara T, Hsieh J, Nakashima K, Taira K, Gage FH (2004) A small modulatory dsRNA specifies the fate of adult neural stem cells. Cell 116: 779-793.
LaBaer J, Garrett MD, Stevenson LF, Slingerland JM, Sandhu C, Chou HS, Fattaey A, Harlow E (1997) New functional activities for the p21 family of CDK inhibitors. Genes Dev 11: 847-862.
Lai K, Kaspar BK, Gage FH, Schaffer DV (2003) Sonic hedgehog regulates adult neural progenitor proliferation in vitro and in vivo. Nat Neurosci 6: 21-27.
Langosch D, Thomas L, Betz H (1988) Conserved quaternary structure of ligand-gated ion channels: the postsynaptic glycine receptor is a pentamer. Proc Natl Acad Sci U S A 85: 7394-7398.
Laywell ED, Rakic P, Kukekov VG, Holland EC, Steindler DA (2000) Identification of a multipotent astrocytic stem cell in the immature and adult mouse brain. Proc Natl Acad Sci U S A 97: 13883-13888.
Le Novere N, Changeux JP (2001) The Ligand Gated Ion Channel database: an example of a sequence database in neuroscience. Philos Trans R Soc Lond B Biol Sci 356: 1121-1130.
Lee M, Lelievre V, Zhao P, Torres M, Rodriguez W, Byun JY, Doshi S, Ioffe Y, Gupta G, los Monteros AE, de Vellis J, Waschek J (2001) Pituitary adenylyl cyclase-activating polypeptide stimulates DNA synthesis but delays maturation of oligodendrocyte progenitors. J Neurosci 21: 3849-3859.
Legendre P (2001) The glycinergic inhibitory synapse. Cell Mol Life Sci 58: 760-793.
Lendahl U, Zimmerman LB, McKay RD (1990) CNS stem cells express a new class of intermediate filament protein. Cell 60: 585-595.
Letinic K, Zoncu R, Rakic P (2002) Origin of GABAergic neurons in the human neocortex. Nature 417: 645-649.
Levine JM, Reynolds R, Fawcett JW (2001) The oligodendrocyte precursor cell in health and disease. Trends Neurosci 24: 39-47.
Levine JM, Stincone F, Lee YS (1993) Development and differentiation of glial precursor cells in the rat cerebellum. Glia 7: 307-321.
Levison SW, Goldman JE (1993) Both oligodendrocytes and astrocytes develop from progenitors in the subventricular zone of postnatal rat forebrain. Neuron 10: 201-212.
Levison SW, Young GM, Goldman JE (1999) Cycling cells in the adult rat neocortex preferentially generate oligodendroglia. J Neurosci Res 57: 435-446.
Levrero M, De L, V, Costanzo A, Gong J, Wang JY, Melino G (2000) The p53/p63/p73 family of transcription factors: overlapping and distinct functions. J Cell Sci 113 (Pt 10): 1661-1670.
Li S, Stys PK (2000) Mechanisms of ionotropic glutamate receptor-mediated excitotoxicity in isolated spinal cord white matter. J Neurosci 20: 1190-1198.
Lie DC, Song H, Colamarino SA, Ming GL, Gage FH (2004) NEUROGENESIS IN THE ADULT BRAIN: New Strategies for Central Nervous System Diseases. Annu Rev Pharmacol Toxicol 44: 399-421.
Lim DA, Tramontin AD, Trevejo JM, Herrera DG, Garcia-Verdugo JM, Alvarez-Buylla A (2000) Noggin antagonizes BMP signaling to create a niche for adult neurogenesis. Neuron 28: 713-726.
Lin SC, Bergles DE (2004) Synaptic signaling between GABAergic interneurons and oligodendrocyte precursor cells in the hippocampus. Nat Neurosci 7: 24-32.
Linker RA, Maurer M, Gaupp S, Martini R, Holtmann B, Giess R, Rieckmann P, Lassmann H, Toyka KV, Sendtner M, Gold R (2002) CNTF is a major protective factor in demyelinating CNS disease: a neurotrophic cytokine as modulator in neuroinflammation. Nat Med 8: 620-624.
Liu HN, Almazan G (1995) Glutamate induces c-fos proto-oncogene expression and inhibits proliferation in oligodendrocyte progenitors: receptor characterization. Eur J Neurosci 7: 2355-2363.
Liu HN, Giasson BI, Mushynski WE, Almazan G (2002) AMPA receptor-mediated toxicity in oligodendrocyte progenitors involves free radical generation and activation of JNK, calpain and caspase 3. J Neurochem 82: 398-409.
Liu J, Marino MW, Wong G, Grail D, Dunn A, Bettadapura J, Slavin AJ, Old L, Bernard CC (1998a) TNF is a potent anti-inflammatory cytokine in autoimmune-mediated demyelination. Nat Med 4: 78-83.
Liu J, Solway K, Messing RO, Sharp FR (1998b) Increased neurogenesis in the dentate gyrus after transient global ischemia in gerbils. J Neurosci

18: 7768-7778.
Liu R, Cai J, Hu X, Tan M, Qi Y, German M, Rubenstein J, Sander M, Qiu M (2003a) Region-specific and stage-dependent regulation of Olig gene expression and oligodendrogenesis by Nkx6.1 homeodomain transcription factor. Development 130: 6221-6231.
Liu S, Wang J, Zhu D, Fu Y, Lukowiak K, Lu YM (2003b) Generation of functional inhibitory neurons in the adult rat hippocampus. J Neurosci 23: 732-736.
Logan A, Frautschy SA, Gonzalez AM, Baird A (1992) A time course for the focal elevation of synthesis of basic fibroblast growth factor and one of its high-affinity receptors (flg) following a localized cortical brain injury. J Neurosci 12: 3828-3837.
Lois C, Alvarez-Buylla A (1994) Long-distance neuronal migration in the adult mammalian brain. Science 264: 1145-1148.
Lotan M, Schwartz M (1992) Postinjury changes in platelet-derived growth factor-like activity in fish and rat optic nerves. J Neurochem 58: 1637-1642.
LoTurco JJ, Owens DF, Heath MJ, Davis MB, Kriegstein AR (1995) GABA and glutamate depolarize cortical progenitor cells and inhibit DNA synthesis. Neuron 15: 1287-1298.
Louis JC, Magal E, Muir D, Manthorpe M, Varon S (1992) CG-4, a new bipotential glial cell line from rat brain, is capable of differentiating in vitro into either mature oligodendrocytes or type-2 astrocytes. J Neurosci Res 31: 193-204.
Louis JC, Magal E, Takayama S, Varon S (1993) CNTF protection of oligodendrocytes against natural and tumor necrosis factor-induced death. Science 259: 689-692.
Lu QR, Cai L, Rowitch D, Cepko CL, Stiles CD (2001) Ectopic expression of Olig1 promotes oligodendrocyte formation and reduces neuronal survival in developing mouse cortex. Nat Neurosci 4: 973-974.
Lu QR, Sun T, Zhu Z, Ma N, Garcia M, Stiles CD, Rowitch DH (2002) Common developmental requirement for Olig function indicates a motor neuron/oligodendrocyte connection. Cell 109: 75-86.
Lu QR, Yuk D, Alberta JA, Zhu Z, Pawlitzky I, Chan J, McMahon AP, Stiles CD, Rowitch DH (2000) Sonic hedgehog--regulated oligodendrocyte lineage genes encoding bHLH proteins in the mammalian central nervous system. Neuron 25: 317-329.
Ludwin SK (1987) Regeneration of myelin and oligodendrocytes in the central nervous system. Prog Brain Res 71: 469-484.
Luskin MB (1993) Restricted proliferation and migration of postnatally generated neurons derived from the forebrain subventricular zone. Neuron 11: 173-189.
Luskin MB, Parnavelas JG, Barfield JA (1993) Neurons, astrocytes, and oligodendrocytes of the rat cerebral cortex originate from separate progenitor cells: an ultrastructural analysis of clonally related cells. J Neurosci 13: 1730-1750.
Ma W, Barker JL (1995) Complementary expressions of transcripts encoding GAD67 and GABAA receptor alpha 4, beta 1, and gamma 1 subunits in the proliferative zone of the embryonic rat central nervous system. J Neurosci 15: 2547-2560.
Mabie PC, Mehler MF, Marmur R, Papavasiliou A, Song Q, Kessler JA (1997) Bone morphogenetic proteins induce astroglial differentiation of oligodendroglial-astroglial progenitor cells. J Neurosci 17: 4112-4120.
MacFarlane SN, Sontheimer H (1997) Electrophysiological changes that accompany reactive gliosis in vitro. J Neurosci 17: 7316-7329.
Machold R, Hayashi S, Rutlin M, Muzumdar MD, Nery S, Corbin JG, Gritli-Linde A, Dellovade T, Porter JA, Rubin LL, Dudek H, McMahon AP, Fishell G (2003) Sonic hedgehog is required for progenitor cell maintenance in telencephalic stem cell niches. Neuron 39: 937-950.
Macilwain C, Bush GW, Kerry J (2004) Head to head: Bush vs Kerry. Nature 431: 238-243.
Mack KJ, Kriegler S, Chang S, Chiu SY (1994) Transcription factor expression is induced by axonal stimulation and glutamate in the glia of the developing optic nerve. Brain Res Mol Brain Res 23: 73-80.
MacVicar BA, Tse FW, Crichton SA, Kettenmann H (1989) GABA-activated Cl- channels in astrocytes of hippocampal slices. J Neurosci 9: 3577-3583.
Maeda Y, Solanky M, Menonna J, Chapin J, Li W, Dowling P (2001) Platelet-derived growth factor-alpha receptor-positive oligodendroglia are frequent in multiple sclerosis lesions. Ann Neurol 49: 776-785.
Magavi SS, Leavitt BR, Macklis JD (2000) Induction of neurogenesis in the neocortex of adult mice. Nature 405: 951-955.
Malatesta P, Hartfuss E, Gotz M (2000) Isolation of radial glial cells by fluorescent-activated cell sorting reveals a neuronal lineage. Development 127: 5253-5263.
Malek NP, Sundberg H, McGrew S, Nakayama K, Kyriakides TR, Roberts JM, Kyriakidis TR (2001) A mouse knock-in model exposes sequential proteolytic pathways that regulate p27Kip1 in G1 and S phase. Nature 413: 323-327.
Malek-Hedayat S, Rome LH (1994) Expression of a beta 1-related integrin by oligodendroglia in primary culture: evidence for a functional role in myelination. J Cell Biol 124: 1039-1046.
Mallon BS, Shick HE, Kidd GJ, Macklin WB (2002) Proteolipid promoter activity distinguishes two populations of NG2-positive cells throughout neonatal cortical development. J Neurosci 22: 876-885.
Malumbres M, Sotillo R, Santamaria D, Galan J, Cerezo A, Ortega S, Dubus P, Barbacid M (2004) Mammalian Cells Cycle without the D-Type Cyclin-Dependent Kinases Cdk4 and Cdk6. Cell 118: 493-504.
Marin-Husstege M, Muggironi M, Liu A, Casaccia-Bonnefil P (2002) Histone deacetylase activity is necessary for oligodendrocyte lineage progression. J Neurosci 22: 10333-10345.
Markakis EA, Gage FH (1999) Adult-generated neurons in the dentate gyrus send axonal projections to field CA3 and are surrounded by synaptic vesicles. J Comp Neurol 406: 449-460.
Marmur R, Kessler JA, Zhu G, Gokhan S, Mehler MF (1998) Differentiation of oligodendroglial progenitors derived from cortical multipotent cells requires extrinsic signals including activation of gp130/LIFbeta receptors. J Neurosci 18: 9800-9811.
Marshall CA, Goldman JE (2002) Subpallial dlx2-expressing cells give rise to astrocytes and oligodendrocytes in the cerebral cortex and white matter. J Neurosci 22: 9821-9830.
Marshall CA, Suzuki SO, Goldman JE (2003) Gliogenic and neurogenic progenitors of the subventricular zone: who are they, where did they come from, and where are they going? Glia 43: 52-61.
Mason JL, Goldman JE (2002) A2B5+ and O4+ Cycling progenitors in the adult forebrain white matter respond differentially to PDGF-AA, FGF-2, and IGF-1. Mol Cell Neurosci 20: 30-42.
Mason JL, Xuan S, Dragatsis I, Efstratiadis A, Goldman JE (2003) Insulin-like growth factor (IGF) signaling through type 1 IGF receptor plays an important role in remyelination. J Neurosci 23: 7710-7718.
Mason JL, Ye P, Suzuki K, D'Ercole AJ, Matsushima GK (2000) Insulin-like growth factor-1 inhibits mature oligodendrocyte apoptosis during primary demyelination. J Neurosci 20: 5703-5708.
Matsumoto Y, Maller JL (2004) A centrosomal localization signal in cyclin E required for Cdk2-independent S phase entry. Science 306: 885-888.
Matthias K, Kirchhoff F, Seifert G, Huttmann K, Matyash M, Kettenmann H, Steinhauser C (2003) Segregated expression of AMPA-type

glutamate receptors and glutamate transporters defines distinct astrocyte populations in the mouse hippocampus. J Neurosci 23: 1750-1758.
Matute C (1998) Characteristics of acute and chronic kainate excitotoxic damage to the optic nerve. Proc Natl Acad Sci U S A 95: 10229-10234.
Matute C, Alberdi E, Domercq M, Perez-Cerda F, Perez-Samartin A, Sanchez-Gomez MV (2001) The link between excitotoxic oligodendroglial death and demyelinating diseases. Trends Neurosci 24: 224-230.
Matute C, Sanchez-Gomez MV, Martinez-Millan L, Miledi R (1997) Glutamate receptor-mediated toxicity in optic nerve oligodendrocytes. Proc Natl Acad Sci U S A 94: 8830-8835.
Matzenbach B, Maulet Y, Sefton L, Courtier B, Avner P, Guenet JL, Betz H (1994) Structural analysis of mouse glycine receptor alpha subunit genes. Identification and chromosomal localization of a novel variant. J Biol Chem 269: 2607-2612.
Mauch DH, Nagler K, Schumacher S, Goritz C, Muller EC, Otto A, Pfrieger FW (2001) CNS synaptogenesis promoted by glia-derived cholesterol. Science 294: 1354-1357.
Mayer M, Bhakoo K, Noble M (1994) Ciliary neurotrophic factor and leukemia inhibitory factor promote the generation, maturation and survival of oligodendrocytes in vitro. Development 120: 143-153.
McDonald JW, Althomsons SP, Hyrc KL, Choi DW, Goldberg MP (1998) Oligodendrocytes from forebrain are highly vulnerable to AMPA/kainate receptor-mediated excitotoxicity. Nat Med 4: 291-297.
McKinnon RD, Matsui T, Dubois-Dalcq M, Aaronson SA (1990) FGF modulates the PDGF-driven pathway of oligodendrocyte development. Neuron 5: 603-614.
McKinnon RD, Piras G, Ida JA, Jr., Dubois-Dalcq M (1993) A role for TGF-beta in oligodendrocyte differentiation. J Cell Biol 121: 1397-1407.
McMorris FA, Smith TM, DeSalvo S, Furlanetto RW (1986) Insulin-like growth factor I/somatomedin C: a potent inducer of oligodendrocyte development. Proc Natl Acad Sci U S A 83: 822-826.
McNaughton LA, Hunt SP (1992) Regulation of gene expression in astrocytes by excitatory amino acids. Brain Res Mol Brain Res 16: 261-266.
Meijer L, Borgne A, Mulner O, Chong JP, Blow JJ, Inagaki N, Inagaki M, Delcros JG, Moulinoux JP (1997) Biochemical and cellular effects of roscovitine, a potent and selective inhibitor of the cyclin-dependent kinases cdc2, cdk2 and cdk5. Eur J Biochem 243: 527-536.
Mekki-Dauriac S, Agius E, Kan P, Cochard P (2002) Bone morphogenetic proteins negatively control oligodendrocyte precursor specification in the chick spinal cord. Development 129: 5117-5130.
Merkle FT, Tramontin AD, Garcia-Verdugo JM, Alvarez-Buylla A (2004) Radial glia give rise to adult neural stem cells in the subventricular zone. Proc Natl Acad Sci U S A DOI 10.1073/pnas.0407893101 .
Milner R, Anderson HJ, Rippon RF, McKay JS, Franklin RJ, Marchionni MA, Reynolds R, Ffrench-Constant C (1997) Contrasting effects of mitogenic growth factors on oligodendrocyte precursor cell migration. Glia 19: 85-90.
Milner R, Edwards G, Streuli C, Ffrench-Constant C (1996) A role in migration for the alpha V beta 1 integrin expressed on oligodendrocyte precursors. J Neurosci 16: 7240-7252.
Milner R, Ffrench-Constant C (1994) A developmental analysis of oligodendroglial integrins in primary cells: changes in alpha v-associated beta subunits during differentiation. Development 120: 3497-3506.
Miranda-Contreras L, Benitez-Diaz PR, Mendoza-Briceno RV, Delgado-Saez MC, Palacios-Pru EL (1999) Levels of amino acid neurotransmitters during mouse cerebellar neurogenesis and in histotypic cerebellar cultures. Dev Neurosci 21: 147-158.
Miranda-Contreras L, Mendoza-Briceno RV, Palacios-Pru EL (1998) Levels of monoamine and amino acid neurotransmitters in the developing male mouse hypothalamus and in histotypic hypothalamic cultures. Int J Dev Neurosci 16: 403-412.
Miranda-Contreras L, Ramirez-Martens LM, Benitez-Diaz PR, Pena-Contreras ZC, Mendoza-Briceno RV, Palacios-Pru EL (2000) Levels of amino acid neurotransmitters during mouse olfactory bulb neurogenesis and in histotypic olfactory bulb cultures. Int J Dev Neurosci 18: 83-91.
Molina-Holgado E, Vela JM, Arevalo-Martin A, Almazan G, Molina-Holgado F, Borrell J, Guaza C (2002) Cannabinoids promote oligodendrocyte progenitor survival: involvement of cannabinoid receptors and phosphatidylinositol-3 kinase/Akt signaling. J Neurosci 22: 9742-9753.
Molofsky AV, Pardal R, Iwashita T, Park IK, Clarke MF, Morrison SJ (2003) Bmi-1 dependence distinguishes neural stem cell self-renewal from progenitor proliferation. Nature 425: 962-967.
Monti B, Contestabile A (2000) Blockade of the NMDA receptor increases developmental apoptotic elimination of granule neurons and activates caspases in the rat cerebellum. Eur J Neurosci 12: 3117-3123.
Monti B, Marri L, Contestabile A (2002) NMDA receptor-dependent CREB activation in survival of cerebellar granule cells during in vivo and in vitro development. Eur J Neurosci 16: 1490-1498.
Morgan DO (1995) Principles of CDK regulation. Nature 374: 131-134.
Morgan DO (1997) Cyclin-dependent kinases: engines, clocks, and microprocessors. Annu Rev Cell Dev Biol 13: 261-291.
Morshead CM, Craig CG, van der KD (1998) In vivo clonal analyses reveal the properties of endogenous neural stem cell proliferation in the adult mammalian forebrain. Development 125: 2251-2261.
Morshead CM, Garcia AD, Sofroniew MV, van der KD (2003) The ablation of glial fibrillary acidic protein-positive cells from the adult central nervous system results in the loss of forebrain neural stem cells but not retinal stem cells. Eur J Neurosci 18: 76-84.
Morshead CM, Reynolds BA, Craig CG, McBurney MW, Staines WA, Morassutti D, Weiss S, van der KD (1994) Neural stem cells in the adult mammalian forebrain: a relatively quiescent subpopulation of subependymal cells. Neuron 13: 1071-1082.
Moss SJ, Smart TG (2001) Constructing inhibitory synapses. Nat Rev Neurosci 2: 240-250.
Muller T, Moller T, Berger T, Schnitzer J, Kettenmann H (1992) Calcium entry through kainate receptors and resulting potassium-channel blockade in Bergmann glial cells. Science 256: 1563-1566.
Nagler K, Mauch DH, Pfrieger FW (2001) Glia-derived signals induce synapse formation in neurones of the rat central nervous system. J Physiol 533: 665-679.
Nakahara J, Tan-Takeuchi K, Seiwa C, Gotoh M, Kaifu T, Ujike A, Inui M, Yagi T, Ogawa M, Aiso S, Takai T, Asou H (2003) Signaling via immunoglobulin Fc receptors induces oligodendrocyte precursor cell differentiation. Dev Cell 4: 841-852.
Nakatomi H, Kuriu T, Okabe S, Yamamoto S, Hatano O, Kawahara N, Tamura A, Kirino T, Nakafuku M (2002) Regeneration of hippocampal pyramidal neurons after ischemic brain injury by recruitment of endogenous neural progenitors. Cell 110: 429-441.
Nakayama K, Ishida N, Shirane M, Inomata A, Inoue T, Shishido N, Horii I, Loh DY, Nakayama K (1996) Mice lacking p27(Kip1) display increased body size, multiple organ hyperplasia, retinal dysplasia, and pituitary tumors. Cell 85: 707-720.
Nakayama K, Nagahama H, Minamishima YA, Matsumoto M, Nakamichi I, Kitagawa K, Shirane M, Tsunematsu R, Tsukiyama T, Ishida N, Kitagawa M, Nakayama K, Hatakeyama S (2000) Targeted disruption of Skp2 results in accumulation of cyclin E and p27(Kip1), polyploidy

and centrosome overduplication. EMBO J 19: 2069-2081.
Nakayama KI, Hatakeyama S, Nakayama K (2001) Regulation of the cell cycle at the G1-S transition by proteolysis of cyclin E and p27Kip1. Biochem Biophys Res Commun 282: 853-860.
Nery S, Fishell G, Corbin JG (2002) The caudal ganglionic eminence is a source of distinct cortical and subcortical cell populations. Nat Neurosci 5: 1279-1287.
Nishiyama A, Chang A, Trapp BD (1999) NG2+ glial cells: a novel glial cell population in the adult brain. J Neuropathol Exp Neurol 58: 1113-1124.
Nishiyama A, Lin XH, Giese N, Heldin CH, Stallcup WB (1996) Co-localization of NG2 proteoglycan and PDGF alpha-receptor on O2A progenitor cells in the developing rat brain. J Neurosci Res 43: 299-314.
Noble M, Murray K (1984) Purified astrocytes promote the in vitro division of a bipotential glial progenitor cell. EMBO J 3: 2243-2247.
Noble M, Murray K, Stroobant P, Waterfield MD, Riddle P (1988) Platelet-derived growth factor promotes division and motility and inhibits premature differentiation of the oligodendrocyte/type-2 astrocyte progenitor cell. Nature 333: 560-562.
Noctor SC, Flint AC, Weissman TA, Dammerman RS, Kriegstein AR (2001) Neurons derived from radial glial cells establish radial units in neocortex. Nature 409: 714-720.
Noda M, Nakanishi H, Nabekura J, Akaike N (2000) AMPA-kainate subtypes of glutamate receptor in rat cerebral microglia. J Neurosci 20: 251-258.
Nolte C, Matyash M, Pivneva T, Schipke CG, Ohlemeyer C, Hanisch UK, Kirchhoff F, Kettenmann H (2001) GFAP promoter-controlled EGFP-expressing transgenic mice: a tool to visualize astrocytes and astrogliosis in living brain tissue. Glia 33: 72-86.
Norton JD (2000) ID helix-loop-helix proteins in cell growth, differentiation and tumorigenesis. J Cell Sci 113 (Pt 22): 3897-3905.
Norton JD, Deed RW, Craggs G, Sablitzky F (1998) Id helix-loop-helix proteins in cell growth and differentiation. Trends Cell Biol 8: 58-65.
Nunes MC, Roy NS, Keyoung HM, Goodman RR, McKhann G, Jiang L, Kang J, Nedergaard M, Goldman SA (2003) Identification and isolation of multipotential neural progenitor cells from the subcortical white matter of the adult human brain. Nat Med 9: 439-447.
Ohtsubo M, Theodoras AM, Schumacher J, Roberts JM, Pagano M (1995) Human cyclin E, a nuclear protein essential for the G1-to-S phase transition. Mol Cell Biol 15: 2612-2624.
Ohtsuka T, Ishibashi M, Gradwohl G, Nakanishi S, Guillemot F, Kageyama R (1999) Hes1 and Hes5 as notch effectors in mammalian neuronal differentiation. EMBO J 18: 2196-2207.
Oka A, Belliveau MJ, Rosenberg PA, Volpe JJ (1993) Vulnerability of oligodendroglia to glutamate: pharmacology, mechanisms, and prevention. J Neurosci 13: 1441-1453.
Oliet SH, Piet R, Poulain DA (2001) Control of glutamate clearance and synaptic efficacy by glial coverage of neurons. Science 292: 923-926.
Oliver TG, Wechsler-Reya RJ (2004) Getting at the root and stem of brain tumors. Neuron 42: 885-888.
Opanashuk LA, Pauly JR, Hauser KF (2001) Effect of nicotine on cerebellar granule neuron development. Eur J Neurosci 13: 48-56.
Ortega S, Prieto I, Odajima J, Martin A, Dubus P, Sotillo R, Barbero JL, Malumbres M, Barbacid M (2003) Cyclin-dependent kinase 2 is essential for meiosis but not for mitotic cell division in mice. Nat Genet 35: 25-31.
Ostenfeld T, Caldwell MA, Prowse KR, Linskens MH, Jauniaux E, Svendsen CN (2000) Human neural precursor cells express low levels of telomerase in vitro and show diminishing cell proliferation with extensive axonal outgrowth following transplantation. Exp Neurol 164: 215-226.
Osterhout DJ, Ebner S, Xu J, Ornitz DM, Zazanis GA, McKinnon RD (1997) Transplanted oligodendrocyte progenitor cells expressing a dominant-negative FGF receptor transgene fail to migrate in vivo. J Neurosci 17: 9122-9132.
Othman T, Yan H, Rivkees SA (2003) Oligodendrocytes express functional A1 adenosine receptors that stimulate cellular migration. Glia 44: 166-172.
Palma V, Lim DA, Dahmane N, Sanchez P, Brionne TC, Herzberg CD, Gitton Y, Carleton A, Alvarez-Buylla A, Altaba A (2005) Sonic hedgehog controls stem cell behavior in the postnatal and adult brain. Development 132: 335-344.
Palmer TD, Ray J, Gage FH (1995) FGF-2-responsive neuronal progenitors reside in proliferative and quiescent regions of the adult rodent brain. Mol Cell Neurosci 6: 474-486.
Palmer TD, Takahashi J, Gage FH (1997) The adult rat hippocampus contains primordial neural stem cells. Mol Cell Neurosci 8: 389-404.
Panganiban G, Irvine SM, Lowe C, Roehl H, Corley LS, Sherbon B, Grenier JK, Fallon JF, Kimble J, Walker M, Wray GA, Swalla BJ, Martindale MQ, Carroll SB (1997) The origin and evolution of animal appendages. Proc Natl Acad Sci U S A 94: 5162-5166.
Panganiban G, Rubenstein JL (2002) Developmental functions of the Distal-less/Dlx homeobox genes. Development 129: 4371-4386.
Pardee AB (1974) A restriction point for control of normal animal cell proliferation. Proc Natl Acad Sci U S A 71: 1286-1290.
Pardee AB (1989) G1 events and regulation of cell proliferation. Science 246: 603-608.
Parent JM, Lowenstein DH (2002) Seizure-induced neurogenesis: are more new neurons good for an adult brain? Prog Brain Res 135: 121-131.
Parent JM, Yu TW, Leibowitz RT, Geschwind DH, Sloviter RS, Lowenstein DH (1997) Dentate granule cell neurogenesis is increased by seizures and contributes to aberrant network reorganization in the adult rat hippocampus. J Neurosci 17: 3727-3738.
Parisi T, Beck AR, Rougier N, McNeil T, Lucian L, Werb Z, Amati B (2003) Cyclins E1 and E2 are required for endoreplication in placental trophoblast giant cells. EMBO J 22: 4794-4803.
Park SK, Miller R, Krane I, Vartanian T (2001) The erbB2 gene is required for the development of terminally differentiated spinal cord oligodendrocytes. J Cell Biol 154: 1245-1258.
Parras CM, Galli R, Britz O, Soares S, Galichet C, Battiste J, Johnson JE, Nakafuku M, Vescovi A, Guillemot F (2004) Mash1 specifies neurons and oligodendrocytes in the postnatal brain. EMBO J 23: 4495-4505.
Parras CM, Schuurmans C, Scardigli R, Kim J, Anderson DJ, Guillemot F (2002) Divergent functions of the proneural genes Mash1 and Ngn2 in the specification of neuronal subtype identity. Genes Dev 16: 324-338.
Pastor A, Chvatal A, Sykova E, Kettenmann H (1995) Glycine- and GABA-activated currents in identified glial cells of the developing rat spinal cord slice. Eur J Neurosci 7: 1188-1198.
Patneau DK, Wright PW, Winters C, Mayer ML, Gallo V (1994) Glial cells of the oligodendrocyte lineage express both kainate- and AMPA-preferring subtypes of glutamate receptor. Neuron 12: 357-371.
Pende M, Fisher TL, Simpson PB, Russell JT, Blenis J, Gallo V (1997) Neurotransmitter- and growth factor-induced cAMP response element binding protein phosphorylation in glial cell progenitors: role of calcium ions, protein kinase C, and mitogen-activated protein kinase/ribosomal S6 kinase pathway. J Neurosci 17: 1291-1301.
Pende M, Holtzclaw LA, Curtis JL, Russell JT, Gallo V (1994) Glutamate regulates intracellular calcium and gene expression in oligodendrocyte progenitors through the activation of DL-alpha-amino-3-hydroxy-5-methyl-4-isoxazolepropionic acid receptors. Proc Natl Acad Sci U S A 91: 3215-3219.

Perrier AL, Tabar V, Barberi T, Rubio ME, Bruses J, Topf N, Harrison NL, Studer L (2004) Derivation of midbrain dopamine neurons from human embryonic stem cells. Proc Natl Acad Sci U S A 101: 12543-12548.
Pfeiffer SE, Warington AE, Bansal R (1993) The oligodendrocyte and its many cellular processes. Trends Cell Biol 3: 191-197.
Pitt D, Werner P, Raine CS (2000) Glutamate excitotoxicity in a model of multiple sclerosis. Nat Med 6: 67-70.
Plachta N, Bibel M, Tucker KL, Barde YA (2004) Developmental potential of defined neural progenitors derived from mouse embryonic stem cells. Development 131: 5449-5456.
Planas-Silva MD, Weinberg RA (1997) The restriction point and control of cell proliferation. Curr Opin Cell Biol 9: 768-772.
Porter JT, McCarthy KD (1995) GFAP-positive hippocampal astrocytes in situ respond to glutamatergic neuroligands with increases in [Ca2+]i. Glia 13: 101-112.
Prineas JW, Barnard RO, Kwon EE, Sharer LR, Cho ES (1993) Multiple sclerosis: remyelination of nascent lesions. Ann Neurol 33: 137-151.
Publication #1 - Belachew S, Yuan X, Gallo V (2001) Unraveling oligodendrocyte origin and function by cell-specific transgenesis. Dev Neurosci 23: 287-298.
Publication #10 - Belachew S, Rogister B, Rigo JM, Malgrange B, Mazy-Servais C, Xhauflaire G, Coucke P, Moonen G (1998) Cultured oligodendrocyte progenitors derived from cerebral cortex express a glycine receptor which is pharmacologically distinct from the neuronal isoform. Eur J Neurosci 10: 3556-3564.
Publication #11 - Belachew S, Malgrange B, Rigo JM, Rogister B, Leprince P, Hans G, Nguyen L, Moonen G (2000) Glycine triggers an intracellular calcium influx in oligodendrocyte progenitor cells which is mediated by the activation of both the ionotropic glycine receptor and Na+-dependent transporters. Eur J Neurosci 12: 1924-1930.
Publication #12 - Nguyen L, Malgrange B, Breuskin I, Lallemend F, Hans G, Moonen G, Belachew S, Rigo JM (2004) Striatal PSA-NCAM+ precursor cells from the newborn rat express functional glycine receptors. Neuroreport 15: 583-588.
Publication #13 - Nguyen L, Malgrange B, Belachew S, Rogister B, Rocher V, Moonen G, Rigo JM (2002) Functional glycine receptors are expressed by postnatal nestin-positive neural stem/progenitor cells. Eur J Neurosci 15: 1299-1305.
Publication #14 - Vautier F, Belachew S, Chittajallu R, Gallo V (2004) *Shaker*-type potassium channel subunits Kv1.3-1.4 and Kv1.6 differentially control oligodendrocyte progenitor cell cycle progression. Glia in press.
Publication #15 - Nguyen L, Malgrange B, Breuskin I, Bettendorff L, Moonen G, Belachew S, Rigo JM (2003) Autocrine/paracrine activation of the GABA(A) receptor inhibits the proliferation of neurogenic polysialylated neural cell adhesion molecule-positive (PSA-NCAM+) precursor cells from postnatal striatum. J Neurosci 23: 3278-3294.
Publication #2 - Yuan X, Chittajallu R, Belachew S, Anderson S, McBain CJ, Gallo V (2002) Expression of the green fluorescent protein in the oligodendrocyte lineage: a transgenic mouse for developmental and physiological studies. J Neurosci Res 70: 529-545.
Publication #3 - Belachew S, Aguirre AA, Wang H, Vautier F, Yuan X, Anderson S, Kirby M, Gallo V (2002) Cyclin-dependent kinase-2 controls oligodendrocyte progenitor cell cycle progression and is downregulated in adult oligodendrocyte progenitors. J Neurosci 22: 8553-8562.
Publication #4 - Nguyen L, Malgrange B, Rocher V, Hans G, Moonen G, Rigo JM, Belachew S (2003) Chemical inhibitors of cyclin-dependent kinases control proliferation, apoptosis and differentiation of oligodendroglial cells. Int J Dev Neurosci 21: 321-326.
Publication #5 - Belachew S, Chittajallu R, Aguirre AA, Yuan X, Kirby M, Anderson S, Gallo V (2003) Postnatal NG2 proteoglycan-expressing progenitor cells are intrinsically multipotent and generate functional neurons. J Cell Biol 161: 169-186.
Publication #6 - Aguirre AA, Chittajallu R, Belachew S, Gallo V (2004) NG2-expressing cells in the subventricular zone are Type C-like cells and contribute to interneuron generation in the postnatal hippocampus. J Cell Biol 165: 575-589.
Publication #7 - Nguyen L, Rigo JM, Rocher V, Belachew S, Malgrange B, Rogister B, Leprince P, Moonen G (2001) Neurotransmitters as early signals for central nervous system development. Cell Tissue Res 305: 187-202.
Publication #8 - Nguyen L, Rigo JM, Malgrange B, Moonen G, Belachew S (2003) Untangling the functional potential of PSA-NCAM-expressing cells in CNS development and brain repair strategies. Curr Med Chem 10: 2185-2196.
Publication #9 - Belachew S, Malgrange B, Rigo JM, Rogister B, Coucke P, Mazy-Servais C, Moonen G (1998) Developmental regulation of neuroligand-induced responses in cultured oligodendroglia. Neuroreport 9: 973-980.
Qi Y, Cai J, Wu Y, Wu R, Lee J, Fu H, Rao M, Sussel L, Rubenstein J, Qiu M (2001) Control of oligodendrocyte differentiation by the Nkx2.2 homeodomain transcription factor. Development 128: 2723-2733.
Raff MC (1989) Glial cell diversification in the rat optic nerve. Science 243: 1450-1455.
Raff MC, Abney ER, Fok-Seang J (1985) Reconstitution of a developmental clock in vitro: a critical role for astrocytes in the timing of oligodendrocyte differentiation. Cell 42: 61-69.
Raff MC, Lillien LE, Richardson WD, Burne JF, Noble MD (1988) Platelet-derived growth factor from astrocytes drives the clock that times oligodendrocyte development in culture. Nature 333: 562-565.
Raff MC, Miller RH, Noble M (1983) A glial progenitor cell that develops in vitro into an astrocyte or an oligodendrocyte depending on culture medium. Nature 303: 390-396.
Raine CS (1997) The Norton Lecture: a review of the oligodendrocyte in the multiple sclerosis lesion. J Neuroimmunol 77: 135-152.
Rakic P (2002a) Adult neurogenesis in mammals: an identity crisis. J Neurosci 22: 614-618.
Rakic P (2002b) Neurogenesis in adult primate neocortex: an evaluation of the evidence. Nat Rev Neurosci 3: 65-71.
Rakic P (2002c) Neurogenesis in adult primates. Prog Brain Res 138: 3-14.
Redwine JM, Armstrong RC (1998) In vivo proliferation of oligodendrocyte progenitors expressing PDGFalphaR during early remyelination. J Neurobiol 37: 413-428.
Reichling DB, Kyrozis A, Wang J, MacDermott AB (1994) Mechanisms of GABA and glycine depolarization-induced calcium transients in rat dorsal horn neurons. J Physiol 476: 411-421.
Ren S, Rollins BJ (2004) Cyclin c/cdk3 promotes rb-dependent g0 exit. Cell 117: 239-251.
Reyners H, Gianfelici dR, Maisin JR (1982) The beta astrocyte: a newly recognized radiosensitive glial cell type in the cerebral cortex. J Neurocytol 11: 967-983.
Reyners H, Gianfelici dR, Regniers L, Maisin JR (1986) A glial progenitor cell in the cerebral cortex of the adult rat. J Neurocytol 15: 53-61.
Reynolds BA, Tetzlaff W, Weiss S (1992) A multipotent EGF-responsive striatal embryonic progenitor cell produces neurons and astrocytes. J Neurosci 12: 4565-4574.
Reynolds BA, Weiss S (1992) Generation of neurons and astrocytes from isolated cells of the adult mammalian central nervous system. Science 255: 1707-1710.
Reynolds R, Hardy R (1997) Oligodendroglial progenitors labeled with the O4 antibody persist in the adult rat cerebral cortex in vivo. J Neurosci Res 47: 455-470.
Richardson WD, Pringle N, Mosley MJ, Westermark B, Dubois-Dalcq M (1988) A role for platelet-derived growth factor in normal gliogenesis

in the central nervous system. Cell 53: 309-319.
Robert A, Magistretti PJ (1997) AMPA/kainate receptor activation blocks K+ currents via internal Na+ increase in mouse cultured stellate astrocytes. Glia 20: 38-50.
Roberts JM (1999) Evolving ideas about cyclins. Cell 98: 129-132.
Robinson S, Tani M, Strieter RM, Ransohoff RM, Miller RH (1998) The chemokine growth-regulated oncogene-alpha promotes spinal cord oligodendrocyte precursor proliferation. J Neurosci 18: 10457-10463.
Rogers SW, Gregori NZ, Carlson N, Gahring LC, Noble M (2001) Neuronal nicotinic acetylcholine receptor expression by O2A/oligodendrocyte progenitor cells. Glia 33: 306-313.
Rosenberg PA, Dai W, Gan XD, Ali S, Fu J, Back SA, Sanchez RM, Segal MM, Follett PL, Jensen FE, Volpe JJ (2003) Mature myelin basic protein-expressing oligodendrocytes are insensitive to kainate toxicity. J Neurosci Res 71: 237-245.
Ross SE, Greenberg ME, Stiles CD (2003) Basic helix-loop-helix factors in cortical development. Neuron 39: 13-25.
Rothstein JD, Dykes-Hoberg M, Pardo CA, Bristol LA, Jin L, Kuncl RW, Kanai Y, Hediger MA, Wang Y, Schielke JP, Welty DF (1996) Knockout of glutamate transporters reveals a major role for astroglial transport in excitotoxicity and clearance of glutamate. Neuron 16: 675-686.
Rowitch DH, Lu QR, Kessaris N, Richardson WD (2002) An 'oligarchy' rules neural development. Trends Neurosci 25: 417-422.
Russo AA, Jeffrey PD, Patten AK, Massague J, Pavletich NP (1996) Crystal structure of the p27Kip1 cyclin-dependent-kinase inhibitor bound to the cyclin A-Cdk2 complex. Nature 382: 325-331.
Samanta J, Kessler JA (2004) Interactions between ID and OLIG proteins mediate the inhibitory effects of BMP4 on oligodendroglial differentiation. Development 131: 4131-4142.
Sanai N, Tramontin AD, Quinones-Hinojosa A, Barbaro NM, Gupta N, Kunwar S, Lawton MT, McDermott MW, Parsa AT, Manuel-Garcia VJ, Berger MS, Alvarez-Buylla A (2004) Unique astrocyte ribbon in adult human brain contains neural stem cells but lacks chain migration. Nature 427: 740-744.
Sanchez-Gomez MV, Alberdi E, Ibarretxe G, Torre I, Matute C (2003) Caspase-dependent and caspase-independent oligodendrocyte death mediated by AMPA and kainate receptors. J Neurosci 23: 9519-9528.
Sanchez-Gomez MV, Matute C (1999) AMPA and kainate receptors each mediate excitotoxicity in oligodendroglial cultures. Neurobiol Dis 6: 475-485.
Santarelli L, Saxe M, Gross C, Surget A, Battaglia F, Dulawa S, Weisstaub N, Lee J, Duman R, Arancio O, Belzung C, Hen R (2003) Requirement of hippocampal neurogenesis for the behavioral effects of antidepressants. Science 301: 805-809.
Sasai Y, Kageyama R, Tagawa Y, Shigemoto R, Nakanishi S (1992) Two mammalian helix-loop-helix factors structurally related to Drosophila hairy and Enhancer of split. Genes Dev 6: 2620-2634.
Sausville EA, Zaharevitz D, Gussio R, Meijer L, Louarn-Leost M, Kunick C, Schultz R, Lahusen T, Headlee D, Stinson S, Arbuck SG, Senderowicz A (1999) Cyclin-dependent kinases: initial approaches to exploit a novel therapeutic target. Pharmacol Ther 82: 285-292.
Scherer SS, Braun PE, Grinspan J, Collarini E, Wang DY, Kamholz J (1994) Differential regulation of the 2',3'-cyclic nucleotide 3'-phosphodiesterase gene during oligodendrocyte development. Neuron 12: 1363-1375.
Schofield PR, Lynch JW, Rajendra S, Pierce KD, Handford CA, Barry PH (1996) Molecular and genetic insights into ligand binding and signal transduction at the inhibitory glycine receptor. Cold Spring Harb Symp Quant Biol 61: 333-342.
Schroder W, Seifert G, Huttmann K, Hinterkeuser S, Steinhauser C (2002) AMPA receptor-mediated modulation of inward rectifier K+ channels in astrocytes of mouse hippocampus. Mol Cell Neurosci 19: 447-458.
Schuurmans C, Guillemot F (2002) Molecular mechanisms underlying cell fate specification in the developing telencephalon. Curr Opin Neurobiol 12: 26-34.
See J, Zhang X, Eraydin N, Mun SB, Mamontov P, Golden JA, Grinspan JB (2004) Oligodendrocyte maturation is inhibited by bone morphogenetic protein. Mol Cell Neurosci 26: 481-492.
Selmaj KW, Raine CS (1988) Tumor necrosis factor mediates myelin and oligodendrocyte damage in vitro. Ann Neurol 23: 339-346.
Senderowicz AM, Sausville EA (2000) Preclinical and clinical development of cyclin-dependent kinase modulators. J Natl Cancer Inst 92: 376-387.
Serafini R, Valeyev AY, Barker JL, Poulter MO (1995) Depolarizing GABA-activated Cl- channels in embryonic rat spinal and olfactory bulb cells. J Physiol 488 (Pt 2): 371-386.
Sergeeva OA (1998) Comparison of glycine- and GABA-evoked currents in two types of neurons isolated from the rat striatum. Neurosci Lett 243: 9-12.
Sergeeva OA, Haas HL (2001) Expression and function of glycine receptors in striatal cholinergic interneurons from rat and mouse. Neuroscience 104: 1043-1055.
Seri B, Garcia-Verdugo JM, McEwen BS, Alvarez-Buylla A (2001) Astrocytes give rise to new neurons in the adult mammalian hippocampus. J Neurosci 21: 7153-7160.
Setoguchi T, Kondo T (2004) Nuclear export of OLIG2 in neural stem cells is essential for ciliary neurotrophic factor-induced astrocyte differentiation. J Cell Biol 166: 963-968.
Sharma G, Vijayaraghavan S (2001) Nicotinic cholinergic signaling in hippocampal astrocytes involves calcium-induced calcium release from intracellular stores. Proc Natl Acad Sci U S A 98: 4148-4153.
Sheaff RJ, Groudine M, Gordon M, Roberts JM, Clurman BE (1997) Cyclin E-CDK2 is a regulator of p27Kip1. Genes Dev 11: 1464-1478.
Sherr CJ (1994a) G1 phase progression: cycling on cue. Cell 79: 551-555.
Sherr CJ (1994b) The ins and outs of RB: coupling gene expression to the cell cycle clock. Trends Cell Biol 4: 15-18.
Sherr CJ (1995) D-type cyclins. Trends Biochem Sci 20: 187-190.
Sherr CJ (1996) Cancer cell cycles. Science 274: 1672-1677.
Sherr CJ, Roberts JM (1995) Inhibitors of mammalian G1 cyclin-dependent kinases. Genes Dev 9: 1149-1163.
Sherr CJ, Roberts JM (1999) CDK inhibitors: positive and negative regulators of G1-phase progression. Genes Dev 13: 1501-1512.
Sherr CJ, Roberts JM (2004) Living with or without cyclins and cyclin-dependent kinases. Genes Dev 18: 2699-2711.
Shi Y, Chichung LD, Taupin P, Nakashima K, Ray J, Yu RT, Gage FH, Evans RM (2004) Expression and function of orphan nuclear receptor TLX in adult neural stem cells. Nature 427: 78-83.
Shihabuddin LS, Horner PJ, Ray J, Gage FH (2000) Adult spinal cord stem cells generate neurons after transplantation in the adult dentate gyrus. J Neurosci 20: 8727-8735.
Shors TJ (2004) Memory traces of trace memories: neurogenesis, synaptogenesis and awareness. Trends Neurosci 27: 250-256.
Shors TJ, Miesegaes G, Beylin A, Zhao M, Rydel T, Gould E (2001) Neurogenesis in the adult is involved in the formation of trace memories. Nature 410: 372-376.

Shors TJ, Townsend DA, Zhao M, Kozorovitskiy Y, Gould E (2002) Neurogenesis may relate to some but not all types of hippocampal-dependent learning. Hippocampus 12: 578-584.
Sim FJ, Zhao C, Penderis J, Franklin RJ (2002) The age-related decrease in CNS remyelination efficiency is attributable to an impairment of both oligodendrocyte progenitor recruitment and differentiation. J Neurosci 22: 2451-2459.
Simerly C, Dominko T, Navara C, Payne C, Capuano S, Gosman G, Chong KY, Takahashi D, Chace C, Compton D, Hewitson L, Schatten G (2003) Molecular correlates of primate nuclear transfer failures. Science 300: 297.
Singh SK, Clarke ID, Hide T, Dirks PB (2004a) Cancer stem cells in nervous system tumors. Oncogene 23: 7267-7273.
Singh SK, Hawkins C, Clarke ID, Squire JA, Bayani J, Hide T, Henkelman RM, Cusimano MD, Dirks PB (2004b) Identification of human brain tumour initiating cells. Nature 432: 396-401.
Skoff RP, Vaughn JE (1971) An autoradiographic study of cellular proliferation in degenerating rat optic nerve. J Comp Neurol 141: 133-155.
Smith T, Groom A, Zhu B, Turski L (2000) Autoimmune encephalomyelitis ameliorated by AMPA antagonists. Nat Med 6: 62-66.
Sobko A, Peretz A, Shirihai O, Etkin S, Cherepanova V, Dagan D, Attali B (1998) Heteromultimeric delayed-rectifier K+ channels in schwann cells: developmental expression and role in cell proliferation. J Neurosci 18: 10398-10408.
Song H, Stevens CF, Gage FH (2002a) Astroglia induce neurogenesis from adult neural stem cells. Nature 417: 39-44.
Song HJ, Stevens CF, Gage FH (2002b) Neural stem cells from adult hippocampus develop essential properties of functional CNS neurons. Nat Neurosci 5: 438-445.
Sontheimer H, Kettenmann H, Backus KH, Schachner M (1988) Glutamate opens Na+/K+ channels in cultured astrocytes. Glia 1: 328-336.
Sontheimer H, Trotter J, Schachner M, Kettenmann H (1989) Channel expression correlates with differentiation stage during the development of oligodendrocytes from their precursor cells in culture. Neuron 2: 1135-1145.
Spassky N, de Castro F, Le Bras B, Heydon K, Queraud-LeSaux F, Bloch-Gallego E, Chedotal A, Zalc B, Thomas JL (2002) Directional guidance of oligodendroglial migration by class 3 semaphorins and netrin-1. J Neurosci 22: 5992-6004.
Spassky N, Goujet-Zalc C, Parmantier E, Olivier C, Martinez S, Ivanova A, Ikenaka K, Macklin W, Cerruti I, Zalc B, Thomas JL (1998) Multiple restricted origin of oligodendrocytes. J Neurosci 18: 8331-8343.
Stankoff B, Aigrot MS, Noel F, Wattilliaux A, Zalc B, Lubetzki C (2002) Ciliary neurotrophic factor (CNTF) enhances myelin formation: a novel role for CNTF and CNTF-related molecules. J Neurosci 22: 9221-9227.
Stegmuller J, Werner H, Nave KA, Trotter J (2003) The proteoglycan NG2 is complexed with alpha-amino-3-hydroxy-5-methyl-4-isoxazolepropionic acid (AMPA) receptors by the PDZ glutamate receptor interaction protein (GRIP) in glial progenitor cells. Implications for glial-neuronal signaling. J Biol Chem 278: 3590-3598.
Steinhauser C, Gallo V (1996) News on glutamate receptors in glial cells. Trends Neurosci 19: 339-345.
Steinhauser C, Jabs R, Kettenmann H (1994) Properties of GABA and glutamate responses in identified glial cells of the mouse hippocampal slice. Hippocampus 4: 19-35.
Stevaux O, Dyson NJ (2002) A revised picture of the E2F transcriptional network and RB function. Curr Opin Cell Biol 14: 684-691.
Stevens B, Porta S, Haak LL, Gallo V, Fields RD (2002) Adenosine: a neuron-glial transmitter promoting myelination in the CNS in response to action potentials. Neuron 36: 855-868.
Stewart RR, Hoge GJ, Zigova T, Luskin MB (2002) Neural progenitor cells of the neonatal rat anterior subventricular zone express functional GABA(A) receptors. J Neurobiol 50: 305-322.
Stidworthy MF, Genoud S, Li WW, Leone DP, Mantei N, Suter U, Franklin RJ (2004) Notch1 and Jagged1 are expressed after CNS demyelination, but are not a major rate-determining factor during remyelination. Brain 127: 1928-1941.
Stiles CD (2003) Lost in space: misregulated positional cues create tripotent neural progenitors in cell culture. Neuron 40: 447-449.
Stolt CC, Lommes P, Sock E, Chaboissier MC, Schedl A, Wegner M (2003) The Sox9 transcription factor determines glial fate choice in the developing spinal cord. Genes Dev 17: 1677-1689.
Sugimoto Y, Taniguchi M, Yagi T, Akagi Y, Nojyo Y, Tamamaki N (2001) Guidance of glial precursor cell migration by secreted cues in the developing optic nerve. Development 128: 3321-3330.
Sun T, Dong H, Wu L, Kane M, Rowitch DH, Stiles CD (2003) Cross-repressive interaction of the Olig2 and Nkx2.2 transcription factors in developing neural tube associated with formation of a specific physical complex. J Neurosci 23: 9547-9556.
Sun T, Echelard Y, Lu R, Yuk DI, Kaing S, Stiles CD, Rowitch DH (2001) Olig bHLH proteins interact with homeodomain proteins to regulate cell fate acquisition in progenitors of the ventral neural tube. Curr Biol 11: 1413-1420.
Suzuki SO, Goldman JE (2003) Multiple cell populations in the early postnatal subventricular zone take distinct migratory pathways: a dynamic study of glial and neuronal progenitor migration. J Neurosci 23: 4240-4250.
Svendsen CN, Smith AG (1999) New prospects for human stem-cell therapy in the nervous system. Trends Neurosci 22: 357-364.
Takebayashi H, Yoshida S, Sugimori M, Kosako H, Kominami R, Nakafuku M, Nabeshima Y (2000) Dynamic expression of basic helix-loop-helix Olig family members: implication of Olig2 in neuron and oligodendrocyte differentiation and identification of a new member, Olig3. Mech Dev 99: 143-148.
Tanaka K, Watase K, Manabe T, Yamada K, Watanabe M, Takahashi K, Iwama H, Nishikawa T, Ichihara N, Kikuchi T, Okuyama S, Kawashima N, Hori S, Takimoto M, Wada K (1997) Epilepsy and exacerbation of brain injury in mice lacking the glutamate transporter GLT-1. Science 276: 1699-1702.
Tang DG, Tokumoto YM, Apperly JA, Lloyd AC, Raff MC (2001) Lack of replicative senescence in cultured rat oligodendrocyte precursor cells. Science 291: 868-871.
Tang DG, Tokumoto YM, Raff MC (2000) Long-term culture of purified postnatal oligodendrocyte precursor cells. Evidence for an intrinsic maturation program that plays out over months. J Cell Biol 148: 971-984.
Tang XM, Beesley JS, Grinspan JB, Seth P, Kamholz J, Cambi F (1999) Cell cycle arrest induced by ectopic expression of p27 is not sufficient to promote oligodendrocyte differentiation. J Cell Biochem 76: 270-279.
Tang XM, Strocchi P, Cambi F (1998) Changes in the activity of cdk2 and cdk5 accompany differentiation of rat primary oligodendrocytes. J Cell Biochem 68: 128-137.
Taupin P, Gage FH (2002) Adult neurogenesis and neural stem cells of the central nervous system in mammals. J Neurosci Res 69: 745-749.
Tekkok SB, Goldberg MP (2001) Ampa/kainate receptor activation mediates hypoxic oligodendrocyte death and axonal injury in cerebral white matter. J Neurosci 21: 4237-4248.
Temple S, Alvarez-Buylla A (1999) Stem cells in the adult mammalian central nervous system. Curr Opin Neurobiol 9: 135-141.
Temple S, Raff MC (1985) Differentiation of a bipotential glial progenitor cell in a single cell microculture. Nature 313: 223-225.
Temple S, Raff MC (1986) Clonal analysis of oligodendrocyte development in culture: evidence for a developmental clock that counts cell divisions. Cell 44: 773-779.

Tikoo R, Casaccia-Bonnefil P, Chao MV, Koff A (1997) Changes in cyclin-dependent kinase 2 and p27kip1 accompany glial cell differentiation of central glia-4 cells. J Biol Chem 272: 442-447.
Tikoo R, Osterhout DJ, Casaccia-Bonnefil P, Seth P, Koff A, Chao MV (1998) Ectopic expression of p27Kip1 in oligodendrocyte progenitor cells results in cell-cycle growth arrest. J Neurobiol 36: 431-440.
Tokumoto YM, Apperly JA, Gao FB, Raff MC (2002) Posttranscriptional regulation of p18 and p27 Cdk inhibitor proteins and the timing of oligodendrocyte differentiation. Dev Biol 245: 224-234.
Tokumoto YM, Durand B, Raff MC (1999) An analysis of the early events when oligodendrocyte precursor cells are triggered to differentiate by thyroid hormone, retinoic acid, or PDGF withdrawal. Dev Biol 213: 327-339.
Tokumoto YM, Tang DG, Raff MC (2001) Two molecularly distinct intracellular pathways to oligodendrocyte differentiation: role of a p53 family protein. EMBO J 20: 5261-5268.
Trapp BD, Nishiyama A, Cheng D, Macklin W (1997) Differentiation and death of premyelinating oligodendrocytes in developing rodent brain. J Cell Biol 137: 459-468.
Trimmer JS, Rhodes KJ (2004) Localization of voltage-gated ion channels in mammalian brain. Annu Rev Physiol 66: 477-519.
Tropepe V, Hitoshi S, Sirard C, Mak TW, Rossant J, van der KD (2001) Direct neural fate specification from embryonic stem cells: a primitive mammalian neural stem cell stage acquired through a default mechanism. Neuron 30: 65-78.
Tsai HH, Frost E, To V, Robinson S, Ffrench-Constant C, Geertman R, Ransohoff RM, Miller RH (2002) The chemokine receptor CXCR2 controls positioning of oligodendrocyte precursors in developing spinal cord by arresting their migration. Cell 110: 373-383.
Tsai HH, Tessier-Lavigne M, Miller RH (2003) Netrin 1 mediates spinal cord oligodendrocyte precursor dispersal. Development 130: 2095-2105.
Tsai LH, Lees E, Faha B, Harlow E, Riabowol K (1993) The cdk2 kinase is required for the G1-to-S transition in mammalian cells. Oncogene 8: 1593-1602.
Tyers M, Jorgensen P (2000) Proteolysis and the cell cycle: with this RING I do thee destroy. Curr Opin Genet Dev 10: 54-64.
Ullian EM, Sapperstein SK, Christopherson KS, Barres BA (2001) Control of synapse number by glia. Science 291: 657-661.
Valerio A, Ferrario M, Dreano M, Garotta G, Spano P, Pizzi M (2002) Soluble interleukin-6 (IL-6) receptor/IL-6 fusion protein enhances in vitro differentiation of purified rat oligodendroglial lineage cells. Mol Cell Neurosci 21: 602-615.
van den Heuvel S., Harlow E (1993) Distinct roles for cyclin-dependent kinases in cell cycle control. Science 262: 2050-2054.
van Heyningen P, Calver AR, Richardson WD (2001) Control of progenitor cell number by mitogen supply and demand. Curr Biol 11: 232-241.
van Praag H, Christie BR, Sejnowski TJ, Gage FH (1999a) Running enhances neurogenesis, learning, and long-term potentiation in mice. Proc Natl Acad Sci U S A 96: 13427-13431.
van Praag H, Kempermann G, Gage FH (1999b) Running increases cell proliferation and neurogenesis in the adult mouse dentate gyrus. Nat Neurosci 2: 266-270.
van Praag H, Schinder AF, Christie BR, Toni N, Palmer TD, Gage FH (2002) Functional neurogenesis in the adult hippocampus. Nature 415: 1030-1034.
Vartanian T, Fischbach G, Miller R (1999) Failure of spinal cord oligodendrocyte development in mice lacking neuregulin. Proc Natl Acad Sci U S A 96: 731-735.
Vartanian T, Li Y, Zhao M, Stefansson K (1995) Interferon-gamma-induced oligodendrocyte cell death: implications for the pathogenesis of multiple sclerosis. Mol Med 1: 732-743.
Vaughn JE, Hinds PL, Skoff RP (1970) Electron microscopic studies of Wallerian degeneration in rat optic nerves. I. The multipotential glia. J Comp Neurol 140: 175-206.
Vaughn JE, Peters A (1968) A third neuroglial cell type. An electron microscopic study. J Comp Neurol 133: 269-288.
Vela JM, Molina-Holgado E, Arevalo-Martin A, Almazan G, Guaza C (2002) Interleukin-1 regulates proliferation and differentiation of oligodendrocyte progenitor cells. Mol Cell Neurosci 20: 489-502.
Verkhratsky A, Kettenmann H (1996) Calcium signalling in glial cells. Trends Neurosci 19: 346-352.
Verkhratsky A, Steinhauser C (2000) Ion channels in glial cells. Brain Res Brain Res Rev 32: 380-412.
Vernadakis A (1996) Glia-neuron intercommunications and synaptic plasticity. Prog Neurobiol 49: 185-214.
Vlach J, Hennecke S, Amati B (1997) Phosphorylation-dependent degradation of the cyclin-dependent kinase inhibitor p27. EMBO J 16: 5334-5344.
Wakayama T, Tabar V, Rodriguez I, Perry AC, Studer L, Mombaerts P (2001) Differentiation of embryonic stem cell lines generated from adult somatic cells by nuclear transfer. Science 292: 740-743.
Wang DD, Krueger DD, Bordey A (2003) GABA depolarizes neuronal progenitors of the postnatal subventricular zone via GABAA receptor activation. J Physiol 550: 785-800.
Wang S, Sdrulla A, Johnson JE, Yokota Y, Barres BA (2001) A role for the helix-loop-helix protein Id2 in the control of oligodendrocyte development. Neuron 29: 603-614.
Wang S, Sdrulla AD, diSibio G, Bush G, Nofziger D, Hicks C, Weinmaster G, Barres BA (1998) Notch receptor activation inhibits oligodendrocyte differentiation. Neuron 21: 63-75.
Wang Y, Penfold S, Tang X, Hattori N, Riley P, Harper JW, Cross JC, Tyers M (1999) Deletion of the Cul1 gene in mice causes arrest in early embryogenesis and accumulation of cyclin E. Curr Biol 9: 1191-1194.
Warrington AE, Barbarese E, Pfeiffer SE (1993) Differential myelinogenic capacity of specific developmental stages of the oligodendrocyte lineage upon transplantation into hypomyelinating hosts. J Neurosci Res 34: 1-13.
Watanabe M (2002) Glial processes are glued to synapses via Ca(2+)-permeable glutamate receptors. Trends Neurosci 25: 5-6.
Weinberg RA (1995) The retinoblastoma protein and cell cycle control. Cell 81: 323-330.
Weiss S, Dunne C, Hewson J, Wohl C, Wheatley M, Peterson AC, Reynolds BA (1996) Multipotent CNS stem cells are present in the adult mammalian spinal cord and ventricular neuroaxis. J Neurosci 16: 7599-7609.
Welcker M, Singer J, Loeb KR, Grim J, Bloecher A, Gurien-West M, Clurman BE, Roberts JM (2003) Multisite phosphorylation by Cdk2 and GSK3 controls cyclin E degradation. Mol Cell 12: 381-392.
Wichterle H, Turnbull DH, Nery S, Fishell G, Alvarez-Buylla A (2001) In utero fate mapping reveals distinct migratory pathways and fates of neurons born in the mammalian basal forebrain. Development 128: 3759-3771.
Wolswijk G (1997) Oligodendrocyte precursor cells in chronic multiple sclerosis lesions. Mult Scler 3: 168-169.
Wolswijk G (1998) Chronic stage multiple sclerosis lesions contain a relatively quiescent population of oligodendrocyte precursor cells. J Neurosci 18: 601-609.
Wolswijk G (2000) Oligodendrocyte survival, loss and birth in lesions of chronic-stage multiple sclerosis. Brain 123 (Pt 1): 105-115.

Wolswijk G, Noble M (1989) Identification of an adult-specific glial progenitor cell. Development 105: 387-400.
Wolswijk G, Noble M (1992) Cooperation between PDGF and FGF converts slowly dividing O-2Aadult progenitor cells to rapidly dividing cells with characteristics of O-2Aperinatal progenitor cells. J Cell Biol 118: 889-900.
Wolswijk G, Riddle PN, Noble M (1991) Platelet-derived growth factor is mitogenic for O-2Aadult progenitor cells. Glia 4: 495-503.
Wonderlin WF, Strobl JS (1996) Potassium channels, proliferation and G1 progression. J Membr Biol 154: 91-107.
Wosik K, Ruffini F, Almazan G, Olivier A, Nalbantoglu J, Antel JP (2004) Resistance of human adult oligodendrocytes to AMPA/kainate receptor-mediated glutamate injury. Brain 127: 2636-2648.
Wren D, Wolswijk G, Noble M (1992) In vitro analysis of the origin and maintenance of O-2Aadult progenitor cells. J Cell Biol 116: 167-176.
Wu Q, Miller RH, Ransohoff RM, Robinson S, Bu J, Nishiyama A (2000) Elevated levels of the chemokine GRO-1 correlate with elevated oligodendrocyte progenitor proliferation in the jimpy mutant. J Neurosci 20: 2609-2617.
Xin M, Yue T, Ma Z, Wu FF, Gow A, Lu QR (2005) Myelinogenesis and axonal recognition by oligodendrocytes in brain are uncoupled in Olig1-null mice. J Neurosci 25: 1354-1365.
Yang A, Kaghad M, Caput D, McKeon F (2002) On the shoulders of giants: p63, p73 and the rise of p53. Trends Genet 18: 90-95.
Yang A, McKeon F (2000) P63 and P73: P53 mimics, menaces and more. Nat Rev Mol Cell Biol 1: 199-207.
Ye P, Bagnell R, D'Ercole AJ (2003) Mouse NG2+ oligodendrocyte precursors express mRNA for proteolipid protein but not its DM-20 variant: a study of laser microdissection-captured NG2+ cells. J Neurosci 23: 4401-4405.
Yew PR (2001) Ubiquitin-mediated proteolysis of vertebrate G1- and S-phase regulators. J Cell Physiol 187: 1-10.
Yoshioka A, Hardy M, Younkin DP, Grinspan JB, Stern JL, Pleasure D (1995) Alpha-amino-3-hydroxy-5-methyl-4-isoxazolepropionate (AMPA) receptors mediate excitotoxicity in the oligodendroglial lineage. J Neurochem 64: 2442-2448.
Yuan X, Curtin J, Xiong Y, Liu G, Waschsmann-Hogiu S, Farkas DL, Black KL, Yu JS (2004) Isolation of cancer stem cells from adult glioblastoma multiforme. Oncogene.
Yuan X, Eisen AM, McBain CJ, Gallo V (1998) A role for glutamate and its receptors in the regulation of oligodendrocyte development in cerebellar tissue slices. Development 125: 2901-2914.
Yung SY, Gokhan S, Jurcsak J, Molero AE, Abrajano JJ, Mehler MF (2002) Differential modulation of BMP signaling promotes the elaboration of cerebral cortical GABAergic neurons or oligodendrocytes from a common sonic hedgehog-responsive ventral forebrain progenitor species. Proc Natl Acad Sci U S A 99: 16273-16278.
Zebedee Z, Hara E (2001) Id proteins in cell cycle control and cellular senescence. Oncogene 20: 8317-8325.
Zetterberg A, Larsson O, Wiman KG (1995) What is the restriction point? Curr Opin Cell Biol 7: 835-842.
Zezula J, Casaccia-Bonnefil P, Ezhevsky SA, Osterhout DJ, Levine JM, Dowdy SF, Chao MV, Koff A (2001) p21cip1 is required for the differentiation of oligodendrocytes independently of cell cycle withdrawal. EMBO Rep 2: 27-34.
Zhang SC, Wernig M, Duncan ID, Brustle O, Thomson JA (2001) In vitro differentiation of transplantable neural precursors from human embryonic stem cells. Nat Biotechnol 19: 1129-1133.
Zhao X, Ueba T, Christie BR, Barkho B, McConnell MJ, Nakashima K, Lein ES, Eadie BD, Willhoite AR, Muotri AR, Summers RG, Chun J, Lee KF, Gage FH (2003) Mice lacking methyl-CpG binding protein 1 have deficits in adult neurogenesis and hippocampal function. Proc Natl Acad Sci U S A 100: 6777-6782.
Zhou Q, Anderson DJ (2002) The bHLH transcription factors OLIG2 and OLIG1 couple neuronal and glial subtype specification. Cell 109: 61-73.
Zhou Q, Choi G, Anderson DJ (2001) The bHLH transcription factor Olig2 promotes oligodendrocyte differentiation in collaboration with Nkx2.2. Neuron 31: 791-807.
Zhou Q, Wang S, Anderson DJ (2000) Identification of a novel family of oligodendrocyte lineage-specific basic helix-loop-helix transcription factors. Neuron 25: 331-343.
Zhuo L, Sun B, Zhang CL, Fine A, Chiu SY, Messing A (1997) Live astrocytes visualized by green fluorescent protein in transgenic mice. Dev Biol 187: 36-42.

6 List of abbreviations

AMPA	α-amino-3-hydroxy-5-methyl-4-isoxazole proprionic acid
bHLH	basic helix-loop-helix
BrdU	bromodeoxyuridine
CAK	cdk-activating kinase
Cdk	cyclin-dependent kinase
Cdki	endogenous inhibitor of cdks
CKI	chemical cdk inhibitor
CNPase	2'-3'-cyclic nucleotide 3'-phosphodiesterase
CNS	central nervous system
DG	dentate gyrus
Dlx	distal-less homeobox gene
Dn	dominant-negative
EGF	epidermal growth factor
EGFP	enhanced green fluorescent protein
ERK	extracellular signal-regulated kinase
ES	embryonic stem
FACS	fluorescence activated cell sorting
FGF2	type 2 fibroblast growth factor
GABA	γ-aminobutyric acid
GAD	glutamic acid decarboxylase
GalC	galactocerebroside
GFAP	glial fibrillary acidic protein
GluR	glutamate receptor
GlyR	glycine receptor
GLYT	glycine transporter
Hes	hairy and enhancer-of-split
Id	inhibitor of DNA binding
Kv	voltage-dependent potassium channel
LeX	Lewis X antigen
MAG	myelin-associated glycoprotein
MBP	myelin basic protein
MOG	myelin oligodendrocytic glycoprotein
MS	multiple sclerosis
Na_v	voltage-dependent sodium channel
NeuN	neuronal nuclei protein
NSC	neural stem cell
NT	nuclear transfer
OB	olfactory bulb
OINPC	oligodendrocyte/interneuron progenitor cell
OPC	oligodendrocyte progenitor cell
PCNA	proliferating cell nuclear antigen
PDGF(R-α)	platelet-derived growth factor (receptor-alpha)
PLP	proteolipid protein
PSA-NCAM	polysialylated form of neural cell adhesion molecule
Rb	retinoblastoma tumor-suppressor protein
RMS	rostral migratory stream
SVZ	subventricular zone
TH	thyroid hormone
VGCC	voltage-gated calcium channel
WT	wild-type

7 Appendix - Publications

7.1 Publication #1: Belachew,S., Yuan,X., and Gallo,V. (2001). Unraveling oligodendrocyte origin and function by cell-specific transgenesis. *Dev. Neurosci.* 23:287-298.

Original Paper

Developmental Neuroscience

Dev Neurosci 2001;23:287–298

Received: June 3, 2001
Accepted: June 26, 2001

Unraveling Oligodendrocyte Origin and Function by Cell-Specific Transgenesis

Shibeshih Belachew Xiaoqing Yuan Vittorio Gallo

Laboratory of Cellular and Synaptic Neurophysiology, National Institute of Child Health and Human Development, National Institutes of Health, Bethesda, Md., USA

Key Words

2′-3′-Cyclic nucleotide 3′-phosphodiesterase · Gliogenesis · Green fluorescent protein · Myelination · Oligodendrocyte progenitor · Proteolipid protein

Abstract

Besides the role of mature oligodendrocytes in myelin synthesis during the development of the central nervous system (CNS), the oligodendrocyte lineage also encompasses the largest pool of postnatal proliferating progenitors whose behavior in vivo remains broadly elusive in health and disease. We describe here transgenic models that allow us to track the functions and origins of such cells by using proteolipid protein and 2′,3′-cyclic nucleotide 3′-phosphodiesterase (CNP) gene promoters to direct oligodendroglial expression of different reporters, in particular the green fluorescent protein (GFP). We emphasize that the CNP-GFP mouse, which targets the entire oligodendroglial lineage from embryonic life to adulthood, provides an outstanding tool to study the in vivo properties of oligodendrocyte progenitor cells in normal and damaged CNS.

Introduction

Oligodendrocytes develop from proliferating progenitor cells (OPCs) that arise at mid-late gestation from the germinal ventricular zones of the embryonic brain and spinal cord [1–3]. As these OPCs migrate throughout the developing brain, they proliferate for a limited number of cell cycles before they stop dividing and terminally differentiate into postmitotic oligodendrocytes. Designed to unravel the features of lineage progression from OPCs to myelinating oligodendrocytes in vivo, the use of transgenic strategies aimed at selectively targeting oligodendroglial cells was a logical consequence of the mapping and characterization of genes coding for myelin proteins. The gene promoters of myelin basic protein (MBP) [4], proteolipid protein (PLP) [5] and 2′,3′-cyclic nucleotide 3′-phosphodiesterase (CNP) [6] have become valuable molecular tools to selectively target gene expression in oligodendrocytes and Schwann cells.

A decade ago, several groups used fragments of the MBP promoter to direct the expression of heterologous genes to myelinating oligodendrocytes in vivo. In the *shiverer* mice, a dysmyelinating mutant with a partial deletion in the MBP gene, the introduction into the germ line of the wild-type MBP gene under the transcriptional control of either a 4- or a 1-kb 5′-flanking sequence was sufficient to rescue the disabled neurological phenotype and induce a correct temporal and spatial expression of the MBP gene

KARGER

Fax + 41 61 306 12 34
E-Mail karger@karger.ch
www.karger.com

Accessible online at:
www.karger.com/journals/dne

Dr. Shibeshih Belachew
Laboratory of Cellular and Synaptic Neurophysiology
NICHD, NIH, Bldg 49 R5A-60
Bethesda, MD 20892-4495 (USA)
Tel. +1 301 402 4783, Fax +1 301 402 4777, E-Mail sbelachew@ulg.ac.be

itself [7]. Similarly, a 1.3-kb fragment of the MBP promoter was able to drive oligodendroglial expression of class I major histocompatibility complex molecules, resulting in a typically hypomyelinated pattern of the central nervous system (CNS) [8, 9].

In order to analyze the sequence of events that culminate in CNS myelination, transgenic mice were generated with constructs containing the MBP promoter fused to the bacterial *lac*Z or chloramphenicol acetyltransferase reporter genes [10–12]. Many features of the myelination program revealed by this approach were previously predicted by immunocytochemical and ultrastructural data derived from independent analysis. Nonetheless, patterns that were previously undocumented were elucidated by these transgenic models, *e.g.* MBP-*lac*Z mice showing that oligodendrocytes accumulated detectable levels of β-galactosidase as they began to myelinate, first in the ventral spinal cord 1 day prior to birth [12]; subsequent myelination proceeded in a strictly rostral-caudal direction, whereas in the dorsal cord, myelination initiated in the cervical enlargement and proceeded in both rostral and caudal directions [12].

The cell specificity of the MBP promoter has also been widely used for developmental and physiopathological studies in vivo, to assess the effects of overexpressing transcription factors [13], cytokines [14, 15], growth factors [16], type 1 human immunodeficiency virus [17] or oncogenic proteins [18, 19] in mature oligodendrocytes. More recently, mice have been engineered to express the bacteriophage P1 Cre-recombinase under the control of the MBP promoter [20, 21]. By combining such a Cre/*loxP* site-specific recombination system [22] with inducible tools for controlling Cre expression and function [23], it is now possible to introduce conditional oligodendroglial alterations that are temporally controlled.

In the past 5 years, the green fluorescent protein (GFP) from the jellyfish *Aequorea victoria* has considerably boosted transgenic strategies and become one of the most widely studied and exploited proteins in cell biology as an established marker for gene expression and protein targeting in intact living cells and organisms [24, 25]. The independence of GFP visualization from enzymatic substrates makes it a particularly suitable tool for transgenic animals, although strong promoters are necessary to drive expression levels that enable the detection of fluorescence. GFP is a relatively small protein of 238 amino acids and readily diffuses throughout the cytoplasm and the processes, providing a highly accurate visualization of cell morphology, which usefully fits the aims of developmental studies of the oligodendroglial lineage.

Unlike MBP-promoter-based strategies, CNP- and PLP-promoter-driven cell-specific transgenic mice allow to assess OPC development and function in vivo, as transcription of the PLP and CNP genes begins during embryonic life and at early developmental stages of the oligodendroglial lineage, far before the onset of myelination (fig. 1) [26–29]. In the present article, we shall focus on comparing transgenic models that have used CNP- and PLP-promoter-directed expression of different reporter genes, in particular GFP.

Molecular Determinants Providing Oligodendroglial Specificity of PLP and CNP Promoters

The PLP gene is present as a single copy in the genome [30–32], is located on the X chromosome [33, 34] and displays an intron/exon structure [for review see ref. 35] similar in mice and humans (fig. 2). This gene consists of 17 kb of DNA encompassing 7 exons, with an unusually large first intron (8.5 kb). The PLP gene not only generates the PLP protein (30 kD), but also a second myelin polypeptide expressed earlier in development, DM20 (25 kD) [36]. DM20 differs from PLP by an internal deletion of 35 amino acids, due to the presence of an alternative splicing site within exon 3 of the gene [37–39]. Recently, it has been demonstrated that the PLP gene also alternatively encodes non-myelinic protein products which are strictly cytoplasmic forms of the classical PLP/DM20 proteins, namely somal-restricted (sr)-PLP and sr-DM20 [40]. Interestingly, these sr-proteolipids are also expressed in different classes of neurons and contain a newly identified exon 1.1 lying between exon 1 and 2, the insertion of which results in 12 additional amino acids at the N-terminus of PLP and DM20 [35, 40].

It has been relatively difficult to map the transcriptional regulatory elements controlling PLP gene expression in vitro. Several experiments using 0.3–5.0 kb of the 5′-flanking region of the PLP gene demonstrated reporter gene expression in a variety of neural and non-neural cell types, including cells that do not normally express PLP gene products [41–43], thus proving that the 5′-flanking promoter elements are not sufficient to direct tissue- and cell-specific expression of this gene. As a matter of fact, the first intron of the PLP gene, which is highly conserved through evolution and accounts for almost half of the gene, appears to be essential to ensure oligodendroglial-specific expression. This conclusion was based on the generation of transgenic mice using a regulatory sequence containing the 2.4-kb 5′-flanking region (promoter), exon 1 and intron 1 of the PLP gene (see 'green' sequence in fig. 2). These mice displayed selective oligodendroglial

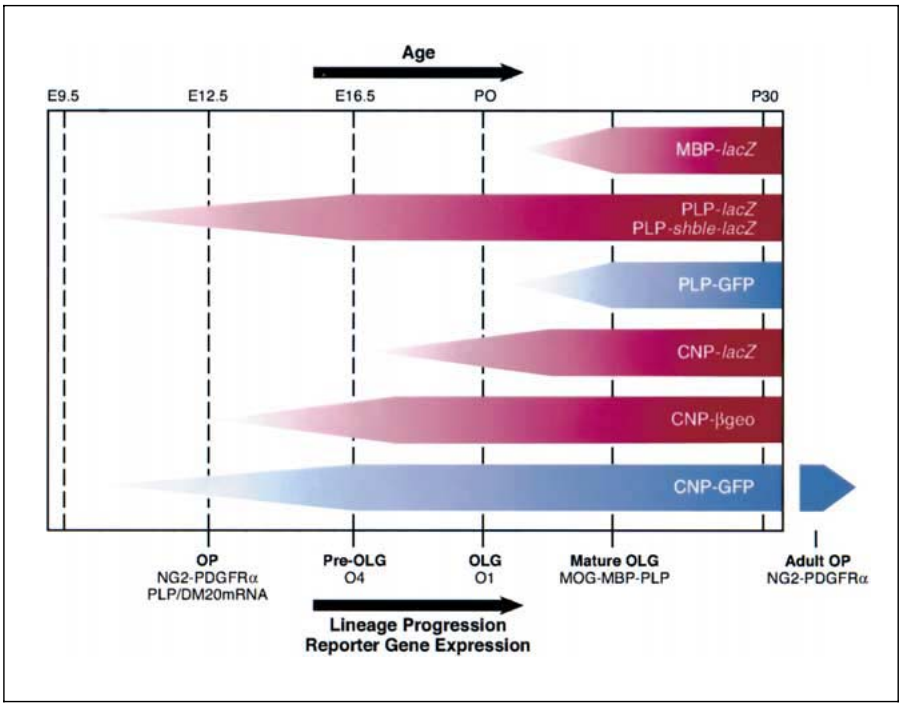

Fig. 1. Developmental regulation of reporter expression in transgenic mouse models assessing oligodendrogliogenesis. OLG = Oligodendrocyte; MOG = myelin-oligodendrocytic glycoprotein. Different color codes are used to distinguish GFP (blue) from other reporter genes (red). See tables 1 and 2 for relevant references.

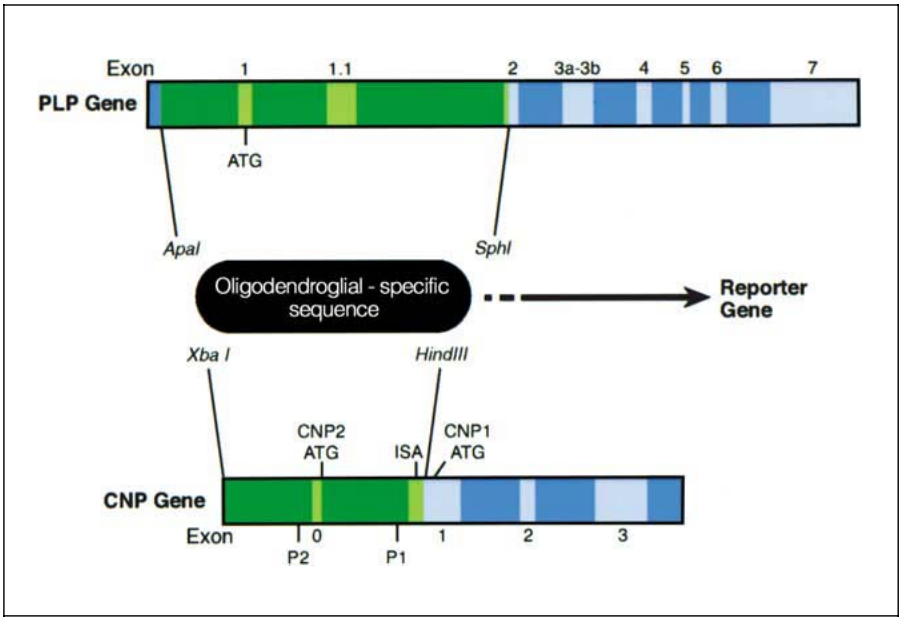

Fig. 2. Schematic illustration of the molecular structure of the CNP and PLP genes depicting (in green) the sequences (extracted with *ApaI-SphI* for PLP and *XbaI-HindIII* for CNP) which specifically direct oligodendroglial expression of different reporter genes in transgenic mice models. Light green and blue = Exons; dark green and blue = introns; *P1* and *P2* = CNP1 and CNP2 promoter core elements, respectively; *ISA* = internal splice acceptor site.

expression of different reporter gene constructs: (i) a fusion gene linking the first 13 amino acids of PLP with *Escherichia coli lac*Z gene [44], (ii) the same first 13 amino acids of PLP linked to a fusion gene comprising *lac*Z and *sh ble* (a zeomycin resistance gene isolated from *Streptoalloteichus hindustanus*) [45] and (iii) GFP alone [46]. For this latter model, it is noteworthy to point out that a different pattern of reporter expression (table 1) was observed, although GFP was under the control of an identical PLP-regulatory sequence, except that the ATG was mutated in GAG in exon 1 and combined with a deletion of exon 2, thereby allowing translation to start downstream of intron 1 [46].

Table 1. Transgenic mice models using the PLP promoter to target the oligodendroglial lineage

Promoter activity	Reporter gene(s)	Temporo-spatial expression	Lineage-specific expression	Functional analysis	References
2.4 kb 5′ flanking sequence (promoter), exon 1, intron 1 and first 37 bp of exon 2 of the mouse *plp* gene	*lac*Z	– CNS and PNS expression detected at E14.5 – increase in transgene expression following a caudal to rostral gradient from P5 → P21 – β-gal activity is targeted to myelin	– in vitro: mixed glial cultures from P3 brains, > 70% of β-gal+ cells are galactocerebroside-positive mature oligodendrocytes	ND	44
	sh ble zeomycin resistance fused to *lac*Z	– E9.5: basal plate of the diencephalon and caudal hypothalamus – E12.5–14.5: CNS germinative ventricular zones – E10.5: rhombencephalon and spinal cord (ventrolateral) – E9.5: PNS dorsal root and cranial ganglia correlated with endogenous *plp/dm-20* gene expression	– in situ: O4+ and NG-2+ cells at E16.5 and RIP+ oligodendrocytes at P1 – in vitro: cultures from E12.5 → mostly O4+ cells	antibiotic-selected transgene-expressing cells continue to proliferate even in the absence of PDGF-AA and O4 immunoreactivity is delayed	45
2.4-kb 5′ flanking sequence (promoter), exon 1 (with ATG mutated to GAG) and intron 1 of the mouse *plp* gene	GFP	– GFP protein detected by Western blot at P23 – GFP mRNA (with abnormal size) increases from P5 to P21 and decrease from P32 onward – GFP fluo. in white matter areas of the CNS at P23 – GFP fluo. in optic nerve at P6	– in situ: 95% of the GFP+ cells (P23 brains) were CC1+ (Ab anti-*adenomatous polyposis coli* protein); GFP+ cells were neither NeuN+ nor GFAP+ – in vitro: most of the freshly isolated FACS-sorted GFP+ cells from P21 spinal cords were O4+ and become galC+ within 48 h in culture	electrophysiological patch-clamp recordings of P9 and P49 brain GFP+ cells display potassium current characteristics of mature oligodendrocytes	46

ND = Not determined.

Even though its function remains relatively elusive, the CNP gene is one of the earliest known myelin-specific proteins which is abundantly expressed in developing oligodendrocytes [47–49]. Two CNP isoforms, CNP1 (46 kD) and CNP2 (48 kD) are both encoded by a single gene, the transcription of which is controlled by two separate promoter regions [50–53]. Two ATG codons responsible for translation initiation of CNP1 and CNP2 polypeptides are located in the second and first of the four exons of the CNP gene, respectively (fig. 2). CNP1 mRNA (2.6 kb) is transcribed from the downstream proximal promoter and contains only the open reading frame for the CNP1 protein, whereas the distal upstream promoter regulates the transcription of CNP2 mRNA (2.4 kb), which is able to translate both CNP1 and CNP2 proteins [54]. Although CNP1 is the most prominent mRNA and protein found postnatally in mature oligodendrocytes, CNP2 mRNA and protein are also expressed by differentiated cells. CNP2 mRNA is to date the only isoform synthesized at low levels in early embryonic life in OPCs [49]. Furthermore, CNP2 is also the only mRNA detected in non-neural tissues, notably in the thymus and testis [49, 55, 56]. Different CNP-transgenic mice have recently been generated (table 2) and all have confirmed that the 3.7-kb 5′-flanking sequence of the mouse CNP gene, containing CNP1 and CNP2 promoter core elements, exon 0 and part of exon 1 (see 'green' sequence in fig. 2), is sufficient to drive tissue- and cell-specific expression of different reporter genes, *i.e. lac*Z [55], βgeo (a fusion gene coding for both a bacterial β-galactosidase and neomycin phosphotransferase) [56] and GFP (fig. 3, 4) [57]. In these transgenic lines, the spatiotemporal pattern of reporter gene expression remarkably reproduced the cumulative features of endogenous CNP1 and CNP2 mRNA synthesis.

Transgenic Models Unravel the Paths of Oligodendrogliogenesis

Oligodendrocyte progenitor (OP) cells initially develop from neuroepithelial progenitors located in the walls of the embryonic neural tube. A yet unresolved controversy catalyzes the interest in the field over whether the oligodendroglial lineage ontogenically derives from either distinct or phylogenetically related progenitor cells [for re-

Table 2. Transgenic mice models using the CNP promoter to target the oligodendroglial lineage

Promoter activity	Reporter gene(s)	Temporo-spatial expression	Lineage-specific expression	Functional analysis	References
3.7-kb 5′ flanking sequence of the mouse CNP gene containing CNP1 and CNP2 promoter core elements, exon 0 and part of exon 1	*lac*Z	– consistent with myelination progression and endogenous CNP expression → caudorostral increase in brain and spinal cord X-gal staining from P7 onward, peaked at P30 with a slight decrease in older animals (P90 and P180) – in the PNS, transgene expression in sciatic and spinal nerves only in young animals (P15); no expression after P30 – E16.5: brain → medulla and pons; spinal cord → ventral zone	– in situ: in P30 brain sections, all the β-gal+ cells were CNP+ oligodendroglial cells displaying a myelinating morphotype	ND	55
	β-galactosidase and neomycin phosphotransferase (NPT, neomycin resistance) fusion gene (βgeo)	– E12.5: CNS → ventral regions of the rhombencephalon and spinal cord, around third ventricle in the telencephalon; PNS → spinal ganglia – E15: CNS → ventral spinal cord and floor plate at the level of the lower thoracic, lumbar and sacral spinal cord; PNS → dorsal and ventral proximal projections of peripheral nerves around the spinal cord + intercostal nerves – P21: robust *lac*Z expression in white matter tracts of the cortex, brainstem and cerebellum	– in situ: in P21 brains, co-localization of X-gal and CNP stainings and X-gal+ cells were NSE, GFAP and ED1 negative X-gal staining of S-100+ Schwann cells in P17 and P60 sciatic nerves – in vitro: G418 selected X-gal+ cells arising from E12.5 rhombencephalon cultures were A2B5+ or O1+ in brain or sciatic nerve cultures from P10 mice, G418 treatment selected the growth of CNP+ oligodendrocyte and S-100+ Schwann cells	ND	56
	GFP	– E10 → adulthood, consistent with areas of oligodendrogliogenesis and white matter development	– in situ: GFP+ cells are NG2+ and/or CNP+, no staining with astroglial or neuronal markers – in vitro: FACS-sorted GFP+ cells generate mature oligodendrocytes	electrophysiological patch-clamp recordings of GFP+ cells display developmental regulations of K^+ currents	57

ND = Not determined.

view see ref. 58, 59]. Most of the studies approaching this issue were performed in the spinal cord where two different markers were used to identify OP cells: (i) platelet-derived growth factor α-receptor (PDGFRα) transcripts, first appearing at the ventricular surface of the cervical spinal cord at E12.5 in the mouse (E14 in the rat, E7 in the chick) [60, 61]; (ii) PLP/DM20 mRNA, expressed at E14.5 in the mouse, in scattered cells located just outside the ventricular layer of the spinal cord [62]. Most of the developmental studies in the field are based on these two markers. However, in situ hybridization analysis with CNP transcript-specific probes also revealed the presence of a thin longitudinal column of CNP2-positive cells in the ventral ventricular zone of E14 rat spinal cord that were matching, both temporally and spatially, PDGFRα-expressing cells [49, 63]. At least at the level of the spinal cord and the brainstem, Richardson et al. [58] and Zalc et al. [59] reasonably agree that PLP/DM20-expressing cells, which are non-dividing (between E14.5 and E18.5), do not migrate [64] and develop later, are very likely post-mitotic non-myelinating oligodendrocytes that could directly derive from proliferative PDGFRα+ OPCs [65]. Consistent with these findings, only 10% of the normal number of oligodendrocytes are formed in the spinal cord of transgenic mice unable to synthesize the main ligand (PDGF-A) of the PDGFRα [66].

The generation of OPCs appears to require sonic hedgehog signaling *(shh)*, a morphogen produced by the floor plate and the notochord, which acts as a major patterning agent for the ventral neural tube by a mechanism involving a concentration-dependent repression and induction of two classes of homeodomain transcription factors: class I including genes of the Pax family and class II including genes of the Nkx family [67, 68]. In this regard, it has been shown that the neutralization of *shh* signaling prevents the development of ventral oligodendrocytes,

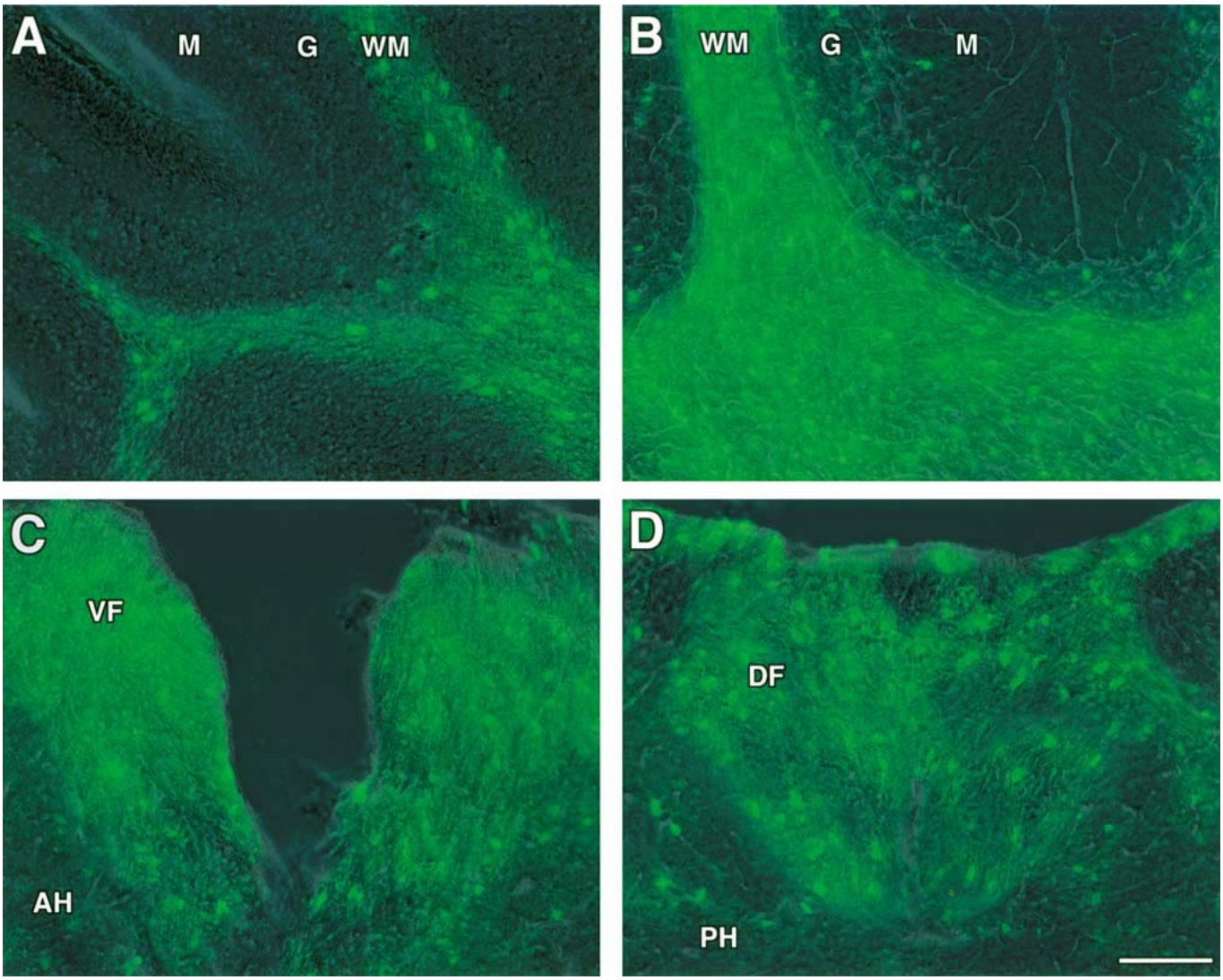

Fig. 3. Oligodendroglial white matter expression of the reporter gene in the CNP-GFP mice. Overlaps of phase contrast photomicrographs and fluorescence views depict the topographic distribution of GFP expression. Between P8 (**A**) and P30 (**B**), as myelination proceeds, cerebellar white matter tracts become thicker and more intensely GFP+. GFP+ oligodendroglial cells also appear in the granule cell layer (**B**). At the level of the cervical (C_1) spinal cord, transversal P30 sections demonstrate GFP expression in the ventral (**C**) and dorsal (**D**) funiculus, while scattered oligodendroglial cells are also visualized in the grey matter areas. Scale bar represents 100 μm for all the panels. M = Molecular layer; G = granular layer; WM = white matter tracts; VF = ventral funiculus; DF = dorsal funiculus; AH = anterior horn of the spinal cord; PH = posterior horn of the spinal cord.

whereas dorsal OP cells can be induced by ectopic dorsal *shh* production [61, 69, 70]. A recent study, using the Nkx2.1 mutant mice in which telencephalic expression of *Shh* is selectively lost [71], demonstrated that oligodendrocyte development is also *shh* dependent at the level of the embryonic forebrain [72]. Interestingly, among the areas of the forebrain from which early oligodendrocytes are commonly accepted to originate, both the amygdaloid region and the *zona limitans intrathalamica* displayed a normal expression of PLP/DM20 transcripts in the Nkx2.1 mice [72]. This raises the hypothesis that, rather than distinct oligodendroglial sources, the dual existence PLP/DM20- versus PDGFRα-expressing cells might reflect the existence of different molecular pathways that

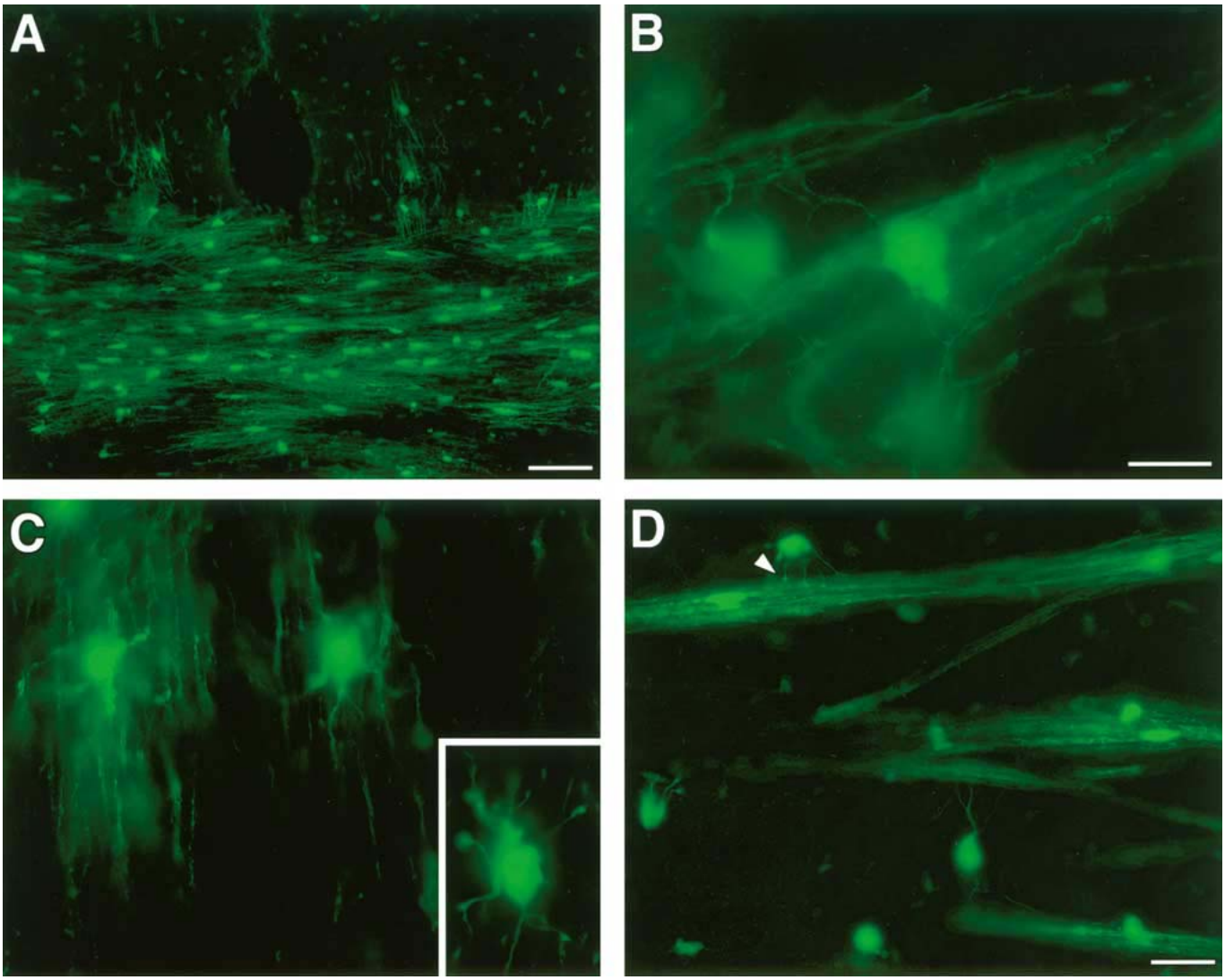

Fig. 4. Reporter gene expression in the corpus callosum of CNP-GFP mice. **A** P30 coronal section. GFP is expressed through the entire cell body of oligodendroglial cells and in the processes, including the myelin sheaths. Detailed views of mature myelinating oligodendrocytes whose GFP+ processes typically wrap around many different axonal tracts (**B–D**). **C** (insert) and **D** (arrowhead) highlight GFP+ end-feet of oligodendroglial processes. Scale bars represent 100 (**A**) and 20 μm (**B**). **C–D** Same magnification (bar = 20 μm).

underlie the generation of oligodendrocytes in different areas of the CNS.

Despite the trend to accept PDGFRα as the earliest marker of OP commitment, it remains possible that determining events for the oligodendroglial lineage have occurred before this receptor is expressed, as suggested by the detection of weakly PLP/DM20-expressing cells in the ventral neuroepithelium close to the floor plate of the spinal cord as early as E12 in the rat [63]. Moreover, Oligo2 and to a lesser extent Oligo1, members of the basic helix-loop-helix family of transcription factors, have been shown to be specifically expressed in OP cells and in the region of the neuroepithelium from which they arise at E11.5, prior to PDGFRα appearance [73, 74]. These genes, whose expression is lost in all populations of developing oligodendrocytes in *shh* null mice [73], are presently suitable candidates for being direct regulators of oligodendrocyte fate. Loss-of-function studies should soon bring new insights unraveling how Oligo1 and Oligo2 are causally related to oligodendroglial development.

Transgenic animals have recently provided important information regarding the early steps of oligodendrogliogenesis. In a CNP-GFP mouse model generated in our laboratory, GFP expression is detectable as early as E10 in the ventricular zone lining the lateral and the IVth ventricle, as well as along the Sylvius aqueduct and in the medulla [57]. We also found GFP expression at E10 all along the ventral spinal cord and at the level of the floor plate [57]. On the other hand, in the PLP/DM20-*sh ble-lac*Z mice [45], the transgene was first detected at E9.5 with a slightly different expression pattern: (i) in the brain, at the level of the basal plate of the diencephalon and caudal hypothalamus, and (ii) in the entire ventral part of the spinal cord and at the cervical level in its dorsal part. Interestingly, the early distribution of transgene expression in the CNP-GFP mice strikingly matches that of Oligo2 and to a lesser extent Oligo1 expression at E11.5 [74]. In situ hybridization experiments have convincingly demonstrated a colocalization of Oligo1/2 and CNP transcripts in mouse E14.5 spinal cord and E13 brain [75]. Furthermore, Oligo2 expression was observed in TuJ1-positive neuronal progenitors scattered in E12.5 rat spinal cord or E14.5 rat olfactory epithelium [75], raising the possibility that CNP promoter activity could be present in multipotential neuron/glia progenitors prior to the commitment to the oligodendrocyte lineage. This possibility is supported by in vitro work showing that OP cells can be reprogrammed to become multipotential CNS stem cells [76].

In order to address this issue of stem cell identity in vivo, we have to emphasize that, to date, no marker can be considered as specific of the stem cell potential from the developmental embryonic period until adulthood. As a matter of fact, in the adult dentate gyrus of a transgenic mouse generated by using the second intron enhancer of the rat nestin gene [77] to drive GFP expression [78], one can observe a loss of strict correlation between reporter expression and stem cells located in this area. Similarly, it is noteworthy to point out that another transgenic model using the human glial fibrillary acidic protein (GFAP) promoter to direct GFP expression in astrocytes demonstrated that a subset of GFP+ radial glial cells from E14 mouse cortex have a bipotential neuronal-astroglial fate [79]. This confirms that promoters that were primarily considered specific for distinct classes of differentiated neural cells can be active well before cells are restricted to a specific lineage. The biological relevance of early PLP, CNP and GFAP promoter activity and the identity of the immature cells expressing these genes need further experimental work to be fully elucidated.

Transgenic Models and the Understanding of OP Function in the Developing and Adult CNS

Besides their crucial role in understanding the origins and multipotentiality of oligodendroglial cells, transgenic strategies using the oligodendrocyte-specific CNP and PLP promoters could also be used to overexpress wild-type or mutant genes of interest that code for key regulatory proteins suspected to be involved in oligodendroglial functions in vivo. These would include transcription factors [80], voltage- and ligand-gated ion channels [81], components of signal transduction cascades, cell-cycle-related proteins [82] and other diffusely expressed molecules, which are unsuitable candidates for transgenic strategies that would not target a specific subset of cells. Concerning this particular purpose, the CNP promoter, as demonstrated in our CNP-GFP mice, has the advantage to be active from early embryonic life until adulthood and throughout the entire oligodendroglial lineage, from the progenitor stage to the mature myelinating oligodendrocyte (fig. 1, 3, 4; table 3) [57].

This property of transgenic models, obtained with CNP-driven overexpression of proteins, appears to be crucial for assessing oligodendroglial function in vivo. Either in developmental abnormalities or in diseases affecting the adult white matter, oligodendroglial function is mostly disrupted at the level of OP proliferation and/or differentiation [83]. Coupled with GFP reporter gene, CNP-dependent transgenic overexpression of a protein could give rise to in vivo assays evaluating genetically modified OPCs with respect to their essential proliferative and migrating capacities under various experimental conditions. The electrophysiological properties of such GFP-expressing OP cells can also be easily analyzed in fresh tissue slices [84]. Moreover, unlike antibiotic selection strategies used in other transgenic models that necessitate many days of growth in vitro [45, 56], we found that fluorescence-activated cell sorting of acutely dissociated GFP-expressing cells constitutes a straightforward technique for ex vivo studies of purified oligodendroglial cells isolated from CNS at different developmental stages [57]. Notably, this opens interesting prospects for further analysis of the regulation of gene expression within the oligodendroglial lineage in vivo.

Based on the pattern of reporter expression from the PLP-*lac*Z and PLP-*sh ble-lac*Z mice (fig. 1), we would like to emphasize that, theoretically, PLP-GFP transgenic systems may also be suitable models for engineering modified OP cells during their development. The absence of GFP expression in OP cells of the PLP-GFP mice of Fuss

Table 3. Immunocytochemical characterization of GFP+ cells in CNP-GFP transgenic mice

	NG2	O_4	O_1	CNP	MBP	Rip	S100β	GFAP	NeuN	$MAP2_{a–b}$
In vitro	+	+	+	+	+	ND	ND	–	–	–
In vivo	+	ND	ND	+	+	+	–	–	–	ND

GFP+ cells were immunoreactive for antibodies targeting the entire oligodendroglial lineage (NG2, O_4, O_1, CNPase, Rip and MBP), whereas no staining was observed with antibodies recognizing neuron- (NeuN, $MAP2_{a–b}$) or astrocyte-specific (S100β, GFAP) epitopes. Data in vitro were obtained from mixed glial cultures 24 h after plating. Data in vivo were from P2, P10 and P30 tissue sections. NeuN = Neuron-specific nuclear protein; $MAP2_{a–b}$ = 2a & 2b isoforms of the microtubule-associated protein; ND = not determined.

et al. [46] could actually reflect a lower GFP sensitivity, or an unfavorable insertional position, since only one single line was obtained in this study.

One of the most promising aspects of the CNP-GFP mice is to provide a very convenient tool for investigating OP cell function within the adult CNS. These adult OPCs, of which so little is known, represent approximately 5–8% of the total CNS glial population [85]. Adult OPCs are commonly identified by staining with antibodies to NG2 chondroitin sulfate proteoglycan or PDGFRα [86, 87]. Although dividing slowly in situ, adult OP cells represent the major proliferating cell population of the adult CNS, with as much as 70% of the adult NG2+ cells being proliferative in the spinal cord and in the cortex, as shown by BrdU incorporation experiments [83, 88]. We anticipate that the CNP-GFP mice, or any equivalent model, could help addressing the following issues concerning adult OP cells: (i) to what extent can these cells be multipotent in vivo, (ii) how can their proliferative capacities be recruited to generate significant myelin repair through the production of new oligodendrocytes in various CNS demyelinating injuries and (iii) what are the factors influencing adult OP cell cycle state and migrating properties, and are these two parameters linked in vivo?

The analysis of neuron-OP cell interactions [81] is another interesting and outstanding issue which might be enlightened by the use of CNP-GFP mice. The presence of OP cell processes at the nodes of Ranvier and at synapses [89, 90], as well as the breakthrough demonstration that OP cells receive direct synaptic input from glutamate-releasing hippocampal neurons [91] suggest that a functional crosstalk exists between neurons and OP cells. As it is now clear that astrocytes are actively tuning synapse formation and function [92–97], the CNP-GFP mice should help to elucidate whether some of the physiological roles attributed to astrocytes at the level of the synaptic cleft might be actually also carried out, at least partially, by immature oligodendrocytes.

In conclusion, we anticipate that besides the broad interest of in vivo studies directly using our CNP-GFP mice, conditional loss/gain-of-function CNP-promoter-driven transgenic models, as well as double transgenes combining CNP-GFP profile with inducible dysmyelination models [98], may bring outstanding insights helping to identify the multiple functions of OP cells in health and disease.

Acknowledgments

This work was supported by the *NICHD* intramural program. We thank Dr. Michel Gravel (McGill University, Montreal) for kindly providing the 3.7-kb mouse CNP promoter sequence. We are grateful to R. Chittajallu for his critical comments on the manuscript. S.B. is supported by the 'Fonds National de la Recherche Scientifique'.

References

1 Miller RH: Oligodendrocyte origins. Trends Neurosci 1996;19:92–96.
2 Rogister B, Ben-Hur T, Dubois-Dalcq M: From neural stem cells to myelinating oligodendrocytes. Mol Cell Neurosci 1999;14:287–300.
3 Lee JC, Mayer-Proschel M, Rao MS: Gliogenesis in the central nervous system. Glia 2000;30:105–121.
4 Sternberger NH, Itoyama Y, Kies MW, Webster H deF: Immunocytochemical method to identify basic protein in myelin-forming oligodendrocytes of newborn rat C.N.S. J Neurocytol 1978;7:251–263.
5 Hartman BK, Agrawal HC, Agrawal D, Kalmbach S: Development and maturation of central nervous system myelin: Comparison of immunohistochemical localization of proteolipid protein and basic protein in myelin and oligodendrocytes. Proc Natl Acad Sci USA 1982;79:4217–4420.
6 Kurihara T, Nussbaum JL, Mandel P: 2′,3′-Cyclic nucleotide 3′-phosphohydrolase in brains of mutant mice with deficient myelination. J Neurochem 1970;17:993–997.
7 Readhead C, Popko B, Takahashi N, Shine HD, Saavedra RA, Sidman RL, Hood L: Expression of a myelin basic protein gene in transgenic shiverer mice: Correction of the dysmyelinating phenotype. Cell 1987;48:703–712.
8 Turnley AM, Morahan G, Okano H, Bernard O, Mikoshiba K, Allison J, Bartlett PF, Miller JF: Dysmyelination in transgenic mice resulting from expression of class I histocompatibility molecules in oligodendrocytes. Nature 1991;353:566–569.
9 Yoshioka T, Feigenbaum L, Jay G: Transgenic mouse model for central nervous system demyelination. Mol Cell Biol 1991;11:5479–5486.
10 Miskimins R, Knapp L, Dewey MJ, Zhang X: Cell and tissue-specific expression of a heterologous gene under control of the myelin basic protein gene promoter in transgenic mice. Brain Res Dev Brain Res 1992;65:217–221.
11 Gow A, Friedrich VL Jr, Lazzarini RA: Myelin basic protein gene contains separate enhancers for oligodendrocyte and Schwann cell expression. J Cell Biol 1992;119:605–616.
12 Foran DR, Peterson AC: Myelin acquisition in the central nervous system of the mouse revealed by an MBP-Lac Z transgene. J Neurosci 1992;12:4890–4897.
13 Jensen NA, Pedersen KM, Celis JE, West MJ: Neurological disturbances, premature lethality, and central myelination deficiency in transgenic mice overexpressing the homeo domain transcription factor Oct-6. J Clin Invest 1998;101:1292–1299.
14 Tani M, Fuentes ME, Peterson JW, Trapp BD, Durham SK, Loy JK, Bravo R, Ransohoff RM, Lira SA: Neutrophil infiltration, glial reaction, and neurological disease in transgenic mice expressing the chemokine N51/KC in oligodendrocytes. J Clin Invest 1996;98:529–539.
15 Taupin V, Renno T, Bourbonnière L, Peterson AC, Rodriguez M, Owens T: Increased severity of experimental autoimmune encephalomyelitis, chronic macrophage/microglial reactivity, and demyelination in transgenic mice producing tumor necrosis factor-alpha in the central nervous system. Eur J Immunol 1997;27:905–913.
16 Ma W, Ribeiro-da-Silva A, Noel G, Julien JP, Cuello AC: Ectopic substance P and calcitonin gene-related peptide immunoreactive fibres in the spinal cord of transgenic mice over-expressing nerve growth factor. Eur J Neurosci 1995;7:2021–2035.
17 Goudreau G, Carpenter S, Beaulieu N, Jolicoeur P: Vacuolar myelopathy in transgenic mice expressing human immunodeficiency virus type 1 proteins under the regulation of the myelin basic protein gene promoter. Nat Med 1996;2:655–661.
18 Hayes C, Kelly D, Murayama S, Komiyama A, Suzuki K, Popko B: Expression of the neu oncogene under the transcriptional control of the myelin basic protein gene in transgenic mice: Generation of transformed glial cells. J Neurosci Res 1992;31:175–187.
19 Jensen NA, Pedersen KM, Celis JE, West MJ: Failure of central nervous system myelination in MBP/c-myc transgenic mice: Evidence for c-myc cytotoxicity. Oncogene 1998;16:2123–2129.
20 Hisahara S, Araki T, Sugiyama F, Yagami Ki, Suzuki M, Abe K, Yamamura K, Miyazaki J, Momoi T, Saruta T, Bernard CC, Okano H, Miura M: Targeted expression of baculovirus p35 caspase inhibitor in oligodendrocytes protects mice against autoimmune-mediated demyelination. EMBO J 2000;19:341–348.
21 Niwa-Kawakita M, Abramowski V, Kalamarides M, Thomas G, Giovannini M: Targeted expression of Cre recombinase to myelinating cells of the central nervous system in transgenic mice. Genesis 2000;26:127–129.
22 Nagy A: Cre recombinase: The universal reagent for genome tailoring. Genesis 2000;26:99–109.
23 Sauer B: Inducible gene targeting in mice using the Cre/lox system. Methods 1998;14:381–392.
24 Chalfie M, Tu Y, Euskirchen G, Ward WW, Prasher DC: Green fluorescent protein as a marker for gene expression. Science 1994;263:802–805.
25 Tsien RY: The green fluorescent protein. Annu Rev Biochem 1998;67:509–544.
26 Jordan C, Friedrich V Jr, Dubois-Dalcq M: In situ hybridization analysis of myelin gene transcripts in developing mouse spinal cord. J Neurosci 1989;9:248–257.
27 Kanfer J, Parenty M, Goujet-Zalc C, Monge M, Bernier L, Campagnoni AT, Dautigny A, Zalc B: Developmental expression of myelin proteolipid, basic protein, and 2′,3′-cyclic nucleotide 3′-phosphodiesterase transcripts in different rat brain regions. J Mol Neurosci 1989;1:39–46.
28 Ikenaka K, Kagawa T, Mikoshiba K: Selective expression of DM-20, an alternatively spliced myelin proteolipid protein gene product, in developing nervous system and in nonglial cells. J Neurochem 1992;58:2248–2253.
29 Timsit SG, Bally-Cuif L, Colman DR, Zalc B: DM-20 mRNA is expressed during the embryonic development of the nervous system of the mouse. J Neurochem 1992;58:1172–1175.
30 Milner RJ, Lai C, Nave KA, Lenoir D, Ogata J, Sutcliffe JG: Nucleotide sequences of two mRNAs for rat brain myelin proteolipid protein. Cell 1985;42:931–939.
31 Diehl HJ, Schaich M, Budzinski RM, Stoffel W: Individual exons encode the integral membrane domains of human myelin proteolipid protein. Proc Natl Acad Sci USA 1986;83:9807–9811.
32 Gardinier MV, Macklin WB, Diniak AJ, Deininger PL: Characterization of myelin proteolipid mRNAs in normal and jimpy mice. Mol Cell Biol 1986;6:3755–3762.
33 Willard HF, Riordan JR: Assignment of the gene for myelin proteolipid protein to the X chromosome: Implications for X-linked myelin disorders. Science 1985;230:940–942.
34 Mattei MG, Alliel PM, Dautigny A, Passage E, Pham-Dinh D, Mattei JF, Jollès P: The gene encoding for the major brain proteolipid (PLP) maps on the q-22 band of the human X chromosome. Hum Genet 1986;72:352–353.
35 Campagnoni AT, Skoff RP: The pathobiology of myelin mutants reveal novel biological functions of the MBP and PLP genes. Brain Pathol 2001;11:74–91.
36 Agrawal HC, Burton RM, Fishman MA, Mitchell RF, Prensky AL: Partial characterization of a new myelin protein component. J Neurochem 1972;19:2083–2089.
37 Trifilieff E, Luu B, Nussbaum JL, Roussel G, Espinosa de los Monteros A, Sabatier JM, Van Rietschoten J: A specific immunological probe for the major myelin proteolipid. Confirmation of a deletion in DM-20. FEBS Lett 1986;198:235–239.
38 Nave KA, Lai C, Bloom FE, Milner RJ: Splice site selection in the proteolipid protein (PLP) gene transcript and primary structure of the DM-20 protein of central nervous system myelin. Proc Natl Acad Sci USA 1987;84:5665–5669.
39 Simons R, Alon N, Riordan JR: Human myelin DM-20 proteolipid protein deletion defined by cDNA sequence. Biochem Biophys Res Commun 1987;146:666–671.
40 Bongarzone ER, Campagnoni CW, Kampf K, Jacobs EC, Handley VW, Schonmann V, Campagnoni AT: Identification of a new exon in the myelin proteolipid protein gene encoding novel protein isoforms that are restricted to the somata of oligodendrocytes and neurons. J Neurosci 1999;19:8349–8357.
41 Nave KA, Lemke G: Induction of the myelin proteolipid protein (PLP) gene in C6 glioblastoma cells: Functional analysis of the PLP promotor. J Neurosci 1991;11:3060–3069.

42 Cook JL, Irias-Donaghey S, Deininger PL: Regulation of rodent myelin proteolipid protein gene expression. Neurosci Lett 1992;137:56–60.

43 Berndt JA, Kim JG, Hudson LD: Identification of cis-regulatory elements in the myelin proteolipid protein (PLP) gene. J Biol Chem 1992;267:14730–14737.

44 Wight PA, Duchala CS, Readhead C, Macklin WB: A myelin proteolipid protein-LacZ fusion protein is developmentally regulated and targeted to the myelin membrane in transgenic mice. J Cell Biol 1993;123:443–454.

45 Spassky N, Goujet-Zalc C, Parmantier E, Olivier C, Martinez S, Ivanova A, Ikenaka K, Macklin W, Cerruti I, Zalc B, Thomas JL: Multiple restricted origin of oligodendrocytes. J Neurosci 1998;18:8331–8343.

46 Fuss B, Mallon B, Phan T, Ohlemeyer C, Kirchhoff F, Nishiyama A, Macklin WB: Purification and analysis of in vivo-differentiated oligodendrocytes expressing the green fluorescent protein. Dev Biol 2000;218:259–274.

47 Vogel US, Thompson RJ: Molecular structure, localization, and possible functions of the myelin-associated enzyme 2′,3′-cyclic nucleotide 3′-phosphodiesterase. J Neurochem 1988;50: 1667–1677.

48 Sprinkle TJ: 2′,3′-Cyclic nucleotide 3′-phosphodiesterase, an oligodendrocyte-Schwann cell and myelin-associated enzyme of the nervous system. Crit Rev Neurobiol 1989;4:235–301.

49 Scherer SS, Braun PE, Grinspan J, Collarini E, Wang DY, Kamholz J: Differential regulation of the 2′,3′-cyclic nucleotide 3′-phosphodiesterase gene during oligodendrocyte development. Neuron 1994;12:1363–1375.

50 Monoh K, Kurihara T, Sakimura K, Takahashi Y: Structure of mouse 2′,3′-cyclic-nucleotide 3′-phosphodiesterase gene. Biochem Biophys Res Commun 1989;165:1213–1220.

51 Kurihara T, Monoh K, Sakimura K, Takahashi Y: Alternative splicing of mouse brain 2′,3′-cyclic-nucleotide 3′-phosphodiesterase mRNA. Biochem Biophys Res Commun 1990;170: 1074–1081.

52 Douglas AJ, Thompson RJ: Structure of the myelin membrane enzyme 2′,3′-cyclic nucleotide 3′-phosphodiesterase: Evidence for two human mRNAs. Biochem Soc Trans 1993;21: 295–297.

53 Gravel M, DeAngelis D, Braun PE: Molecular cloning and characterization of rat brain 2′,3′-cyclic nucleotide 3′-phosphodiesterase isoform 2. J Neurosci Res 1994;38:243–247.

54 O'Neill RC, Minuk J, Cox ME, Braun PE, Gravel M: CNP2 mRNA directs synthesis of both CNP1 and CNP2 polypeptides. J Neurosci Res 1997;50:248–257.

55 Gravel M, Di Polo A, Valera PB, Braun PE: Four-kilobase sequence of the mouse CNP gene directs spatial and temporal expression of lacZ in transgenic mice. J Neurosci Res 1998; 53:393–404.

56 Chandross KJ, Cohen RI, Paras P Jr, Gravel M, Braun PE, Hudson LD: Identification and characterization of early glial progenitors using a transgenic selection strategy. J Neurosci 1999;19:759–774.

57 Yuan X, Chittajallu R, Gallo V: In vivo identification, characterization and FACS purification of oligodendrocyte lineage cells using a CNP-GFP transgenic mouse model. Abstr Soc Neurosci Meet (Ref N 1496) 2001.

58 Richardson WD, Smith HK, Sun T, Pringle NP, Hall A, Woodruff R: Oligodendrocyte lineage and the motor neuron connection. Glia 2000;29:136–142.

59 Spassky N, Olivier C, Perez-Villegas E, Goujet-Zalc C, Martinez S, Thomas Jl, Zalc B: Single or multiple oligodendroglial lineages: A controversy. Glia 2000;29:143–148.

60 Pringle NP, Richardson WD: A singularity of PDGF alpha-receptor expression in the dorsoventral axis of the neural tube may define the origin of the oligodendrocyte lineage. Development 1993;117:525–533.

61 Pringle NP, Yu WP, Guthrie S, Roelink H, Lumsden A, Peterson AC, Richardson WD: Determination of neuroepithelial cell fate: Induction of the oligodendrocyte lineage by ventral midline cells and sonic hedgehog. Dev Biol 1996;177:30–42.

62 Timsit S, Martinez S, Allinquant B, Peyron F, Puelles L, Zalc B: Oligodendrocytes originate in a restricted zone of the embryonic ventral neural tube defined by DM-20 mRNA expression. J Neurosci 1995;15:1012–1024.

63 Yu WP, Collarini EJ, Pringle NP, Richardson WD: Embryonic expression of myelin genes: Evidence for a focal source of oligodendrocyte precursors in the ventricular zone of the neural tube. Neuron 1994;12:1353–1362.

64 Hardy RJ, Friedrich VL Jr: Oligodendrocyte progenitors are generated throughout the embryonic mouse brain, but differentiate in restricted foci. Development 1996;122:2059–2069.

65 Calver AR, Hall AC, Yu WP, Walsh FS, Heath JK, Betsholtz C, Richardson WD: Oligodendrocyte population dynamics and the role of PDGF in vivo. Neuron 1998;20:869–882.

66 Fruttiger M, Karlsson L, Hall AC, Abramsson A, Calver AR, Boström H, Willetts K, Bertold CH, Heath JK, Betsholtz C, Richardson WD: Defective oligodendrocyte development and severe hypomyelination in PDGF-A knockout mice. Development 1999;126:457–467.

67 Briscoe J, Ericson J: The specification of neuronal identity by graded sonic hedgehog signalling. Semin Cell Dev Biol 1999;10:353–362.

68 Briscoe J, Pierani A, Jessell TM, Ericson J: A homeodomain protein code specifies progenitor cell identity and neuronal fate in the ventral neural tube. Cell 2000;101:435–445.

69 Orentas DM, Hayes JE, Dyer KL, Miller RH: Sonic hedgehog signaling is required during the appearance of spinal cord oligodendrocyte precursors. Development 1999;126:2419–2429.

70 Poncet C, Soula C, Trousse F, Kan P, Hirsinger E, Pourquié O, Duprat AM, Cochard P: Induction of oligodendrocyte progenitors in the trunk neural tube by ventralizing signals: Effects of notochord and floor plate grafts, and of sonic hedgehog. Mech Dev 1996;60:13–32.

71 Sussel L, Marin O, Kimura S, Rubenstein JL: Loss of Nkx2.1 homeobox gene function results in a ventral to dorsal molecular respecification within the basal telencephalon: Evidence for a transformation of the pallidum into the striatum. Development 1999;126:3359–3370.

72 Nery S, Wichterle H, Fishell G: Sonic hedgehog contributes to oligodendrocyte specification in the mammalian forebrain. Development 2001; 128:527–540.

73 Lu QR, Yuk D, Alberta JA, Zhu Z, Pawlitzky I, Chan J, McMahon AP, Stiles CD, Rowitch DH: Sonic hedgehog-regulated oligodendrocyte lineage genes encoding bHLH proteins in the mammalian central nervous system. Neuron 2000;25:317–329.

74 Zhou Q, Wang S, Anderson DJ: Identification of a novel family of oligodendrocyte lineage-specific basic helix-loop-helix transcription factors. Neuron 2000;25:331–343.

75 Takebayashi H, Yoshida S, Sugimori M, Kosako H, Kominami R, Nakafuku M, Nabeshima Y: Dynamic expression of basic helix-loop-helix Olig family members: Implication of Olig2 in neuron and oligodendrocyte differentiation and identification of a new member, Olig3. Mech Dev 2000;99:143–148.

76 Kondo T, Raff M: Oligodendrocyte precursor cells reprogrammed to become multipotential CNS stem cells. Science 2000;289:1754–1757.

77 Zimmerman L, Parr B, Lendahl U, Cunningham M, McKay R, Gavin B, Mann J, Vassileva G, McMahon A: Independent regulatory elements in the nestin gene direct transgene expression to neural stem cells or muscle precursors. Neuron 1994;12:11–24.

78 Kawaguchi A, Miyata T, Sawamoto K, Takashita N, Murayama A, Akamatsu W, Ogawa M, Okabe M, Tano Y, Goldman SA, Okano H: Nestin-EGFP transgenic mice: Visualization of the self-renewal and multipotency of CNS stem cells. Mol Cell Neurosci 2001;17:259–273.

79 Malatesta P, Hartfuss E, Gotz M: Isolation of radial glial cells by fluorescent-activated cell sorting reveals a neuronal lineage. Development 2000;127:5253–5263.

80 Wegner M: Expression of transcription factors during oligodendroglial development. Microsc Res Tech 2001;52:746–752.

81 Gallo V, Ghiani CA: Glutamate receptors in glia: New cells, new inputs and new functions. Trends Pharmacol Sci 2000;21:252–258.

82 Ghiani C, Gallo V: Inhibition of cyclin E-cyclin-dependent kinase 2 complex formation and activity is associated with cell cycle arrest and withdrawal in oligodendrocyte progenitor cells. J Neurosci 2001;21:1274–1282.

83 Levine JM, Reynolds R, Fawcett JW: The oligodendrocyte precursor cell in health and disease. Trends Neurosci 2001;24:39–47.

84 Chittajallu R, Yuan X, McBain CJ, Gallo V: Electrophysiological characterization of oligodendrocyte cells in a CNP-GFP transgenic mouse model. Abstr Soc Neurosci Meet (Ref N 2727) 2001.
85 Dawson MR, Levine JM, Reynolds R: NG2-expressing cells in the central nervous system: Are they oligodendroglial progenitors? J Neurosci Res 2000;61:471–479.
86 Levine JM, Stincone F, Lee YS: Development and differentiation of glial precursor cells in the rat cerebellum. Glia 1993;7:307–321.
87 Nishiyama A, Yu M, Drazba JA, Tuohy VK: Normal and reactive NG2+ glial cells are distinct from resting and activated microglia. J Neurosci Res 1997;48:299–312.
88 Horner PJ, Power AE, Kempermann G, Kuhn HG, Palmer TD, Winkler J, Thal LJ, Gage FH: Proliferation and differentiation of progenitor cells throughout the intact adult rat spinal cord. J Neurosci 2000;20:2218–2228.
89 Ong WY, Levine JM: A light and electron microscopic study of NG2 chondroitin sulfate proteoglycan-positive oligodendrocyte precursor cells in the normal and kainate-lesioned rat hippocampus. Neuroscience 1999;92:83–95.
90 Butt AM, Duncan A, Hornby MF, Kirvell SL, Hunter A, Levine JM, Berry M: Cells expressing the NG2 antigen contact nodes of Ranvier in adult CNS white matter. Glia 1999;26:84–91.
91 Bergles DE, Roberts JD, Somogyi P, Jahr CE: Glutamatergic synapses on oligodendrocyte precursor cells in the hippocampus. Nature 2000;405:187–191.
92 Araque A, Carmignoto G, Haydon P: Dynamic signaling between astrocytes and neurons. Annu Rev Physiol 2001;63:795–813.
93 Haydon PG: GLIA: Listening and talking to the synapse. Nat Rev Neurosci 2001;2:185–193.
94 Ullian EM, Sapperstein SK, Christopherson KS, Barres BA: Control of synapse number by glia. Science 2001;291:657–661.
95 Oliet SHR, Piet R, Poulain DA: Control of glutamate clearance and synaptic efficacy by glial coverage of neurons. Science 2001;292:923–926.
96 Iino M, Goto K, Kakegawa W, Okado H, Sudo M, Ishiuchi S, Miwa A, Takayasu Y, Saito I, Tsuzuki K, Ozawa S: Glia-synapse interaction through Ca^{2+}-permeable AMPA receptors in Bergmann glia. Science 2001;292:926–929.
97 Gallo V, Chittajallu R: Unwrapping glial cells from the synapse: What lies inside? Science 2001;292:872–873.
98 Mathis C, Hindelang C, LeMeur M, Borrelli E: A transgenic mouse model for inducible and reversible dysmyelination. J Neurosci 2000;20:7698–7705.

7.2 Publication #2: Yuan,X., Chittajallu,R., Belachew,S., Anderson,S., McBain,C.J., and Gallo,V. (2002). Expression of the green fluorescent protein in the oligodendrocyte lineage: a transgenic mouse for developmental and physiological studies. *J. Neurosci. Res.* 70:529-545.

Journal of Neuroscience Research 70:529–545 (2002)

Expression of the Green Fluorescent Protein in the Oligodendrocyte Lineage: A Transgenic Mouse for Developmental and Physiological Studies

Xiaoqing Yuan,[1] Ramesh Chittajallu,[1] Shibeshih Belachew,[1] Stacie Anderson,[2] Chris J. McBain,[1] and Vittorio Gallo[1,3]*

[1]Laboratory of Cellular and Synaptic Neurophysiology, National Institute of Child Health and Human Development, National Institutes of Health, Bethesda, Maryland
[2]Gene Transfer Laboratory, Hematopoiesis Section, Flow Cytometry Core Unit, National Human Genome Research Institute, National Institutes of Health, Bethesda, Maryland
[3]Center for Neuroscience Research, Children's Research Institute, Children's National Medical Center, Washington, DC

We generated a transgenic mouse expressing the enhanced green fluorescent protein (EGFP) under the control of the 2′-3′-cyclic nucleotide 3′-phosphodiesterase (CNP) promoter. $EGFP^+$ cells were visualized in live tissue throughout embryonic and postnatal development. Immunohistochemical analysis in brain tissue and in sciatic nerve demonstrated that EGFP expression was restricted to cells of the oligodendrocyte and Schwann cell lineages. EGFP was also strongly expressed in "adult" oligodendrocyte progenitors (OPs) and in gray matter oligodendrocytes. Fluorescence-activated cell sorting allowed high-yield purification of $EGFP^+$ oligodendrocyte-lineage cells from transgenic brains. Electrophysiological patch clamp recordings of $EGFP^+$ cells in situ demonstrated that OP cells displayed large outward tetraethylammonium (TEA)-sensitive K^+ currents and very small inward currents, whereas mature oligodendrocytes were characterized by expression of large inward currents and small outward K^+ currents. The proliferation rate of $EGFP^+$ cells in developing white matter decreased with the age of the animals and was strongly inhibited by TEA. Oligodendrocyte development and physiology can be studied in live tissue of CNP-EGFP transgenic mice, which represent a source of pure $EGFP^+$ oligodendrocyte-lineage cells throughout development.

Key words: glia; potassium channels; 2′-3′-cyclic nucleotide 3′-phosphodiesterase promoter; Schwann cells

The cellular heterogeneity and functional complexity of the nervous system represent an obstacle for accurate developmental and physiological studies of specific cellular populations. The birth of distinct neural cell types occurs at different embryonic and postnatal ages; however, the time windows of their developmental maturation largely overlap (Jacobson, 1991; Brown et al., 2001), limiting the experimental analysis of individual classes of cells during development. These problems have been partially circumvented by using cell cultures comprising purified neural cell types (Banker and Goslin, 1992). However, the developmental and physiological properties of isolated cellular populations in vitro can largely differ from their in vivo counterpart because of changes in the microenvironment and the absence of appropriate cellular interactions (Luskin et al., 1988; Walz and MacVicar, 1988; Barres et al., 1990a,b; Butt, 1991; Espinosa de los Monteros et al., 1993).

Numerous transgenic mouse lines have recently been developed, based on the use of promoter/reporter gene constructs that are selectively expressed in distinct classes of neural cells (Brenner et al., 1994; Zhuo et al., 1997; Gravel et al., 1998; Spassky et al., 1998; Chandross et al., 1999; Fuss et al., 2000; Yamaguchi et al., 2000; Kawaguchi et al., 2001; Nolte et al., 2001; Mallon et al., 2002). In some of these transgenic mice, the major macroglial cell types, astrocytes and oligodendrocytes, have been identified by the selective expression of reporter genes, such as lacZ and the green fluorescent protein (GFP; Chalfie et al., 1994), that are directed by neural cell-specific promoters. Specifically, promoters for 2′-3′-cyclic nucleotide 3′-phosphodiesterase (CNP), proteolipid protein (PLP), and glial fibrillary acidic protein (GFAP) have all been used for

Contract grant sponsor: National Institute of Child Health and Human Development.

*Correspondence to: Dr. Vittorio Gallo, Center for Neuroscience Research, Children's Research Institute, Children's National Medical Center, 111 Michigan Avenue, N.W., Washington, DC 20010-2970.
E-mail: vgallo@cnmcresearch.org

Received 26 May 2002; Accepted 3 June 2002

this purpose (Brenner et al., 1994; Zhuo et al., 1997; Gravel et al., 1998; Spassky et al., 1998; Chandross et al., 1999; Fuss et al., 2000; Nolte et al., 2001; Mallon et al., 2002).

However, the transcriptional regulation and the sensitivity of the promoter/reporter gene system used in previous transgenic mice have imposed limits on both developmental and physiological studies. For example, identification of oligodendrocyte-lineage cells in the CNP-lacZ mouse requires manipulations of the tissue that prevent direct identification of living cells and physiological studies in intact preparations (Gravel et al., 1998; Chandross et al., 1999). We therefore sought to create a transgenic mouse that would allow direct identification of the oligodendrocyte and Schwann cell lineages in vivo throughout embryonic and postnatal development. For this purpose, to direct selective expression of enhanced GFP (EGFP) in oligodendrocytes and Schwann cells from the progenitor stage to the mature phenotype, we used the CNP promoter, whose transcriptional activity is specific to oligodendrocytes and Schwann cells and is sustained throughout development (Gravel et al., 1998).

In the present study we report that, in such a CNP-EGFP transgenic mouse, EGFP expression could be readily detected from embryonic day 10 to adulthood and was restricted to cells of the oligodendrocyte and Schwann cell lineages. Importantly, cells with a phenotype of "adult" oligodendrocyte progenitors (OP) could be identified in mature transgenic mouse brains. This class of cells was not identified by reporter gene expression in previous transgenic mice (Chandross et al., 1999). Visualization of EGFP-expressing cells in situ allowed direct electrophysiological recordings in acutely isolated brain slices and a study of the role of K^+ channels in the regulation of OP cell proliferation. Finally, the CNP-EGFP mouse described here allowed rapid isolation by fluorescence-activated cell sorting (FACS) of pure and viable oligodendrocyte-lineage cells. Importantly, the antigenic properties of these cellular fractions were identical to their counterpart before FACS isolation, indicating that the purified EGFP-expressing cells were representative of the EGFP-expressing cells in situ.

MATERIALS AND METHODS

Generation of Transgenic Mice

The CNP-EGFP transgene used for generation of transgenic mice was constructed as follows. A 3.7 kb XbaI-HindIII fragment containing mouse CNP promoters 1 and 2 (Gravel et al., 1998) was ligated upstream of a 1 kb SmaI-XhoI fragment containing the EGFP coding sequence (Clontech Laboratories, Inc., Palo Alto, CA). EGFP is a red-shifted variant (mutations F64L and S65T) of wild-type GFP that has been optimized for brighter fluorescence and higher expression in mammalian cells. The DNA construct was designed to have the first AUG of the EGFP coding sequence in frame with CNP promoter 2. The 3′-end of this fusion gene contained a poly-A signal from bovine growth hormone. A 4.7 kb XbaI-XhoI fragment (see Fig. 1) was excised, purified, and injected into fertilized oocytes from FVB/N and FVB/N × C57B6 (F1) genetic backgrounds.

To identify positive transgenic animals, founders were analyzed by both polymerase chain reaction (PCR) and Southern blot analysis, using genomic DNAs extracted from tail biopsies. Primers for PCR were designed based on the EGFP coding sequence: forward primer, 5′-GGGTGGTGCCCATCCTGGTCGAGC-3′; reverse primer, 5′-CCAGCATGCCTGCTATTGTCTTCCC-3′. A 925 bp fragment containing the EGFP coding sequences and part of the poly-A signal was used as probe for Southern hybridization. In total 12 positive founder mice were identified, with a balanced distribution in both genetic backgrounds (data not shown). The six male founders (founders A2, A3, and D2 were from FVB/N background, and C1, C4, and G5 were from FVB/N × CB6 background) were used to breed with FVB/N females. Transgene was transmitted to the offspring of all six lines (data not shown). No gross behavioral differences were noticeable in the CNP-EGFP mice compared with wild-type littermates.

The transgene copy number of the C1 CNP-EGFP line was determined by dot blot. Tail biopsy DNAs (20 μg) were denatured in 0.1 N NaOH, 0.5 M NaCl, and boiled for 5 minutes. After cooling on ice, DNAs were blotted by spotting on Hybond-N^+ membranes (Amersham Pharmacia Biotech, Buckinghamshire, England) and ultrviolet (UV) cross-linked. Known amounts of the EGFP DNA were also immobilized on the same blot. The blot was then hybridized to random primed, ^{32}P-labeled EGFP sequences. The hybridized blot was then exposed to a phosphor screen and later to X-ray film. Densitometry and comparison with the known amounts of EGFP sequence determined the transgene copy number. Densitometry was carried out using a STORM 860 scanner and ImageQuant (Molecular Dynamics, Inc. Sunnyvale, CA).

A preliminary analysis was carried out by visualizing the in vivo expression of EGFP in brain sections of P30 CNP-EGFP mice. Line C1 was selected for further studies because of the higher levels of fluorescence observed. Line G5 was eliminated because of low levels of EGFP expression. Line A3 was eliminated for poor breeding efficiency. Lines A2, C4, and D2 were maintained for future studies and for comparison with line C1. In all these lines, the morphology of the EGFP-expressing cells resembled that of oligodendrocytes or Schwann cells. All animal procedures were performed according to NIH guidelines.

Analysis of EGFP Expression and Immunohistochemistry in Tissue Sections and in Whole Tissue

Mice at P2, P10, and P30 were anesthetized following NIH guidelines, and perfused intracardiacly with 1× PBS and then 4% paraformaldehyde. Brains were dissected out, postfixed with 4% paraformaldehyde at 4°C overnight, and then transferred into a solution of 4% paraformaldehyde, 10% glycerol, in PBS for an overnight incubation at 4°C. Fixed brains were preserved in 20% glycerol in 1× PBS. Pregnant mice at gestational days 9.5–15.5 were anesthetized and perfused using 1× PBS. Embryos were dissected out and fixed with 4% paraformaldehyde at 4°C overnight, then treated as described above for brain tissue.

For tissue sections, brains or embryos were rinsed in 1× PBS, then frozen in Tissue Freezing Medium (Triangle Biomedical Sciences, Durham, NC) and mounted on a Microm HM400 microtome (Microm International GmbH, Walldorf, Germany). Sections were cut (50 μm) and stored in 1× PBS, 0.05% sodium azide solution.

For immunohistochemistry, frozen sections were blocked at room temperature for at least 1 hr in blocking solution [1% bovine serum albumin (BSA), 0.3% Triton X-100, and 20% normal serum in 1× PBS]. Primary antibodies were diluted using carrier solution (1% BSA, 0.3% Triton X-100 in 1× PBS). Rabbit polyclonal antibody to NG2 (a kind gift of Dr. J. Levine, SUNY, Stony Brook, NY) was diluted 1:500. The monoclonal antibody to CNP (Sternberger Monoclonals, Lutherville, MD) was diluted 1:250. Monoclonal antibody to myelin basic protein (MBP; Sternburger Monoclonals) was diluted 1:1,000. The monoclonal antibody RIP (hybridoma supernatant was produced by ATCC) was diluted 1:1. The rabbit polyclonal antibody to GFAP (Chemicon International, Inc., Temecula, CA) was diluted 1:250. The monoclonal antibody against β-tubulin III TUJ1 (BabCO, Richmond, CA) was diluted 1:250. The monoclonal anti-L1 antibody (Boehringer Mannheim, Indianapolis, IN) was diluted 1:10. Brain sections were incubated in primary antibodies at 4°C overnight. Rinse was carried out in carrier solution at room temperature, with three changes of solution every 10 min. All secondary antibodies (Jackson Immunoresearch Laboratories, West Grove, PA) were diluted 1:200 in carrier solution. TRITC-conjugated goat anti-mouse IgG was used for all monoclonal antibodies. TRITC-conjugated goat anti-rabbit IgG was used for all rabbit polyclonal antibodies. Incubation was carried out at room temperature for 1 hr, followed by three washes as described above. Sections were then transferred into 1× PBS and mounted with Mowiol. All fluorescence microscopy images were obtained on a Zeiss Axiophot or on a Nikon microscope equipped with a Bio-Rad MRC 1024 laser scanning confocal system.

Cultures of Oligodendrocyte Progenitor Cells and Schwann Cells

Cortical OP cultures were prepared from P1 CNP-EGFP transgenic mice (Ghiani et al., 1999a) using the protocol previously described for rat OP cultures, with slight modifications (McCarthy and deVellis, 1980; Gallo and Armstrong, 1995; Gallo et al., 1996). OPs were plated onto poly-L-lysine-treated 12 mm coverslips at a density of 50,000 cells/coverslip and cultured in DMEM-N1 medium, in the presence of platelet-derived growth factor (PDGF) and basic fibroblast growth factor (bFGF; 10 ng/ml of each; both from Upstate Biotechnology, Lake Placid, NY) for 24–48 hr.

Schwann cell cultures were prepared and maintained as previously described (Stevens et al., 1998). Cells were cultured in 5HS MEM N3 + G medium for 5 days before immunocytochemical staining.

Immunostaining of cultured oligodendrocyte-lineage cells and Schwann cells was performed as previously described (Gallo and Armstrong, 1995; Yuan et al., 1998). For cell surface markers, coverslips were washed in 1× HBSS (Gibco BRL, Rockville, MD) briefly. Rabbit polyclonal antibody to NG2 (1:1,000) and mouse monoclonal antibodies (IgM) O4 (1:10) and O1 (1:10) were diluted as indicated in 1× HBSS. Cells were incubated with primary antibodies for 30–60 min at room temperature, followed by three washes in 1× HBSS. TRITC-conjugated goat anti-rabbit antibody was used for NG2 antibody, and TRITC-conjugated goat anti-mouse IgM antibody was used for O4 and O1. All secondary antibodies were from Jackson Immunoresearch Laboratories and were diluted 1:200 using 1× HBSS. After incubation at room temperature for 30 min and three washes with 1× HBSS, coverslips were fixed with 4% paraformaldehyde in 1× PBS at room temperature for 15 min. After three further washes in 1× PBS, coverslips were mounted in Mowiol.

For intracellular antigens, coverslips were fixed with 4% paraformaldehyde in 1× PBS at room temperature for 10 min, then permeabilized using 0.1% Triton X-100 at room temperature for 10 min. Coverslips were then treated with a blocking solution at room temperature for 1 hr. The monoclonal antibodies to CNP (Stemberger Monoclonals; 1:250), S100β (Chemicon; 1:2,000), and GFAP (Chemicon; 1:500) were diluted in carrier solution. Cells were incubated in primary antibodies for 1 hr at 4°C. Cells were then washed as previously described and incubated in TRITC-conjugated goat anti-mouse IgG (1:200) for 30 min at 4°C. After three washes, coverslips were rinsed in 1× PBS and mounted in Mowiol.

Preparation of Total Cell Suspensions and FACS

Brains were dissected from P3 or P5 CNP-EGFP mice and wild-type littermates. After meninges removal, brain tissue was cut into small pieces and incubated in enzyme solution (15 U/ml papain, 100 U/ml DNaseI) at 37°C for 20 min. Digested tissue was gently passed through needles in the gauge order of 19 × 1, 21 × 1, and 23 × 1 inches. Cell suspensions were then diluted 5× using DMEM-N1 + 10% fetal bovine serum (FBS) and filtered through a 70 μm cell strainer (Becton Dickinson, Franklin Lakes, NJ). After centrifugation, cells were resuspended in DMEM-N1 + 10% FBS to a density of 10^7 cells/ml for sorting. A fraction of the cell suspension was plated onto poly-L-lysine (30 μg/ml)-coated 25 mm coverslips at a density of 2×10^6 cells/coverslip and incubated at 37°C, 10% CO_2 for 1 hr. These cells were used as pre-FACS cells for further immunocytochemical characterization.

Cells were analyzed for light forward- and side-scatter using a FACS Vantage SE instrument (Becton Dickinson, San Jose, CA). For EGFP fluorescence, excitation wavelength of the argon ion laser was set at 488 nm, and emission was through a 530 nm bandpass filter. Cells from the negative littermates were used to set the background fluorescence, and a size threshold was used to gate out erythrocytes and cellular debris. The sorting speed was 2,000–4,000 cells/sec.

For double NG2/EGFP and O4/EGFP FACS analysis, cell suspensions were initially incubated with appropriate primary antibodies (see immunocytochemistry discussion) and then with Cy-5-conjugated secondary antibodies (1:200; Jackson Immunoresearch Laboratories) prior to any sorting. Cy-5 fluorescence was excited with an HeNe laser (633 nm) and filtered with a 675 nm longpass filter.

Sorted cells were rinsed at least once with growth medium (DMEM-N1 + 10% FBS), resuspended, and plated onto poly-L-lysine-coated 12 mm coverslips at a density of 50,000 cells/

coverslip. After 1 hr of incubation at 37°C, 10% CO_2, culture medium was changed to DMEM-N1 + 0.5% FBS with the addition of 10 ng/ml PDGF and bFGF, respectively. Cells were cultured at 37°C, 10% CO_2, for a further 48 hr, with an addition of growth factors every 24 hr. Cells cultured for 1 hr after FACS and cells cultured for 48 hr in PDGF + bFGF were used for further immunocytochemical analysis. In some experiments, cells were also treated with L-3,3′,5-triiodothyronine sodium salt (T3 hormone; Calbiochem, La Jolla, CA) after mitogen withdrawal.

Electrophysiological Recordings From EGFP$^+$ Cells in Acutely Isolated Slices

Young (P5–P8) or adult (P27–P30) CNP-EGFP mice were sacrificed following NIH Animal Welfare Guidelines, and 300 μm sagittal sections were obtained using a Leica VT1000S vibratome. After a 1 hr recovery period, slices were transferred to a recording chamber and perfused with an extracellular solution of the following composition (in mM): NaCl 124, KCl 3, $CaCl_2$ 2.5, $MgSO_4$ 1.3, $NaHCO_3$ 26, $NaHPO_4$ 1.25, glucose 15, 1 μM tetrodotoxin, saturated with 95% O_2/5% CO_2 at room temperature.

EGFP$^+$ cells in the subventricular zone (SVZ) of young mice and myelinating EGFP$^+$ cells in corpus callosum of adult mice were identified with an upright Olympus BX50WI microscope fitted with an Olympus BX-FLA reflected light fluorescent attachment and a U-MWIBA filter cube (excitation 460–490 nm; emission 515–550 nm). EGFP$^+$ cells were then approached under visual control using differential interference contrast optics coupled with infrared video microscopy.

Patch electrodes had resistances between 5 and 7 MΩ when filled with intracellular solution of the following composition (in mM): K-gluconate 130, NaCl 10, Mg-ATP 2, Na-GTP 0.3, HEPES 10, EGTA 0.6, adjusted to pH 7.4 and 275 mOsm. The series resistances (which were typically 20 MΩ), input resistances, and membrane capacitances were calculated from the capacitive transients and steady-state currents resulting from a 5 mV test pulse filtered at 10 kHz. To elicit sustained outward voltage-dependent K^+ currents (I_K), cells were voltage clamped at –70 mV, and a prepulse to –50 mV for 100 msec was applied to inactivate the A-type transient outward K^+ currents (I_A), followed immediately by a series of voltage steps from –70 mV to 50 mV for 200 msec (10 mV increments; 0.1 Hz). To ascertain whether EGFP$^+$ cells possessed I_A, the prepulse was altered to –110 mV prior to the voltage steps. The transient currents could then be isolated by digital subtraction of these traces from the traces obtained with the –50 mV prepulse (Knutson et al., 1997). In young animals, capacitive and transient leak currents were subtracted online using the P/N leak subtraction method. To measure inward rectifying K^+ currents (I_{Kir}), a voltage step was applied to –140 mV for 200 msec from a holding potential of –70 mV. I_{Kir} were isolated by digitally subtracting the current obtained in the presence of bath-applied Cs^+ (5 mM) from that obtained under control conditions.

To test the effects of drug application (10 mM TEA, 30 μM kainate, and 10 μM DNQX) on I_K, a test pulse to +50 mV was elicited at 0.1 Hz, and drugs were perfused directly into the recording chamber via the extracellular solution. In all the experiments, currents were recorded using an Axopatch 1D amplifer (Axon Instruments, Burlingame, CA), filtered at 5 kHz, and digitized at 10 kHz. All membrane potentials were adjusted for a calculated junction potential of 13.7 mV, and offline analysis was performed using the Clampfit analysis program (Axon Instruments).

Analysis of EGFP$^+$ Cell Proliferation in Slice Cultures

Brains were dissected from P2, P10, and P20 CNP-EGFP mice. Cerebellar sagittal sections (400 μm) and cerebral coronal sections (400 μm) were sliced using a McIlwain tissue chopper (Mickle Laboratory Engineering Co. Ltd.). Slices were cultured using the interface method (Yuan et al., 1998). Two or three tissue slices were placed on each LCR sterile filter (0.5 μm pore size), which was laid on sterilized sieves (Netwell Inserts, 24 mm diameter, 500 μm mesh size; Fisher Scientific, Pittsburgh, PA), and cultured in DMEM-N1 medium containing 10% FBS (Hyclone, Logan, UT) in six-well tissue culture plates (Falcon, Becton Dickinson, Franklin Lakes, NJ). After 48 hr in culture in the presence or in the absence of tetraethylammonium (TEA, 10 mM), tissue slices were fixed in 4% paraformaldehyde at 4°C for 16 hr, followed by three washes in 1× PBS at room temperature. Fixed slices were further treated with 100% methanol at –20°C for 15 min.

After three washes in PBS, slices were subjected to staining for proliferating cell nuclear antigen (PCNA) with specific antibodies. Blocking and antibody binding were carried out as described above for immunohistochemistry on frozen sections. Monoclonal anti-PCNA (Sigma, St. Louis, MO) antibody was used at 1:1,000 dilution. A TRITC-conjugated goat anti-mouse IgG (1:2,000; Jackson Immunoresearch Laboratories) was used as secondary antibody. Stained slices were mounted in Mowiol and subjected to image analysis using a Nikon microscope equipped with a Bio-Rad MRC 1024 laser scanning confocal system. Areas of developing white matter were scanned, and an average of 10 images was taken for each experimental condition under 40× magnification. Total EGFP$^+$ and EGFP$^+$/PCNA$^+$ cells were quantified.

RESULTS

Generation of CNP-EGFP Transgenic Mice: EGFP Fluorescence Is Detected in the Oligodendrocyte Lineage From Embryonic Age to Adulthood

Transgenic mice were generated using the DNA construct shown in Figure 1A (upper panel). EGFP expression was under the control of the entire CNP promoter region, comprising the two promoters CNP1 and CNP2, previously characterized by Gravel et al. (1998). The making of the CNP-EGFP DNA construct and the generation of the transgenic lines are described in detail in Materials and Methods. We determined gene copy number in the founder (F0 generation) of the transgenic mouse line C1 by dot blot analysis of genomic tail DNA with an EGFP cDNA probe (Fig. 1A, lower panel). Comparison with a standard demonstrated that five gene copies were integrated in the C1 (+/–) mouse (Fig. 1A, lower panel).

We first analyzed the distribution pattern of EGFP$^+$ cells in sagittal and coronal tissue sections obtained from

the postnatal brain of the C1 line. At P10, a high density of EGFP$^+$ cells were found in subcortical, brainstem, and cerebellar white matter regions and in the olfactory bulb (Fig. 1B). At P30, high levels of EGFP expression were notable in cells of the corpus callosum, which displayed the typical oligodendrocyte morphology (Fig. 1C).

Figure 2 shows the distribution pattern of EGFP$^+$ cells at different stages of embryonic development in mouse tissue sections derived from the same transgenic line C1. Embryonic age E10 was the first developmental time point analyzed (Fig. 2A; letters in parentheses below refer to Fig. 2A). EGFP expression was detected in the ventricular and subventricular zones of the lateral (a), third (d), and fourth (c) ventricles. The neuroepithelia surrounding the nasal cavity (e) also displayed EGFP expression. Many EGFP$^+$ cells were found in the basal telencephalic plate (f), medulla (g), and ventral region of the spinal cord (h). Finally, in the peripheral nervous system (PNS), EGFP-expressing cells were present in neural crest cells and efferent nerves of the spinal cord (l), in sacral plexus (j), and in vagus nerve (k).

The distribution pattern of EGFP expression in the embryonic spinal cord of CNP-EGFP mice is shown in Figure 2B–D. At E12.5, EGFP-expressing cells were restricted to the ventral neuroepithelium of the spinal cord (Fig. 2B), whereas, at later developmental stages (E15.5 and E18.5), EGFP$^+$ cells were dispersed throughout the gray matter, with very few cells still present in the ventricular zone (Fig. 2C,D). At E18.5, the number of EGFP$^+$ cells was significantly higher than at E15.5, and cells strongly expressing the transgene were scattered throughout the entire spinal cord (Fig. 2D). In the adult spinal cord, a high density of EGFP$^+$ cells was found in the ventral and dorsal funiculus, whereas scattered green fluorescent oligodendroglial cells were visualized in areas of the gray matter (Belachew et al., 2001).

In conclusion, the pattern of CNP-driven EGFP distribution in the developing mouse CNS indicates that EGFP expression is detected at early embryonic stages of development and is maintained throughout maturation of the brain. Importantly, in the embryo, the distribution pattern of EGFP-expressing cells is similar to that of well-established OP markers, such as *Pdgfrα*, *Olig1*, and *Olig2* (Yu et al., 1994; Lu et al., 2000; Zhou et al., 2000). These observations, combined with the morphological and antigenic characteristics (see below) of the EGFP-expressing

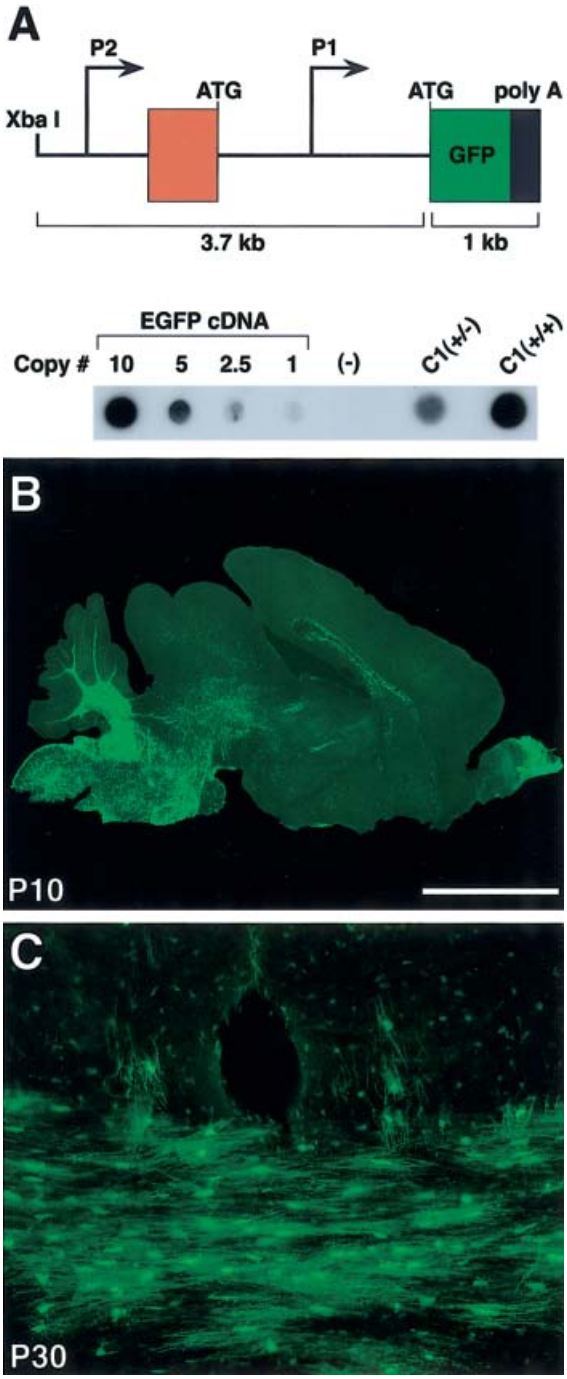

Fig. 1. Schematic diagram of the DNA construct used to generate the CNP-EGFP transgenic mice and analysis of transgene copy number. **A:** Upper panel: The CNP promoters that specifically direct oligodendroglial expression are indicated as CNP1 and CNP2, and the EGFP sequence is shown in green. The orange box denotes exon 0 of the CNP gene. The purple box indicates the polyadenylation sequence from bovine growth hormone. The relative size of the individual sequences and the total size of the construct are also indicated. Lower panel: Dot-blot analysis of transgene copy number in the CNP-EGFP transgenic mouse line C1. Tail genomic DNA from the C1 founder and F2 homozygous mouse was hybridized with an EGFP cDNA probe and compared with EGFP DNA standards. **B:** Sagittal section (50 μm) of a P10 transgenic mouse brain. Abundant EGFP expression was confined to white matter tracts. **C:** Coronal section (50 μm) of a P30 transgenic mouse brain, showing strong EGFP expression in cells of the corpus callosum. Scale bar = 3 mm in B; 190 μm in C.

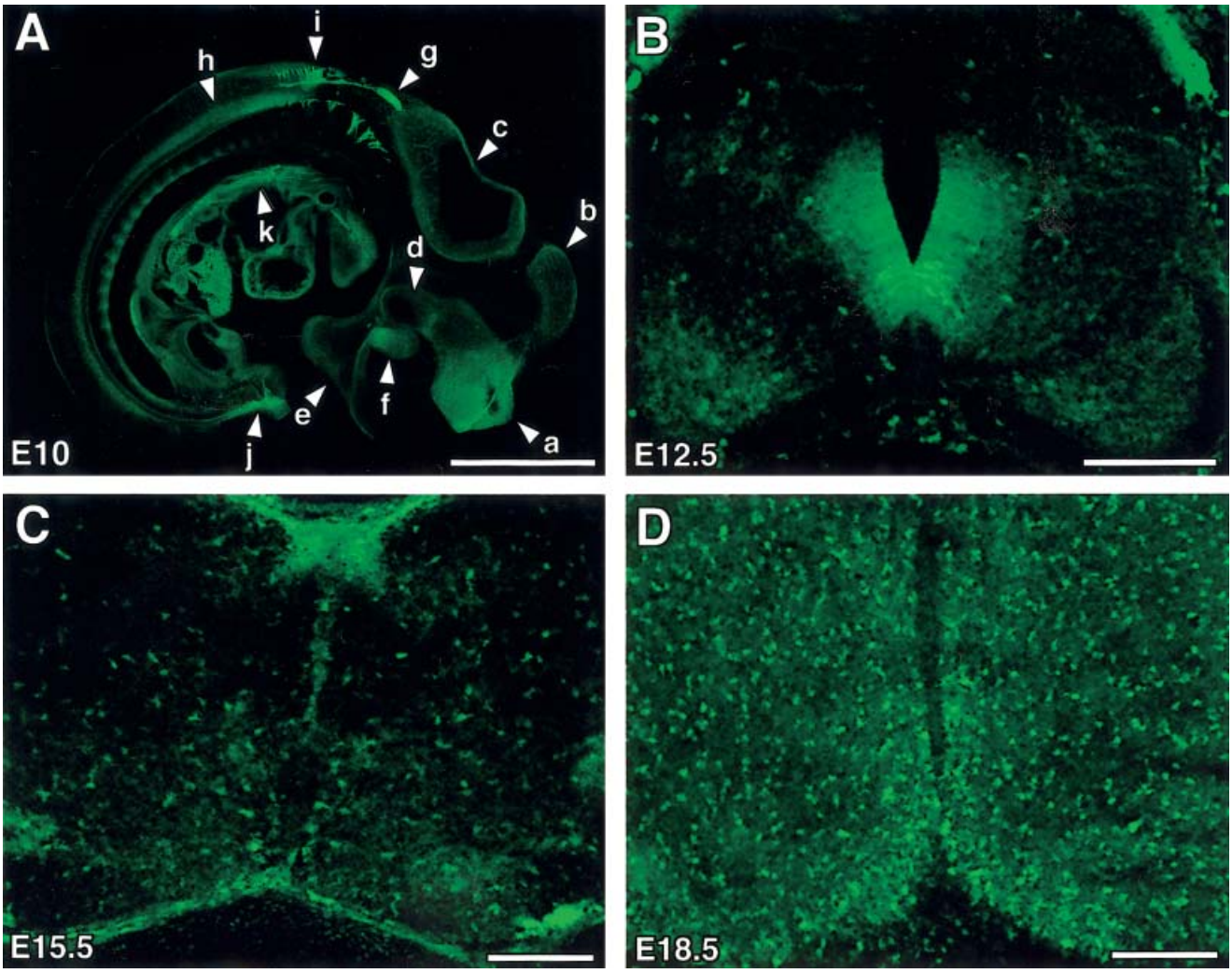

Fig. 2. EGFP fluorescence is detected in cells of the oligodendrocyte lineage during embryonic development. **A:** Whole-mount sagittal section (50 μm) of an E9.5 transgenic mouse embryo. In the brain, EGFP was expressed in the ventricular and subventricular zones of lateral ventricle (a), aqueduct (b), fourth ventricle (c), and third ventricle (d) as well as the neuroepithelia surrounding the nasal cavity (e). EGFP expression was also found in the regions of basal telencephalic plate (f) and medulla (g). EGFP was also expressed throughout the spinal cord, mainly in the ventral region (h). In the PNS, EGFP expression was observed in neural crest cells and nerves projecting from the spinal cord (i), in sacral plexus (j), and in vagus nerve (k). **B–D:** Transverse sections of embryonic mouse midthoracic spinal cord. At E12.5 (B), EGFP-expressing cells are restricted to the ventral neuroepithelium of the spinal cord; at E15.5 (C) and E18.5 (D), EGFP-expressing cells are dispersed throughout the gray matter. Scale bars = 1.5 mm in A; 100 μm in B–D.

cells in the postnatal brain, indicate that EGFP is expressed at high levels in cells of the oligodendrocyte lineage.

Immunohistochemical Characterization of EGFP-Expressing Cells During Postnatal Development In Vivo Reveals an Oligodendrocytic Phenotype

To identify definitively the $EGFP^+$ cells in postnatal transgenic mouse brains, fluorescent cells were extensively characterized by immunohistochemistry, using antibodies that identify different classes of neural cells. At P2, the majority (80.9% ± 1.8%; average ± SEM) of the $EGFP^+$ cells (260 total $EGFP^+$ cells counted) of the SVZ and developing subcortical white matter were stained with the OP marker NG2 (Levine et al., 1993; Fig. 3A–C). Importantly, all the $NG2^+$ cells in the SVZ were $EGFP^+$.

To verify that EGFP expression was still confined to cells of the oligodendrocyte lineage at mature developmental stages (i.e., that deregulation of transgene expression had not occurred), we performed a series of immunostainings using P30 brain sections (Fig. 3D–I). In white matter regions, such as corpus callosum, the cell bodies and processes of all green fluorescent cells were stained with the mature oligodendrocyte markers anti-CNP (Fig.

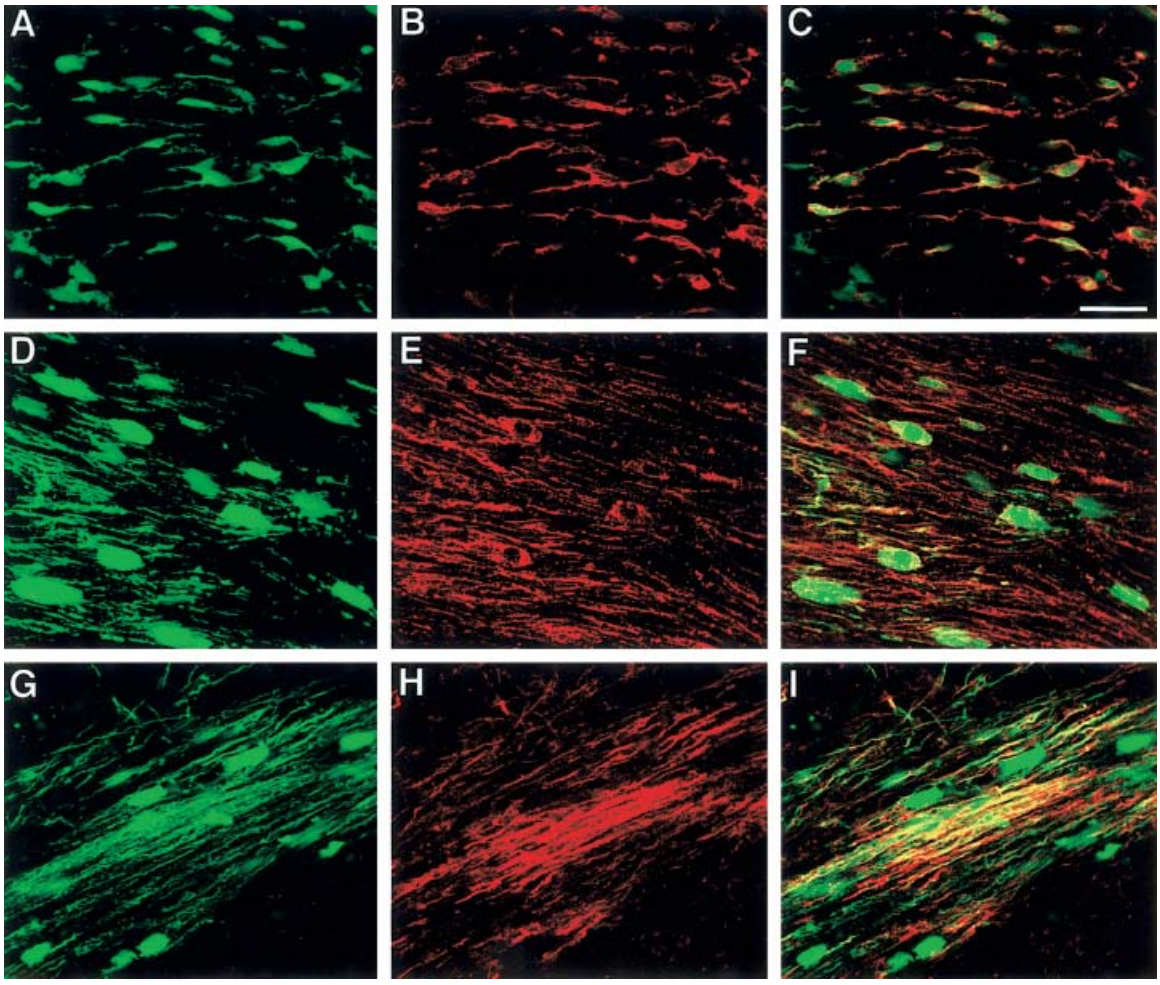

Fig. 3. Immunocytochemical characterization of EGFP-expressing cells in the postnatal mouse brain indicates an oligodendrocyte phenotype. Microtome frozen sagittal brain sections (50 μm) were obtained from P2 (**A–C**) and P30 (**D–I**) transgenic CNP-EGFP mice. A–C: Staining with anti-NG2 antibody (B; red fluorescence) in the SVZ shows that the vast majority of EGFP-expressing cells (A; green fluorescence) is also $NG2^+$ (C; merged). By P30, in corpus callosum, the majority of EGFP-expressing cells (D; green fluorescence) are also stained with anti-CNP antibodies (E; red fluorescence) both in their cell bodies and in their processes (F; merged). At the same age, staining with anti-MBP (H; red fluorescence) shows that EGFP-expressing cells (G; green fluorescence) in corpus callosum are also MBP^+ (I; merged). Scale bar = 30 μm in A–C,G–I; 20 μm in D–F.

3D–F). $EGFP^+$ cell processes were also stained with anti-MBP (Fig. 3G–I) and RIP (data not shown). Direct cell counting demonstrated that 100% of the $EGFP^+$ cells were stained with anti-CNP or RIP antibodies (120–125 total $EGFP^+$ cells counted for each marker). Also at P30, both in the SVZ and in subcortical white matter, $EGFP^+$ cells did not express GFAP (Fig. 4A–C) and were not stained with the neuronal marker NeuN (Fig. 4D–F). Identical results were also obtained in cerebellar white matter (data not shown). Thus, in corpus callosum (Figs. 3, 4) and in cerebellar white matter (data not shown), EGFP expression at P30 was clearly still oligodendrocyte specific. The CNP immunoreactivity of EGFP-expressing cells (Fig. 3D–F) was predicted by our transgenic strategy and confirmed that the transgene was correctly expressed in cells that translate the CNP protein.

It is noteworthy that the well-characterized quiescent adult $NG2^+$ OPs (Levine et al., 2001) were also $EGFP^+$ (Fig. 5A–C). These cells were identified both in the SVZ (Fig. 5A,B) and in cortical gray matter (Fig. 5C) at P30. In the SVZ, 58.2% ± 3.3% (average ± SEM) of the $EGFP^+$ cells were $NG2^+$ (96 total $EGFP^+$ cells counted). In gray matter, two populations of $EGFP^+$ cells were identified. One cell population displayed a stellate morphology and was also stained with NG2 (Fig. 5C; 50.3% ± 2.5% of $EGFP^+$ cells; 257 total $EGFP^+$ cells counted), whereas the other displayed typical white matter oligodendrocyte morphology with parallel processes and was stained with anti-CNP (Fig. 5D). These latter cells represented only a small percentage of the $EGFP^+$ cells in the cortical gray matter. At P30, both in the SVZ and in the gray matter, all the $NG2^+$ cells were also $EGFP^+$ (data

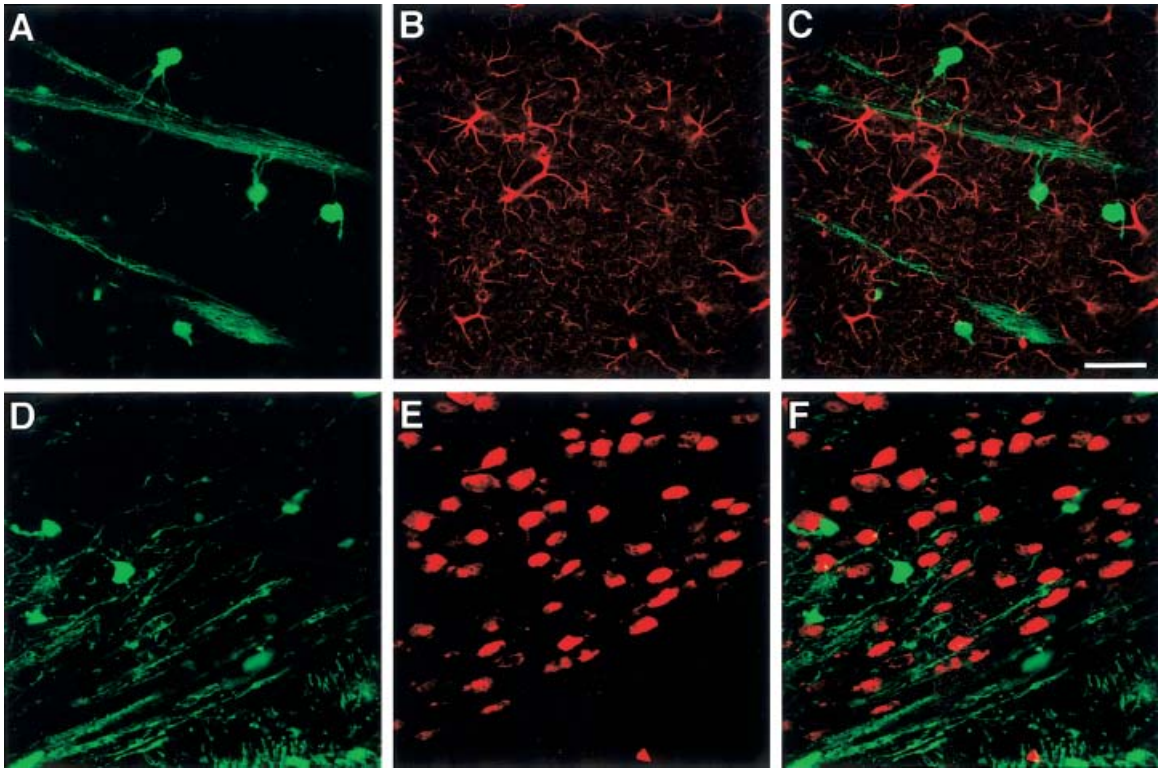

Fig. 4. EGFP-expressing cells in the postnatal mouse brain are not astrocytes or neurons. Microtome frozen sagittal brain sections (50 μm) were obtained from P30 transgenic CNP-EGFP mice. **A–C:** Staining with anti-GFAP antibody (B; red fluorescence) in corpus callosum shows that EGFP-expressing cells (A; green fluorescence) do not express GFAP (C; merged). **D–F:** In the same white matter region, staining with anti-NeuN antibody (B; red fluorescence) shows that EGFP-expressing cells (D) are NeuN-negative (F; merged). Scale bar = 30 μm.

not shown), indicating that subpopulations of $NG2^+$ cells cannot be distinguished based on CNP gene expression, as previously described for PLP-driven transgene (Mallon et al., 2002). In conclusion, the immunocytochemical characterization of $EGFP^+$ cells in CNP-EGFP mouse brain indicated that transgene expression was exclusive to cells of the oligodendrocyte lineage and was maintained from embryonic to adult developmental stages.

Characterization of EGFP-Expressing Cells in the PNS

The CNP gene is actively transcribed also in myelinating cells of the PNS, i.e., Schwann cells (Gravel et al., 1998). EGFP expression comparable to that found in the CNS was also detected in the PNS of CNP-EGFP mice. Intact sciatic nerves isolated from P2 and P30 mice contained a large number of $EGFP^+$ cells, as demonstrated in whole-mount preparations (Fig. 6A,B). At P30, both myelinating and nonmyelinating $EGFP^+$ Schwann cells were found in the nerves, as demonstrated by staining with anti-MBP and anti-L1 antibodies, respectively (data not shown). At this age, most CNP^+ cells in the nerve were MBP^+ and $L1^-$, but a small percentage of the CNP^+ cells were $L1^+$. When cells were isolated from P2 sciatic nerves and cultured under conditions that favored Schwann cell proliferation and differentiation, all $EGFP^+$ cells in the cultures expressed the Schwann cell marker S100β (Fig. 6C–E). These results indicate that also the pattern of EGFP expression in the PNS reflects that of the endogenous CNP gene (Gravel et al., 1998).

Selective EGFP Expression in Oligodendrocyte-Lineage Cells During Development in Culture

We wanted to determine whether EGFP expression was selectively maintained in cells of the oligodendrocyte lineage in culture. Cell culture methods also allow further immunocytochemical analysis of EGFP expression at different stages of oligodendrocyte development. We therefore used a previously established standard cell culture procedure (McCarthy and deVellis, 1980; Gallo and Armstrong, 1995; Ghiani et al., 1999a) to obtain pure OP cell cultures from CNP-EGFP mice.

OP cells were purified as previously described (Gallo and Armstrong, 1995; Ghiani et al., 1999a) by shaking them off mixed glial cultures that also contained astrocytes at day 12 in vitro. Figure 7A shows that, in mixed glial cultures before the purification procedure, none of the

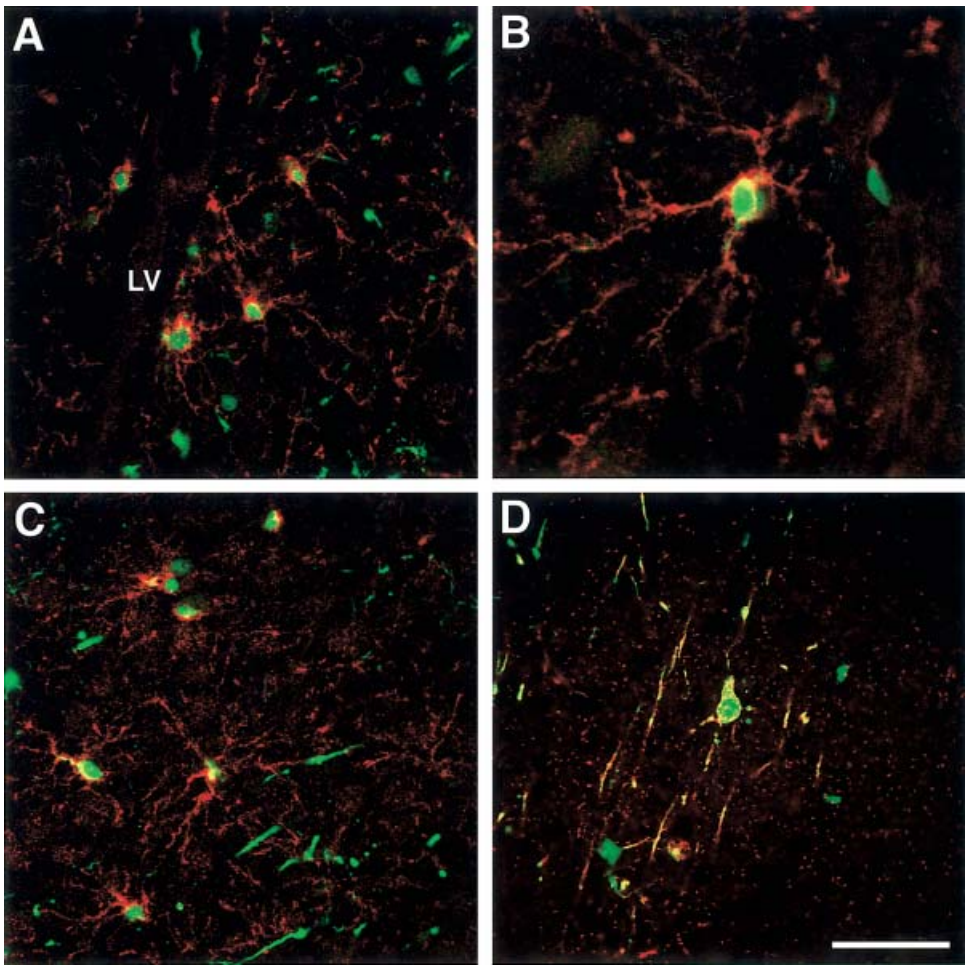

Fig. 5. EGFP fluorescence is detected in adult oligodendrocyte progenitor cells and in gray matter oligodendrocytes. Frozen brain coronal sections (50 μm) were obtained from P30 CNP-EGFP mice. Confocal images were obtained from the subventricular zone (A,B) and the cerebral cortex (C,D). **A:** Staining with NG2 antibody (red fluorescence) shows that, at P30, many $EGFP^+$ cells (green fluorescence) are still $NG2^+$ in the SVZ. **B:** High-magnification image of an $NG2^+$ (red)/$EGFP^+$ (green) cell in the SVZ at P30. **C:** Staining with NG2 antibody (red fluorescence) shows that, at P30, many $EGFP^+$ cells (green fluorescence) in the cortical gray matter are $NG2^+$. Note that the $NG2^+$/$EGFP^+$ cells display a radial morphology, with multiple, fine, branching processes. **D:** Staining with anti-CNP antibody (red fluorescence) shows that some $EGFP^+$ cells (green fluorescence) in the gray matter are also CNP^+. These CNP^+/$EGFP^+$ cells display the typical morphology of white matter oligodendrocytes. Scale bar = 50 μm in A,C,D; 20 μm in B.

$EGFP^+$ cells expressed the astrocytic marker GFAP. These results were consistent with the in vivo data shown in Figure 4.

After purification and 1 day of culturing in the presence of PDGF and bFGF, all the cells were $EGFP^+$, indicating that transgene expression was maintained in OP cells in culture (Fig. 7E). Within the EGFP-expressing cell population, most (84%) of the cells were $NG2^+$ (Fig. 7B,E), and a much smaller percentage was $O4^+$ (15%; Fig. 7C,E) or $O1^+$ (3%; Fig. 7D,E). These data indicate that, under cell culture conditions known to induce OP proliferation, $EGFP^+$ cells maintained a proliferative OP phenotype (Dubois-Dalcq, 1987; Gard and Pfeiffer, 1990; Hardy and Reynolds, 1991; Levine et al., 1993), i.e., were either $NG2^+$ or $O4^+$.

Purification of EGFP-Expressing Cells by FACS Generates a Pure Population of Cells With Antigenic Properties Identical to Those In Vivo

Purification of $EGFP^+$ cells by the standard cell culture procedures described above requires several days of maintaining OP cells in mixed glial cultures in vitro before the purification procedure itself. Such experimental manipulations may result in changes of the developmental and physiological properties of OP cells that may not entirely resemble those found in vivo. One of the advantages of selective EGFP expression in specific neural cell types in vivo is that FACS can be used to obtain pure populations of EGFP-expressing cells directly from brain tissue. We, therefore, used the FACS technique to purify

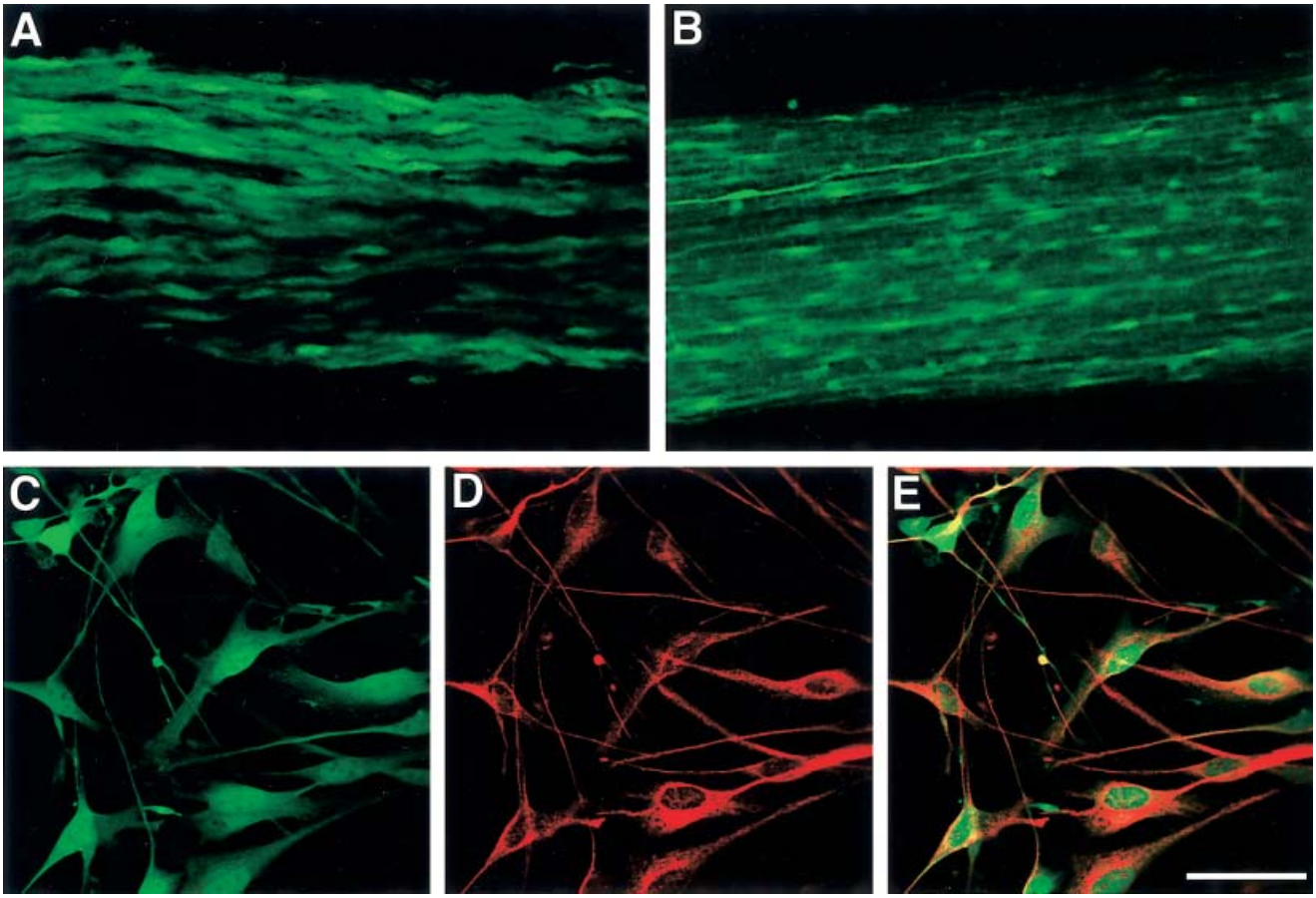

Fig. 6. EGFP expression in sciatic nerve and in Schwann cells during development. Whole mounts of sciatic nerves were prepared from CNP-EGFP transgenic mice at P2 (**A**) and P30 (**B**). Strong EGFP expression was detected in many cells at both developmental stages. **C–E:** Schwann cells were cultured and stained with anti-S100β antibodies. All $EGFP^+$ cells (C; green fluorescence) were also $S100\beta^+$ (D; red fluorescence). E: Merged. Scale bar = 50 μm in A; 100 μm in B; 30 μm in C–E.

EGFP-expressing cells from CNP-EGFP mice and analyze the antigenic properties (i.e., the cellular subtypes) of the purified cellular fractions.

The experiments shown in Figure 8 were performed on cell suspensions prepared from P3 or P5 mice. Background fluorescence was set from cell suspensions prepared from nontransgenic littermates (area outside of R2; Fig. 8A). Based on these criteria, at P5, 4.2% ± 0.9% of the total brain cells in the suspensions was sorted as $EGFP^+$ (R3 fraction; Fig. 8A; average ± SEM from a total of 21 transgenic brains from four independent sorting experiments).

To validate our fluorescence selection criteria, we analyzed the antigenic properties of cell suspensions before and after FACS. Cell suspensions were plated and fixed before and after FACS, and cells were stained with a variety of neural markers. Importantly, both before and after the sorting, 40–50% of the $EGFP^+$ cells from P5 mice were stained with the anti-NG2 or O4 antibodies, which identify proliferative stages of the oligodendrocyte lineage (Fig. 8B). Only 7% of the cells were stained with the mature oligodendrocyte marker O1 in both cell suspensions (Fig. 8B). Finally, none of the $EGFP^+$ cells was stained for the astrocytic marker GFAP or the neuronal marker NeuN (Fig. 8B). These experiments confirm that EGFP expression in the CNP transgenic mice is limited to oligodendrocyte-lineage cells and that the FACS procedure results in a 100% pure population of $EGFP^+$ cells (651 total cells counted) whose antigenic properties are identical to those in vivo.

By using the analytical mode of the FACS technique, we also analyzed ex vivo (i.e., immediately after enzymatic dissociation) NG2 and O4 immunophenotypes in P3 whole-brain cell suspensions. By taking into account the background fluorescence (upper left quadrants in Fig. 8C,D), cells from transgenic brains that were specifically stained with NG2 and O4 antibodies were all within the EGFP-expressing population (upper right quadrants in Fig. 8C,D). Therefore, NG2 and O4 staining of live cells in conjunction with direct FACS analysis confirmed that,

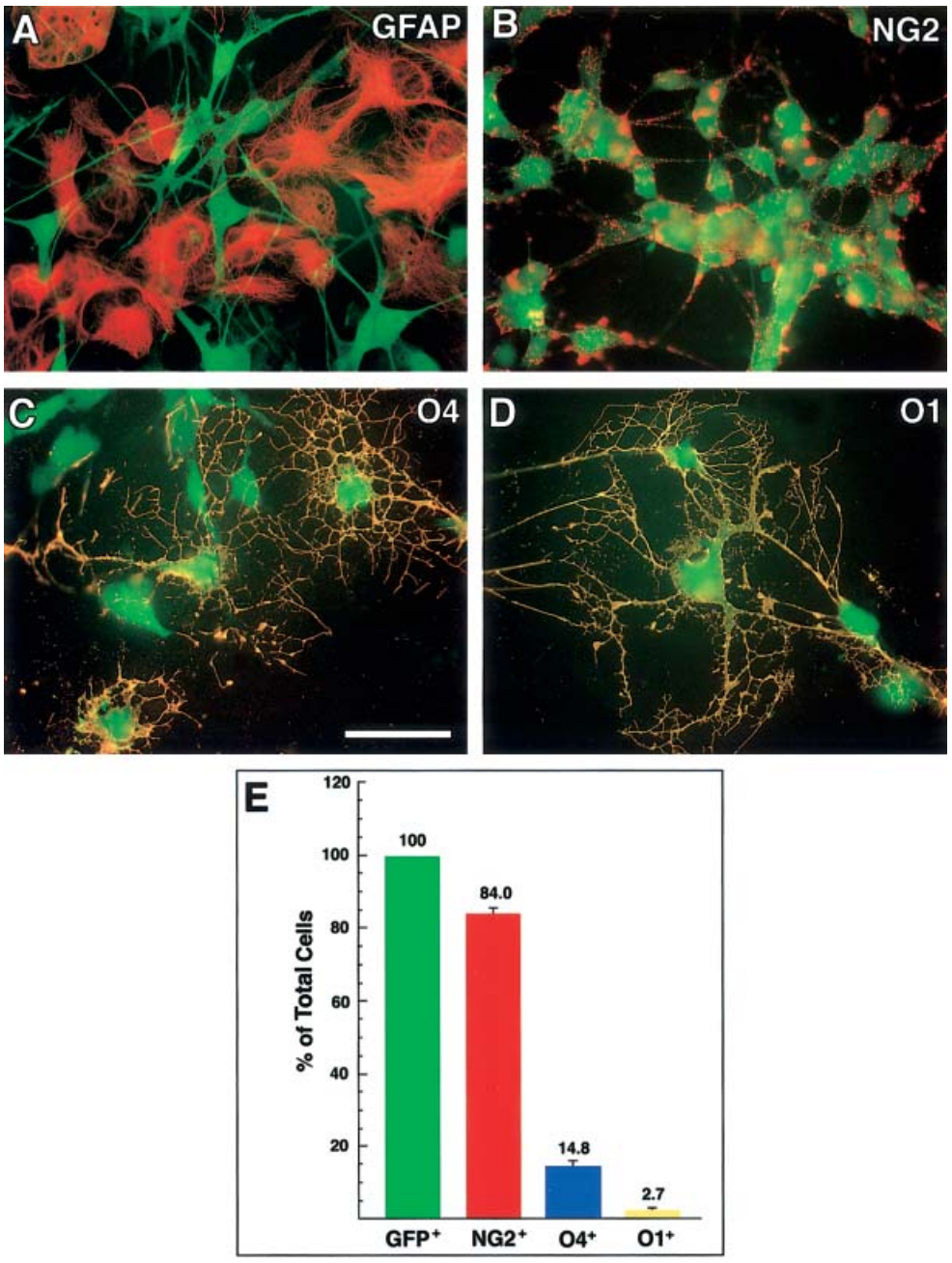

Fig. 7. EGFP-expressing OP cells develop into oligodendrocytes in culture. **A:** Mixed glial cortical cultures after 12 days in vitro and staining with anti-GFAP antibodies. None of the EGFP-expressing cells (green fluorescence) is stained for GFAP (red fluorescence). **B:** After the purification procedure (shaking and replating) and culturing in PDGF + bFGF for 1 day, most of the EGFP-expressing cells (green fluorescence) were stained with the OP marker NG2 (red fluorescence). **C,D:** A small percentage of the EGFP-expressing cells (green fluorescence) were $O4^+$ or $O1^+$ (red fluorescence) and displayed a multipolar differentiated morphology. **E:** Cell counting after 1 day in PDGF + bFGF shows that all cells express EGFP and that most of the cells display an OP ($NG2^+$) or preoligodendrocyte ($O4^+$) phenotype. Values shown are averages ± SEM obtained from one representative experiment (total cells counted 4,091; 20 microscopic fields/antibody). Scale bar = 30 μm.

in vivo, EGFP-expressing cells belong to the oligodendrocyte lineage.

When $EGFP^+$ cells FACS purified from P5 mice were cultured in the presence of PDGF and bFGF for 2 days, cells maintained EGFP expression, and all the major oligodendrocyte antigenic phenotypes could be identified in the cultures (data not shown). These were 72.8% ± 1.4% $NG2^+$ cells, 29.0% ± 1.6% $O4^+$ cells, and

12.4 ± 0.9 $O1^+$ cells (percentages of total cells; two independent experiments; 5,249 total $EGFP^+$ cells counted; 60 microscopic fields/antibody). After mitogen withdrawal and treatment with T3 hormone, CNP^+ and MBP^+ cells started to appear in the cultures (data not shown). These results further confirm that all the $EGFP^+$ cells purified by FACS belong to the oligodendrocyte lineage and that, in culture, they express antigenic properties of immature and mature oligodendrocytes.

Electrophysiological Characterization and Developmental Regulation of K^+-Channel Currents in $EGFP^+$ Cells

The CNP-EGFP mice allow electrophysiological recordings in acutely isolated slices at a variety of developmental stages, permitting examination of the changes in electrophysiological properties, and in particular K^+-channel expression, that occur as OP cells mature into oligodendrocytes in a relatively intact system. $EGFP^+$ cells located in the SVZ of mice aged 5–8 days and in the corpus callosum of mice aged 27–30 days were investigated. Figure 9A illustrates the morphology of the two types of $EGFP^+$ cells from which K^+ currents were analyzed and clearly shows the distinction between a $EGFP^+$ SVZ OP displaying few processes and small cell body (Fig. 9A, left panels) and a much larger $EGFP^+$ mature oligodendrocyte in the corpus callosum, with distinctive myelinating parallel processes (Fig. 9A, right panels).

All SVZ $EGFP^+$ cells tested (n = 14) expressed both I_K (sustained) and I_A (transient; Fig. 9B, top). The activation profile for I_K was described by a single Boltzmann equation and revealed a mean half-activation of –19 ± 2 mV (n = 8; k = 11; Fig. 9B, bottom). Figure 9C shows that I_K was sensitive to the K^+-channel blocker TEA (30% ± 4% of baseline, 4 min after TEA application; n = 6) in a reversible manner (89% ± 8% of baseline, 20 min after TEA washout; n = 6). Application of kainate (30 μM) also caused an inhibition of I_K (66% ± 6% of baseline, 8 min after kainate application; n = 8; Fig. 9D). The inhibition was significantly attenuated in the presence of the glutamate receptor antagonist DNQX (10 μM; 93% ± 2% of baseline, 8 min after kainate application in the presence of DNQX; n = 5; Fig. 9D), indicating the involvement of AMPA receptors in mediating the observed effect. The glutamate receptor-mediated block of K^+ channels observed in EGFP-expressing cells has been previously described from cultured rat OP cells (Borges and Kettenmann, 1995; Gallo et al., 1996) and $NG2^+$ OP cells in the SVZ of acutely isolated rat brain slices (Chittajallu et al., 2002).

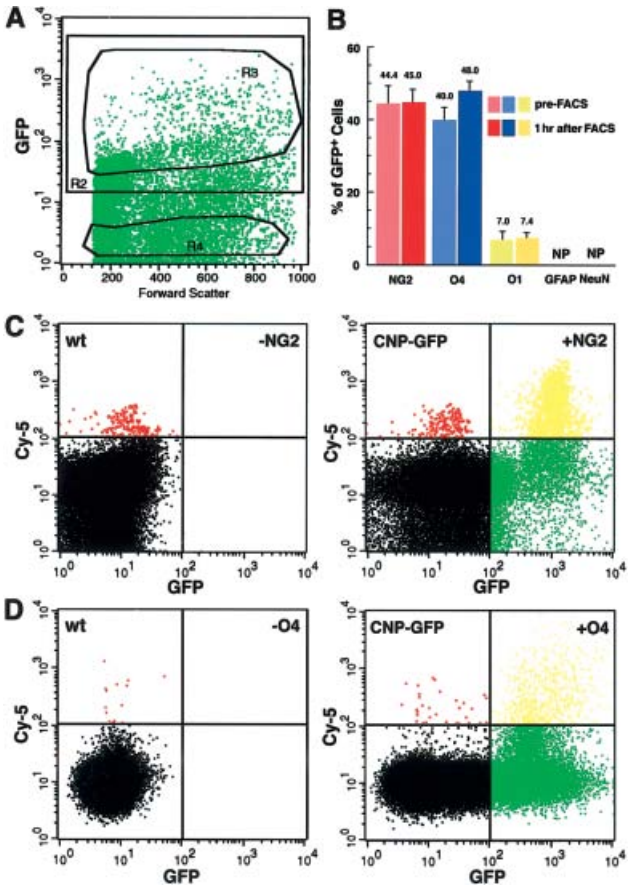

Fig. 8. Ex vivo-isolated $EGFP^+$ cells belong to the oligodendroglial lineage and can be efficiently purified by FACS. **A:** FACS analysis dot plot representation of EGFP fluorescence (y-axis; logarithmic scale) in total brain cell suspension from P5 CNP-EGFP transgenic mice. R4 box represents the population of cells selected as $EGFP^-$ based on the analysis of a control brain cell suspension from wild-type littermates processed in parallel (not shown). R2 represents a cell population in which <0.01% of wild-type cells were $EGFP^+$. R3 shows the window gate used for sorting CNP-$EGFP^+$ cells. **B:** Pre-FACS freshly isolated total-brain cell suspensions (light colors) and post-FACS $EGFP^+$ selected cells (dark colors) were plated for 1 hr before being fixed and immunostained with NG2 (red), O4 (blue), O1 (yellow), GFAP and NeuN antibodies. The phenotypic distribution of pre- and postsorting $EGFP^+$ cells was identical, demonstrating that our fluorescence criteria for FACS selection were appropriate. NP, not present. Data are averages ± SEM from the sorting experiment in A. The total number of cells cell counted was 2,072 for presorting (10 microscopic fields) and 2,192 for postsorting (20 microscopic fields). **C,D:** Acutely isolated living cell suspensions from P3 brains of transgenic mice (CNP-EGFP; right panels) were stained separately with NG2 (C) and O4 (D) antibodies and FACS analyzed without sorting. Three-color dot plot histograms show the distribution of living cells according to fluorescence intensity for EGFP (x-axis; logarithmic scale) and Cy-5 (secondary antibody recognizing NG2 and O4 immunoreactivity; y-axis; logarithmic scale). Lines represent thresholds beyond which <0.01% of the control cells were positive. Color codes were arbitrarily determined with respect to these threshold levels: black, $EGFP^-/Cy\text{-}5^-$; green, $EGFP^+/Cy\text{-}5^-$; red, $EGFP^-/Cy\text{-}5^+$ (defining background); and yellow, $EGFP^+/Cy\text{-}5^+$. As control conditions (left panels), cell suspensions were simultaneously isolated from wild-type brains (wt) and stained with Cy-5-conjugated secondary antibodies alone. Upper left quadrants of left panels thus determined the level of nonspecific immunostaining. By taking into account background levels, specific $NG2^+$ and $O4^+$ cells were found among exclusively the $EGFP^+$ population (upper right quadrants; yellow; right panels).

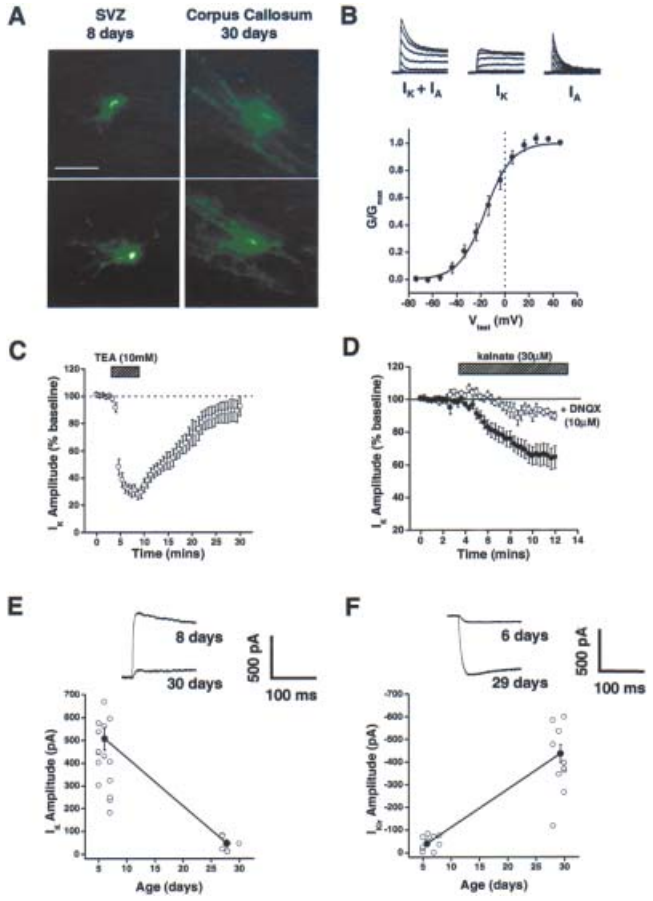

Fig. 9. Expression and developmental regulation of K^+-channel expression in $EGFP^+$ cells from acutely isolated slices. **A:** The two types of $EGFP^+$ cells from which K^+ currents were recorded. Left panels show typical SVZ $EGFP^+$ OP cells in young mice (5–8 days). Right panels show myelinating $EGFP^+$ cells in the corpus callosum of mice aged 27–30 days. **B:** Single example, from among a total of 14 SVZ $EGFP^+$ cells tested, expressing both I_K and I_A (top). Activation profile of I_K is fitted with a single Boltzmann equation and has a mean half-activation of –19 ± 2 mV (n = 8; bottom). **C:** I_K in SVZ $EGFP^+$ cells from young mice are sensitive to 10 mM TEA in a reversible manner (n = 6). **D:** Kainate at 30 μM also inhibits I_K, an effect that is attenuated in the presence of 10 μM DNQX (n = 5–8). **E:** I_K amplitude is significantly lower in myelinating $EGFP^+$ cells (46 ± 15 pA; n = 5) than in SVZ $EGFP^+$ cells (507 ± 59 pA; n = 15). **F:** I_{Kir} amplitude is significantly higher in myelinating $EGFP^+$ cells (–437 ± 38 pA; n = 10) than in SVZ $EGFP^+$ cells (–39 ± 10 pA; n = 10). Scale bar = 20 μm.

Previous analysis in cultured oligodendrocyte-lineage cells demonstrated that I_K and I_{Kir} expression are both developmentally regulated and correlate with the proliferative potential of these cells (Sontheimer et al., 1989; Knutson et al., 1997). The CNP-EGFP transgenic mouse allows for accurate identification of the oligodendrocyte lineage at different stages of lineage progression (Fig. 9A). Consistently with previous studies, a marked down-regulation of I_K is observed as $EGFP^+$ cells acquire a myelinating morphology that is characteristic of postmitotic, mature oligodendrocytes (Fig. 9E). Conversely a marked up-regulation of I_{Kir} is apparent as OP cells progress to a mature phenotype (Fig. 9F).

Proliferation Rate of EGFP-Expressing Cells Decreases During Development and Is Modulated by K^+-Channel Activity

In previous experiments, we demonstrated that organotypic slice cultures from rat cerebellum provide a valuable model with which to study OP development and investigate the role of ligand- and voltage-gated ionic channels in the regulation of OP proliferation (Yuan et al., 1998). These cultures offer the opportunity to study OP development in a cytoarchitecturally intact environment (Gähwiler et al., 1997). We wanted, therefore, to determine whether slice cultures from CNP-EGFP transgenic mice could be used to study OP proliferation in situ.

Figure 10A shows that, in slice cultures from P2 cerebellar tissue, many EGFP-expressing cells of the white matter were stained with anti-PCNA antibody, indicating that these cells were dividing. A similar pattern was also observed in subcortical white matter (data not shown). Figure 10B,C shows that OP cell proliferation in subcortical and cerebellar white matter, as measured by PCNA staining of $EGFP^+$ cells in slice cultures, decreased with aging of the animals from which the tissue was isolated. By P30, the proliferation rate of $EGFP^+$ cells in the white matter of both brain regions was four- to sevenfold lower than at P2 (Fig. 10B,C). Incubation of the slices with the K^+-channel blocker TEA for 48 hr, at the same concentration that caused an inhibition of I_K (Fig. 9C), caused a strong decrease in PCNA staining of $EGFP^+$ cells in both cerebellar (Fig. 10B) and subcortical (Fig. 10C) white matter at all developmental stages analyzed. These data are consistent with the physiological effects of TEA on K^+-channel activity in oligodendrocyte-lineage cells shown in Figure 9 and indicate that these channels are involved in the regulation of OP cell proliferation in situ (Ghiani et al., 1999b; Gallo and Ghiani, 2000).

DISCUSSION

In the present study, we generated a transgenic mouse that allows direct identification of oligodendrocytes in live tissue. To generate such a mouse, we took advantage of a gene promoter that comprises DNA elements that direct tissue- and cell-specific gene expression in oligodendrocytes and Schwann cells. The 4 kb CNP promoter region that we have used contains the two promoters for this gene, CNP1 and CNP2 (Gravel et al., 1998). These promoters are active at distinct developmental stages, because CNP2 mRNA transcripts are detected in embryonic brain, whereas CNP1 mRNA is found only after birth (Scherer et al., 1994). It has been previously shown that the combination of CNP1 and CNP2: 1) restricts reporter gene expression to the oligodendrocyte and Schwann cell lineages and 2) confers a gene expression pattern during development that recapitulates the complex spatiotemporal expression profile of the endogenous CNP

gene (Gravel et al., 1998; Chandross et al., 1999). Importantly, and in contrast to the case for other myelin genes, the onset of CNP gene transcription occurs at early embryonic developmental stages and is maintained in adulthood. This property makes the CNP promoter an ideal molecular tool with which to direct cell-specific heterologous gene expression in oligodendrocytes and Schwann cells during the entire development of the mammalian nervous system.

Previous studies have shown that *lacZ* gene expression, driven by the CNP promoter, displays a developmental time course identical to that of the endogenous gene (Gravel et al., 1998; Chandross et al., 1999). Our study is consistent with these previous findings, in that 1) we could detect EGFP expression as early as E10 in regions previously identified as containing oligodendrocyte precursors (Timsit et al., 1995; Miller, 1996; Gravel et al., 1998; Spassky et al., 1998; Chandross et al., 1999) and 2) green fluorescence was maintained throughout postnatal development in cells that displayed anatomical and morphological features of oligodendrocytes at different stages of maturation. Importantly, in our CNP-EGFP mouse, the origin and distribution pattern of $EGFP^+$ cells in the embryonic spinal cord is similar to the expression pattern of the oligodendrocyte-lineage gene markers *Pdgfr*α, *Olig1*, and *Olig2* (Yu et al., 1994; Lu et al., 2000; Zhou et al., 2000).

Several lines of evidence unequivocally demonstrate that the EGFP-expressing cells in the transgenic mouse described here are indeed oligodendrocytes. First, $EGFP^+$ cells were stained in situ with several antibodies that bind to developmentally regulated antigens expressed by cells of the oligodendrocyte lineage. These include NG2 for OPs and the myelin components CNP, MBP and the RIP antigen for mature oligodendrocytes. Experiments performed using the FACS technique demonstrated that, in early postnatal transgenic mouse brains, $NG2^+$ and $O4^+$ cells were all EGFP expressing, and no EGFP-negative cells were stained with NG2 or O4 antibodies. Second, $EGFP^+$ cells were not stained with astrocytic or neuronal markers (GFAP and NeuN, respectively) at any of the developmental stages analyzed either before or after FACS purification. Third, the vast majority of EGFP-expressing cells in adult mice was found in white matter regions. Finally, $EGFP^+$ cells isolated from transgenic mice at early postnatal developmental stages displayed an OP phenotype and gave rise to mature oligodendrocytes in culture.

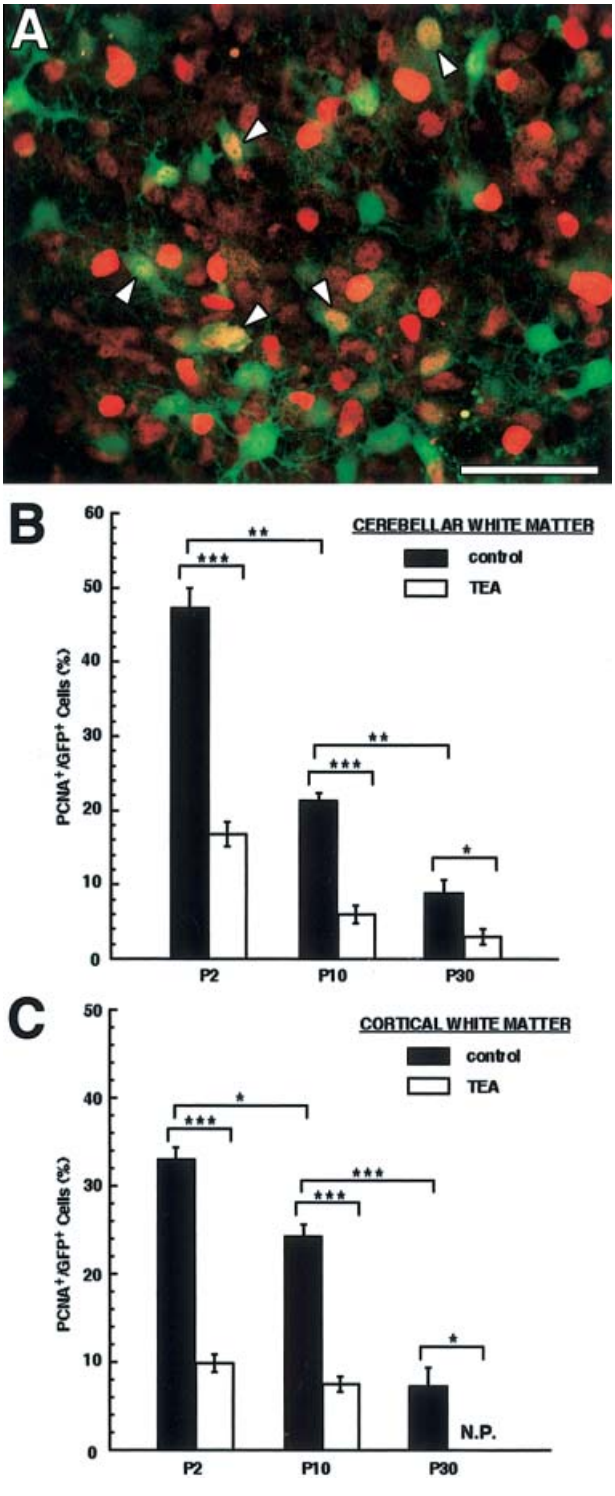

Fig. 10. Proliferation rate of $EGFP^+$ oligodendrocyte lineage cells decreases with age and is inhibited by blockage of K^+ channels. **A:** Confocal microscopic images of PCNA staining of 400 μm cerebellar sagittal slice cultures from P2 CNP-EGFP transgenic mouse brains. At P2, many oligodendrocyte-lineage cells (green) are PCNA positive (red). Arrowheads show examples of $PCNA^+/EGFP^+$ cells. **B,C:** Quantitative analysis of $EGFP^+$ cell proliferation in slice cultures from P2, P10, and P20 transgenic mouse brains. Two independent experiments were performed for each experimental condition (control and TEA treatment in cortical and cerebellar slices, respectively) at each developmental stage. An average of 400 cells was counted for each experimental condition from 10 distinct confocal images. Proliferation rates of oligodendrocytes decreased significantly from P2 to P20 in both subcortical and cerebellar white matter. TEA strongly inhibited oligodendrocyte-lineage cell proliferation at all three developmental stages analyzed. Data represent averages ± SEM; $***P < 0.001$, $**P < 0.01$, and $*P < 0.05$ (Student's *t*-test). Scale bar = 50 μm.

Compared with other transgenic mice previously generated by using oligodendrocyte-specific promoters, our CNP-EGFP mouse offers many advantages. The CNP-lacZ mouse reported by Chandross et al. (1999) allows analysis of oligodendrocyte development in situ; however, identification of the transgene-expressing cells cannot be directly performed in live, unfixed tissue and requires a biochemical reaction. In our transgenic mouse, $EGFP^+$ cells can easily be detected in live tissue throughout development. Furthermore, the reporter gene EGFP appears to be a more sensitive detection of promoter activity than *lacZ*, insofar as we were able easily to detect EGFP-expressing OP cells as early as E10 in mouse embryos.

A major advantage displayed by the CNP-EGFP mouse described here is that EGFP-expressing cells can be routinely purified by FACS from animals at different developmental stages. Furthermore, the antigenic characterization of the cells separated by this procedure clearly indicates that the purified cellular fraction is exclusively composed of cells of the oligodendrocyte lineage and that this fraction comprises the same cellular subtypes present in vivo. In fact, 100% of the cells separated by FACS under our experimental conditions were $EGFP^+$, and identical percentages of $NG2^+$, $O4^+$, and $O1^+$ cells were found within this population before and after sorting. This result indicates that the FACS-purified cellular fraction can, therefore, be used to study the cellular and biochemical properties of oligodendrocytes during development in situ. This finding opens several avenues for future applications of the CNP-EGFP mouse, including 1) study of the developmental potential of the EGFP-expressing cells in vitro and in vivo, 2) analysis of gene expression and gene profiling of oligodendrocytes during development in vivo, and 3) analysis of possible therapeutic applications of OP cell transplantation in vivo in pathological models of demyelination.

The electrophysiological characterization of the EGFP-expressing cells reported here supports several conclusions. First, it shows that it is possible to perform direct physiological studies on oligodendrocytes at various developmental stages without post hoc immunohistochemical characterization of the cells. Second, the finding that aspects of K^+ channel and GluR expression in $EGFP^+$ cells are identical to those previously described for rat oligodendrocyte-lineage cells in vitro and in vivo (Knutson et al. 1997; Yuan et al., 1998; Chittajallu et al., 2002) indicates that EGFP expression does not change the physiological properties of oligodendrocyte-lineage cells in our transgenic mouse. Third, our electrophysiological analysis shows that the CNP-EGFP transgenic mouse is a valuable tool with which to study in detail the regulation and physiological role of ligand- and voltage-gated channels in oligodendrocytes during development. For example, in a recent study, it was demonstrated that mice lacking the inwardly rectifying K^+-channel subunit Kir4.1 display a dysmyelinating phenotype (Neusch et al., 2001).

The CNP-EGFP mouse allows electrophysiological analysis of I_K and of I_{Kir} during development, and we have shown here that changes in both these currents occur as cells of the oligodendrocyte lineage mature. Finally, the possibility of direct electrophysiological analysis of oligodendrocytes in slice preparations opens new prospects to studies of neuron–oligodendrocyte interactions during development. For example, a recent report indicated that functional glutamatergic synapses exist between neurons and putative immature oligodendrocytes in the rat hippocampus (Bergles et al., 2000). Therefore, different types of cellular interactions might be established between neurons and oligodendrocytes during development. The CNP-EGFP mouse described here will greatly facilitate the analysis and physiological characterization of the synaptic connections between neurons and oligodendrocytes in the hippocampus and other parts of the CNS.

In the present study, we show that $EGFP^+$ cells in the developing white matter of early postnatal mice express large I_K similar to those previously described in proliferating rat OP cells (Gallo et al., 1996; Knutson et al., 1997; Yuan et al., 1998). We wanted to determine, based on previous findings showing that these K^+ channels are involved in the regulation of OP cell cycle progression (Knutson et al., 1997; Yuan et al., 1998; Ghiani et al., 1999b), 1) whether their blockage would also affect the proliferation of EGFP-expressing cells and 2) whether this could be directly studied in a slice preparation. Our analysis indicates that blockage of I_K in EGFP-expressing cells with TEA inhibited their proliferation, as directly visualized in cortical and cerebellar slices after PCNA staining. These results not only confirm the identity of the EGFP-expressing cells at early developmental stages as OPs but also indicate that EGFP tagging allows investigation of the relationship between membrane channel function and OP development in an intact preparation.

In conclusion, we have generated a transgenic mouse that allows developmental and functional studies of oligodendrocytes in vivo during the whole developmental time span of this class of cells. Our CNP-EGFP mouse not only represents a very important tool for study of oligodendrocyte development and function but also indicates that the CNP-EGFP DNA construct can be used as a molecular delivery system to overexpress selectively wild-type or dominant-negative mutant genes in cells of the oligodendrocyte lineage. Finally, the exciting prospect of crossing our CNP-EGFP mouse with other transgenic mutants (see, e.g., Neusch et al., 2001) will greatly enhance our knowledge of the effects of genetic manipulations on oligodendrocytes.

ACKNOWLEDGMENTS

We thank Michel Gravel and Peter Braun for the generous gift of the CNP promoter. We are particularly grateful to Joel Levine for the generous gift of the polyclonal NG2 antibody. We thank Douglas Fields and Beth Stevens for their help with analysis of EGFP expression in sciatic nerve and Schwann cells. R.C. was supported by a

Wellcome Trust Fellowship, and S.B. was supported by the Fonds National de la Recherche Scientifique (Belgium).

REFERENCES

Banker G, Goslin K. 1992. Culturing nerve cells. Cambridge, MA: MIT Press.

Barres BA, Koroshtez WJ, Chun LL, Corey DP. 1990a. Ion channel expression by white matter glia: the type-1 astrocyte. Neuron 5:527–544.

Barres BA, Koroshtez WJ, Swartz KJ, Chun LL, Corey DP. 1990b. Ion channel expression by white matter glia: the O-2A glial progenitor cell. Neuron 4:507–524.

Belachew S, Yuan X, Gallo V. 2001. Unraveling oligodendrocyte origin and function by cell-specific transgenesis. Dev Neurosci 23:287–298.

Bergles DE, Roberts JDB, Somogyi P, Jahr CE. 2000. Glutamatergic synapses on oligodendrocyte precursor cells in the hippocampus. Nature 405:187–191.

Borges K, Kettenmann H. 1995. Blockade of K^+ channels induced by AMPA/kainate receptor activation in mouse oligodendrocyte precursor cells is mediated by Na^+ entry. J Neurosci Res 42:579–593.

Brenner M, Kisseberth WC, Su Y, Besnard F, Messing A. 1994. GFAP promoter directs astrocyte-specific expression in transgenic mice. J Neurosci 14:1030–1037.

Brown M, Keynes R, Lumsden A. 2001. The developing brain. New York: Oxford University Press, Inc.

Butt AM. 1991. Macroglial cell types, lineage, and morphology in the CNS. Ann N Y Acad Sci 633:90–95.

Chalfie M, Tu Y, Euskirchen G, Ward WW, Prasher DC. 1994. Green fluorescent protein as a marker for gene expression. Science 263:802–805.

Chandross KJ, Cohen RI, Paras P Jr, Gravel M, Braun PE, Hudson LD. 1999. Identification and characterization of early glial progenitors using a transgenic selection strategy. J Neurosci 19:759–774.

Chittajallu R, Chen Y, Wang H, Yuan X, Ghiani CA, Heckman T, McBain CJ, Gallo V. 2002. Regulation of Kv1 subunit expression in oligodendrocyte progenitor cells and their role in G1/S phase progression of the cell cycle. Proc Natl Acad Sci USA 99:2350–2355.

Dubois-Dalcq M. 1987. Characterization of a slowly proliferative cell along the oligodendrocyte differentiation pathway. EMBO J 6:2587–2595.

Espinosa de los Monteros A, Zhang M, deVellis J. 1993. O-2A progenitor cells transplanted into the neonatal rat brain develop into oligodendrocytes but not astrocytes. Proc Natl Acad Sci USA 90:50–54.

Fuss B, Mallon B, Phan T, Ohlemeyer C, Kirchoff F, Nishiyama A, Macklin WB. 2000. Purification and analysis of in vivo-differentiated oligodendrocytes expressing the green fluorescent protein. Dev Biol 218:259–274.

Gähwiler BH, Capogna M, Debanne D, Mckinney RA, Thompson SM. 1997. Organotypic slice cultures: a technique has come of age. Trends Neurosci 20:471–477.

Gallo V, Armstrong R. 1995. Developmental and growth factor induced regulation of nestin in oligodendrocyte lineage cells. J Neurosci 15:394–406.

Gallo V, Ghiani CA. 2000. Glutamatergic receptors in glia: new cells, new inputs and new functions. Trends Pharmacol Sci 21:252–258.

Gallo V, Zhou JM, McBain CJ, Wright PW, Knutson PL, Armstrong R. 1996. Oligodendrocyte progenitor cell proliferation and lineage progression are regulated by glutamate receptor-mediated K^+ channel block. J Neurosci 16:2659–2670.

Gard AL, Pfeiffer SE. 1990. Two proliferative stages of the oligodendrocyte lineage ($A2B5^+O4^-$ and $O4^+GalC^-$) under different mitogenic control. Neuron 17:1397–1405.

Ghiani CA, Eisen AM, Yuan X, DePinho RA, McBain CJ, Gallo V. 1999a. Neurotransmitter receptor activation triggers $p27^{Kip1}$ and $p21^{CIP1}$ accumulation and G_1 cell cycle arrest in oligodendrocyte progenitors. Development 126:1077–1090.

Ghiani CA, Yuan X, Eisen AM, Knutson PL, DePinho, RA, McBain CJ, Gallo V. 1999b. Voltage-activated K^+ channels and membrane depolarization regulate accumulation of the cyclin-dependent kinase inhibitors $p27^{Kip1}$ and $p21^{CIP1}$ in glial progenitor cells. J Neurosci 19:5380–5392.

Gravel M, DiPolo A, Valera PB, Braun PE. 1998. A 4 kb sequence of the mouse CNP gene directs spatial and temporal expression of lacZ in transgenic mice. J Neurosci Res 53:393–404.

Hardy R, Reynolds R. 1991. Proliferation and differentiation potential of rat forebrain oligodendroglial progenitors both in vitro and in vivo. Development 111:1061–1080.

Jacobson M. 1991. Developmental neurobiology. New York: Plenum Press.

Kawaguchi A, Miyata T, Sawamoto K, Takashita N, Murayama A, Akamatsu W, Ogawa M, Okabe M, Tano Y, Goldman SA, Okano H. 2001. Nestin-EGFP transgenic mice: visualization of the self-renewal and multipotency of CNS stem cells. Mol Cell Neurosci 17:259–273.

Knutson P, Ghiani C, Zhou JM, Gallo V, McBain C. 1997. K^+ channel expression and proliferation are regulated by intracellular sodium and membrane depolarization in oligodendrocyte progenitor cells. J Neurosci 17:2669–2682.

Levine JM, Stincone F, Lee YS. 1993. Development and differentiation of glial precursor cells in the rat cerebellum. Glia 7:307–321.

Levine JM, Reynolds R, Fawcett JW. 2001. The oligodendrocyte precursor cell in health and disease. Trends Neurosci 24:39–47.

Lu QR, Yuk D, Alberta JA, Zhu Z, Pawlitzky I, Chan J, McMahon AP, Stiles CD, Rowitch DH. 2000. Sonic hedge-hog-regulated oligodendrocyte lineage genes encoding bHLH proteins in the mammalian central nervous system. Neuron 25:317–329.

Luskin MB, Pearlman AL, Sanes JR. 1988. Cell lineage in the cerebral cortex of the mouse studied in vivo and in vitro with a recombinant retrovirus. Neuron 1:635–647.

Mallon BS, Shick HE, Kidd GJ, Macklin WB. 2002. Proteolipid promoter activity distinguishes two populations of NG2-positive cells throughout neonatal cortical development. J Neurosci 22:876–885.

McCarthy KD, deVellis J. 1980. Preparation of separate astroglial and oligodendroglia cell cultures from rat cerebral tissue. J Cell Biol 85:890–902.

Miller R. 1996. Oligodendrocyte origins. Trends Neurosci 19:92–96.

Neusch C, Rozengurt N, Jacobs RE, Lester HA, Kofuji P. 2001. Kir4.1 potassium channel subunit is crucial for oligodendrocyte development and in vivo myelination. J Neurosci 21:5429–5438.

Nolte C, Matyash M, Pivneva T, Schipke CG, Ohlemeyer C, Hanisch UK, Kirchoff F, Kettenmann H. 2001. GFAP promoter-controlled EGFP-expressing transgenic mice: a tool to visualize astrocytes and astrogliosis in living brain tissue. Glia 33:72–86.

Scherer SS, Braun PE, Grinspan J, Collarini E, Wang DY, Kamholz J. 1994. Differential regulation of the 2′,3′-cyclic nucleotide 3′-phosphodiesterase gene during oligodendrocyte development. Neuron 12:1363–1375.

Sontheimer H, Trotter J, Schachner M, Kettenmann H. 1989. Channel expression correlates with differentiation stage during the development of oligodendrocytes from their precursor cells in culture. Neuron 2:1135–1145.

Spassky N, Goujet-Zalc C, Parmantier E, Olivier C, Martinez S, Ivanova A, Ikenaka K, Macklin W, Cerruti I, Zalc B, Thomas JL. 1998. Multiple restricted origins of oligodendrocytes. J Neurosci 18:8331–8343.

Stevens B, Tanner S, Fields RD. 1998. Control of myelination by specific patterns of neural impulses. J Neurosci 18:9303–9311.

Timsit S, Martinez S, Aliquant B, Petron F, Puelles L, Zalc B. 1995. Oligodendrocytes originate in a restricted zone of the embryonic ventral neural tube defined by DM-20 mRNA expression. J Neurosci 15:1012–1024.

Walz W, MacVicar B. 1988. Electrophysiological properties of glial cells. Comparison of brain slices with primary cultures. Brain Res 443:321–324.

Yamaguchi M, Saito H, Suzuki M, Mori K. 2000. Visualization of neurogenesis in the central nervous system using nestin promoter-EGFP transgenic mice. Dev Neurosci 11:1991–1996.

Yu WP, Collarini EJ, Pringle NP, Richardson WD. 1994. Embryonic expression of myelin genes: evidence for a focal source of oligodendrocyte precursors in the ventricular zone of the neural tube. Neuron 12:1353–1362.

Yuan X, Eisen AM, McBain CJ, Gallo V. 1998. A role for glutamate and its receptors in the regulation of oligodendrocyte development in cerebellar tissue slices. Development 125:2901–2914.

Zhuo L, Sun B, Zhang CL, Fine A, Chiu SY, Messing A. 1997. Live astrocytes visualized by green fluorescent protein in transgenic mice. Dev Biol 187:36–42.

Zhou Q, Wang S, Anderson DJ. 2000. Identification of a novel family of oligodendrocyte lineage-specific basic helix-loop-helix transcription factors. Neuron 25:331–343.

7.3 Publication #3: Belachew,S., Aguirre,A.A., Wang,H., Vautier,F., Yuan,X., Anderson,S., Kirby,M., and Gallo,V. (2002). Cyclin-dependent kinase-2 controls oligodendrocyte progenitor cell cycle progression and is downregulated in adult oligodendrocyte progenitors. *J. Neurosci.* 22:8553-8562.

The Journal of Neuroscience, October 1, 2002, *22*(19):8553–8562

Cyclin-Dependent Kinase-2 Controls Oligodendrocyte Progenitor Cell Cycle Progression and Is Downregulated in Adult Oligodendrocyte Progenitors

Shibeshih Belachew,[1] Adan A. Aguirre,[1] Hang Wang,[1] François Vautier,[1] Xiaoqing Yuan,[1] Stacie Anderson,[2] Martha Kirby,[2] and Vittorio Gallo[1]

[1]*Laboratory of Cellular and Synaptic Neurophysiology, National Institute of Child Health and Human Development, and* [2]*Gene Transfer Laboratory, Hematopoiesis Section, Flow Cytometry Core Unit, National Human Genome Research Institute, National Institutes of Health, Bethesda, Maryland 20892-4495*

Proliferation of oligodendrocyte progenitor (OP) cells is a crucial process controlling myelination in the CNS. Previous studies demonstrated a correlation between OP proliferation rate and cyclin E/cyclin-dependent kinase-2 (cdk2) activity. To establish a causal link between cyclin E/cdk2 activity and OP proliferation, we selectively modulated cdk2 activity *in vitro* by transfection of cultured OP cells. Dominant-negative (Dn)-cdk2 overexpression inhibited mitogen-induced OP cell proliferation, whereas wild-type (wt)-cdk2 prevented cell cycle arrest caused by anti-mitotic signals. Dn-cdk2- or wt-cdk2-mediated regulation of G_1/S transition, per se, did not influence initiation of OP differentiation. To study the function of cyclin E/cdk2 in OP cells during development *in vivo*, we analyzed cdk2 and cyclin E expression in cells acutely isolated from transgenic mice expressing the green fluorescent protein (GFP) under the control of the 2′-3′-cyclic nucleotide 3′-phosphodiesterase gene promoter. Both cyclin E/cdk2 protein levels and activity were decreased in GFP^+ oligodendrocyte lineage cells between postnatal days 4 and 30. Immunostaining of $NG2^+/GFP^+$ OP cells in brain tissue sections showed a 90% decrease in overall cell proliferation and cdk2 expression between perinatal and adult cells. However, cdk2 expression within the proliferating (i.e., expressing the proliferating cell nuclear antigen) OP cell population was maintained throughout development. Our data indicate that: (1) cyclin E/cdk2 activity plays a pivotal function in OP cell cycle decisions occurring at G_1/S checkpoint; (2) initiation of OP differentiation is independent of cyclinE/cdk2 checkpoint, and (3) intrinsic differences in cyclin E/cdk2 expression and activity may underlie the slowly proliferative state that characterizes so-called "quiescent" adult OP cells *in vivo*.

Key words: cell cycle; cell differentiation; checkpoint genes; CDK; cyclin; fluorescence-activated cell sorting; glia; myelin

In the oligodendroglial lineage, oligodendrocyte progenitor (OP) cells undergo a limited period of proliferation during development, before they exit the cell cycle and terminally differentiate into myelinating oligodendrocytes (Temple and Raff, 1986). Nevertheless, some oligodendrocyte precursor cells have also been shown to lack replicative senescence *in vitro* and to proliferate indefinitely in the presence of mitogens and in the absence of hydrophobic stimulation (i.e., thyroid hormone) (Tang et al., 2001). This would suggest that OP proliferation is regulated by extracellular environmental signals acting on molecular intrinsic targets, which are yet undefined, but ultimately linked to the cell cycle machinery.

A significant number of cells with an OP phenotype is still present in the adult CNS, both in the white and gray matter (Levine et al., 2001). Adult OPs proliferate much more slowly than perinatal OPs (Shi et al., 1998; Noble, 2000) and, after CNS damage, they display drastic changes in morphology and increases in NG2 immunoreactivity and mitotic rate (Dawson et al., 2000; Levine et al., 2001). In areas of demyelination, $NG2^+$ adult OPs proliferate and increase in number, but do not appear to differentiate into myelinating oligodendrocytes. *In vitro* studies demonstrated lineage continuity between perinatal and adult OPs, however the molecular basis of their differences in cell proliferation and cell cycle length are still unknown (Noble, 2000).

Cell cycle progression, including G1-S phase transition, is governed by a complex network of biochemical interactions involving the activity of essential components, the cyclin-dependent kinases (cdks) (Morgan, 1997; Kohn, 1999; Roberts, 1999). Because of its intrinsic complexity, cell cycle progression can be regulated at many molecular levels (Sherr and Roberts, 1999) and distinct cdks play pivotal roles in G1-S transition in different neural cell types (Ross, 1996; Ohnuma et al., 2001). The precise roles and relative importance of specific cdks in different neural cell types is still a matter of debate. For example, cdk2 has been shown to play a prominent role in the regulation of Schwann cell

Received June 4, 2002; revised July 17, 2002; accepted July 22, 2002.

This work was supported by the National Institute of Child Health and Human Development Intramural Program. S.B. was supported by the Fonds National de la Recherche Scientifique (Belgium). A.A. was supported by a predoctoral fellowship from Consejo Nacional de Ciencia y Tecnologia (Mexico). We are grateful to Dr. Sander van den Heuvel for generously providing the pCMV-neo-BAM vectors containing the cDNAs for the dominant-negative mutants of cdk2, 4, and 6 and wild-type cdk2. We are particularly grateful to Cristina Ghiani for valuable discussion and for help during the initial phase of this project and to Ann Baron-Van Evercooren for valuable discussion. We thank Li-Jin Chew, Ramesh Chittajallu, Doug Fields, Cristina Ghiani, Chris McBain, Sergio Schinelli, and Beth Stevens for their critical comments on this manuscript.

Correspondence should be addressed to Dr. Vittorio Gallo, Center for Neuroscience Research, Children's Research Institute, Children's National Medical Center, 111 Michigan Avenue, Washington, DC 20010-2970. E-mail: vgallo@cnmcresearch.org.

S. Belachew's present address: Center for Cellular and Molecular Neurobiology, Department of Neurology, University of Liège, Belgium; and Center for Neuroscience Research, Children's Research Institute, Children's National Medical Center, Washington, DC 20010-2970.

A. Aguirre's and V. Gallo's present address: Center for Neuroscience Research, Children's Research Institute, Children's National Medical Center, Washington, DC 20010-2970.

 0270-6474/02/228553-10$15.00/0

proliferation (Tikoo et al., 2000), whereas the cdk4/6 signaling pathway is crucial for cortical neural progenitor cell proliferation (Ferguson et al., 2000). In astrocytes, cdk4 is an essential component of cell division (Holland et al., 1998). Clearly, the identification of critical cell type-specific cell cycle regulator(s) under defined physiological conditions will help elucidate mechanisms underlying the growth characteristics of different neural cells in development and disease.

Previous analysis in cultured OP cells demonstrated a decrease of cyclin E/cdk2 kinase activity after permanent cell cycle exit or after reversible cell cycle arrest triggered by extracellular signals (Ghiani et al., 1999a,b; Ghiani and Gallo, 2001). Conversely, cyclin D-associated cdk4/6 kinase activity was only marginally affected during permanent cell cycle withdrawal (Ghiani and Gallo, 2001). In contrast with proliferation, specific molecular targets involved in OP differentiation remain elusive, and little is known about the relationship between cell cycle-related pathways and OP differentiation (Tokumoto et al., 1999; Zezula et al., 2001; Huang et al., 2002).

In the present study, we first used a cell transfection procedure to modify cdk2 activity in cultured perinatal OP cells. We then extended our analysis of cyclin E/cdk2 expression and activity to a transgenic mouse selectively expressing the green fluorescent protein (GFP) in the oligodendrocyte lineage (Belachew et al., 2001; Yuan et al., 2002). Our results establish a direct causal link between cyclin E/cdk2 activity and OP cell proliferation, pointing to a pivotal function of cdk2 in changes of OP cell cycle kinetics.

MATERIALS AND METHODS

Cell culture. The CG-4 oligodendrocyte progenitor cell line was cultured as previously described (Louis et al., 1992). Twenty-four hours before transfection, CG-4 cells were plated onto poly-L-lysine-treated 12 mm glass coverslips at a density of 50,000 cells per coverslip.

Purified cortical OP cell cultures were prepared as previously described from embryonic day 20 Sprague Dawley rats, using a standard experimental protocol (McCarthy and de Vellis, 1980) with slight modifications (Ghiani et al., 1999a,b). OP cells were expanded for 2 weeks in poly-L-lysine-treated 100 mm plastic Petri dishes (passaged every 4 d) in DME-N_1 supplemented with B_{104} conditioned medium (30%, v:v) (Louis et al., 1992). One day before transfection, OP cells were transferred onto poly-L-lysine-treated 12 mm glass coverslips at a density of 50,000 cells per coverslip in DME-N_1 medium in the presence of platelet-derived growth factor (PDGF, 10 ng/ml) (Upstate Biotechnology, Lake Placid, NY).

DNA constructs and transfection procedure. We used pCytomegalovirus (CMV)-neo-BAM vectors containing cDNAs of wild-type cdk2 and dominant-negative mutants of cdk2, cdk4, and cdk6 (van den Heuvel and Harlow, 1993). *Bam*HI-*Bam*HI fragments encompassing wild-type (wt)- and dominant negative (Dn)-cdk genes were subcloned into Bluescript SK (+/−) vectors (Stratagene, La Jolla, CA), to allow the following step of downstream cloning of an internal ribosomal entry site (IRES)–enhanced green fluorescent protein (EGFP) sequence (catalog #6064-1; Clontech, Palo Alto, CA). Wt-cdk2-, Dn-cdk2-, Dn-cdk4-, and Dn-cdk6-IRES–EGFP fragments were then inserted back into the native pCMV-neo-BAM backbone vector, to form plasmids named pCMV:WT2:IRES–GFP, pCMV:DN2:IRES–GFP, pCMV:DN4:IRES–GFP, and pCMV:DN6:IRES–GFP, respectively (Fig. 1*A*).

All plasmid constructs were introduced into cultured cells by liposomal transfection in 24-well dishes, using 0.3 μg of DNA and 0.8 μl of lipofectamine in OPTI-MEM (Life Technologies, Gaithersburg, MD) for each well (50,000 cells per coverslip). The duration of the transfection procedure was 6 hr. After transfection, the cells were placed in a mitogenic environment, i.e., DME-N_1 supplemented with PDGF (10 ng/ml) for primary OP cells, and DME-N_1 supplemented with 30% (v:v) B_{104} conditioned medium for the CG-4 cells. The average efficiency of the transfection procedure (evaluated at 48 hr after transfection) in primary OP cells (GFP^+ cells per total cells, mean ± SD) was 9.6 ± 4.2‰ for Dn-cdk2 construct, 13.4 ± 4.2‰ for Dn-cdk4, 16.1 ± 7.0‰ for Dn-cdk6, and 19.5 ± 7.8‰ for wt-cdk2. The rate of transfection in CG-4 cells was between 30 and 50% for all the constructs.

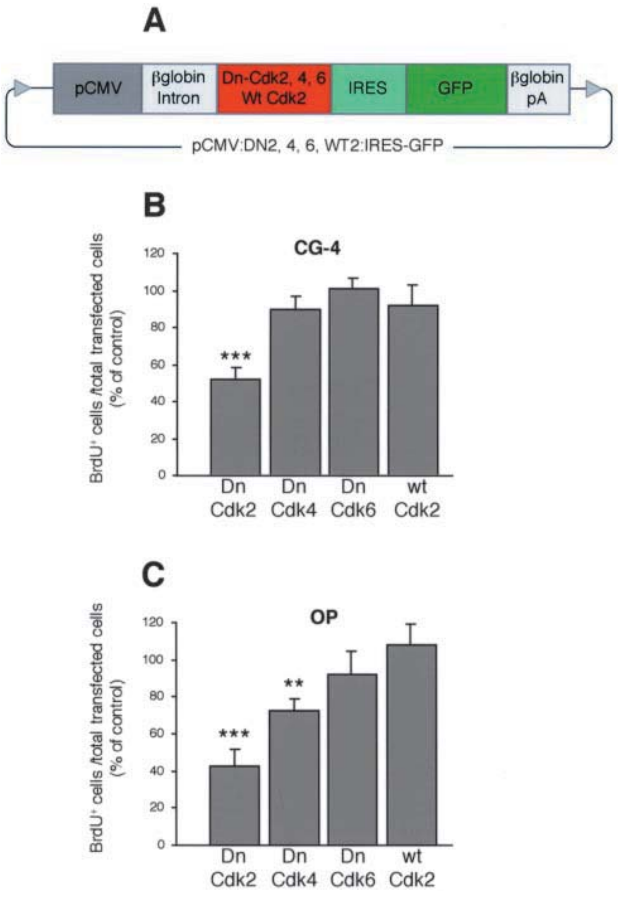

Figure 1. Cdk2 is a crucial mediator of mitogen-induced OP cell cycle progression. *A,* Several plasmid constructions (pCMV:DN2, 4, 6, WT2:IRES-GFP, 8.8–8.9 kb) carrying cDNAs for the wild-type cdk2 or dominant-negative mutants of cdk2, 4, and 6, under the control of the CMV promoter were generated. The GFP was used as reporter gene and was cloned downstream of an IRES, allowing GFP to be synthesized without fusing with the different kinase proteins. The control vector (pCMV:IRES-GFP, 7.9 kb) only contained the IRES–GFP directly driven by the CMV promoter. The plasmids also encompassed the β-globin intron to enhance transgene expression, and the β-globin polyadenylation (pA) sequence. *B, C,* Transfected CG-4 and OP cells were cultured in mitogenic medium (see Materials and Methods) and stained after incorporating BrdU (20 μM) from 24 to 42 hr post-end of transfection. The BrdU incorporation index (= $BrdU^+$ cells/total transfected GFP^+ cells) for cells overexpressing the different Dn- and wt-cdks is expressed as a percentage of the corresponding values obtained for cells transfected with the pCMV:IRES-GFP control vector, which were 62.6 ± 3% for primary OP cells and 90.4 ± 5% for CG-4 cells (mean ± SEM). Dn-cdk2 overexpression induced cell cycle arrest both in primary OP and CG-4 cells, whereas Dn-cdk4 marginally inhibited proliferation only in primary OP cells. Histograms represent mean ± SEM of counts from three separate experiments (>1000 GFP^+ cells counted for each condition, triplicate coverslips for each). $^{**}p < 0.01$, $^{***}p < 0.001$, Student's *t* test.

2′-3′-cyclic nucleotide 3′-phosphodiesterase–GFP transgenic mouse. The 2′-3′-cyclic nucleotide 3′-phosphodiesterase (CNP)–GFP transgenic mouse was generated by using the 3.7 kb *Xba*I-*Hin*dIII sequence, which contains the type I and II promoter core elements of the mouse CNP gene (Gravel et al., 1998; Belachew et al., 2001; Yuan et al., 2002). This fragment was ligated upstream of a 1 kb *Sma*I–*Xho*I fragment encompassing the coding sequence of EGFP gene (catalog #6064–1; Clontech) (Belachew et al., 2001; Yuan et al., 2002). A polyadenylation signal from bovine growth hormone was cloned downstream of the fusion gene. A 4.7 kb *Xba*I–*Xho*I fragment was excised, purified, and injected into fertilized

oocytes from F1 females from FVB/NxCB6 genetic background. To identify positive transgenic animals, mice were analyzed by both PCR and Southern blot analysis. All animal procedures were performed according to National Institutes of Health guidelines. Immunohistochemical and electrophysiological characterization of GFP^+ cells in tissue sections from transgenic mice revealed GFP expression in the oligodendroglial lineage (Yuan et al., 2002).

Isolation of oligodendroglial cells by fluorescence-activated cell sorting. Brains were dissected out from postnatal day 4 (P4)–P8, P15, and P30 CNP–GFP mice and from wild-type littermates. Meninges were removed. Brain tissues were cut into small pieces and incubated in enzyme solution (papain, 15 U/ml; type I deoxyribonuclease, 100 U/ml diluted in PBS solution) at 37°C for 20 min. Digested tissues were gently dissociated by passing through successive needles (gauge, 19 × 1 inch, 21 × 1 inch, and 23 × 1 inch). Cell suspensions were then filtered through a 70 μm cell strainer, centrifuged, and resuspended in DME-N_1 plus 10% fetal bovine serum (FBS) at a density of 10^7 cells/ml for subsequent fluorescence-activated cell sorting (FACS). Cells were analyzed for light forward and side scatter using a FACS Vantage SE instrument (Becton Dickinson, San Jose, CA). To detect GFP fluorescence, cells were analyzed through a 530 nm bandpass filter, because the excitation wavelength was set at 488 nm of the argon–ion laser. Cells from negative littermates were used to set the background fluorescence, and a size threshold was used to gate out debris and small fragments. The sorting speed was 2000–4000 cells/sec. After FACS, cells were washed twice and harvested in ice-cold PBS solution.

Western blot and cdk2 activity assay. FACS-sorted cell pellets were resuspended in 100 μl of sample buffer [50 mM HEPES, pH 7.4, 150 mM NaCl, 1 mM EDTA, 2.5 mM EGTA, 1% Nonidet P-40, 1 mM Na_3VO_4, 4 μM NaF, 10 μg/ml leupeptin, 10 μg/ml aprotinin, 10 μg/ml pepstatin, and 1 mM 4-(2-aminoethyl)benzenesulfonyl fluoride (AEBSF)] and lysed for 45 min on ice, followed by a brief sonication. The lysate was clarified by centrifugation at 12,000 rpm for 5 min, and the supernatant was collected. An aliquot was taken for protein determination using the Pierce (Rockford, IL) BCA protein assay kit. Protein extracts (18 μg) were resolved on a 4–20% mini-SDS polyacrylamide gel and transferred to Immobilon polyvinylidene difluoride membranes. Equal protein loading was verified by Ponceau S solution (Sigma, St. Louis, MO) reversible staining of the blots. Blots were processed as previously described (Ghiani et al., 1999a,b; Ghiani and Gallo, 2001), using anti-cdk2 (1:500, clone M2, sc-163; Santa Cruz Biotechnology, Santa Cruz, CA) and anti-cyclin E (1:500, clone M20, sc-481; Santa Cruz Biotechnology) antibodies.

Immunostaining in tissue sections and in cell cultures. For cdk2 immunohistochemical experiments, P6 and P30 sections from CNP–GFP transgenic mice were prepared as previously described (Yuan et al., 2002). Frozen sections were blocked at room temperature for at least 1 hr in blocking solution (1% BSA, 0.3% Triton X-100, and 20% normal goat serum in 1× PBS). Anti-cdk2 (1:200, clone M2, sc-163; Santa Cruz Biotechnology), anti- proliferating cell nuclear antigen (PCNA) (1:50, 05–347; Upstate Biotechnology, Lake Placid, NY), and NG2 (1:1000, AB5320; Chemicon, Temecula, CA) primary antibodies were diluted using carrier solution (1% BSA, 0.3% Triton X-100 in 1× PBS). Brain sections were incubated with primary antibody at 4°C overnight. For PCNA staining, tissue sections were treated with cold methanol at 20°C for 10 min before blocking. Rinse was performed in carrier solution at room temperature with three changes of solution every 15 min. Anti-rabbit and anti-mouse tetramethylrhodamine isothiocyanate- and Cy5-conjugated secondary antibodies (Jackson ImmunoResearch Laboratories, West Grove, PA) were diluted 1:200 in carrier solution. Incubation was performed at room temperature for 1 hr and followed by three washes, as described above. Sections were then transferred into 1× PBS, mounted with Mowiol, and later imaged using a Nikon fluorescence microscope equipped with a Bio-Rad (Hercules, CA) MRC1024 laser confocal scanning system.

For immunocytochemistry of acutely purified OP cells from CNP–GFP mice or transfected CG-4 and OP cell cultures, NG2, O4, O1, and BrdU stainings were performed as previously described (Yuan et al., 1998, 2002). For BrdU immunostaining, because the necessary alkaline denaturation of cell DNA (NaOH 0.07N) was partially quenching GFP fluorescence, GFP immunostaining (1:100; polyclonal anti-GFP, Santa Cruz Biotechnology) was performed before BrdU staining to allow accurate detection of transfected cells.

RESULTS

Cdk2 is a crucial mediator of OP cell cycle progression either in a pro- or anti-mitotic environment

To establish a causal link between cyclin E/cdk2 activity and OP proliferation, we used cell transfection procedure and performed gain/loss of function experiments. We designed plasmids containing dominant-negative mutants of cdk2, 4, and 6 (Dn-cdk2, 4 and 6) (Fig. 1*A*) placed under the control of the cytomegalovirus (CMV) promoter with GFP as a reporter gene. These dominant inhibitory mutants hold a single amino acid mutation located in the catalytic cleft of the enzyme that renders them inactive (van den Heuvel and Harlow, 1993). However, Dn-cdks retain their ability to bind their cyclin partners and inactivate the function of endogenous cdks by sequestering the required cyclins (van den Heuvel and Harlow, 1993).

Because previous studies on OP cell cycle kinetics were performed with rat tissue (Ghiani et al., 1999b; Ghiani and Gallo, 2001), transfection experiments were done with purified rat primary cortical OP cells prepared following an established standard culture protocol (McCarthy and de Vellis, 1980) and with progenitors from the rat oligodendroglial cell line CG-4 (Louis et al., 1992). Proliferation was assessed by using bromodeoxyuridine (BrdU) incorporation assays to quantitate GFP-expressing S-phase precursors. In the presence of mitogenic stimulation after transfection, Dn-cdk2 overexpression strongly decreased the number of dividing cells both in primary OP and CG-4 cultures by 58 and 49%, respectively (Fig. 1*B,C*). Dn-cdk4 overexpression only inhibited proliferation of primary OP cells by 27%, whereas Dn-cdk6 was devoid of effect (Fig. 1*B,C*).

In parallel with loss of function experiments, which pointed to a crucial role of cdk2 in mitogen-induced OP proliferation, we also observed that overexpression of the wild-type version of cdk2 (wt-cdk2) in the presence of mitogens did not result in any significant gain of function (Fig. 1*B,C*). Conversely, when deprived from platelet-derived growth factor (PDGF) stimulation, overexpression of wt-cdk2 was sufficient to maintain a higher percentage of primary OP cells within the cell cycle (Fig. 2*A, E–G*). These results are consistent with the notion that wt-cdk2 overexpression can compensate the downregulation of endogenous cdk2 that constitutively occurs in OP cells after PDGF withdrawal (Ghiani and Gallo, 2001).

We demonstrated that OP cell cycle progression *in vitro* and *in situ* (Gallo and Ghiani, 2000) could be influenced by extracellular signals, such as glutamate (Bergles et al., 2000; Gallo and Ghiani, 2000) and norepinephrine (Ghiani et al., 1999b) or by pharmacological K^+ channel blockade (Ghiani et al., 1999a). In OP cells overexpressing wt-cdk2, reversible G_1/S cell cycle arrest induced by kainic acid, isoproterenol, and tetraethylammonium in the presence of mitogen, was partially but significantly prevented (Fig. 2*B–D*).

OP cell differentiation is cdk2- and cell cycle number-independent

To determine whether modifications of OP cell cycle progression could also affect the differentiation process, we studied the emergence of O_4^+ pre-oligodendrocytes and O_1^+ mature oligodendrocytes in transfected cultures. Before transfection, primary OP cultures maintained in PDGF contained <5% of O_4^+ and no O_1^+ cells (>90% of the cells were GD_3^+ or $A2B5^+$ under these

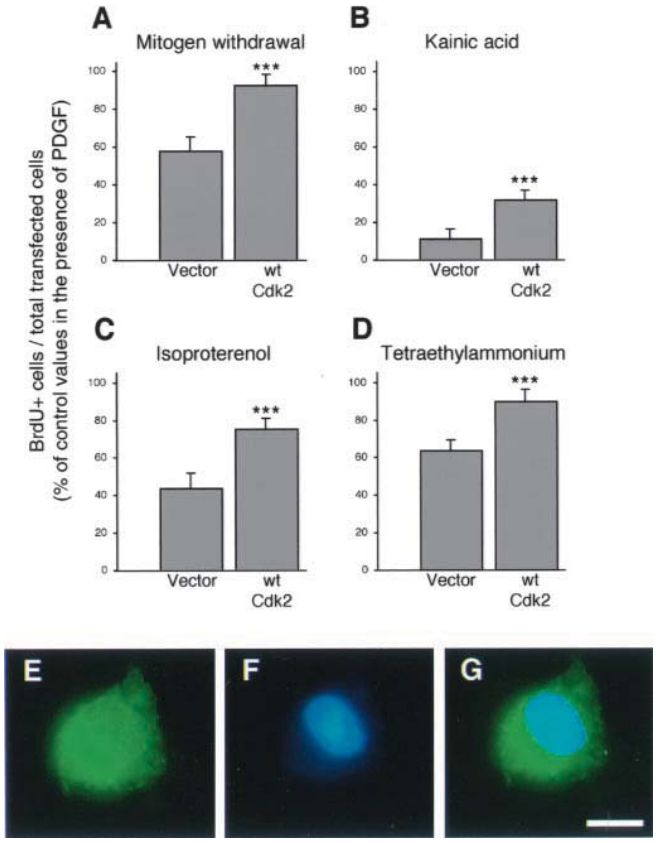

Figure 2. Wt-cdk2 overexpression reverted OP cell cycle arrest associated with the activation of glutamatergic and β-adrenergic receptors, K^+ channels blockade, or mitogen starvation. After transfection, primary OP cells were placed in DME-N_1 plus PDGF (10 ng/ml). Twenty-four hours after end of transfection, OP cells were either shifted to growth factor free DME-N_1 (*A*), or maintained in PDGF-containing medium supplemented with the glutamate receptor agonist kainic acid (100 μM) (*B*), the β-adrenergic agonist isoproterenol (50 μM) (*C*), or K^+ channel blocker tetraethylammonium (5 mM) (*D*). Two hours after the medium change, OP cells were incubated with BrdU (20 μM) for the next 18 hr. Cells transfected with pCMV:WT2:IRES-GFP were compared with those transfected with pCMV:IRES-GFP control vector. Each BrdU incorporation index is expressed as a percentage of values obtained with cells that were transfected with the same constructs, but cultured in the presence of PDGF alone during the entire duration of the experiment. Histograms represent mean ± SEM of counts (total GFP^+ cells counted ranged between 539 and 885 for each condition) from two independent experiments with triplicate coverslips each. $^{***}p < 0.001$, Student's *t* test. Separate (GFP in *E* and BrdU staining in *F*) and merged (*G*) fluorescence views of a proliferating pCMV:WT2:IRES-GFP-transfected OP cell cultured in growth factor free DME-N_1. Scale bar, 7 μm.

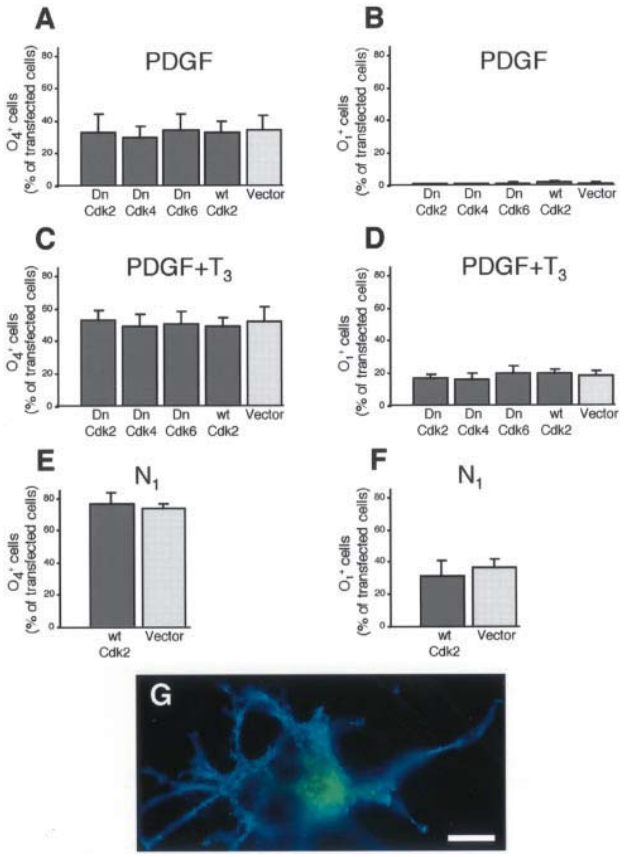

Figure 3. Cdk2-mediated regulation of OP cell cycle kinetics does not affect differentiation. O_4 and O_1 immunophenotypes were assessed 4 d after transfection (pCMV:DN2, 4, 6, WT2:IRES-GFP and pCMV:IRES-GFP) of OP cells kept in a mitogenic environment (DME-N_1 plus PDGF 10 ng/ml) with (*C, D*) or without (*A, B*) tri-iodothyronine (T_3; 50 ng/ml). Conversely, we also analyzed O_4 and O_1 emergence 4 d after transfecting (pCMV:IRES-GFP versus pCMV:WT2:IRES-GFP) OP cells that had been transferred into cell cycle arresting conditions (i.e., DME-N_1), 24 hr after end of transfection (*E, F*). *G,* Double fluorescence view of an O_1^+ (*blue*) mature oligodendrocyte overexpressing wt-cdk2 (GFP in *green*). Scale bar, 7 μm. Histograms represent mean ± SEM of counts (total GFP^+ cells counted ranged between 427 and 1106 for each condition) from three independent experiments with triplicate coverslips each.

conditions) (Ghiani et al., 1999b; Ghiani and Gallo, 2001) (data not shown). When OP cultures were maintained in the presence of PDGF for 4 d after transfection, the overexpression of Dn-cdk2, 4, 6, and wt-cdk2 did not influence oligodendrocyte differentiation, which remained very low (<2% of O_1^+ cells) (Fig. 3*A,B*). In this mitogenic environment, thyroid hormone (T_3) increased, as expected, the proportion of O_4^+ cells (Fig. 3, compare *A*, *C*) and induced the appearance of 15–20% of O_1^+ cells (Fig. 3, compare *B*, *D*). Furthermore, the presence of T_3 did not stimulate growth-arrested OP cells overexpressing Dn-cdk2 or 4 to differentiate more rapidly than OP cells transfected with the control vector (Fig. 3*C,D*). Finally, in mitogen-free medium, we also observed an increase of OP cell differentiation (Fig. 3, compare *A, E* and *B, F*), but overexpression of wt-cdk2, despite maintaining OP cells within the cell cycle (Fig. 2*A*), did not induce a more immature phenotype (Fig. 3*E–G*)

Developmental regulation of cyclin E/cdk2 expression and activity in OP cells *in vivo*

To quantitate cyclin E and cdk2 expression in the oligodendroglial lineage *in vivo*, we took advantage of a transgenic mouse expressing the GFP under the control of the CNP promoter (Belachew et al., 2001; Yuan et al., 2002). In this transgenic mouse, GFP expression was targeted to the oligodendroglial lineage (Belachew et al., 2001; Yuan et al., 2002). Acutely dissociated GFP^+ oligodendroglial cells from CNP–GFP mice at different developmental stages (P4–P30) were purified by FACS. Unlike in tissue sections (Yuan et al., 2002), we observed that the proportion of $NG2^+$ and $O4^+$ cells among acutely purified CNP–GFP^+ oligodendroglial cells was not significantly different between FACS-sorted cell suspensions derived from early (P4) or adult (P30) transgenic mice (Fig. 4*A*). On the other hand, the proportion of $O1^+$ cells significantly increased between P4 and

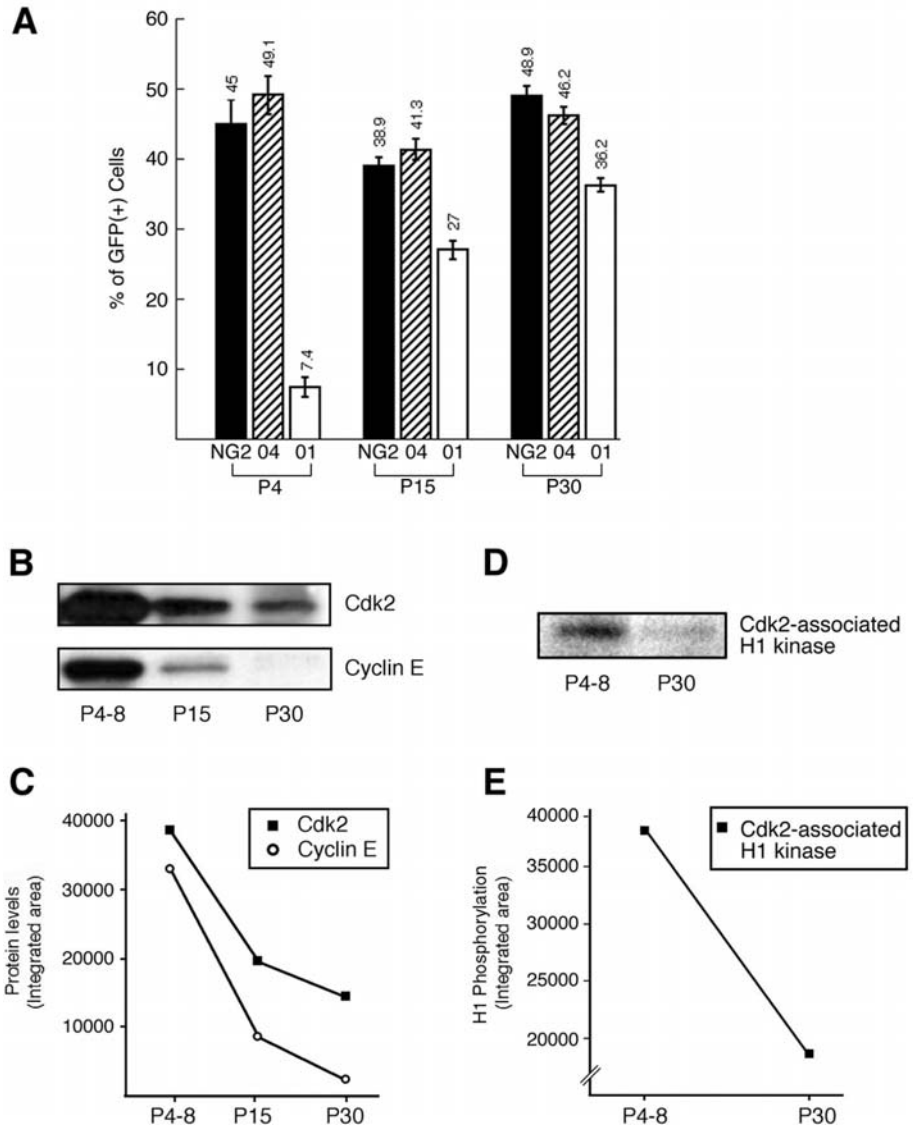

Figure 4. Cyclin E/cdk2 levels and activity decrease in oligodendroglial cells during development *in vivo*. *A,* Immunophenotype of acutely isolated CNP-GFP$^+$ oligodendroglial cells after FACS purification. We previously demonstrated that GFP expression in CNP–GFP transgenic mice was restricted to oligodendrocyte lineage cells (Belachew et al., 2001; Yuan et al., 2002), and that the FACS procedure resulted in a 100% pure population of GFP$^+$ cells whose antigenic properties were identical to those *in vivo* (Yuan et al., 2002). Values represent the percentage (mean ± SEM) of NG2$^+$, $O_4{}^+$, and $O_1{}^+$ cells in FAC-sorted cell suspensions derived from P4, P15, and P30 CNP–GFP transgenic mice. Total cells counted ranged from 652 to 2185 for each condition. *B,* Western blot analysis of cdk2 and cyclin E expression was performed with samples containing pure oligodendroglial cells freshly isolated from postnatal P4–P8, P15, and P30 brains. Samples were obtained by FACS of GFP$^+$ cells from CNP–GFP transgenic mice. FAC-sorted cells were pooled from a total of 15 brains for each experimental time point. *C,* Values were determined by densitometric analysis of the autoradiographs shown in *B* and are expressed in arbitrary units. *D,* Cdk2-associated histone H1-kinase activity was measured in FACS-purified CNP–GFP$^+$ cells at P4–P8 and P30, as previously described (Ghiani and Gallo, 2001). Western blot FAC-sorted cells were pooled from a total of 15 brains for each experimental time point. *E,* Values were determined by densitometric analysis of the autoradiograph shown in *D* and are expressed in arbitrary units.

P30 (Fig. 4*A*). The steady percentage of NG2$^+$ and O4$^+$ cells in the GFP$^+$ cell suspensions between P4 and P30 most likely reflects the better survival of immature oligodendroglial cells during the dissociation procedure. At least in part, this could be caused by a loss of cell-to-cell contacts of mature oligodendrocytes in cell suspension. Importantly, as previously demonstrated (Yuan et al., 2002), all the NG2$^+$ OP cells isolated from our CNP–GFP mice were GFP$^+$. We never distinguished a subpopulation of NG2$^+$/GFP-negative cells, as reported in the transgenic mouse strain expressing the GFP under the proteolipid protein (PLP) promoter (Mallon et al., 2002).

Western blot analysis of protein extracts from FACS-purified GFP$^+$ cells revealed higher levels of cdk2 and cyclin E expression at the early postnatal period (P4–P8) (Fig. 4*B,C*). In FACS-purified CNP–GFP$^+$ oligodendrocyte lineage cells, a 65% decrease of cdk2 and a 95% reduction of cyclin E protein expression were observed between P4–P8 and P30 (Fig. 4*B,C*). Similarly, we also observed a drastic (>50%) reduction in cyclinE/cdk2 activity between P4 and P30 (Fig. 4*D,E*).

To determine whether the developmental regulation of cyclinE/cdk2 occurred in OPs during *in vivo* development, we performed double immunostaining of GFP$^+$ cells in tissue sections from CNP–GFP transgenic mice at P6 and P30. Immunodetection of NG2 chondroitin sulfate proteoglycan was used to identify both perinatal and adult OPs in the subventricular zone (SVZ), subcortical white matter, and cerebellar white matter (Levine et al., 2001). NG2$^+$/GFP$^+$ OP cells were immunostained with anti-cdk2 antibodies or with antibodies raised against the PCNA, a DNA replication-associated protein expressed in the nucleus of dividing cells, which was used as a marker of cell proliferation (Hyde-Dunn and Jones, 1997). In the SVZ at P6, the majority of NG2$^+$/GFP$^+$ OP cells displayed cytoplasmic staining with anti-cdk2 antibodies (Fig. 5*A–D*) and nuclear staining with anti-PCNA antibodies (Fig. 5*E–H*). Consistent with the Western blot results shown in Figure 4, cell counting after immunohistochemical analysis of tissue sections demonstrated a 9- to 10-fold decrease in the percentage of NG2$^+$/GFP$^+$ OP cells expressing cdk2 or PCNA in the SVZ, subcortical white matter, and cerebellar white matter between P6 and P30 (Fig. 6*A,B*).

Double staining of GFP$^+$ cells with anti-cdk2 and anti-PCNA in the same brain regions showed that, both at P6 and at P30, >90% of the GFP$^+$/PCNA$^+$ cells were also cdk2$^+$ (Figs. 7, 8*A*).

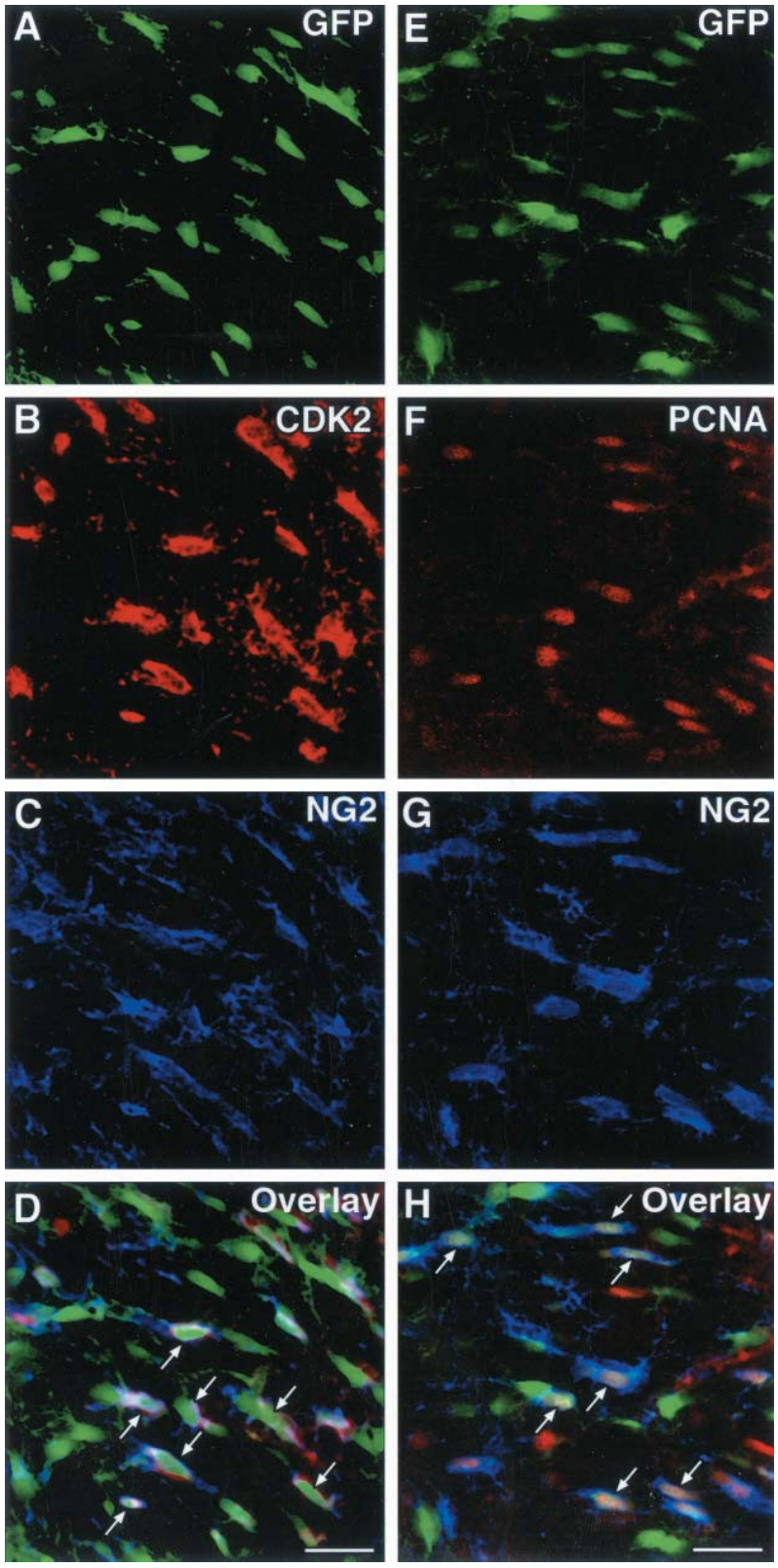

Figure 5. The majority of perinatal NG2$^+$ OP cells are proliferative and express cdk2 *in vivo*. Brain sections of SVZ from P6 CNP–GFP mice were immunostained with either (*A–D*, representing the same field) NG2 (*blue*) and anti-cdk2 (*red*) antibodies, or (*E–H*, representing the same field) with NG2 (*blue*) and anti-PCNA (*red*) antibodies. Images were obtained from the subventricular zone. At P6, the majority of GFP$^+$/NG2$^+$ cells were also stained with anti-cdk2 (*A–D, arrows* in *D*) or with anti-PCNA antibodies (*E–H, arrows* in *H*) (see Fig. 6 for quantitation). Scale bar, 20 μm.

This finding indicates that, within the GFP$^+$ oligodendroglial cell population, proliferating cells always expressed cdk2, whereas most of the cdk2-negative cells were nonproliferating (Fig. 7). At P6, 80–90% of the cdk2-expressing cells were also PCNA$^+$ (Fig. 8*B*), but at P30, PCNA expression was detected only in 40–60% of the cdk2$^+$ cells (Fig. 8*B*).

Altogether, these data indicate that cdk2 is highly expressed in proliferating oligodendroglial cells *in vivo* throughout develop-

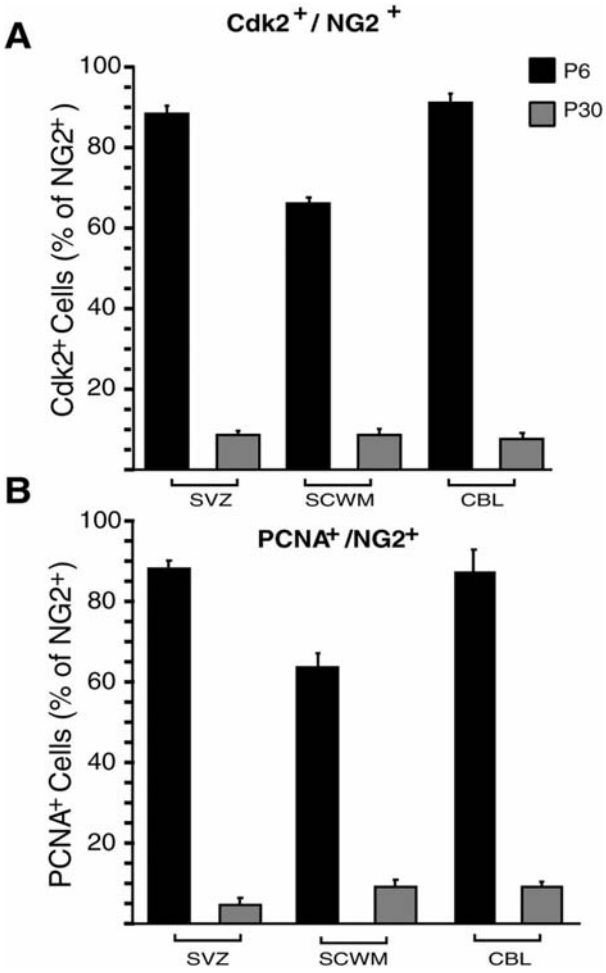

Figure 6. Cdk2 expression and cell proliferation are downregulated between perinatal and adult oligodendrocyte progenitor cells. Subventricular zone (*SVZ*), subcortical white matter (*SCWM*), and cerebellar white matter (*CBL*) from CNP–GFP mice were analyzed by immunostaining at P6 and P30, to assess the number of cdk2- (*A*) and PCNA-expressing (*B*) cells within the $NG2^+/GFP^+$ population at distinct developmental stages. Histograms represent mean ± SEM. Total GFP^+ cells counted ranged between 483 and 641 at P6, and between 409 and 455 at P30.

ment, and that the significant downregulation of cdk2 expression in adult $NG2^+$ OP cells is correlated with the event of cell cycle withdrawal.

DISCUSSION

In the present study, using *in vitro* transgenesis to overexpress dominant-negative mutants of different cdk genes, we provide evidence that cyclin E/cdk2 activity constitutes an essential component of the mechanism of mitogen-dependent OP cell proliferation. In parallel, we also demonstrate that a decrease of cdk2 activity causally underlies OP cell cycle exit triggered by extracellular signals acting at glutamate and β-adrenergic receptors, or K^+ channels. Therefore, our results show that, in OPs, cell cycle pathways activated either in a pro- or in an anti-mitotic environment converge on the common molecular target cdk2.

The finding that cdk4/6 activity was less limiting than cdk2 in the regulation of OP entry into S-phase is consistent with the function of cyclinD/cdk4/6 complexes in different cell types (Jones and Kazlauskas, 2000). In fact, it is likely that reduced cdk4/6 activity is still sufficient to initiate pRb phosphorylation in early G_1 (Jones and Kazlauskas, 2000). This would trigger release of E2F factors, transcriptional activation of cyclin E, and formation of the cyclin E/cdk2 complex, which in turn would maintain pRb phosphorylation until G_1/S checkpoint (Jones and Kazlauskas, 2000).

Our experiments also demonstrate that cdk2-mediated regulation of OP cell cycle progression did not modify the time course of oligodendrocyte differentiation in the presence of PDGF. Hence, OP cell cycle arrest is a necessary but insufficient condition to trigger differentiation. The uncoupling between OP cell proliferation and differentiation has been demonstrated in cells treated with growth factors or overexpressing cdk inhibitors such as p18, p21, or p27 (Tikoo et al., 1998; Zezula et al., 2001; Tokumoto et al., 2002), however in all these experimental paradigms effects on multiple intracellular pathways could not be excluded. In our cdk2 loss-of-function or gain-of-function experiments, we are selectively targeting one component of the cell cycle machinery and demonstrating that by the specific modification of cdk2 activity we can arrest proliferation without altering differentiation.

Oligodendrocyte differentiation induced by PDGF withdrawal or T_3 treatment was not modified by cdk2-mediated manipulations of OP cell cycle kinetics achieved by overexpressing Dn- or wt-cdk2. Thus, agents that stimulate OP differentiation may cause irreversible OP cell cycle withdrawal by complex and likely redundant mechanisms, which appear to be unrelated to cyclin E/cdk2 G_1/S checkpoint. Furthermore, because cdk2-dependent cell cycle arrest did not result in a more immature OP phenotype, nor did cdk2-dependent cell cycle progression accelerate differentiation, our results also provide evidence that OP cells do not "count" the number of cell cycles before they differentiate. Thus, it appears that the yet undefined molecular cues which regulate the differentiation program of OP cells are cell cycle number-independent.

A recent study suggests that at least two molecularly distinct intracellular pathways may be involved in the timer mechanism that triggers OP cell irreversible cell cycle exit and differentiation (Tokumoto et al., 2001). T_3-mediated OP cell differentiation appears to depend on a p53 family protein (for review, see Levrero et al., 2000), whereas spontaneous differentiation of OP cells in the presence of PDGF or OP cell differentiation induced by PDGF withdrawal are p53-independent (Tokumoto et al., 2001). T_3 treatment and PDGF starvation can trigger changes in expression of Cip/Kip and Ink4 CKIs (Ghiani et al., 2001; Tokumoto et al., 2001) that in turn influence cdk2 activity. However, our data show that transgenic modulation of cdk2 activity, per se, did not influence T_3- and PDGF withdrawal-induced differentiation. Therefore, the unknown endpoint mechanism of irreversible cell cycle exit associated with these pro-differentiating conditions are likely to involve distinct pathways that are independent from cyclin E/cdk2 activity. It can be hypothesized that nuclear transcription factors, such as helix-loop-helix proteins, known to stimulate oligodendrocyte differentiation (Kondo and Raff, 2000; Wang et al., 2001) could bypass cyclin E/cdk2 checkpoint and trigger irreversible OP cell cycle exit by directly affecting the phosphorylation state of pRb (Huang et al., 2002).

To correlate our findings on the essential role of cyclin E/cdk2 activity in OP proliferation in culture with OP proliferation *in vivo*, we took advantage of a transgenic mouse model in which GFP was selectively expressed in the oligodendroglial lineage throughout embryonic and postnatal development (Belachew et al., 2001; Yuan et al., 2002). After a FACS procedure that allowed

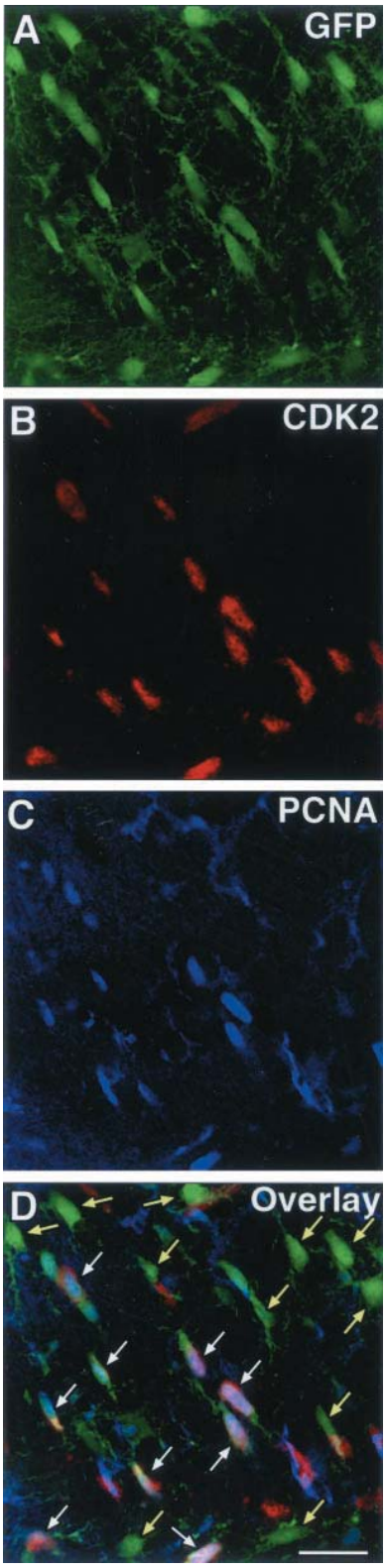

Figure 7. Coexpression of PCNA and cdk2 in CNP-GFP$^+$ cells *in vivo*. Brain sections from P6 CNP–GFP mice *A–D*, representing the same field were immunostained with anti-cdk2 (*B, red*) and anti-PCNA (*C, blue*) antibodies. Images represent the same microscopic field obtained from the subventricular zone at P6. The majority of proliferating PCNA$^+$/GFP$^+$ oligodendroglial cells coexpressed cdk2 (*white arrows*; see Fig. 8 for quantitation), whereas most of the cdk2-negative oligodendroglial cells were found to be nonproliferative, i.e., PCNA-negative (*yellow arrows*). Scale bar, 20 μm.

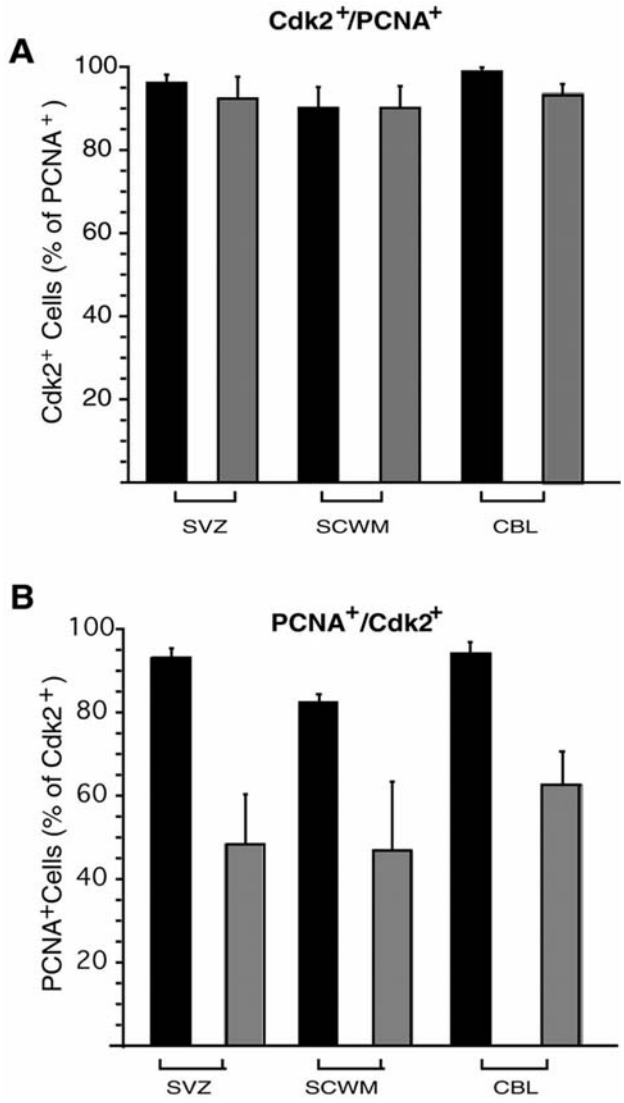

Figure 8. Proliferating GFP$^+$ oligodendroglial cells express sustained levels of cdk2 during development. Subventricular zone (*SVZ*), subcortical white matter (*SCWM*), and cerebellar white matter (*CBL*) from CNP–GFP mice were analyzed by immunostaining at P6 and P30, to assess the number of PCNA- and cdk2-co-expressing cells within the GFP$^+$ population at distinct developmental stages. *A* shows the percentage of PCNA$^+$ cells also expressing cdk2, whereas *B* indicates the percentage of cdk2$^+$ cells also expressing PCNA. Histograms represent mean ± SEM. Total GFP$^+$ cells counted ranged between 483 and 597 at P6 and between 409 and 455 at P30.

us to purify GFP$^+$ oligodendroglial cells at the progenitor stage (Yuan et al., 2002), we were able to demonstrate a downregulation of cyclin E/cdk2 activity and cyclin E and cdk2 protein expression in OP cells acutely isolated from adult brain.

We also performed a developmental immunohistochemical study of the proportion of cdk2-expressing cells within NG2$^+$/GFP$^+$ OP cells in the SVZ, cerebellar white matter, and subcortical white matter. We detected a drastic decrease of both proliferation and cdk2 expression in NG2$^+$ OP cells between the perinatal period and adulthood. Furthermore, we observed that nearly all the few OP cells which remain proliferative in the adult brain sustained a high level of cdk2 expression. Conversely, about half of cdk2-expressing OPs of the adult brain were found to be

nonproliferative, which suggests that the decrease of cyclin E/cdk2 complex activity and proliferation in postnatal OPs may be initially triggered by a reduction in cyclin E expression. This hypothesis is supported by our Western blot analysis of cyclin E and cdk2 expression in FACS-purified GFP^+ cells (Fig. 4), indicating a more rapid developmental decline in cyclin E than in cdk2 levels. Thus, altogether our data strongly suggest that regulation of cyclin E and cdk2 expression and cyclin E/cdk2 activity within the oligodendroglial lineage *in vivo* causally underlies the progressive breakdown of OP cell proliferative potential that occurs during postnatal maturation (Wolswijk et al., 1990; Calver et al., 1998; Shi et al., 1998).

Despite an established lineage continuity, adult OP cells are known to differ from their neonatal counterparts in cell cycle time, rate of migration and time course of differentiation (Ffrench-Constant and Raff, 1986; Wolswijk et al., 1990; Shi et al., 1998). Our data show that, besides extrinsic environmental differences at the level of mitogen supply and response (Chan et al., 1990; Wolswijk and Noble, 1992; Engel and Wolswijk, 1996; van Heyningen et al., 2001), a major reason for the slower cell cycle kinetics of adult OPs relies on the intrinsic developmental regulation of the molecular machinery controlling cell cycle G_1/S checkpoint. These findings may shed a new light on our understanding of the "quiescent" state of OP cells in human normal adult white matter and in multiple sclerosis lesions (Wolswijk, 1998; Chang et al., 2000; Maeda et al., 2001). Consistent with our hypothesis, a recent study by Sim et al. (2002) demonstrated that the significant attenuation in remyelination efficiency observed in adult OPs as compared to their perinatal counterpart is at least in part due to an impairment in recruitment, that involves both proliferation and migration.

Our results not only provide insights into OP cell cycle decisions and the relationship between OP proliferation and differentiation, but also open new perspectives with respect of our understanding of: (1) the deregulation of proliferation underlying the genesis of OP-derived gliomas (Shoshan et al., 1999), and (2) the failure of remyelination in spite of the persistence of OP cells in CNS demyelinating lesions (Chang et al., 2000). We propose here that, besides acting on extrinsic cues, the molecular strategies aimed at modulating adult OP cell proliferation may need to focus on specifically targeting the cyclinE/cdk2 complex. With regard to genetic engineering techniques, as demonstrated in previous studies (Belachew et al., 2001; Yuan et al., 2002; Mallon et al., 2002), the use of CNP or PLP promoter-driven genes appears to be best suited for loss/gain-of-function experiments selectively targeting adult OP cells.

REFERENCES

Belachew S, Yuan X, Gallo V (2001) Unraveling oligodendrocyte origin and function by cell-specific transgenesis. Dev Neurosci 23:287–298.
Bergles DE, Roberts JD, Somogyi P, Jahr CE (2000) Glutamatergic synapses on oligodendrocyte precursor cells in the hippocampus. Nature 405:187–191.
Calver AR, Hall AC, Yu WP, Walsh FS, Heath JK, Betsholtz C, Richardson WD (1998) Oligodendrocyte population dynamics and the role of PDGF in vivo. Neuron 20:869–882.
Chan CL, Wigley CB, Berry M (1990) Oligodendrocyte-type 2 astrocyte (O-2A) progenitor cells from neonatal and adult rat optic nerve differ in their responsiveness to platelet-derived growth factor. Brain Res Dev Brain Res 55:275–282.
Chang A, Nishiyama A, Peterson J, Prineas J, Trapp BD (2000) NG2-positive oligodendrocyte progenitor cells in adult human brain and multiple sclerosis lesions. J Neurosci 20:6404–6412.
Dawson MRL, Levine JM, Reynolds R (2000) NG2-expressing cells in the central nervous system: are they oligodendroglial progenitors? J Neurosci Res 61:471–479.
Engel U, Wolswijk G (1996) Oligodendrocyte-type-2 astrocyte (O-2A) progenitor cells derived from adult rat spinal cord: in vitro characteristics and response to PDGF, bFGF and NT-3. Glia 16:16–26.
Ferguson KL, Callaghan SM, O'Hare MJ, Park DS, Slack RS (2000) The Rb-cdk4/6 signaling pathway is critical in neural precursor cell cycle regulation. J Biol Chem 275:33593–33600.
Ffrench-Constant C, Raff MC (1986) Proliferating bipotential glial progenitor cells in adult rat optic nerve. Nature 319:499–502.
Gallo V, Ghiani CA (2000) Glutamate receptors in glia: new cells, new inputs and new functions. Trends Pharmacol Sci 21:252–258.
Ghiani CA, Yuan X, Eisen AM, Knutson PL, DePinho RA, McBain CJ, Gallo V (1999a) Voltage-activated K^+ channels and membrane depolarization regulate accumulation of the cyclin-dependent kinase inhibitors p27(Kip1) and p21(CIP1) in glial progenitor cells. J Neurosci 19:5380–5392.
Ghiani CA, Eisen AM, Yuan X, DePinho RA, McBain CJ, Gallo V (1999b) Neurotransmitter receptor activation triggers p27(Kip1) and p21(CIP1) accumulation and G1 cell cycle arrest in oligodendrocyte progenitors. Development 126:1077–1090.
Ghiani CA, Gallo V (2001) Inhibition of cyclin E-cyclin-dependent kinase 2 complex formation and activity is associated with cell cycle arrest and withdrawal in oligodendrocyte progenitor cells. J Neurosci 21:1274–1282.
Gravel M, Di Polo A, Valera PB, Braun PE (1998) Four-kilobase sequence of the mouse CNP gene directs spatial and temporal expression of lacZ in transgenic mice. J Neurosci Res 53:393–404.
Holland EC, Hively WP, Gallo V, Varmus HE (1998) Modeling mutations in the G_1 arrest pathway in human gliomas: overexpression of *CDK4* but not loss of *INK4a-ARF* induces hyperploidy in cultured mouse astrocytes. Genes Dev 12:3644–3649.
Huang Z, Tang XM, Cambi F (2002) Down-regulation of the retinoblastoma protein (rb) is associated with rat oligodendrocyte differentiation. Mol Cell Neurosci 19:250–262.
Hyde-Dunn J, Jones GE (1997) Visualization of cell replication using antibody to proliferating cell nuclear antigen. Methods Mol Biol 75:341–347.
Jones SM, Kazlauskas A (2000) Connecting signaling and cell cycle progression in growth factor-stimulated cells. Oncogene 19:5558–5567.
Kohn KW (1999) Molecular interaction map of the mammalian cell cycle control and DNA repair systems. Mol Biol Cell 10:2703–2734.
Kondo T, Raff M (2000) Basic helix-loop-helix proteins and the timing of oligodendrocyte differentiation. Development 127:2989–2998.
Levine JM, Reynolds R, Fawcett JW (2001) The oligodendrocyte precursor cell in health and disease. Trends Neurosci 24:39–47.
Levrero M, De Laurenzi V, Costanzo A, Gong J, Wang JY, Melino G (2000) The p53/p63/p73 family of transcription factors: overlapping and distinct functions. J Cell Sci 113:1661–1670.
Louis JC, Magal E, Muir D, Manthorpe M, Varon S (1992) CG-4, a new bipotential glial cell line from rat brain, is capable of differentiating in vitro into either mature oligodendrocytes or type-2 astrocytes. J Neurosci Res 31:193–204.
Maeda Y, Solanky M, Menonna J, Chapin J, Li W, Dowling P (2001) Platelet-derived growth factor-alpha receptor-positive oligodendroglia are frequent in multiple sclerosis lesions. Ann Neurol 49:776–785.
Mallon BS, Shick HE, Kidd GJ, Macklin WB (2002) Proteolipid promoter activity distinguishes two populations of NG2-positive cells throughout neonatal cortical development. J Neurosci 22:876–885.
McCarthy KD, de Vellis J (1980) Preparation of separate astroglial and oligodendroglial cell cultures from rat cerebral tissue. J Cell Biol 85:890–902.
Morgan DO (1997) Cyclin-dependent kinases: engines, clocks, and microprocessors. Annu Rev Cell Dev Biol 13:261–291.
Noble M (2000) Precursor cell transitions in oligodendrocyte development. J Cell Biol 148:839–841.
Ohnuma S, Philpott A, Harris WA (2001) Cell cycle and cell fate in the nervous system. Curr Opin Neurobiol 11:66–73.
Roberts JM (1999) Evolving ideas about cyclins. Cell 98:129–132.
Ross ME (1996) Cell division and the nervous system: regulating the cycle from neural differentiation to death. Trends Neurosci 19:62–68.
Sherr CJ, Roberts JM (1999) CDK inhibitors: positive and negative regulators of G1-phase progression. Genes Dev 13:1501–1512.
Shi J, Marinovich A, Barres BA (1998) Purification and characterization of adult oligodendrocyte precursor cells from the rat optic nerve. J Neurosci 18:4627–4636.
Shoshan Y, Nishiyama A, Chang A, Mork S, Barnett GH, Cowell JK, Trapp BD, Staugaitis SM (1999) Expression of oligodendrocyte progenitor cell antigens by gliomas: implications for the histogenesis of brain tumors. Proc Natl Acad Sci USA 96:10361–10366.
Sim FJ, Zhao C, Penderis J, Franklin RJM (2002) The age-related decrease in CNS remyelination efficiency is attributable to an impairment of both oligodendrocyte progenitor recruitment and differentiation. J Neurosci 22:2451–2459.
Tang DG, Tokumoto YM, Apperly JA, Lloyd AC, Raff MC (2001) Lack of replicative senescence in cultured rat oligodendrocyte precursor cells. Science 291:868–871.
Temple S, Raff MC (1986) Clonal analysis of oligodendrocyte develop-

ment in culture: evidence for a developmental clock that counts cell divisions. Cell 44:773–779.
Tikoo R, Osterhout DJ, Casaccia-Bonnefil P, Seth P, Koff A, Chao MV (1998) Ectopic expression of p27Kip1 in oligodendrocyte progenitor cells results in cell-cycle growth arrest. J Neurobiol 36:431–440.
Tikoo R, Zanazzi G, Shiffman D, Salzer J, Chao MV (2000) Cell cycle control of Schwann cell proliferation; role of cyclin-dependent kinase-2. J Neurosci 20:4627–4634.
Tokumoto YM, Durand B, Raff MC (1999) An analysis of the early events when oligodendrocyte precursor cells are triggered to differentiate by thyroid hormone, retinoic acid, or PDGF withdrawal. Dev Biol 213:327–339.
Tokumoto YM, Tang DG, Raff MC (2001) Two molecularly distinct intracellular pathways to oligodendrocyte differentiation: role of a p53 family protein. EMBO J 20:5261–5268.
Tokumoto YM, Apperly JA, Gao FB, Raff MC (2002) Posttranscriptional regulation of p18 and p27 Cdk inhibitor proteins and the timing of oligodendrocyte differentiation. Dev Biol 245:224–234.
van den Heuvel S, Harlow E (1993) Distinct roles for cyclin-dependent kinases in cell cycle control. Science 262:2050–2054.
van Heyningen P, Calver AR, Richardson WD (2001) Control of progenitor cell number by mitogen supply and demand. Curr Biol 11:232–241.
Wang S, Sdrulla A, Johnson JE, Yokota Y, Barres BA (2001) A role for the helix-loop-helix protein Id2 in the control of oligodendrocyte development. Neuron 29:603–614.
Wolswijk G (1998) Chronic stage multiple sclerosis lesions contain a relatively quiescent population of oligodendrocyte precursor cells. J Neurosci 18:601–609.
Wolswijk G, Noble M (1992) Cooperation between PDGF and FGF converts slowly dividing O-2Aadult progenitor cells to rapidly dividing cells with characteristics of O-2Aperinatal progenitor cells. J Cell Biol 118:889–900.
Wolswijk G, Riddle PN, Noble M (1990) Coexistence of perinatal and adult forms of a glial progenitor cell during development of the rat optic nerve. Development 109:691–698.
Yuan X, Eisen AM, McBain CJ, Gallo V (1998) A role for glutamate and its receptors in the regulation of oligodendrocyte development in cerebellar tissue slices. Development 125:2901–2914.
Yuan X, Chittajallu R, Belachew S, Anderson S, McBain CJ, Gallo V (2002) Expression of the green fluorescent protein in the oligodendrocyte lineage: a transgenic mouse for developmental and physiological studies. J Neurosci Res, in press.
Zezula J, Casaccia-Bonnefil P, Ezhevsky SA, Osterhout DJ, Levine JM, Dowdy SF, Chao MV, Koff A (2001) p21cip1 is required for the differentiation of oligodendrocytes independently of cell cycle withdrawal. EMBO J 2:27–34.

7.4 Publication #4: Nguyen,L., Malgrange,B., Rocher,V., Hans,G., Moonen,G., Rigo,J.M., and Belachew,S. (2003). Chemical inhibitors of cyclin-dependent kinases control proliferation, apoptosis and differentiation of oligodendroglial cells. *Int. J. Dev. Neurosci.* 21:321-326.

PERGAMON

Int. J. Devl Neuroscience 21 (2003) 321–326

INTERNATIONAL JOURNAL of DEVELOPMENTAL NEUROSCIENCE

www.elsevier.com/locate/ijdevneu

Chemical inhibitors of cyclin-dependent kinases control proliferation, apoptosis and differentiation of oligodendroglial cells

Laurent Nguyen [a], Brigitte Malgrange [a], Véronique Rocher [a], Grégory Hans [a], Gustave Moonen [a,b], Jean-Michel Rigo [a,1], Shibeshih Belachew [a,b,*,1]

[a] *Center for Cellular and Molecular Neurobiology, University of Liège, 17 Place Delcour, B-4020 Liège, Belgium*
[b] *Department of Neurology, University of Liège, C.H.U. (B35) Sart Tilman, B-4000 Liège, Belgium*

Received 13 March 2003; received in revised form 2 June 2003; accepted 3 June 2003

Abstract

Since cyclin-dependent kinases (Cdks) and their endogenous inhibitors (Cdkis) play an essential role as regulators of cell cycle withdrawal and onset of differentiation within oligodendroglial cells, we assessed here the effects of exogenous chemical Cdk inhibitors (CKIs) on cultured rat cortical oligodendrocyte progenitor cells (OPCs). We showed that purine derivatives and especially roscovitine strongly inhibited OPCs proliferation. In the presence of mitogenic signals, roscovitine synergized with thyroid hormone to stimulate oligodendrocyte differentiation. Roscovitine also prevented oligodendroglial apoptosis induced by growth factor deprivation. We thus demonstrated that small molecular weight chemical CKIs have important effects on crucial events of oligodendroglial development in vitro. This might open prospects for using these apparently well tolerated agents in remyelination strategies.

Keywords: Roscovitine; Cell cycle; Oligodendroglia; Differentiation; Apoptosis; Rat cerebral cortex

1. Introduction

Proliferation, differentiation and survival of neural cells during the development of central nervous system (CNS) are known to depend on both intrinsic and extrinsic signalling (Edlund and Jessell, 1999). In particular, differentiation of oligodendrocyte progenitor cells (OPCs) is tightly coupled to cell cycle withdrawal which has been suggested to depend on complex mechanisms including the interaction of at least two cell-intrinsic components that are controlled by extracellular signals: (i) a timer regulated by platelet-derived growth factor (PDGF) that measures elapsed time, and (ii) an effector component that can be triggered by hydrophobic signals, such as retinoic acid or thyroid hormone acting at the level of the induction of permanent cell cycle exit, associated with the onset of differentiation (Durand and Raff, 2000).

Cell cycle arrest appears to be a crucial event to which many molecular pathways, which regulate oligodendrocyte development, converge. Progression throughout the mammalian cell cycle is known to be regulated by phosphorylation/dephosphorylation of the retinoblastoma protein (pRb), a process operated by cyclin-dependent kinases (Cdks) which require association with cyclins and phosphorylation to be active (Morgan, 1997). Superimposed upon this core unit, the endogenous Cdk-inhibitors (Cdkis) inhibit Cdk activity and thereby can prevent S phase entry and counteract with the effects of activating cyclins (Sherr and Roberts, 1999). So far, two families of Cdkis have been identified in mammalian cells: the Cip/Kip family which includes $p27^{Kip1}$, $p21^{Cip1}$ and $p57^{Kip2}$ and the Ink4 family which includes $p16^{Ink4a}$, $p15^{Ink4b}$, $p18^{Ink4c}$ and $p19^{Ink4d}$ (Sherr and Roberts, 1999). In the oligodendroglial lineage, $p21^{Cip1}$ and $p27^{Kip1}$ accumulate as OPCs proliferate (Ghiani et al., 1999) and inhibit cyclin E-Cdk2 complex activity, which appears to play a pivotal function in OPC cell cycle decisions occurring at G_1/S checkpoint (Ghiani and Gallo, 2001; Belachew et al., 2002). Furthermore, intrinsic differences in vivo in cyclin E/cdk2 expression and activity in adult OPCs may underlie the slowly proliferative state that characterizes these so-called "quiescent" OPCs from adult white matter (Belachew et al., 2002).

Based upon this established function of Cdks in cell cycle regulation and given that approximately 90% of all neoplasias are associated with Cdk hyperactivation (Hartwell and Kastan, 1994), several strategies have recently been

* Corresponding author. Tel.: +32-4-3665905; fax: +32-4-3665912.
E-mail address: sbelachew@ulg.ac.be (S. Belachew).
[1] J.-M.R. and S.B. contributed equally to this work.

0736-5748/$30.00
doi:10.1016/S0736-5748(03)00075-3

designed to develop pharmacological compounds that are capable of inhibiting the catalytic Cdk subunit, i.e. its ATP-binding site. Such chemical Cdk inhibitors (CKIs) are extensively evaluated in cancer chemotherapy as well as in other indications including neurodegenerative disorders, since these agents also inhibit apoptosis in post-mitotic neuronal cells (Sausville et al., 1999).

In the present work, considering the prominent role of Cdk regulation in OPC cell cycle arrest and withdrawal (Belachew et al., 2002), we assessed the effect of synthetic exogenous CKIs on proliferation, differentiation and cell death within the oligodendroglial lineage in vitro. More specifically, we used purine derivatives (roscovitine, RP107 and aminopurvalanol) and paullones (alsterpaullone) that are relatively selective for Cdk2.

2. Experimental procedures

2.1. Cell culture

Primary oligosphere-derived OPCs cultures were prepared from 1- to 3-day-old rat pups as previously described (Belachew et al., 2000), using a slight modification of the isolation procedure of Avellana-Adalid et al. (1996). The animals were killed following National Institutes of Health animal welfare guidelines. The cerebral cortices of 1–3-day-old rat pups were dissected and collected in PBS supplemented with glucose at 4.5 g/l, carefully freed of meninges and vessels, and dissociated by sieving successively through a 225 and a 25 μm nylon mesh. Cells were collected in PBS containing 25 mM HEPES. The cell suspension was layered on top of a pre-centrifuged (30 min at 26,000 × *g*) Percoll density gradient (1.04 g/ml; Pharmacia, Sweden) and centrifuged for 15 min at 26,000 × *g*. Cell debris which remained in the top aqueous phase were discarded and the interphase below the debris and just above the red blood cells was resuspended in PBS–HEPES. The suspension was centrifuged three times (10 min at 400 *g*) in PBS–HEPES to eliminate Percoll. The final pellet was resuspended in DMEM supplemented with N_1, biotin (10 ng/ml) and 30% (v/v) of B104-conditioned medium (CM) (Louis et al., 1992). Five milliliters of the cell suspension was then seeded on an uncoated 25 cm^2 tissue culture flask (Falcon; Becton-Dickinson, USA) at a concentration of 4×10^6 cells/ml. After 24 and 48 h, the flask was smoothly shaken and the suspension transferred into a new flask, thus eliminating adherent cells. After these pre-platings, the progenitor cells have grown as spheroid aggregates termed "oligospheres" (150–300 μm diameter). To induce an oligodendrocyte commitment, oligospheres were seeded on polyornithine-coated (0.1 mg/ml) glass coverslips in the center of 35 mm plastic Petri dishes (NUNC, Denmark) at a density of 10–25 oligospheres per coverslip, and then were switched to growth factor-free DMEM-N_1 medium.

2.2. Immunocytochemistry

Cultures on coverslips were fixed in 4% (w/v) paraformaldehyde for 10 min at room temperature. Non-specific binding was blocked by a 60 min treatment in a PBS solution containing non-fat dry milk (15 mg/ml). This was followed by a 60 min incubation at 37 °C with rabbit polyclonal anti-galactocerebroside (GalC) (1:200) (Sigma Chemical Co., St. Louis, MO) and A2B5 (1:100) IgM antibodies (Boehringer Mannheim). As secondary antibodies, a rhodamine-conjugated anti-rabbit IgG (Jackson, ImmunoResearch, USA) at 1:400 and a FITC-conjugated anti-mouse IgM (Jackson, ImmunoResearch) at 1:250 dilution were incubated for 60 min at room temperature. Triple PBS rinses were performed between each step. The preparations were mounted in Fluoprep and imaged using a Bio-Rad MRC1024 laser scanning confocal microscope. The total cell number was measured after counterstaining the cultures with the nuclear dye Hoescht 33258 (0.4 μg/ml in PBS for 15 min) at the end of the procedure. For cell number assessment, 10 microscopic fields (±200 cells per field) (Axiovert 135 fluorescence microscope, 40× objective, Zeiss) were counted for each coverslip and two coverslips were analyzed for each experimental condition. Each experimental condition was tested in three independent experiments, yielding to a total number of cells counted that ranged between 2517 and 3004 for each condition.

2.3. BrdU incorporation assay

To label cells in S phase in vitro, bromodeoxyuridine (BrdU, 10 μM, Sigma), which is incorporated into replicating DNA, was added to the cultures for 72 h prior to staining. The treatment of cultures (in DMEM-N_1 + PDGF 10 ng/ml) with BrdU started 24 h after allowing the oligospheres to adhere and spread on a coated substrate. Chemical CKIs were added to the cultures together with BrdU for the same 72 h time period. Using such a long (72 h) BrdU incorporation assay allowed us: (i) to be devoid of any artefact that would result from the lack of synchronization of our OPC culture at the start of the proliferation assay, and (ii) to cover a time-frame corresponding to the duration of two–three complete cell cycles; thus, obtaining a more reliable and accurate assessment of the total pool of OPCs that remained cycling in our experimental conditions (given that cell cycle duration can be varied considerably between single cells). A2B5 labeling was performed as described in the Section 2.2 except that the secondary antibody was replaced by a TRITC-conjugated anti-mouse IgM (Jackson, ImmunoResearch) at 1:250 dilution. Coverslips were then post-fixed for another 10 min incubation in 4% (w/v) paraformaldehyde, incubated in NaOH 0.07N for 10 min, once again post-fixed for another 10 min, permeabilized in Triton-X100 (0.1%) and finally incubated for 45 min with a FITC-conjugated anti-BrdU antibody (1:3,

Becton-Dickinson). Cell imaging and countings were performed as described in the Section 2.2.

2.4. TUNEL labeling

Apoptosis was analyzed in OPC cultures maintained for 5 days in various experimental conditions. We used the terminal deoxynucleotidyl transferase-mediated dUTP nick-end labeling (TUNEL) method using the ApopTag fluorescent detection kit (Oncor, Gaitherburg, MD). The cultures were fixed with 4% paraformaldehyde for 20 min at room temperature. Equilibration buffer was then applied for 30 min. Cultures were incubated with working strength TdT enzyme for 1 h at 37 °C. The reaction was stopped with working strength stop/wash buffer. Cultures were then washed and further incubated with anti-digoxigenin–FITC. The total number of oligodendrocytes was measured after counterstaining the culture with the nuclear dye Hoescht 33258 (0.4 μg/ml for 15 min) at the end of the procedure.

2.5. Drugs

Roscovitine, alsterpaullone, RP107 (1-methyl-6-aminopurine) and aminopurvalanol were kindly provided by Laurent Meijer (Roscoff, France). PDGF-AA was from Prepro Tech (Rocky Hill, NJ) and triiodothyronine (T_3) from Sigma.

3. Results

3.1. Chemical Cdk-inhibitors inhibit PDGF-induced OPCs proliferation

To measure the effect of several small molecular weight CKIs on the proliferation of OPCs, the cultured cells were studied in the outgrowth zone of expanded oligospheres (Fig. 1A–C). OPCs were allowed to incorporate BrdU for 72 h in DMEM-N_1 supplemented with PDGF in the presence of roscovitine (Fig. 2A), alsterpaullone (Fig. 2B), aminopurvalanol (Fig. 2C) or RP 107 (Fig. 2D). We specifically assessed CKIs effect on the proliferation of $A2B5^+$ OPCs by performing double stainings for BrdU and A2B5. We observed a dose-dependent decrease of the BrdU labeling index with all the tested CKIs. The IC_{50} values of their anti-mitotic effect were (mean ± S.D., $n = 3$) 0.18 ± 0.2 μM for roscovitine, 2.36 ± 0.4 μM for alsterpaullone, 1.79 ± 0.3 μM for aminopurvalanol and 2.4 ± 0.1 μM for RP 107.

3.2. Roscovitine has opposite effects on the survival of proliferating OPCs and differentiating oligodendrocytes

Growth factor deprivation in vitro is known to trigger the differentiation of OPCs, but also induces apoptosis to a significant extent (Casaccia-Bonnefil, 2000). To investigate the possible interaction of chemical CKIs with this developmental cell death, the percentage of apoptotic cells was measured in oligosphere-derived oligodendroglial cultures that had been allowed to grow for 5 days in mitogen-free DMEM-N_1. In such conditions, we observed an anti-apoptotic effect of roscovitine (Fig. 3A) occurring at a concentration range (1–3 μM) that had been shown to

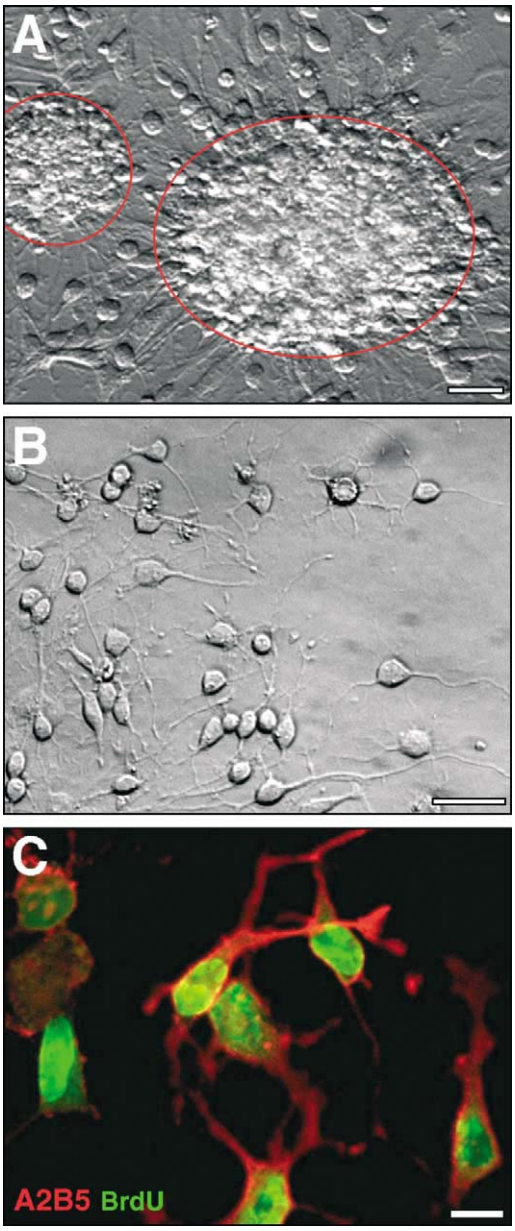

Fig. 1. PDGF-induced proliferation of cultured oligodendrocyte progenitor cells derived from oligospheres. (A and B) Phase–contrast views of expanded oligospheres after attachment onto a coated substrate and cultured in DMEM-N_1 supplemented with PDGF (10 ng/ml). OPCs rapidly spread out of the spheres and were assessed for BrdU incorporation in the monolayer appearing in the outgrowth zone located outside the spheres that are represented in (A) as red circled regions. (B) Phase–contrast view displaying the typical OPC density observed in such peripheral areas around oligospheres, where proliferation was quantified. (C) Confocal microscopy image of PDGF-stimulated proliferating OPCs immunostained with A2B5 (red) and anti-BrdU (green) antibodies. Scale bar = 50 μm for (A and B) and 15 μm for C.

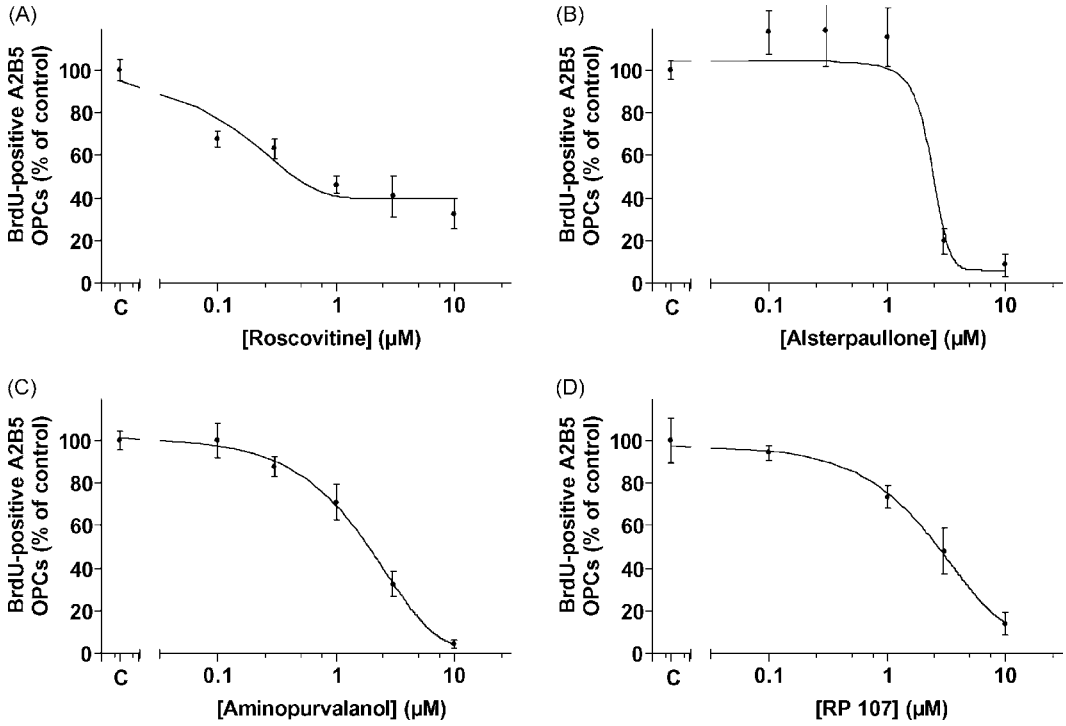

Fig. 2. CKIs inhibit oligodendrocyte progenitor cell proliferation. After being switched (24 h after seeding the oligospheres on a coated surface) from a B_{104}CM containing medium to DMEM-N_1 supplemented with PDGF (10 ng/ml), OPCs were allowed to incorporate BrdU (10 μM) for 72 h. The BrdU incorporation index (%) was expressed as a percentage of the control value specifically within the highly proliferative A2B5$^+$ OPCs. We showed the dose–response curves of the anti-mitotic effects of roscovitine (A), alsterpaullone (B), aminopurvalanol (C) and RP 107 (D).

inhibit cell cycle progression in the presence of PDGF (see Fig. 2A). Conversely, if OPCs were maintained for the same time-frame (5 days) in a proliferative state in the presence of PDGF (10 ng/ml) (Fig. 3B), the absolute intensity of the apoptotic process was by far lower (9.78 ± 1.17% of the cells; mean ± S.D., $n = 5$) than in mitogen-free medium (75.14 ± 5.1% of total cells; mean ± S.D., $n = 5$) and roscovitine then had no effect on the proportion of apoptotic cells except at high non-physiological concentrations (30 μM).

3.3. In a mitogenic environment, roscovitine synergizes with T_3 to stimulate oligodendrocyte differentiation

We finally assessed the effects of CKIs on the kinetics of oligodendrocyte maturation by analysing the immunophenotype of the cultures after 5 days in DMEM-N1 supplemented (Fig. 4A) or not (Fig. 4B) with PDGF and in the presence of roscovitine, T_3 (30 ng/ml) or both T_3 and roscovitine (3 μM). We quantified the relative proportions of GalC-positive cells in each condition. The basal level

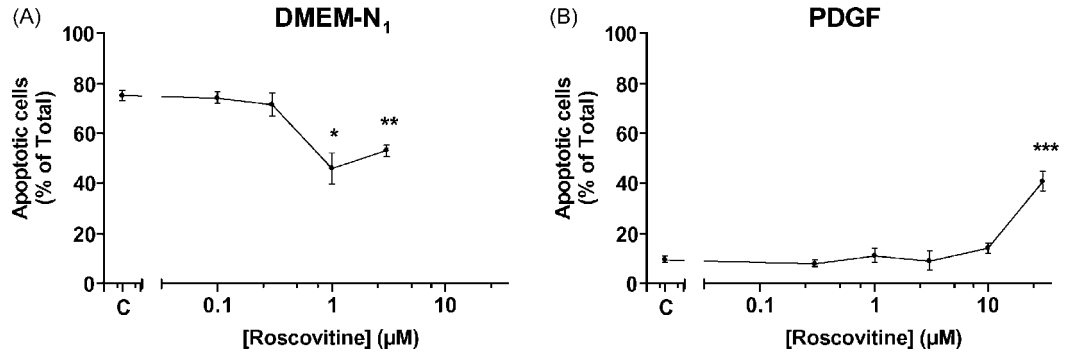

Fig. 3. Dual effects of roscovitine on oligodendroglial apoptosis. Apoptotic cell death was determined by performing *TUNEL* viability assays with cultures incubated for 5 days in the presence of roscovitine, respectively, in DMEM-N1 supplemented (B) or not (A) with PDGF (10 ng/ml). Histograms represent apoptotic cells as a percentage of the total cell number evaluated by counterstaining cell nuclei with the Hoescht 33258 dye. Statistical data (Student's *t*-test) arose from comparison with the control for each condition. (*) $P < 0.05$; (**) $P < 0.01$; (***) $P < 0.001$.

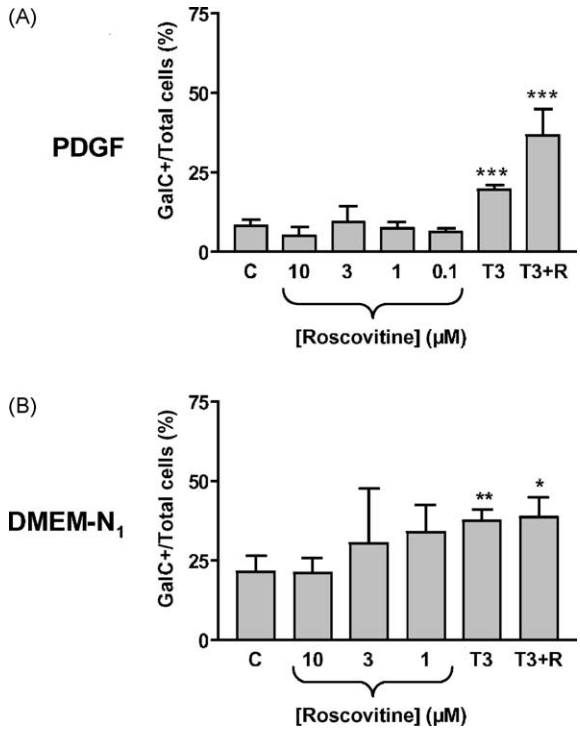

Fig. 4. Roscovitine synergizes with the pro-differentiating effect of T_3 in a mitogenic environment. The percentage of GalC-expressing immature oligodendrocytes was evaluated after 5 days of differentiation in the presence of PDGF (10 ng/ml) (A) or in mitogen-free DMEM-N1 (B). In such conditions, we assessed the effect of roscovitine at several concentrations, the effect of T_3 (30 ng/ml) alone or in combination with roscovitine at 3 μM ($T_3 + R$). Statistical data (Student's *t*-test) were expressed as a comparison with the control condition: (*) $P < 0.05$; (**) $P < 0.01$; (***) $P < 0.001$.

of $GalC^+$ cells was (mean ± S.D., $n = 5$) 8.4 ± 1.8% of total cells with PDGF and 21.68 ± 5.1% of total cells in the absence of PDGF. Anti-mitotic concentrations of roscovitine had no effect on the proportion of $GalC^+$ cells, neither in growth factor-free medium nor in PDGF-enriched DMEM-N_1. In the presence of PDGF, T_3 increased the percentage of $GalC^+$ cells to 19.7 ± 1.4% of total cells if applied alone and 36.8 ± 8.2% when combined with 3 μM roscovitine. To a much lesser extent, T_3 also slightly stimulated oligodendrocyte maturation in DMEM-N_1 with no additional effect of roscovitine.

4. Discussion

Consistent with the increasing evidence that endogenous Cdkis may play a major role in OPC cell cycle exit, we demonstrated here that synthetic small molecular weight CKIs, mainly inhibitors of Cdk2, regulate oligodendroglial growth in vitro. Roscovitine, which was the most potent inhibitor of Cdk2 among the tested CKIs, had the most effective anti-mitotic activity on cultured OPCs with an IC_{50} in the micromolar range. We also demonstrated that roscovitine alone had no effect on oligodendrocyte maturation but potentiated T_3-induced differentiation in the presence of PDGF.

These results are consistent with the key role of cyclin E-Cdk2 complex, the main biochemical target of roscovitine, during oligodendroglial development (Ghiani and Gallo, 2001; Belachew et al., 2002). Thus, blockade of this enzymatic complex by roscovitine: (i) appears to be sufficient to induce OPC cell cycle arrest by mimicking the effect of endogenous Cdkis such as p27 acting on the cdk2-dependent G_1/S checkpoint; (ii) can increase the pro-differentiating effect of thyroid hormone in a mitogenic environment, hereby mimicking somehow the pro-differentiating effect of another endogenous Cdki, p21 (Zezula et al., 2001). Given that Cdk2-dependent G_1/S cell cycle arrest is known to be a necessary but insufficient condition to trigger differentiation in the oligodendroglial lineage (Belachew et al., 2002), roscovitine likely controls differentiation by interacting with other intracellular kinases. As a matter of fact, roscovitine is also known to regulate Cdk5, Cdk7 and, to a lesser extent, ERK1/ERK2 (Meijer et al., 1997; Knockaert et al., 2002) that could be part of the yet unknown T_3-induced intracellular cascade. We hypothesized that such properties of synthetic chemical CKIs might indeed allow them to stimulate differentiation and thus myelinating function of quiescent OPCs known to persist both in adult normal white matter and in MS lesions.

We have also shown in the presence of PDGF that roscovitine induced apoptosis of oligodendrocytes, but only at very high concentrations. On the other hand, apoptosis induced by growth factor deprivation was effectively reduced by low concentrations of roscovitine. Such opposite effects of roscovitine on apoptosis have already been described in other cell types. CKIs classically trigger apoptosis, preferentially in many dividing but also non-dividing cells, or facilitate cell death mediated by other agents (Meijer et al., 1999; Shibata et al., 1996). It is well established that α-tumor necrosis factor inhibits mitogen-elicited OPC proliferation, and enhances apoptosis with a concomittant up-regulation of p21/p27 and a parallel decrease of Cdk2 activity (Yu et al., 2000). It has also been shown that in the presence of mitogenic stimulation, OPCs induced to growth arrest by overexpressing $p27^{Kip1}$ are programmed to die because of an inappropriate coordination between signal transduction pathways activated by exogenous stimuli and intrinsic components of cell cycle machinery, creating a genotoxic stimulus and activating a p53-dependent death program (Casaccia-Bonnefil, 2000). Furthermore, it is now recognized that chemical CKIs can protect post-mitotic PC12 neuronal cells from apoptosis induced by nerve growth factor withdrawal (Park et al., 1996).

The interaction of synthetic CKIs with life/death decisions within the oligodendroglial lineage strengthens the evidence that cell cycle exit, onset of differentiation and apoptosis are tightly linked processes controlled by Cdks and their inhibitors (King and Cidlowski, 1998). Considering that synthetic CKIs are already used in clinical

trials as chemotherapeutic agents and seem well tolerated (Senderowicz and Sausville, 2000), the question of the potential pro-differentiating and anti-apoptotic actions of these drugs on oligodendroglial lineage cells in vivo should soon be addressed using experimental autoimmune encephalomyelitis as an animal model of immune-mediated demyelination. Likewise, as many glial tumors may actually arise from a dysregulation of proliferation at the level of bipotential oligodendroglial progenitors (Shoshan et al., 1999), CKIs may also become interesting candidates for future anti-mitotic treatment of OPC-derived gliomas.

Acknowledgements

We are particularly grateful to Dr. Laurent Meijer (CNRS, Station Biologique, Roscoff, Bretagne, France) for kindly providing the different chemical CKIs. This work was supported by the Fonds pour la Formation à la Recherche dans l'Industrie et dans l'Agriculture (F.R.I.A., Belgium), the Ligue Belge de la Sclérose en Plaques, the Charcot Fondation and Concerted Action of the French Community of Belgium. We thank P. Ernst-Gengoux for her technical support and expertise. B. Malgrange is a research associate and S. Belachew is a post-doctoral researcher of the FNRS-Belgium.

References

Avellana-Adalid, V., Nait-Oumesmar, B., Lachapelle, F., Baron-Van Evercooren, A., 1996. Expansion of rat oligodendrocyte progenitors into proliferative "oligospheres" that retain differentiation potential. J. Neurosci. Res. 45, 558–570.

Belachew, S., Malgrange, B., Rigo, J.-M., Rogister, B., Leprince, P., Hans, G., Nguyen, L., Moonen, G., 2000. Glycine triggers an intracellular calcium influx in oligodendrocyte progenitor cells which is mediated by the activation of both the ionotropic glycine receptor and Na^+-dependent transporters. Eur. J. Neurosci. 12, 1924–1930.

Belachew, S., Aguirre, A.A., Wang, H., Vautier, F., Yuan, X., Anderson, S., Kirby, M., Gallo, V., 2002. Cyclin-dependent kinase-2 controls oligodendrocyte progenitor cell cycle progression and is downregulated in adult oligodendrocyte progenitors. J. Neurosci. 22, 8553–8562.

Casaccia-Bonnefil, P., 2000. Cell death in the oligodendrocyte lineage: a molecular perspective of life/death decisions in development and disease. Glia 29, 124–135.

Durand, B., Raff, M., 2000. A cell-intrinsic timer that operates during oligodendrocyte development. Bioessays 22, 64–71.

Edlund, T., Jessell, T.M., 1999. Progression from extrinsic to intrinsic signaling in cell fate specification: a view from the nervous system. Cell 96, 211–224.

Ghiani, C.A., Gallo, V., 2001. Inhibition of cyclin *E*-cyclin-dependent kinase 2 complex formation and activity is associated with cell cycle arrest and withdrawal in oligodendrocyte progenitor cells. J. Neurosci. 21, 1274–1282.

Ghiani, C.A., Eisen, A.M., Yuan, X., DePinho, R.A., McBain, C.J., Gallo, V., 1999. Neurotransmitter receptor activation triggers p27(Kip1) and p21(CIP1) accumulation and G1 cell cycle arrest in oligodendrocyte progenitors. Development 126, 1077–1090.

Hartwell, L.H., Kastan, M.B., 1994. Cell cycle control and cancer. Science 266, 1821–1828.

King, K.L., Cidlowski, J.A., 1998. Cell cycle regulation and apoptosis. Annu. Rev. Physiol. 60, 601–617.

Knockaert, M., Greengard, P., Meijer, L., 2002. Pharmacological inhibitors of cyclin-dependent kinases. Trends Pharmacol. Sci. 23, 417–425.

Louis, J.C., Magal, E., Muir, D., Manthorpe, M., Varon, S., 1992. CG-4, a new bipotential glial cell line from rat brain, is capable of differentiating in vitro into either mature oligodendrocytes or type-2 astrocytes. J. Neurosci. Res. 31, 193–204.

Meijer, L., Borgne, A., Mulner, O., Chong, J.P., Blow, J.J., Inagaki, N., Inagaki, M., Delcros, J.G., Moulinoux, J.P., 1997. Biochemical and cellular effects of roscovitine, a potent and selective inhibitor of the cyclin-dependent kinases cdc2, cdk2 and cdk5. Eur. J. Biochem. 243, 527–536.

Meijer, L., Leclerc, S., Leost, M., 1999. Properties and potential-applications of chemical inhibitors of cyclin-dependent kinases. Pharmacol. Ther. 82, 279–284.

Morgan, D.O., 1997. Cyclin-dependent kinases: engines, clocks, and microprocessors. Annu. Rev. Cell. Dev. Biol. 13, 261–291.

Park, D.S., Farinelli, S.E., Greene, L.A., 1996. Inhibitors of cyclin-dependent kinases promote survival of post-mitotic neuronally differentiated PC12 cells and sympathetic neurons. J. Biol. Chem. 271, 8161–8169.

Sausville, E.A., Zaharevitz, D., Gussio, R., Meijer, L., Louarn-Leost, M., Kunick, C., Schultz, R., Lahusen, T., Headlee, D., Stinson, S., Arbuck, S.G., Senderowicz, A., 1999. Cyclin-dependent kinases: initial approaches to exploit a novel therapeutic target. Pharmacol. Ther. 82, 285–292.

Senderowicz, A.M., Sausville, E.A., 2000. Preclinical and clinical development of cyclin-dependent kinase modulators. J. Natl. Cancer Inst. 92, 376–387.

Sherr, C.J., Roberts, J.M., 1999. CDK inhibitors: positive and negative regulators of G1-phase progression. Genes Dev. 13, 1501–1512.

Shibata, Y., Nishimura, S., Okuyama, A., Nakamura, T., 1996. p53-Independent induction of apoptosis by cyclin-dependent kinase inhibition. Cell Growth Differ. 7, 887–891.

Shoshan, Y., Nishiyama, A., Chang, A., Mork, S., Barnett, G.H., Cowell, J.K., Trapp, B.D., Staugaitis, S.M., 1999. Expression of oligodendrocyte progenitor cell antigens by gliomas: implications for the histogenesis of brain tumors. Proc. Natl. Acad. Sci. U.S.A. 96, 10361–10366.

Yu, C., Takeda, M., Soliven, B., 2000. Regulation of cell cycle proteins by TNF-alpha and TGF-beta in cells of oligodendroglial lineage. J. Neuroimmunol. 108, 2–10.

Zezula, J., Casaccia-Bonnefil, P., Ezhevsky, S.A., Osterhout, D.J., Levine, J., Dowdy, S.F., Chao, M.V., Koff, A., 2001. p21cip1 is required for the differentiation of oligodendrocytes independently of cell cycle withdrawal. EMBO Rep. 2, 27–34.

7.5 Publication #5: Belachew,S., Chittajallu,R., Aguirre,A.A., Yuan,X., Kirby,M., Anderson,S., and Gallo,V. (2003). Postnatal NG2 proteoglycan-expressing progenitor cells are intrinsically multipotent and generate functional neurons. *J. Cell Biol.* 161:169-186.

JCB Article

Postnatal NG2 proteoglycan–expressing progenitor cells are intrinsically multipotent and generate functional neurons

Shibeshih Belachew,[1,2] Ramesh Chittajallu,[1,2] Adan A. Aguirre,[1] Xiaoqing Yuan,[2] Martha Kirby,[3] Stacie Anderson,[3] and Vittorio Gallo[1,2]

[1]Center for Neuroscience Research, Children's Research Institute, Children's National Medical Center, Washington, DC 20010
[2]Laboratory of Cellular and Synaptic Neurophysiology, National Institute of Child Health and Human Development, National Institutes of Health, Bethesda, MD 20892
[3]Gene Transfer Laboratory, Hematopoiesis Section, Flow Cytometry Core Unit, National Human Genome Research Institute, National Institutes of Health, Bethesda, MD 20892

Neurogenesis is known to persist in the adult mammalian central nervous system (CNS). The identity of the cells that generate new neurons in the postnatal CNS has become a crucial but elusive issue. Using a transgenic mouse, we show that NG2 proteoglycan–positive progenitor cells that express the 2′,3′-cyclic nucleotide 3′-phosphodiesterase gene display a multipotent phenotype in vitro and generate electrically excitable neurons, as well as astrocytes and oligodendrocytes. The fast kinetics and the high rate of multipotent fate of these NG2$^+$ progenitors in vitro reflect an intrinsic property, rather than reprogramming. We demonstrate in the hippocampus in vivo that a sizeable fraction of postnatal NG2$^+$ progenitor cells are proliferative precursors whose progeny appears to differentiate into GABAergic neurons capable of propagating action potentials and displaying functional synaptic inputs. These data show that at least a subpopulation of postnatal NG2-expressing cells are CNS multipotent precursors that may underlie adult hippocampal neurogenesis.

Introduction

The identity of postnatal central nervous system (CNS)* multipotent neural stem cells (NSCs) in vivo is a matter of intense debate. To date, a lineage continuum has not yet been established between embryonic neuroepithelial and "adult" NSCs, which emerge in restricted germinative areas during the first postnatal week (Alvarez-Buylla and Temple, 1998; Alvarez-Buylla et al., 2001). Embryonic radial glia can generate neurons (Malatesta et al., 2000; Noctor et al., 2001), and adult NSCs express molecular markers (glial fibrillary acidic protein; GFAP) and ultrastructural characteristics of astrocytes (Doetsch et al., 1999; Laywell et al., 2000). However, the use of GFAP antigenicity as a feature of postnatal NSCs is not without caveats and mostly applies to the subventricular zone (SVZ; Doetsch et al., 1999).

Similar to CNS stem cells, NG2 proteoglycan–expressing progenitor cells persist and slowly proliferate throughout the adult CNS (Ffrench-Constant and Raff, 1986; Wolswijk and Noble, 1989). During CNS development, the well-characterized anatomical distribution of NG2$^+$ progenitors (Spassky et al., 1998) overlaps with areas where totipotent NSCs reside and ongoing neurogenesis occurs (Alvarez-Buylla and Temple, 1998; Temple and Alvarez-Buylla, 1999). Cells that express the NG2 chondroitin proteoglycan represent the largest pool of postnatal proliferative progenitors

S. Belachew and R. Chittajallu contributed equally to this paper.

The online version of this article includes supplemental material.

Address correspondence to Dr. Vittorio Gallo, Center for Neuroscience Research, Children's Research Institute, Room 5345, Children's National Medical Center, 111 Michigan Ave., N.W., Washington, DC 20010-2970. Tel.: (202) 884-4996. Fax: (202) 884-4988.
E-mail: vgallo@cnmcresearch.org

S. Belachew's present address is Center for Cellular and Molecular Neurobiology, Department of Neurology, University of Liège, B-4000 Liège, Belgium.

*Abbreviations used in this paper: CNP, 2′,3′-cyclic nucleotide 3′-phosphodiesterase; CNS, central nervous system; DNQX, 6,7-dinitro-2,3-quinoxalinedione; GABA, γ-aminobutyric acid; GAD, glutamate decarboxylase; GFAP, glial fibrillary acidic protein; MAP, microtubule-associated protein; NeuN, neuronal nuclei protein; NSC, neural stem cell; OPC, oligodendrocyte progenitor cell; PCNA, proliferating cell nuclear antigen; PLP, proteolipid protein; SCM, stem cell medium; SVZ, subventricular zone; TOAD-64, turned on after division, 64 kD; TTX, tetrodotoxin.

Key words: stem cell; oligodendrocyte progenitor; differentiation; adult neurogenesis; glia

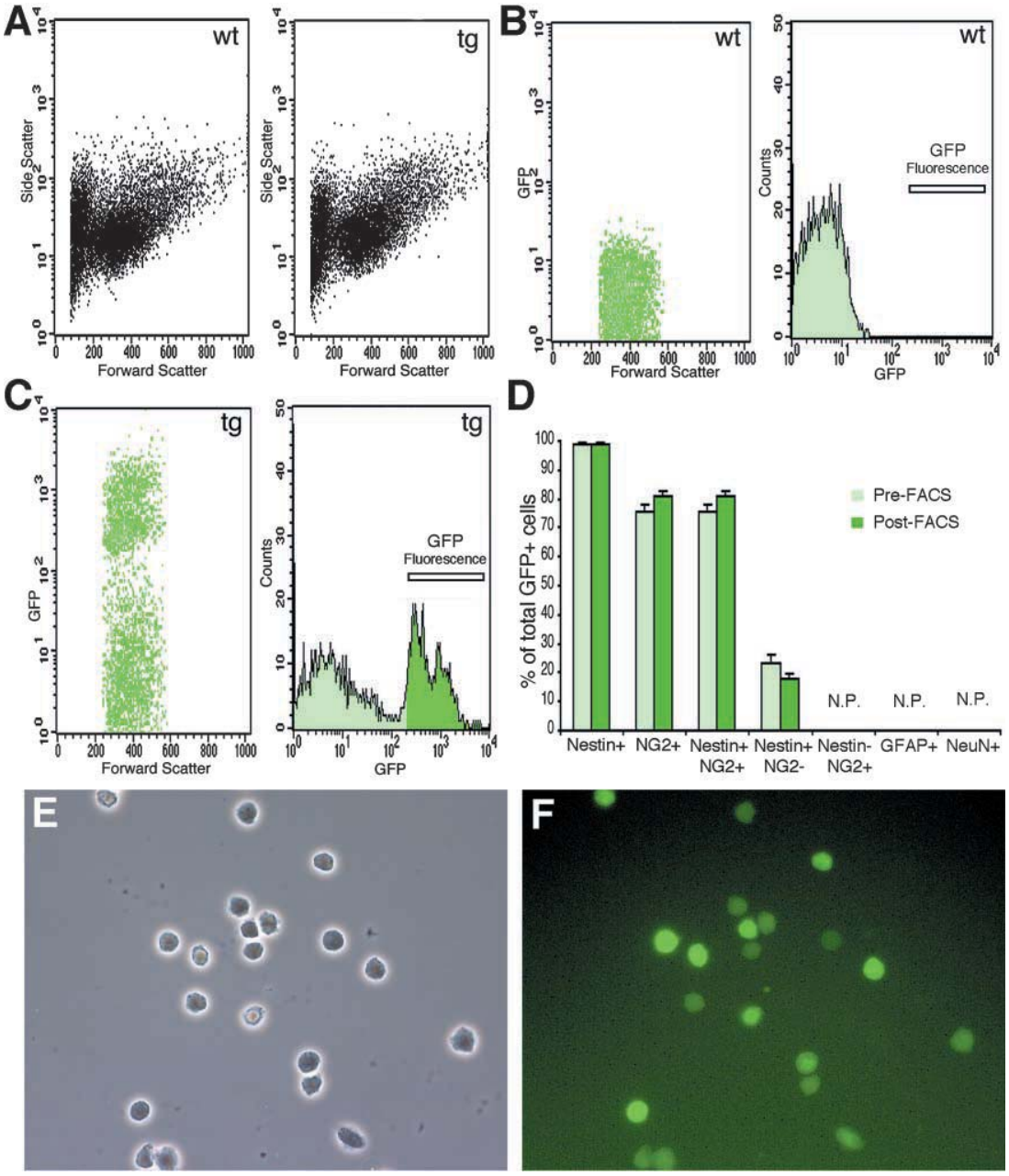

Figure 1. **FACS® purification of early postnatal GFP$^+$ cells from CNP-GFP transgenic brains reveals an NG2$^+$/nestin$^+$ phenotype.** FACS® analysis of acutely dissociated cell suspensions of P2 whole brain from CNP-GFP transgenic mice (tg) and wild-type (wt) littermates displayed identical light forward and side scatter distributions (A). To eliminate erythrocytes and cell debris, forward scatter gating parameters were chosen for further GFP fluorescence analysis (B and C, left panels). Cells from CNP-GFP suspensions that were considered GFP$^+$ and FACS®-selected, were in a range of fluorescence (C, bar in right panel) far above (ratio >5×) maximal background intensity yielded by the wild-type cell suspension (B, bar in right panel). Using such criteria, all FACS®-sorted cells were consistently found to be GFP$^+$, as determined by fluorescence microscopy analysis of cell suspensions plated on coverslips immediately after sorting, and fixed 1 h later (two independent experiments, total cells counted = 1,069, 100% were GFP$^+$; E and F). (D) Immunocytochemical characterization of pre-FACS® and post-FACS® cell suspensions (total GFP$^+$ counted cells = 1069, two independent experiments). N.P., not present. We demonstrated here that pre-FACS® versus post-FACS® GFP$^+$ cells were antigenically identical and mostly expressed an NG2$^+$/nestin$^+$ phenotype. This validated our fluorescence sorting criteria, which did not preferentially select a subset of CNP-GFP$^+$ cells. Phase-contrast (E) and fluorescence (F) views of FACS®-selected cells that were all GFP$^+$.

scattered throughout neurogenic as well as nonneurogenic areas of the CNS (Dawson et al., 2000), but their possible intrinsic stem cell potential has not yet been explored.

To determine to what extent postnatal NG2$^+$ cells may display multipotent stem cell-like properties in vitro and in vivo, we used a transgenic mouse expressing the GFP under the control of the 2′,3′-cyclic nucleotide 3′-phosphodiesterase (CNP) promoter (Belachew et al., 2001; Yuan et al., 2002). In this CNP-GFP transgenic mouse, all NG2$^+$ progenitor cells assessed in the first postnatal week were consis-

tently found to be GFP$^+$ in distinct CNP-GFP transgenic lines (Yuan et al., 2002), indicating that they also expressed the CNP gene.

In white matter regions of the CNP-GFP mice, the spatial and temporal expression pattern of GFP matched oligodendrocyte development from the progenitor stage to mature myelinating oligodendrocytes (Belachew et al., 2001; Yuan et al., 2002). Furthermore, CNP-GFP$^+$ cells expressed oligodendrocyte progenitor markers in the subventricular zone, and mature oligodendrocyte markers in the developing and adult white matter (Yuan et al., 2002). However, CNP-GFP$^+$ cells expressing the NG2 proteoglycan were also found in gray matter regions (Yuan et al., 2002).

Here, we report that acutely purified preparations of CNP-GFP–expressing cells from early postnatal brain can form clonal neurospheres in vitro. Furthermore, we demonstrate that within the CNP-GFP$^+$ population, NG2$^+$ cells represent multipotent progenitors that can rapidly generate astrocytes and mature, action potential–propagating neurons after 48 h of culture. Finally, we provide evidence that a proportion of NG2$^+$/CNP-GFP$^+$ progenitor cells may be a source of new functional neurons in the postnatal hippocampus, where neurogenesis is known to continue in adulthood.

Results

Early postnatal CNP-GFP$^+$ oligodendroglial cells form multipotent neurospheres and rapidly generate neurons, astrocytes, and oligodendrocytes in vitro

All the in vitro data were obtained from a single transgenic line (Belachew et al., 2001; Yuan et al., 2002), but were replicated in another CNP-GFP line (Fig. S2, available at http://www.jcb.org/cgi/content/full/jcb.200210110/DC1, and unpublished data). FACS® was used to generate pure GFP$^+$ cell preparations from early postnatal brain of CNP-GFP mice (Fig. 1, A–F). We characterized the nestin immunophenotype of FACS®-purified GFP$^+$ cells because nestin is an intermediate filament protein expressed in neuroepithelium-derived NSCs during development (Lendahl et al., 1990). We observed that 99.0 ± 0.6% of P2 FACS®-sorted GFP$^+$ cells were nestin$^+$. Furthermore, 81.1 ± 1.6% of FACS®-sorted GFP$^+$ cells were NG2$^+$, whereas 17.9 ± 1.6% were NG2$^-$ (Fig. 1 D; mean ± SEM, total GFP$^+$ counted cells = 1,069, two independent experiments). We also observed that only 6.24 ± 1.02% (mean ± SEM, total GFP$^+$ counted cells = 678) of acutely FACS®-purified GFP$^+$ cells expressed the CNP protein, a marker of more mature oligodendrocytes. No freshly sorted GFP$^+$ cells expressed neuronal (neuronal nuclei protein, NeuN) or astrocytic (GFAP) markers (Fig. 1 D).

To study the developmental fate of early postnatal CNP-GFP$^+$ cells, pure FACS®-sorted GFP$^+$ cells from P2 brains were cultured in stem cell medium (SCM) under two different conditions (Fig. 2 A): (1) "suspension" cultures; cells seeded on uncoated plastic to form floating clonal spheres; and (2) "adherent" monolayer cultures; cells directly plated on polyornithine-coated plastic. In suspension cultures, CNP-GFP$^+$ cells rapidly gave rise to GFP$^+$ neurospheres (Fig. 2, B and C) that displayed high levels of nestin expression (Fig. 2 D). Single clonally expanded GFP$^+$ spheres (8–10 d of suspension culture in SCM) plated on coated plastic generated both NeuN$^+$ neurons and GFAP$^+$ astrocytes in SCM (Fig. 2, E–G). Interestingly, these neurons and astrocytes derived from CNP-GFP$^+$ cells were GFP$^-$, illustrating that CNP gene expression is down-regulated when GFP$^+$ cells undergo nonoligodendroglial differentiation. Similarly, in adherent cultures, FACS®-purified CNP-GFP$^+$ cells that were nestin$^+$ and mostly NG2$^+$ (Fig. 1 D and Fig. 2, H–I) rapidly generated NeuN$^+$/GFP$^-$ neurons, GFAP$^+$/GFP$^-$ astrocytes, and mature O1$^+$/GFP$^+$ oligodendrocytes within 48 h (Fig. 2, J–L).

NG2$^+$ cells represent the multipotent cells in the CNP-GFP$^+$ lineage

To enable accurate determination of cell numbers and percentages, we restricted our quantitative analysis to adherent cultures (Fig. 2 M). We assessed cellular immunophenotypes after 48 h in SCM to prevent misinterpretation of the results due to a possible amplification of an initially undetectable contamination of our FACS®-sorted samples by GFP$^-$ cells (Fig. 1 D). The fate of total FACS®-sorted CNP-GFP$^+$ cells arising from P2 whole brain was compared with the fate of selected subpopulations of CNP-GFP$^+$ cells double-sorted according to their NG2$^+$ (Fig. 3 A) or O4$^+$ phenotype (Yuan et al., 2002).

First, we compared the fate of FACS®-sorted NG2$^+$/CNP-GFP$^+$ cells with that of total CNP-GFP$^+$ cells (Fig. 2 M). In cultures derived from purified NG2$^+$/CNP-GFP$^+$ cells, we observed: (1) a higher percentage of NeuN$^+$ neurons; (2) a lower percentage of GFAP$^+$ astrocytes; and (3) a strikingly lower percentage of nestin$^+$ cells. The different fates of NG2$^+$/CNP-GFP$^+$ cells and total CNP-GFP$^+$ cells must result from specific properties of NG2$^-$ progenitor cells that were shown to be also nestin$^+$ in the initial FACS®-purified suspensions (Fig. 1 D). Therefore, this NG2$^-$/nestin$^+$ population might account for a functionally distinct class of CNP-GFP$^+$ precursors that appears significantly less neurogenic, but more astrogliogenic than NG2$^+$/nestin$^+$ cells. The rapid down-regulation of nestin expression when FACS®-sorted NG2$^+$/nestin$^+$/CNP-GFP$^+$ cells were cultured in SCM suggests that the multipotent fate of these cells is not the result of their de-differentiation into NG2$^-$/nestin$^+$/CNP-GFP$^+$ cells.

O4$^+$/CNP-GFP$^+$ cells were also selectively FACS®-purified and cultured for 48 h in SCM. As compared with the progeny of NG2$^+$/CNP-GFP$^+$ cells, with O4$^+$/CNP-GFP$^+$ cells (Fig. 2 M) we observed (1) a significant decrease in the percentage of NeuN$^+$ neurons and GFAP$^+$ astrocytes; (2) a smaller percentage of NG2$^+$ cells; and (3) a higher proportion of O4$^+$ and O1$^+$ oligodendrocyte lineage cells. Given that the NG2 and O4 phenotypes are known to partially overlap, the fact that purified O4$^+$/CNP-GFP$^+$ cells still generated a small percentage of neurons and astrocytes was either due to the presence of NG2$^+$/O4$^+$ cells within the FACS®-selected O4$^+$/CNP-GFP$^+$ population (unpublished data), or to an intrinsic property of O4$^+$ cells. Altogether, these results suggest that a sizeable proportion of NG2$^+$ cells in culture represent postnatal multipotent precursor cells.

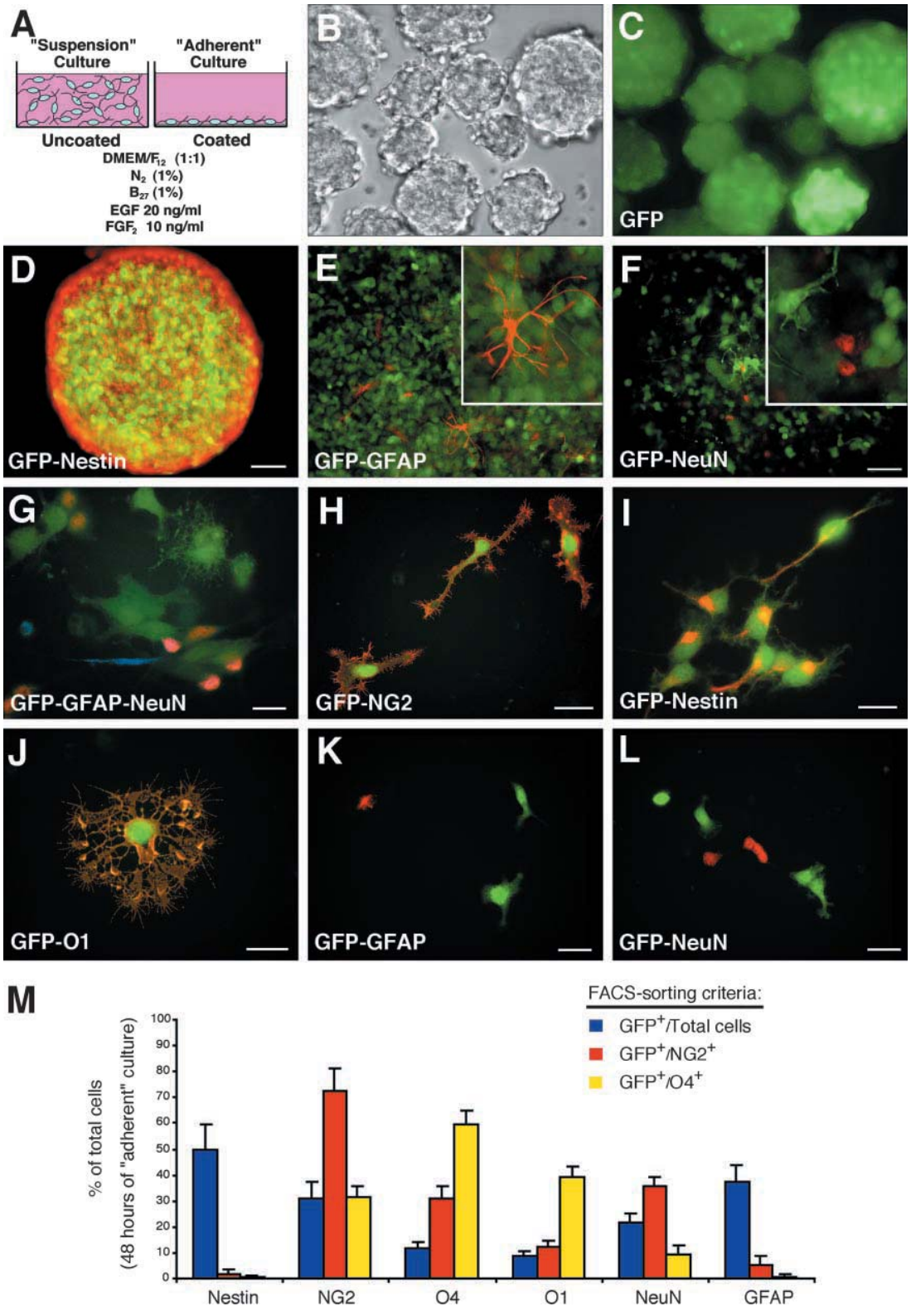

Figure 2. **Early postnatal CNP-GFP$^+$ cells generate multipotent neurospheres and give rise to neurons, astrocytes, and oligodendrocytes in vitro.** (A) Culture conditions. Phase-contrast (B) and fluorescence (C) views of GFP$^+$ neurospheres grown in suspension (5 d in vitro) on uncoated substrate in EGF- and FGF2-containing medium (SCM). (D) A clonally expanded GFP$^+$ neurosphere expressed high levels of nestin immunostaining (red). Clonal spheres gave rise to GFAP$^+$/GFP$^-$ astrocytes (E, red) and NeuN$^+$/GFP$^-$ neurons (F, red) within 2 d post-plating on polyornithine-coated coverslips. G shows GFAP$^+$ (blue) astrocytes, NeuN$^+$ (red) neurons, and GFP$^+$ oligodendroglial cells derived from a single clonal GFP$^+$ sphere. When cultured in adherent conditions, i.e., on polyornithine-coated surface directly after FACS® sorting, NG2$^+$(H, red)/nestin$^+$(I, red) GFP$^+$ cells also expressed a multipotent fate within 2 d in SCM, and generated mature O1$^+$(J, red)/GFP$^+$

Clonal analysis of cultured NG2$^+$/CNP-GFP$^+$ cells

NG2$^+$/CNP-GFP$^+$ cells were FACS®-purified (Fig. 3, A–D) and cultured at clonal dilution for 1 week in SCM. We performed two independent experiments yielding similar results, and assessed a total of 297 clones (Fig. 3 E; 18 ± 3 cells/clone, mean ± SEM, ranging from 10 to 34). The efficiency of clone generation was 0.43 ± 0.02% (number of clones/number of NG2$^+$/CNP-GFP$^+$ cells seeded). The vast majority of the clones comprised three cell types, i.e., astrocytes (GFAP$^+$), neurons (NeuN$^+$), and O4$^+$/CNP-GFP$^+$ cells (Fig. 3, E–J). No clone was found to be devoid of CNP-GFP$^+$ cells, nor to contain exclusively CNP-GFP$^+$ cells. It is noteworthy that multipotent clones obtained from clonal cultures of NG2$^+$/CNP-GFP$^+$ cells contained slightly more astrocytes than neurons (Fig. 3 F), whereas the same progenitor cells generated preferentially neurons at nonclonal dilution (Fig. 2 M).

Inverse correlation between CNP gene promoter activity and lineage progression of CNP-GFP$^+$ cells that undergo neuronal or astroglial differentiation in vitro

A gradual loss of GFP expression was observed during astroglial maturation of CNP-GFP$^+$ cells (Fig. S1). Mature astrocytes derived from CNP-GFP$^+$ cells were GFP$^-$ and displayed typical stellate shapes with intense GFAP expression in cell bodies and processes (Fig. S1, A–D). In the same cultures, we also identified GFAP$^+$ cells expressing low levels of GFP. In all these GFAP$^+$/CNP-GFP$^+$ cells, GFAP expression was restricted to their cell body (Fig. S1, E–H, arrowheads), suggesting an intermediate stage of astroglial maturation. Similarly, among NeuN$^+$ and type $2_{a,b}$ microtubule-associated protein-positive ($MAP2_{a,b}$) neurons generated from CNP-GFP$^+$ cells, we identified either cells that were totally GFP$^-$ (Fig. 4, A–D; Fig. 4 H, arrow) or cells that expressed very low levels of GFP fluorescence (Fig. 4, E–H, arrowheads).

In conclusion, neuronal or astroglial differentiation of FACS®-sorted CNP-GFP$^+$ cells is accompanied by a progressive loss of CNP gene promoter activity and a decrease in GFP expression (Fig. 4 and Fig. S1). Our data demonstrate a lineage continuum in vitro, with the existence of weakly GFP$^+$ intermediate developmental stages, between strongly CNP-GFP–expressing multipotent cells and their GFP$^-$ neuronal or astroglial progeny.

Neurons generated from NG2$^+$/CNP-GFP$^+$ cells are electrically excitable in vitro

To confirm that FACS®-sorted CNP-GFP$^+$ cells could give rise to differentiated functional neurons, we performed whole-cell patch-clamp electrophysiological experiments. To ensure their full neuronal maturation, SCM cultures of CNP-GFP$^+$ cells were switched to a pro-neuronal medium containing a combination of brain-derived neurotrophic factor and neurotrophin-3 (Vicario-Abejon et al., 2000) (Fig. 4, I–K). After 3 d under these culture conditions and consistent with a more advanced stage of neuronal differentiation, none of the NeuN$^+$ cells continued to express GFP at detectable levels (unpublished data). GFP$^-$ (Fig. 4, I and J) and GFP$^+$ (Fig. 4 K) cells were then analyzed under these conditions. Depolarization of GFP$^-$ cells by electrotonic current pulses (step size = 10–30 pA, step duration = 300 ms) elicited single or repetitive action potentials. Post-hoc immunocytochemical characterization demonstrated NeuN expression in these electrically excitable GFP$^-$ cells (Fig. 4, I and J). In contrast, all GFP$^+$ cells were NeuN$^-$ and electrically unexcitable (Fig. 4 K). Identical results were obtained from the electrophysiological analysis of neurons generated from FACS®-purified NG2$^+$/CNP-GFP$^+$ cells cultured in pro-neuronal medium. From a total of six cells recorded, all displayed action potentials on depolarization with electrotonic pulses (unpublished data).

In situ analysis of early postnatal CNP-GFP$^+$ cells reveals an NG2$^+$/nestin$^+$ proliferative phenotype

We performed an analysis of the properties of postnatal CNP-GFP$^+$ cells in situ, with a particular focus on postnatal germinative regions (i.e., SVZ and hippocampus). Consistent with our data on acutely isolated CNP-GFP$^+$ cells from the same developmental stage (Fig. 1 D), a high proportion of CNP-GFP$^+$ cells were also NG2$^+$ and nestin$^+$ at P2 in situ (Fig. 5, A–D). Direct cell counting demonstrated that 89.6 ± 1.7% (mean ± SEM, total cells counted = 483) of CNP-GFP$^+$ cells were also NG2$^+$ in the SVZ at P2, and 18.4 ± 1.6% (mean ± SEM, total cells counted = 273) of CNP-GFP$^+$ cells were NG2$^+$ in the hippocampus at P2. Because nestin immunostaining was mostly visualized in the cell processes (Fig. 5 C), we were unable to obtain an accurate quantification of the nestin phenotype in situ. Given the controversy over whether stem cells of the adult CNS are located in the ependymal or subependymal layer of lateral ventricle walls (Chiasson et al., 1999; Doetsch et al., 1999; Johansson et al., 1999; Laywell et al., 2000; Capela and Temple, 2002), it is important to point out that NG2$^+$/CNP-GFP$^+$ cells were found in the subependymal zone (i.e., SVZ) but never in the ependymal layer, from P2 to P30 (unpublished data).

Proliferation of CNP-GFP$^+$ cells in situ was investigated by studying expression of proliferating cell nuclear antigen (PCNA). As assessed by PCNA immunostaining, 67.7 ± 5.8% of CNP-GFP$^+$ cells were proliferative in P2 hippocampus (Fig. 5, E–G; mean ± SEM, n = 354 cells counted, two independent experiments). A high mitotic index of CNP-GFP$^+$ cells was also observed in the SVZ at P2, with 93.1 ± 4.1% of these cells being PCNA$^+$ (Fig. 5, H–J; mean ± SEM, n = 793 cells counted, two independent experiments).

oligodendrocytes, GFAP$^+$(K, red)/GFP$^-$ astrocytes and NeuN$^+$(L, red)/GFP$^-$ neurons. Bar: 50 μm (B–D and E–F), 25 μm (G, K, and L), and 20 μm (H–J). M shows quantitative analysis of the multipotent properties of CNP-GFP$^+$ cells. Histograms represent immunocytochemical characterization (% of total cells in y axis, immunophenotypes in x axis) of the progeny of early postnatal (P2) FACS®-purified CNP-GFP$^+$ cells cultured directly under adherent conditions for 48 h in SCM. Comparison was made between the fate of total CNP-GFP$^+$ cells (blue) versus selected subsets of CNP-GFP$^+$ cells that were FACS®-purified according to their NG2$^+$/CNP-GFP$^+$ (red) or O4$^+$/CNP-GFP$^+$ (yellow) phenotype. Nestin, NG2, O4, O1, NeuN, and GFAP phenotypes were analyzed. Values (mean ± SEM) represent averages of 2–3 independent experiments. Counting was performed separately for each staining, and the number of total cells counted (from at least 15 separate microscopic fields) ranged between 403 and 714. Significant differences reported in the Results section were all with a P value <0.001 (*t* test).

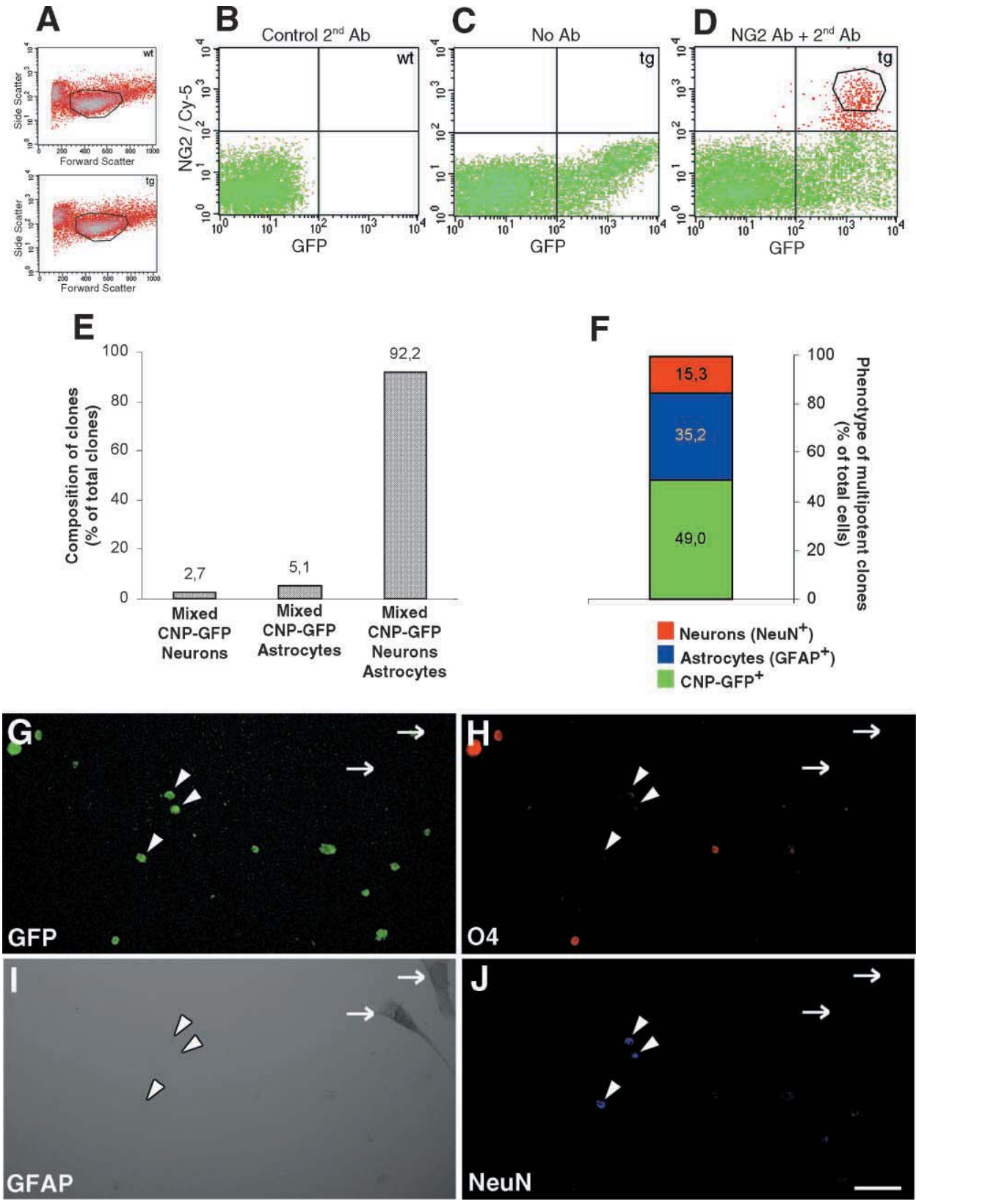

Figure 3. **Clonal analysis of NG2$^+$/CNP-GFP$^+$ cells in vitro.** (A) FACS® dot plots of acutely dissociated cells from wild-type (wt, top) and CNP-GFP transgenic brains (tg, bottom), in forward and side scatter with a polygon indicating the gate selecting the viable cells. (B–D) Sorting profiles of acutely isolated cell suspensions from P2 brains of wild-type (B) and CNP-GFP transgenic mice (C and D) dot plotted according to fluorescence intensity for GFP (x axis, logarithmic scale) and Cy-5 (fluorescence associated to secondary antibody recognizing NG2 immunoreactivity, y axis, logarithmic scale). (B) Control wild-type cells that were incubated only with the Cy-5–conjugated secondary antibody

A subset of CNP-GFP$^+$ hippocampal cells expresses neuronal markers and are electrically excitable in vivo

To determine whether highly proliferative postnatal CNP-GFP–expressing cells were also able to generate neurons or astrocytes in vivo, we investigated the existence of intermediate stages of neuronal and astroglial differentiation (i.e., expressing low levels of GFP) in CNS germinative areas. We were unable to find even a single cell expressing both GFAP and GFP between P2 and P10, either in the hippocampus or in the SVZ (unpublished data). Conversely, we found that numerous postnatal CNP-GFP$^+$ cells were also NeuN$^+$ in the hippocampus (Fig. 6, A–I). Hippocampal NeuN$^+$/CNP-GFP$^+$ committed neurons all expressed low levels of GFP (Fig. 6 J), and were mostly distributed at P6 within stratum radiatum and lucidum of CA1 and CA3 (Fig. 6, A–F; Fig. 6, C and F, arrowheads), and in the molecular layer and hilar region of the dentate gyrus. Scattered NeuN$^+$/CNP-GFP$^+$ neurons were also observed in the CA1 (unpublished data) and CA3 (Fig. 6, A–F) pyramidal layers and in the granule layer of the dentate gyrus. Postnatal NeuN$^+$/CNP-GFP$^+$ hippocampal neurons were identified in two different CNP-GFP transgenic lines (unpublished data).

NeuN$^+$/CNP-GFP$^+$ neurons were also studied by whole-cell voltage-clamp electrophysiology in P3 to P8 hippocampal slices. We recorded exclusively from CNP-GFP$^+$ cells that were selected according to their low level of GFP expression because the average GFP fluorescence intensity of NeuN$^+$/CNP-GFP$^+$ hippocampal neurons was 3.5-fold lower than NeuN$^-$/CNP-GFP$^+$ cells (Fig. 6 J; Fig. 6, G–I, arrowhead). Depolarization of such weakly CNP-GFP$^+$ hippocampal cells triggered repetitive action potentials in all of the eight cells tested (Fig. 6, K and L). Application of 1 μM tetrodotoxin (TTX) totally abolished these action potentials (five cells tested, unpublished data). Post-hoc immunostainings demonstrated that the biocytin-filled CNP-GFP$^+$ hippocampal cells that were recorded and that displayed action potentials (four cells tested) were consistently NeuN$^+$ (Fig. 6, M–O).

The anatomical and developmental distribution of NeuN$^+$/CNP-GFP$^+$ neurons in the hippocampus correlates with restriction of postnatal neurogenesis to the dentate gyrus

NeuN$^+$/CNP-GFP$^+$ cells were not only observed at early postnatal stages, but also in the adult hippocampus (P30). In all hippocampal regions, but particularly in CA1 and CA3, we observed that the absolute density of NeuN$^+$/CNP-GFP$^+$ cells and the total number of CNP-GFP$^+$ cells decreased during postnatal maturation, between P6 and P30 (Fig. 7, A and B). At P30, the density of NeuN$^+$/CNP-GFP$^+$ cells followed a clear anatomical gradient: dentate gyrus > CA3 > CA1 (Fig. 7 B). In parallel, total CNP-GFP$^+$ cells were distributed according to the same gradient (Fig. 7 B). Finally, except in CA1, the percentage of CNP-GFP$^+$ cells that expressed NeuN in the hippocampus remained constant between P6 and P30, and was maximal in the dentate gyrus (Fig. 7, C and D). These findings suggest that the intrinsic neurogenic potential of CNP-GFP$^+$ cells in CA3 and dentate gyrus may not decrease in adulthood. These results could also indicate that the decrease in the absolute number of multipotent CNP-GFP$^+$ cells might underlie the reduction of newly formed NeuN$^+$/CNP-GFP$^+$ neurons in the adult hippocampus.

A lineage continuum between NG2$^+$/CNP-GFP$^+$ progenitor cells and NeuN$^+$/CNP-GFP$^+$ neurons in the adult dentate gyrus

In the dentate gyrus of adult (P30) hippocampus, we observed that some CNP-GFP$^+$ cells also expressed TOAD-64 (turned on after division, 64 kD) protein (Fig. 8, A–H), a transient marker of early post-mitotic neurons that is expressed before most neuron-specific proteins during neurogenesis (Minturn et al., 1995a, 1995b; Cameron and McKay, 2001). TOAD-64 is also referred to as collapsin response-mediated protein 4 (Seki, 2002). In P30 dentate gyrus and CA3 areas, 11.3 ± 3.8% of CNP-GFP$^+$ cells were TOAD-64$^+$ (mean ± SEM, n = 244 total counted cells, two independent experiments). Hippocampal TOAD-64$^+$/CNP-GFP$^+$ immature neurons (Fig. 8, A–H, white arrows) reliably expressed levels of GFP fluorescence higher than NeuN$^+$/CNP-GFP$^+$-differentiated neurons (Fig. 8, A–D, arrowheads), consistent with the hypothesis that a gradual loss of CNP gene expression correlates with neuronal differentiation of CNP-GFP$^+$ cells. Moreover, the vast majority of TOAD-64$^+$/CNP-GFP$^+$ immature neurons were found to be NG2$^+$ (90%, total cells counted = 262) in the adult dentate gyrus (Fig. 8, E–H, white arrows), whereas NeuN$^+$/CNP-GFP$^+$ neurons were NG2$^-$ (Fig. 8, I–L, arrows), except for a small percentage of cells (5%; total counted cells = 754). However, in these cells, NG2 staining appeared ambiguous and suggested either a low level of NG2 proteoglycan expression or a close enwrapping of the cells within an intricate network of NG2$^+$ processes from neighboring CNP-GFP$^+$ cells (Fig. 8, I–L, arrowhead). Colocalization of TOAD-64 and NeuN expression in CNP-GFP$^+$ cells was only observed in cells displaying a weak nuclear pattern of TOAD-64 expression (Fig. 8, A–D, white arrowheads) different from the classical perinuclear distribution of this protein (Fig. 8 B, white arrows). We could also visualize TOAD-64$^+$ adult hippocam-

without anti-NG2 primary antibody. Crossed black lines in B–D represent thresholds of fluorescence. It was observed that <0.01% (limit of detection) of the control cells from B fell over this threshold. Thus, these lines determined the level of fluorescence above which cells from CNP-GFP brains (C) were selected as GFP$^+$ (lower right quadrant). When CNP-GFP cell suspensions were immunostained for NG2 (D), NG2$^+$/CNP-GFP$^+$ cells were detected in upper right quadrant. To ensure accurate purification of NG2$^+$/CNP-GFP$^+$ cells, the sort gate for these cells (D, polygon) was defined by taking an additional margin (0.2–0.3 log units) with respect to background fluorescence levels. (E) FACS®-purified early postnatal (P2) NG2$^+$/CNP-GFP$^+$ cells were cultured at clonal density for 1 wk in SCM and the phenotype of resulting cell clones was then determined. (F) Relative proportion of the different subpopulations found in the multipotent clones, i.e., containing CNP-GFP$^+$ cells, as well as neurons (NeuN$^+$) and astrocytes (GFAP$^+$). (G–J) GFP fluorescence (G, green), O4 (H, red), GFAP (I, peroxidase reaction), and NeuN (J, blue) stainings of the same microscopic field showing a representative multipotent clone derived from the growth of a single NG2$^+$/CNP-GFP$^+$ cell after one week in SCM. NeuN$^+$ cells (arrowheads) are still retaining CNP-GFP fluorescence at this stage, whereas in GFAP$^+$ astrocytes GFP expression has been lost (arrows). Bar, 50 μm for G–J.

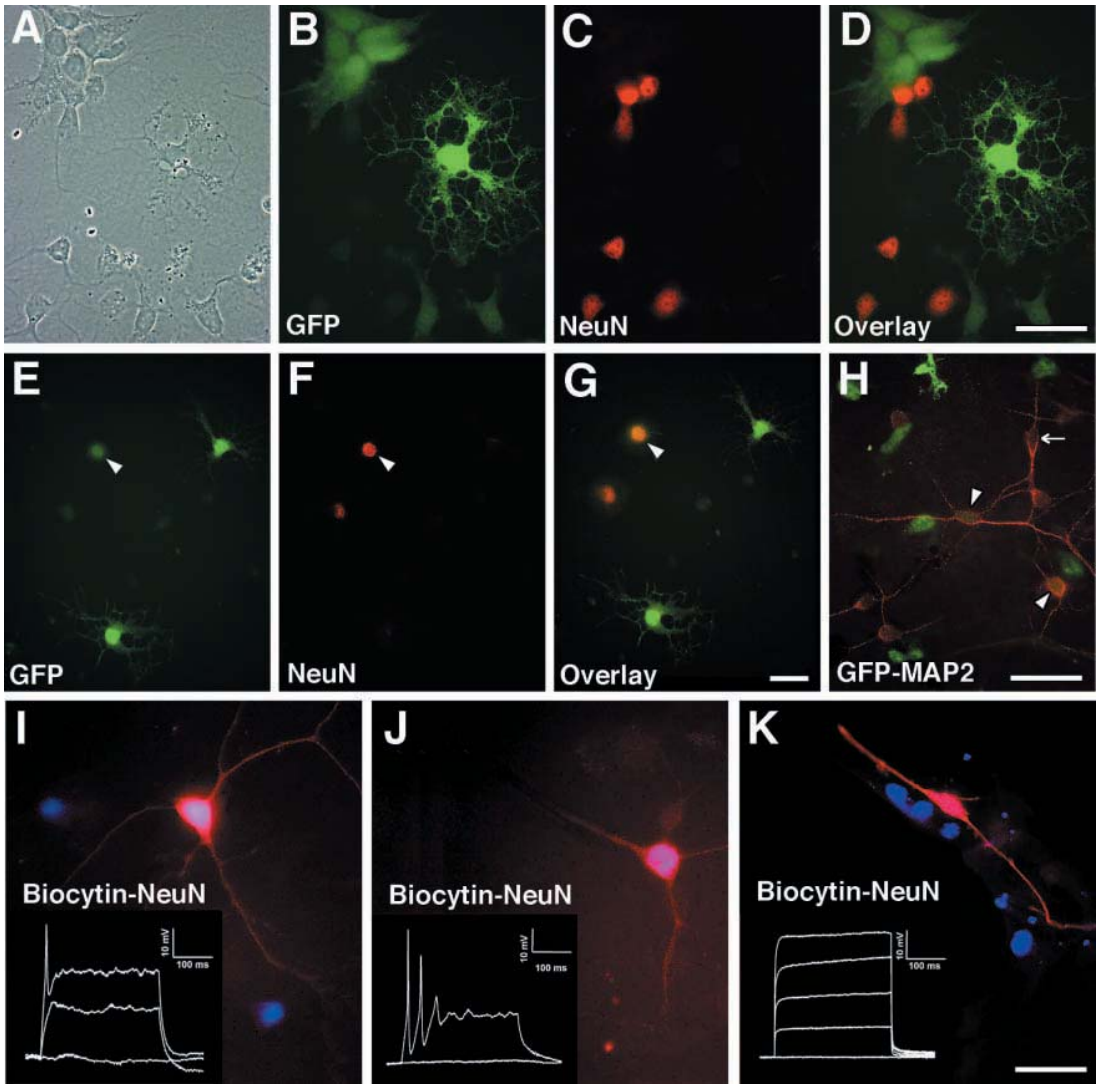

Figure 4. **CNP-GFP$^+$ cells gradually lose GFP expression as they differentiate into mature, excitable neurons in culture.** Phase-contrast view (A), GFP green fluorescence (B), NeuN staining (C, red), and overlay (D) of the same microscopic field showing NeuN$^+$/CNP-GFP$^-$ neuronal progeny derived from P2 FACS®-purified CNP-GFP$^+$ cells after 48 h in SCM. Cells expressing low levels of GFP, but displaying a neuronal phenotype could also be found (E–H). These cells expressed the neuronal markers NeuN (same microscopic field with GFP green fluorescence in E, red NeuN staining in F, and overlay in G) and MAP2$_{a,b}$ (H, red staining). Arrowheads indicate NeuN$^+$/CNP-GFP$^+$ (E–G) and MAP2$_{a,b}{}^+$/CNP-GFP$^+$ cells (H). Arrow in H points to a MAP2$_{a,b}$-expressing neuron that has completely lost GFP expression. (I–K) Electrophysiological whole-cell patch-clamp experiments in current-clamp mode were performed, in order to study excitability of cell progeny arising from SCM-cultured FACS®-sorted CNP-GFP$^+$ cells. After 2 d in SCM, cultures were switched to EGF- and FGF2-free medium supplemented with a combination of 30 ng/ml brain-derived neurotrophic factor and 30 ng/ml neurotrophin-3 for one week. GFP$^+$ and GFP$^-$ cells were analyzed and filled with biocytin during electrophysiological recording for identification and further immunocytochemical characterization. We recorded only GFP$^-$ cells that did not display a typical astrocytic morphology. Depolarization of GFP$^-$ cells elicited single (7 out of 9 cells; I, inset), or repetitive (2 out of 9 cells; J, inset) action potentials. In five of these cells, we investigated biocytin (red) and NeuN (blue) immunoreactivities, and in all cases colocalization (purple) was observed (I–J). In contrast, all GFP$^+$ cells tested (12 cells) did not elicit action potentials (K, inset). Out of the GFP$^+$ cells that were immunostained after recording (6 cells), all were NeuN$^-$ (K; biocytin in red, NeuN in blue). (I–K) GFP expression could not be visualized because of dialysis associated with whole-cell recording. Bars: 25 μm (A–D), (E–G), (H), and (I–K).

pal neurons that were CNP-GFP$^-$ (Fig. 8, A–H, red arrows) and consistently NG2$^-$ (Fig. 8, E–H, red arrows).

Adult CNP-GFP$^+$ neurons located in the hilus and inner layer of the dentate gyrus express a marker of GABAergic differentiation

To determine whether CNP-GFP$^+$ neurons found in the adult hippocampus may express phenotypic markers of functional neuronal differentiation, we performed immunohistochemical stainings for glutamate decarboxylase-67 (GAD-67), a γ-aminobutyric acid (GABA) synthesizing enzyme. In the hippocampus, GAD-67 is mostly expressed by GABAergic interneurons (Stone et al., 1999). We observed that a significant percentage of hippocampal adult CNP-GFP$^+$ cells expressed GAD-67, and all displayed low levels of GFP fluorescence (Fig. 9, A–I, arrowheads). At P30, these GAD-67$^+$/

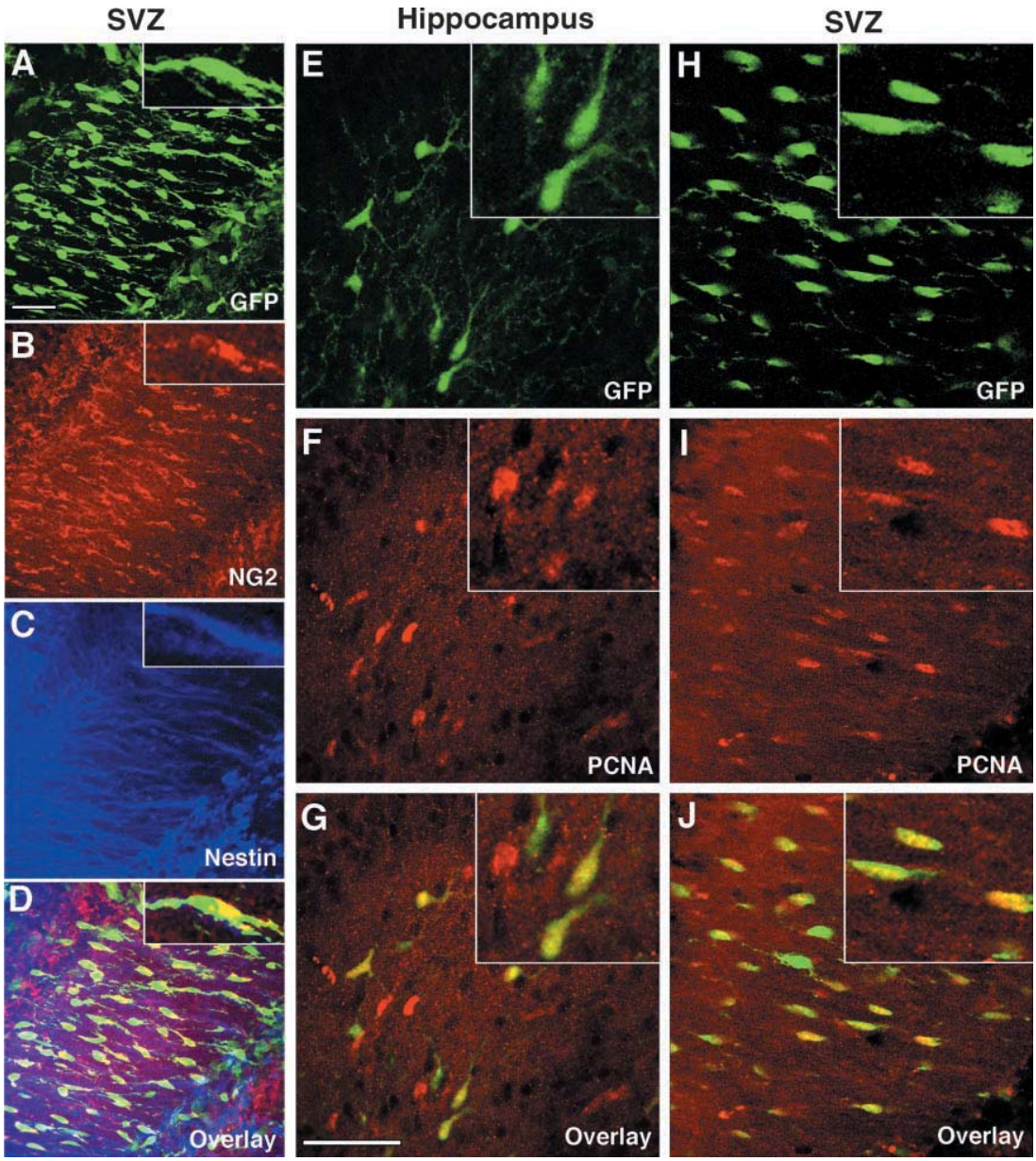

Figure 5. **Early postnatal CNP-GFP$^+$ cells are proliferative and display an NG2$^+$/nestin$^+$ phenotype in vivo in the SVZ and hippocampus.** As illustrated by Z-series (A–D, 22-μm thickness, image steps = 0.5 μm) confocal scanning images of the same field in SVZ area from P2 CNP-GFP transgenic mice, CNP-GFP$^+$ cells expressed an NG2$^+$/nestin$^+$ phenotype. 1-μm thick single plane images of a single cell at high magnification are provided in insets of A–D. The same phenotype was observed in the hippocampus (not depicted). (A) GFP green fluorescence, (B) NG2 staining, (C) nestin staining, (D) overlay. As shown in E–J (high magnification in insets), CNP-GFP$^+$ cells were proliferative in vivo. 0.5-μm thick single plane confocal scanning images of CA3 stratum radiatum area of hippocampus (E–G) and SVZ (H–J) from P2 CNP-GFP transgenic mice. (E and H) GFP green fluorescence, (F and I) PCNA staining, (G and J) overlay. A high percentage of CNP-GFP$^+$ cells were PCNA$^+$ in both germinative areas. Bars: 50 μm (A–D) and (E–J).

CNP-GFP$^+$ neurons were particularly concentrated in the inner granular zone of the dentate gyrus (Fig. 9, D–I, arrowheads), but few scattered cells were also seen in CA3 (Fig. 9, A–C, arrow and arrowheads) and CA1 areas. In the adult dentate gyrus (P30), a large proportion (~90%) of NeuN$^+$/CNP-GFP$^+$ hippocampal neurons were GAD-67$^+$, and all GAD-67$^+$/CNP-GFP$^+$ were found to be NeuN$^+$ (unpublished data). Mature neurons expressing GAD-67 and low levels of GFP were consistently CNP protein-negative (Fig. S3). Even though keeping a detectable level of transcriptional activation of the CNP gene, these GABAergic neurons have thus completely down-regulated CNP protein expression.

Postnatal hippocampal CNP-GFP$^+$ neurons receive functional synaptic inputs

To investigate whether CNP-GFP$^+$ neurons from postnatal hippocampus receive functional synaptic innervation, whole-cell voltage-clamp recordings were obtained from CNP-GFP$^+$ cells displaying low levels of GFP fluorescence in dentate gyrus (3 cells) and CA3 (14 cells) regions of P10-P12

178 The Journal of Cell Biology | Volume 161, Number 1, 2003

The Journal of Cell Biology

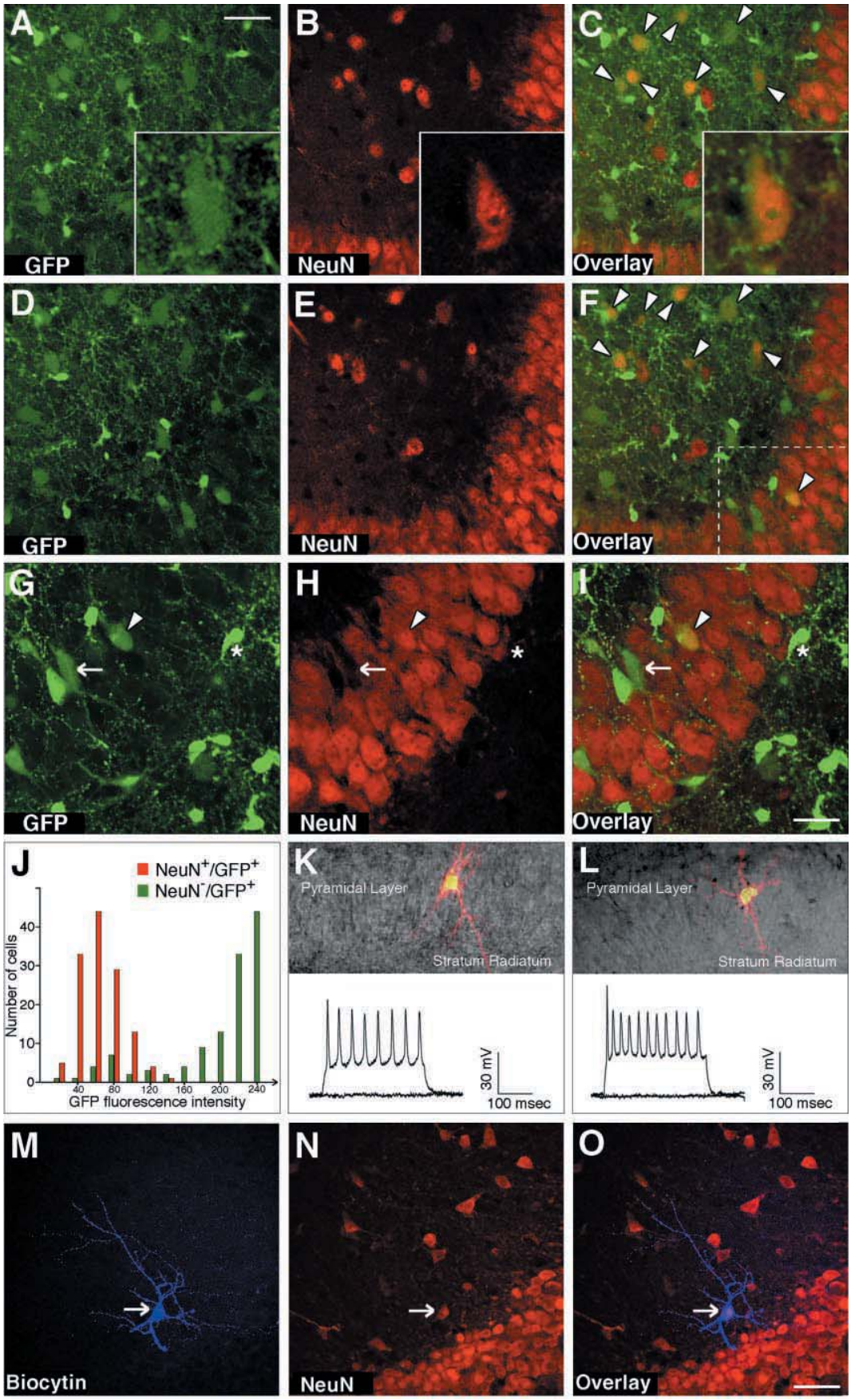

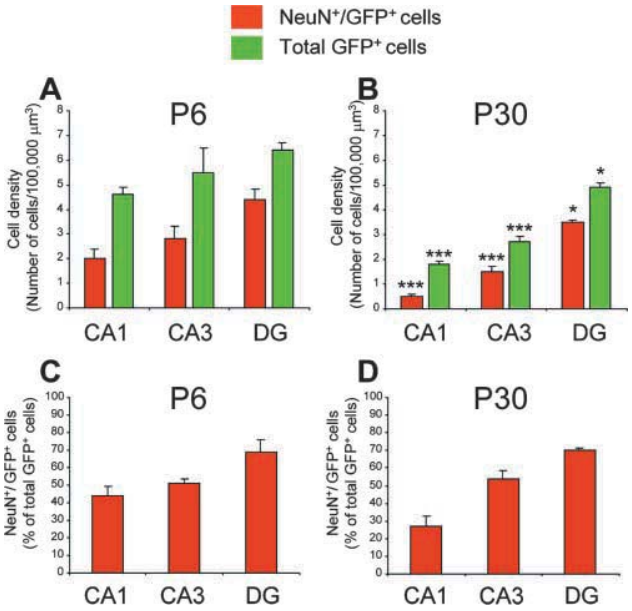

Figure 7. **Developmental and anatomical distribution of NeuN$^+$/CNP-GFP$^+$ neurons in the postnatal hippocampus.** The anatomical distribution of NeuN$^+$/CNP-GFP$^+$ cells was analyzed in Z-series confocal scanning images (20–32 μm of thickness, step size = 0.5 μm between successive images of the same field) from P6 (A and C) and P30 (B and D) hippocampus. Square fields of 228 μm^2 were separately acquired in CA1, CA3, and the dentate gyrus (DG). We calculated the absolute density of total CNP-GFP$^+$ cells and NeuN$^+$/CNP-GFP$^+$ cells in each area at P6 (A) and P30 (B). We found developmental changes in the percentage of NeuN$^+$/CNP-GFP$^+$ cells within the CNP-GFP$^+$ population only in CA1 between P6 (C) and P30 (D). Histogram values represent mean ± SEM (total GFP$^+$ cells counted = 841, two independent experiments). Statistical data pointed out in B were derived from the comparison of each P30 experimental parameter with its identical counterpart at P6. ***, $P < 0.001$; *, $P < 0.05$ (*t* test).

CNP-GFP mice. We were unable to consistently obtain recordings at older ages (i.e., P30) in these particular areas, due to the presence of brightly fluorescent neighboring cells and their associated processes (Fig. 8 and Fig. 9), which hindered reliable identification of CNP-GFP$^+$ cells expressing low levels of fluorescence. All 17 weak CNP-GFP$^+$ cells tested displayed spontaneous inward currents (Fig. 9 J). Furthermore, in seven weakly CNP-GFP$^+$ hippocampal cells, we were able to determine whether cells that exhibited spontaneous synaptic currents were also capable of eliciting action potentials on depolarization. We observed that five out of seven cells possessed both post-synaptic currents and the ability to generate action potentials. Two out of seven cells possessed synaptic currents but no action potentials, raising the hypothesis that, in the course of postnatal hippocampal neurogenesis, immature committed CNP-GFP$^+$ neuronal precursors may receive synaptic inputs first and then secondarily become capable to propagate action potentials. Importantly, we found NeuN immunoreactivity in all weakly CNP-GFP$^+$ hippocampal cells displaying synaptic currents in which we were able to perform post-hoc immunostainings (four cells; Fig. 6, M–O).

The frequency and amplitude of the spontaneous currents were clearly reduced in the presence of TTX (three cells tested), suggesting that a proportion of the spontaneous currents resulted from action potential–mediated neurotransmitter release from afferent terminals (Fig. 9 K). Furthermore, 6,7-dinitro-2,3-quinoxalinedione (DNQX; three cells tested), an antagonist of α-amino-3-hydroxy-5-methyl-4-isoxazole propionic acid and kainate subtypes of glutamate receptors, abolished all the spontaneous inward currents (Fig. 9 K). We did not expect significant activation of NMDA (*N*-methyl-D-aspartate) or chloride channel–coupled receptors such as $GABA_A$, because of the experimental conditions used (holding potential = −60 mV; calculated E_{Cl-} = −70 mV). Hence, the complete block induced by DNQX does not allow one to draw any conclusions on the existence of GABAergic inputs onto or the expression of NMDA receptors by the CNP-GFP$^+$ postnatal hippocampal neurons. Nonetheless, the finding that these postnatal CNP-GFP$^+$ neurons display spontaneous synaptic currents clearly illustrates that these cells are capable of receiving synaptic inputs in vivo.

Discussion

Using a transgenic mouse selectively expressing GFP under the influence of the CNP gene promoter, we demonstrate

Figure 6. **A subset of postnatal NeuN$^+$ hippocampal neurons express low levels of CNP-GFP and are electrically excitable.** (A–F) 0.5-μm thick single plane confocal scanning images representing two different levels (levels of planes in A–C and D–F are separated by 4 μm) of the same field of CA3 region of hippocampus from P6 CNP-GFP transgenic mice revealed that some cells were NeuN (red)-immunoreactive and expressed GFP fluorescence (A–C, insets of high magnification of a single cell). Distinct microscopic planes (A–C and D–F) within the same cells (C and F, arrowheads) showed a diffuse colocalization of the two signals, providing a more accurate demonstration of NeuN/CNP-GFP coexpression. Most of these NeuN$^+$/CNP-GFP$^+$ cells were located in the stratum radiatum, but sparse NeuN$^+$/CNP-GFP$^+$ cells were also found in the pyramidal layer (G–I, arrowhead). (G–I) Z-series (10 μm thick) confocal scanning image centered on the dashed area of (F) at higher magnification. Lower levels of GFP fluorescence were detected in all NeuN$^+$/CNP-GFP$^+$ cells (C, F, and G–I, arrowheads), as compared with CNP-GFP$^+$ cells from the same field (G–I, star), that were NeuN$^-$. Cells that expressed low levels of GFP that were NeuN$^-$ were also found (G–I, arrow). (J) Quantitative image analysis of GFP fluorescence intensity (linear arbitrary scale from 0 to 250 U; paired columns represent incremental intervals of 20 arbitrary fluorescence units) revealed a bimodal distribution, demonstrating that the average GFP fluorescence of NeuN$^+$/CNP-GFP$^+$ neurons (red) was 3.5-fold lower than that of NeuN$^-$/CNP-GFP$^+$ cells (green; total cells counted = 252, two independent experiments, equal number of cells analyzed for each population). Electrophysiological recordings were performed in weakly CNP-GFP$^+$ cells from the CA1 and CA3 pyramidal layer of P3–P8 hippocampal slices (K–L). Upper parts of K–L represent single examples of fluorescence images showing the neuron-like arborized morphology of two different CNP-GFP$^+$ cells recorded in CA3 and visualized after filling with a rhodamine-coupled dye. Lower parts of K–L display repetitive action potentials elicited by depolarizing the same cells with electrotonic current pulses (step size = 10–30 pA, step duration = 300 ms). (M–O) Representative example of a biocytin-filled (arrow in M) recorded cell in the CA3 stratum radiatum area, showing that cells that expressed low levels of GFP and that were able to propagate action potentials were consistently NeuN$^+$ (arrow in N and O) by post-hoc immunostaining. Bars: 50 μm (A–F), 33 μm (G–I), and 60 μm (M–O).

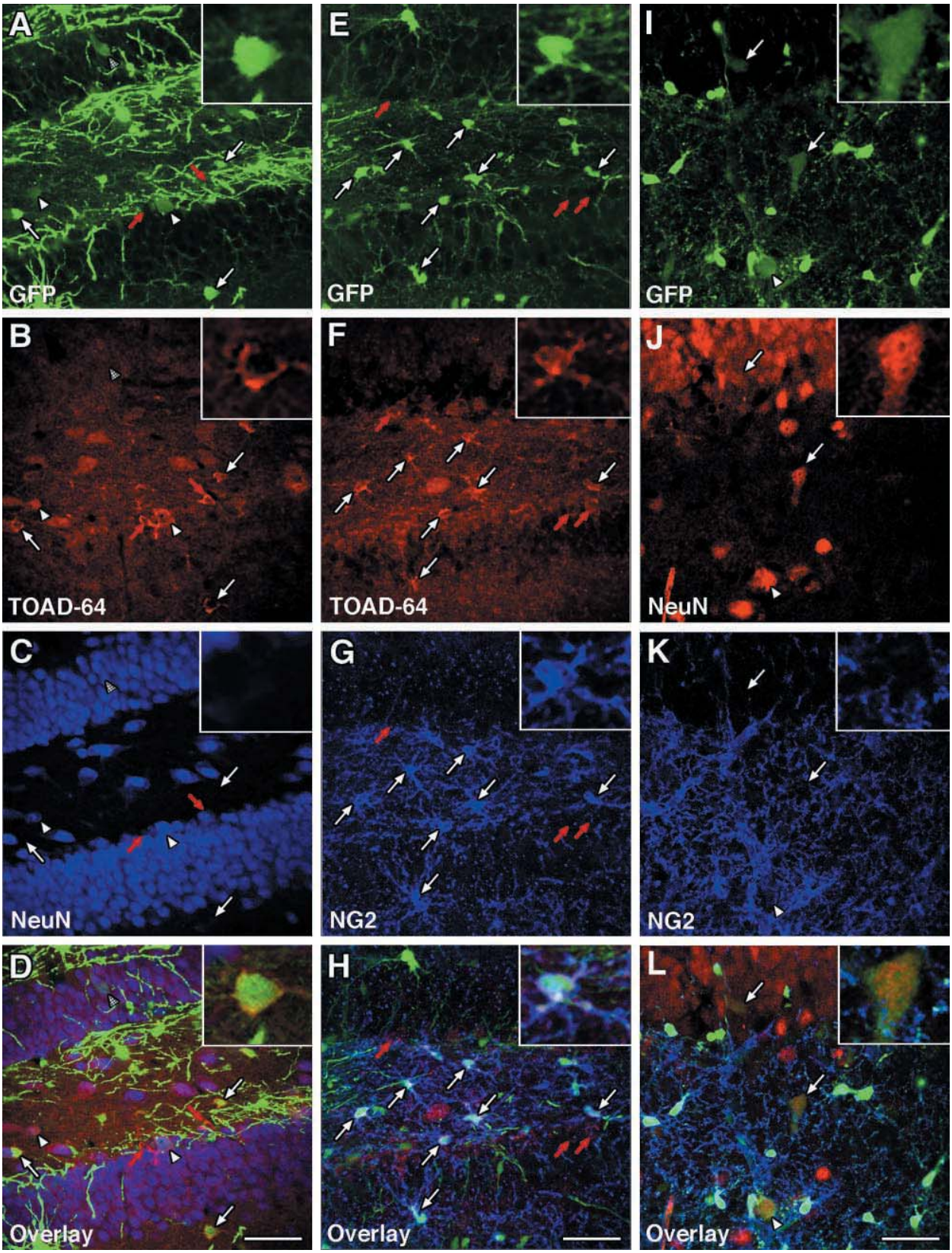

Figure 8. **The existence of NG2$^+$/TOAD-64$^+$/CNP-GFP$^+$ immature hippocampal neurons establishes a lineage continuum between NG2$^+$/CNP-GFP$^+$ progenitor cells and NG2$^-$/NeuN$^+$/CNP-GFP$^+$ neurons in the adult dentate gyrus.** Confocal photomicrographs (merged images from 4–6 optical sections of 0.5 μm each) of three representative fields of P30 hippocampal slices in which CNP-GFP$^+$ cells were immunolabeled for either TOAD-64 and NeuN (A–D, dentate gyrus), TOAD-64 and NG2 (E–H, dentate gyrus), or NeuN and NG2 (I–L, CA3). 0.5-μm thin single plane high magnification images of single cells are shown for each panel as insets located in the upper right corners (A–L). In A–D and

that postnatal NG2$^+$ progenitor cells expressing the CNP gene display antigenic and developmental features of multipotent CNS progenitor cells in vitro, including (1) a nestin$^+$ immunophenotype (Reynolds and Weiss, 1992; Johe et al., 1996); (2) the capacity to form neurospheres when cultured in uncoated conditions in EGF- and FGF2-containing medium (Reynolds and Weiss, 1992; Johe et al., 1996); and (3) the ability of a single cell to give rise to electrically excitable neurons, and to astrocytes and oligodendrocytes.

Our clonal analysis demonstrates that the multipotent fate of NG2$^+$/CNP-GFP$^+$ cells in vitro is not restricted to a minor subpopulation, but is a characteristic of a significant percentage of these progenitor cells in the early postnatal period. Moreover, because the multipotent properties of NG2$^+$/CNP-GFP$^+$ cells were reproduced in two different transgenic mouse lines, our results reflect biological properties of cells expressing the CNP gene, independent of genetic influences associated with the transgene insertion site.

To date, NG2 proteoglycan expression is the most widely used marker of postnatal progenitors in vivo (Levine et al., 2001). The mostly NG2$^+$ immunophenotype of acutely purified CNP-GFP$^+$ cells, and the quantitative comparison of the differential fate of NG2$^+$/CNP-GFP$^+$ and O4$^+$/CNP-GFP$^+$ cells versus total CNP-GFP$^+$ cells indicate that NG2$^+$ cells, which are preferentially neurogenic in SCM, represent a significant source of multipotentiality among progenitor cells expressing the CNP gene during the early postnatal period. In a previous work, optic nerve oligodendrocyte progenitor cells (OPCs) were shown to undergo nonoligodendroglial differentiation in vitro, although this occurred through a process that required a 2-mo "reprogramming" by sequential treatments with platelet-derived growth factor, FBS, and FGF2 (Kondo and Raff, 2000). Here, we demonstrate that multipotentiality in vitro is an intrinsic feature of a sizeable subpopulation of the previously so-called NG2$^+$ OPCs. This property is readily and rapidly (48 h) displayed by NG2$^+$ progenitor cells under conditions previously shown to support stem cell growth. These results emphasize that postnatal progenitor cells expressing NG2 chondroitin proteoglycan can no longer be considered as progenitor cells restricted to an oligodendroglial fate (Dawson et al., 2000). Importantly, results obtained from O4$^+$ progenitors derived from subcortical white matter in the adult forebrain show that these cells can generate neurons in response to FGF-2 (Mason, J.L., and J.E. Goldman, personal communication; and unpublished data). Such findings indicate that in the adult brain, the neurogenic potential is maintained also in cells labeled by a marker that identifies more mature stages of the oligodendrocyte lineage. This would be consistent with previous works showing that exposure of mature oligodendrocytes to FGF-2 resulted in the down-regulation of CNP, MBP, and proteolipid protein (PLP) levels and allowed re-entrance into the cell cycle (Bansal and Pfeiffer, 1997a,b).

Consistent with our in vitro studies on acutely FACS®-purified CNP-GFP$^+$ cells, early postnatal CNP-GFP$^+$ cells from SVZ and hippocampal germinative areas appeared to be NG2$^+$/nestin$^+$, and displayed a highly proliferative phenotype in situ. We demonstrate, in the postnatal hippocampus and particularly in the dentate gyrus at the adult stage, that a subset of CNP-GFP$^+$ cells, namely NG2$^+$, can express the antigenic phenotype of differentiated neurons. Furthermore, these CNP-GFP$^+$ cells were identified as neurons not only by their expression of specific neuronal proteins, but also by their capability of eliciting action potentials in situ. We also show that the anatomical distribution of NeuN$^+$/CNP-GFP$^+$ hippocampal neurons is developmentally regulated and strikingly correlates with the well-established restricted pattern of adult hippocampal neurogenesis in the dentate gyrus (Altman and Das, 1965; Kaplan and Hinds, 1977; Kuhn et al., 1996; Gage, 2000).

In the adult brain, we observed that early post-mitotic CNP-GFP$^+$ immature hippocampal neurons expressing TOAD-64 (Cameron and McKay, 2001) were also NG2$^+$ and displayed high levels of GFP, whereas more differentiated NeuN$^+$/CNP-GFP$^+$ neurons were NG2$^-$ and all exhibited low levels of GFP fluorescence. This finding indicates that NG2 proteoglycan expression and CNP gene promoter activity, as assessed by GFP fluorescence intensity, are inversely correlated with the progression of neuronal differentiation in vivo. These results are consistent with our in vitro data showing that the lineage continuum between NG2$^+$ cells and their neuronal and astroglial progeny encompassed intermediate stages of commitment, which displayed low levels of GFP expression and the differentiated neural cell markers GFAP or NeuN. Hence, altogether these results delineate a possible developmental link between a defined class of adult progenitor cells expressing NG2 chondroitin proteoglycan and the CNP gene, and newborn postnatal hippocampal neurons (Fig. 10). Although we cannot assess with the present model to what extent NG2$^+$/CNP-GFP$^+$ postnatal progenitor cells may totally repress CNP gene transcription during terminal stages of neuronal differentiation in vivo, we propose the following developmental scheme of postnatal/adult neurogenesis from NG2$^+$/CNP-GFP$^+$ cells in the hippocampus: NG2$^+$/CNP-GFP^{+++} $\rightarrow$ TOAD-64$^+$/NG2$^+$/CNP-GFP^{2+} $\rightarrow$ NeuN$^+$/NG2$^-$/CNP-GFP$^+$ $\rightarrow$ NeuN$^+$/NG2$^-$/CNP-GFP$^-$ (Fig. 10).

Using similar GFP fluorescence criteria for tracking their fate, we found no evidence that CNP-GFP$^+$ cells could generate GFAP$^+$ astrocytes in the noninjured postnatal brain. However, this discrepancy between in vitro and in vivo could be due to full repression of CNP-GFP expression in astrocytes in vivo before GFAP expression.

To place our results in the context of other works indicating that a subset of GFAP$^+$ astrocytes can generate newly formed adult hippocampal neurons (Seri et al., 2001) and/or stimulate adult neurogenesis by instructing hippocampal stem cells to adopt a neuronal fate (Song et al., 2002a, 2002b), we would like to emphasize the existence of TOAD-64$^+$/NG2$^-$/CNP-GFP$^-$ immature neurons in the adult dentate gyrus of CNP-GFP mice. The presence of

E–H, white arrows point to NG2$^+$/TOAD-64$^+$/CNP-GFP$^+$ early post-mitotic neurons that expressed levels of GFP higher than differentiated NG2$^-$/NeuN$^+$/CNP-GFP$^+$ neurons (A–D, arrowheads; I–L, arrows). Red arrows in A–D and E–H depict TOAD-64$^+$ neuronal cells that did not express CNP-GFP. Bars, 50 μm for all panels.

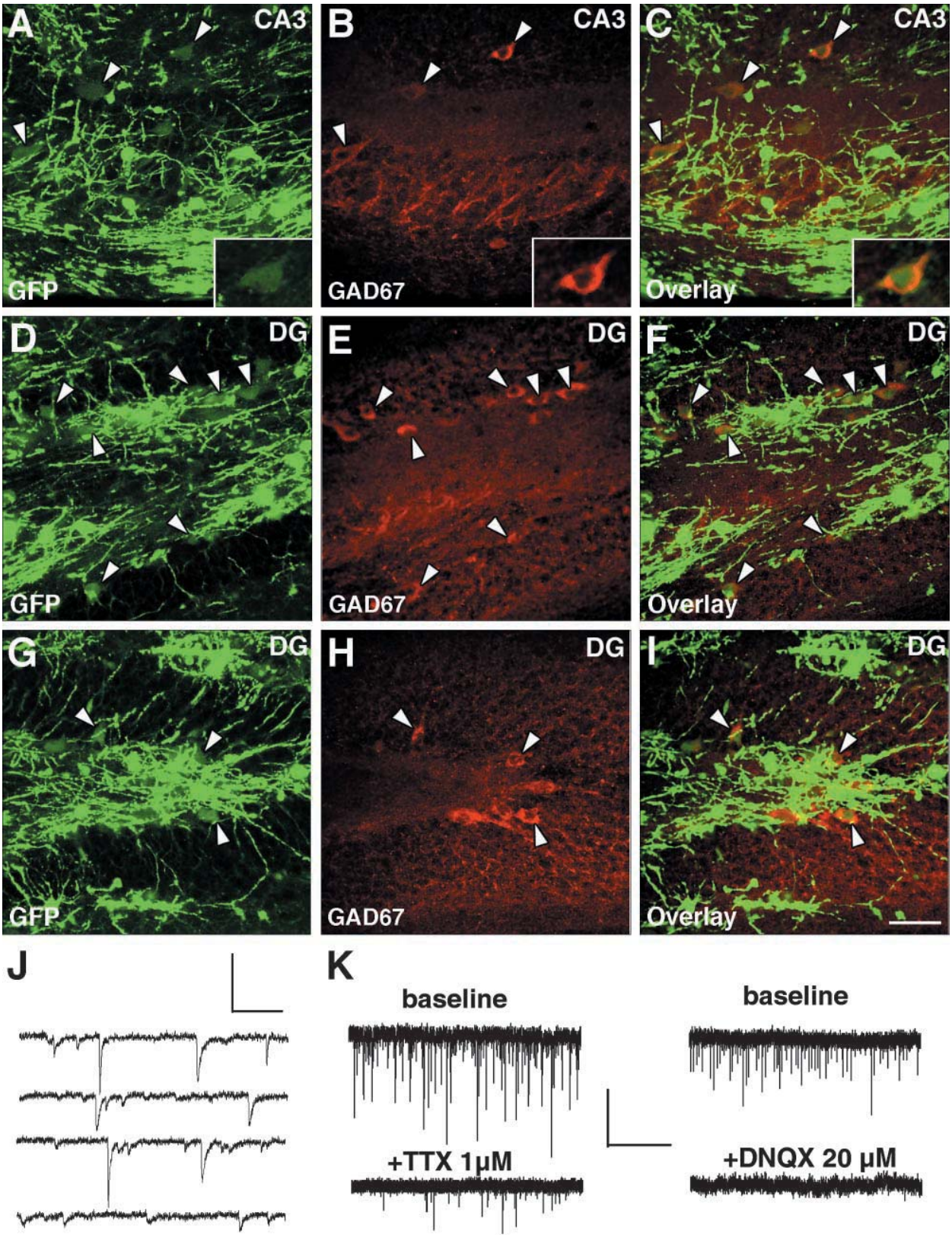

Figure 9. **CNP-GFP$^+$ postnatal hippocampal neurons are mostly GABAergic and receive functional synaptic inputs.** Representative confocal images from CA3 (A–C) and dentate gyrus (D–F and G–I; merged images of 4–6 optical sections of 0.5–0.75 μm); three adjacent fields of the same P30 hippocampal slice showed the typical spatial distribution of CNP-GFP$^+$ cells immunoreactive for GAD-67 (examples depicted by arrowheads). 0.5-μm thin single plane high magnification images of a single cell are shown in A–C as insets located in the lower right corners. All GAD-67$^+$/CNP-GFP$^+$ neurons displayed relatively low levels of GFP fluorescence. Bar, 50 μm for all panels A–I. (J) Continuous recording

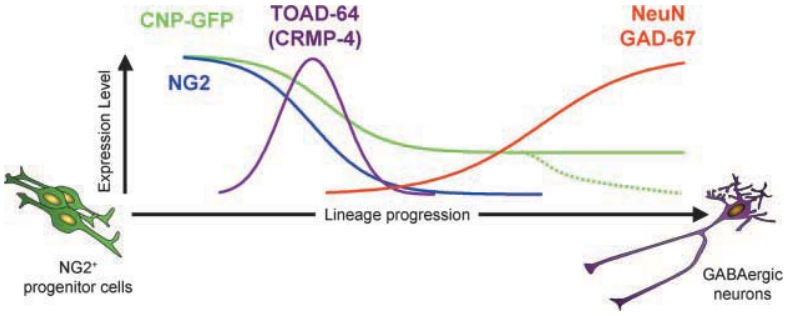

Figure 10. **Developmental regulation of neural markers in CNP-GFP lineage cells.** This scheme represents a summary of the antigenic markers expressed at different stages of neuronal differentiation of NG2+/CNP-GFP+ cells in the postnatal hippocampus.

these cells raises the issue that multiple progenitor phenotypes likely coexist to fully account for adult hippocampal neurogenesis. Rather than from another class of neuronal hippocampal progenitors, immature TOAD-64+/NG2−/CNP-GFP− cells could also directly derive from NG2+/CNP-GFP+ cells, and reflect the existence of a different pathway of neurogenesis exhibiting distinct regulation of CNP promoter activity.

In parallel with our work, a transgenic mouse expressing GFP driven by the mouse myelin (PLP) gene promoter was developed to investigate oligodendroglial lineage cells in vivo (Mallon et al., 2002). In these PLP-GFP mice, two subpopulations of NG2+ cells have been identified, based on PLP promoter (pPLP)-driven GFP expression (Mallon et al., 2002). The PLP gene is transcriptionally active in one subpopulation of NG2+ progenitors (pPLP+), which have the potential to generate mature myelinating oligodendrocytes (Mallon et al., 2002), whereas NG2+ cells that lack pPLP activity (pPLP−) could be involved in different functions. To date, there is no evidence from other reports that pPLP+ or pPLP− progenitors may undergo nonoligodendroglial differentiation (Fuss et al., 2000; Mallon et al., 2002). Our previous data provided evidence that in the CNP-GFP mice, GFP expression in white matter regions is sustained in the entire oligodendroglial lineage throughout development (Yuan et al., 2002). Furthermore, the entire postnatal NG2+ population, including both pPLP+ and pPLP− OPCs, displays high levels of GFP expression (Yuan et al., 2002). Therefore, we cannot yet distinguish whether the multipotent properties of NG2+/CNP-GFP+ postnatal progenitor cells are related to differences between the pPLP+ and pPLP− subpopulations.

Recently, it has been shown that newly generated cells in the adult mouse hippocampus display a neuronal morphology, and possess action potentials and functional synaptic inputs similar to those found in mature dentate granule neurons (van Praag et al., 2002). It has also been shown in vitro that the progeny of adult rat NSCs, when cocultured with primary neurons and astrocytes from neonatal hippocampus, develop into electrically active neurons and integrate into neuronal networks with functional synaptic transmission (Song et al., 2002b). Consistent with these findings, our data show that postnatal hippocampal CNP-GFP+ neurons located in the dentate gyrus express both NeuN and GAD-67, and display spontaneous TTX- and DNQX-sensitive post-synaptic currents, confirming that they receive functional synaptic inputs. Recent data have demonstrated that, besides excitatory granule neurons, also functional inhibitory GABAergic neurons (i.e., basket cells) are newly generated in the dentate gyrus of adult rats (Liu et al., 2003). Therefore, we suggest that NG2+/CNP-GFP+ cells represent a sizeable pool of progenitor cells that generate new functional GABAergic neurons in the adult murine hippocampus. It remains to be investigated whether postnatal NG2+/CNP-GFP+ cells express Lewis X antigen as adult murine SVZ stem cells do (Capela and Temple, 2002), and whether they are ontogenically linked to the embryonic mouse basal forebrain multipotent stem cells that generate both GABAergic neurons and oligodendrocytes during development (He et al., 2001; Yung et al., 2002).

It is still unclear to what extent our present findings can be related to the presence of α-amino-3-hydroxy-5-methyl-4-isoxazole propionic acid receptor-mediated synaptic inputs onto adult hippocampal NG2+ cells that do not display action potentials (Bergles et al., 2000). Given the neurogenic potential of postnatal NG2+ hippocampal cells and the existence of TOAD-64+/NG2+/CNP-GFP+ neuronal progenitors in the hippocampus, one could hypothesize that the results of Bergles and colleagues were obtained from NG2+ cells committed to a neuronal fate. However, these NG2+ cells analyzed electrophysiologically (Bergles et al., 2000) were located outside of neurogenic areas (i.e., CA1), where adult NG2+ hippocampal cells may be instead restricted to an oligodendroglial fate and receive, as described, synaptic inputs from CA3 pyramidal cells.

In conclusion, our data strongly support the novel hypothesis that NG2+ cells are a source of newly-generated functional neurons in the postnatal mouse hippocampus in vivo. These findings shed new light on our understanding of the function of proliferative NG2+ cells scattered throughout the entire postnatal CNS. The lack of specific immunohistochemical markers has represented a crucial hindrance for the analysis of NSCs in the adult brain. The characterization of a defined postnatal multipotent cell phenotype will help unravel the functional heterogeneity of specific subsets of newly born neurons in the postnatal hippocampus. Multipotent NG2+/CNP-GFP+ endogenous progenitor cells

(total = 2.4 s) of spontaneous post-synaptic currents under voltage clamp (−60 mV) in a CNP-GFP+ neuron of the hilar dentate gyrus area (Scale: 0.5 s, 50 pA). (K) Synaptic activity of dentate gyrus CNP-GFP+ neurons was blocked by application of 1 μM TTX and 20 μM DNQX (Scale: 30 s, 50 pA). Spontaneous synaptic currents recorded in baseline conditions were compared with those of the same cell (bottom traces) 2 min after drug application.

may thus be considered as a major cellular target for strategies aimed at recruiting CNS postnatal repair not only in demyelinating disorders, but in a broader array of neurodegenerative diseases.

Materials and methods

CNP-GFP transgenic mouse model

As previously described by Yuan et al. (2002), the CNP-GFP transgenic mouse was generated using the 3.7-kb XbaI-HindIII sequence that contains the type I and II promoter core elements of the mouse CNP gene (Gravel et al., 1998). This fragment was ligated upstream of a 1-kb SmaI-XhoI fragment encompassing the coding sequence of the EGFP gene (Cat. No. 6064–1; CLONTECH Laboratories, Inc.; Belachew et al., 2001; Yuan et al., 2002). Transgenic line C1 (FVB/NxCB6 background) was used for all the data presented in this paper. However, it is noteworthy to point out that we were able to obtain the same results in vitro and in vivo with a distinct CNP-GFP transgenic line, A2 (Fig. S2). All animal procedures were performed according to National Institutes of Health (NIH) guidelines.

Isolation of CNP-GFP$^+$ progenitor cells by FACS® and cell culture

Brains were dissected out from P2 CNP-GFP pups and wild-type littermates. Brain tissues were dissociated as described previously (Yuan et al., 2002) to obtain final cell suspensions resuspended in N1 + 10% FBS at a density of 10^7 cells/ml for subsequent FACS® sorting. Pre-FACS® cells were plated onto 0.1 mg/ml polyornithine-coated 25-mm coverslips and incubated at 37°C for 1 h to allow attachment before further immunocytochemical characterization.

Cells were analyzed for light forward and side scatter using a FACSVantage™ SE instrument (Becton Dickinson). Cells from the negative littermates were used to set the background fluorescence, and a size threshold was used to gate out erythrocytes and cellular debris. For double NG2/EGFP and O4/EGFP FACS® analysis, cell suspensions were initially incubated with appropriate primary antibodies (see Immunocytochemistry) and then with Cy-5–conjugated secondary antibodies (1:200; Jackson ImmunoResearch Laboratories) before any sorting. Given that NG2 chondroitin sulfate can be easily cleaved off after protease treatment (Stallcup and Beasley, 1987), we compared the percentage of NG2$^+$ cells that were detected after immunostaining with cell suspensions from P4 CNP-GFP brains dissociated with and without papain treatment, respectively. We did not observe any significant differences between these two conditions. Without protease treatment during the dissociation procedure, the percentage of NG2$^+$ cells was 97.1 ± 2% (mean ± SEM; total cells counted = 520) of what it was in the presence of protease.

After FACS®, cells were rinsed twice with PBS solution and resuspended in stem cell-like medium, i.e., DME/F12 (1:1, vol/vol) supplemented with 1% N_2, 1% B_{27} (GIBCO BRL/Life Technologies), 20 ng/ml EGF, and 10 ng/ml FGF2 (Upstate Biotechnology). For adherent cultures, FACS®-sorted cells were plated onto 0.1 mg/ml polyornithine-coated 12-mm coverslips at a density of 20,000 cells/coverslip. Cells were cultured in SCM at 37°C/10% CO_2 for 48 h with renewal of growth factors every 24 h. For suspension cultures, FACS®-sorted cells were seeded onto uncoated 24-well plates (5×10^4 cells/well) and grown in SCM with daily addition of growth factors at the concentrations listed above.

Clonal analysis

For clonal expansion of single cell–derived neurospheres, the same isolation procedure was used, but FACS®-sorted CNP-GFP$^+$ cells were initially seeded in suspension conditions at a clonal density (5 cells/μl). Immediately after their formation (2–3 d in vitro), single clonal spheres were transferred (by pipetting) into separate wells to prevent formation of aggregates.

For clonal analysis, FACS®-purified NG2$^+$/CNP-GFP$^+$ cells were seeded onto polyornithine-coated coverslips at clonal density and cultured in SCM for 1 wk with daily addition of EGF and FGF2. At this density, we never observed clonal superimpositions. The average number of clones detected per coverslip was 6.06 ± 0.2 (n = 49 coverslips; mean ± SEM). The possibility of occurrence of rare cell duplets during the initial seeding of clonal cultures would not explain the high incidence of multipotent clones obtained in SCM (Fig. 3).

Immunohistochemistry

Mice at P2, P6, P10, or P30 were anesthetized by inhalation of Forane® (Ohmeda PPD Inc.), and perfused intracardiacly with 1× PBS, followed by 4% PFA. Brains were dissected out and postfixed with 4% PFA at 4°C overnight, then transferred into a solution of 4% PFA and 10% glycerol in 1× PBS for an overnight incubation at 4°C. Fixed brains were preserved in 20% glycerol in 1× PBS.

Frozen 50-μm tissue sections were prepared as described previously (Yuan et al., 2002). Sections were incubated at RT for at least 1 h in blocking solution (1% BSA, 0.3% Triton X-100, and 20% normal goat serum in 1× PBS). Primary antibodies were diluted using carrier solution (1% BSA and 0.3% Triton X-100 in 1× PBS). Primary antibody dilutions were 1:500 for rabbit polyclonal anti-NG2 antibody (a gift from Dr. Joel M. Levine, State University of New York at Stony Brook, Stony Brook, NY), 1:1,000 for mouse monoclonal anti-PCNA (Sigma-Aldrich), 1:1,000 for mouse monoclonal anti-nestin (CHEMICON International), 1:500 for mouse monoclonal anti-NeuN (CHEMICON International), 1:1,000 for rabbit polyclonal anti-GAD-67 (CHEMICON International), 1:1,000 for mouse monoclonal anti-CNP (Sternberger Monoclonals, Inc.) and 1:1,000 for rabbit anti-TOAD-64 (CHEMICON International). Brain sections were incubated in primary antibodies at 4°C overnight. Rinse was performed in carrier solution at RT, with three changes of solution every 5–15 min. All secondary antibodies (Jackson ImmunoResearch Laboratories) were diluted 1:200 in carrier solution. Cy-5– or AMCA- or TRITC-conjugated goat anti–mouse IgGs were used for monoclonal antibodies. Cy-5– or TRITC-conjugated goat anti–rabbit IgGs were used for NG2 staining. Incubation was performed at RT for 1 h, followed by three washes as described above. Sections were then transferred into 1× PBS, mounted with Mowiol, and later imaged using a fluorescence microscope (Nikon) equipped with a laser confocal scanning system (MRC1024; Bio-Rad Laboratories).

Immunocytochemistry

NG2, O4, O1, and BrdU immunostainings were performed as described previously (Yuan et al., 1998, 2002). For other stainings, coverslips were fixed with 4% PFA in 1× PBS at RT for 10 min, then permeabilized using 0.2% Triton X-100 at RT for 10 min. Blockage was performed using blocking solution at RT for 1 h. Mouse monoclonal anti-nestin antibodies (1:1000; CHEMICON International), anti-GFAP (1:500; CHEMICON International), anti-NeuN (1:250; CHEMICON International) and anti-isoforms $2_{a,b}$ of MAP$2_{a,b}$ (1:500; Clone AP-20, Lab Vision Corp.) were diluted in carrier solution, and cells were incubated at 4°C for 1 h. Cells were then washed as described ini the Immunohistochemistry section, and incubated in AMCA- or TRITC-conjugated goat anti–mouse IgG (1:200) at 4°C for 30 min. After three washes, coverslips were rinsed in 1× PBS and mounted with Mowiol.

Electrophysiology

For electrophysiological recordings in cultures derived from FACS®-purified CNP-GFP$^+$, cells were first maintained for 2 d in SCM and then shifted to EGF- and FGF2-free DME/F12 (1:1, vol/vol) medium supplemented with 10% FBS, 1% N2, and a combination of 30 ng/ml brain-derived neurotrophic factor and 30 ng/ml neurotrophin-3. Between 3 and 6 d after culturing in this neurotrophic medium, the coverslips were transferred to a recording chamber and perfused with extracellular solution (see Online supplemental material).

Patch electrodes had resistances between 4 and 7 MΩ when filled with intracellular solution of the following composition (mM): K-gluconate 130; NaCl 10; Mg-ATP 2; Na-GTP 0.3, Hepes 10; EGTA 0.6, biocytin 5 mg/ml, adjusted to pH 7.4 and 275 mosM. To elicit action potentials, whole-cell current-clamp recordings from both GFP$^+$ and GFP$^-$ cells were performed using the Axopatch amplifier (model 200A; Axon Instruments). From a resting potential of −60 mV, a series of current steps (step size = 10–30 pA; step duration = 300 ms), was applied to depolarize the cell membrane.

After the recordings, the coverslips were immediately fixed with 4% PFA as described in the previous section. To identify cells from which electrophysiological recordings were obtained, biocytin staining or rhodamine$_{600}$ (XRITC) Avidin D fluorescence detection (Vector Laboratories) was used in combination with anti-NeuN antibody (see Immunocytochemistry).

Slice electrophysiological recordings were obtained from P3–P12 CNP-GFP mice. In brief, mice were killed after NIH Animal Welfare Guidelines and 300 μm hippocampal sagittal sections were obtained. After a 1-h recovery period, slices were transferred to a recording chamber and perfused with extracellular solution as described in Online supplemental material. Weakly CNP-GFP$^+$ cells (visualized as described in the legend to Fig. 6 and in Yuan et al., 2002) were identified in the subgranular layer or hilar region of the dentate gyrus and also in CA1/CA3 pyramidal layers, and whole-cell current-clamp was used to investigate the ability of these cells to elicit action potentials. All parameters were as described above for the FACS®-cultured cells, except that the intracellular solution contained 2

mg/ml dextran-conjugated tetramethylrhodamine (Molecular Probes, Inc.) instead of biocytin. This allowed for the immediate visualization of the recorded cells under a fluorescence microscope.

For the recording of spontaneous synaptic currents, CNP-GFP$^+$ cells displaying weak GFP fluorescence in hilar region of the dentate gyrus and CA3 regions were voltage clamped at −60 mV and continuous traces were obtained. Extracellular solution was as described in Online supplemental material, and intracellular solution comprised of (mM): $CsMeSO_4$ 135, NaCl 8, MgATP 4, NaGTP 0.3, Hepes 10, and EGTA 0.6.

Online supplemental material

Fig. S1 illustrates the correlation between loss of CNP-GFP expression and morphological differentiation of GFAP$^+$ astrocytes derived from CNP-GFP$^+$ progenitor cells. Fig. S2 provides evidence that CNP-GFP$^+$ cells derived from transgenic line A2 have similar multipotent properties. Fig. S3 demonstrates that CNP protein is only expressed in mature oligodendrocytes and cannot be detected in GAD67$^+$ hippocampal neurons, which maintain a low level of CNP gene transcription, as detected by GFP fluorescence. Fig. S4 shows subregional differences in the anatomical distribution of NeuN$^+$/CNP-GFP$^+$ cells in the postnatal hippocampus. Online supplemental material available at http://www.jcb.org/cgi/content/full/jcb.200210110/DC1.

We are particularly grateful to Brian Weinberg (National Institute of Child Health and Human Development, NIH, Bethesda, MD) and Robyn Rufner (George Washington University School of Medicine, Washington, DC) for their valuable help in acquisition of confocal images. We thank our colleagues Jeff Mason and James Goldman (Columbia University, New York, NY) for sharing their unpublished observations and for valuable discussion. We thank Douglas Fields, Beth Stevens, and Chris J. McBain for discussion. We thank Regina Armstrong, Li-Jin Chew, Douglas Fields, Chris McBain, Sergio Schinelli, and Beth Stevens for their critical comments on the manuscript.

This work was partially supported by the NICHD intramural program, by P30HD40677, and by the Wadsworth Foundation. S. Belachew was supported by the Fonds National de la Recherche Scientifique (Belgium), and by NICHD. R. Chittajallu was supported by a Wellcome Trust Fellowship. Adan Aguirre was supported by a pre-doctoral fellowship from Consejo Nacional de Ciencia y Tecnologia and from the William A. Haseltine Postdoctoral Fellowship in Neuroscience and Genetics.

Submitted: 18 October 2002
Revised: 24 February 2003
Accepted: 24 February 2003

References

Altman, J., and G.D. Das. 1965. Autoradiographic and histological evidence of postnatal hippocampal neurogenesis in rats. *J. Comp. Neurol.* 124:319–335.

Alvarez-Buylla, A., and S. Temple. 1998. Stem cells in the developing and adult nervous system. *J. Neurobiol.* 36:105–110.

Alvarez-Buylla, A., J.M. Garcia-Verdugo, and A.D. Tramontin. 2001. A unified hypothesis on the lineage of neural stem cells. *Nat. Rev. Neurosci.* 2:287–293.

Bansal, R., and S.E. Pfeiffer. 1997a. FGF-2 converts mature oligodendrocytes to a novel phenotype. *J. Neurosci. Res.* 50:215–228.

Bansal, R., and S.E. Pfeiffer. 1997b. Regulation of oligodendrocyte differentiation by fibroblast growth factors. *Adv. Exp. Med. Biol.* 429:69–77.

Belachew, S., X. Yuan, and V. Gallo. 2001. Unraveling oligodendrocyte origin and function by cell-specific transgenesis. *Dev. Neurosci.* 23:287–298.

Bergles, D.E., J.D. Roberts, P. Somogyi, and C.E. Jahr. 2000. Glutamatergic synapses on oligodendrocyte precursor cells in the hippocampus. *Nature.* 405:187–191.

Cameron, H.A., and R.D. McKay. 2001. Adult neurogenesis produces a large pool of new granule cells in the dentate gyrus. *J. Comp. Neurol.* 435:406–417.

Capela, A., and S. Temple. 2002. LeX/ssea-1 is expressed by adult mouse CNS stem cells, identifying them as nonependymal. *Neuron.* 35:865–875.

Chiasson, B.J., V. Tropepe, C.M. Morshead, and D. van der Kooy. 1999. Adult mammalian forebrain ependymal and subependymal cells demonstrate proliferative potential, but only subependymal cells have neural stem cell characteristics. *J. Neurosci.* 19:4462–4471.

Dawson, M.R., J.M. Levine, and R. Reynolds. 2000. NG2-expressing cells in the central nervous system: are they oligodendroglial progenitors? *J. Neurosci. Res.* 61:471–479.

Doetsch, F., I. Caille, D.A. Lim, J.M. Garcia-Verdugo, and A. Alvarez-Buylla. 1999. Subventricular zone astrocytes are neural stem cells in the adult mammalian brain. *Cell.* 97:703–716.

Ffrench-Constant, C., and M.C. Raff. 1986. Proliferating bipotential glial progenitor cells in adult rat optic nerve. *Nature.* 319:499–502.

Fuss, B., B. Mallon, T. Phan, C. Ohlemeyer, F. Kirchhoff, A. Nishiyama, and W.B. Macklin. 2000. Purification and analysis of in vivo-differentiated oligodendrocytes expressing the green fluorescent protein. *Dev. Biol.* 218:259–274.

Gage, F.H. 2000. Mammalian neural stem cells. *Science.* 287:1433–1438.

Gravel, M., A. Di Polo, P.B. Valera, and P.E. Braun. 1998. Four-kilobase sequence of the mouse CNP gene directs spatial and temporal expression of lacZ in transgenic mice. *J. Neurosci. Res.* 53:393–404.

He, W., C. Ingraham, L. Rising, S. Goderie, and S. Temple. 2001. Multipotent stem cells from the mouse basal forebrain contribute GABAergic neurons and oligodendrocytes to the cerebral cortex during embryogenesis. *J. Neurosci.* 21:8854–8862.

Johansson, C.B., S. Momma, D.L. Clarke, M. Risling, U. Lendahl, and J. Frisen. 1999. Identification of a neural stem cell in the adult mammalian central nervous system. *Cell.* 96:25–34.

Johe, K.K., T.G. Hazel, T. Muller, M.M. Dugich-Djordjevic, and R.D. McKay. 1996. Single factors direct the differentiation of stem cells from the fetal and adult central nervous system. *Genes Dev.* 10:3129–3140.

Kaplan, M.S., and J.W. Hinds. 1977. Neurogenesis in the adult rat: electron microscopic analysis of light radioautographs. *Science.* 197:1092–1094.

Kondo, T., and M.C. Raff. 2000. Oligodendrocyte precursor cells reprogrammed to become multipotential CNS stem cells. *Science.* 289:1754–1757.

Kuhn, H.G., H. Dickinson-Anson, and F.H. Gage. 1996. Neurogenesis in the dentate gyrus of the adult rat: age-related decrease of neuronal progenitor proliferation. *J. Neurosci.* 16:2027–2033.

Laywell, E.D., P. Rakic, V.G. Kukekov, E.C. Holland, and D.A. Steindler. 2000. Identification of a multipotent astrocytic stem cell in the immature and adult mouse brain. *Proc. Natl. Acad. Sci. USA.* 97:13883–13888.

Lendahl, U., L.B. Zimmerman, and R.D. McKay. 1990. CNS stem cells express a new class of intermediate filament protein. *Cell.* 60:585–595.

Levine, J.M., R. Reynolds, and J.W. Fawcett. 2001. The oligodendrocyte precursor cell in health and disease. *Trends Neurosci.* 24:39–47.

Liu, S., J. Wang, D. Zhu, Y. Fu, K. Lukowiak, and Y. Lu. 2003. Generation of functional inhibitory neurons in the adult rat hippocampus. *J. Neurosci.* 23:732–736.

Malatesta, P., E. Hartfuss, and M. Gotz. 2000. Isolation of radial glial cells by fluorescent-activated cell sorting reveals a neuronal lineage. *Development.* 127:5253–5263.

Mallon, B.S., H.E. Shick, G.J. Kidd, and W.B. Macklin. 2002. Proteolipid promoter activity distinguishes two populations of NG2-positive cells throughout neonatal cortical development. *J. Neurosci.* 22:876–885.

Minturn, J.E., D.H. Geschwind, H.J. Fryer, and S. Hockfield. 1995a. Early postmitotic neurons transiently express TOAD-64, a neural specific protein. *J. Comp. Neurol.* 355:369–379.

Minturn, J.E., H.J. Fryer, D.H. Geschwind, and S. Hockfield. 1995b. TOAD-64, a gene expressed early in neuronal differentiation in the rat, is related to unc-33, a *C. elegans* gene involved in axon outgrowth. *J. Neurosci.* 15:6757–6766.

Noctor, S.C., A.C. Flint, T.A. Weissman, R.S. Dammerman, and A.R. Kriegstein. 2001. Neurons derived from radial glial cells establish radial units in neocortex. *Nature.* 409:714–720.

Reynolds, B.A., and S. Weiss. 1992. Generation of neurons and astrocytes from isolated cells of the adult mammalian central nervous system. *Science.* 255:1707–1710.

Seki, T. 2002. Expression patterns of immature neuronal markers PSA-NCAM, CRMP-4 and NeuroD in the hippocampus of young adult and aged rodents. *J. Neurosci. Res.* 70:327–334.

Seri, B., J.M. Garcia-Verdugo, B.S. McEwen, and A. Alvarez-Buylla. 2001. Astrocytes give rise to new neurons in the adult mammalian hippocampus. *J. Neurosci.* 21:7153–7160.

Song, H., C.F. Stevens, and F.H. Gage. 2002a. Astroglia induce neurogenesis from adult neural stem cells. *Nature.* 417:39–44.

Song, H., C.F. Stevens, and F.H. Gage. 2002b. Neural stem cells from adult hippocampus develop essential properties of functional CNS neurons. *Nat. Neurosci.* 5:438–445.

Spassky, N., C. Goujet-Zalc, E. Parmantier, C. Olivier, S. Martinez, A. Ivanova, K. Ikenaka, W. Macklin, I. Cerruti, B. Zalc, and J.L. Thomas. 1998. Multiple restricted origin of oligodendrocytes. *J. Neurosci.* 18:8331–8343.

Stallcup, W.B., and L. Beasley. 1987. Bipotential glial precursor cells of the optic

nerve express the NG2 proteoglycan. *J. Neurosci.* 7:2737–2744.

Stone, D.J., J. Walsh, and F.M. Benes. 1999. Localization of cells preferentially expressing GAD(67) with negligible GAD(65) transcripts in the rat hippocampus. A double in situ hybridization study. *Brain Res. Mol. Brain Res.* 71:201–209.

Temple, S., and A. Alvarez-Buylla. 1999. Stem cells in the adult mammalian central nervous system. *Curr. Opin. Neurobiol.* 9:135–141.

van Praag, H., A.F. Schinder, B.R. Christie, N. Toni, T.D. Palmer, and F.H. Gage. 2002. Functional neurogenesis in the adult hippocampus. *Nature.* 415:1030–1034.

Vicario-Abejon, C., C. Collin, P. Tsoulfas, and R.D. McKay. 2000. Hippocampal stem cells differentiate into excitatory and inhibitory neurons. *Eur. J. Neurosci.* 12:677–688.

Wolswijk, G., and M. Noble. 1989. Identification of an adult-specific glial progenitor cell. *Development.* 105:387–400.

Yuan, X., A.M. Eisen, C.J. McBain, and V. Gallo. 1998. A role for glutamate and its receptors in the regulation of oligodendrocyte development in cerebellar tissue slices. *Development.* 125:2901–2914.

Yuan, X., R. Chittajallu, S. Belachew, S. Anderson, C.J. McBain, and V. Gallo. 2002. Expression of the green fluorescent protein in the oligodendrocyte lineage: a transgenic mouse for developmental and physiological studies. *J. Neurosci. Res.* 70:529–545.

Yung, S.Y., S. Gokhan, J. Jurcsak, A.E. Molero, J.J. Abrajano, and M.F. Mehler. 2002. Differential modulation of BMP signaling promotes the elaboration of cerebral cortical GABAergic neurons or oligodendrocytes from a common sonic hedgehog-responsive ventral forebrain progenitor species. *Proc. Natl. Acad. Sci. USA.* 99:16273–16278.

JCB
Online Supplemental Material

Belachew et al. http://www.jcb.org/cgi/doi/10.1083/jcb.200210110

FACS®

For EGFP fluorescence, excitation wavelength of the argon ion laser was set at 488 nm and emission was through a 530-nm bandpass filter. Cy-5 fluorescence was excited with an HeNe laser (633 nm) and filtered with a 675-nm longpass filter. The sorting speed was 3,000–4,000 cells/second.

Electrophysiology

The composition of extracellular solution was as follows (mM): NaCl 124, KCl 3, $CaCl_2$ 2.5, $MgSO_4$ 1.3, $NaHCO_3$ 26, NaHPO4 1.25, and glucose 15, saturated with 95% O_2/5% CO_2 at RT. GFP expression in cultured cells was determined with an upright microscope (model BX50WI; Olympus) fitted with a reflected light fluorescent attachment (model BX-FLA; Olympus) and a U-MWIBA filter cube (excitation 460–490 nm; emission 515–550 nm).

Image analysis

We measured GFP fluorescence intensity by using MetaMorph® v.4.1.2 image analysis software (Universal Imaging Corp.). We studied $NeuN^+$/CNP-GFP^+ and $NeuN^-$/CNP-GFP^+ cells in single-plane confocal scanning images of sagittal tissue sections from CNP-GFP mice. All confocal images were acquired using identical scanning parameters. Random hippocampal fields were assessed in CA1, CA3, and dentate gyrus areas. The mean background fluorescence intensity was subtracted for each measurement, and final values were expressed in arbitrary scale units. Cell counts were obtained after classifying cells according to their GFP fluorescence by intervals of 20 U from 0 to 240.

The Journal of Cell Biology

[HELP with High Resolution Image Viewing]

Full Text of this Article

[View Larger Version of this Image]

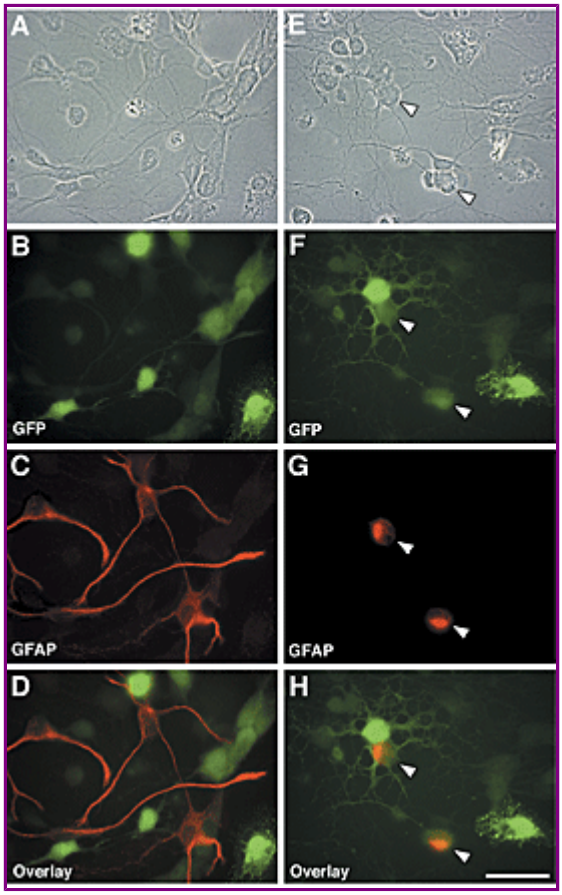

Figure S1. Correlation between loss of CNP-GFP expression and morphological differentiation of GFAP$^+$ astrocytes derived from CNP-GFP$^+$ progenitor cells. Both sets of panels (A-D and E-H) represent photomicrographs from the same microscopic field. Phase contrast (A and E), green GFP fluorescence (B and F), red GFAP staining (C and G), and overlays (D and H) are shown. After 48 h of adherent culture in SCM, mature astrocytes derived from FACS®-purified P2 CNP-GFP$^+$ progenitor cells were GFP$^-$, and displayed stellate shapes with GFAP expression in cell body and processes (A-D). In the same cultures, we also identified cells still expressing low levels of GFP, but that were also GFAP$^+$ (E-H, arrowheads). In all these GFAP$^+$/CNP-GFP$^+$ cells, GFAP expression was restricted to their cell body, with no staining of processes (E-H, arrowheads). Bars, 20 μm.

Full Text of this Article

The Journal of Cell Biology

[HELP with High Resolution Image Viewing]

Full Text of this Article

[View Larger Version of this Image]

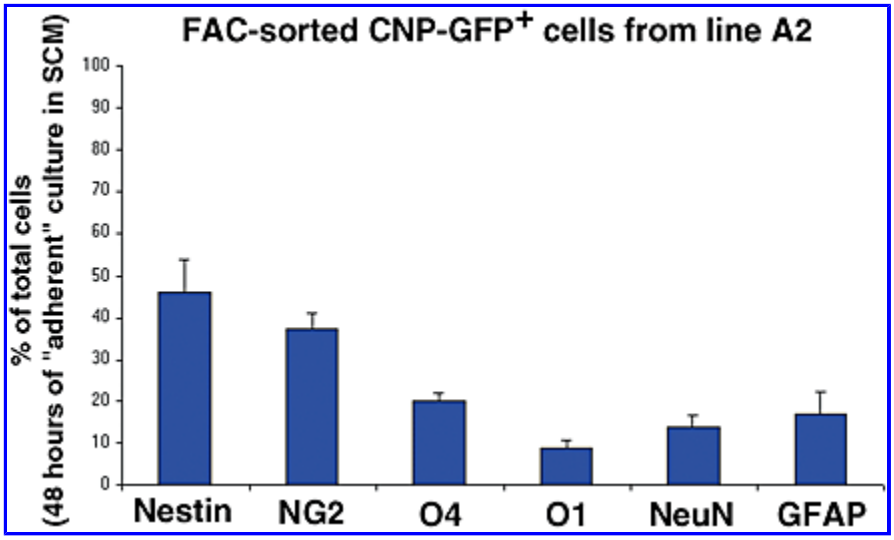

Figure S2. Quantitative analysis of the multipotent properties of CNP-GFP$^+$ cells derived from transgenic line A2. Histograms represent immunocytochemical characterization (% of total cells in y axis, immunophenotypes in x axis) of the progeny of early postnatal (P2) FACS®-purified CNP-GFP$^+$ cells from line A2 cultured immediately after FACS® under adherent conditions for 48 h in SCM. Nestin, NG2, O4, O1, NeuN, and GFAP immunophenotypes were assessed. Values (mean ± SD) represent averages of one experiment. Countings were performed separately for each staining, and the number of total cells counted (from at least 15 separate microscopic fields) ranged between 255 and 412.

Full Text of this Article

The Journal of Cell Biology

[HELP with High Resolution Image Viewing]

Full Text of this Article

[View Larger Version of this Image]

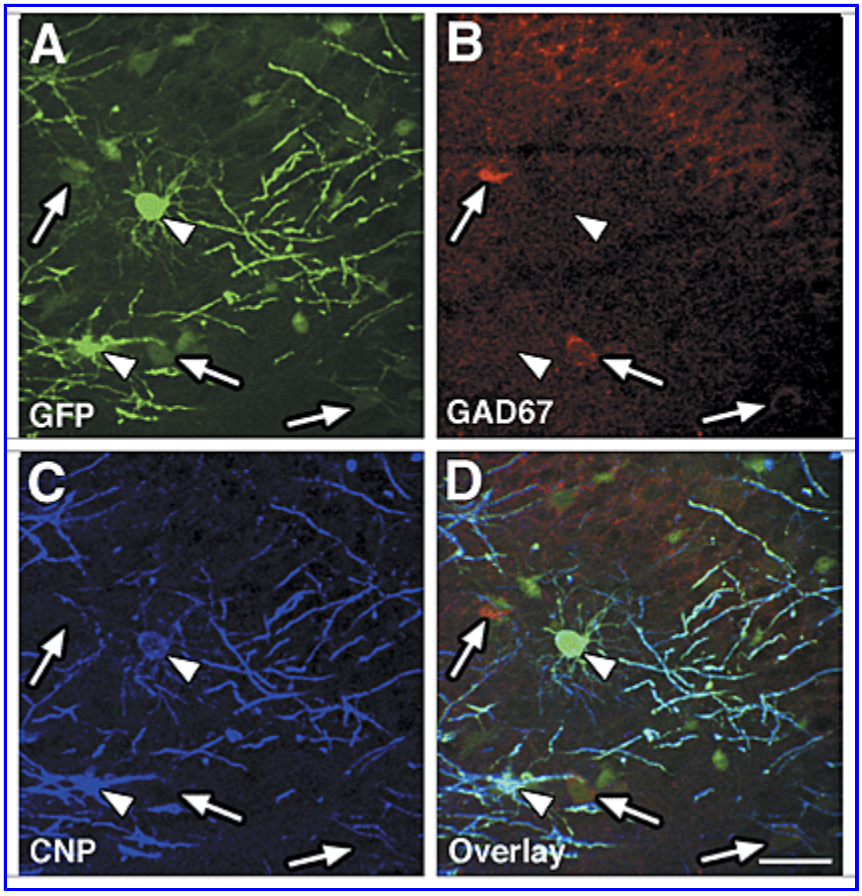

Figure S3. Developmental regulation of CNP protein expression in CNP-GFP$^+$ cells in situ. Confocal images of a representative field in adult (P30) CA3 stratum radiatum area showing GFP (A), GAD67 (B), and CNP protein (C) expression. CNP protein is only expressed in differentiated oligodendrocytes that display a mature myelin-forming-like morphology, and that are highly GFP$^+$, reflecting a high level of transcriptional activation of the CNP gene (arrowheads). Conversely, CNP protein expression is not detected in GAD67$^+$ hippocampal neurons that maintain low levels of GFP fluorescence, reflecting weak transcriptional activation of the CNP gene (arrows). Bars, 40 μm.

Full Text of this Article

The Journal of Cell Biology

[HELP with High Resolution Image Viewing]

Full Text of this Article

[View Larger Version of this Image]

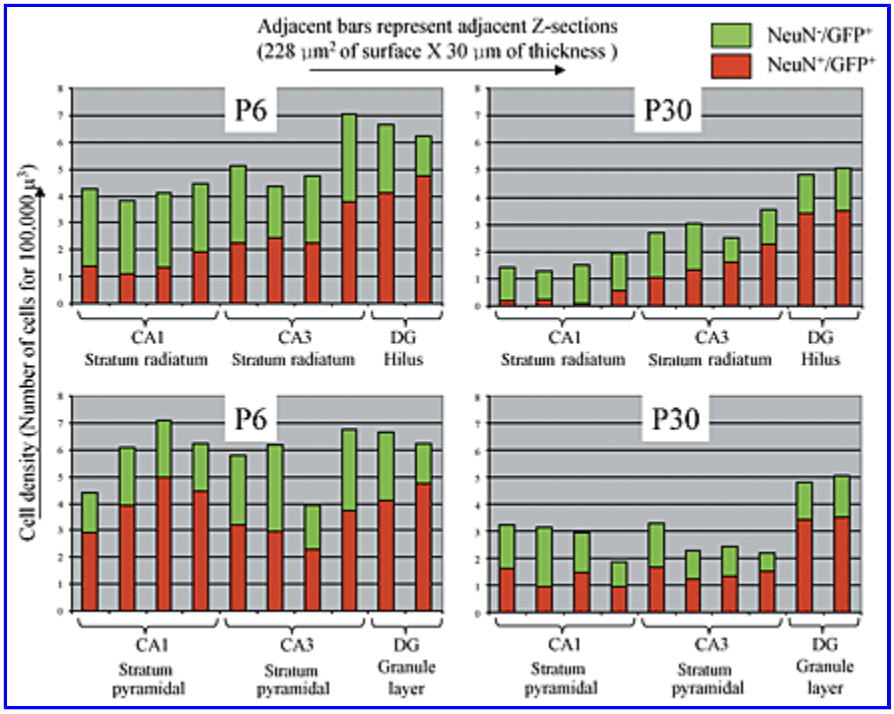

Figure S4. Subregional differences in the anatomical distribution of NeuN$^+$/CNP-GFP$^+$ cells in the postnatal hippocampus. The absolute density (per volume unit) of NeuN$^+$/CNP-GFP$^+$ cells is not significantly lower in the pyramidal layer as compared with stratum radiatum. In CA1, the density of NeuN$^+$/CNP-GFP$^+$ cells is significantly higher in stratum pyramidal than in stratum radiatum. However, CA3/CA1 pyramidal layers and DG granule layer represent anatomically much smaller tissue volumes than CA3/CA1 stratum radiatum and DG molecular and hilar DG areas. This is consistent with the finding that most of NeuN$^+$/CNP-GFP$^+$ cells were found in these latter regions. We emphasize here that electrophysiological recordings (i.e., presence of action potentials and of spontaneous currents) from NeuN$^+$/CNP-GFP$^+$ cells were similar in CA3 stratum radiatum and CA3 stratum pyramidal.

Full Text of this Article

Home | Help | Feedback | Subscriptions | Archive | Search

7.6 Publication #6: Aguirre,A.A., Chittajallu,R., Belachew,S., and Gallo,V. (2004). NG2-expressing type C multipotent progenitor cells of the subventricular zone: a possible source of interneuron renewal the adult hippocampus. *J. Cell Biol.* 165:575-589.

JCB Article

NG2-expressing cells in the subventricular zone are type C–like cells and contribute to interneuron generation in the postnatal hippocampus

Adan A. Aguirre,[1] Ramesh Chittajallu,[1] Shibeshih Belachew,[2] and Vittorio Gallo[1]

[1]Center for Neuroscience Research, Children's Research Institute, Children's National Medical Center, Washington, DC 20010
[2]Center for Cellular and Molecular Neurobiology, University of Liège, 4020 Liège, Belgium

The subventricular zone (SVZ) is a source of neural progenitors throughout brain development. The identification and purification of these progenitors and the analysis of their lineage potential are fundamental issues for future brain repair therapies. We demonstrate that early postnatal NG2-expressing ($NG2^+$) progenitor cells located in the SVZ self-renew in vitro and display phenotypic features of transit-amplifier type C–like multipotent cells. $NG2^+$ cells in the SVZ are highly proliferative and express the epidermal growth factor receptor, the transcription factors Dlx, Mash1, and Olig2, and the Lewis X (LeX) antigen. We show that grafted early postnatal $NG2^+$ cells generate hippocampal GABAergic interneurons that propagate action potentials and receive functional glutamatergic synaptic inputs. Our work identifies Dlx^+/$Mash1^+$/LeX^+/$NG2^+$/GFAP-negative cells of the SVZ as a new class of postnatal multipotent progenitor cells that may represent a specific cellular reservoir for renewal of postnatal and adult inhibitory interneurons in the hippocampus.

Introduction

Neurogenesis continues in restricted areas of the postnatal vertebrate brain throughout adulthood (Reynolds and Weiss, 1992; Doetsch et al., 1999a; Alvarez-Buylla and Garcia-Verdugo, 2002). Adult neural stem cells (NSCs) that give rise to neurons are found in specific brain regions, including the subventricular zone (SVZ). This germinal layer is a large reservoir of proliferating NSCs (Doetsch et al., 1999a,b, 2002a; Capela and Temple, 2002), and is therefore a potential source of multipotential precursors for use in cell repair therapies.

Two major multipotent NSC phenotypes have been described in the adult SVZ, based on expression of the intermediate filament protein GFAP (glial fibrillary acidic protein; Doetsch et al., 1999a, 2002a; Capela and Temple, 2002). Type B cells express GFAP and give rise to the rapidly dividing, transit-amplifying type C cells, which are not immunopositive for GFAP (Doetsch et al., 1999a). It has been demonstrated that SVZ type C cells (a) generate neurospheres in the presence of EGF; (b) express the Dlx2 transcription factor and the epidermal growth factor receptor (EGFR); and (c) are the direct precursors of neurons generated in the olfactory bulb (Doetsch et al., 1999a, 2002a).

Adult NSCs express the Lewis X (LeX) carbohydrate antigen, which is detected in both $GFAP^+$ and GFAP-negative cells of the SVZ (Capela and Temple, 2002), indicating that this brain region contains a LeX^+/GFAP-negative cell population with neurogenic potential. Because type C cells are a GFAP-negative and highly proliferative cell population, it is likely that the LeX^+/GFAP-negative stem cells are in fact type C progenitors (Capela and Temple, 2002; Doetsch et al., 2002a).

Cells that express the NG2 chondroitin sulfate proteoglycan represent the largest pool of postnatal/adult proliferative progenitors in the brain (Dawson et al., 2000). NG2-expressing cells were thought to be strictly oligodendrocyte progenitors; however, recent studies have expanded their role by demonstrating that early postnatal $NG2^+$ cells form neurospheres and generate neurons in vitro (Belachew et al., 2003). These properties were established by using a 2′,3′-cyclic nucleotide 3′-phosphodiesterase (CNP)-EGFP transgenic mouse, in

The online version of this article includes supplemental material.

Address correspondence to Vittorio Gallo, Center for Neuroscience Research, Children's Research Institute, Rm. 5345, Children's National Medical Center, 111 Michigan Ave., N.W., Washington, DC 20010. Tel.: (202) 884-4996. Fax: (202) 884-4988. email: vgallo@cnmcresearch.org

Key words: neural stem cells; homeobox transcription factors; bHLH genes; progenitor cell transplantation; synaptic transmission

Abbreviations used in this paper: CNP, 2′,3′-cyclic nucleotide 3′-phosphodiesterase; DG, dentate gyrus; DIV, days in vitro; EGFR, epidermal growth factor receptor; LeX, Lewis X; NSC, neural stem cell; SVZ, subventricular zone.

The Journal of Cell Biology, Volume 165, Number 4, May 24, 2004 575–589
http://www.jcb.org/cgi/doi/10.1083/jcb.200311141

Supplemental Material can be found at:
http://www.jcb.org/cgi/content/full/jcb.200311141/DC1

which $NG2^+$ progenitors expressed CNP promoter-driven EGFP (Yuan et al., 2002; Belachew et al., 2003). Consistent with these results, a parallel study demonstrated that $A2B5^+$ precursor cells isolated from the adult human subcortical white matter expressed the CNP gene and generated neurons in vitro and in vivo (Nunes et al., 2003). Given these findings, it is clear that CNP gene-expressing cells that are NG2 and A2B5 immunopositive display properties of multipotent progenitor cells (Belachew et al., 2003; Goldman, 2003; Nunes et al., 2003). These cells could contribute to neurogenesis in the postnatal/adult brain, although the precise characterization and neurogenic potential of $NG2^+$ progenitors in the SVZ and the classification of the neuronal subtypes that they generate remain undefined.

In the present work, we demonstrate that early postnatal $NG2^+/EGFP^+$ cells in the SVZ of CNP-EGFP mice are mitotically active and express markers of multipotent precursor cells of the adult SVZ (Dlx, EGFR, and LeX). Based on these markers, we establish a relationship between $NG2^+$ and LeX^+ precursor cells, and determine a lineage continuum between $NG2^+/Dlx^+$ progenitors and hippocampal GABAergic interneurons. We also show that isochronically transplanted perinatal $NG2^+/EGFP^+$ progenitors migrate to the hippocampus, where they give rise to Dlx^+ GABAergic interneurons. Our findings indicate that early postnatal $NG2^+$ cells are Lex^+/GFAP-negative type C–like cells in the SVZ, and identify such type C–like cells as a source of hippocampal GABAergic interneurons in the postnatal brain.

Results

Early postnatal and adult NG2-expressing cells in the SVZ display a type C–like immunophenotype

Fig. 1 shows that the majority (~75%; Fig. S3, available at http://www.jcb.org/cgi/content/full/jcb.200311141/DC1) of $EGFP^+$ cells in the SVZ were $NG2^+$ at P8 (Fig. 1, A–G) and at P40 (not depicted). At both ages, all the $NG2^+$ cells were $EGFP^+$ and were found subependymally in the lateral ventricle wall (Fig. 1 A). Staining with anti-Olig2 (Lu et al., 2000) labeled virtually all the $NG2^+/EGFP^+$ cells at P8 (Fig. 1 B) and P40 (not depicted). $Olig2^+/EGFP^+$ cells that did not express NG2 were also found in the SVZ (Fig. 1 B). A significant percentage (26.5 ± 2.4%; mean ± SEM; $n = 356$) of the $NG2^+/EGFP^+$ cells in the SVZ were also labeled with anti-Mash1 (Fig. 1 E and Fig. S2, available at http://www.jcb.org/cgi/content/full/jcb.200311141/DC1).

We determined the proliferative potential of $NG2^+$ cells in the postnatal SVZ. 2 h after a single BrdU injection, 31.9 ± 5.2 and 25.7 ± 4.2% ($n = 360$ and 239) of the $NG2^+/EGFP^+$ cells were $BrdU^+$ at P8 and P40, respectively (Fig. 1 C and Fig. 2 G, inset). Consistent with these findings, a large percentage of $NG2^+/EGFP^+$ cells (P8, 59.0 ± 3.3%, $n = 283$; P40, 37.5 ± 7.3%, $n = 140$; Fig. 1 D and Fig. 2 G, inset) were $Ki67^+$ (Schluter et al., 1993).

To further define the immunophenotype of $NG2^+/EGFP^+$ cells in the SVZ, we immunolabeled tissue sections with anti-NG2 and the MMA monoclonal antibody, which recognizes the LeX antigen (Capela and Temple, 2002). At P8 (Figs. 1 F and 2 G) and P40 (Fig. 2 G and not depicted), 47 and 25% of the $NG2^+/EGFP^+$ cells were LeX^+, respectively. None of the $NG2^+$ cells in the SVZ expressed GFAP or GLAST (Fig. 2, A and B). $NG2^+/EGFP^+$ cells represented 12.9 ± 0.8% of total SVZ cells at P8, and the total LeX^+ SVZ population was divided into a 27.4 ± 1.5% of cells that were $GFAP^+$ and a nonoverlapping subset of 37.9 ± 3.1% of cells that were $NG2^+$ (Fig. S3). Altogether, these results indicate that the $NG2^+/EGFP^+$ cells that express LeX, but do not express GFAP, account for approximately half of total LeX^+/GFAP-negative cells. Thus, $NG2^+/EGFP^+/Lex^+$/GFAP-negative cells likely represent the population of LeX^+/GFAP-negative cells characterized by Capela and Temple (2002), and might correspond to type C–like transit-amplifying cells that are present in the early postnatal SVZ and persist throughout adulthood (Doetsch et al., 2002a).

Adult type C cells express the EGFR and the Dlx2 homeobox-containing transcription factor (Doetsch et al., 2002a). At P8, virtually all (96.0 ± 8.2%, $n = 395$) of the $NG2^+/EGFP^+$ cells also expressed EGFR in the SVZ (Figs. 1 G and 2 G). At P40, more than half of the $NG2^+/EGFP^+$ cells expressed the EGFR (52.0 ± 5.8%, $n = 210$; Fig. 2 G). After immunostaining with a pan anti-Dlx antibody, recognizing both the early (*dlx1/2*) and late (*dlx5/6*) members of the *dlx* homeobox gene family (Panganiban et al., 1997), we found that 45.0 ± 5.2 ($n = 335$) and 37.0 ± 3.3% ($n = 160$) of the $NG2^+/EGFP^+$ cells were also Dlx^+ at P8 and P40, respectively (Fig. 2, C and G). Dlx was also expressed in $LeX^+/EGFP^+$ cells (unpublished data). We confirmed by RT-PCR that the Dlx2 gene was expressed in SVZ $NG2^+$ cells at P8 (Fig. S2). Among the total Dlx^+ cell population of the SVZ, only 7.7 ± 0.9% expressed NG2 at P8 (Fig. S3). Because it has been demonstrated that Dlx proteins are expressed in bipotential oligodendrocyte-GABAergic neuron progenitors (He et al., 2001; Marshall and Goldman, 2002; Panganiban and Rubenstein, 2002), we determined if the pan anti-Dlx antibody also stained $EGFP^+$/NG2-negative oligodendrocytes. $EGFP^+/MBP^+$ (myelin basic protein) oligodendrocytes were consistently Dlx-negative (unpublished data).

In summary, it appears that at the end of the first postnatal week, $NG2^+/LeX^+/Dlx^+/Mash1^+$/GFAP-negative type C–like cells may represent ~2–3% of the total SVZ cell population.

NG2 expression is detected in cells displaying an immature neuronal phenotype in the SVZ

Neuroblasts are Dlx^+/PSA-$NCAM^+$ and can be found migrating through the SVZ into the olfactory bulb (Doetsch et al., 1997, 1999a). In the SVZ, 22.0 ± 2.2 and 11.0 ± 1.8% of the $NG2^+/EGFP^+$ cells expressed PSA-NCAM (Fig. 2, D and G) at P8 and P40, respectively. Confirming the identity of a fraction of $NG2^+/EGFP^+$ cells as immature neuroblasts, we found that 16.0 ± 3.2 and 7.0 ± 1.6% of $NG2^+/EGFP^+$ cells in the SVZ also expressed class III β-tubulin (stained by TUJ1 antibody) at P8 and P40, respectively (Fig. 2, E and G; and not depicted). Similar percentages were also obtained with the immature neuronal marker HuC/D (unpublished data).

These data indicate that ~15% of endogenous $NG2^+/EGFP^+$ cells are postmitotic neuroblasts in the SVZ at P8.

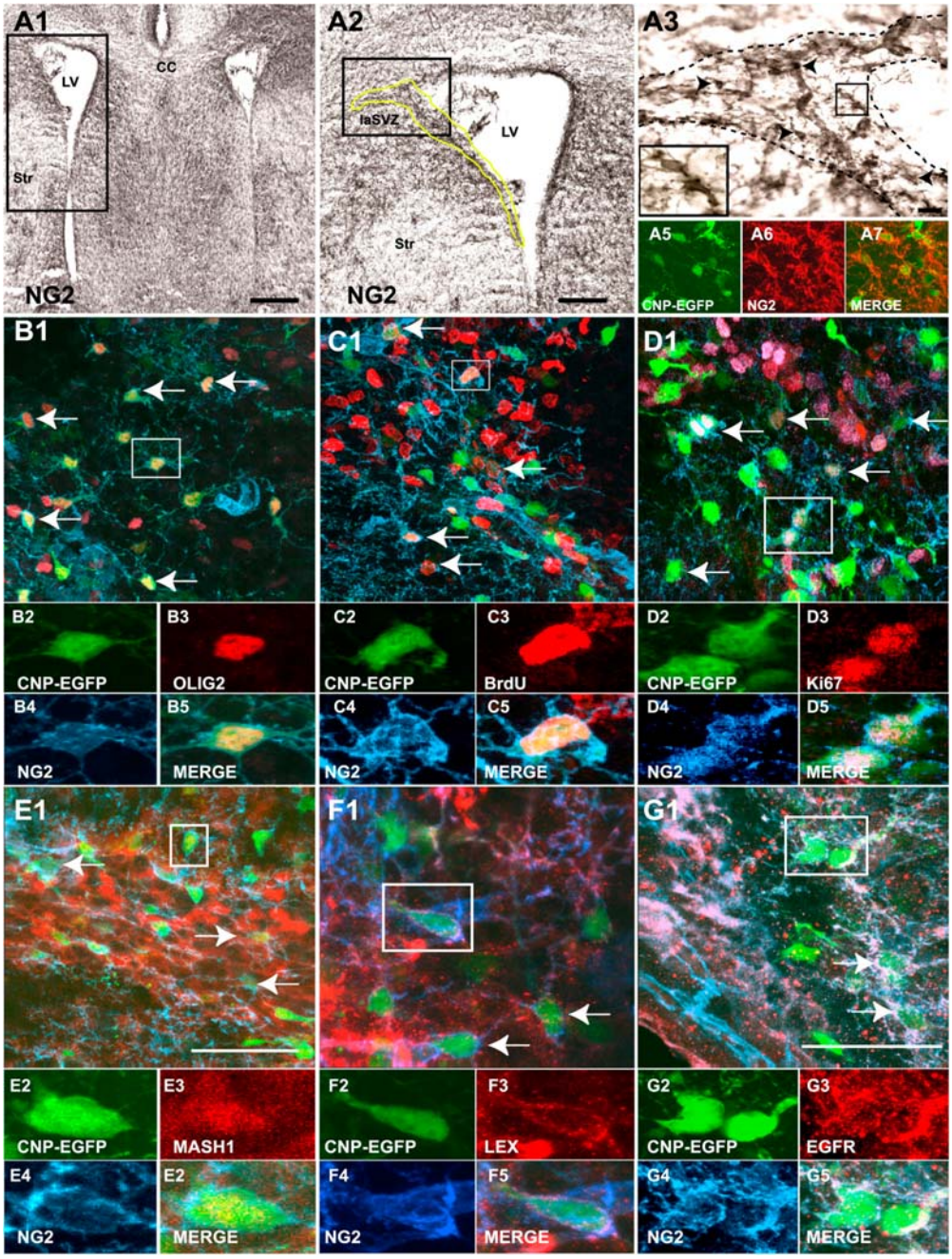

Figure 1. **NG2$^+$/EGFP$^+$ cells express NSCs markers in the SVZ.** Coronal sections of the SVZ at P8. (A1–A3) Anti-NG2 staining (DAB reaction, brown) shows that NG2 cells are found lining the wall of the lateral ventricle (yellow line) and throughout the entire lateral SVZ. The dotted line (A3) indicates the area analyzed in this paper. (A5–A7) Most of the EGFP$^+$ cells (A5, green) were labeled with NG2 antibodies (A6, red), and all NG2$^+$ cells were EGFP$^+$ (A7). (B–G) All micrographs were obtained from the lateral SVZ (laSVZ). (B) All NG2$^+$/EGFP$^+$ cells (blue/green, respectively) express Olig2 (red). (C and D) NG2$^+$/EGFP$^+$ cells proliferate in the SVZ, as shown by BrdU incorporation (C, red) and by Ki67 immunolabeling (D, red). (E and G) A large percentage of NG2$^+$/EGFP$^+$ cells (blue/green, respectively) express the transcription factor Mash1 (E, red), the adult NSC markers LeX antigen (F, red), and EGFR (G, red). Arrows indicate NG2$^+$/EGFP$^+$ cells double-labeled with any of the markers used. NG2$^+$/EGFP$^+$ cells in boxed areas are shown at higher magnification. LV, lateral ventricle; Str, striatum; CC, corpus callosum. Bars: (A1) 500 μm; (A2) 300 μm; (A3) 50 μm; (B–E) 50 μm; (F and G) 100 μm.

Consistently, we found that the majority of SVZ NG2$^+$/EGFP$^+$ cells that expressed class III β-tubulin were immunoreactive for Dlx at P8 (Fig. 2 F and Fig. S3). Finally, we could also detect LeX$^+$ cells that were TUJ1$^+$ (Capela and Temple, 2002; unpublished data).

The LeX-expressing subset of early postnatal NG2$^+$/EGFP$^+$ cells generates neurospheres and is self-renewing

To demonstrate self-renewal of early postnatal NG2$^+$/EGFP$^+$ cells, we determined whether or not single cells derived from the dissociation of primary neurospheres

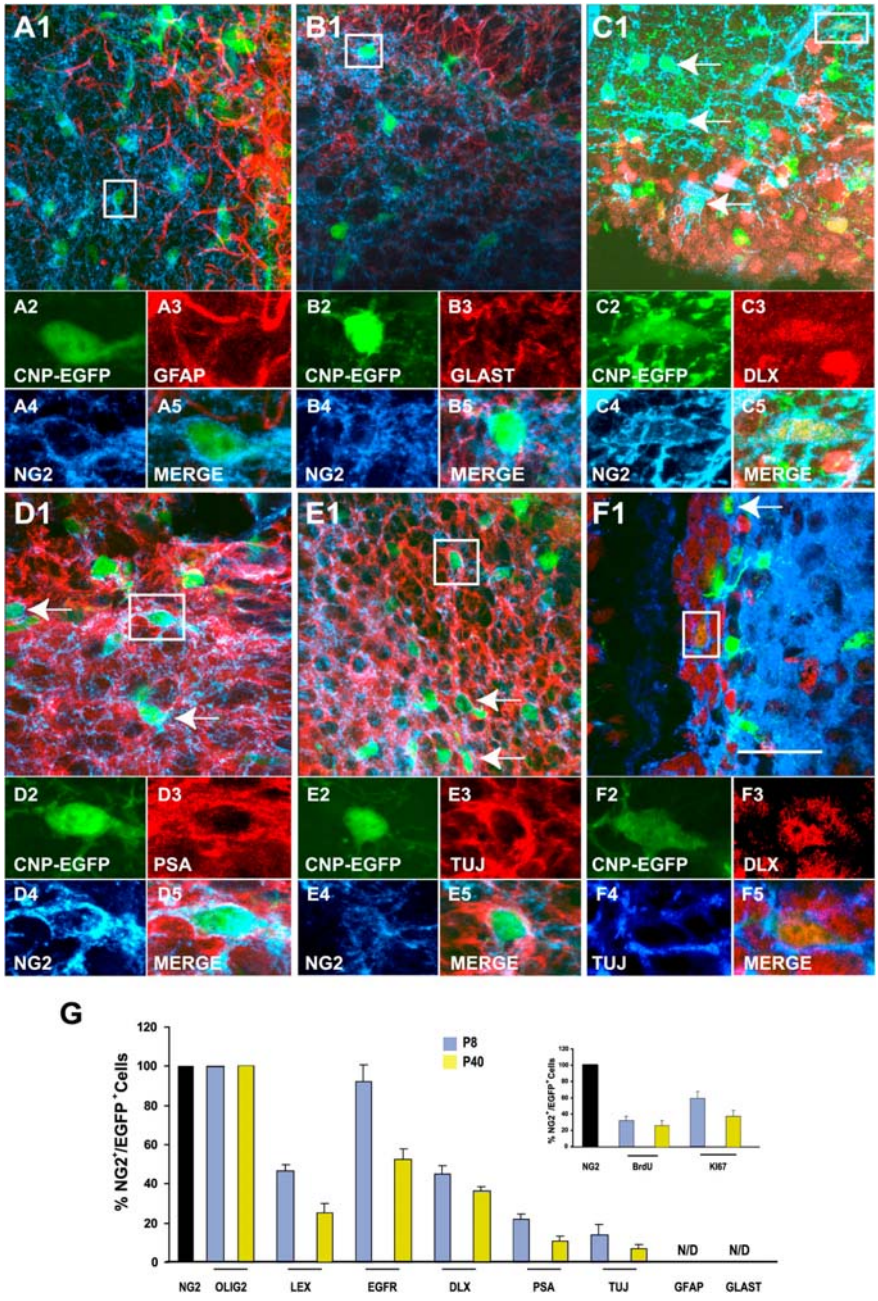

Figure 2. **A subpopulation of NG2$^+$/EGFP$^+$ cells displays an immature neuronal phenotype in the SVZ.** P8 coronal sections. (A and B) NG2$^+$/EGFP$^+$ cells (blue/green, respectively) in the SVZ are not labeled for the astroglial markers GFAP (A, red) or GLAST (B, red). (C) A large percentage of the NG2$^+$/EGFP$^+$ cells (blue/green, respectively) in the SVZ are labeled with anti-Dlx antibodies (red) for neuronal progenitor cells. (D) A significant percentage of the NG2$^+$/EGFP$^+$ cells (blue/green, respectively) in the SVZ express the early neuronal markers PSA-NCAM (D, red) and βIII-tubulin (E, TUJ1; red). (F) The majority of the EGFP$^+$/TUJ1$^+$ cells (green/blue, respectively) are Dlx$^+$ (red). Arrows indicate double-labeled NG2$^+$/EGFP$^+$ cells. NG2$^+$/EGFP$^+$ cells in boxed areas are shown at higher magnification. Bar, 50 μm. (G) NG2$^+$/EGFP$^+$ cells in the lateral ventricle of the SVZ. Virtually all NG2$^+$/EGFP$^+$ cells expressed Olig2 at P8 and P40, and EGFRs at P8. At P40 the percentage of EGFR$^+$/NG2$^+$ cells decreases by 50%. A similar decrease is also observed for Lex, Dlx, PSA-NCAM, and TUJ1. None of the NG2$^+$/EGFP$^+$ cells are labeled with anti-GFAP or anti-GLAST antibodies. (inset) Percentage of NG2$^+$/EGFP$^+$ cells that incorporated BrdU after 2 h of pulse labeling. No significant differences are detected between P8 and P40. This result was also confirmed by anti-Ki67 immunostaining. Percentages were obtained by counting NG2$^+$/EGFP$^+$ cells located into the SVZ region. Data are means ± SEM (total NG2$^+$/EGFP$^+$ cells counted equals 850 at P8 and 400 at P40; for each age, four to six brain sections from four different brains were used).

(Belachew et al., 2003) generated secondary neurospheres. FACS®-purified NG2$^+$/EGFP$^+$ cells from P2 brains represented 4.1 ± 0.2% of the total cells (12 separate sortings). After 7 d in EGF, these cells seeded at clonal dilution formed neurospheres, displaying the typical morphology and growth properties of NSCs (Reynolds and Weiss, 1992; Belachew et al., 2003). NG2$^+$/EGFP$^+$ cells dissociated from primary neurospheres generated secondary neurospheres, thus indicating self-renewal (Fig. 3 A1, inset).

NG2$^+$ cell–derived clonal neurospheres plated on coverslips comprised TUJ$^+$ neurons, GFAP$^+$ astrocytes, O4$^+$ preoligodendrocytes, and nestin$^+$ progenitors (unpublished data). Each clone contained ∼15–20% of neurons. The vast majority of the neurons in each clone were GABAergic, based on GAD-67 coexpression (93 ± 0.6% of total TUJ1-expressing cells; Fig. 3, A–C; and Fig. S1, available at http://www.jcb.org/cgi/content/full/jcb.200311141/DC1). All of the GAD-67$^+$/EGFP$^+$ neurons were Dlx$^+$ (Fig. 3 B and Fig. S1), and a small subset coexpressed the Ca^{2+}-binding protein PV (parvalbumin; Fig. 3 C). In contrast with the mixed neuronal fate potential of typical E14.5 forebrain NSCs, ∼5% of neurons derived from early postnatal NG2$^+$/EGFP$^+$ cells were immunoreactive for markers of dopaminergic and glutamatergic neurons (Fig. S1). These results indicate that NG2$^+$/EGFP$^+$ cells predominantly generate inhibitory GABAergic interneurons in culture, as demonstrated by their expression of GAD-67, Dlx, and PV (Ma et al., 1994; Jinno and Kosaka, 2002; Panganiban and Rubenstein, 2002; Liu et al., 2003).

By proposing that early postnatal SVZ NG2$^+$/EGFP$^+$ cells are type C–like cells (Doetsch et al., 2002a) and that the

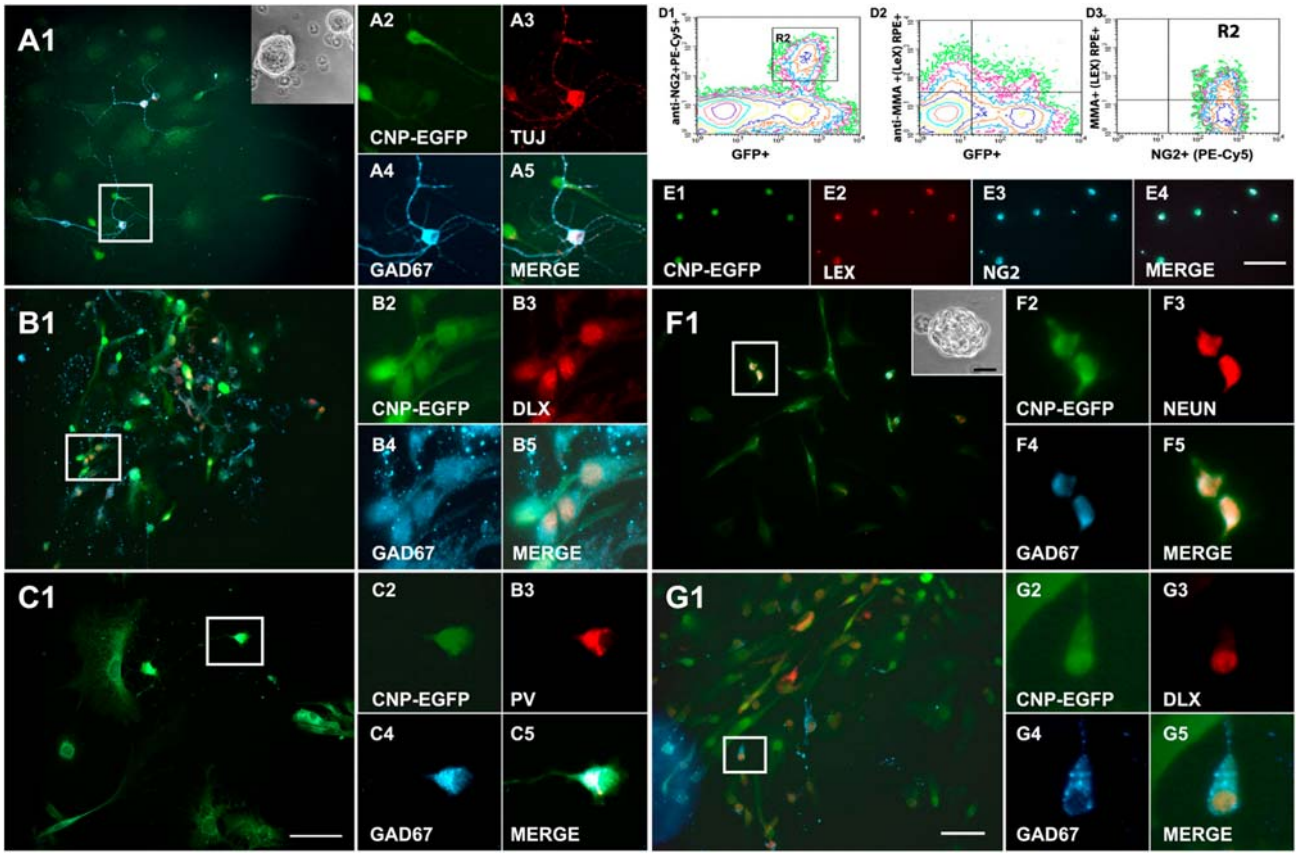

Figure 3. **FACS®-purified NG2$^+$/EGFP$^+$ and LeX$^+$/NG2$^+$/EGFP$^+$ cells self-renew and generate GABAergic interneurons in vitro.** FACS®-purified NG2$^+$/EGFP$^+$ (A–C) and LeX$^+$/NG2$^+$/EGFP$^+$ (D–G) cells generate neurospheres. After primary neurosphere formation, cell dissociation to single cell suspension and replating in SCM at clonal dilution generated secondary neurospheres (A1 and F1, insets). (A) A single secondary neurosphere was plated and processed for immunocytochemistry 6 d after plating. All the TUJ1$^+$ cells (red) are labeled with anti–GAD-67 (blue) antibodies. (B and C) The phenotype of the neurons derived from NG2$^+$/EGFP$^+$ cells is GABAergic. Neurons are double labeled with anti-Dlx (red) and anti–GAD-67 (blue) antibodies (B), and anti-parvalbumin (PV, red) and anti–GAD-67 (C, blue). (D) Sorting profile for NG2$^+$/EGFP$^+$ cells (D1; NG2 immunolabeling was scattered with PE-Cy5, R2 box) or MMA$^+$/EGFP$^+$ cells (D2; LeX antigen was scattered with R-phycoerythrin, RPE). To scatter the triple positive (LeX$^+$/NG2$^+$/EGFP$^+$) cells, the NG2$^+$/EGFP$^+$ fraction (R2 box in D1) was double sorted using PE-Cy5 for NG2 and RPE for LeX (D3). Note that a significant percentage of NG2$^+$/EGFP$^+$ cells (D1, R2 window) express the LeX antigen (D3). (E) A typical sample of LeX$^+$/NG2$^+$/EGFP$^+$ cells after FACS® shows high purity. (F) LeX$^+$/NG2$^+$/EGFP$^+$ FACS®-purified cells were assayed for neurosphere formation. LeX$^+$/NG2$^+$/EGFP$^+$ neurospheres displayed similar properties to those derived from NG2$^+$/EGFP$^+$ cells and generated differentiated GABAergic neurons, as shown by immunocytochemistry with anti-NeuN (red) and anti–GAD-67 (blue) antibodies. (G) The GABAergic neuronal fate is confirmed by anti-Dlx (red) and anti–GAD-67 (blue) coexpression. EGFP$^+$ cells (green) in boxed areas are shown at higher magnification. Bars, 50 μm.

LeX$^+$/GFAP-negative cells described by Capela and Temple (2002) are NG2$^+$, we are suggesting that NG2$^+$/EGFP$^+$ cells, which also express LeX, are multipotent and have the potential to self-renew. To demonstrate this property, we purified P2 LeX$^+$/NG2$^+$/EGFP$^+$ cells by triple FACS® (Fig. 3, D1–D3). All FACS®-purified Lex$^+$ cells were consistently NG2$^+$/EGFP$^+$ (Fig. 3, E1–E4), whereas only 26% of the NG2$^+$/EGFP$^+$ cells were also Lex$^+$ (Table I).

FACS®-purified LeX$^+$/NG2$^+$/EGFP$^+$ cells formed primary and secondary neurospheres (Fig. 3 F1, inset). Also, these neurospheres generated GFAP$^+$, O4$^+$, and nestin$^+$ cells in each clone (unpublished data). All clones contained

Table I. **Antigenic characterization of FACS®-purified perinatal and adult NG2$^+$/EGFP$^+$ cells**

	NG2	Ki67	LEX	DLX	EGFR	PSA	TUJ	GFAP
Postnatal (P2)	100	65.99 ± 0.42	26.0 ± 1.8	13.13 ± 2.2	97.52 ± 5.3	26.26 ± 0.30	10.17 ± 0.50	N/D
Adult (P40)	100	26.43 ± 2.2	14.58 ± 1.8	9.62 ± 1.2	42.20 ± 3.4	16.23 ± 0.4	6.2 ± 1.0	N/D

Postnatal day 2 (P2) and 40 (P40) brains from CNP-EGFP transgenic mice were dissociated and processed for NG2/EGFP FACS® purification, as described in Materials and methods. After FACS®, cells were plated on polyornithine-coated coverslips (20,000 cells per 35-mm coverslip) and processed for immunocytochemistry after 2 h. Percentages of NG2$^+$/EGFP$^+$ cells labeled with each marker are shown. Cells were not detected at P2 or P40 with the astrocyte marker GFAP (N/D). Values represent means ± SEM obtained from a total of five to six separate FACS® experiments and 10 microscopic fields per experiment. Total number of cells counted for each marker ranged between 2,787 and 3,251 at P2 and 2,020 and 2,485 at P40.

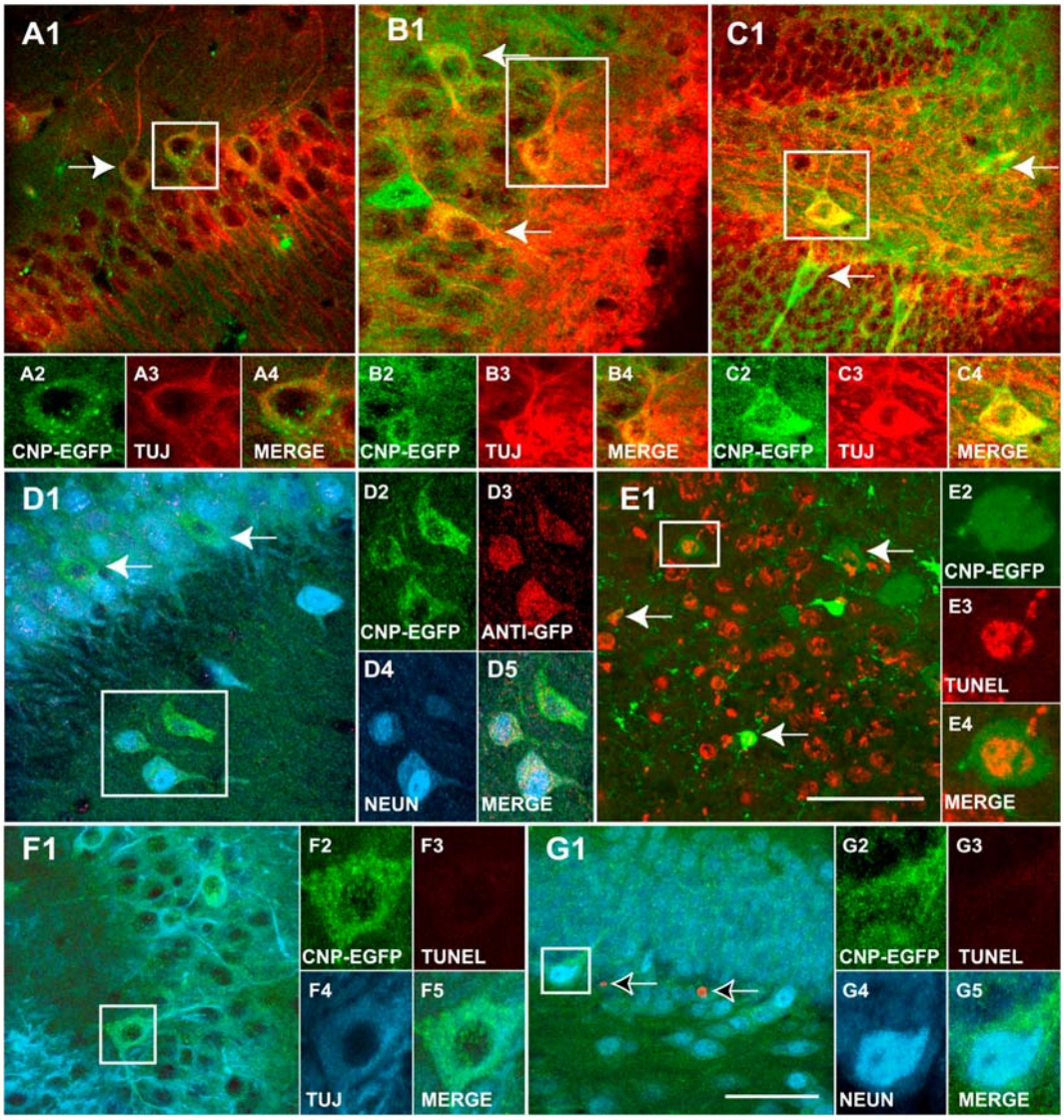

Figure 4. **Grafted NG2$^+$/EGFP$^+$ cells differentiate to neurons in the hippocampus.** (A–C) 3 wk after transplantation, all the grafted EGFP$^+$ cells (green) in the hippocampus are labeled with TUJ1 (red) antibodies. EGFP$^+$/TUJ1$^+$ cells (green/red, respectively) are found in the pyramidal layer of the CA1 (A1) and CA3 (B1). Grafted cells are also found in the hilar region of the DG (C1). (D) A large percentage of transplanted EGFP$^+$ cells (green) are also labeled with anti-NeuN (blue) antibodies in the CA3 area and hilar region of the DG (not depicted), confirming the neural fate of the grafted NG2$^+$/EGFP$^+$ cells. The tissue was also stained with anti-GFP antibodies (D3, red), confirming that these neurons are derived from the transplanted NG2$^+$/EGFP$^+$ fraction. (E–G) Neurons derived from grafted NG2$^+$/EGFP$^+$ cells are viable, as determined by TUNEL assay. (E) Positive control (Dnase I-treated tissue). EGFP$^+$/TUJ1$^+$ (F, green/blue, respectively) and EGFP$^+$/NeuN$^+$ (G, green/blue, respectively) grafted cells are TUNEL-negative (red) 6 wk after transplantation. Arrows in A1–D1 indicate EGFP$^+$ neurons derived from grafted cells. Arrows in E1 indicate EGFP$^+$/TUNEL$^+$ cells after DNAse treatment of the tissue (positive control). Arrows in G1 indicate endogenous EGFP-negative TUNEL$^+$ cells in DG. EGFP$^+$ cells in boxed areas are shown at higher magnification. Bars: (A–D , F, and G) 50 μm; (E) 100 μm.

~10% of NeuN$^+$/GAD-67$^+$/Dlx$^+$ neurons (Fig. 3, F and G). FACS®-purified Lex-negative/NG2$^+$/EGFP$^+$ cells did not generate neurospheres, indicating that, under our culture conditions, LeX$^+$ cells represent the multipotent neurosphere-generating cells among the NG2$^+$/EGFP$^+$ lineage.

NG2-expressing progenitors transplanted into the lateral ventricle migrate to the hippocampus and differentiate into GABAergic interneurons

To determine their developmental fate in vivo, we transplanted perinatal NG2$^+$/EGFP$^+$ cells FACS®-purified from P2 CNP-EGFP brains into wild-type mouse brains. Table I shows that, in agreement with the in vivo results (Figs. 1 and 2), a high percentage of the FACS®-purified NG2$^+$/EGFP$^+$ cells were Ki67$^+$, i.e., they displayed a proliferative phenotype. None of the cells were stained with anti-GFAP (Table I) or with anti-NeuN antibodies (Belachew et al., 2003). Both at P2 and P40, a significant percentage of the cells were stained for all the markers expressed by NG2$^+$/EGFP$^+$ cells in the SVZ in vivo, i.e., LeX, Dlx, EGFR, PSA-NCAM, and TUJ1 (Table I). These percentages were very similar to those found in the SVZ

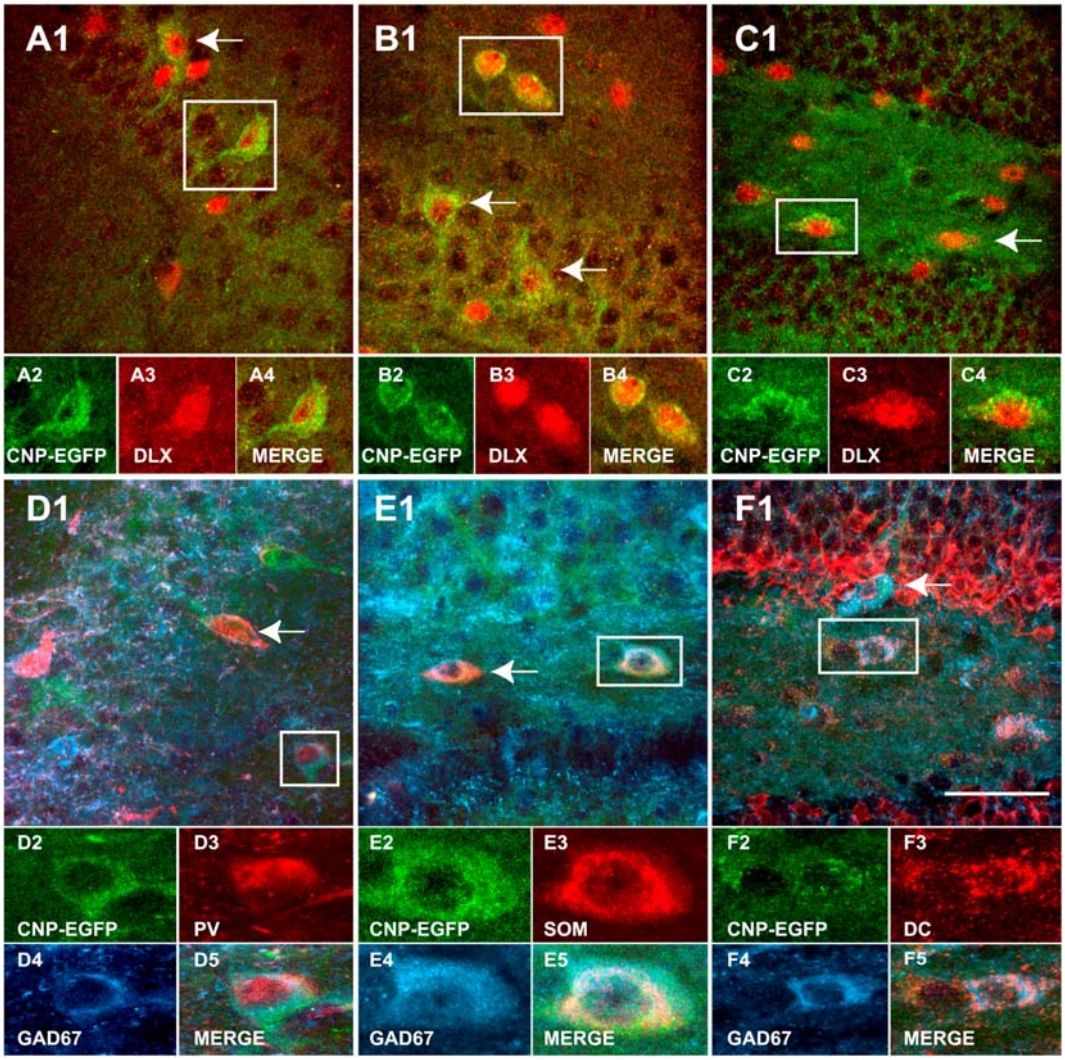

Figure 5. **Grafted NG2$^+$/EGFP$^+$ cells give rise to GABAergic interneurons in the hippocampus.** (A–C) 3 wk after transplantation, EGFP$^+$/Dlx$^+$ cells were found in the stratum radiatum, stratum oriens, and stratum pyramidale of the CA1 (A) and CA3 (B) and in the hilar region of the DG (C). (D–F) Immunostaining with anti–GAD-67 antibodies 3 wk after transplantation. Note that at this time the vast majority of the grafted EGFP$^+$ cells (green) were labeled with anti–GAD-67 (blue). Immunoreactivity of the graft-derived GAD-67$^+$ neurons for calcium-binding proteins and neuropeptides confirmed the interneuron fate of the grafted EGFP$^+$ cells. (D and E) A proportion of the graft-derived neurons are double labeled with anti–GAD-67 (blue) and parvalbumin (D, PV; red), somatostatin (E, SOM; red), or doublecortin (F, DC; red). Arrows in A1–F1 indicate EGFP$^+$ neurons derived from grafted cells. EGFP$^+$ cells in boxed areas are shown at higher magnification. Bar, 50 μm.

(compare Table I with Fig. 2 G and Fig. S3), indicating that the majority of FACS®-purified NG2$^+$/EGFP$^+$ cells display an SVZ-like immunophenotype.

We injected FACS®-purified NG2$^+$/EGFP$^+$ cells into the LV of P2 wild-type mice and analyzed the grafted cells over the following 3–4 wk. In some experiments, cells were also labeled with the fluorescent dye PKH26 before transplantation (Fig. S4 A, available at http://www.jcb.org/cgi/content/full/jcb.200311141/DC1). Labeled migrating cells were seen within the wall of the lateral ventricle and striatum as soon as 48 h after injection (Fig. S4 A). Some of the cells had migrated tangentially through the subcortical white matter (Fig. S4 A, arrow and inset). As negative controls, we transplanted NG2$^+$/CNP-EGFP$^+$ cells, which underwent six freeze–thaw cycles. These cells did not migrate, but were found as clumps surrounding the area of the lateral ventricle (unpublished data). EGFP fluorescence intensity was sufficient to detect the grafted cells up to 5 wk after transplantation. Within the first 2–3 wk, a large number of the transplanted cells were found dispersed throughout the olfactory bulb and striatum (not depicted), hippocampus (Figs. 4 and 5), and cortex and white matter (Fig. S5, available at http://www.jcb.org/cgi/content/full/jcb.200311141/DC1).

4 d after transplantation, EGFP$^+$ migrating neuroblasts were encountered in the stratum oriens of the hippocampus and in striatum (Fig. S4, B1 and B2, respectively). The majority of the migrating cells were PSA-NCAM$^+$ (Fig. S4 C) and TUJ1$^+$ (Fig. S4 D). We were not able to identify a single EGFP$^+$/TUJ1$^+$ cell in the hippocampus or surrounding the area of injection at 48 h after transplantation (unpublished data). These findings demonstrate that neuronal differentiation of NG2$^+$/EGFP$^+$ cells observed after 3 wk does

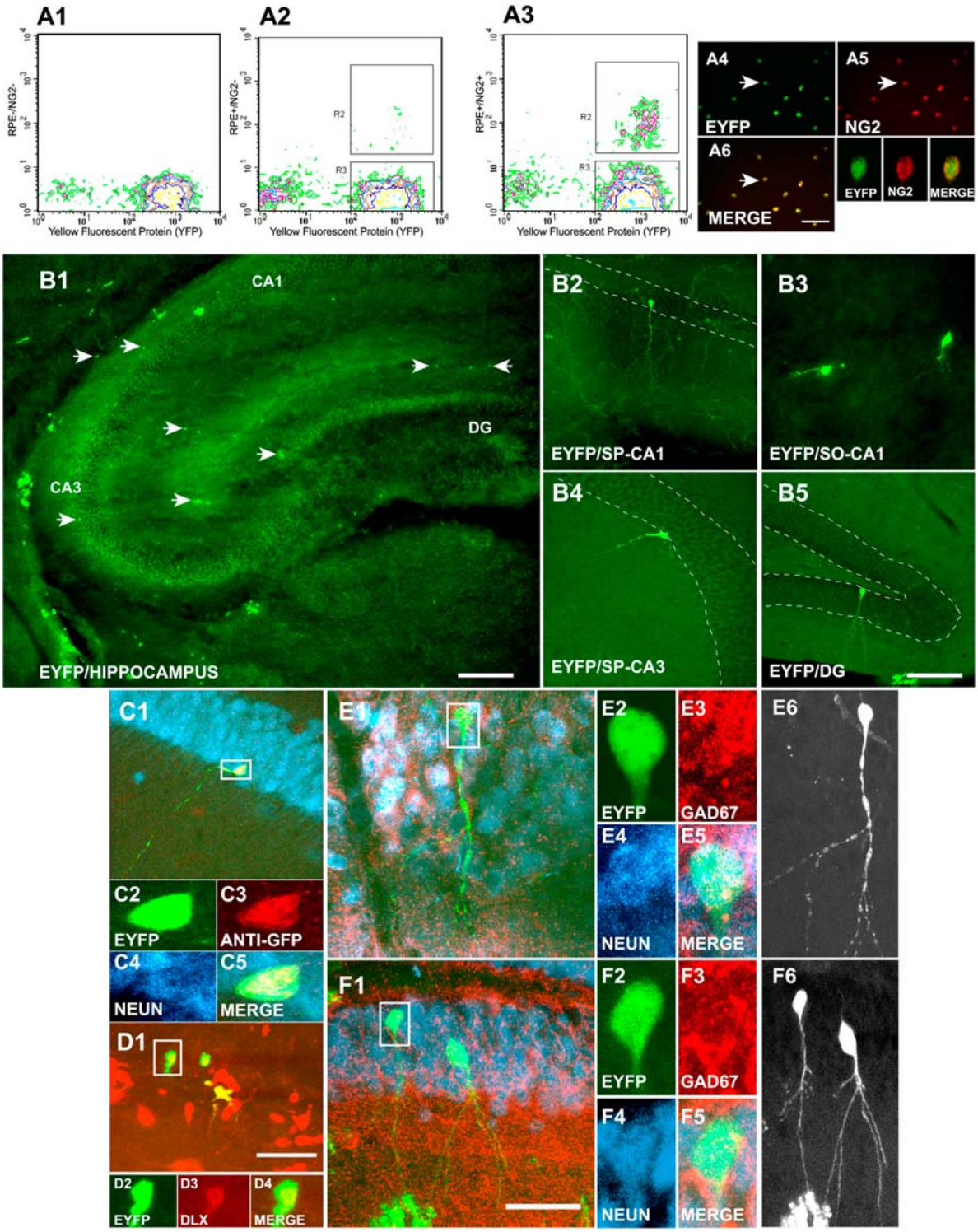

Figure 6. **Grafted NG2$^+$/EYFP$^+$ cells give rise to GABAergic interneurons in the hippocampus.** (A1–A3) Typical sorting profile for NG2$^+$/EYFP$^+$ cells (NG2 immunolabeling was scattered with RPE-Cy5 [R2 box]). (A4–A6) A typical sample of NG2$^+$/EYFP$^+$ cells after FACS® shows high purity. (B) 1 wk after grafting, EYFP$^+$ cells (green) were found in the hippocampus (arrows) displaying a typical neuronal morphology in the stratum oriens of the CA1 (B3) and CA3 (not depicted), in the stratum pyramidale of the CA1 and CA3 (B2 and B4, respectively), and in the DG (B5). The tissue was also stained with anti-GFP antibodies (C, red), confirming that these neurons are derived from the transplanted NG2$^+$/EYFP$^+$ fraction. Migratory EYFP$^+$ cells acquired immature neuronal markers 1 wk after grafting, as shown by Dlx (D, red) and TUJ1 (not depicted). (E and F) 3 wk after transplantation, all the grafted EYFP$^+$ cells (green) found in the hippocampus are labeled with anti-NeuN antibodies (blue). EYFP$^+$/NeuN$^+$ cells (green/blue) are found in the pyramidal layer of the CA1 (not depicted) and CA3 (E) and in the subgranular layer of the DG (F). EYFP$^+$ cells are also labeled with anti–GAD-67 (red) antibodies in the CA3 area (E) and DG (F), confirming their neural fate. In E6 and F6, EYFP was converted to grayscale. Anti-GFP antibodies recognize all the GFP variants, including EGFP, EYFP, and ECFP. EYFP$^+$ cells are shown at higher magnification in boxed areas. Bars: (A, C, E, and F) 50 μm; (B1) 300 μm; (B2–B5) 100 μm.

not arise from the small fraction of NG2$^+$/EGFP$^+$ cells that may already express markers of early neuronal commitment (Table I). Finally, no EGFP$^+$ cells were found outside the area of injection, including the hippocampus, within the first 24–48 h after grafting. These results indicate that the grafted NG2$^+$/EGFP$^+$ cells acquire a neuronal fate during the first week after transplantation.

3 wk after transplantation, grafted NG2$^+$/EGFP$^+$ cells were found scattered in the hippocampus (Fig. S4, E–G). EGFP$^+$ cells were seen in the stratum radiatum (Fig. S4, E and F), stratum lucidum (Fig. S4 E), stratum oriens (Fig. S4 F), and stratum pyramidale (Fig. S4, E and F) of the CA1 and CA3 regions. Cells were also found in the hilar region of the dentate gyrus (DG; Fig. S4 G). Complete overlap between green fluorescence and EGFP was confirmed in all grafted cells found in the hippocampus by using anti-GFP antibodies (Fig. 4 D). None of the EGFP$^+$ cells found in the hippocampus was labeled for astrocyte (GFAP) or oligodendrocyte (MBP) markers (unpublished data). However, EGFP$^+$/MBP$^+$ cells with a typical oligodendrocyte morphology were found both in subcortical white matter and in cerebral cortex 2–3 wk after grafting (Fig. S5).

3 wk after transplantation, the majority of the grafted EGFP$^+$ cells in the hippocampus were immunolabeled with TUJ1 (Fig. 4, A–C) and were found in the stratum oriens, stratum radiatum, and stratum pyramidale of the CA1 and CA3 regions (Fig. 4, A and B). Cells with the same phenotype were also found in the hilar region of the DG (Fig. 4 C). In the same hippocampal regions, a large percentage of the EGFP$^+$ cells also expressed NeuN (Fig. 4 D), indicating that grafted cells had differentiated into mature neurons. TUNEL assays demonstrated that graft-derived TUJ1$^+$ and NeuN$^+$ neurons in the hippocampus were still viable 6 wk after transplantation (Fig. 4, F and G).

Transcription factors of the Dlx homeobox gene family are implicated in GABAergic interneuron identity and differentiation (Panganiban and Rubenstein, 2002). The majority of the hippocampal graft-derived EGFP$^+$ cells were labeled with anti-Dlx antibody (Fig. 5, A–C) and anti–GAD-67 (Fig. 5, D–F), indicating that NG2$^+$/EGFP$^+$ cells generated GABAergic interneurons in vivo. Many EGFP$^+$ grafted cells found in CA1, CA3, and DG were GAD-67$^+$/PV$^+$ (Fig. 5 D), GAD-67$^+$/SOM$^+$ (somatostatin; Fig. 5 E), or GAD-67$^+$/DC$^+$ (doublecortin; Fig. 5 F), confirming their interneuron identity (Jinno and Kosaka, 2002).

We repeated the aforementioned grafting experiments by using NG2$^+$/EYFP$^+$ (enhanced YFP$^+$) cells FACS® purified from P2 β-actin-EYFP mouse brain (Fig. 6 A). NG2$^+$/EYFP$^+$ cells transplanted into the lateral ventricle migrated to different regions of the hippocampus (Fig. 6 B) and differentiated into NeuN$^+$/Dlx$^+$/GAD-67$^+$ GABAergic interneurons displaying typically arborized morphologies (Fig. 6, C–F).

GABAergic hippocampal interneurons derived from transplanted NG2-expressing progenitor cells are functionally integrated

We investigated whether or not EGFP$^+$ cells in the hippocampus that could be identified after transplantation elicited action potentials and received synaptic innervation. We performed whole cell current and voltage clamp from nine graft-derived EGFP$^+$ hippocampal cells (Fig. 7 A). Examples of two of such cells are shown in Fig. 7 (H and I) for hilar region and stratum oriens of the CA3, respectively. Cells displayed a morphologically differentiated neuronal phenotype (Fig. 7, H and I). In all cases, depolarizing current pulses (30–180 pA for 1,000 ms; step = 30 pA) from a membrane potential of ~−70 mV resulted in the generation of action potentials (Fig. 7 B, step size 120 pA) at a range of frequencies (Fig. 7 C). At the maximum current injection used, the mean firing frequency was 50 ± 10 Hz (Fig. 7 C; $n = 9$; range 35–106 Hz). Interestingly, minimal spike frequency adaptation was noted within the duration of the depolarizing current injections (Fig. 7 D). In all cells tested ($n = 6$), spontaneous inward currents were present (single example in Fig. 7, E and F), which were consistently abolished by the inclusion of 10 μM NBQX (Fig. 7 E, arrow). The average inward current (267 events) from the single example trace shown in Fig. 7 E displayed a decay with $\tau = 2.2$ ms when fitted to a single exponential (Fig. 7 G).

Endogenous CNP-EGFP$^+$ neurons in the hippocampus are GABAergic interneurons

Similar to the SVZ, a significant percentage (18.4 ± 4.0%; $n = 342$) of NG2$^+$/EGFP$^+$ cells in the postnatal and adult DG of the hippocampus coexpressed NG2 and PSA-NCAM (Fig. 8 A). Hippocampal TUJ1$^+$/EGFP$^+$ cells were also observed and expressed Dlx (Fig. 8 B). The majority of the Dlx$^+$ cells were stained with anti–GAD-67 antibodies both at P8 and P40 (Fig. 8 C and Table II), confirming their GABAergic identity. Finally, a large percentage of Dlx$^+$/EGFP$^+$ cells were NeuN$^+$ (Fig. 8 D and Table II).

To define the phenotype of the EGFP$^+$ GABAergic neurons, we performed immunolabeling for the interneuron markers PV (Fig. 8 E), DC (Fig. 8 F), SOM (Fig. 8 G), and CAL (calretinin; Fig. 8 H). A large percentage of the hippocampal EGFP$^+$ neurons were double-labeled with these markers and anti–GAD-67 (Fig. 8, E–H; and Table II). The majority of GAD-67$^+$/EGFP$^+$ neurons were found in CA3 and DG regions (Belachew et al., 2003). Table II shows that the percentage of GAD-67$^+$/EGFP$^+$ cells expressing PV increased by 2–5-fold in all regions between P8 and P40. The percentage of GAD-67$^+$/EGFP$^+$ cells that were DC$^+$ also increased to a similar extent (Table II). In contrast, the percentage of GAD-67$^+$/EGFP$^+$ cells that were SOM$^+$ remained constant (Table II). No EGFP$^+$/CAL$^+$ cells were found (Fig. 8 H). In all hippocampal regions, we observed that the absolute density of GAD-67$^+$/EGFP$^+$ cells and the total number of EGFP$^+$ cells decreased between P8 and P40 (unpublished data).

Together, these results show that endogenous hippocampal GAD-67$^+$/EGFP$^+$ interneurons display a cellular phenotype similar to that of interneurons derived from transplanted NG2$^+$/EGFP$^+$ progenitors or neurons generated from NG2$^+$/EGFP$^+$ neurospheres.

Discussion

Recent works demonstrated that the majority of adult CNS multipotent progenitor cells are rapidly dividing in the SVZ

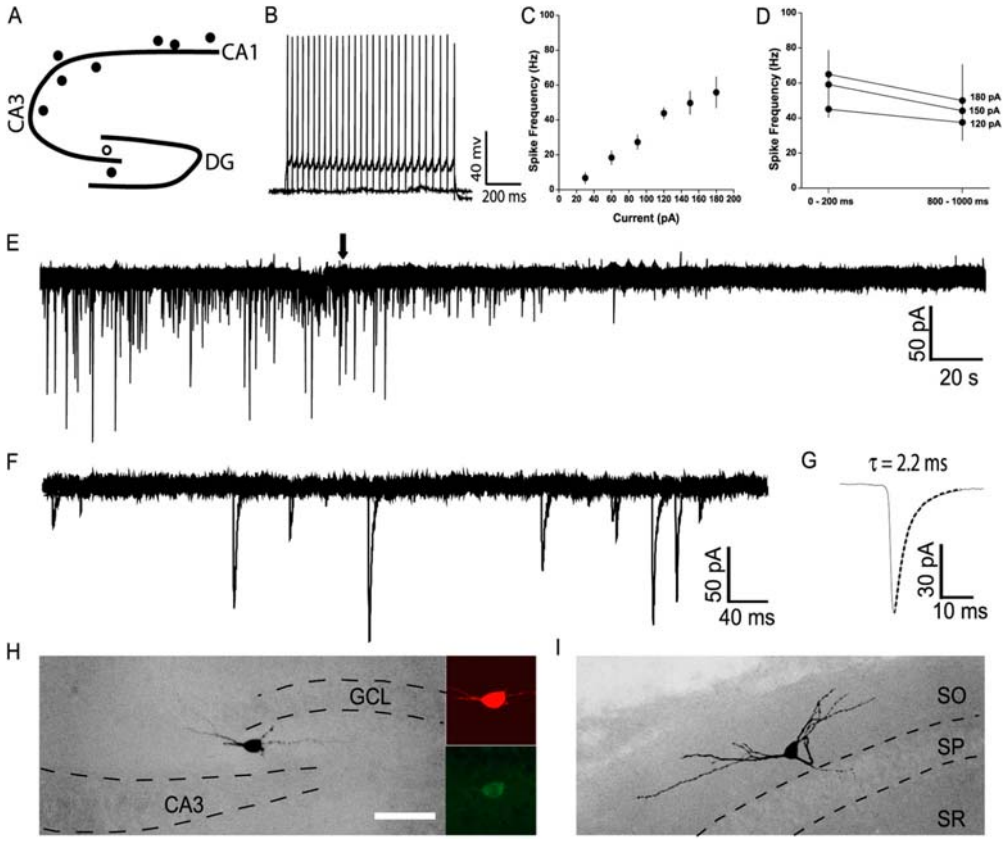

Figure 7. **Grafted NG2$^+$/EGFP$^+$ cells in the hippocampus possess physiological properties of mature inhibitory interneurons.** (A) Schematic of hippocampus illustrating the positions of the grafted EGFP$^+$ cells that physiological recordings were attained from. The open circle indicates the cell from which the single example current (B) and voltage clamp (E and F) traces were obtained. (B) Action potential generation in response to a depolarizing current injection (120 pA for 1,000 ms) from a membrane potential of −70 mV. (C) Pooled data of injection current (30–180 pA; step = 30 pA) versus spike frequency during the 1,000-ms depolarizing pulse. (D) Pooled data illustrating spike frequency during the first and last 200-ms epochs (0–200 and 800–1,000 ms) of depolarizing current injections (120, 150, and 180 ms pA). (E) Continuous voltage clamp trace (holding potential −70 mV; 3 min) illustrating the presence of spontaneous inward currents that were abolished by inclusion of 10 μM NBQX (arrow, 2 min; NBQX is present for the remainder of trace). (F) Magnification of part of the trace in E, illustrating the time course of individual spontaneous inward currents (four superimposed consecutive traces of 700 ms each). (G) Average time course (267 events; average amplitude equals 73 pA) of the inward currents, as determined by single exponential fitting of the decay (dotted line). (H and I) Biocytin (brown) images of two cells from which recordings were taken. GCL, granule cell layer; SO, stratum orien; SP, stratum pyramidale; SR, stratum radiatum. Images were converted to grayscale and inverted for clarity. Insets in H illustrate a high magnification of the biocytin-conjugated fluorescence (red; top inset) and the corresponding EGFP$^+$ fluorescence (green; bottom inset). Bar, 50 μm.

(Capela and Temple, 2002; Doetsch et al., 2002a). In the present work, we show that a large percentage of NG2$^+$/EGFP$^+$ cells in the SVZ incorporated BrdU after a 2-h pulse at P8 and P40. Furthermore, a similar percentage of the cells were immunopositive for Ki67 antibodies (Schluter et al., 1993). From our data, it can be concluded that NG2$^+$ progenitors represent a major population of rapidly cycling cells in the postnatal and adult SVZ. To further characterize the properties of NG2$^+$ cells in the SVZ, we analyzed expression of several NSC markers (Capela and Temple, 2002; Doetsch et al., 2002a). Based on LeX expression, Capela and Temple (2002) have previously identified two main subpopulations of multipotent NSCs in the adult SVZ. Lex$^+$/GFAP$^+$ cells represent only a small percentage (6%) of the entire Lex$^+$ stem cell population, whereas LeX$^+$/GFAP-negative cells are the majority and represent a large percentage of cells (Capela and Temple, 2002). Importantly, only a small percentage of the LeX$^+$/GFAP$^+$ cells proliferate in vivo, whereas the majority of LeX$^+$/GFAP-negative cells incorporate BrdU (Capela and Temple, 2002). Based on these observations, it was proposed that the SVZ contains a stem cell population with a novel identity, neither astrocytic nor ependymal, but Lex$^+$/GFAP-negative (Capela and Temple, 2002). Our experiments demonstrate that this population corresponds to NG2 proteoglycan-expressing cells, based on the findings that half of Lex$^+$/GFAP-negative cells are NG2$^+$ in the early postnatal SVZ and, vice versa, that a large fraction of NG2$^+$ cells in the postnatal and adult SVZ express LeX, do not express GFAP, and incorporate BrdU.

A separate study by Doetsch et al. (2002a) demonstrated that the Lex$^+$/GFAP-negative cells belong to the transit-amplifying, multipotent type C cells in the adult SVZ. These cells are also GFAP negative and display intrinsic properties of multipotent NSCs. Furthermore, type C cells express Dlx and the EGFR (Doetsch et al., 2002a). In the present work, we show that a high percentage of NG2$^+$ cells in the early

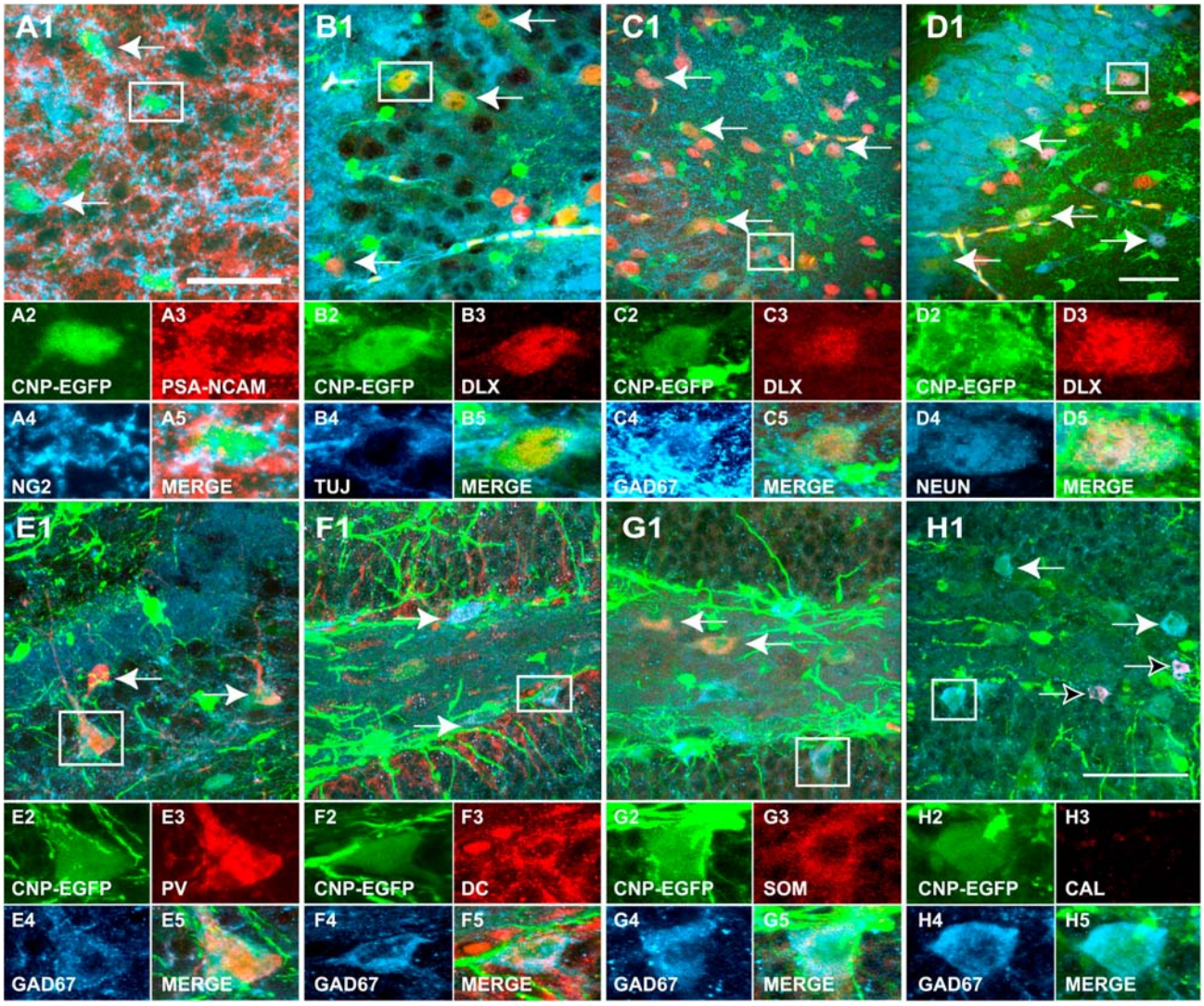

Figure 8. **Endogenous EGFP$^+$ cells in the postnatal hippocampus display a GABAergic interneuron phenotype.** P8 sagittal sections and CA3 and DG regions of the hippocampus. (A) A proportion of the NG2$^+$/EGFP$^+$ cells (blue/green, respectively) in the DG express PSA-NCAM (red). (B) A proportion of the EGFP$^+$ cells coexpress Dlx (red) and class III β-tubulin (blue). (C) The majority of the EGFP$^+$ cells (green) that express Dlx (red) also express GAD-67 (blue). (D) All the EGFP$^+$/NeuN$^+$ cells (green/blue, respectively) also express Dlx (red). (E and F) A proportion of the EGFP$^+$ cells in CA3 (E) and DG (F) express parvalbumin (E, PV; red), doublecortin (F, DC; red), and GAD-67 (blue). (G) In the hilar region of the DG and in CA3 (not depicted), a significant proportion of the EGFP$^+$ cells express the neuropeptide somatostatin (SOM, red) and GAD-67 (blue). (H) EGFP$^+$ cells that are positive for GAD-67 (blue) are not labeled with antibodies against calretinin (CAL, red). White arrows in A1–H1 indicate EGFP$^+$ cells that are also labeled for all the markers analyzed. In H1, black arrows indicate EGFP-negative CAL$^+$/GAD-67$^+$ cells. Cells in boxed areas are shown at higher magnification. Quantitative analysis of these data is shown in Table II. Bars, 50 μm.

postnatal and adult SVZ expresses the EGFR, and that a significant proportion expresses Dlx. These results, combined with the proliferative properties of NG2$^+$ cells and LeX expression in these progenitors, indicate that NG2$^+$ cells in the perinatal SVZ represent a transit-amplifying type C–like cell phenotype, as described by Doetsch et al. (2002a). This notion is further supported by previous studies (Casaccia-Bonnefil et al., 1997; Doetsch et al., 2002b) showing that the absence of p27Kip1 significantly increased the proliferation of both NG2$^+$ cells and of the transit-amplifying type C cells in the mouse SVZ. This evidence not only corroborates that NG2$^+$ and type C cells are overlapping populations, but also that their highly proliferative rate is essential to maintain a reservoir of multipotent progenitor cells in the SVZ. The unambiguous identification of NG2$^+$/Lex$^+$ cells as type C cells would necessitate the demonstration of ultrastructural features that were first described for this phenotype in the adult SVZ (Doetsch et al., 1999a, 2002a). However, our findings indicate that perinatal NG2$^+$/Lex$^+$ cells fulfil all the functional and antigenic criteria to be considered as type C–like progenitor cells of the SVZ.

NG2$^+$/EGFP$^+$ cells can be reliably purified by FACS®, form primary neurospheres, and generate secondary neurospheres after cell dissociation, i.e., they display self-renewal. Cells in secondary neurospheres maintain their multipotentiality and generate GABAergic neurons that express Dlx

Table II. **Immunocytochemical characterization of GAD-67$^+$/EGFP$^+$ neurons in the perinatal and adult hippocampus**

	PV		DC		SOM		DIx		NeuN	
	P8	P40	P8	P40	P8	P40	P8	P40	P8	P40
DG										
GL	23 ± 4	52 ± 5	0	67 ± 7	71 ± 7	58 ± 8	94 ± 2	86 ± 2	70 ± 8	65 ± 8
HL	14 ± 4	30 ± 4	9 ± 3	78 ± 5	68 ± 5	74 ± 6	92 ± 1	92 ± 2	86 ± 5	83 ± 7
CA3										
SR	11 ± 3	45 ± 8	12 ± 3	76 ± 5	67 ± 6	66 ± 3	92 ± 4	83 ± 6	84 ± 6	83 ± 5
SP	11 ± 2	53 ± 6	15 ± 3	67 ± 4	76 ± 2	72 ± 7	90 ± 4	86 ± 4	86 ± 2	92 ± 4
CA1										
SR	0	28 ± 2	0	0	0	58 ± 5	95 ± 2	89 ± 1	90 ± 8	92 ± 8
SP	0	69 ± 2	0	25 ± 2	62 ± 7	63 ± 2	95 ± 2	85 ± 2	88 ± 2	94 ± 6

Sagittal sections from postnatal day 8 (P8) and 40 (P40) brains of CNP-EGFP transgenic mice were stained with different antibody combinations, as described in Materials and methods. Cells were analyzed in dentate gyrus (DG) granule layer (GL) and hylus (HL), and in CA3 and CA1 stratum radiatum (SR) and stratum pyramidale (SP). Percentages of GAD-67$^+$/EGFP$^+$ cells labeled with each marker are shown. Values represent mean ± SEM obtained from four different brains (six tissue sections per brain). Total cells counted were 1,080 for P8 and 770 for P40. PV, parvalbumin; DC, doublecortin; SOM, somatostatin.

and GAD-67. Regarding the self-renewal and multipotential properties of the NG2$^+$ cell population, our results suggest that the high percentage of NG2$^+$/EGFP$^+$ cells in the early postnatal SVZ that also express LeX correspond to the cell population that generate neurospheres and displays multipotentiality. The NG2$^+$/EGFP$^+$/Lex-negative cells that did not form neurospheres could either require different growth conditions or could be progenitors committed to an oligodendroglial fate. These results indicate that, under our experimental conditions, only the LeX$^+$ subpopulation of NG2$^+$/EGFP$^+$ cells is capable of self-renewal and is multipotential. Our analysis establishes a link between NG2$^+$/Lex$^+$/EGFP$^+$ cells in the early postnatal SVZ and a GABAergic neuronal progeny expressing Dlx and GAD-67.

To demonstrate that NG2$^+$/EGFP$^+$ cells are intrinsically neurogenic in vivo, and to define the neuronal subtypes they can generate, we isochronically grafted early postnatal NG2$^+$/EGFP$^+$ cells into wild-type host brains. Our results clearly show that transplanted NG2$^+$/EGFP$^+$ progenitors generate differentiated and synaptically integrated neurons. The antigenic properties of these grafted NG2$^+$ cell–derived hippocampal neurons indicate that they are interneurons based on expression of GAD-67 and markers such as PV, SOM, and DC. The hippocampal graft-derived neurons display the ability to respond to depolarizing current pulses with spikes at high frequencies of discharge that display minimal spike frequency accommodation. Both of these features are indicative of an inhibitory interneuron phenotype and are distinct to the physiological properties commonly seen in principal cells of the hippocampus (McBain and Fisahn, 2001). In addition, these cells also receive functional AMPA receptor-mediated inputs. Together, these data illustrate the neuronal maturation and functional integration of the early postnatal NG2$^+$/EGFP$^+$-derived cells after transplantation into a wild-type host.

Several studies that analyzed development of transplanted neural progenitors concluded that these precursors were unable to generate the appropriate neuronal cell types in various brain regions (Olsson et al., 1997; Desai and McConnell, 2000). In contrast, our results indicate that NG2$^+$/EGFP$^+$ cells express molecular cues, such as Dlx, that are necessary for cellular and regional identity. We also show that temporal and regional information is maintained after transplantation because both grafted NG2$^+$/EGFP$^+$ precursors and hippocampal interneurons derived from these cells still express Dlx. It has been previously shown that Dlx expression identifies a bipotential neural progenitor population capable of generating GABAergic interneurons and oligodendrocytes during embryonic CNS maturation (He et al., 2001; Yung et al., 2002). Therefore, postnatal Dlx$^+$/NG2$^+$/EGFP$^+$ cells are likely to be developmentally related to such bipotential embryonic Dlx$^+$ progenitors. Dlx expression in neural progenitors is also associated with a GABAergic fate and plays a crucial role in terminal differentiation of these neurons (Panganiban and Rubenstein, 2002; Stuhmer et al., 2002). Because we transplanted acutely purified NG2$^+$/EGFP$^+$ cells immediately after FACS®, we suggest that NG2$^+$/EGFP$^+$ cells possess intrinsic properties to generate GABAergic interneurons (Belachew et al., 2003).

The grafted NG2$^+$ cell–derived interneurons express the same antigenic profile and similar physiological properties of endogenous EGFP$^+$/GAD-67$^+$ interneurons found in CA1, CA3, and DG. This finding indicates that the grafted NG2$^+$ cells follow an existing endogenous developmental pathway that results in interneuron generation in the postnatal hippocampus, and recruitment of GABAergic interneurons in the hippocampus significantly contributes to early postnatal and possibly adult neurogenesis. In agreement with our results, a recent study demonstrated that A2B5$^+$, CNP gene-expressing progenitors isolated from the adult human white matter, generate GABAergic hippocampal neurons after transplantation into fetal rat brain (Nunes et al., 2003). These findings contribute to the changing view that a significant percentage of newly generated neurons in the postnatal and adult hippocampus are inhibitory interneurons, as demonstrated by Liu et al. (2003) for PV$^+$ GABAergic basket cells in the adult DG.

Our work suggests that postnatal newly-formed GABAergic interneurons derive from exogenous NG2$^+$ progenitors that migrate out of the SVZ into the hippocampus and most likely to other brain regions. It remains to be determined to what extent our data suggest that endogenous newborn post-

natal interneurons in the hippocampus may derive from NG2$^+$ SVZ progenitor cells, likely located in the posterior SVZ. This would raise the possibility that a subpopulation of type C–like progenitor cells from the SVZ are able to migrate backward and radially (Marshall and Goldman, 2002; Suzuki and Goldman, 2003), instead of following their classical route of tangential forward migration through the rostral migratory stream toward the olfactory bulb.

In conclusion, we have taken advantage of a transgenic mouse to define the cellular properties of CNP gene-expressing NG2$^+$ progenitors in the early postnatal and adult SVZ, and to demonstrate that they are a subpopulation of type C–like cells. Based on EGFP expression, we were also able to graft NG2$^+$ cells into the early postnatal brain and follow their developmental fate. We established that neurons generated from early postnatal NG2$^+$/EGFP$^+$ cells in vivo have the same cellular and functional phenotype of endogenous populations of hippocampal inhibitory interneurons. The possibility of obtaining a viable and highly purified population of endogenous neural progenitors and to direct the generation of GABAergic neurons from these precursors could have very important implications for future therapeutic approaches to epilepsy, stroke, and degenerative damage of the brain.

Materials and methods

CNP-EGFP transgenic mouse

Line C1 of the CNP-GFP transgenic mouse was used this work (Yuan et al., 2002). The same results were obtained with line D2. All animal procedures were performed according to Children's National Medical Center, Institutional Animal Care and Use Committee, and National Institutes of Health guidelines.

Isolation of NG2$^+$/EGFP$^+$ and NG2$^+$/EYFP$^+$ progenitor cells by FACS® and cell culture

Brains were dissected out from P2 and P40 CNP-EGFP mice or P2 β-actin-EYFP mice (Tg ActbEYFP; JAX Mice). Cells were dissociated (Belachew et al., 2003) and analyzed for light forward and side scatter using a FACStar plus instrument (Becton Dickinson). For double NG2/EGFP and LeX/EGFP FACS® analysis, cell suspensions were incubated with appropriate primary antibodies (see Immunocytochemistry), and then with R-PE– and PECy5-conjugated secondary antibodies (Caltag).

SVZ microdissection

SVZ areas were microdissected from 300-μm-thick coronal sections of P8 CNP-EGFP brains. Cells were dissociated (Belachew et al., 2003), seeded (20,000 cells per well) on coverslips, and processed for immunocytochemistry 2 h after plating.

Neurosphere preparation and differentiation

FACS®-purified NG2$^+$/EGFP$^+$ cells (P2) or E14.5 forebrain cells were seeded (10 cells/μl) on uncoated 24-well plates (BD Biosciences) and grown in SCM (StemCell Technologies Inc.) for 6 d in vitro (DIV) with daily addition of 20 ng/ml EGF. For E14.5 cultures, 10 ng/ml bFGF was also added. Primary neurosphere colonies (Reynolds and Weiss, 1992) were subcloned by mechanical dissociation and replating at 10 cells/μl in 24-well plates. Stem cell self-renewal was assessed after a further 6 DIV. For differentiation experiments, single neurosphere colonies were transferred to individual wells of a 24-well culture plate precoated with 0.1mg/ml polyornithine in serum-free medium + 1% FBS (GIBCO). Cells were processed by immunocytochemistry after 6 DIV (Belachew et al., 2003).

Immunocytochemistry

For cell sorting, cell suspensions were incubated with anti-NG2 antibody (1:1,000; Chemicon) or with antibody from the hybridoma clone MMA (for LeX antigen; 1:50; Becton Dickinson). For immunocytochemistry, cell cultures were processed (Yuan et al., 2002) with the following primary antibodies: anti-NeuN, antityrosine hydroxylase, anti–PSA-NCAM (all from Chemicon), anti-Ki67 (Novocastra), and anti-panDlx (obtained from G. Panganiban, University of Wisconsin Medical School, Madison, WI), all at 1:250. At a dilution of 1:500, TUJ1 (BabCo), anti-NG2, anti-GFAP (Sigma-Aldrich), anti–GAD-67, and anti–choline acetyltransferase (both from Chemicon). Anti-MMA mouse monoclonal (for LeX antigen; Becton Dickinson), antivesicular glutamate transporter 1 (Chemicon), and anti-EGFR (Santa Cruz Biotechnology, Inc.) were used at 1:50, 1:10,000, and 1:100, respectively.

RT-PCR

RNA was isolated from P8 FACS®-purified NG2$^+$/EGFP$^+$ cells and from neurospheres after 4 d in differentiation medium using Trizol® (Invitrogen). 1 μg RNA from each sample was reverse-transcribed using the SuperScript™ First-Strand cDNA Synthesis kit (Invitrogen). The mouse gene-specific primers used were obtained from Integrated DNA Technologies, Inc. Sequences were as follows: Mash1, sense 5′ AGC AGC TGC TGG ACG AGC A 3′, antisense 5′ CCT GCT TCC AAA GTC CAT TC 3′; Dlx2, sense 5′ GGC ACC AGT TCG TCT CCG GTC AA 3′, antisense 5′ CGC CGA AGT CCC AGG ATG CTG 3′; GAD-67, sense 5′ AAG GCA TGG CGG CTG TGC CCA AAC 3′, antisense 5′ ACC ACC CCA GGC AGC ATC CAC ATG 3′; GAD-65, sense 5′ CCA TTA CCC CAA TGA GCT TCT 3′, antisense 5′ CCC CAA GCA GCA TCC ACG T 3′; Actin, sense 5′ CGT GGG CCG CCC TAG GCA CCA 3′, antisense 5′ TTG GCC TTA GGG TTC AGG GGG 3′. Genes were amplified by denaturation at 94°C for 1 min, annealing at 60°C for 1 min, and extension at 72°C for 1 min for 35 cycles. PCR products were resolved by 1.2% agarose gel electrophoresis and visualized under UV light.

Immunohistochemistry

Frozen 50-μm tissue sections were prepared as described previously (Yuan et al., 2002). Primary antibody dilutions were as follows: 1:500 for anti-NG2 antibody, anti-Ki67, anti-CNP (Sternberger Monoclonal Inc.), anti-MBP (Sternberger Monoclonal Inc.), anti-NeuN, anti-HuC/D (Molecular Probes), and anti-GFAP; 1:1,000 for anti–Mash-1 (from D. Anderson, California Institute of Technology, Pasadena, CA), anti-PV (Sigma-Aldrich), anti–GAD-67, anti–PSA-NCAM, antisomatostatin, antidoublecortin, and anticalretinin (all from Chemicon). Anti-GLAST (Chemicon) and anti-Olig2 (obtained from D. Rowitch, Dana Farber Cancer Institute, Harvard Medical School, Boston, MA) were both used at a 1:5,000 dilution. Anti-BrdU and MMA antibodies (1:100) were purchased from Becton Dickinson.

BrdU administration and detection

Mice were injected intraperitoneally with a single dose of 50 μg/g of BrdU (Sigma-Aldrich) in sterile 0.9% NaCl solution and killed 2 h after the injection. Sections were incubated in 2 N HCl for 30 min at 37°C, immersed in 0.1 M Na$^+$-borate at pH 8.5, and stained with anti-BrdU and anti-NG2.

Microscopy and cell counting

A confocal laser-scanning microscope (model MRC 1024; Bio-Rad Laboratories) equipped with a krypton-argon laser and an inverted microscope (model IX-70; Olympus) was used to image localization of FITC (488-nm laser line excitation; 522/35 emission filter), Texas red (568-nm excitation; 605/32 emission filter) of Cy5 (647 excitation; 680/32 emission filter). Optical sections (z = 0.5 μm) of confocal epifluorescence images were sequentially acquired using a 40× (NA = 1.35), a 60× (NA = 1.40), or 100× oil objective (NA = 1.35) with LaserSharp v3.2 software (Bio-Rad Laboratories). Confocal Assistant 4.02 software was subsequently used to merge images. Merged images were processed in Photoshop 7.0 with minimal manipulations of contrast. For cell counting, NG2$^+$/EGFP$^+$ cells were counted in the SVZ and hippocampus. We consistently found that 100% of the NG2$^+$ cells were EGFP$^+$. The analysis of the SVZ was performed at different rostrocaudal levels of the lateral ventricle. An average of 15–20 sections were counted for the SVZ and hippocampus to obtain an estimate of the total number of NG2$^+$ cells. Percentages of cells expressing different antigens were estimated by scoring the number of cells double-labeled with the marker in question. In cultured cells, 2 coverslips/culture and 8–10 microscopic fields/coverslip were counted from three separate cultures. Statistical analysis was performed by paired t test.

Transplantation and analysis of grafted cells

FACS®-purified NG2$^+$/EGFP$^+$ or NG2$^+$/EYFP$^+$ donor cells were prepared from P2 CNP-EGFP or β-actin-EYFP transgenic mice. Immediately after FACS®, cells were stained with PKH26 (Sigma-Aldrich) and incubated with the diluent C (5:1,000) for 5 min at RT. Cells were washed with DME + 10% FCS and resuspended in DME at 20,000 cells/μl. As a negative control, NG2$^+$ cells were exposed to six freeze–thaw cycles before grafting.

Microinjection was performed under deep hypothermia, and 1–2 μl of the cell suspension was injected directly into the ventricles of wild-type *P2* FVB/NxCB6 pups. In some experiments, trypan blue (0.1%) was added to the cell suspension to confirm targeting of injections. The injection was performed with a glass capillary pipet (100–150 μm outer diameter with beveled tip) driven by a micromanipulator (Harvard Instruments). For the studies of migration and proliferation, mice were reared 24–72 h after injection and processed for immunohistochemistry. For anatomical and electrophysiological studies of the grafted cells, mice were killed 1–4 wk after the injection. Grafted $NG2^+$ cells were readily visible under confocal microscopy using a 488-nm laser-line excitation. An anti-GFP rabbit polyclonal antibody (IgG; 1:250; BD Biosciences) was used to confirm $NG2^+$ cell differentiation by immunohistochemistry. In three experiments, we quantified the percentage of transplanted $NG2^+/EYFP^+$ cells found in the hippocampus after 1 wk as $NeuN^+$ neurons. After injecting 20,000 $NG2^+/EYFP^+$ cells, we detected an average of 215.0 ± 9.1 $NeuN^+$ cells per hippocampus (total four brains counted), i.e., 1.07 ± 0.05% of the total injected cells, and 0.04 ± 0.002% NeuN-negative cells.

TUNEL assay

Sagittal sections (50 μm, $n = 6$ sections per animal) were prepared 6 wk after transplantation and were processed for TUNEL by using an apoptosis detection kit (Roche Bioscience) following the protocol from the kit.

Electrophysiology

Acutely isolated hippocampal slices (sagittal; 150–200 μM; Belachew et al., 2003) were prepared from P10–P15 mice that had received a ventricular injection of FACS®-sorted $NG2^+/EGFP^+$ cells. After a 1-h recovery, slices were perfused in a recording chamber with extracellular solution (Belachew et al., 2003). $EGFP^+$ cells in the stratum oriens and stratum radiatum of CA1 and CA3 were identified as described previously (Belachew et al., 2003). Due to the low levels of EGFP fluorescence, the InvestiGater integrating box (DAGE-MTI) was used to amplify the fluorescent signal detected by the CCD camera (model CCD-100; DAGE-MTI). Patch electrodes and intracellular solution were as described previously (Belachew et al., 2003). Action potentials and spontaneous AMPA-receptor currents were analyzed under current-clamp (current injection 30–180 pA steps; 1,000 ms duration) and voltage-clamp, respectively, as described previously (Belachew et al., 2003). All data were filtered at 2 kHz and digitized at 10–20 KhZ. Offline analysis was performed using Clampfit 8 (Axon Instruments, Inc.) and MiniAnalysis (Synaptosoft Inc.).

Online supplemental material

Fig. S1 shows that neurons derived from P2 $NG2^+/EGFP^+$ spheres give rise primarily to GABAergic neurons. Fig. S2 shows the presence of *Dlx2* and *Mash1* mRNA in FACS®-purified $NG2^+/EGFP^+$ cells. Fig. S3 shows the antigenic characterization of acutely dissociated P8 striatal-SVZ. Fig. S4 shows the cellular distribution and migration into the hippocampus of transplanted $NG2^+/EGFP^+$ cells at different times after transplantation. Fig. S5 shows the progenies derived from transplanted $NG2^+/EGFP^+$ cells in the subcortical white matter 3 wk after transplantation. Online supplemental material is available at http:www.jcb.org/cgi/content/full/jcb.200311141/DC1.

We thank Drs. David Rowitch, David Anderson, and Grace Panganiban for the gift of anti-Olig 2, anti-Mash1, and anti-Dlx antibodies, respectively. We thank Xiaoqing Yuan for generating the CNP-EGFP mouse and Dr. Li-Jin Chew for its maintenance. We are thankful to Mr. William King and Dr. Robyn Ruffner for their invaluable assistance with FACS® sorting and acquisition of confocal images, respectively. We are especially grateful to Dr. Tarik Haydar for his assistance with the grafting experiments. We thank Drs. Mike Bell, Li-Jin Chew, Magdalena Gotz, Tarik Haydar, Chris McBain, and David Panchision for discussion and critical comments on the manuscript.

This work was partially supported by National Institutes of Health (grant MRDDRC P30HD40677) and by the Wadsworth Foundation. A. Aguirre is a William A. Haseltine Postdoctoral Fellow in Neuroscience and Genetics. S. Belachew is a Research Associate of the Fonds National de la Recherche Scientifique.

Submitted: 28 November 2003
Accepted: 15 April 2004

References

Alvarez-Buylla, A., and J.M. Garcia-Verdugo. 2002. Neurogenesis in adult subventricular zone. *J. Neurosci.* 22:629–634.

Belachew, S., R. Chittajallu, A.A. Aguirre, X. Yuan, M. Kirby, S. Anderson, and V. Gallo. 2003. Postnatal NG2 proteoglycan-expressing progenitor cells are intrinsically multipotent and generate functional neurons. *J. Cell Biol.* 161: 169–186.

Capela, A., and S. Temple. 2002. Lex/ssea-1 is expressed by adult mouse CNS stem cells, identifying them as nonependymal. *Neuron.* 35:865–875.

Casaccia-Bonnefil, P., R. Tikoo, H. Kiyokawa, V. Friedrich Jr., M.V. Chao, and A. Koff. 1997. Oligodendrocyte precursor differentiation is perturbed in the absence of the cyclin-dependent kinase inhibitor p27Kip1. *Genes Dev.* 11: 2335–2346.

Dawson, M.R., J.M. Levine, and R. Reynolds. 2000. NG2-expressing cells in the central nervous system: are they oligodendroglial progenitors? *J. Neurosci. Res.* 61:471–479.

Desai, A.R., and S.K. McConnell. 2000. Progressive restriction in fate potential by neural progenitors during cerebral cortical development. *Development.* 127: 2863–2872.

Doetsch, F., J.M. Garcia-Verdugo, and A. Alvarez-Buylla. 1997. Cellular composition and three-dimensional organization of the subventricular germinal zone in the adult mammalian brain. *J. Neurosci.* 17:5046–5061.

Doetsch, F., I. Caille, D.A. Lim, J.M. Garcia-Verdugo, and A. Alvarez-Buylla. 1999a. Subventricular zone astrocytes are neural stem cells in the adult mammalian brain. *Cell.* 97:703–716.

Doetsch, F., J.M. Garcia-Verdugo, and A. Alvarez-Buylla. 1999b. Regeneration of a germinal layer in the adult mammalian brain. *Proc. Natl. Acad. Sci. USA.* 96:11619–11624.

Doetsch, F., L. Petreanu, I. Caille, J.M. Garcia-Verdugo, and A. Alvarez-Buylla. 2002a. EGF converts transit-amplifying neurogenic precursors in the adult brain into multipotent stem cells. *Neuron.* 36:1021–1034.

Doetsch, F., J.M. Verdugo, I. Caille, A. Alvarez-Buylla, M.V. Chao, and P. Casaccia-Bonnefil. 2002b. Lack of the cell-cycle inhibitor p27Kip1 results in selective increase of transit-amplifying cells for adult neurogenesis. *J. Neurosci.* 22:2255–2264.

Goldman, S. 2003. Glia as neural progenitor cells. *Trends Neurosci.* 26:590–596.

He, W., C. Ingraham, L. Rising, S. Goderie, and S. Temple. 2001. Multipotent stem cells from the mouse basal forebrain contribute GABAergic neurons and oligodendrocytes to the cerebral cortex during embryogenesis. *J. Neurosci.* 21:8854–8862.

Jinno, S., and T. Kosaka. 2002. Immunocytochemical characterization of hippocamposeptal projecting GABAergic nonprincipal neurons in the mouse brain: a retrograde labeling study. *Brain Res.* 945:219–231.

Liu, S., J. Wang, D. Zhu, Y. Fu, K. Lukowiak, and Y.M. Lu. 2003. Generation of functional inhibitory neurons in the adult rat hippocampus. *J. Neurosci.* 23: 732–736.

Lu, Q.R., D. Yuk, J.A. Alberta, Z. Zhu, I. Pawlitzky, J. Chan, A.P. McMahon, C.D. Stiles, and D.H. Rowitch. 2000. Sonic hedgehog-regulated oligodendrocyte lineage genes encoding bHLH proteins in the mammalian central nervous system. *Neuron.* 25:317–329.

Ma, W., T. Behar, L. Chang, and J.L. Barker. 1994. Transient increase in expression of GAD-65 and GAD-67 mRNAs during postnatal development of rat spinal cord. *J. Comp. Neurol.* 346:151–160.

Marshall, C.A., and J.E. Goldman. 2002. Subpallial dlx2-expressing cells give rise to astrocytes and oligodendrocytes in the cerebral cortex and white matter. *J. Neurosci.* 22:9821–9830.

McBain, C.J., and A. Fisahn. 2001. Interneurons unbound. *Nat. Rev. Neurosci.* 2:11–23.

Nunes, M.C., N.S. Roy, H.M. Keyoung, R.R. Goodman, G. McKhann, II, L. Jiang, J. Kang, M. Nedergaard, and S.A. Goldman. 2003. Identification and isolation of multipotential neural progenitor cells from the subcortical white matter of the adult human brain. *Nat. Med.* 9:439–447.

Olsson, M., K. Campbell, and D.H. Turnbull. 1997. Specification of mouse telencephalic and mid-hindbrain progenitors following heterotopic ultrasound-guided embryonic transplantation. *Neuron.* 19:761–772.

Panganiban, G., and J.L. Rubenstein. 2002. Developmental functions of the Distal-less/Dlx homeobox genes. *Development.* 129:4371–4386.

Panganiban, G., S.M. Irvine, C. Lowe, H. Roehl, L.S. Corley, B. Sherbon, J.K. Grenier, J.F. Fallon, J. Kimble, M. Walker, et al. 1997. The origin and evolution of animal appendages. *Proc. Natl. Acad. Sci. USA.* 94:5162–5166.

Reynolds, B.A., and S. Weiss. 1992. Generation of neurons and astrocytes from isolated cells of the adult mammalian central nervous system. *Science.* 255: 1707–1710.

Schluter, C., M. Duchrow, C. Wohlenberg, M.H. Becker, G. Key, H.D. Flad, and J. Gerdes. 1993. The cell proliferation–associated antigen of antibody Ki-67:

a very large, ubiquitous nuclear protein with numerous repeated elements, representing a new kind of cell cycle–maintaining proteins. *J. Cell Biol.* 123: 513–522.

Stuhmer, T., S.A. Anderson, M. Ekker, and J.L. Rubenstein. 2002. Ectopic expression of the Dlx genes induces glutamic acid decarboxylase and Dlx expression. *Development.* 129:245–252.

Suzuki, S.O., and J.E. Goldman. 2003. Multiple cell populations in the early postnatal subventricular zone take distinct migratory pathways: a dynamic study of glial and neuronal progenitor migration. *J. Neurosci.* 24:4240–4250.

Yuan, X., R. Chittajallu, S. Belachew, S. Anderson, C.J. McBain, and V. Gallo. 2002. Expression of the green fluorescent protein in the oligodendrocyte lineage: a transgenic mouse for developmental and physiological studies. *J. Neurosci. Res.* 70:529–545.

Yung, S.Y., S. Gokhan, J. Jurcsak, A.E. Molero, J.J. Abrajano, and M.F. Mehler. 2002. Differential modulation of BMP signaling promotes the elaboration of cerebral cortical GABAergic neurons or oligodendrocytes from a common sonic hedgehog-responsive ventral forebrain progenitor species. *Proc. Natl. Acad. Sci. USA.* 99:16273–16278.

The Journal of Cell Biology

[HELP with High Resolution Image Viewing]

Full Text of this Article

[View Larger Version of this Image]

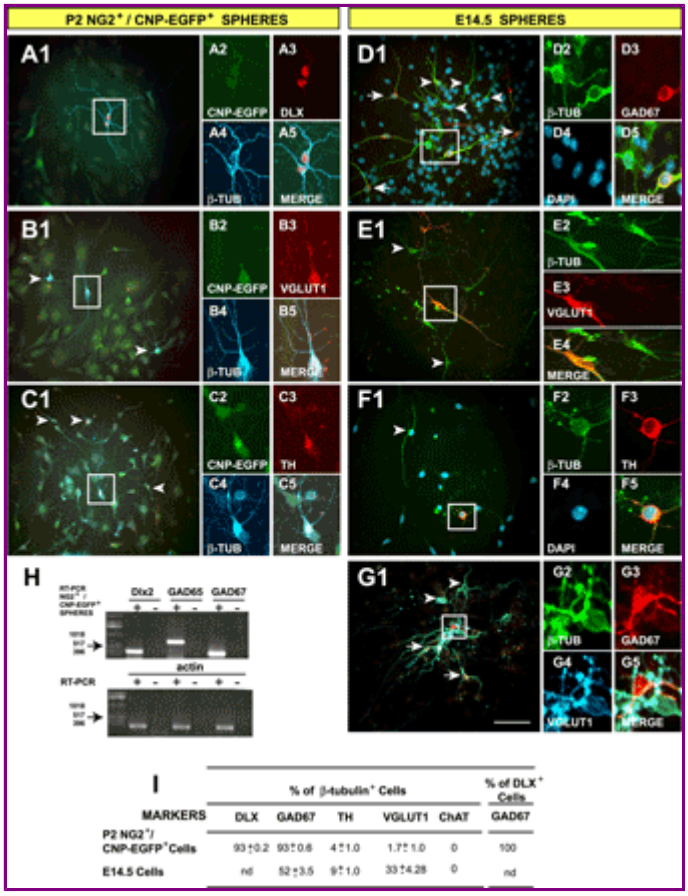

Figure S1. NG2$^+$/EGFP$^+$ cells give rise to GABAergic interneurons in vitro. Neurospheres derived from P2 NG2$^+$/EGFP$^+$ cells (A-C) and E14.5 mouse brain (D-G) were grown under the same conditions and processed for immunocytochemistry 6 d after plating. Neuronal phenotypes were identified using ß-tubulin (A-G, blue) and Dlx (A, red), VGLUT1 (B, E, and G, red), and TH (C and F, red) antibodies. (H) RT-PCR results for Dlx, GAD-65, GAD-67, and actin genes on RNA derived from NG2$^+$/EGFP$^+$ neurospheres after differentiation. RNA without RT was used as negative control (-). (I) Quantification of neuronal phenotypes from NG2$^+$/EGFP$^+$ and E14.5 neurospheres. Data are averages $^+$ SEM. Cells in boxed areas are shown at higher magnification. Arrowheads in A-G show ß-tubulin$^+$ cells that are negative for the analyzed markers. Arrows in D and G show double labelling for ß-tubulin and GAD-67. Bar, 50 µm.

Full Text of this Article

The Journal of Cell Biology

[HELP with High Resolution Image Viewing]

Full Text of this Article

[View Larger Version of this Image]

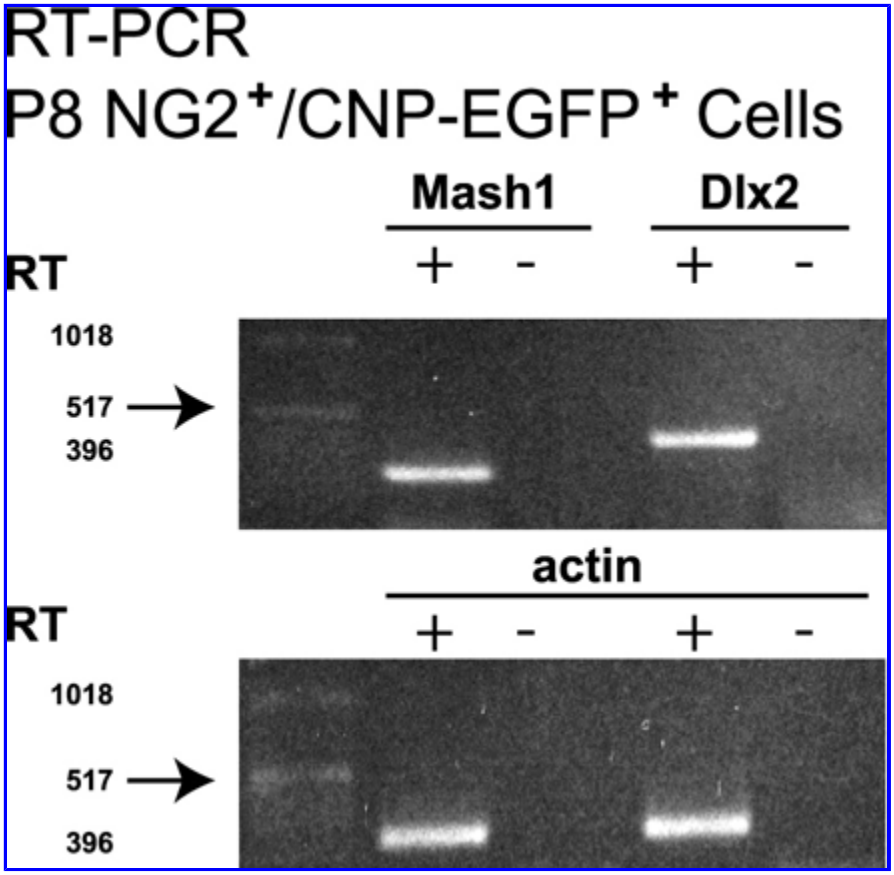

Figure S2. The transcription factor Dlx2 and Mash1 are expressed in postnatal SVZ $NG2^+/EGFP^+$ cells. RT-PCR results from RNA derived from P8 FACS®-purified $NG2^+/EGFP^+$ cells. Mash1 and Dlx2 genes were amplified using mouse oligonucleotide primers selective for these genes. RNA that was not reverse transcribed was used as a negative control (-).

Full Text of this Article

The Journal of Cell Biology

[HELP with High Resolution Image Viewing]

Full Text of this Article

[View Larger Version of this Image]

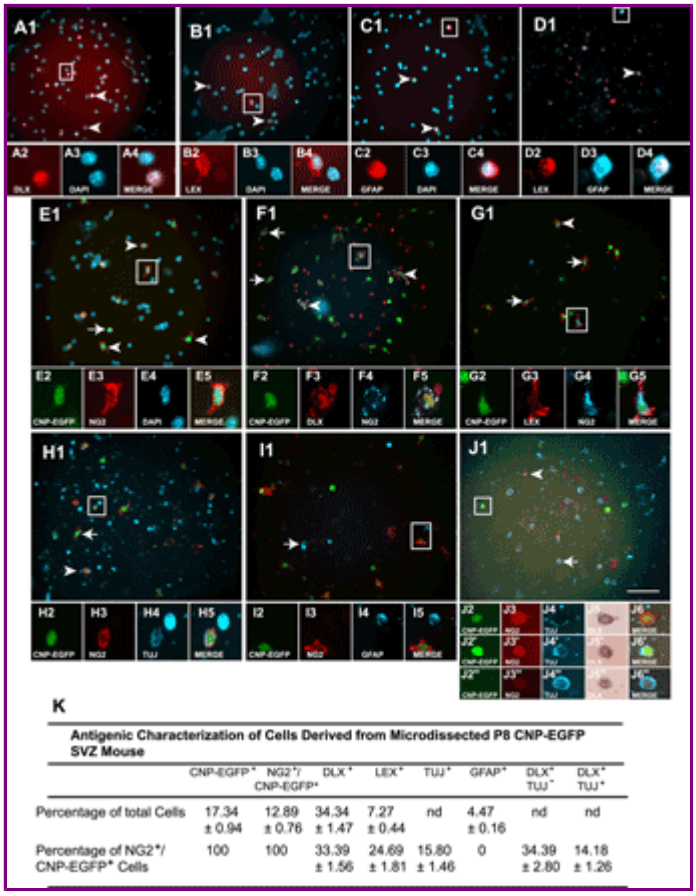

Figure S3. Antigenic characterization of cell derived from microdissected SVZ of P8 CNP-EGFP mice. (A-J) The striatal SVZ was microdissected and enzymatically dissociated to single cells that were stained for markers 2 h after plating. For triple labelling in J1, Dlx (brown) was developed with DAB. Cells in boxed areas are shown at higher magnification. Bar, 50 µm. (K) Percentages of total ($DAPI^+$) and of $NG2^+/EGFP^+$ cells were calculated for each marker. Data are expressed as averages $^+$ SEM. Arrows indicate double-positive cells, and arrowheads indicate triple-positive cells.

Full Text of this Article

The Journal of Cell Biology

[HELP with High Resolution Image Viewing]

Full Text of this Article

[View Larger Version of this Image]

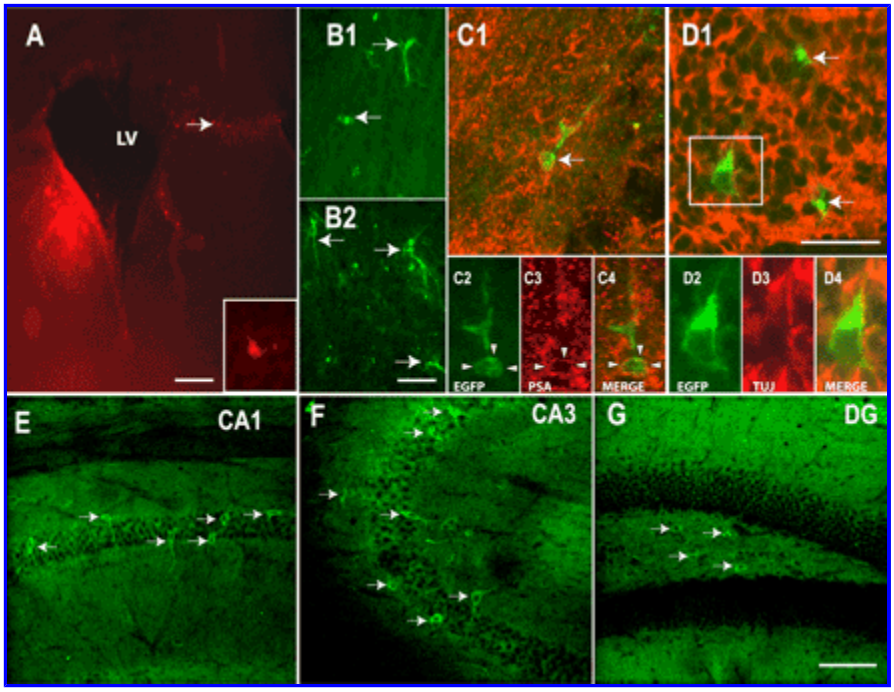

Figure S4. Grafted NG2$^+$/EGFP$^+$ cells migrate from the postnatal lateral ventricle to the hippocampus. NG2$^+$/EGFP$^+$ cells were FACS®-purified from P2 brains, stained with the dye PKH26 (red), and transplanted into the lateral ventricle (LV) of P2 wild-type mice. (A) 48 h after transplantation, green cells are found surrounding the LV area, and some cells start migrating tangentially to different areas of the cortex (arrow). One of the migrating cells is depicted in the inset (A; PKH26, red). 4 d after grafting, migrating EGFP$^+$ cells (green) were observed in the stratum oriens of the CA3 (B1) and in the stratum pyramidale of the CA3 (B2). Migratory EGFP$^+$ cells (green) acquired immature neuronal markers 4 d after grafting, as shown by PSA-NCAM (C; arrowheads in C2-C4 point to cell body, red) and TUJ1 (D, red) expression. (E-G) 3 wk after grafting, a large percentage of EGFP$^+$ cells (green) is found in the hippocampus and displays the typical morphology of interneurons. EGFP$^+$ cells are integrated into the structure of the CA1 (E), CA3 (F), and DG (G) of the hippocampus. Arrows indicate grafted EGFP$^+$ cells. Arrowheads in C2-C4 indicate co localization of EGFP and PSA-NCAM. Bars: (A) 200 µm; (B-D) 50 µm; (E-G) 100 µm.

Full Text of this Article

Home | Help | Feedback | Subscriptions | Archive | Search

The Journal of Cell Biology

[HELP with High Resolution Image Viewing]

Full Text of this Article

[View Larger Version of this Image]

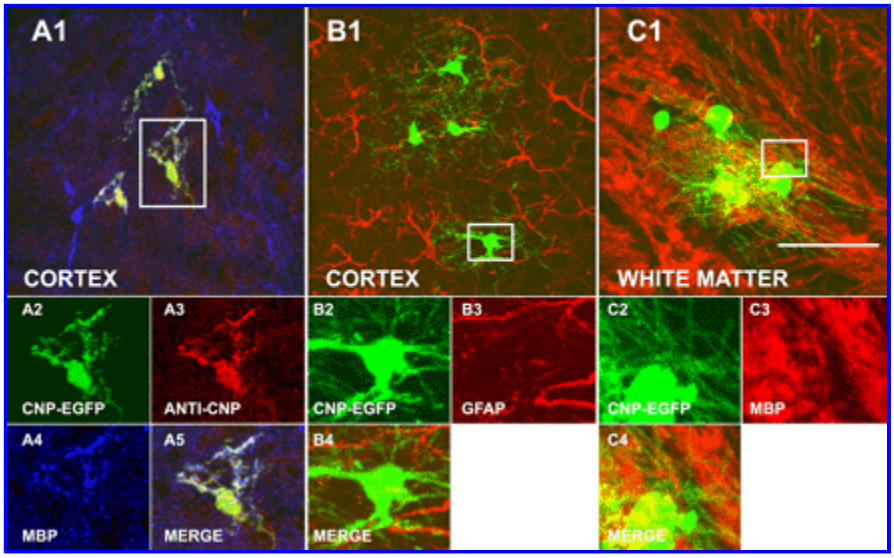

Figure S5. Grafted NG2$^+$/EGFP$^+$ cells differentiate to oligodendrocytes in the white matter and cerebral cortex. 3 wk after transplantation, sagittal brain sections were prepared for immunohistochemistry. (A-C) EGFP$^+$ grafted cells (green) found in the cortex and white matter display an oligodendrocyte morphology. (A) EGFP$^+$/CNP-protein$^+$ (red) and MBP$^+$ (blue) cells are found in cerebral cortex. (B) EGFP$^+$ grafted cells with oligondendrocyte morphology are found in cerebral cortex and are not immunolabeled with anti-GFAP antibodies (red). (C) Oligodendrocytes expressing MBP (red) were also found in white matter. EGFP$^+$ cells are shown at higher magnification in boxed areas. Bar, 50 μm.

Full Text of this Article

Home | Help | Feedback | Subscriptions | Archive | Search

7.7 Publication #7: Nguyen, L., Rigo, J.-M., Rocher, V., Belachew, S., Malgrange, B., Rogister, B., Leprince, P., and Moonen, G. (2001) Neurotransmitters as early signals for central nervous system development. *Cell Tissue Res.* 305:187-202.

Cell Tissue Res (2001) 305:187–202
DOI 10.1007/s004410000343

REVIEW

**Laurent Nguyen · Jean-Michel Rigo
Véronique Rocher · Shibeshih Belachew
Brigitte Malgrange · Bernard Rogister
Pierre Leprince · Gustave Moonen**

Neurotransmitters as early signals for central nervous system development

Received: 10 November 2000 / Accepted: 6 December 2000 / Published online: 20 February 2001

Abstract During brain ontogenesis, the temporal and spatial generation of the different types of neuronal and glial cells from precursors occurs as a sequence of successive progenitor stages whose proliferation, survival and cell-fate choice are controlled by environmental and cellular regulatory molecules. Neurotransmitters belong to the chemical microenvironment of neural cells, even at the earliest stages of brain development. It is now established that specific neurotransmitter receptors are present on progenitor cells of the developing central nervous system and could play, during neural development, a role that has remained unsuspected until recently. The present review focuses on the occurrence of neurotransmitters and their corresponding ligand-gated ion channel receptors in immature cells, including neural stem cells of specific embryonic and neonatal brain regions. We summarize in vitro and in vivo data arguing that neurotransmitters could regulate morphogenetic events such as proliferation, growth, migration, differentiation and survival of neural precursor cells. The understanding of neurotransmitter function during early neural maturation could lead to the development of pharmacological tools aimed at improving adult brain repair strategies.

This work was supported by the Fonds pour la Formation à la Recherche dans l'Industrie et dans l'Agriculture, the Fonds National de la Recherche Scientifique (FNRS), the Fondation Médicale Reine Elisabeth (FMRE), the Fondation Charcot and the Ligue Belge de la Sclérose en Plaques

L. Nguyen (✉) · J.-M. Rigo · V. Rocher · S. Belachew
B. Malgrange · B. Rogister · P. Leprince · G. Moonen
Center for Cellular and Molecular Neurobiology,
University of Liège, 17 Place Delcour, 4020 Liège, Belgium
e-mail: Laurent.Nguyen@student.ulg.ac.be
Tel.: +32-4-3665918, Fax: +32-4-3665912

S. Belachew · B. Rogister · G. Moonen
Department of Neurology, University of Liège,
C.H.U. (B35) Sart Tilman, 4000 Liège, Belgium

Keywords Ligand-gated ion channels · Neural progenitors · Neurotransmitters · Proliferation · Migration · Differentiation · Survival

Introduction

Harmonious development of the mammalian central nervous system (CNS) during embryogenesis not only requires accurate course of genetic schedules but also depends on appropriate influences by various epigenetic signalling processes. In that respect, much effort has been recently devoted to characterize intrinsic and extrinsic factors regulating the behaviour of neural progenitor cell populations during brain maturation. Recently, several secreted molecules such as growth factors, hormones and neurotransmitters have been implied in the extrinsic regulation of cell proliferation within the developing telencephalon (reviewed by Cameron et al. 1998a). Among them, neurotransmitters are prominent candidates for transcellular signals that could influence the development of CNS cells, since they surround neural cells throughout the CNS maturation period (Cicirata et al. 1991; Miranda-Contreras et al. 1998, 1999, 2000) and since functional ligand-gated ionic channel receptors have been described in neural progenitors before the establishment of cortical and subcortical synapses (Belachew et al. 1998a; Flint et al. 1998; Haydar et al. 2000; Ma et al. 1998, 2000; Maric et al. 2000; Sah et al. 1997). Furthermore, several studies strongly suggest that neurotransmitters could behave as growth regulators during specific developmental periods (Antonopoulos et al. 1997; Brezun and Daszuta 2000; Butler et al. 1999; Cameron et al. 1998a; Fiszman et al. 1999; Haydar et al. 2000; Lauder et al. 1998; LoTurco et al. 1995; Ma et al. 1998, 2000; Wang et al. 1996; Weiss et al. 1998).

Our present view of the CNS has changed dramatically over the past few years. It is now well established that self-renewing neural stem and progenitor cells (Fig. 1) do persist in the adult mammalian brain and spinal cord

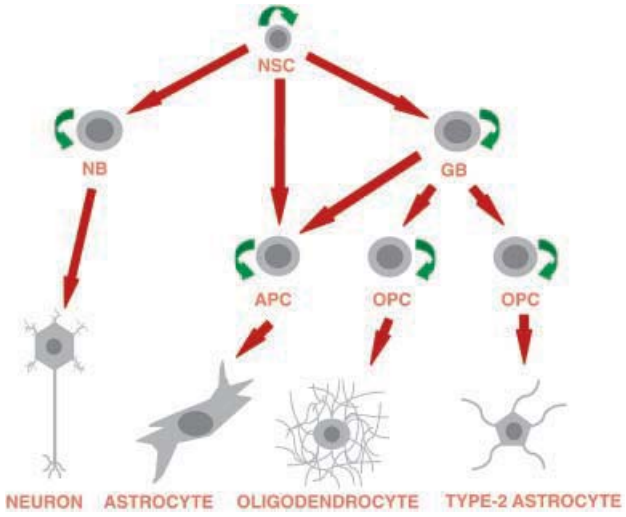

Fig. 1 General schematic view of the early central nervous system lineage progression: neural stem cell lineage. The possible lineage relationships between the various defined precursors and mature neural cells. Immature progenitors are able to self-renew (*green arrow* that loops around a cell) and/or to generate more differentiated cells. (*NSC* Neural stem cell population, *APC* astrocyte precursor cells, *NB* neuroblasts, *GB* glioblasts, *OPC* oligodendrocyte progenitor cells)

(Gage 2000; Weiss et al. 1996). Since various neural precursors exhibit functional neurotransmitter receptors and transporters, the pharmacological modulation of the concentration of relevant neurotransmitters or of the downstream membrane and intracellular events that they induce could provide new pathways for therapeutic interventions during neural development. Regarding expected clinical prospects, the improvement of cell replacement therapies, using properly selected and/or bioengineered exogenous progenitors or the recruitment of endogenous stem cells that are induced to migrate and differentiate into specific phenotypes, are both crucial issues that could be modified by interacting with neurotransmitter-controlled events.

This review summarizes our current knowledge on the various functions of ionotropic neurotransmitter receptors expressed on neural stem cells (NSCs) and neuronal and glial progenitors. In that respect, we have focused on the ionotropic glutamate receptors (iGluR) – including α-amino-3-hydroxy-5-methyl-4-isoxazolepropionate receptor (AMPAR), *N*-methyl-D-aspartate receptor (NMDAR) and kainate receptors (KAR) – the type-A γ-aminobutyric acid receptor ($GABA_AR$), the glycine receptor (GlyR), the nicotinic acetylcholine receptor (nAChR) and the type-3 serotonin receptor ($5\text{-}HT_3R$). We also reviewed the roles played by the main agonists of these receptors during early stages of CNS development.

γ-Aminobutyric acid

GABA, the main, fast-acting inhibitory neurotransmitter in the adult neocortex (Connors et al. 1988; Krnjevic and Schwartz 1967), is also one of the most abundant neurotransmitters detected during mammalian brain development (Cicirata et al. 1991; Miranda-Contreras et al. 1998, 1999, 2000).Three classes of GABA receptors (GABAR) are currently distinguished in the CNS: the $GABA_AR$ and $GABA_CR$, which are both ionotropic receptors, and the metabotropic $GABA_BR$ (reviewed by Chebib and Johnston, 1999). Among ionotropic receptors, so far six different subunit families have been identified to form CNS $GABA_AR$ receptors: α1–6, β1–3, γ1–3, δ, ε, and θ; two additional subunits, ρ1 and ρ2, have been classified as part of the $GABA_CR$ (Bonnert et al. 1999; Bormann and Feigenspan 1995; Davies et al. 1997; Luddens et al. 1995; McKernan and Whiting 1996).

Several types of $GABA_AR$ transcripts and subunits have been previously described in situ as components of functional $GABA_AR$ in rat neuroepithelial cells, as well as in neuroblasts and glioblasts, during spinal and cortical neurogenesis (LoTurco et al. 1995; Ma and Barker 1995; Ma et al. 1998; Serafini et al. 1998a, 1998b; Verkhratsky and Steinhauser 2000). The abundance of GABA and its receptors in the early developing rodent CNS both in vivo and in vitro has led to speculations on the role of this transmitter in immature neural cell proliferation, migration, differentiation and survival (Table 1). It is now well established that GABA exerts a variety of trophic influences through the stimulation of the $GABA_AR$ during neural development (reviewed by Barker et al., 1998; Lauder et al. 1998).

Neural stem cells

Ma et al., using cultures of rat embryonic telencephalic NSCs expanded by treatment with basic fibroblast growth factor (bFGF), have shown that the activation of functional $GABA_AR$ induces an increase in $[Ca^{2+}]_i$. This effect was reversibly blocked by specific antagonists of the $GABA_AR$ (Ma et al. 1998). Similarly, rat embryonic hippocampal progenitor cells – likely to contain NSCs – have been reported to express functional $GABA_AR$ in vitro. In these NSCs, GABAergic currents remain present to a significant extent even after multiple passages (Sah et al. 1997). Such in vitro results strengthen the hypothesis of a functional role for $GABA_AR$ during primordial neural development.

Neuroblasts

Several studies have already reported that $GABA_AR$ activation can control the cell cycle kinetics in neuronal progenitors (Haydar et al. 2000; LoTurco et al. 1995). Fiszman et al. have suggested that, in vitro, GABA pro-

Table 1 GABA-induced events in neural progenitors (*PC* patch-clamp, *IM* immunostainings, *PA* proliferation assay, *CaI* calcium imaging, *Sbio* survival bioassay, *VIA* video-analysis imaging, *Cbio* chemotaxis bioassay, *VZ* ventricular zone, *SVZ* subventricular zones, *OPC* oligodendroglia-progenitor cells)

GABA			
Cell stage	Model/Techniques	Results	References
NSCs	El6 rat hippocampal neural precursor cells (including NSCs) in vitro: PC	GABA-triggered currents mainly remain present in hippocampal neural precursor cells even after multiple passages	Sah et al. 1997
	E13–13.5 rat neuroepithelial cells in vitro: PC/IM	GABA-induced depolarization via $GABA_AR$ activation elicits calcium entry in NSC cells	Ma et al. 1998
Neuroblasts	P6–8 rat cerebellum granule cells in vitro: PA	GABA promotes proliferation	Fiszman et al. 1999
	Rat embryonic cortical cell cultured in vitro: IM/PA	Activation of $GABA_AR$ by GABA or muscimol inhibits proliferative effect of bFGF	Antonopoulos et al. 1997
	E16–19 rat VZ cells in situ: PC/PA/CaI	GABA decreases DNA synthesis via calcium-dependent pathway	LoTurco et al. 1995
	E13–14 mouse VZ and SVZ cells in situ: PA/IM	GABA affects cell cycle of SVZ population by decreasing DNA synthesis; also enhances proliferation of VZ cells	Haydar et al. 2000
	E18 rat striatal neurons in vitro: Sbio/CaI	GABA enhances survival through $GABA_AR$ activation	Ikeda et al. 1997
	Embryonic rat hippocampal neurons in vitro: VIA	Antagonism of $GABA_AR$ induces decrease in dendritic outgrowth in pyramidal neurons	Barbin et al. 1993; Mattsson and Kater 1989
	Embryonic rat cerebellum cells and embryonic chick tectum cells in vitro: VIA	Activation of $GABA_AR$ in serum-supplemented medium increases neurite elongation	Michler 1990
	Embryonic rat spinal and cortical cells in vitro: Cbio/VIA	GABA enhances neuronal migration	Behar et al. 1994, 1996
Glioblasts	Astrocytes/astroblasts in vitro/in situ: PC	Astrocytes depolarized by GABA application	Bormann et al. 1988; Kettenmann et al. 1984a, 1984b; MacVicar et al. 1989
	Murine and rat OPCs in vitro/ in situ: PC/CaI	GABA-elicited inward current depolarizes OPC membrane and induces rise of $[Ca^{2+}]_i$	Belachew et al. 1998a, 1998b; Kettenmann et al. 1984a, 1984b; Kirchhoff et al. 1992; Pastor et al. 1995

motes rat immature cerebellar granule cell proliferation by indirect activation of the mitogen-activated protein kinase (MAPK) cascade (Fiszman et al. 1999). Conversely, an in situ study has demonstrated that $GABA_AR$ currents triggered by GABA or muscimol (a $GABA_AR$ agonist) negatively regulate DNA synthesis in neural progenitors of the rat embryonic neocortical ventricular zone (E16 and E19), through a depolarization-based mechanism (LoTurco et al. 1995). Unlike mature neurons, neuroblasts have high $[Cl^-]_i$ probably maintained by unopposed, inward Cl^- transport (Luhmann and Prince 1991). The existence of such a chloride gradient is consistent with the demonstration that either GABA or muscimol in embryonic and neonatal cortical slices induces membrane depolarization (Owens et al. 1996). On the other hand, $GABA_AR$ antagonists increase DNA synthesis, indicating that endogenous GABA is sufficient to modulate the cell cycle of neocortical progenitors (LoTurco et al. 1995). This GABA-restrictive effect on progenitor cell proliferation, assessed in situ, is supported by an in vitro study showing that the activation of $GABA_AR$ decreases the proliferation rate of embryonic dissociated cortical cells cultured in the presence of bFGF (Antonopoulos et al. 1997). The situation could, however, be more complex, since Haydar et al. have recently shown that, in embryonic mice brain organotypic slices, GABA and glutamate affect the cell cycle of subventricular zone (SVZ) cells by decreasing DNA synthesis, and, hence, actually have an opposite effect on the proliferation of ventricular zone (VZ) precursors (Haydar et al. 2000).

All these data strongly suggest that in vivo the activation of $GABA_AR$ by endogenous GABA could play an important role during neocortical development, regulating the proliferation of neuronal progenitors.

Besides its proposed role in progenitor cell proliferation, various in vitro models suggest that GABA could have trophic factor-like additional functions. Indeed, GABA significantly enhances the survival of rat embryonic (E18) striatal neurons in vitro. This effect, which is

not induced by the $GABA_BR$ agonist baclofen, is triggered by GABA or muscimol and blocked by $GABA_AR$ antagonists such as bicuculline and picrotoxin. Various molecules, including L-type voltage-gated Ca^{2+} channel (VGCC) blockers (nifedipine and nicardipine) or protein kinase inhibitors (H-7 and genistein) also block the $GABA_AR$-mediated increase in cell survival. Based upon their pharmacological results, the authors proposed that the activation of $GABA_AR$ initiate a cascade which first triggers a depolarization-evoked Ca^{2+} influx through L-type VGCC and second triggers Ca^{2+}-dependent intracellular signalling pathways such as H-7 and genistein-sensitive protein kinases (Ikeda et al. 1997).

GABA also appears to be important for the migration and the maturation of neuronal precursors, since it enhances the rat embryonic spinal and cortical neural cell motility (Behar et al. 1994, 1996, 2000) and partially modulates neuritic outgrowth in cultured rat hippocampal pyramidal neurons, rat cerebellar neurons and embryonic chick tectum (Barbin et al. 1993; Mattson and Kater 1989; Michler 1990).

Glioblasts

Electrophysiological studies have reported the occurrence of functional ionotropic $GABA_AR$ in glia. These receptors were found not only in rodent astrocytes in culture (Bormann and Kettenmann 1988; Hosli et al. 1997) and in situ (Butt and Jennings 1994; MacVicar et al. 1989; Pastor et al. 1995) but also in newborn rat and murine oligodendroglia progenitor cells (OPCs) in vitro (Belachew et al. 1998a; Gilbert et al. 1984; Kettenmann et al. 1984a; Williamson et al. 1998) and in situ (Pastor et al. 1995).

As has been reported for neuroblasts (LoTurco et al. 1995), GABA depolarizes rodent oligodendrocytes and astrocytes in culture (Kettenmann et al. 1984a, 1984b). The OPC membrane depolarization mediated by GABA seems to trigger the opening of VGCCs, leading to a rise of cytosolic $[Ca^{2+}]_i$ (Kirchhoff and Kettenmann 1992). This depolarization could be sufficient to open Na^+ voltage-gated channels (Na_v), and Na^+ subsequent entry is known to block the outward potassium conductance, thereby inhibiting OPC proliferation (Knutson et al. 1997). However, GABA modulation of OPC proliferation has not been reported (Gallo et al. 1996), suggesting that the level of depolarization mediated by GABA does not reach the activation threshold of Na_v (Barres et al. 1990).Via these mechanisms, $GABA_AR$ activation during development could modulate biological properties of the glia lineage committed-cells.

Glycine

Strychnine-sensitive GlyRs are members of the nicotinic ligand-gated ion channel family (le Novere and Changeux 1999). They mediate postsynaptic inhibition by increasing chloride permeability of the postsynaptic cell membrane in adult spinal cord, brain stem and some higher brain regions (reviewed by Betz, 1991; Kuhse et al. 1995; Schofield et al. 1996). The GlyR is a pentameric transmembrane protein composed of glycosylated integral transmembrane α- (48 kDa) and β-subunits (58 kDa; Schofield et al. 1996). Currently, four α- (α1, α2, α3 and α4; Kuhse et al. 1990, 1995; Matzenbach et al. 1994) and one β-subunit variant (Schofield et al. 1996) have been described. GlyR heterogeneity also arises from alternative splicing that results in the formation of two isoforms of the α1-, the α2- and the α3-subunits (Betz et al. 1994; Nikolic et al. 1998). On the other hand, the homologous glial GlyR found in OPCs could differ from its neuronal counterpart by containing a putative β-subunit variant (Belachew et al. 1998b; Pribilla et al. 1992). In newborn rats, the GlyR is α2-homomeric and differs from the adult form, which classically includes three α1- and two β-subunits (Langosch et al. 1988). Adult GlyRs are mainly clustered at the postsynaptic membrane by gephyrin, a 93-kDa protein (Kneussel and Betz 2000; Langosch et al. 1988). Otherwise, it is now well established that GlyRs assume some functions during CNS developmental period (Table 2).

Neuroblasts

GlyRs are expressed by neuronal progenitors of the rodent developing neocortex and the spinal cord neurons in situ (Malosio et al. 1991) and in vitro (Tapia and Aguayo 1998; Withers and St John 1997). In the developing neocortex, glycine is found at very low concentration as compared to the spinal cord (Aprison et al. 1969), suggesting that another endogenous ligand might stimulate GlyR during corticogenesis. One candidate is taurine – a GlyR agonist (Schmieden et al. 1992) – which is abundant in the developing neocortex and present at lower concentration postnatally. Moreover, unlike glycine, taurine synthesis is more important in the cerebral cortex than in the spinal cord (Agrawal et al. 1971). These results are consistent with a putative role for taurine during corticogenesis, since Flint et al. have nicely demonstrated that GlyRs are functionally expressed by immature migrating and differentiating neurons of rat embryonic and early postnatal cortical slices (Flint et al. 1998).The transmitter role of taurine, acting at the GlyR during cortical development, may help explain observations on the consequence of taurine deprivation during embryogenesis. Indeed, abnormal kitten cortex development has been reported in association with maternal dietary taurine deprivation (Palackal et al. 1986). Flint et al. have suggested furthermore that GlyR signalling could play a role in synapse establishment, since the expression of taurine and GlyR occurs during the peak of synaptogenesis in the developing neocortex (Flint et al. 1998).

Other in vivo and in vitro studies, dealing with the trophic effects of glycine signalling during CNS development, suggest that the glycinergic transmission may

Table 2 Glycine-induced events in neural progenitors (*PC* patch-clamp, *CaI* calcium imaging, *VIA* video-analysis imaging, *Sbio* survival bioassay, *InSitu* in situ hybridization, *IM* immunostainings)

Glycine			
Cell stage	Model/Techniques	Results	References
Neuroblasts	Perinatal rat neuroblasts in situ: PC/CaI	Taurine triggers inward currents and induces membrane depolarization. Depolarization opens VGCCs and elevates intracellular calcium concentrations	Flint et al. 1998
	P6–7 gerbil lateral superior olive neurons in vivo and in situ: VIA	Spontaneous GlyR activation reduces neuronal dendritic branching and total dendritic length	Sanes and Chokshi 1992
	E13–14 mice spinal cord neuroblasts in vitro: PC/CaI/VIA/Sbio	GlyR activation increases number of primary neurites and total neurite length	Tapia et al. 2000
	E20–21 rat cerebellar neuronal cultures in vitro: PC/InSitu/IM/Sbio	Glycine and L-serine promote survival, dendritogenesis and electrophysiological development of Purkinje neurons in cultures	Furuya et al. 2000
Glioblasts	Neonatal rat spinal cord astrocytes, oligodendrocytes and OPCs in situ: PC/single-cell RT-PCR	Expression of functional GlyR in glial cells and progenitors from acute spinal cord slices	Kirchhoff et al. 1996; Pastor et al. 1995
	Newborn rat cortical OPCs in vitro: PC/IM/CaI	Expression of functional GlyR. Structural and pharmacological differences from homologous neuronal GlyR. Glycine application induces rise of intracellular calcium (through VGCCs and glycine transporters)	Belachew et al. 1998a, 1988b, 2000

regulate the growth of postsynaptic processes in the lateral superior olive of gerbils (Sanes and Chokshi 1992; Sanes and Hafidi 1996). In addition, an in vitro study performed by Tapia et al. shows that GlyR activation increases the number of primary neurites and the total neurite length in developing mouse spinal neurons (Tapia et al. 2000). Finally, a recent study argues for trophic roles of astroglia-released glycine and L-serine (a GlyR agonist) on cerebellar Purkinje neurons (PN) in vitro. These amino acids promote the survival, the dendritogenesis and the electrophysiological development of rat cerebellar PN in culture (Furuya et al. 2000). Glycine and L-serine could also play such a role in vivo, since their measured levels in cerebellar extracellular spaces are compatible with the concentrations eliciting significant trophic actions in vitro (Furuya et al. 2000; Hashimoto et al. 1995). In the cerebellum, the Bergmann glia is likely to be the main source of glycine and L-serine in vivo, since it is the only cell type expressing 3-phosphoglycerate dehydrogenase (3PGDH), an essential enzyme for de novo biosynthesis of these molecules (Jaeken et al. 1996).

Glioblasts

Functional GlyRs have been described in newborn rat astrocytes, oligodendrocytes and OPCs in spinal cord slices (Kirchhoff et al. 1996; Pastor et al. 1995). Glycine-induced currents were also recorded from newborn rat cortical oligosphere-derived OPCs, where GlyR seems to be not only pharmacologically but also structurally distinct from the homologous neuronal receptor (Belachew et al. 1998b). Moreover, glycine application on cultured OPCs induces a rise of $[Ca^{2+}]_i$ via the opening of VGCC. This effect is mediated by a depolarization related to the activation of GlyR and Na^+-dependent glycine transporters GLYT1 and/or GLYT2 (Belachew et al. 2000). These results raise the question of a possible function of glycine in the maturation of OPCs into myelinating cells.

Glutamate

In the adult mammalian CNS, excitatory neurotransmission is mainly mediated by two amino acid neurotransmitters: (1) glutamate, which is the most abundant amino acid in the adult CNS; and (2) aspartate. Both enhance a nonselective cationic conductance through the opening of ionotropic glutamate receptors (iGluRs) (Engelsen 1986; Fonnum 1984). Different studies have reported that during neurogenesis high levels of glutamate could be found in several CNS developing areas (Miranda-Contreras et al. 1998, 1999, 2000).

Glutamate receptors are classified in two main groups, namely ionotropic and metabotropic. Metabotropic receptors (mGluRs) are G protein-coupled and regulate the synthesis of various intracellular second messengers (Pin and Duvoisin 1995), whereas iGluRs are heteromeric ligand-gated ion channels (Dingledine et al. 1999; le Novere and Changeux 1999). Based on their pharmacological and electrophysiological properties, iGluRs can be subdivided into three families: AMPAR, NMDAR and KAR. These receptors are expressed not

Table 3 Glutamate-induced events in neural progenitors (*PC* patch-clamp, *CaI* calcium imaging, *FACS* flow-activated cell sorting, *PA* proliferation assay, *IM* immunostainings, *Sbio* survival bioassay, *EM* electron microscopy, *Melec* microelectrode, *W-B* Western-blott, *N-B* Northern-blott, *InSitu* in situ hybridization)

Glutamate			
Cell stage	Model/Techniques	Results	References
NSCs	E16 rat hippocampal neural precursor cells (including NSCs) in vitro: PC	NMDA and kainate-gated currents recorded in hippocampal neural precursor cells, including NSCs	Sah et al. 1997
Neuroblasts	E13 rat differentiating neurons and neuroblasts derived from NSCs in vitro: PC/RT-PCR/CaI/FACS	Expression of functional AMPAR. Activation triggers inward currents and cytosolic Ca^{2+} increases	Maric et al. 2000; O'Connor et al. 2000
	E16–19 rat VZ cells in situ: PC/PA/CaI	AMPA/KAR activation decrease DNA via calcium-dependent pathway	LoTurco et al. 1995
	E13–14 mouse VZ and SVZ cells in situ: PA/IM	Glutamate agonists affect the cell cycle of SVZ population by decreasing DNA synthesis; also enhance the proliferation of VZ cells	Haydar et al. 2000
	Neonatal/adult rat dentate gyrus cells in vivo: PA/Sbio/IM	NMDAR antagonism, during 1st postnatal week or in adulthood, leads to increase in [^{3}H]thymidine incorporation in rat dentate gyrus cells maturing mostly in granule neurons	Cameron et al. 1995, 1998a, 1998b; Gould et al. 1994
	E12–22 rat striatum neuroblasts in vivo: PA/IM	Antagonism of NMDAR induces a decrease in proliferation during the proliferative phase in vivo	Sadikot et al. 1998
	P7–11 rat cerebellar immature granule neurons in vitro/in vivo: Sbio	Activation of NMDAR promotes cell survival	Balazs et al. 1988a, 1988b; Monti and Contestabile 2000
	Embryonic mice spinal cord neurons in vivo: Sbio	Antagonism of NMDAR reduces cell survival	Brenneman et al. 1990
	Neonatal/adult rat dentate gyrus in vivo: PA/Sbio/IM	Antagonism of NMDAR increases cell death	Gould and Cameron 1996; Gould et al. 1994
	18-Day-old rat whole-brain dissociated cultures in vivo: EM	L-Monosodium glutamate promotes neuronal growth and differentiation	Aruffo et al. 1987
	Rat cerebellar immature granule neurons in vivo	Activation of NMDAR promotes neurite outgrowth	Pearce et al. 1987
	Rat hippocampal differentiating neurons in vitro: VIA/CaI	Activation of NMDAR promotes dendritic outgrowth and branching	Brewer et al. 1989; Mattsson et al. 1988a, 1988b; Wilson et al. 2000
	Developing rat and mouse cerebellar neurons in situ: PC/VIA	Increase in tonic NMDA receptor-channel activity during stages of granule cell differentiation, migration and synaptogenesis; driven by endogenous glutamate release, regulated by NMDAR density and local glutamate uptake	Rossi and Slater 1993; Komuro and Rakic 1993
Glioblasts	Postnatal rat cerebral astocyte cultures in vitro: Melec	Functional AMPAR and KAR	Kettenmann et al. 1984a, 1984b
	Newborn mouse cerebral astrocyte cultures in vitro: PC	Activation of AMPA/KAR leads to substantial blockade of K^+ currents via intracellular Na^+-amassing pathway	Robert and Magistretti 1997
	Rat spinal cord astrocyte cultures in vitro: PC/PA	K^+ channel-blocking reduces astroglial proliferation	Pappas et al. 1994
	Postnatal rat cortical astrocyte cultures and rat optic nerve astrocytes in vitro: InSitu	Immediate early gene (e.g. c-*fos*, c-*jun*, *jun-B*) expression modulated by the activation of AMPAR and KAR	Mack et al. 1994; McNaughton and Hunt 1992
	Neonatal rat hippocampal astrocyte cultures in vitro: VIA/EM	Glutamate, acting at AMPA/KAR, induces increase in number of filopodia	Cornell-Bell et al. 1990
	Adult human retinal glial cells in vitro: PA/PC/IM/W-B	Proliferation of cultured glial Müller cells, enhanced by NMDAR activation. NMDAR activation also inhibits inward-rectifying K^+ currents	Puro et al. 1996; Uchihori and Puro 1993

Table 3 (continued)

Glutamate			
Cell stage	Model/Techniques	Results	References
Glioblasts	Rat cerebral and optic nerve OPCs in vitro: PC/PCR/InSitu	Functional AMPAR and KAR in vitro	Barres et al. 1990; Gallo et al. 1994; Jensen and Chiu 1993; Patneau et al. 1994
	P0 rat neurohypophysis OPCs in vitro: PA/PCR/IM/CaI	Blockade of functional NMDAR inhibits PSA-NCAM expression and stops migration	Wang et al. 1996
	Postnatal rat cerebral cortex cultures in vitro: CaI/IM/N-B	AMPA/KAR activation allows calcium-dependent regulation of c-*fos*, blocks voltage-gated K^+ channels, inhibits proliferation and lineage progression	Liu and Almazan 1995; Pende et al. 1994
	Postnatal rat cerebral cortex in vitro and in situ: PC/PA/IM	AMPA/KAR activation blocks spontaneous proliferation and lineage progression through Na^+ blockade of outward K^+ currents mechanism. Mechanism downstream of blockade of outward K^+ currents involves accumulation of cyclin-dependent kinase inhibitors	Gallo et al. 1996; Ghiani et al. 1999; Knutson et al. 1997

only by neurons but also by glial cells (reviewed by Dingledine et al., 1999; Verkhratsky and Steinhauser 2000). In addition to their role in neurotransmission during adulthood, excitatory amino acid transmitters could also exert neurotrophic functions in the course of CNS development (Table 3; reviewed by Cameron et al., 1998a; McDonald and Johnston 1990).

iGluRs are widely expressed throughout the adult and developing mammalian CNS (reviewed by Bettler and Mulle, 1995; Borges and Dingledine 1998; Ozawa et al. 1998) among which AMPARs and KARs seem to be the first, being expressed during early mammalian CNS ontogenesis (Bardoul et al. 1998a, 1998b; Gallo et al. 1995).

Neural stem cells

During brain embryogenesis, AMPAR and KAR are especially found on neural precursor cells in periventricular areas (Lidow and Rakic 1995; LoTurco et al. 1995). NMDA and kainate-gated currents have been recorded in primary cultures of embryonic rat hippocampal precursors, including NSCs, grown under proliferative conditions. Kainate-induced currents in NSCs could still be observed in the presence of various culture conditions even after multiple passages (Sah et al. 1997).

Neuroblasts

Recent studies have reported that mitotic neuroblasts derived from rat embryonic cortical NSCs and expanded in vitro in a defined medium do express functional iGluRs. Actually, inward currents as well as increase in cytosolic Ca^{2+} following AMPA and glutamate application were found in differentiating neurons and in a subpopulation of proliferating cells expressing the early neuronal marker β-tubulin III (TuJ1). This accounts for an early emergence of AMPA/KAR during terminal cell division of neuronal committed precursors (Maric et al. 2000; O'Connor et al. 2000).

Glutamate, via AMPA/KAR activation, could regulate periventricular progenitor proliferation as attested by its decreasing effect on [^{3}H]thymidine incorporation in rat E16 and E19 cortical explant neuroblasts (LoTurco et al. 1995). However, the VZ and SVZ subpopulations are differentially affected in situ, since glutamate agonists both increase the proliferation rate of VZ cells and decrease the SVZ cell proliferation (Haydar et al. 2000).

The *gyrus dentatus* retains a neurogenic population of cells throughout life in rodents (Altman and Das 1965, 1966; Cameron et al. 1993; Schlessinger et al. 1975), in primates (Gould et al. 1998, 1999) and even in human brains (Eriksson et al. 1998). Several studies performed in vivo have shown that the antagonism of NMDAR, either during the 1st postnatal week or in the adult, leads to an increase in [^{3}H]thymidine incorporation in rat *gyrus dentatus* maturing cells, mostly in granule neurons (Cameron et al. 1995, 1998b; Gould et al. 1994). Activation of these receptors following intraperitoneal injection of NMDA decreases the proliferation rate of neuroblasts in the adult rat *gyrus dentatus* (Cameron et al. 1995). The exact mechanism by which glutamate acts to block *gyrus dentatus* cell proliferation is currently unknown (reviewed by Cameron et al., 1998a). Based on similarities with the action of corticosterone, an adrenal steroid that reduces the *gyrus dentatus* cell neurogenesis (Cameron and Gould 1994), it has been hypothesized that glutamate and corticosterone may regulate cell division through a common pathway (Cameron et al. 1998b). Conversely, in the time course of rat striatum development, the antagonism of NMDAR decreases the proliferation of striatal neuroblasts during their proliferative phase in vivo (Sadikot et al. 1998). Additional evidence

suggests that, through the activation of iGluRs, glutamate could also interact with various other developmental processes such as cell survival, growth, differentiation and migration. A striking dependence on glutamate, acting at NMDAR, has been demonstrated for rat cerebellar P7–8 immature granule cell survival in culture (Balazs et al. 1988a, 1988b) and more recently in vivo for rat cerebellar P7–11 differentiating neurons (Monti and Contestabile 2000). These developmental stages correspond to a time period during which the excitatory input carried by incoming mossy fibres becomes massive in vivo (Arsenio Nunes and Sotelo 1985). This effect is likely to be dependent on Ca^{2+} entry through NMDAR (Burgoyne et al. 1993), since the activation of non-NMDAR does not affect granule cell survival but instead promote synaptogenesis in other systems (Mattson et al. 1988a). Similarly, NMDAR antagonism has been reported to reduce the survival of developing spinal cord neurons in vitro (Brenneman et al. 1990), and of *gyrus dentatus* neurons in vivo (Gould et al. 1994; Gould and Cameron 1996).

Glutamate is currently recognized as also playing a role in neural differentiation (Bading et al. 1995). Aruffo et al. have found that glutamate application on postnatal rat whole-brain dissociated cell cultures promotes neuronal growth and differentiation as compared to control cultures (Aruffo et al. 1987). Many studies have reported that the glutamate NMDAR activation promotes neurite outgrowth from cerebellar granule cells (Pearce et al. 1987) and dendritic outgrowth and branching of hippocampal cells (Brewer and Cotman 1989; Mattson et al. 1988b; Wilson et al. 2000).

Besides their neurite growth-promoting effect, NMDARs are also involved in synaptogenesis during development (Scheetz and Constantine-Paton 1994).

The migration of postmitotic neurons from brain germinative areas to their final destination in appropriate spatial and temporal patterns is a very complex process, involving multiple intrinsic and extrinsic signals (Rakic et al. 1994). Among these extracellular cues, neurotransmitters, and especially glutamate, are to be considered. If NMDARs are blocked by specific antagonists (Rossi and Slater 1993) or by high Mg^{2+} concentrations in cerebellar brain slices, the rate of mice granule cell migration from the external to the internal granule layer along the process of Bergmann glia is slowed down. Conversely, removal of Mg^{2+} or an increase in NMDA or glycine concentrations accelerates this phenomenon (Komuro and Rakic 1993). Behar et al. have also described a similar NMDAR-dependent effect in cultured murine embryonic cortical cells. In this study, glutamate and NMDA probably act as neuronal chemoattractants (Behar et al. 1999).

Glioblasts

During the last few years, several groups have found strong evidence for the expression of AMPAR and KAR in astrocytes both in culture and in situ (Kettenmann et al. 1984b; Porter et al. 1998). Glial AMPAR activation induces an increase in $[Na^+]_i$, which in turn blocks outward rectifying K^+ currents (Robert and Magistretti 1997). Since the block of K^+ channels reduces astroglial proliferation (Pappas et al. 1994), it has been suggested that AMPAR activation could be involved in glial differentiation (Verkhratsky and Steinhauser 2000). In addition, immediate early gene (e.g. c-*fos*, c-*jun*, *jun-B*) expression can be modulated by the activation of AMPAR and KAR, which therefore could trigger long-term changes in cellular function (Mack et al. 1994; Mc Naughton and Hunt 1992). Glutamate and kainate have been shown to induce the reorganization of the astrocytic membrane and hence, under physiological conditions where glutamate is synaptically released, have been proposed to play a role in active synapse detection and stabilization (Cornell-Bell et al. 1990; von Blankenfeld and Kettenmann 1991). The expression of NMDAR in glial cells is, in contrast, still debated. However, the proliferation of cultured glial Müller cells seems to involve these receptors (Uchihori and Puro 1993) and, furthermore, NMDAR activation inhibits their inwardly rectifying potassium currents (Puro et al. 1996). OPCs also express iGluRs. Actually, compelling evidence of AMPAR and KAR occurrence in these progenitors in vitro as well as in situ has been reported (Barres et al. 1990; Gallo et al. 1994; Jensen and Chiu 1993; Patneau et al. 1994). As is the case for astrocytes, NMDAR expression in OPCs is still a matter of debate, since one study has shown the expression of such receptors by OPCs derived from rat neurohypophysial explants. In these cells, migration depends on polysialic acid-neural cell adhesion molecule (PSA-NCAM) expression, which could be regulated by NMDAR activity (Wang et al. 1996). AMPAR, KAR and/or VGCC activation contribute to a calcium-dependent regulation of c-*fos* expression and inhibit OPC proliferation (Liu and Almazan 1995; Pende et al. 1994).

The observation that AMPA/KAR activation reversibly reduces voltage-gated K^+ outward currents (Borges et al. 1994) via Na^+ accumulation (Borges and Kettenmann 1995) leads to speculation about AMPA/KAR function in the control of OPC proliferation and differentiation (reviewed by Gallo and Ghiani, 2000). V. Gallo's group have demonstrated that AMPA/KAR activation blocks spontaneous OPC proliferation and lineage progression through a Ca^{2+}-independent mechanism that involves Na^+ blockade of outward K^+ currents (Gallo et al. 1996; Knutson et al. 1997). The mechanism downstream of the blocking of outward K^+ currents seems to involve the accumulation of the cyclin-dependent kinase inhibitors p27/Kip and P21/Cip1 (Ghiani et al. 1999), known to induce a G1 arrest in the OPCs' cell cycle (Tikoo et al. 1998). Similar effects of glutamate on OPC proliferation and differentiation were reported in situ in postnatal cerebellar slices (Yuan et al. 1998).

Finally, the discovery of glutamatergic synapses between OPCs and neurons in situ (Bergles et al. 2000)

adds one more argument to the probable role that glutamate exerts during the development of OPCs in vivo.

Acetylcholine

Acetylcholine receptors include two classes of receptors that are named according to their main agonist, the naturally occurring plant alkaloids nicotine and muscarine. Nicotinic receptors (nAChRs) are the archetypal model of the ligand-gated ion channel superfamily (le Novere and Changeux 1999). They are pentamers of subunits surrounding a central cation-selective pore, and, besides a significant permeability to Ca^{2+} (Pugh and Berg 1994; Rathouz and Berg 1994; Zheng et al. 1994), they do not readily distinguish among monovalent cations (Waxham 1999). nAChRs form a family of receptors that are differentially expressed in many regions of the CNS and the peripheral nervous system (PNS). Neuronal nAChRs are solely composed of α- and β-subunits and are pharmacologically distinct from muscle nAChRs, which also include other subunits. In addition, neural nAChRs can also be subclassified based upon their sensitivity to the snake venom α-bungarotoxin (α-Bgtx-nAChRs and α-Bgtx-insensitive nAChRs; reviewed by Chew and Gallo, 1998; Cordero-Erausquin et al. 2000). Muscarinic receptors (mAChRs), which are composed of seven membrane-spanning domains, are metabotropic and coupled to G protein(s), thus belonging to another superfamily that activates second messenger pathways (Caulfield and Birdsall 1998; Waxham 1999).

nAChRs are widely distributed throughout the mammalian CNS (Quik et al. 2000; Zoli et al. 1995) and notably in adult and developing human brain (Court et al. 1995, 1997; Gotti et al. 1997; Kinney et al. 1993; Paterson and Nordberg 2000). The activity of these ionotropic receptors contributes to a wide range of brain processes from cognitive functions such as learning, memory formation or reward (Jones et al. 1999; Levin 1992), to cellular events such as degeneration (Zoli et al. 1999) and neural development (Table 4; Coronas et al. 2000; Jones et al. 1999; Lauder 1993).

Neuroblasts

The temporal coincidence of the presence of both choline acetyltransferase (ChAT) and various nAChR subunits during early embryogenesis (Role and Berg 1996) strongly suggests a role for acetylcholine during neuronal development. Actually, several studies have shown that acetylcholine can regulate different aspects of nervous system morphogenesis at least in vitro. For instance, acetylcholine induces neuritic outgrowth in neonatal rat primary olfactory bulb cultures through α7-like nAChR activation (Coronas et al. 2000). Conversely, acetylcholine inhibits neuritic extension of embryonic mouse spinal cord neurons (Owen and Bird 1995). In addition, Zheng et al. have shown that acetylcholine is a powerful chemoattractant for embryonic nerve growth-cone guidance in vitro through the activation of Ca^{2+}-permeable nAChR (Zheng et al. 1994).

Recent physiological studies support the idea that nAChRs are involved in the development of the sensory cortex in mammals (reviewed by Jones et al. 1999). The transient activation of nAChR during crucial periods of

Table 4 Acetylcholine-induced events in neural progenitors (*IM* immunostainings, *BD* binding, *Sbio* survival bioassay, *VIA* video-analysis imaging, *Ph* photograpical analysis, *CaI* calcium imaging, *PC* patch-clamp, *VIA* video-analysis imaging, *Phstim* photostimulation, *Sbio* survival bioassay, *AU* autoradiography)

Acetylcholine

Cell Stages	Model/Techniques	Results	References
Neuroblasts	P1–3 rat olfactory bulb in vitro: IM/BD/Sbio/VIA	Activation of α7-like nAChR promotes neuronal neuritic outgrowth	Coronas et al. 2000
	E15–17 mouse spinal cord neurons in vitro: Ph	Activation of α7-like nAChR inhibits neuronal neuritic outgrowth and motility	Owen and Bird 1995
	Developing *Xenopus* neurons in vitro: CaI/VIA	Acetylcholine exerts chemoattractance for guidance of embryonic nerve growth cones	Zheng et al. 1994
	P8–24 rat cortex and P6–57 ferret cortex in situ: PC/IM/Phstim	Transient activation of nAChR during crucial periods of cortical development promotes formation and strengthening of synapse	Aramakis et al. 1998; Roerig et al. 1997
	Adult/embryonic rodent striatal, cortical and hippocampal neurons in vitro: Sbio	Nicotinic agonists prevent rat cortical cell death resulting from glutamate exposure	Belluardo et al. 2000
	E16 rat hippocampi progenitors in vitro: Sbio	Nicotinic agonists enhance hippocampal progenitor death resulting rom glutamate exposure	Berger et al. 1998
Glioblasts	Rat brain stem and spinal cord astrocytes in situ: AU	Expression of nAChRs	Hosli et al. 1988
	Newborn rat OPCs in vitro: PC/CaI	Functional expression of nAChR in culture	Belachew et al. 1998a, 1988b

cortical development may promote the formation and the strengthening of synapses, both in the developing rat auditory cortex (Aramakis and Metherate 1998) and in the developing ferret visual cortex (Roerig and Katz 1997; Roerig et al. 1997).

Experimental evidences have underlined the differences existing between mature and progenitor cells regarding the effect of nAChR activation on their survival. It has been reported that, via a calcium-dependent pathway, nicotine can prevent rodent striatal, cortical or hippocampal neuronal death resulting from glutamate exposure (Akaike et al. 1994; Kaneko et al. 1997; Marin et al. 1994). In contrast, the activation of α-Bgtx-nAChR by nicotine leads to the apoptotic cell death of rat hippocampal progenitor cells. This cytotoxic effect of nicotine is a Ca^{2+}-dependent process and involves the induction of the tumour suppressor p53 and the cdk inhibitor p21 (Berger et al. 1998). More recently, the implication of α-Bgtx-nAChR activation in apoptotic cell death in mice somatosensory cortex was furthermore supported by a study on transgenic mice expressing mutated α7-nAChR. The mutation consisted of leucine to threonine (position 250) substitution, which leads to an increase in agonist affinity and to a decrease in the desensitization rate of the receptors, creating a "gain of function". Homozygote mutants are not viable and present an abnormal apoptotic cell death, which is observed throughout their somatosensory cortex, possibly due to calcium influx (Orr-Urtreger et al. 2000). Finally, nAChR activation has also been shown to enhance early gene expression prior to neuronal differentiation (reviewed by Role and Berg, 1996).

Glioblasts

An autoradiographic study has revealed the expression of nAChRs on astrocytes from rat brain stem and spinal cord in organotypic cultures (Hosli and Hosli 1988). Moreover, these nAChRs seem to be fully functional in astrocytes, since hyperpolarization induced by nicotine application was antagonized by mecamylamine hydrochloride, a specific nAChR antagonist (Hosli et al. 1988). The physiological function fulfilled by these receptors in glia is currently not understood. The coexistence of both cholinergic and peptidergic receptors on astrocytes is of great interest, since both neurotransmitter systems are involved in cognitive functions and impaired in Alzheimer's patients. This raises the question of the potential involvement – besides neurons – of astrocytes in neurodegenerative disorders (Hosli and Hosli 2000).

Belachew et al. have demonstrated the occurrence of acetylcholine-elicited currents specifically antagonized by the nAChR blocker hexamethonium in OPCs located in the outgrowth zone of expanded cultured oligospheres. The authors have also suggested that acetylcholine, through a depolarizing mechanism, could influence some biological properties of OPCs, perhaps through a modulation of $[Ca^{2+}]_i$ (Belachew et al. 1998a).

Serotonin

A large number of studies have been devoted to the classification of the mammalian 5-hydroxytryptamine receptors (5-HTR; reviewed by Barnes and Sharp, 1999). Most of the seven described 5-HTR families ($5\text{-}HT_{1–7}$) are metabotropic and coupled to G protein. Only the $5\text{-}HT_3R$ is ionotropic and mediates rapid excitatory responses through a ligand-gated ion channel (Derkach et al. 1989; le Novere and Changeux 1999). As in other ligand-gated ion channels from the nicotinic family, the $5\text{-}HT_3Rs$ are comprised of five transmembrane subunits that form a multimeric ring surrounding a central cation-selective channel. This ionic pore is mainly permeant to Na^+ and K^+, with a variable permeability for Ca^{2+} according to the receptor subunit stoichiometry (Derkach et al. 1989; Hargreaves et al. 1994; Ronde and Nichols 1998). To date, two distinct subunits are known to be part of native $5\text{-}HT_3Rs$, the $5\text{-}HT_{3A}$ [Maricq et al. 1991; including an alternatively spliced variant (Hope et al. 1993)] and the $5\text{-}HT_{3B}$ (Davies et al. 1999). Despite some species-to-species variations, the highest levels of $5\text{-}HT_3R$ expression are found generally within the brain stem (especially in the vagal complex), the hippocampus, the amygdala and the superficial layers of the cerebral cortex (reviewed by Barnes and Sharp, 1999).

The early appearance of both serotonin (5-HT; Lauder et al. 1981) and its receptor during prenatal development (Tecott et al. 1995; Wallace and Lauder 1983), together with the widespread effects of 5-HT during CNS morphogenesis (reviewed by Whitaker-Azmitia et al., 1996), strongly suggest that this biogenic amine plays a regulating role in the development and the maturation of the mammalian brain, prior to the period when it assumes its neuromodulatory role (Table 5).

Neuroblasts

A number of investigations indicate that 5-HT plays an important role during cortical development. The early occurrence of serotoninergic innervation in developing cortical pathways (D'Amato et al. 1987; Nakazawa et al. 1992) suggests a role for serotonin in brain circuit formation (reviewed by Roerig and Feller 2000) and synaptogenesis (Haydon et al. 1987; Mazer et al. 1997). Serotoninergic fibres invade the ferret visual cortex several weeks before eye opening. It appears that $5\text{-}HT_3R$ signalling may be required during activity-dependent stages of visual cortex circuit formation (Roerig and Katz 1997; Roerig et al. 1997). Chubakov et al. have identified various 5-HT-induced trophic effects on rat neocortical explants that could be partly mediated by $5\text{-}HT_3R$, including neuronal differentiation and synaptogenesis (Chubakov et al. 1986a). A recent report suggests, moreover, that 5-HT is required for normal early brain maturation, since the depletion of 5-HT during this critical period leads to a decrease in synaptic density and impairs the cognitive capabilities in adult rats (Mazer et al. 1997).

Table 5 Serotonin-induced events in neural progenitors (*PC* patch-clamp, *Phstim* photostimulation, *HSOI* high-speed optical imaging, *IM* immunostainings, *Melec* microelectrode, *EM* electron microscopy, *CaI* calcium imaging)

Serotonin			
Cell stage	Model/Techniques	Results	References
Neuroblasts	P6–57 ferret visual cortex in situ: PC/Phstim/HSOI	5-HT_3R signalling may be required during activity-dependent stages of cortex circuits formation	Roerig and Katz 1997; Roerig et al. 1997
	Newborn rat cortical explants in situ: Melec/EM	Serotonin hastrophic-induced effects, which could be partly mediated by 5-HT_3R, including neuronal differentiation and synaptogenesis	Chubakov et al. 1986a, 1986b
Glioblasts	Newborn rat cortical OPCs in vitro: PC/CaI	5-HT_3R functionally expressed	Belachew et al. 1998a, 1988b

Glioblasts

So far, very few studies have been devoted to the effects mediated by 5-HT_3R on glia. Our group has identified functional 5-HT_3Rs in neonatal cortical rat oligosphere-derived OPCs. Serotonin application triggers inward currents that are reversibly inhibited by 3′5-tropyl-dichlorobenzoate, a 5-HT_3R-specific antagonist. Regarding these results, we have suggested an increase in 5-HT_3R expression with in vitro differentiation (Belachew et al. 1998a). In vitro, serotonin has been proposed to stimulate glial proliferation and myelination (Chubakov et al. 1986b). In addition, recent work has shown that 5-HT could exert various developmental effects on cultured postnatal forebrain OPCs, including an increase in myelin basic protein (MBP)-expressing cells and a putative cooperative effect between 5-HT and brain-derived neurotrophic factor (BDNF) to enhance DNA synthesis by these OPCs (Keise et al. 2000).

Conclusions

Until recently, the adult mammalian brain was considered as a non-renewable organ devoid of any regenerative neuronal capacities, hence making it particularly vulnerable to injury or disease (Rakic 1985). This concept has dramatically changed over the last 20 years; many studies testifying the occurrence of NSCs in adult CNS have been conducted by numerous groups (Doetsch et al. 1999a; Johansson et al. 1999; Reynolds and Weiss 1992; Weiss et al. 1996). These cells are characterized by their ability to self-renew and to generate at least all the cell phenotypes that constitute their original tissue (McKay 1997). Despite the existence of such NSCs in adulthood, the CNS still retains a limited capacity of self-renewal after traumatic injuries or neurodegenerative damage (Cameron and McKay 1999; Doetsch et al. 1999b; Scharfman et al. 2000). This could be the result of adult stem cells being generally in a quiescent state except in the *gyrus dentatus* (Cameron et al. 1993) and in the SVZ (Lois and Alvarez-Buylla 1993), where they can generate, respectively, hippocampal interneurons (Kaplan and Bell 1984) and neurons that migrate towards the olfactory bulbs (Lois and Alvarez-Buylla 1994; Luskin and Boone 1994).

The generation of distinct types of neurons and glial cells from NSCs involves a sequence of intermediate progenitor stages that are controlled by environmental and intrinsic regulatory signals (Edlund and Jessell 1999). In that respect, one could imagine the restoration of brain function after injuries caused by trauma or chronic neurodegenerative diseases by awakening resident stem cells or by performing stem-like cell grafts. This is why recently much effort has been devoted to characterize intrinsic and extrinsic factors regulating the behaviour of neural progenitor cell populations during brain maturation. This review provides evidence showing that neurotransmitters and their corresponding ligand-gated ion channel receptors exert, in vitro and in vivo, various roles during primary nervous structure establishment prior to the emergence of their role in neurotransmission. In that way, the early activation of some ligand-gated ion channel receptors, expressed by several kinds of neural progenitors, could account in vivo for the regulation of proliferation, migration, differentiation or even survival processes during neural development.

Since many neuropharmacological tools are already available to treat various disorders such as epilepsy, depression, anxiety and schizophrenia and if, as proposed here, neurotransmitters actually play a role during early CNS development, those drugs could well find a second life as adult brain repair aids. There is therefore an urgent need for further studies aimed at establishing a functional significance for these neurotransmitter receptors and in particular a need for appropriate in vivo models.

Acknowledgements B. Malgrange, P. Leprince and B. Rogister are research associates, and S. Belachew is a post-doctoral researcher of the FNRS.

References

Agrawal HC, Davison AN, Kaczmarek LK (1971) Subcellular distribution of taurine and cysteine sulphinate decarboxylase in developing rat brain. Biochem J 122:759–763

Akaike A, Tamura Y, Yokota T, Shimohama S, Kimura J (1994) Nicotine-induced protection of cultured cortical neurons against *N*-methyl-D-aspartate receptor-mediated glutamate cytotoxicity. Brain Res 644:181–187

Altman J, Das GD (1965) Autoradiographic and histological evidence of postnatal hippocampal neurogenesis in rats. J Comp Neurol 124:319–335

Altman J, Das GD (1966) Autoradiographic and histological studies of postnatal neurogenesis. I. A longitudinal investigation of the kinetics, migration and transformation of cells incorporating tritiated thymidine in neonate rats, with special reference to postnatal neurogenesis in some brain regions. J Comp Neurol 126:337–389

Antonopoulos J, Pappas IS, Parnavelas JG (1997) Activation of the $GABA_A$ receptor inhibits the proliferative effects of bFGF in cortical progenitor cells. Eur J Neurosci 9:291–298

Aprison MH, Shank RP, Davidoff RA (1969) A comparison of the concentration of glycine, a transmitter suspect, in different areas of the brain and spinal cord in seven different vertebrates. Comp Biochem Physiol 28:1345–1355

Aramakis VB, Metherate R (1998) Nicotine selectively enhances NMDA receptor-mediated synaptic transmission during postnatal development in sensory neocortex. J Neurosci 18:8485–8495

Arsenio Nunes ML, Sotelo C (1985) Development of the spinocerebellar system in the postnatal rat. J Comp Neurol 237:291–306

Aruffo C, Ferszt R, Hildebrandt AG, Cervos-Navarro J (1987) Low doses of L-monosodium glutamate promote neuronal growth and differentiation in vitro. Dev Neurosci 9:228–239

Bading H, Segal MM, Sucher NJ, Dudek H, Lipton SA, Greenberg ME (1995) *N*-Methyl-D-aspartate receptors are critical for mediating the effects of glutamate on intracellular calcium concentration and immediate early gene expression in cultured hippocampal neurons. Neuroscience 64:653–664

Balazs R, Jorgensen OS, Hack N (1988a) *N*-Methyl-D-aspartate promotes the survival of cerebellar granule cells in culture. Neuroscience 27:437–451

Balazs R, Hack N, Jorgensen OS (1988b) Stimulation of the *N*-methyl-D-aspartate receptor has a trophic effect on differentiating cerebellar granule cells. Neurosci Lett 87:80–8

Barbin G, Pollard H, Gaiarsa JL, Ben Ari Y (1993) Involvement of $GABA_A$ receptors in the outgrowth of cultured hippocampal neurons. Neurosci Lett 152:150–154

Bardoul M, Drain MJ, Konig N (1998a) Modulation of intracellular calcium in early neural cells by non-NMDA ionotropic glutamate receptors. Perspect Dev Neurobiol 5:353–371

Bardoul M, Levallois C, Konig N (1998b) Functional AMPA/kainate receptors in human embryonic and foetal central nervous system. J Chem Neuroanat 14:79–85

Barker JL, Behar T, Li YX, Liu QY, Ma W, Maric D, Maric I, Schaffner AE, Serafini R, Smith SV, Somogyi R, Vautrin JY, Wen XL, Xian H (1998) GABAergic cells and signals in CNS development. Perspect Dev Neurobiol 5:305–322

Barnes NM, Sharp T (1999) A review of central 5-HT receptors and their function. Neuropharmacology 38:1083–1152

Barres BA, Koroshetz WJ, Swartz KJ, Chun LL, Corey DP (1990) Ion channel expression by white matter glia: the O-2A glial progenitor cell. Neuron 4:507–524

Behar TN, Schaffner AE, Colton CA, Somogyi R, Olah Z, Lehel C, Barker JL (1994) GABA-induced chemokinesis and NGF-induced chemotaxis of embryonic spinal cord neurons. J Neurosci 14:29–38

Behar TN, Li YX, Tran HT, Ma W, Dunlap V, Scott C, Barker JL (1996) GABA stimulates chemotaxis and chemokinesis of embryonic cortical neurons via calcium-dependent mechanisms. J Neurosci 16:1808–1818

Behar TN, Scott CA, Greene CL, Wen X, Smith SV, Maric D, Liu QY, Colton CA, Barker JL (1999) Glutamate acting at NMDA receptors stimulates embryonic cortical neuronal migration. J Neurosci 19:4449–4461

Behar TN, Schaffner AE, Scott CA, Greene CL, Barker JL (2000) GABA receptor antagonists modulate postmitotic cell migration in slice cultures of embryonic rat cortex. Cereb Cortex 10:899–909

Belachew S, Malgrange B, Rigo JM, Rogister B, Coucke P, Mazy-Servais C, Moonen G (1998a) Developmental regulation of neuroligand-induced responses in cultured oligodendroglia. Neuroreport 9:973–980

Belachew S, Rogister B, Rigo JM, Malgrange B, Mazy-Servais C, Xhauflaire G, Coucke P, Moonen G (1998b) Cultured oligodendrocyte progenitors derived from cerebral cortex express a glycine receptor which is pharmacologically distinct from the neuronal isoform. Eur J Neurosci 10:3556–3564

Belachew S, Malgrange B, Rigo JM, Rogister B, Leprince P, Hans G, Nguyen L, Moonen G (2000) Glycine triggers an intracellular calcium influx in oligodendrocyte progenitor cells which is mediated by the activation of both the ionotropic glycine receptor and Na^+-dependent transporters. Eur J Neurosci 12: 1924–1930

Belluardo N, Mudo G, Blum M, Fuxe K (2000) Central nicotinic receptors, neurotrophic factors and neuroprotection. Behav Brain Res 113:21–34

Berger F, Gage FH, Vijayaraghavan S (1998) Nicotinic receptor-induced apoptotic cell death of hippocampal progenitor cells. J Neurosci 18:6871–6881

Bergles DE, Roberts JD, Somogyi P, Jahr CE (2000) Glutamatergic synapses on oligodendrocyte precursor cells in the hippocampus. Nature 405:187–191

Bettler B, Mulle C (1995) Review: neurotransmitter receptors. II. AMPA and kainate receptors. Neuropharmacology 34:123–139

Betz H (1991) Glycine receptors: heterogeneous and widespread in the mammalian brain. Trends Neurosci 14:458–461

Betz H, Kuhse J, Fischer M, Schmieden V, Laube B, Kuryatov A, Langosch D, Meyer G, Bormann J, Rundstrom N (1994) Structure, diversity and synaptic localization of inhibitory glycine receptors. J Physiol (Paris) 88:243–248

Blankenfeld G von, Kettenmann H (1991) Glutamate and GABA receptors in vertebrate glial cells. Mol Neurobiol 5:31–43

Bonnert TP, McKernan RM, Farrar S, le Bourdelles B, Heavens RP, Smith DW, Hewson L, Rigby MR, Sirinathsinghji DJ, Brown N, Wafford KA, Whiting PJ (1999) theta, a novel gamma-aminobutyric acid type A receptor subunit. Proc Natl Acad Sci USA 96:9891–9896

Borges K, Dingledine R (1998) AMPA receptors: molecular and functional diversity. Prog Brain Res 116:153–170

Borges K, Kettenmann H (1995) Blockade of K^+ channels induced by AMPA/kainate receptor activation in mouse oligodendrocyte precursor cells is mediated by Na^+ entry. J Neurosci Res 42:579–593

Borges K, Ohlemeyer C, Trotter J, Kettenmann H (1994) AMPA/kainate receptor activation in murine oligodendrocyte precursor cells leads to activation of a cation conductance, calcium influx and blockade of delayed rectifying K^+ channels. Neuroscience 63:135–149

Bormann J, Feigenspan A (1995) GABAC receptors. Trends Neurosci 18:515–519

Bormann J, Kettenmann H (1988) Patch-clamp study of gamma-aminobutyric acid receptor Cl^- channels in cultured astrocytes. Proc Natl Acad Sci USA 85:9336–9340

Brenneman DE, Forsythe ID, Nicol T, Nelson PG (1990) *N*-Methyl-D-aspartate receptors influence neuronal survival in developing spinal cord cultures. Brain Res Dev Brain Res 51:63–68

Brewer GJ, Cotman CW (1989) NMDA receptor regulation of neuronal morphology in cultured hippocampal neurons. Neurosci Lett 99:268–273

Brezun JM, Daszuta A (2000) Serotonin may stimulate granule cell proliferation in the adult hippocampus, as observed in rats grafted with foetal raphe neurons. Eur J Neurosci 12:391–396

Burgoyne RD, Graham ME, Cambray-Deakin M (1993) Neurotrophic effects of NMDA receptor activation on developing cerebellar granule cells. J Neurocytol 22:689–695

Butler AK, Uryu K, Rougon G, Chesselet MF (1999) *N*-Methyl-D-aspartate receptor blockade affects polysialylated neural cell adhesion molecule expression and synaptic density during striatal development. Neuroscience 89:1169–1181

Butt AM, Jennings J (1994) Response of astrocytes to gamma-aminobutyric acid in the neonatal rat optic nerve. Neurosci Lett 168:53–56

Cameron HA, Gould E (1994) Adult neurogenesis is regulated by adrenal steroids in the dentate gyrus. Neuroscience 61:203–209

Cameron HA, McKay RD (1999) Restoring production of hippocampal neurons in old age. Nat Neurosci 2:894–897

Cameron HA, Woolley CS, McEwen BS, Gould E (1993) Differentiation of newly born neurons and glia in the dentate gyrus of the adult rat. Neuroscience 56:337–344

Cameron HA, McEwen BS, Gould E (1995) Regulation of adult neurogenesis by excitatory input and NMDA receptor activation in the dentate gyrus. J Neurosci 15:4687–4692

Cameron HA, Hazel TG, McKay RD (1998a) Regulation of neurogenesis by growth factors and neurotransmitters. J Neurobiol 36:287–306

Cameron HA, Tanapat P, Gould E (1998b) Adrenal steroids and *N*-methyl-D-aspartate receptor activation regulate neurogenesis in the dentate gyrus of adult rats through a common pathway. Neuroscience 82:349–354

Caulfield MP, Birdsall NJ (1998) International Union of Pharmacology. XVII. Classification of muscarinic acetylcholine receptors. Pharmacol Rev 50:279–290

Chebib M, Johnston GA (1999) The "ABC" of GABA receptors: a brief review. Clin Exp Pharmacol Physiol 26:937–940

Chew LJ, Gallo V (1998) Regulation of ion channel expression in neural cells by hormones and growth factors. Mol Neurobiol 18:175–225

Chubakov AR, Gromova EA, Konovalov GV, Sarkisova EF, Chumasov EI (1986a) The effects of serotonin on the morphofunctional development of rat cerebral neocortex in tissue culture. Brain Res 369:285–297

Chubakov AR, Gromova EA, Konovalov GV, Chumasov EI, Sarkisova EF (1986b) Effect of serotonin on the development of a rat cerebral cortex tissue culture. Neurosci Behav Physiol 16:490–497

Cicirata F, Meli C, Castorina C, Serapide MF, Sorrenti V, Di Giacomo C, Gambera G, Vanella A (1991) Neurotransmitter amino acid levels in rat thalamus and cerebral cortex after cerebellectomy. Int J Dev Neurosci 9:365–369

Connors BW, Malenka RC, Silva LR (1988) Two inhibitory postsynaptic potentials, and $GABA_A$ and $GABA_B$ receptor-mediated responses in neocortex of rat and cat. J Physiol (Lond) 406:443–468

Cordero-Erausquin M, Marubio LM, Klink R, Changeux JP (2000) Nicotinic receptor function: new perspectives from knockout mice. Trends Pharmacol Sci 21:211–217

Cornell-Bell AH, Thomas PG, Smith SJ (1990) The excitatory neurotransmitter glutamate causes filopodia formation in cultured hippocampal astrocytes. Glia 3:322–334

Coronas V, Durand M, Chabot JG, Jourdan F, Quirion R (2000) Acetylcholine induces neuritic outgrowth in rat primary olfactory bulb cultures. Neuroscience 98:213–219

Court JA, Perry EK, Spurden D, Griffiths M, Kerwin JM, Morris CM, Johnson M, Oakley AE, Birdsall NJ, Clementi F (1995) The role of the cholinergic system in the development of the human cerebellum. Brain Res Dev Brain Res 90:159–167

Court JA, Lloyd S, Johnson M, Griffiths M, Birdsall NJ, Piggott MA, Oakley AE, Ince PG, Perry EK, Perry RH (1997) Nicotinic and muscarinic cholinergic receptor binding in the human hippocampal formation during development and aging. Brain Res Dev Brain Res 101:93–105

D'Amato RJ, Blue ME, Largent BL, Lynch DR, Ledbetter DJ, Molliver ME, Snyder SH (1987) Ontogeny of the serotonergic projection to rat neocortex: transient expression of a dense innervation to primary sensory areas. Proc Natl Acad Sci USA 84:4322–4326

Davies PA, Hanna MC, Hales TG, Kirkness EF (1997) Insensitivity to anaesthetic agents conferred by a class of GABA(A) receptor subunit. Nature 385:820–823

Davies PA, Pistis M, Hanna MC, Peters JA, Lambert JJ, Hales TG, Kirkness EF (1999) The $5\text{-}HT_3B$ subunit is a major determinant of serotonin-receptor function. Nature 397:359–363

Derkach V, Surprenant A, North RA (1989) 5-HT3 receptors are membrane ion channels. Nature 339:706–709

Dingledine R, Borges K, Bowie D, Traynelis SF (1999) The glutamate receptor ion channels. Pharmacol Rev 51:7–61

Doetsch F, Caille I, Lim DA, Garcia-Verdugo JM, Alvarez-Buylla A (1999a) Subventricular zone astrocytes are neural stem cells in the adult mammalian brain. Cell 97:703–716

Doetsch F, Garcia-Verdugo JM, Alvarez-Buylla A (1999b) Regeneration of a germinal layer in the adult mammalian brain. Proc Natl Acad Sci USA 96:11619–11624

Edlund T, Jessell TM (1999) Progression from extrinsic to intrinsic signaling in cell fate specification: a view from the nervous system. Cell 96:211–224

Engelsen B (1986) Neurotransmitter glutamate: its clinical importance. Acta Neurol Scand 74:337–355

Eriksson PS, Perfilieva E, Bjork-Eriksson T, Alborn AM, Nordborg C, Peterson DA, Gage FH (1998) Neurogenesis in the adult human hippocampus. Nat Med 4:1313–1317

Fiszman ML, Borodinsky LN, Neale JH (1999) GABA induces proliferation of immature cerebellar granule cells grown in vitro. Brain Res Dev Brain Res 115:1–8

Flint AC, Liu X, Kriegstein AR (1998) Nonsynaptic glycine receptor activation during early neocortical development. Neuron 20:43–53

Fonnum F (1984) Glutamate: a neurotransmitter in mammalian brain. J Neurochem 42:1–11

Furuya S, Tabata T, Mitoma J, Yamada K, Yamasaki M, Makino A, Yamamoto T, Watanabe M, Kano M, Hirabayashi Y (2000) L-Serine and glycine serve as major astroglia-derived trophic factors for cerebellar Purkinje neurons. Proc Natl Acad Sci USA 97:11528–11533

Gage FH (2000) Mammalian neural stem cells. Science 287:1433–1438

Gallo V, Ghiani CA (2000) Glutamate receptors in glia: new cells, new inputs and new functions. Trends Pharmacol Sci 21:252–258

Gallo V, Patneau DK, Mayer ML, Vaccarino FM (1994) Excitatory amino acid receptors in glial progenitor cells: molecular and functional properties. Glia 11:94–101

Gallo V, Pende M, Scherer S, Molne M, Wright P (1995) Expression and regulation of kainate and AMPA receptors in uncommitted and committed neural progenitors. Neurochem Res 20: 549–560

Gallo V, Zhou JM, McBain CJ, Wright P, Knutson PL, Armstrong RC (1996) Oligodendrocyte progenitor cell proliferation and lineage progression are regulated by glutamate receptor-mediated K^+ channel block. J Neurosci 16:2659–2670

Ghiani CA, Eisen AM, Yuan X, DePinho RA, McBain CJ, Gallo V (1999) Neurotransmitter receptor activation triggers p27(Kip1) and p21(CIP1) accumulation and G1 cell cycle arrest in oligodendrocyte progenitors. Development 126:1077–1090

Gilbert P, Kettenmann H, Schachner M (1984) Gamma-aminobutyric acid directly depolarizes cultured oligodendrocytes. J Neurosci 4:561–569

Gotti C, Fornasari D, Clementi F (1997) Human neuronal nicotinic receptors. Prog Neurobiol 53:199–237

Gould E, Cameron HA (1996) Regulation of neuronal birth, migration and death in the rat dentate gyrus. Dev Neurosci 18:22–35

Gould E, Cameron HA, McEwen BS (1994) Blockade of NMDA receptors increases cell death and birth in the developing rat dentate gyrus. J Comp Neurol 340:551–565

Gould E, Tanapat P, McEwen BS, Flugge G, Fuchs E (1998) Proliferation of granule cell precursors in the dentate gyrus of

adult monkeys is diminished by stress. Proc Natl Acad Sci USA 95:3168–3171

Gould E, Reeves AJ, Fallah M, Tanapat P, Gross CG, Fuchs E (1999) Hippocampal neurogenesis in adult Old World primates. Proc Natl Acad Sci USA 96:5263–5267

Hargreaves AC, Lummis SC, Taylor CW (1994) Ca2+ permeability of cloned and native 5-hydroxytryptamine type 3 receptors. Mol Pharmacol 46:1120–1128

Hashimoto A, Oka T, Nishikawa T (1995) Extracellular concentration of endogenous free D-serine in the rat brain as revealed by in vivo microdialysis. Neuroscience 66:635–643

Haydar TF, Wang F, Schwartz ML, Rakic P (2000) Differential modulation of proliferation in the neocortical ventricular and subventricular zones. J Neurosci 20:5764–5774

Haydon PG, McCobb DP, Kater SB (1987) The regulation of neurite outgrowth, growth cone motility, and electrical synaptogenesis by serotonin. J Neurobiol 18:197–215

Hope AG, Downie DL, Sutherland L, Lambert JJ, Peters JA, Burchell B (1993) Cloning and functional expression of an apparent splice variant of the murine 5-HT_3 receptor A subunit. Eur J Pharmacol 245:187–192

Hosli E, Hosli L (1988) Autoradiographic localization of binding sites for muscarinic and nicotinic agonists and antagonists on cultured astrocytes. Exp Brain Res 71:450–454

Hosli E, Hosli L (2000) Colocalization of neurotransmitter receptors on astrocytes in explant cultures of rat CNS. Neurochem Int 36:301–311

Hosli L, Hosli E, Della BG, Quadri L, Heuss L (1988) Action of acetylcholine, muscarine, nicotine and antagonists on the membrane potential of astrocytes in cultured rat brain stem and spinal cord. Neurosci Lett 92:165–170

Hosli E, Otten U, Hosli L (1997) Expression of GABA(A) receptors by reactive astrocytes in explant and primary cultures of rat CNS. Int J Dev Neurosci 15:949–960

Ikeda Y, Nishiyama N, Saito H, Katsuki H (1997) $GABA_A$ receptor stimulation promotes survival of embryonic rat striatal neurons in culture. Brain Res Dev Brain Res 98:253–258

Jaeken J, Detheux M, Van Maldergem L, Foulon M, Carchon H, Schaftingen E van (1996) 3-Phosphoglycerate dehydrogenase deficiency: an inborn error of serine biosynthesis. Arch Dis Child 74:542–545

Jensen AM, Chiu SY (1993) Expression of glutamate receptor genes in white matter: developing and adult rat optic nerve. J Neurosci 13:1664–1675

Johansson CB, Momma S, Clarke DL, Risling M, Lendahl U, Frisen J (1999) Identification of a neural stem cell in the adult mammalian central nervous system. Cell 96:25–34

Jones S, Sudweeks S, Yakel JL (1999) Nicotinic receptors in the brain: correlating physiology with function. Trends Neurosci 22:555–561

Kaneko S, Maeda T, Kume T, Kochiyama H, Akaike A, Shimohama S, Kimura J (1997) Nicotine protects cultured cortical neurons against glutamate-induced cytotoxicity via alpha7-neuronal receptors and neuronal CNS receptors. Brain Res 765:135–140

Kaplan MS, Bell DH (1984) Mitotic neuroblasts in the 9-day-old and 11-month-old rodent hippocampus. J Neurosci 4:1429–1441

Keise LL, Zaremba TM, Lercher LD, DiCicco-Bloom E, Dreyfus CF (2000) Basal forebrain (BF) oligodendrocytes (OLGS) respond to 5-hydroxytryptamine (5-HT) in culture. Soc Neurosci Abstr 318:11

Kettenmann H, Gilbert P, Schachner M (1984a) Depolarization of cultured oligodendrocytes by glutamate and GABA. Neurosci Lett 47:271–276

Kettenmann H, Backus KH, Schachner M (1984b) Aspartate, glutamate and gamma-aminobutyric acid depolarize cultured astrocytes. Neurosci Lett 52:25–29

Kinney HC, O'Donnell TJ, Kriger P, White WF (1993) Early developmental changes in [^{3}H]nicotine binding in the human brain stem. Neuroscience 55:1127–1138

Kirchhoff F, Kettenmann H (1992) GABA triggers a $[Ca^{2+}]_i$ increase in murine precursor cells of the oligodendrocyte lineage. Eur J Neurosci 4:1049–1058

Kirchhoff F, Mulhardt C, Pastor A, Becker CM, Kettenmann H (1996) Expression of glycine receptor subunits in glial cells of the rat spinal cord. J Neurochem 66:1383–1390

Kneussel M, Betz H (2000) Clustering of inhibitory neurotransmitter receptors at developing postsynaptic sites: the membrane activation model. Trends Neurosci 23:429–435

Knutson P, Ghiani CA, Zhou JM, Gallo V, McBain CJ (1997) K^+ channel expression and cell proliferation are regulated by intracellular sodium and membrane depolarization in oligodendrocyte progenitor cells. J Neurosci 17:2669–2682

Komuro H, Rakic P (1993) Modulation of neuronal migration by NMDA receptors. Science 260:95–97

Krnjevic K, Schwartz S (1967) The action of gamma-aminobutyric acid on cortical neurones. Exp Brain Res 3:320–336

Kuhse J, Schmieden V, Betz H (1990) Identification and functional expression of a novel ligand binding subunit of the inhibitory glycine receptor. J Biol Chem 265:22317–22320

Kuhse J, Betz H, Kirsch J (1995) The inhibitory glycine receptor: architecture, synaptic localization and molecular pathology of a postsynaptic ion-channel complex. Curr Opin Neurobiol 5:318–323

Langosch D, Thomas L, Betz H (1988) Conserved quaternary structure of ligand-gated ion channels: the postsynaptic glycine receptor is a pentamer. Proc Natl Acad Sci USA 85:7394–7398

Lauder JM (1993) Neurotransmitters as growth regulatory signals: role of receptors and second messengers. Trends Neurosci 16:233–240

Lauder JM, Wallace JA, Krebs H (1981) Roles for serotonin in neuroembryogenesis. Adv Exp Med Biol 133:477–506

Lauder JM, Liu J, Devaud L, Morrow AL (1998) GABA as a trophic factor for developing monoamine neurons. Perspect Dev Neurobiol 5:247–259

Levin ED (1992) Nicotinic systems and cognitive function. Psychopharmacology (Berl) 108:417–431

Lidow MS, Rakic P (1995) Neurotransmitter receptors in the proliferative zones of the developing primate occipital lobe. J Comp Neurol 360:393–402

Liu HN, Almazan G (1995) Glutamate induces c-*fos* proto-oncogene expression and inhibits proliferation in oligodendrocyte progenitors: receptor characterization. Eur J Neurosci 7:2355–2363

Lois C, Alvarez-Buylla A (1993) Proliferating subventricular zone cells in the adult mammalian forebrain can differentiate into neurons and glia. Proc Natl Acad Sci USA 90:2074–2077

Lois C, Alvarez-Buylla A (1994) Long-distance neuronal migration in the adult mammalian brain. Science 264:1145–1148

LoTurco JJ, Owens DF, Heath MJ, Davis MB, Kriegstein AR (1995) GABA and glutamate depolarize cortical progenitor cells and inhibit DNA synthesis. Neuron 15:1287–1298

Luddens H, Korpi ER, Seeburg PH (1995) $GABA_A$/benzodiazepine receptor heterogeneity: neurophysiological implications. Neuropharmacology 34:245–254

Luhmann HJ, Prince DA (1991) Postnatal maturation of the GABAergic system in rat neocortex. J Neurophysiol 65:247–263

Luskin MB, Boone MS (1994) Rate and pattern of migration of lineally-related olfactory bulb interneurons generated postnatally in the subventricular zone of the rat. Chem Senses 19: 695–714

Ma W, Barker JL (1995) Complementary expressions of transcripts encoding GAD67 and $GABA_A$ receptor alpha 4, beta 1, and gamma 1 subunits in the proliferative zone of the embryonic rat central nervous system. J Neurosci 15:2547–2560

Ma W, Liu QY, Maric D, Sathanoori R, Chang YH, Barker JL (1998) Basic FGF-responsive telencephalic precursor cells express functional GABA(A) receptor/Cl^- channels in vitro. J Neurobiol 35:277–286

Ma W, Maric D, Li BS, Hu Q, Andreadis JD, Grant GM, Liu QY, Shaffer KM, Chang YH, Zhang L, Pancrazio JJ, Pant HC, Stenger DA, Barker JL (2000) Acetylcholine stimulates cortical precursor cell proliferation in vitro via muscarinic receptor

activation and MAP kinase phosphorylation. Eur J Neurosci 12:1227–1240

Mack KJ, Kriegler S, Chang S, Chiu SY (1994) Transcription factor expression is induced by axonal stimulation and glutamate in the glia of the developing optic nerve. Brain Res Mol Brain Res 23:73–80

MacVicar BA, Tse FW, Crichton SA, Kettenmann H (1989) GABA-activated Cl^- channels in astrocytes of hippocampal slices. J Neurosci 9:3577–3583

Malosio ML, Marqueze-Pouey B, Kuhse J, Betz H (1991) Widespread expression of glycine receptor subunit mRNAs in the adult and developing rat brain. EMBO J 10:2401–2409

Maric D, Liu QY, Grant GM, Andreadis JD, Hu Q, Chang YH, Barker JL, Joseph J, Stenger DA, Ma W (2000) Functional ionotropic glutamate receptors emerge during terminal cell division and early neuronal differentiation of rat neuroepithelial cells. J Neurosci Res 61:652–662

Maricq AV, Peterson AS, Brake AJ, Myers RM, Julius D (1991) Primary structure and functional expression of the $5HT_3$ receptor, a serotonin-gated ion channel. Science 254:432–437

Marin P, Maus M, Desagher S, Glowinski J, Premont J (1994) Nicotine protects cultured striatal neurones against *N*-methyl-D-aspartate receptor-mediated neurotoxicity. Neuroreport 5: 1977–1980

Mattson MP, Kater SB (1989) Excitatory and inhibitory neurotransmitters in the generation and degeneration of hippocampal neuroarchitecture. Brain Res 478:337–348

Mattson MP, Lee RE, Adams ME, Guthrie PB, Kater SB (1988a) Interactions between entorhinal axons and target hippocampal neurons: a role for glutamate in the development of hippocampal circuitry. Neuron 1:865–876

Mattson MP, Dou P, Kater SB (1988b) Outgrowth-regulating actions of glutamate in isolated hippocampal pyramidal neurons. J Neurosci 8:2087–2100

Matzenbach B, Maulet Y, Sefton L, Courtier B, Avner P, Guenet JL, Betz H (1994) Structural analysis of mouse glycine receptor alpha-subunit genes. Identification and chromosomal localization of a novel variant. J Biol Chem 269:2607–2612

Mazer C, Muneyyirci J, Taheny K, Raio N, Borella A, Whitaker-Azmitia P (1997) Serotonin depletion during synaptogenesis leads to decreased synaptic density and learning deficits in the adult rat: a possible model of neurodevelopmental disorders with cognitive deficits. Brain Res 760:68–73

McDonald JW, Johnston MV (1990) Physiological and pathophysiological roles of excitatory amino acids during central nervous system development. Brain Res Brain Res Rev 15:41–70

McKay R (1997) Stem cells in the central nervous system. Science 276:66–71

McKernan RM, Whiting PJ (1996) Which GABAA-receptor subtypes really occur in the brain?. Trends Neurosci 19:139–143

McNaughton LA, Hunt SP (1992) Regulation of gene expression in astrocytes by excitatory amino acids. Brain Res Mol Brain Res 16:261–266

Michler A (1990) Involvement of GABA receptors in the regulation of neurite growth in cultured embryonic chick tectum. Int J Dev Neurosci 8:463–472

Miranda-Contreras L, Mendoza-Briceno RV, Palacios-Pru EL (1998) Levels of monoamine and amino acid neurotransmitters in the developing male mouse hypothalamus and in histotypic hypothalamic cultures. Int J Dev Neurosci 16:403–412

Miranda-Contreras L, Benitez-Diaz PR, Mendoza-Briceno RV, Delgado-Saez MC, Palacios-Pru EL (1999) Levels of amino acid neurotransmitters during mouse cerebellar neurogenesis and in histotypic cerebellar cultures. Dev Neurosci 21:147–158

Miranda-Contreras L, Ramirez-Martens LM, Benitez-Diaz PR, Pena-Contreras ZC, Mendoza-Briceno RV, Palacios-Pru EL (2000) Levels of amino acid neurotransmitters during mouse olfactory bulb neurogenesis and in histotypic olfactory bulb cultures. Int J Dev Neurosci 18:83–91

Monti B, Contestabile A (2000) Blockade of the NMDA receptor increases developmental apoptotic elimination of granule neurons and activates caspases in the rat cerebellum. Eur J Neurosci 12:3117–3123

Nakazawa M, Koh T, Kani K, Maeda T (1992) Transient patterns of serotonergic innervation in the rat visual cortex: normal development and effects of neonatal enucleation. Brain Res Dev Brain Res 66:77–90

Nikolic Z, Laube B, Weber RG, Lichter P, Kioschis P, Poustka A, Mulhardt C, Becker CM (1998) The human glycine receptor subunit alpha3. Glra3 gene structure, chromosomal localization, and functional characterization of alternative transcripts. J Biol Chem 273:19708–19714

Novere N le, Changeux JP (1999) The ligand-gated ion channel database. Nucleic Acids Res 27:340–342

O'Connor SM, Stenger DA, Shaffer KM, Maric D, Barker JL, Ma W (2000) Primary neural precursor cell expansion, differentiation and cytosolic Ca(2+) response in three-dimensional collagen gel. J Neurosci Methods 102:187–195

Orr-Urtreger A, Broide RS, Kasten MR, Dang H, Dani JA, Beaudet AL, Patrick JW (2000) Mice homozygous for the L250T mutation in the alpha7 nicotinic acetylcholine receptor show increased neuronal apoptosis and die within 1 day of birth. J Neurochem 74:2154–2166

Owen A, Bird M (1995) Acetylcholine as a regulator of neurite outgrowth and motility in cultured embryonic mouse spinal cord. Neuroreport 6:2269–2272

Owens DF, Boyce LH, Davis MB, Kriegstein AR (1996) Excitatory GABA responses in embryonic and neonatal cortical slices demonstrated by gramicidin perforated-patch recordings and calcium imaging. J Neurosci 16:6414–6423

Ozawa S, Kamiya H, Tsuzuki K (1998) Glutamate receptors in the mammalian central nervous system. Prog Neurobiol 54:581–618

Palackal T, Moretz R, Wisniewski H, Sturman J (1986) Abnormal visual cortex development in the kitten associated with maternal dietary taurine deprivation. J Neurosci Res 15:223–239

Pappas CA, Ullrich N, Sontheimer H (1994) Reduction of glial proliferation by K^+ channel blockers is mediated by changes in pH_i. Neuroreport 6:193–196

Pastor A, Chvatal A, Sykova E, Kettenmann H (1995) Gly. Eur J Neurosci 7:1188–1198

Paterson D, Nordberg A (2000) Neuronal nicotinic receptors in the human brain. Prog Neurobiol 61:75–111

Patneau DK, Wright PW, Winters C, Mayer ML, Gallo V (1994) Glial cells of the oligodendrocyte lineage express both kai. Neuron 12:357–371

Pearce IA, Cambray-Deakin MA, Burgoyne RD (1987) Glutamate acting on NMDA receptors stimulates neurite outgrowth from cerebellar granule cells. FEBS Lett 223:143–147

Pende M, Holtzclaw LA, Curtis JL, Russell JT, Gallo V (1994) Glutamate regulates intracellular calcium and gene expression in oligodendrocyte progenitors through the activation of DL-alpha-amino-3-hydroxy-5-methyl-4-isoxazolepropionic acid receptors. Proc Natl Acad Sci USA 91:3215–3219

Pin JP, Duvoisin R (1995) The metabotropic glutamate receptors: structure and functions. Neuropharmacology 34:1–26

Porter JT, Cauli B, Staiger JF, Lambolez B, Rossier J, Audinat E (1998) Properties of bipolar VIPergic interneurons and their excitation by pyramidal neurons in the rat neocortex. Eur J Neurosci 10:3617–3628

Pribilla I, Takagi T, Langosch D, Bormann J, Betz H (1992) The atypical M2 segment of the beta-subunit confers picrotoxinin resistance to inhibitory glycine receptor channels. EMBO J 11:4305–4311 [erratum appears in EMBO J (1994) 13:1493]

Pugh PC, Berg DK (1994) Neuronal acetylcholine receptors that bind alpha-bungarotoxin mediate neurite retraction in a calcium-dependent manner. J Neurosci 14:889–896

Puro DG, Yuan JP, Sucher NJ (1996) Activation of NMDA receptor-channels in human retinal Müller glial cells inhibits inward-rectifying potassium currents. Vis Neurosci 13:319–326

Quik M, Polonskaya Y, Gillespie A, Jakowec M, Lloyd GK, Langston JW (2000) Localization of nicotinic receptor subunit mRNAs in monkey brain by in situ hybridization. J Comp Neurol 425:58–69

Rakic P (1985) DNA synthesis and cell division in the adult primate brain. Ann NY Acad Sci 457:193–211

Rakic P, Cameron RS, Komuro H (1994) Recognition, adhesion, transmembrane signaling and cell motility in guided neuronal migration. Curr Opin Neurobiol 4:63–69

Rathouz MM, Berg DK (1994) Synaptic-type acetylcholine receptors raise intracellular calcium levels in neurons by two mechanisms. J Neurosci 14:6935–6945

Reynolds BA, Weiss S (1992) Generation of neurons and astrocytes from isolated cells of the adult mammalian central nervous system. Science 255:1707–1710

Robert A, Magistretti PJ (1997) AMPA/kainate receptor activation blocks K^+ currents via internal Na^+ increase in mouse cultured stellate astrocytes. Glia 20:38–50

Roerig B, Feller MB (2000) Neurotransmitters and gap junctions in developing neural circuits. Brain Res Brain Res Rev 32:86–114

Roerig B, Katz LC (1997) Modulation of intrinsic circuits by serotonin 5-HT_3 receptors in developing ferret visual cortex. J Neurosci 17:8324–8338

Roerig B, Nelson DA, Katz LC (1997) Fast synaptic signaling by nicotinic acetylcholine and serotonin 5-HT3 receptors in developing visual cortex. J Neurosci 17:8353–8362

Role LW, Berg DK (1996) Nicotinic receptors in the development and modulation of CNS synapses. Neuron 16:1077–1085

Ronde P, Nichols RA (1998) High calcium permeability of serotonin 5-HT_3 receptors on presynaptic nerve terminals from rat striatum. J Neurochem 70:1094–1103

Rossi DJ, Slater NT (1993) The developmental onset of NMDA receptor-channel activity during neuronal migration. Neuropharmacology 32:1239–1248

Sadikot AF, Burhan AM, Belanger MC, Sasseville R (1998) NMDA receptor antagonists influence early development of GABAergic interneurons in the mammalian striatum. Brain Res Dev Brain Res 105:35–42

Sah DW, Ray J, Gage FH (1997) Regulation of voltage- and ligand-gated currents in rat hippocampal progenitor. J Neurobiol 32:95–110

Sanes DH, Chokshi P (1992) Glycinergic transmission influences the development of dendrite shape. Neuroreport 3:323–326

Sanes DH, Hafidi A (1996) Glycinergic transmission regulates dendrite size in organotypic culture. J Neurobiol 31:503–511

Scharfman HE, Goodman JH, Sollas AL (2000) Granule-like neurons at the hilar/CA3 border after status epilepticus and their synchrony with area CA3 pyramidal cells: functional implications of seizure-induced neurogenesis. J Neurosci 20:6144–6158

Scheetz AJ, Constantine-Paton M (1994) Modulation of NMDA receptor function: implications for vertebrate neural development. FASEB J 8:745–752

Schlessinger AR, Cowan WM, Gottlieb DI (1975) An autoradiographic study of the time of origin and the pattern of granule cell migration in the dentate gyrus of the rat. J Comp Neurol 159:149–175

Schmieden V, Kuhse J, Betz H (1992) Agonist pharmacology of neonatal and adult glycine receptor alpha-subunits: identification of amino acid residues involved in taurine activation. EMBO J 11:2025–2032

Schofield PR, Lynch JW, Rajendra S, Pierce KD, Handford CA, Barry PH (1996) Molecular and genetic insights into ligand binding and signal transduction at the inhibitory glycine receptor. Cold Spring Harb Symp Quant Biol 61:333–342

Serafini R, Maric D, Maric I, Ma W, Fritschy JM, Zhang L, Barker JL (1998a) Dominant GABA(A) receptor/Cl– channel kinetics correlate with the relative expressions of alpha2, alpha3, alpha5 and beta3-subunits in embryonic rat neurones. Eur J Neurosci 10:334–349

Serafini R, Ma W, Maric D, Maric I, Lahjouji F, Sieghart W, Barker JL (1998b) Initially expressed early rat embryonic GABA(A) receptor Cl^- ion channels exhibit heterogeneous channel properties. Eur J Neurosci 10:1771–1783

Tapia JC, Aguayo LG (1998) Changes in the properties of developing glycine receptors in cultured mouse spinal neurons. Synapse 28:185–194

Tapia JC, Cardenas AM, Nualart F, Mentis GZ, Navarrete R, Aguayo LG (2000) Neurite outgrowth in developing mouse spinal cord neurons is modulated by glycine receptors. Neuroreport 11:3007–3010

Tecott L, Shtrom S, Julius D (1995) Expression of a serotonin-gated ion channel in embryonic neural and non-eural tissues. Mol Cell Neurosci 6:43–55

Tikoo R, Osterhout DJ, Casaccia-Bonnefil P, Seth P, Koff A, Chao MV (1998) Ectopic expression of p27Kip1 in oligodendrocyte progenitor cells results in cell-cycle growth arrest. J Neurobiol 36:431–440

Uchihori Y, Puro DG (1993) Glutamate as a neuron-to-glial signal for mitogenesis: role of glial *N*-methyl-D-aspartate receptors. Brain Res 613:212–220

Verkhratsky A, Steinhauser C (2000) Ion channels in glial cells. Brain Res Brain Res Rev 32:380–412

Wallace JA, Lauder JM (1983) Development of the serotonergic system in the rat embryo: an immunocytochemical study. Brain Res Bull 10:459–479

Wang C, Pralong WF, Schulz MF, Rougon G, Aubry JM, Pagliusi S, Robert A, Kiss JZ (1996) Functional *N*-methyl-D-aspartate receptors in O-2A glial precursor cells: a critical role in regulating polysialic acid-neural cell adhesion molecule expression and cell migration. J Cell Biol 135:1565–1581

Waxham N (1999) Neurotransmitter receptors. In: Zigmond MJ, Bloom FE, Landis SC, Roberts JL, Squire LR (eds) Fundamental neuroscience. Academic, San Diego, pp 235–268

Weiss S, Dunne C, Hewson J, Wohl C, Wheatley M, Peterson AC, Reynolds BA (1996) Multipotent CNS stem cells are present in the adult mammalian spinal cord and ventricular neuroaxis. J Neurosci 16:7599–7609

Weiss ER, Maness P, Lauder JM (1998) Why do neurotransmitters act like growth factors? Perspect Dev Neurobiol 5:323–335

Whitaker-Azmitia PM, Druse M, Walker P, Lauder JM (1996) Serotonin as a developmental signal. Behav Brain Res 73:19–29

Williamson AV, Mellor JR, Grant AL, Randall AD (1998) Properties of GABA(A) receptors in cultured rat oligodendrocyte progenitor cells. Neuropharmacology 37:859–873

Wilson MT, Kisaalita WS, Keith CH (2000) Glutamate-induced changes in the pattern of hippocampal dendrite outgrowth: a role for calcium-dependent pathways and the microtubule cytoskeleton. J Neurobiol 43:159–172

Withers MD, St John PA (1997) Embryonic rat spinal cord neurons change expression of glycine receptor subtypes during development in vitro. J Neurobiol 32:579–592

Yuan X, Eisen AM, McBain CJ, Gallo V (1998) A role for glutamate and its receptors in the regulation of oligodendrocyte development in cerebellar tissue slices. Development 125:2901–2914

Zheng JQ, Felder M, Connor JA, Poo MM (1994) Turning of nerve growth cones induced by neurotransmitters. Nature 368: 140–144

Zoli M, Novere N le, Hill JA Jr, Changeux JP (1995) Developmental regulation of nicotinic ACh receptor subunit mRNAs in the rat central and peripheral nervous systems. J Neurosci 15:1912–1939

Zoli M, Picciotto MR, Ferrari R, Cocchi D, Changeux JP (1999) Increased neurodegeneration during ageing in mice lacking high-affinity nicotine receptors. EMBO J 18:1235–1244

7.8 Publication #8: Nguyen, L., Rigo. J.-M., Malgrange, B., Moonen, G., and Belachew, S. (2003). Untangling the functional potential of PSA-NCAM-expressing cells in CNS development and brain repair strategies. *Curr. Med. Chem.* 10:2185-2196.

Current Medicinal Chemistry, **2003,** *10,* **2185-2196**

Untangling the Functional Potential of PSA-NCAM-Expressing Cells in CNS Development and Brain Repair Strategies

Laurent Nguyen[1], Jean-Michel Rigo[1], Brigitte Malgrange[1], Gustave Moonen[1,2] and Shibeshih Belachew[1,2]*

[1]Center for Cellular and Molecular Neurobiology, [2]Department of Neurology, University of Liège, C.H.U. (B35) Sart Tilman, B-4000 Liège, Belgium

Abstract: Central nervous system (CNS) neural stem cells (NSCs), which are mostly defined by their ability to self-renew and to generate the three main cell lineages of the CNS, were isolated from discrete regions of the adult mammalian CNS including the subventricular zone (SVZ) of the lateral ventricle and the dentate gyrus in the hippocampus. At early stages of CNS cell fate determination, NSCs give rise to progenitors that express the polysialylated form of the neural cell adhesion molecule (PSA-NCAM). PSA-NCAM$^+$ cells persist in adult brain regions where neuronal plasticity and sustained formation of new neurons occur. PSA-NCAM has been shown to be involved in the regulation of CNS myelination as well as in changes of cell morphology that are necessary for motility, axonal guidance, synapse formation, and functional plasticity in the CNS. Although being preferentially committed to a restricted either glial or neuronal fate, cultured PSA-NCAM$^+$ progenitors do preserve a relative degree of multipotentiality. Considering that PSA-NCAM$^+$ cells can be neatly used for brain repair purposes, there is much interest for studying signaling factors regulating their development. With this regard, it is noteworthy that neurotransmitters, which belong to the micro-environment of neural cells *in vivo*, regulate morphogenetic events preceding synaptogenesis such as cell proliferation, migration, differentiation and death. Consistently, several ionotropic but also G-protein-coupled neurotransmitter receptors were found to be expressed in CNS embryonic and postnatal progenitors. In the present review, we outlined the ins and outs of PSA-NCAM$^+$ cells addressing to what extent our understanding of extrinsic and in particular neurotransmitter-mediated signaling in these CNS precursor cells might represent a new leading track to develop alternative strategies to stimulate brain repair.

Key Words: PSA-NCAM, acetylcholine, glutamate, serotonin, stem cell, neurotransmitter, oligodendrocyte, neuroblast.

INTRODUCTION

In the mammalian central nervous system (CNS) development, precursor cells are precisely subdivided into regionally specific groups, expanded in numbers and then differentiated into distinct neurons and glia that form functional networks. The generation of distinct types of neurons and glial cells from neural stem cells (NSCs) involves a sequence of intermediate progenitor stages that are controlled by intracellular regulatory signals [1,2] and extrinsic factors [3,4]. During the initiation of cell commitment, multipotent neural stem cells differentiate primarily into progenitors expressing the polysialylated form of the neural cell adhesion molecule (PSA-NCAM) [5], which is a cell membrane molecule playing important roles in developmental processes as well as in neuronal plasticity occurring throughout adulthood (see [6] for review). Although being already committed either to a glial [7] or a neuronal [8] preferential fate, PSA-NCAM$^+$ precursor cells can retain complex and context-dependent multipotential properties in culture [9]. *In vivo*, PSA-NCAM$^+$ cells located within the adult subventricular zone (SVZ) have the ability to produce granular and periglomerular neurons devoted to the olfactory bulb through a chain migration process via the rostral migratory stream (RMS) [10], and can be recruited to generate astrocytes or oligodendrocytes after lysolecithin-induced demyelination [11] and experimental autoimmune encephalomyelitis [12].

Besides its expression in neural precursor cells, an activity-dependent synthesis of PSA-NCAM occurs in mature neurons and appears to regulate various aspects of synaptic plasticity that are proposed to underlie the re-organization of neuronal networks at several levels of the CNS (reviewed by [13-15]). In the present review, we shall focus on immature progenitor cells expressing PSA-NCAM, trying to unravel the developmental function of these cells which represent a complex phenotype (Fig. (**1**)) with specific properties that can be independent of putative PSA-NCAM-mediated signaling.

BIOSYNTHESIS AND FUNCTION OF PSA-NCAM

NCAM, which is a member of the immunoglobulin superfamily of adhesion molecules [16,17], is coded by a single copy gene composed of 26 exons [18]. However, tens of distinct isoforms can be generated by alternative splicing and NCAM-180 appears to be one of the most widely expressed isoforms [18].

*Address correspondence to this author at the Center for Cellular and Molecular Neurobiology, Department of Neurology, University of Liège, 17 Place Delcour, B-4020 Liège, Belgium; Tel: +32 4 366 59 05; Fax: +32 4 366 59 12; E-mail: sbelachew@ulg.ac.be

0929-8673/03 $41.00+.00

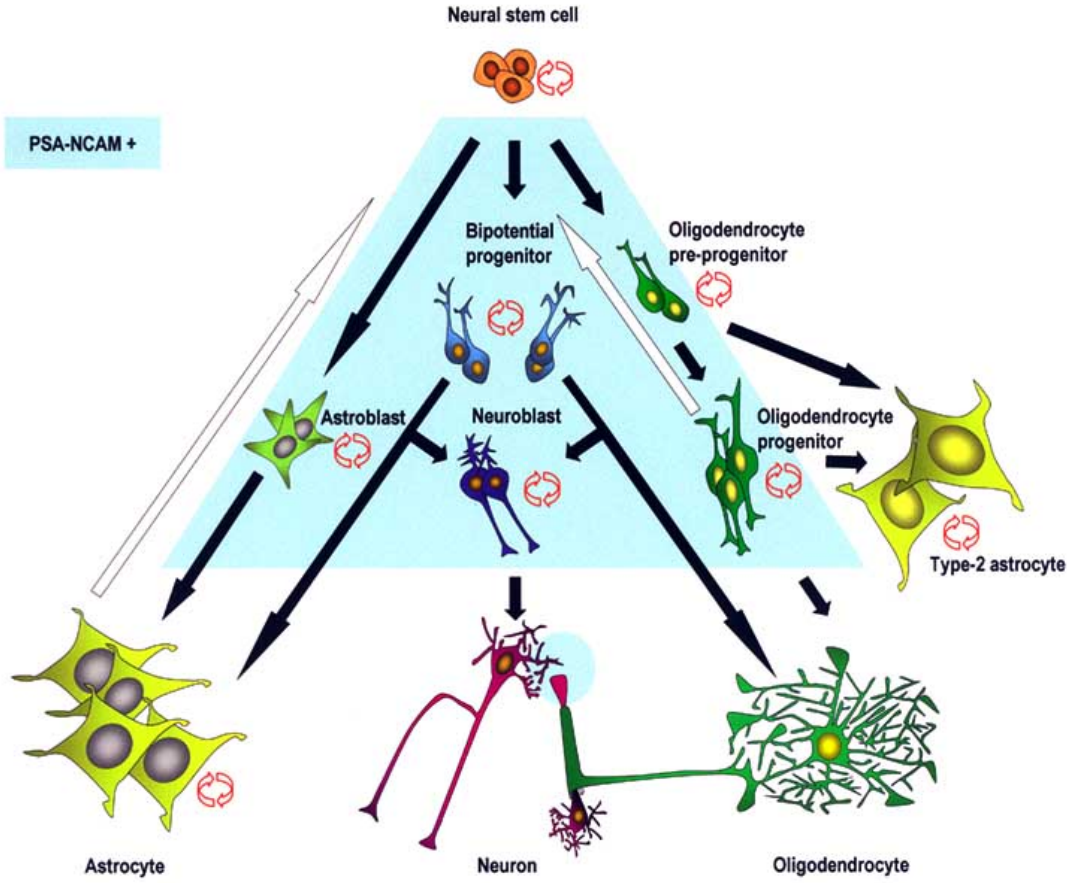

Fig. (1). Correlation between PSA-NCAM expression and cell lineage progression in the central nervous system

Schematic view of the progression of CNS cell specification, proposing possible relationships existing between intermediary phenotypes. Cells expressing PSA-NCAM were specifically shaded on a blue background. The level of PSA-NCAM expression decreases with the progression towards more differentiated phenotypes. In fully differentiated cells, PSA-NCAM is only expressed at the level of synaptic contacts (blue circle). Neural stem cells (NSCs) are *per se* self-renewing and multipotent, thus generating astrocytes, oligodendrocytes as well as distinct subsets of neurons, through the differentiation of intermediary progenitors [144,145]. The proliferative potential of progenitors is pointed by red-circular double-arrows. During the differentiation process, NSCs produce restricted progenitors, including early-committed bipotential progenitors that are subdivided in two classes, neuron-oligodendrocyte [59,146-149] and neuron-astrocyte precursor cells [150-153]. Oligodendrocyte pre-progenitors represent restricted progenitors that mostly generate oligodendrocytes and type-1 astrocytes around birth *in vivo*, and that may be able to generate type-2 astrocytes *in vitro*. However, this latter phenotype remains a subject of intense controversy [7,60,61,154]. Neural stem cells can produce highly proliferative astroblasts devoted to become astrocytes [155,156]. The possible existence of phenotypically characterized restricted astrocyte precursor or so-called astroblasts *in vivo* mostly rely on the description of $Pax2^+$ precursors in the developing optic nerve [157] and $FGFR3^+$ cells in the embryonic CNS neuroepithelium [158], that are both astrocyte-committed progenitor cells giving rise only to mature astrocytes *in vivo*. Finally, some recent data suggested that a sub-population of oligodendrocyte progenitors and GFAP-expressing astrocytes may possibly retain stem cell properties and/or de-differentiate (open arrows) into multipotent progenitor cells able to give rise to functional neurons [89,159,160].

PSA residues, i.e. long homopolymers of alpha-2,8-linked sialic acid, were found to be a major macromolecular component of vertebrate CNS, largely on the basis of an unusual composition and size [19]. Unlike most carbohydrates expressed on the cell surface, PSA is exclusively attached to the neural cell adhesion molecule (NCAM) [20-22]. A single PSA chain may be made of over 50 monomers and the chain length may vary substantially between NCAM isolated from different sources (Fig. (**2**)) [23]. Several levels of regulation are involved in the biosynthetic machinery required to produce PSA on NCAM. PST (i.e. ST8SiaIV/PST) and STX (i.e. ST8SiaII/STX) Golgi-associated polysialyltransferases are members of the sialyltransferase family, and each is sufficient to bind PSA chains specifically to NCAM [24-27]. Both PST and STX add PSA to the fifth Ig domain of NCAM, which contains 3

of the 6 potential N-linked glycosylation sites of the protein [28]. PSA synthesized by PST appears to be longer than that generated by STX and both enzymes can cooperate to produce a higher level of polysialylation than either of them separately [26,28]. The intensity of NCAM polysialylation is mostly dependent on the transcriptional activation of sialyltransferase genes that are developmentally regulated. STX transcripts are abundant in the embryonic brain where overall PSA expression is high, and decrease drastically after birth, while transcription of the PST gene is lower in embryonic tissue but remain more constant in the postnatal CNS [25,29]. Furthermore, there are also distinct patterns of mRNA expression in the different postnatal brain regions for the two enzymes with notably persistence of PST transcripts in the subependymal layer, the glomerular layer of the olfactory bulb, the granule cell layer of the dentate gyrus and

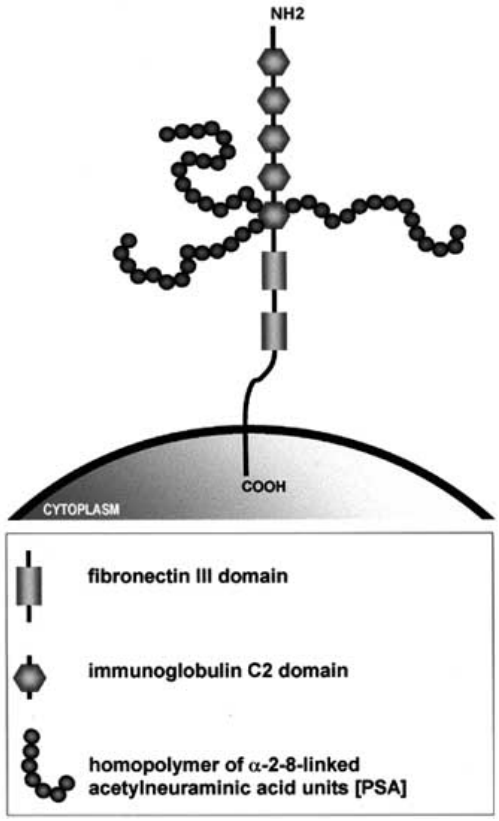

Fig. (2). Molecular structure of PSA-NCAM

The neural cell adhesion molecule (NCAM) is a member of the immunoglobulin superfamily of adhesion molecules. The extracellular part of NCAM is made of five immunoglobulin (Ig)-like domains and two fibronectin type III homology regions. NCAM protein is coded by a single gene composed of 26 exons. Alternative splicing and post-translational modifications generate several isoforms. NCAM-180 is one of the major isoform. Two sialyltransferases, ST8SiaIV/PST and ST8SiaII/STX, are responsible for the synthesis of linear homopolymers of α-2-8-linked acetylneuraminic acid (= sialic acid residues forming polysialic (PSA) carbohydrate chains) which bind to two Asn amino acids in the fifth Ig domain of the extracellular part of NCAM.

in some scattered cells of the cortex, whereas STX had become almost undetectable except in the hippocampus in adulthood [30,31]. However, despite an overall correlation between sialyltransferase mRNA levels and PSA-NCAM expression, non-transcriptional calcium-dependent mechanisms of regulation may also be involved in the control of NCAM polysialylation in specific developmental events [32].

A consensus view of PSA-NCAM biology is to consider this molecule a modulator of cell-cell and cell to matrix interactions establishing the physical anchorage to the environment that is necessary for cell cycle progression, differentiation and migration of cells. The different NCAM isoforms can mediate cis-, trans-, homo- and heterophilic interactions in which the large negatively charged PSA residues could play the role of a spacer decreasing adhesion forces between cells, thus allowing a dynamic re-shaping of membrane contacts that favors migratory processes [15,33,34]. Recent experimental evidences have supported the idea that PSA-NCAM plays a delaying role in organizing membrane-membrane adhesive links, thereby acting as an inhibitory cue of myelination of CNS axons [35,36]. The same pattern of anti-adhesive properties may be implicated in the role of PSA-NCAM in axonal pathfinding, nerve branching [37,38], cell migration [39,40], axonal fasciculation and synaptic plasticity [41].

In order to address the function of PSA and NCAM *in vivo,* different types of loss-of-function models have been developed. In NCAM-deficient mice, chain formation in the rostral migratory stream (RMS) is altered and a massive accumulation of neural precursors occurs, resulting in a defect in migration of cells in this tissue finally giving rise to an abnormally small olfactory bulb [42]. In contrast to NCAM-deficient mice, knock-out mice lacking the PST polysialyltransferase have olfactory precursor cells in the RMS that do express PSA and follow their normal migration pathway likely thanks to the synthesis of PSA by the STX transferase [43]. Furthermore, the absence of NCAM is correlated with the unexpected presence of differentiated oligodendrocytes and astrocytes in the RMS [44]. This latter feature possibly results from the lack of PSA since the removal of PSA on NCAM by endoneuraminidase (endoN) affects only moderately cell migration but accelerates neural precursor cell differentiation [45,46]. With respect to synaptic plasticity, it was shown that endoN-induced PSA deficiency or genetic lack of NCAM alter spatial learning and long-term potentiation (LTP) in the hippocampus [41,42,47,48]. Interestingly, in PST-deficient mice, which express normal levels of PSA during development but develop a progressive loss of PSA in the presence of NCAM in most adult brain regions, LTP was impaired only at CA1 but not at CA3 synapses [43]. Conversely, in NCAM-deficient mice, LTP was disrupted in CA3 [48], suggesting the important role of the NCAM protein backbone for synaptic transmission in CA3 and of the PSA moiety in CA1.

In vitro, binding soluble NCAM has been shown to inhibit the proliferation of nestin-expressing hippocampal progenitor cells and to promote their differentiation to a neuronal phenotype [49]. Finally, the addition of PSA on NCAM may also generate binding sites for soluble

extracellular ligands, thereby concentrating them at the cell surface [50]. Likewise, it was shown that PSA-NCAM sensitizes hippocampal and cortical neurons to the effect of growth factors such as brain-derived neurotrophic factor (BDNF) [51,52].

PSA-NCAM EXPRESSION DURING CNS DEVELOPMENT: A PHENOTYPIC MARKER OF IMMATURE NEURAL PRECURSOR CELLS MULTIPOTENT OR COMMITTED TO A RESTRICTED NEURONAL OR GLIAL FATE

During embryonic spinal cord development, PSA-NCAM-negative multipotent neuroepithelial (NEP) stem cells [53,54] generate self-renewing neuronal restricted precursor cells (NRPs, or neuroblasts) that do express PSA-NCAM and fully differentiate subsequently into multiple neuronal phenotypes [8,55]. The expression of PSA-NCAM appears in motor neurons, presumptive commissural neurons and floor plate at embryonic day 12, and then spreads throughout the spinal cord during late embryonic and early postnatal stages [56]. In the telencephalon, the developmental pattern of PSA-NCAM expression within the ganglionic eminences at E14-E16 (lateral = LGE and medial = MGE) with a dynamic migration towards perinatal subventricular zones (SVZ) suggests that PSA-NCAM$^+$ cells invade the VZ wedge and are involved in the formation of the perinatal SVZ [57]. This migratory behaviour is similar to that of progenitor cells expressing the ventral forebrain markers homeobox genes dlx1/2 [58]. Recent experiments in short term lineage analysis have convincingly shown that a large percentage of SVZ perinatal PSA-NCAM$^+$ cells were the progeny of dlx2-expressing cells and generated astrocytes and oligodendrocytes in the cerebral cortex and white matter [57]. However, since dlx1/2 progenitors from the ganglionic eminences not only give rise to glia but also have the ability to generate GABAergic neurons *in vitro* [59], there might exist different subpopulations of dlx-expressing LGE and MGE precursors that could underlie the genesis of distinct subsets of PSA-NCAM$^+$ SVZ cells with specific fate potentials.

Unfortunately, most experimental approaches studying the phenotype of cultured PSA-NCAM$^+$ cells from postnatal brain dealt with entire cerebral hemispheres, including deep nuclei, white matter and SVZ areas altogether. Hence, with such a material, the behavior of purified immunopanned PSA-NCAM$^+$ cells has to be interpreted as the sum of putative specific properties of cells derived from several locations. In oligodendroglial culture conditions, PSA-NCAM$^+$ cells from early postnatal whole brain [7,60-62] represent so-called oligodendrocyte early pre-progenitor cells that express the intermediate filament protein nestin [63]. Postnatal cerebral PSA-NCAM$^+$ oligodendrocyte pre-progenitor cells are negative for A2B5 [64] and GD3 gangliosides [65] which are markers of the oligodendrocyte progenitors (OPs), but do express platelet-derived growth factor α receptors (PDGFRα) [61] like OPs. Spontaneous and growth factor-induced migration of PSA-NCAM$^+$ cells is more important than that of GD3$^+$ OPs *in vitro* [45] and the enzymatic removal of PSA residues from NCAM decreased migration and induced the differentiation of PSA-NCAM$^+$ cells into GD3$^+$ OPs and GFAP$^+$ astrocytes [45]. When cultured in the absence of the classical OP cell mitogen, i.e. PDGF, but in the presence of type 2-fibroblast growth factor (FGF2) or epidermal growth factor (EGF), neonatal cerebral PSA-NCAM$^+$ cells retained a mostly glial fate and allowed a significant but yet marginal neuronal differentiation [7]. Nevertheless, the neuronal potential of immunopanned neonatal PSA-NCAM$^+$ cells remained much lower than that of striatal neonatal stem cells in the same culture conditions [7]. In contrast, neonatal PSA-NCAM$^+$ cells derived specifically from the cortex exhibited a robust proliferation in response to EGF and displayed real multipotent properties with the capacity to clonally give rise to neurons, astrocytes and oligodendrocytes [9]. Finally, it was shown that cultured neonatal PSA-NCAM$^+$ cells can self-renew in response to EGF and FGF [66].

PSA-NCAM-EXPRESSING CELLS DO PERSIST IN THE ADULT CNS

PSA-NCAM which is broadly expressed during development also persists in scattered adult CNS regions associated with plasticity [67] such as notably the SVZ and RMS [5,68,69], the dentate gyrus [70,71], the amygdala [72], the hypothalamo-neurohypophysial system [73], the olfactory bulb [74], the piriform cortex [75,76], the brainstem dorsal vagal complex [77,78], the laminae I and II of the dorsal horn of the spinal cord as well as around the central canal [69,79].

In the dentate gyrus (DG), it has been shown that newly-formed granule neurons are continuously generated throughout life and became integrated into adult functional hippocampal synaptic circuits [80]. These adult-born synaptic networks are likely to have the potential to affect hippocampal functions such as memory and learning [81]. Immature neuronal progenitors in the adult DG were found to express PSA-NCAM [71,82], simultaneously with other markers of newly-born hippocampal granule cells such as the basic helix-loop-helix protein (bHLH) NeuroD [83-85] and collapsin response-mediated protein-4 (CRMP-4) [85-87] also referred to as TOAD-64 (Turned on after division, 64 kDa) [88,89]. Furthermore, cell-to-cell interaction studies [90] have suggested that the clustering and micro-environment provided by PSA-NCAM$^+$ immature neurons contribute to the early developmental events involved in adult neurogenesis such as proliferation, apoptosis, differentiation and neurophilic migration. It remains to be assessed to what extent the biological properties and in particular fate specification of these PSA-NCAM$^+$ immature hippocampal neurons may involve PSA-NCAM-mediated signaling.

In the adult rodent brain, PSA-NCAM-expressing cells are also observed all along the chain migratory pathway of SVZ neuroblasts that start in the lateral wall of the lateral ventricle where they form weblike patterns extending rostrally between the corpus callosum and the striatum towards the anterior ventral telencephalon into the olfactory bulb [91,92]. Dividing cells along the RMS are so-called type A cells [5] that are PSA-NCAM$^+$ or closely associated with PSA-NCAM$^+$ cells forming chains of tethered migrating cells [91]. In the mammalian SVZ of the lateral

ventricle, type B cells which express GFAP represent the adult stem cells [93], but the most actively dividing cells of the SVZ correspond to type C cells that are the progeny of B cells and that do not express PSA-NCAM [5]. Whereas type C cells are present throughout the SVZ, they are not found in the RMS, suggesting that chains of migrating neuroblasts in the RMS could be derived from type C cells [5] that would turn on PSA-NCAM expression once they become committed to a neuronal fate. It has recently been shown that the majority of EGF-responsive cells in the SVZ are not derived from relatively quiescent type B stem cells *in vivo,* but from the highly mitotic transit-amplifying C cells that are $Dlx2^+$ and that retain stem cell competence under the influence of growth factors [94]. When exposed to EGF, type C cells downregulate Dlx2, arrest neuronal production, and become highly proliferative and invasive [94].

In contrast with the tight developmental link between PSA-NCAM expression and SVZ-derived neurogenesis in the intact adult brain, it is noteworthy that PSA-NCAM can also be associated with the emergence of glial progenitor cells in pathological conditions, notably after demyelination [11,12,95-97]. After lysolecithin-induced demyelination of the corpus callosum, PSA-$NCAM^+$ progenitors of the rostral SVZ and RMS proliferate, migrate towards the lesion and differentiate into oligodendrocytes, astrocytes but not neurons [11,97]. Experimental autoimmune encephalomyelitis also mobilizes PSA-$NCAM^+$ neural progenitors from the SVZ to undergo oligodendrogenesis in adult mice, thus underlying that oligodendrogenesis in response to inflammatory demyelination also occurs in sites where it does not take place in normal conditions, outlining thereby the impact of environment on cell fate specification [12]. Furthermore, it was shown that adult SVZ harbors a focal reservoir of FGF2- and PDGF-responsive PSA-$NCAM^+$ precursor cells that are able to differentiate toward a neuronal and oligodendroglial fate, and that generate myelin-forming mature oligodendrocytes after transplantation into the brain of neonate *shiverer* mutant mice [96].

EXTRACELLULAR SIGNALING IN PSA-$NCAM^+$ PRECURSOR CELLS

The biology of PSA-$NCAM^+$ precursor cells is regulated by multiple secreted factors present within the CNS during critical stages of development. To date, most of the available knowledge about trophic molecules supporting the growth of PSA-$NCAM^+$ precursor cells was provided by *in vitro* models [7,9,62,98]. Multipotent PSA-$NCAM^+$ precursor cells able to give rise to neurons, astrocytes and oligodendrocytes were purified from early postnatal cerebral cortex devoid of generative zones [9]. Such multipotent PSA-$NCAM^+$ cells were shown to express the EGF receptor (EGFR) and were highly proliferative in response to EGF treatment. Moreover, both FGF2 and $PDGF_{AA}$ stimulated cortical PSA-$NCAM^+$ multipotent progenitors to differentiate into oligodendrocyte precursors *in vitro* [9]. The earliest identifiable pool of postnatal glial precursors expressing PSA-NCAM were isolated from the newborn cortex and described as restricted either to oligodendroglial or astroglial commitment [60,64]. As previously mentioned, these particular PSA-$NCAM^+$ cells, also termed "oligodendrocyte pre-progenitors", express the platelet-derived growth factor-α receptors (PDGF-αR) [64,99], the activation of which is necessary for their proliferation, survival and restriction to an oligodendroglial fate *in vitro* [61,64]. The treatment of cultured PSA-$NCAM^+$ oligodendrocyte pre-progenitors with bone morphogenetic proteins (BMPs) BMP2 or BMP4 has been reported to induce astrocyte commitment, while the addition of fibroblast growth factor along with BMPs inhibited the switch to the astrocyte lineage [100]. Other groups have isolated and purified by immunopanning PSA-$NCAM^+$ oligodendrocyte pre-progenitor cells from the whole telencephalon of newborn rats [7,45]. These cells also expressed PDGF-αRs, thyroid hormone-α receptors isoforms (THR-α), fibroblast growth factor receptors (FGFR1, 2, and 3), and were able to grow as proliferating floating spheres and to generate mostly oligodendrocytes and astrocytes in pro-differentiating conditions [7]. Such PSA-$NCAM^+$ oligodendrocyte pre-progenitor cells responded to FGF2 with an increased survival and proliferation, and both effects were enhanced by thyroid hormone (T3) [7]. In addition to FGF2, EGF also allowed the proliferation of PSA-$NCAM^+$ pre-progenitors as floating neurospheres [7]. Decker *et al.* [45] have demonstrated that the addition of B104 conditioned medium [101] or growth factors such as FGF2 and $PDGF_{AA}$ to N1-containing medium enhanced the migration velocity of PSA-$NCAM^+$ pre-progenitors isolated from the cerebral cortex and cultured in proliferating spheres [45].

NRPs expressing PSA-NCAM could be isolated from E13.5 rats spinal cord [8]. After clonal isolation, these cells actively proliferated in a medium containing both FGF and Neurotrophin-3 (NT-3), and generated multiple neuronal phenotypes but not astrocytes or oligodendrocytes after replacing FGF by retinoic acid in the culture medium [8].

The striatal development proceeds for several weeks after birth in rodents and a dense expression of PSA-NCAM still persists within the striatum during the first two postnatal weeks [102-104]. Our recent works have demonstrated that a high amount of PSA-$NCAM^+$ precursor cells could be purified from newborn rat striatum [105], proliferate as floating spheres (Fig. (**3**)) in the presence of EGF [105], and differentiate mainly into neurons (Fig. (**5**)) after adhesion a coated substrate in a medium devoid of mitogen [105].

In the adult mammalian CNS , PSA-$NCAM^+$ precursor cells are mostly restricted to SVZ and RMS areas where they are dedicated to oligodendrogliogenesis [11] or neurogenesis [10], but similar cells are also responsible for the generation of newborn neurons in the adult dentate gyrus [71,85]. The intracerebroventricular infusion of a combination of EGF and FGF2 stimulated the proliferation of PSA-$NCAM^+$ neuronal progenitors located within the germinal areas of the adult rat brain and in spinal cord ventricular neuroaxis, where they generated supraependymal "neuron-like" progenitors expressing class III β-tubulin [69]. PSA-$NCAM^+$ oligodendrocyte pre-progenitors were also mobilized in non-pathological condition by infused mitogenic factors such as $PDGF_{AB}$, FGF2, and transforming growth factor-α that favored their proliferation, migration and differentiation within the SVZ and the RMS [96,97,106]. Likewise, PSA-$NCAM^+$ oligodendrocyte pre-progenitors can be recruited

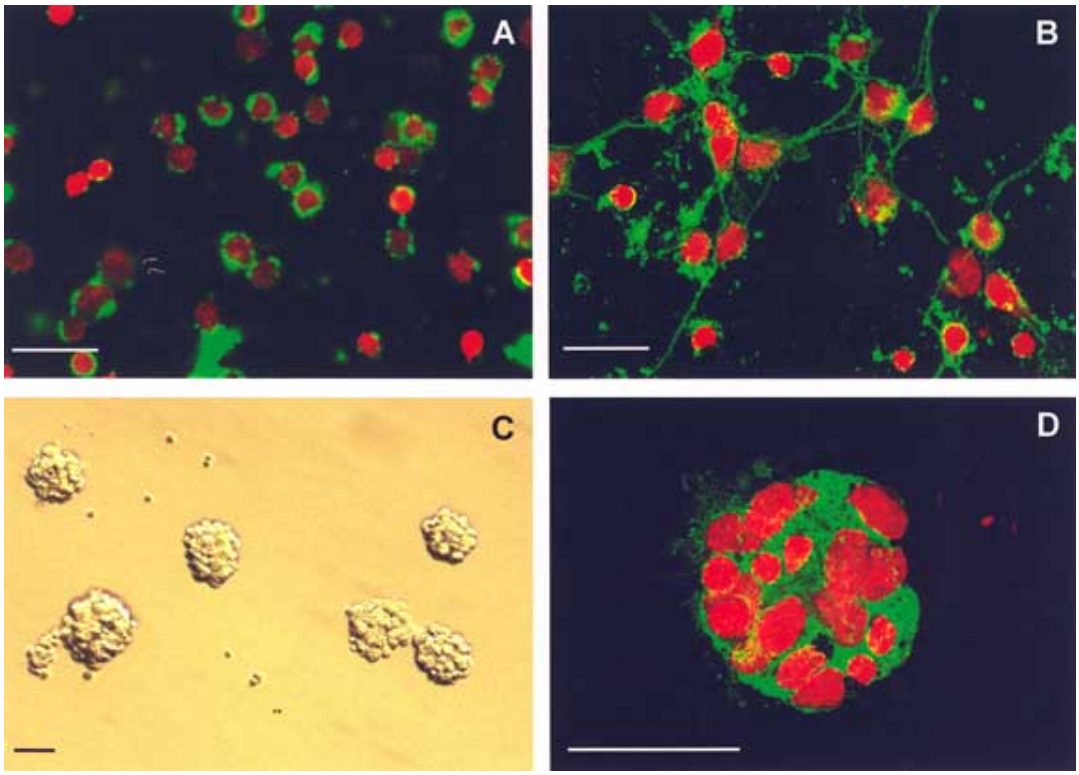

Fig. (3). Purification and growth *in vitro* of proliferative and neurogenic PSA-NCAM$^+$ progenitors from early postnatal striatum

(A-D) Cells were dissociated from postnatal striatum and isolated by a previously described technique [105] which required two steps of purification. First, cells were processed by the technique described by Reynolds and Weiss [161,162] to isolate primary striatal cell suspensions enriched in NSCs. These cells were then layered on top of a pre-centrifugated Percoll density gradient. After ultra-centrifugation, cells with a density ranging from 1,052 to 1,102 g/mL were harvested, seeded in a defined medium containing EGF (20 ng/mL) and cultured as floating spheres for 3 days *in vitro* (3 DIV). (A) Confocal optical section showing such acutely purified cells from the striatum. More than 95 % of these cells are PSA-NCAM$^+$ (PSA-NCAM in green and nuclear dye in red). (B) After 24 hours of culture on a poly-ornithine-coated substrate, these cells conserved PSA-NCAM immunoreactiviy and extended networks of web-like processes towards each other (PSA-NCAM in green and nuclear dye in red). (C, D) Finally, after 3 DIV of EGF-driven expansion, cells have formed spheres (C) that remain mainly composed of PSA-NCAM$^+$ cells (D, PSA-NCAM in green and nuclear dye in red). Scale bars = 20 µm for panels A and B, and 25 µm for panels C and D.

from the SVZa to form new oligodendrocytes after lysolecithin-induced demyelination of the corpus callosum [11].

Other extracellular cues such as neurotransmitters and extracellular matrix (ECM) molecules also seem to be of interest for the regulation of basic developmental events affecting PSA-NCAM$^+$ lineage cells. Hence, the binding of ECM to integrin receptors regulated the migration of PSA-NCAM$^+$ cells *in vitro* [45] but also *in vivo* [107] within the SVZ and the RMS [108]. On the other hand, neurotransmitter receptors and neurotransmitters, which are fully part of the chemical environment surrounding immature cells during and after the CNS developmental period, have been described in neural precursors before the establishment of cortical and subcortical synapses. Early expression of neurotransmitters and their corresponding receptors could be consistent with a significant biological function for their interaction during neural development (reviewed in [3]). As a matter of fact, it has been demonstrated that ligand-gated ionotropic channels (LGICs) are already expressed in nestin$^+$ multipotent neural stem cells (NSCs) and in committed precursors before synaptogenesis [3]. Functional glycine receptors [98] and nicotinic acetylcholine receptors [109,110] have been described in nestin$^+$ NSCs. Embryonic FGF2-responsive telencephalic NSCs express type A γ-aminobutyric acid receptors ($GABA_AR$) *in vitro* [111] and their activation by GABA has been reported to inhibit the mitotic effect of FGF2 [112]. In organotypic slice cultures, GABA and glutamate also interact with cell cycle progression in cortical ventricular progenitors with actually opposite effects on the proliferation kinetics of ventricular zone (VZ) and subventricular zone (SVZ) cells [113]. Serotonin promotes neurogenesis within the adult dentate gyrus and in the SVZ likely by activation of its metabotropic receptor(s) [114,115]. Other functional metabotropic neurotransmitter receptors were also described in nestin$^+$ NSCs, where their activation stimulated cell proliferation through intracellular

cascades involving pertussis toxin-sensitive G-proteins, Ca^{2+} signaling, protein kinase C activation, and mitogen-activated protein kinase (MAPK) phosphorylation [116].

Later in cell lineage progression, glycine-induced inward currents were recorded in OPs cultured in oligospheres [117]. We also reported that the concurrent activation by glycine of both glycine receptors and glycine transporters in OPs was able to trigger a cell-membrane depolarization sufficient to open L-type voltage-gated calcium channels allowing the entry of calcium [118]. The N-methyl-D-aspartate subtype of glutamatergic receptor (NMDAR) also plays a critical role in many aspects of CNS development [3]. In neurohypophysial oligodendroglial progenitor cells, the activation of NMDAR regulates the expression of PSA-NCAM which is required for the migration of these cells [39,40]. NMDAR also plays a role in synaptogenesis occurring within the striatum by regulating the establishment of asymmetric synapses expressing PSA-NCAM [104]. NMDAR activation is important for the age-dependent modulation of PSA expression at synapses in the dorsal vagal complex (DVC) where it could support structural reorganizations and synaptic plasticity in response to visceral afferent signals [77,78]. The pharmacological blockade of NMDAR has been reported to stimulate neurogenesis leading to an increased number of newborn PSA-NCAM$^+$ immature neurons in the adult rat dentate gyrus [119]. Finally, the inhibition of NMDAR was shown to modulate the expression of PSA within the adult pyriform cortex where it is likely to be involved in structural plastic events or migration processes [76].

A recent work has suggested that allopregnanolone, a positive allosteric modulator of $GABA_AR$, promoted the proliferation of PSA-NCAM$^+$ oligodendrocyte pre-progenitors cultured as floating spheres by enhancing the endogenous activation of $GABA_AR$ (Abstract of the *Fifth European Meeting on Glial Cell Function in Health and Disease*, Gago, N., El-Etr, M., Sananês, N., Avellana-Adalid, V., Baron-van Evercooren, A. and Schumacher, M. 2002, *Glia* 38 (S1), 14).

By using the whole-cell patch-clamp technique, we reported that inward currents triggered by glutamate, acetylcholine, and serotonin (Fig. (**4**)) occurred in proliferative neurogenic PSA-NCAM$^+$ progenitors derived from postnatal rat striata (Fig. (**3**)). Currents elicited by glutamate were obtained in a vast majority of the cells (±70%). In contrast, acetylcholine and serotonin induced inward currents only in the minority of the recorded population (±15%) (see Fig. (**4**) for details). The identification of the biological function(s) of these neurotransmitter receptors during the maturation of neurogenic PSA-NCAM$^+$ progenitors has yet to be determined.

TRANSPLANTING PSA-NCAM$^+$ CELLS VERSUS STIMULATING AN ENDOGENOUS POOL: WHO'S THE BEST SUITED GUEST FOR BRAIN REPAIR STRATEGIES ?

Multiple strategies preventing neural cell death have so far been explored with insufficient success toward developing therapeutics for neurological disorders. Cell-replacement approaches to restore function in neurodegenerative diseases have been based on intra-cerebral transplantation of primary fetal cells, restricted progenitor cells pre-differentiated *in vitro* or stem cells [120]. These studies have shown that cell transplantation can serve to give rise to remyelination or to achieve neuronal replacement and partial reconstruction of neuronal circuitry in the adult brain. On the other hand, local endogenous progenitor cells have also been shown to underlie partial brain repair processes allowing to a certain extent remyelination or neuronal replacement to occur after initial insults [121]. It is exhaustively documented that various lesions or growth factor treatments stimulate the proliferation of endogenous progenitors and the generation of new neurons either in known neurogenic regions [122-126] or in sites where neurogenesis normally does not take place [127-132]. In demyelinating disorders, in spite of the overall failure to generate extensive remyelination (reviewed in [133]), endogenous precursor cells do support a limited sketch of myelin repair [12,134-136] occurring however over a restricted area around the lesion without long-distance cell recruitment [137,138]. To date, we remain yet far from being capable to drive endogenous progenitors toward repairing CNS lesions on a functional basis. The spontaneously latent regenerative capacities of endogenous progenitors imply that complex modulations of extrinsic signaling should be a prerequisite to mobilize these cells enough to make them proliferate and differentiate into the appropriate cell types at a sufficient rate.

The enthusiasm arising from stem cell biology data has recently been mitigated by the results of stem cell transplantation studies that highlighted our inability to control the fate of stem cell populations following their implantation into the CNS [139]. Since we can exert little or no control on environmental cues and cellular deficiencies operating at the site of interest, most significant advances for the cell transplantation field could notably come from alternative strategies that would include pre-differentiation of stem cells prior to transplant. With respect to that in view of their *in vivo* context-dependent plasticity and given their relatively restricted fate and self-renewal potential *in vitro,* purified PSA-NCAM$^+$ cells may represent a most promising graft material [66]. In the developing brain of *shiverer* mutant mice, as compared with committed GD3$^+$ OPs, transplanted neonatal PSA-NCAM$^+$ cells from cerebral hemispheres displayed similar myelination potential but were also able to generate neurons and astrocytes, and had higher migratory properties [66]. Furthermore, immunoselected neonatal PSA-NCAM$^+$ cells from rat brain expanded into spheres *in vitro* and grafted in focally demyelinated adult spinal cord have completely remyelinated the lesions by generating both CNS and peripheral nervous system (PNS) myelin-forming cells, i.e. oligodendrocytes and Schwann cells [140]. Intracerebroventricularly- or intrathecally-injected neonatal PSA-NCAM$^+$ cells were also shown to migrate into inflamed white matter and to differentiate into astroglial and oligodendroglial cells after induction of experimental autoimmune encephalomyelitis [141]. Altogether, these results obtained with animal models of myelin disorders provided evidence that transplanted PSA-NCAM$^+$ cells derived from whole brain at the early postnatal period displayed worthy regenerative potential with

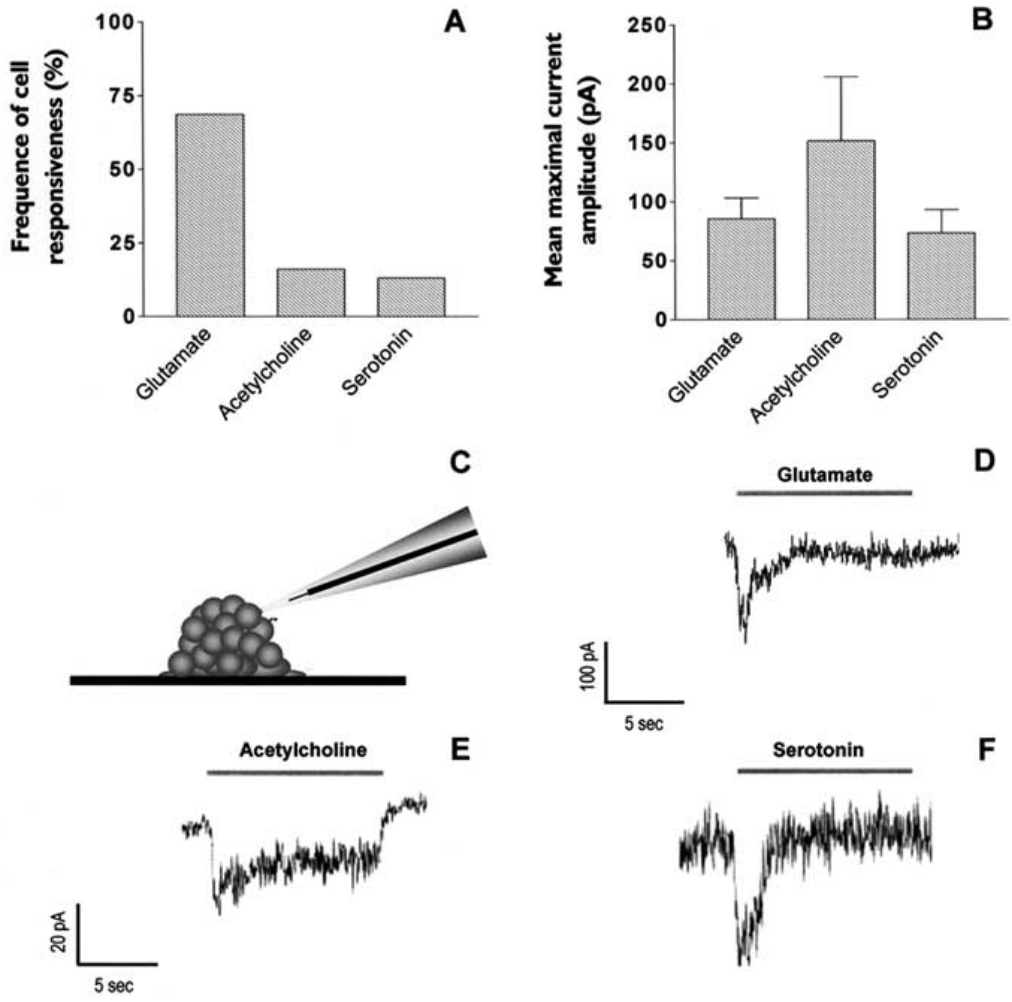

Fig. (4). Glutamate, acetylcholine, and serotonin trigger inward currents in PSA-NCAM$^+$ progenitor cells

Using the patch-clamp technique in the voltage-clamp mode (holding potential at -70 mV), we recorded cells within PSA-NCAM$^+$ spheres, as previously described [105]. The mean membrane potential was -58 mV (n=52 cells). (A) Histograms showing cell responsiveness for the following neurotransmitters: glutamate (n=35 cells), acetylcholine (n=31 cells), and serotonin (n=38 cells). The percentage of PSA-NCAM$^+$ cells eliciting an inward current in response to glutamate application was much higher than that of serotonin and acetylcholine. (B) All applied neurotransmitters were tested at 1mM, i.e. a saturating concentration allowing to measure a peak maximum current amplitude that represented an indirect assessment of corresponding receptor densities. Glutamate-evoked currents were observed in 68,8% of total cells (n=35) with a mean amplitude of 85,7 ± 17,5 pA. Acetylcholine and serotonin were also able to induce inward currents, respectively in 16,1% (n=31 cells) and in 13,2% (n=38 cells) of total cells with mean current amplitudes of 151,6 ± 54 pA for acetylcholine and 73,4 ± 19,7 pA for serotonin. (C) Drawing representing a PSA-NCAM$^+$ cell recorded with a whole-cell patch-clamp micro-electrode within a sphere cultured in suspension for 3 DIV and then plated on a polyornithine-coated substrate for 1 hour to allow attachment before recording. (D-F) Traces illustrating inward currents elicited in PSA-NCAM$^+$ cells by glutamate (1 mM) (D), acetylcholine (1 mM) (E), and serotonin (1 mM) (F). Traces in (E) and (F) have the same scale displayed in (E).

a preferentially glial fate and a high migrating velocity likely due to the anti-adhesive properties of PSA residues [34].

In contrast, nothing has ever been assessed with regard to the putative use of PSA-NCAM$^+$ precursor cells in neuronal replacement strategies [120]. Recently, we demonstrated that PSA-NCAM$^+$ precursor cells isolated from early postnatal striatum [105] displayed a highly pro-neuronal fate *in vitro* (Fig. (**5**)), unlike PSA-NCAM$^+$ cells derived from whole brain at the same developmental period [7]. We emphasize here that striata-derived postnatal PSA-NCAM$^+$ cells might be awesomely a suited guest for neuronal replacement therapies given their cocktail of adapted features that combine a neuron-oriented pre-differentiation and a predisposition to motility thanks to PSA-NCAM biochemical properties [34,44]. Furthermore, likewise neural

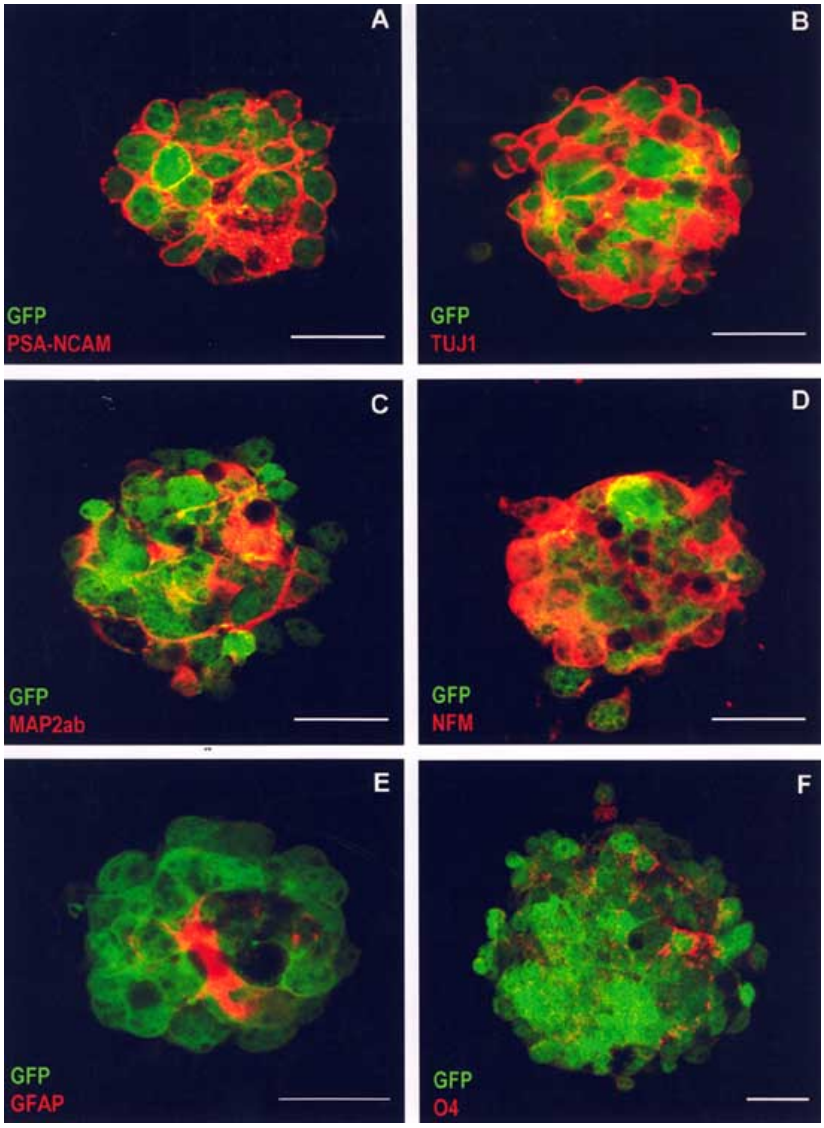

Fig. (5). Striata-derived PSA-NCAM$^+$ spheres expressing the green fluorescent protein: Neuronal-restricted precursor cells suited for transplantation experiments

(A-F) Immunocytochemical characterization of 3DIV-old PSA-NCAM$^+$ spheres isolated from striata of transgenic mice expressing the green fluorescent protein (GFP) driven by the ubiquitous β-actin promoter (The Jackson Laboratory, Strain C57BL/6-TgN(ACTbEGFP)1Osb). (A-F) Confocal microscopy optical sections of 3DIV-old PSA-NCAM$^+$ spheres showing the co-expression of GFP (green) and several lineage-specific markers (red) : PSA-NCAM (A), the neuronal proteins βIII-tubulin (recognized by the Tuj1 antibody) (B), type 2a,b-microtubule-associated protein (MAP2ab) (C) and neurofilament-M (NFM) (D), the astrocytic glial fibrillary-acidic protein (GFAP) (E), and the oligodendroglial ganglioside recognized by the O4 antibody (F). These results demonstrated that early postnatal striatal PSA-NCAM$^+$ cells purified by ultracentrifugation on Percoll density gradient (see Fig. (**3**)) led to the formation of spheres that were made of mainly proliferative neuroblasts, since almost no staining was observed for glial markers (E, F). Such neuron-oriented GFP$^+$/PSA-NCAM$^+$ precursor cells may be of great interest to be tested as cell therapy vectors in animal models of neurodegenerative diseases (in particular Huntington's and Parkinson's diseases). Scale bars = 20 μm for all panels.

stem cells [142,143], it is possible that PSA-NCAM$^+$ precursor cells could be temporally but also regionally specified by local inductive cues favoring them to generate region-appropriate progeny. One would thus expect striata-derived PSA-NCAM$^+$ neuroblasts to be the best accurately designed tool for cell therapy strategies aiming for the broad array of degenerative diseases affecting striatal areas.

ACKNOWLEDGEMENTS

We thank G. Rougon (Université de la Méditerranée, France), and J. Eriksson (University of Turku, Finland) for their generous gifts of antibodies. We are grateful to Nancy Van Overstraeten for taking over the breeding of β-actin-EGFP transgenic mice. B. Malgrange and S. Belachew, respectively are research associates and post-doctoral researchers of the *Fonds National de la Recherche Scientifique* (F.N.R.S., Belgium). This work was supported by the *Fonds pour la Formation à la Recherche dans l'Industrie et dans l'Agriculture* (F.R.I.A., Belgium), the *FNRS*, the *Fondation Médicale Reine Elisabeth* (FMRE), the *Fondation Charcot* and the *Ligue Belge de la Sclérose en Plaques*.

ABBREVIATIONS

BDNF	=	Brain-derived neurotrophic factor
BMP	=	Bone morphogenetic protein
CNS	=	Central nervous system
ECM	=	Extracellular matrix
EGF	=	Epidermal growth factor
FGF	=	Fibroblast growth factor
GABA	=	γ-Aminobutyric acid
GFAP	=	Glial fibrillary acidic protein
LGE	=	Lateral ganglionic eminence
LTP	=	Long-term potentiation
MGE	=	Medial ganglionic eminence
NCAM	=	Neural cell adhesion molecule
NMDA	=	N-Methyl D-aspartate
NRP	=	Neuronal restricted progenitor
NSC	=	Neural stem cell
NT-3	=	Neurotrophin-3
OP	=	Oligodendrocyte progenitor
PDGF	=	Platelet-derived growth factor
PSA	=	Polysialic acid
RMS	=	Rostral migratory stream
SVZ	=	Sub-ventricular zone

REFERENCES

[1] Schuurmans, C.; Guillemot, F. *Curr. Opin. Neurobiol.,* **2002**, *12*, 26.
[2] Sauvageot, C.M.; Stiles, C.D. *Curr. Opin. Neurobiol.,* **2002**, *1***5**M.; Rocher, V.; Belachew, S.; Malgrange, B.; Rogister, B.; Leprince, P.; Moonen, G. *Cell Tissue Res.,* **2001**, *305*, 187.
[4] Cameron, H.A.; Hazel, T.G.; McKay, R.D. *J. Neurobiol.,* **1998**, *36*, 287.
[5] Doetsch, F.; Garcia-Verdugo, J.M.; Alvarez-Buylla, A. *J. Neurosci.*, **1997**, *17*, 5046.
[6] Bruses, J.L.; Rutishauser, U. *Biochimie*, **2001**, *83*, 635.
[7] Ben Hur, T.; Rogister, B.; Murray, K.; Rougon, G.; Dubois-Dalcq, M. *J. Neurosci.*, **1998**, *18*, 5777.
[8] Mayer-Proschel, M.; Kalyani, A.J.; Mujtaba, T.; Rao, M.S. *Neuron*, **1997**, *19*, 773.
[9] Marmur, R.; Mabie, P.C.; Gokhan, S.; Song, Q.; Kessler, J.A.; Mehler, M.F. *Dev. Biol.*, **1998**, *204*, 577.
[10] Doetsch, F.; Alvarez-Buylla, A. *Proc. Natl. Acad. Sci. USA,* **1996**, *93*, 14895.
[11] Nait-Oumesmar, B.; Decker, L.; Lachapelle, F.; Avellana-Adalid, V.; Bachelin, C.; Baron-Van Evercooren, A. *Eur. J. Neurosci.,* **1999**, *11*, 4357.
[12] Picard-Riera, N.; Decker, L.; Delarasse, C.; Goude, K.; Nait-Oumesmar, B.; Liblau, R.; Pham-Dinh, D.; Baron-Van Evercooren, A. *Proc. Natl. Acad. Sci. USA,* **2002**, *99*, 13211.
[13] Buonomano, D.V.; Merzenich, M.M. *Annu. Rev. Neurosci.,* **1998**, *21*, 149.
[14] Benson, D.L.; Schnapp, L.M.; Shapiro, L.; Huntley, G.W. *Trends Cell Biol.,* **2000**, *10*, 473.
[15] Kiss, J.Z.; Troncoso, E.; Djebbara, Z.; Vutskits, L.; Muller, D. *Brain Res. Brain Res. Rev.,* **2001**, *36*, 175.
[16] Edelman, G.M. *Annu. Rev. Cell Biol.*, **1986**, *2*, 81.
[17] Edelman, G.M. *Annu. Rev. Physiol.,* **1986**, *48*, 417.
[18] Goridis, C.; Brunet, J.F. *Semin. Cell Biol.*, **1992**, *3*, 189.
[19] Finne, J. *J. Biol. Chem.*, **1982**, *257*, 11966.
[20] Rutishauser, U.; Landmesser, L. *Trends Neurosci.*, **1991**, *14*, 528.
[21] Acheson, A.; Sunshine, J.L.; Rutishauser, U. *J. Cell Biol.*, **1991**, *114*, 143.
[22] Rutishauser, U. *Curr. Opin. Neurobiol.*, **1993**, *3*, 709.
[23] Rougon, G. *Eur. J. Cell Biol.*, **1993**, *61*, 197.
[24] Nakayama, J.; Fukuda, M.N.; Fredette, B.; Ranscht, B.; Fukuda, M. *Proc. Natl. Acad. Sci. USA,* **1995**, *92*, 7031.
[25] Angata, K.; Nakayama, J.; Fredette, B.; Chong, K.; Ranscht, B.; Fukuda, M. *J. Biol. Chem.*, **1997**, *272*, 7182.
[26] Kojima, N.; Tachida, Y.; Yoshida, Y.; Tsuji, S. *J. Biol. Chem.*, **1996**, *271*, 19457.
[27] Eckhardt, M.; Muhlenhoff, M.; Bethe, A.; Koopman, J.; Frosch, M.; Gerardy-Schahn, R. *Nature*, **1995**, *373*, 715.
[28] Angata, K.; Suzuki, M.; Fukuda, M. *J. Biol. Chem.*, **1998**, *273*, 28524.
[29] Kitagawa, H.; Paulson, J.C. *J. Biol. Chem.*, **1994**, *269*, 17872.
[30] Ong, E.; Nakayama, J.; Angata, K.; Reyes, L.; Katsuyama, T.; Arai, Y.; Fukuda, M. *Glycobiology*, **1998**, *8*, 415.
[31] Hildebrandt, H.; Becker, C.; Murau, M.; Gerardy-Schahn, R.; Rahmann, H. *J. Neurochem.*, **1998**, *71*, 2339.
[32] Bruses, J.L.; Rutishauser, U. *J. Cell Biol.*, **1998**, *140*, 1177.
[33] Crossin, K.L.; Krushel, L.A. *Dev. Dyn.,* **2000**, *218*, 260.
[34] Fujimoto, I.; Bruses, J.L.; Rutishauser, U. *J. Biol. Chem.,* **2001**, *276*, 31745.
[35] Charles, P.; Hernandez, M.P.; Stankoff, B.; Aigrot, M.S.; Colin, C.; Rougon, G.; Zalc, B.; Lubetzki, C. *Proc. Natl. Acad. Sci. USA,* **2000**, *97*, 7585.
[36] Charles, P.; Reynolds, R.; Seilhean, D.; Rougon, G.; Aigrot, M.S.; Niezgoda, A.; Zalc, B.; Lubetzki, C. *Brain*, **2002**, *125*, 1972.
[37] Doherty, P.; Cohen, J.; Walsh, F.S. *Neuron*, **1990**, *5*, 209.
[38] Zhang, H.; Miller, R.H.; Rutishauser, U. *J. Neurosci.,* **1992**, *12*, 3107.
[39] Wang, C.; Rougon, G.; Kiss, J.Z. *J. Neurosci.,* **1994**, *14*, 4446.
[40] Wang, C.; Pralong, W.F.; Schulz, M.F.; Rougon, G.; Aubry, J.M.; Pagliusi, S.; Robert, A.; Kiss, J.Z. *J. Cell Biol.,* **1996**, *135*, 1565.
[41] Muller, D.; Wang, C.; Skibo, G.; Toni, N.; Cremer, H.; Calaora, V.; Rougon, G.; Kiss, J.Z. *Neuron*, **1996**, *17*, 413.
[42] Cremer, H.; Lange, R.; Christoph, A.; Plomann, M.; Vopper, G.; Roes, J.; Brown, R.; Baldwin, S.; Kraemer, P.; Scheff, S. *Nature*, **1994**, *367*, 455.
[43] Eckhardt, M.; Bukalo, O.; Chazal, G.; Wang, L.; Goridis, C.; Schachner, M.; Gerardy, S.; Cremer, H.; Dityatev, A. *J. Neurosci.,* **2000**, *20*, 5234.
[44] Chazal, G.; Durbec, P.; Jankovski, A.; Rougon, G.; Cremer, H. *J. Neurosci.,* **2000**, *20*, 1446.
[45] Decker, L.; Avellana-Adalid, V.; Nait-Oumesmar, B.; Durbec, P.; Baron-Van Evercooren, A. *Mol. Cell Neurosci.*, **2000**, *16*, 422.
[46] Decker, L.; Durbec, P.; Rougon, G.; Baron-Van Evercooren, A. *Mol. Cell Neurosci.,* **2002**, *19*, 225.
[47] Becker, C.G.; Artola, A.; Gerardy-Schahn, R.; Becker, T.; Welzl, H.; Schachner, M. *J. Neurosci. Res.,* **1996**, *45*, 143.
[48] Cremer, H.; Chazal, G.; Carleton, A.; Goridis, C.; Vincent, J.D.; Lledo, P.M. *Proc. Natl. Acad. Sci. USA,* **1998**, *95*, 13242.
[49] Amoureux, M.C.; Cunningham, B.A.; Edelman, G.M.; Crossin, K.L. *J. Neurosci.,* **2000**, *20*, 3631.

[50] Kiss, J.Z.; Rougon, G. *Curr. Opin. Neurobiol.,* **1997**, *7*, 640.
[51] Muller, D.; Djebbara, H.; Jourdain, P.; Vutskits, L.; Durbec, P.; Rougon, G.; Kiss, J.Z. *Proc. Natl. Acad. Sci. USA,* **2000**, *97*, 4315.
[52] Vutskits, L.; Djebbara-Hannas, Z.; Zhang, H.; Paccaud, J.P.; Durbec, P.; Rougon, G.; Muller, D.; Kiss, J.Z. *Eur. J. Neurosci.,* **2001**, *13*, 1391.
[53] Kalyani, A.; Hobson, K.; Rao, M.S. *Dev. Biol.*, **1997**, *186*, 202.
[54] Cai, J.; Wu, Y.; Mirua, T.; Pierce, J.L.; Lucero, M.T.; Albertine, K.H.; Spangrude, G.J.; Rao, M.S. *Dev. Biol.*, **2002**, *251*, 221.
[55] Kalyani, A.J.; Piper, D.; Mujtaba, T.; Lucero, M.T.; Rao, M.S. *J. Neurosci.*, **1998**, *18*, 7856.
[56] Seki, T.; Arai, Y. *Brain Res. Dev. Brain Res.*, **1993**, *73*, 141.
[57] Marshall, C.A.; Goldman, J.E. *J. Neurosci.*, **2002**, *22*, 9821.
[58] Anderson, S.A.; Eisenstat, D.D.; Shi, L.; Rubenstein, J.L. *Science*, **1997**, *278*, 474.
[59] He, W.; Ingraham, C.; Rising, L.; Goderie, S.; Temple, S. *J. Neurosci.*, **2001**, *21*, 8854.
[60] Trotter, J.; Bitter-Suermann, D.; Schachner, M. *J. Neurosci. Res.*, **1989**, *22*, 369.
[61] Grinspan, J.B.; Franceschini, B. *J. Neurosci. Res.*, **1995**, *41*, 540.
[62] Vitry, S.; Avellana-Adalid, V.; Hardy, R.; Lachapelle, F.; Baron-Van Evercooren, A. *J. Neurosci. Res.*, **1999**, *58*, 735.
[63] Gallo, V.; Armstrong, R.C. *J. Neurosci.*, **1995**, *15*, 394.
[64] Grinspan, J.B.; Stern, J.L.; Pustilnik, S.M.; Pleasure, D. *J. Neurosci.*, **1990**, *10*, 1866.
[65] Hardy, R.; Reynolds, R. *Development*, **1991**, *111*, 1061.
[66] Vitry, S.; Avellana-Adalid, V.; Lachapelle, F.; Baron-Van Evercooren, A. *Mol. Cell Neurosci.*, **2001**, *17*, 983.
[67] Rutishauser, U.; Landmesser, L. *Trends Neurosci.*, **1996**, *19*, 422.
[68] Szele, F.G.; Chesselet, M.F. *J. Comp Neurol.*, **1996**, *368*, 439.
[69] Alonso, G. *J. Comp. Neurol..,* **1999**, *414*, 149.
[70] Seki, T.; Arai, Y. *Neurosci Res.*, **1991**, *12*, 503.
[71] Seki, T.; Arai, Y. *J. Neurosci.*, **1993**, *13*, 2351.
[72] Nacher, J.; Lanuza, E.; McEwen, B.S. *Neuroscience*, **2002**, *113*, 479.
[73] Theodosis, D.T.; Rougon, G.; Poulain, D.A. *Proc. Natl. Acad. Sci. USA,* **1991**, *88*, 5494.
[74] Hu, H.; Tomasiewicz, H.; Magnuson, T.; Rutishauser, U. *Neuron*, **1996**, *16*, 735.
[75] Seki, T.; Arai, Y. *Anat. Embryol. (Berl),* **1991**, *184*, 395.
[76] Nacher, J.; Alonso-Llosa, G.; Rosell, D.; McEwen, B. *Brain Res.*, **2002**, *927*, 111.
[77] Bouzioukh, F.; Tell, F.; Jean, A.; Rougon, G. *J. Neurosci.,* **2001**, *21*, 4721.
[78] Bouzioukh, F.; Tell, F.; Rougon, G.; Jean, A. *Eur. J. Neurosci.,* **2001**, *14*, 1194.
[79] Nait-Oumesmar, B.; Vignais, L.; Duhamel-Clerin, E.; Avellana-Adalid, V.; Rougon, G.; Baron-Van Evercooren, A. *Eur. J. Neurosci.,* **1995**, *7*, 480.
[80] van Praag, H.; Schinder, A.F.; Christie, B.R.; Toni, N.; Palmer, T.D.; Gage, F.H. *Nature*, **2002**, *415*, 1030.
[81] Kempermann, G. *J. Neurosci.,* **2002**, *22*, 635.
[82] Kuhn, H.G.; Dickinson, A.; Gage, F.H. *J. Neurosci.,* **1996**, *16*, 2027.
[83] Miyata, T.; Maeda, T.; Lee, J.E. *Genes Dev.,* **1999**, *13*, 1647.
[84] Schwab, M.H.; Bartholomae, A.; Heimrich, B.; Feldmeyer, D.; Druffel-Augustin, S.; Goebbels, S.; Naya, F.J.; Zhao, S.; Frotscher, M.; Tsai, M.J.; Nave, K.A. *J. Neurosci.,* **2000**, *20*, 3714.
[85] Seki, T. *J. Neurosci. Res.,* **2002**, *70*, 327.
[86] Parent, J.M.; Yu, T.W.; Leibowitz, R.T.; Geschwind, D.H.; Sloviter, R.S.; Lowenstein, D.H. *J. Neurosci.,* **1997**, *17*, 3727.
[87] Nacher, J.; Rosell, D.R.; McEwen, B.S. *J. Comp. Neurol.,* **2000**, *424*, 628.
[88] Cameron, H.A.; McKay, R.D. *J. Comp. Neurol.,* **2001**, *435*, 406.
[89] Belachew, S.; Chittajallu, R.; Aguirre, A.A.; Yuan, X.; Kirby, M.; Anderson, S.; Gallo, V. *J. Cell Biol.*, **2003**, *161*, 169.
[90] Seki, T. *J. Neurosci. Res.,* **2002**, *69*, 772.
[91] Rousselot, P.; Lois, C.; Alvarez-Buylla, A. *J. Comp. Neurol.,* **1995**, *351*, 51.
[92] Lois, C.; Garcia-Verdugo, J.M.; Alvarez-Buylla, A. *Science*, **1996**, *271*, 978.
[93] Doetsch, F.; Caille, I.; Lim, D.A.; Garcia-Verdugo, J.M.; Alvarez-Buylla, A. *Cell*, **1999**, *97*, 703.
[94] Doetsch, F.; Petreanu, L.; Caille, I.; Garcia-Verdugo, J.M.; Alvarez-Buylla, A. *Neuron*, **2002**, *36*, 1021.
[95] Decker, L.; Picard, N.; Lachapelle, F.; Baron-Van Evercooren, A. *Prog. Brain Res.,* **2001**, *132*, 175.
[96] Lachapelle, F.; Avellana-Adalid, V.; Nait-Oumesmar, B.; Baron-Van Evercooren, A. *Mol. Cell Neurosci.,* **2002**, *20*, 390.
[97] Decker, L.; Picard-Riera, N.; Lachapelle, F.; Baron-Van Evercooren, A. *J. Neurosci. Res.*, **2002**, *69*, 763.
[98] Nguyen, L.; Malgrange, B.; Belachew, S.; Rogister, B.; Rocher, V.; Moonen, G.; Rigo, J.M. *Eur. J. Neurosci.,* **2002**, *15*, 1299.
[99] Nait-Oumesmar, B.; Vignais, L.; Baron-Van Evercooren, A. *J. Neurosci.,* **1997**, *17*, 125.
[100] Grinspan, J.B.; Edell, E.; Carpio, D.F.; Beesley, J.S.; Lavy, L.; Pleasure, D.; Golden, J.A. *J. Neurobiol.,* **2000**, *43*, 1.
[101] Louis, J.C.; Magal, E.; Muir, D.; Manthorpe, M.; Varon, S. *J. Neurosci. Res.,* **1992**, *31*, 193.
[102] Aaron, L.I.; Chesselet, M.F. *Neuroscience*, **1989**, *28*, 701.
[103] Szele, F.G.; Dowling, J.J.; Gonzales, C.; Theveniau, M.; Rougon, G.; Chesselet, M.F. *Neuroscience*, **1994**, *60*, 133.
[104] Butler, A.K.; Uryu, K.; Rougon, G.; Chesselet, M.F. *Neuroscience*, **1999**, *89*, 1169.
[105] Nguyen, L.; Malgrange, B.; Breuskin, I.; Bettendorff, L.; Moonen, G.; Belachew, S.; Rigo, J.M. *J. Neurosci.*, **2003**, *23*, 3278.
[106] Craig, C.G.; Tropepe, V.; Morshead, C.M.; Reynolds, B.A.; Weiss, S.; van, d. *J. Neurosci.,* **1996**, *16*, 2649.
[107] Garcion, E.; Faissner, A.; ffrench-Constant, C. *Development*, **2001**, *128*, 2485.
[108] Murase, S.; Horwitz, A.F. *J. Neurosci.,* **2002**, *22*, 3568.
[109] Atluri, P.; Fleck, M.W.; Shen, Q.; Mah, S.J.; Stadfelt, D.; Barnes, W.; Goderie, S.K.; Temple, S.; Schneider, A.S. *Dev. Biol.,* **2001**, *240*, 143.
[110] Schneider, A.S.; Atluri, P.; Shen, Q.; Barnes, W.; Mah, S.J.; Stadfelt, D.; Goderie, S.K.; Temple, S.; Fleck, M.W. *Ann. NY Acad. Sci.,* **2002**, *971*, 135.
[111] Ma, W.; Liu, Q.Y.; Maric, D.; Sathanoori, R.; Chang, Y.H.; Barker, J.L. *J. Neurobiol.,* **1998**, *35*, 277.
[112] Antonopoulos, J.; Pappas, I.S.; Parnavelas, J.G. *Eur. J. Neurosci.,* **1997**, *9*, 291.
[113] Haydar, T.F.; Wang, F.; Schwartz, M.L.; Rakic, P. *J. Neurosci.,* **2000**, *20*, 5764.
[114] Brezun, J.M.; Daszuta, A. *Neuroscience*, **1999**, *89*, 999.
[115] Brezun, J.M.; Daszuta, A. *Eur. J. Neurosci.,* **2000**, *12*, 391.
[116] Ma, W.; Maric, D.; Li, B.S.; Hu, Q.; Andreadis, J.D.; Grant, G.M.; Liu, Q.Y.; Shaffer, K.M.; Chang, Y.H.; Zhang, L.; Pancrazio, J.J.; Pant, H.C.; Stenger, D.A.; Barker, J.L. *Eur. J. Neurosci.,* **2000**, *12*, 1227.
[117] Belachew, S.; Rogister, B.; Rigo, J.M.; Malgrange, B.; Mazy, S.; Xhauflaire, G.; Coucke, P.; Moonen, G. *Eur. J. Neurosci.,* **1998**, *10*, 3556.
[118] Belachew, S.; Malgrange, B.; Rigo, J.M.; Rogister, B.; Leprince, P.; Hans, G.; Nguyen, L.; Moonen, G. *Eur. J. Neurosci.,* **2000**, *12*, 1924.
[119] Nacher, J.; Rosell, D.R.; Alonso-Llosa, G.; McEwen, B.S. *Eur. J. Neurosci.,* **2001**, *13*, 512.
[120] Bjorklund, A.; Lindvall, O. *Nat. Neurosci.,* **2000**, *3*, 537.
[121] Chmielnicki, E.; Goldman, S.A. *Prog. Brain Res.,* **2002**, *138*, 451.
[122] Liu, J.; Solway, K.; Messing, R.O.; Sharp, F.R. *J. Neurosci.,* **1998**, *18*, 7768.
[123] Fallon, J.; Reid, S.; Kinyamu, R.; Opole, I.; Opole, R.; Baratta, J.; Korc, M.; Endo, T.L.; Duong, A.; Nguyen, G.; Karkehabadhi, M.; Twardzik, D.; Patel, S.; Loughlin, S. *Proc. Natl. Acad. Sci. USA,* **2000**, *97*, 14686.
[124] Magavi, S.S.; Leavitt, B.R.; Macklis, J.D. *Nature*, **2000**, *405*, 951.
[125] Jin, K.; Minami, M.; Lan, J.Q.; Mao, X.O.; Batteur, S.; Simon, R.P.; Greenberg, D.A. *Proc. Natl. Acad. Sci. USA,* **2001**, *98*, 4710.
[126] Arvidsson, A.; Collin, T.; Kirik, D.; Kokaia, Z.; Lindvall, O. *Nat. Med.,* **2002**, *8*, 963.
[127] Johansson, C.B.; Momma, S.; Clarke, D.L.; Risling, M.; Lendahl, U.; Frisen, J. *Cell*, **1999**, *96*, 25.
[128] Yamamoto, S.; Nagao, M.; Sugimori, M.; Kosako, H.; Nakatomi, H.; Yamamoto, N.; Takebayashi, H.; Nabeshima, Y.; Kitamura, T.; Weinmaster, G.; Nakamura, K.; Nakafuku, M. *J. Neurosci.,* **2001**, *21*, 9814.
[129] Benraiss, A.; Chmielnicki, E.; Lerner, K.; Roh, D.; Goldman, S.A. *J. Neurosci.,* **2001**, *21*, 6718.
[130] Pencea, V.; Bingaman, K.D.; Wiegand, S.J.; Luskin, M.B. *J. Neurosci.,* **2001**, *21*, 6706.
[131] Nakatomi, H.; Kuriu, T.; Okabe, S.; Yamamoto, S.; Hatano, O.; Kawahara, N.; Tamura, A.; Kirino, T.; Nakafuku, M. *Cell*, **2002**, *110*, 429.

[132] Parent, J.M.; Vexler, Z.S.; Gong, C.; Derugin, N.; Ferriero, D.M. *Ann. Neurol.,* **2002**, *52*, 802.
[133] Franklin, R.J. *Nat. Rev. Neurosci.,* **2002**, *3*, 705.
[134] Carroll, W.M.; Jennings, A.R. *Brain*, **1994**, *117 (Pt 3)*, 563.
[135] Gensert, J.M.; Goldman, J.E. *Neuron*, **1997**, *19*, 197.
[136] Keirstead, H.S.; Levine, J.M.; Blakemore, W.F. *Glia*, **1998**, *22* , 161.
[137] Franklin, R.J.; Gilson, J.M.; Blakemore, W.F. *J. Neurosci. Res.,* **1997**, *50*, 337.
[138] Franklin, R.J.; Blakemore, W.F. *Mult. Scler.,* **1997**, *3*, 84.
[139] Keirstead, H.S. *J. Neurosci. Res.,* **2001**, *63*, 233.
[140] Keirstead, H.S.; Ben Hur, T.; Rogister, B.; Leary, M.T.; Dubois-Dalcq, M.; Blakemore, W.F. *J. Neurosci.,* **1999**, *19*, 7529.
[141] Ben Hur, T.; Einstein, O.; Mizrachi-Kol, R.; Ben Menachem, O.; Reinhartz, E.; Karussis, D.; Abramsky, O. *Glia*, **2003**, *41*, 73.
[142] Hitoshi, S.; Tropepe, V.; Ekker, M.; van der Kooy, D. *Development*, **2002**, *129*, 233.
[143] Temple, S. *Nature*, **2001**, *414*, 112.
[144] McKay, R. *Science*, **1997**, *276*, 66.
[145] van der Kooy, D.; Weiss, S. *Science*, **2000**, *287*, 1439.
[146] Williams, B.P.; Read, J.; Price, J. *Neuron*, **1991**, *7*, 685.
[147] Zhou, Q.; Anderson, D.J. *Cell*, **2002**, *109*, 61.
[148] Lu, Q.R.; Sun, T.; Zhu, Z.; Ma, N.; Garcia, M.; Stiles, C.D.; Rowitch, D.H. *Cell*, **2002**, *109*, 75.
[149] Rowitch, D.H.; Lu, Q.R.; Kessaris, N.; Richardson, W.D. *Trends Neurosci.,* **2002**, *25*, 417.
[150] Reynolds, B.A.; Weiss, S. *Science* , **1992**, *255*, 1707.
[151] Vescovi, A.L.; Reynolds, B.A.; Fraser, D.D.; Weiss, S. *Neuron*, **1993**, *11*, 951.
[152] Park, J.K.; Williams, B.P.; Alberta, J.A.; Stiles, C.D. *J. Neurosci.,* **1999**, *19*, 10383.
[153] Malatesta, P.; Hartfuss, E.; Gotz, M. *Development*, **2000**, *127*, 5253.
[154] Avellana-Adalid, V.; Nait-Oumesmar, B.; Lachapelle, F.; Baron-Van Evercooren, A. *J. Neurosci. Res.,* **1996**, *45*, 558.
[155] Rajan, P.; McKay, R.D. *J. Neurosci.,* **1998**, *18*, 3620.
[156] Tanigaki, K.; Nogaki, F.; Takahashi, J.; Tashiro, K.; Kurooka, H.; Honjo, T. *Neuron*, **2001**, *29*, 45.
[157] Mi, H.; Barres, B.A. *J. Neurosci.,* **1999**, *19*, 1049.
[158] Pringle, N.P.; Yu, W.P.; Howell, M.; Colvin, J.S.; Ornitz, D.M.; Richardson, W.D. *Development*, **2003**, *130*, 93.
[159] Kondo, T.; Raff, M. *Science*, **2000**, *289*, 1754.
[160] Laywell, E.D.; Rakic, P.; Kukekov, V.G.; Holland, E.C.; Steindler, D.A. *Proc. Natl. Acad. Sci. USA,* **2000**, *97*, 13883.
[161] Reynolds, B.A.; Weiss, S. *Science* , **1992**, *255*, 1707.
[162] Reynolds, B.A.; Tetzlaff, W.; Weiss, S. *J. Neurosci.,* **1992**, *12*, 4565.

7.9 Publication #9 (was part of our *PhD* thesis) : Belachew, S., Malgrange, B., Rigo, J.-M., Rogister, B., Coucke, P., Mazy-Servais, C., and Moonen, G. (1998). Developmental regulation of neuroligand-induced responses in cultured oligodendroglia. *Neuroreport* 9:973-980.

Developmental Neuroscience

neuroReport

Website publication 27 March 1998

NeuroReport **9**, 973–980 (1998)

Developmental regulation of neuroligand-induced responses in cultured oligodendroglia

Shibeshih Belachew,[1,2] Brigitte Malgrange,[1] Jean-Michel Rigo,[1] Bernard Rogister,[1,2] Paul Coucke,[1] Cécile Mazy-Servais[1] and Gustave Moonen[1,2,CA]

Department of [1]Human Physiology and Pathophysiology, University of Liège, 17 Place Delcour, B-4020, Liège; [2]Department of Neurology, University of Liège, CHU (B35) Sart Tilman, B-4000 Liège, Belgium

[CA]Corresponding Author

USING whole-cell patch-clamp techniques, we show that oligosphere-derived oligodendrocyte progenitor cells (OP) display GABA-, glutamate-, 5-HT-, glycine- and acetylcholine-gated inward currents. When OP differentiate into oligodendrocytes (ODC), the amplitude of peak currents elicited by saturating concentrations of these transmitters decreases except for 5-HT. Intracellular Ca^{2+} concentration changes induced by microperfusion of glutamate, 5-HT, TRH, met-enkephalin and substance P were monitored using a fluo-3-based calcium imaging system. When OP cells differentiate into ODC, a global decrease of the proportion of responding cells is observed. During type-2 astrocytes commitment, this proportion decreases for 5-HT, TRH- and met-enkephalin stimulations whereas it remains constant for substance P and glutamate. These data demonstrate a development regulation of neurotransmitter- and neuropeptide-induced responses within the oligodendroglial lineage. *NeuroReport* 9: 973–980 © 1998 Rapid Science Ltd.

Key words: Development; Fluo-3; Neuropeptide; Neurotransmitter; Oligodendrocyte; Patch-clamp

Introduction

Oligodendrocytes are the neural cells responsible for the synthesis and maintenance of myelin in the central nervous system (CNS). In cerebral cortex, they arise from progenitors which are located in the subventricular zone and migrate into the white matter where they proliferate and differentiate into mature oligodendrocytes.[1] The various stages of differentiation along the oligodendroglial lineage have been defined *in vitro*[2] as well as *in vivo*.[3] *In vitro*, the oligodendrocyte progenitor (OP) is a bipotential cell that, depending on the culture medium, can develop either into type-2 astrocytes (A2B5+, GFAP+, GAL-C–) or into oligodendrocytes (A2B5–, GFAP–, Gal-C+). The actual occurrence of type-2 astrocytes *in vivo* remains to be demonstrated, however.[4,5] Oligodendrocyte (ODC) commitment *in vitro* occurs in a defined medium, while the type-2 astrocyte differentiation is induced by supplementing the medium with fetal calf serum (FCS).

During the last few years, it has been shown that growth factors such as platelet-derived growth factor (PDGF),[6] insulin-like growth factor 1 (IGF-1),[7] basic fibroblast growth factor (bFGF),[6] ciliary neuronotrophic factor (CNTF)[5] and neurotrophin-3 (NT-3)[8] promote and/or modulate OP proliferation and differentiation. *In vivo*, these soluble factors probably arise from the neuronal and astroglial microenvironment of OP cells. Since neurotransmitters and neuropeptides are also an integral part of the chemical environment surrounding OP cells, possible paracrine effects should be considered in which case the corresponding receptors to these transmitters should be present on OP and ODC cells.

Oligodendrocytes express α1A-adrenergic,[9] β-adrenergic,[10] serotoninergic (5-HT), somatostatin and muscarinic G protein-coupled receptors,[11] GABA and glutamate-activated ion channels, voltage-dependent calcium and potassium channels and tetrodotoxin-sensitive sodium channels.[12,13] Regarding calcium signalling within oligodendroglial cells, a few studies have reported heterogeneous ATP, histamine, bradykinin and substance P receptor-mediated intracellular calcium responses.[14]

The only well-characterized biological effects of these neuroligands are the glutamate- and carbachol-induced modulation of OP cell proliferation which is correlated with an increased c-*fos* expression.[15,16] In order to obtain more insight into the biological meaning of such a complex array of receptor expression, we investigated the developmental regulation of O2A lineage cell responses to these various neuroligands. Therefore, using whole-cell patch-clamp techniques, we studied the evolution of various ligand-induced ionotropic responses during oligoden-

drocyte differentiation. Considering neuroligand-induced calcium signalling, we also performed a development study of oligodendroglial responses as compared with type-2 astrocytes which were used as positive controls for the calcium imaging method.

In these experiments, we used the recently described culture technique of OP oligospheres,[17] which allows large numbers of homotypic OP aggregates to be obtained after only 2 days *in vitro*. Compared with the most commonly used culture technique described by Cole and de Vellis,[18] this procedure enabled us to analyse OP after a short time *in vitro*, thus presumably having metabolic properties closer to the *in vivo* phenotype. Immunocytochemical characterization[17] has shown that cells within oligospheres express nestin and PSA-NCAM, two antigens specific of the early OP stage. Interestingly, such immature OP are known to persist in adult brain and to be a potential source of remyelinating oligodendrocytes after experimental demyelination in the subcortical white matter of adult rats.[19]

Materials and Methods

Cell culture: To prepare B104-conditioned medium, the B104 rat CNS neuroblastoma cell line was maintained in logarithmic phase of growth in Dulbecco's modified minimum essential medium (DMEM, Gibco) supplemented with 10% fetal calf serum and 2 mM glutamine. For conditioned medium production, confluent B104 cultures were washed twice with phosphate buffered saline (PBS) and incubated in serum-free DMEM containing 2 mM glutamine and N_1 supplement (insulin 5 μg/ml, transferrin 5 μg/ml, progesterone 20 nM, putrescine 100 μM and selenium 30 nM).[20] After 3 days, the medium was collected, filtered (0.22 μm) and stored at –20°C until use.

Primary oligodendrocyte cultures were prepared using a slight modification of the isolation procedure described by Avellana-Adalid *et al.*[17] The cerebral cortices of 1- to 3-day-old rat pups were dissected and collected in PBS supplemented with glucose at 4.5 g/l, carefully freed of meninges and vessels, and dissociated by sieving successively through a 225 μm and a 25 μm nylon mesh. Cells were collected in PBS containing 25 mM HEPES. The cell suspension was layered on top of a pre-centrifuged (30 min at 26 000 × **g**) Percoll density gradient (1.04 g/ml; Pharmacia) and centrifuged for 15 min at 26 000 × **g**. Cell debris which remained in the top aqueous phase was discarded and the interphase below the debris and just above the red blood cells was resuspended in PBS–HEPES. The suspension was centrifuged three times (10 min at 400 × **g**) in PBS–HEPES to eliminate Percoll. The final pellet was resuspended in DMEM supplemented with N_1, biotin (10 ng/ml) and 30% (v/v) B104 conditioned medium (B104-CM). Five milliliters of the cell suspension were then seeded on an uncoated 25 cm^2 tissue culture flask (Falcon; Becton/Dickinson) at a concentration of 4×10^6 cells/ml. After 24 and 48 h the flask was gently shaken and the suspension transferred into a new flask, allowing the elimination of adhering cells. After these preplatings, the progenitor cells make up spheroid aggregates termed oligospheres (150–300 μm diameter). To obtain an oligodendrocyte commitment, oligospheres were switched to DMEM–N_1 medium and seeded on polyornithine-coated (0.1 mg/ml) glass coverslips in the center of 35 mm plastic Petri dishes (NUNC; 10–25 oligospheres/coverslip). To induce type-2 astrocyte commitment, the same procedure was used except that DMEM–N_1 was supplemented with 10% (v/v) FCS.

Immunocytochemistry: Cultures on coverslips were fixed in 4% (v/v) paraformaldehyde for 10 min at room temperature. Non-specific binding was blocked by a 60 min incubation in PBS containing non-fat dry milk (15 mg/ml). This was followed by 60 min incubation at 37°C in the presence of a rabbit polyclonal anti-Gal-C antibody (Sigma) and a mouse monoclonal anti-A2B5 antibody (Boehringer-Mannheim) both at 1:100 dilution. As secondary antibodies, a rhodamine-conjugated anti-rabbit IgG (Jackson) at 1:400 and a FITC-conjugated anti-mouse Ig (Boehringer-Mannheim) at 1:30 dilution was used for a 60 min at room temperature. For GFAP staining, the same fixation protocol was followed by a 30 min incubation in PBS containing non-fat dry milk and Tween 20 (1:2000). Monoclonal anti-GFAP (1:1000) was diluted in the same solution and applied for 45 min at 37°C. A 10 min Triton-X100 (0.1% in PBS) permeabilization preceded the 45 min incubation with a FITC-conjugated anti-mouse IgG (1:250; Jackson). Triple PBS rinses were performed between steps. For anti-neurofilament staining, we used the mouse antibodies SMI 31 and SMI 32 (Sternberger-Meyer, Jarretsville, MD) as described by Malgrange *et al.*[21]

Electrophysiology: For recording of membrane currents, the cells were transferred to the stage of an inverted Hoffman contrast microscope and maintained at room temperature (20–25°C) in a recording chamber which was continuously perfused allowing application of drugs. The extracellular perfusion solution contained (mM): NaCl 116.0; D-glucose 11.1; KCl 5.4; $CaCl_2.2H_2O$ 1.8; $MgCl_2.6H_2O$ 2.0; HEPES 10.0; pH 7.2. All the neurotransmitters were from Sigma except glycine which was from UCB. The

reagents were applied by a rapid microperfusion system (SPS-8, List-Medical) at 1 mM in standard external solution.

Recording electrodes were made from borosilicate capillaries (Hilgenberg, Malsfeld, Germany) using a Flaming-Brown microelectrode puller (Model P97, Sutter Instruments Co). Recording pipettes (10–20 MΩ) were filled with a solution containing (mM): KCl 130.0; $CaCl_2.2H_2O$ 1.0; D-glucose 11.1; EGTA 10.0; and Na_2- or Mg-ATP 5.0; HEPES 10.0; pH 7.4.

Voltage-clamp recordings were performed with a Bio-Logic RK-400 patch-clamp amplifier using the tight-seal whole-cell recording configuration.[22] Series resistances were in the range 10–20 MΩ and were electronically compensated (up to 85–90%). Current traces were digitized and stored on an AT-compatible computer system. Control of drug application, data acquisition and data analysis were achieved using an ITC-16 acquisition board (Instrutech Corporation) and the TIDA for Windows software (HEKA Elektronik).

Calcium imaging: Cells were loaded with the calcium indicator dye fluo-3 AM (6 μM; Molecular Probes) by bath application for 45 min at 37°C. Fluo-3 AM is a non-ratiometric indicator dye that increases cellular fluorescence intensity with increased intracellular calcium concentration. Loaded cells were then washed three times with Hank's balanced salt solution (HBS). The responses of cells to experimental conditions were recorded as digitized images acquired with a Bio-Rad MRC 1000 laser scanning confocal system coupled to Zeiss Axiovert 135 microscope with a plan-NEOFLUAR objective (40×, 1.3 n.a., oil immersion). The TCSM program (Bio-Rad) was used to control the confocal microscope in order to acquire a series of images at 2–5 s intervals. The different reagents were applied by a fast microperfusion system (SPS-8, List-Medical) diluted in Hank's solution at the following concentrations (μM): glutamate (Sigma) 1000; 5-HT (Sigma) 100; thyrotropin releasing hormone (TRH) (UCB) 50; substance P (Sigma) 2; met-enkephalin (Sigma) 10. The series of digitized fluorescence images was analyzed by a program determining the average level of fluorescence of each cell above background level for every time point sampled. The locations of cells are delimited by placing rectangular boxes around every cell in a field. A background box was also defined in a non-cellular area of the scanned image. The averaged intensity of the pixels within a boxed cellular region was calculated by the program and the averaged intensity of the pixels within the background box defined for the image was subtracted from this value. In order to compensate for variable dye loading between cells, these background-corrected values were normalized by conversion to percent changes relative to a baseline measurement for each boxed cellular region at the start of a time series (F_t/F_0). Statistical analysis was performed using GraphPAD Prism software and GraphPAD InStat.

Results

Electrophysiological recordings: The cultured cells were studied in the outgrowth zone of expanded oligospheres at various differentiation stages, i.e. 1, 3 and 7 days after switching to DMEM-N_1. In this growth factor-free medium, immunocytochemical staining demonstrated that after 7 days, 97% of the cells were Gal-C+ while at day 1 95% of the cells were A2B5+. Three-day-old cultures contained a mixed population with 60% A2B5+ cells and 60% Gal-C+ cells, thus including double-stained cells. After 7 days in DMEM-N_1 only 3% of the cells were GFAP positive. In the areas from where electrophysiological and calcium imaging recordings were made, no cells were positive after immunocytochemical staining using anti-phosphorylated and unphosphorylated neurofilament antibodies.

Under our recording conditions, day 1 progenitor cells and day 7 oligodendrocytes had respective mean (± s.d.) membrane potentials of –70 ± 6 mV (n = 14) and –56 ± 5 mV (n = 22). All our patch-clamp experiments were performed in the whole-cell configuration and in voltage-clamp conditions at a holding membrane potential of –70 mV. We recorded inward currents elicited by bath application (10 s) of five different neurotransmitters (GABA, glutamate, glycine, serotonin and acetylcholine) at 1 mM concentration (Fig. 1A). At such concentrations, the induced currents are maximum currents (I_{max}), the amplitude of which reflects receptors density. The glycine, 5-HT and acetylcholine responses could be reversibly inhibited respectively by strychnine, 3-5-tropyl-dichlorobenzoate (5-HT_3 antagonist) and hexamethonium (nicotinic blocker; Fig. 2). As shown in Fig. 1B, values of I_{max} were maximum at the intermediate differentiation stage (3 days *in vitro*) except for 5-HT, when I_{max} increased from day 1 to day 3 and remained thereafter constant. If the proportion of responding cells rather than I_{max} is used to compare cells between the different differentiation stages (Fig. 1C), neurotransmitters fall into three categories: roughly all cells were responsive to GABA and glutamate whatever the differentiation stage; for glycine and acetylcholine, the percentage of responsive cells culminates at the intermediate stage; the proportion of 5-HT responsive cells increases with the cell differentiation.

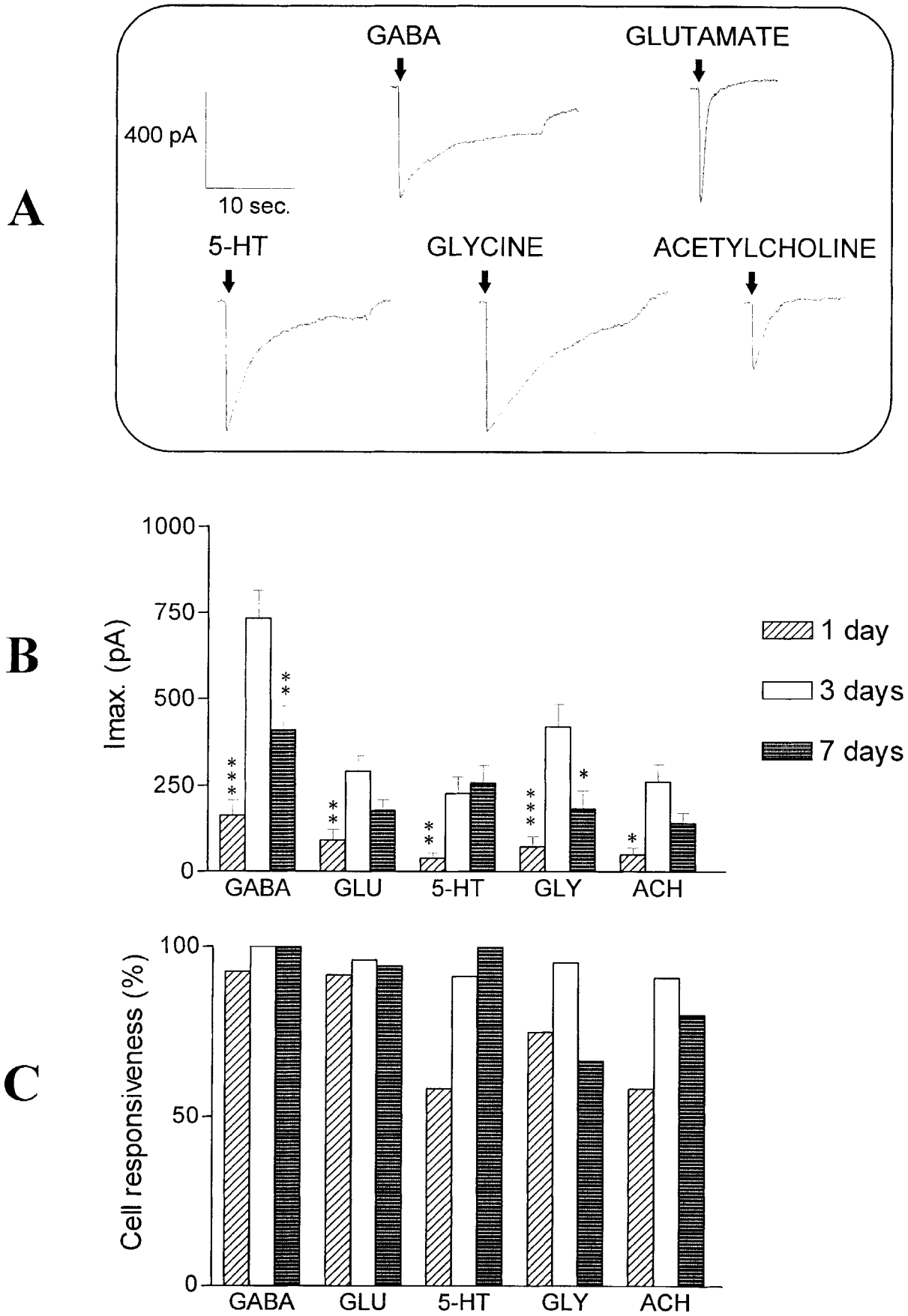
A
GABA
GLUTAMATE
400 pA
10 sec.
5-HT
GLYCINE
ACETYLCHOLINE
B
Imax. (pA)
1000
750
500
250
0
GABA
GLU
5-HT
GLY
ACH
1 day
3 days
7 days
C
Cell responsiveness (%)
100
50
0
GABA
GLU
5-HT
GLY
ACH

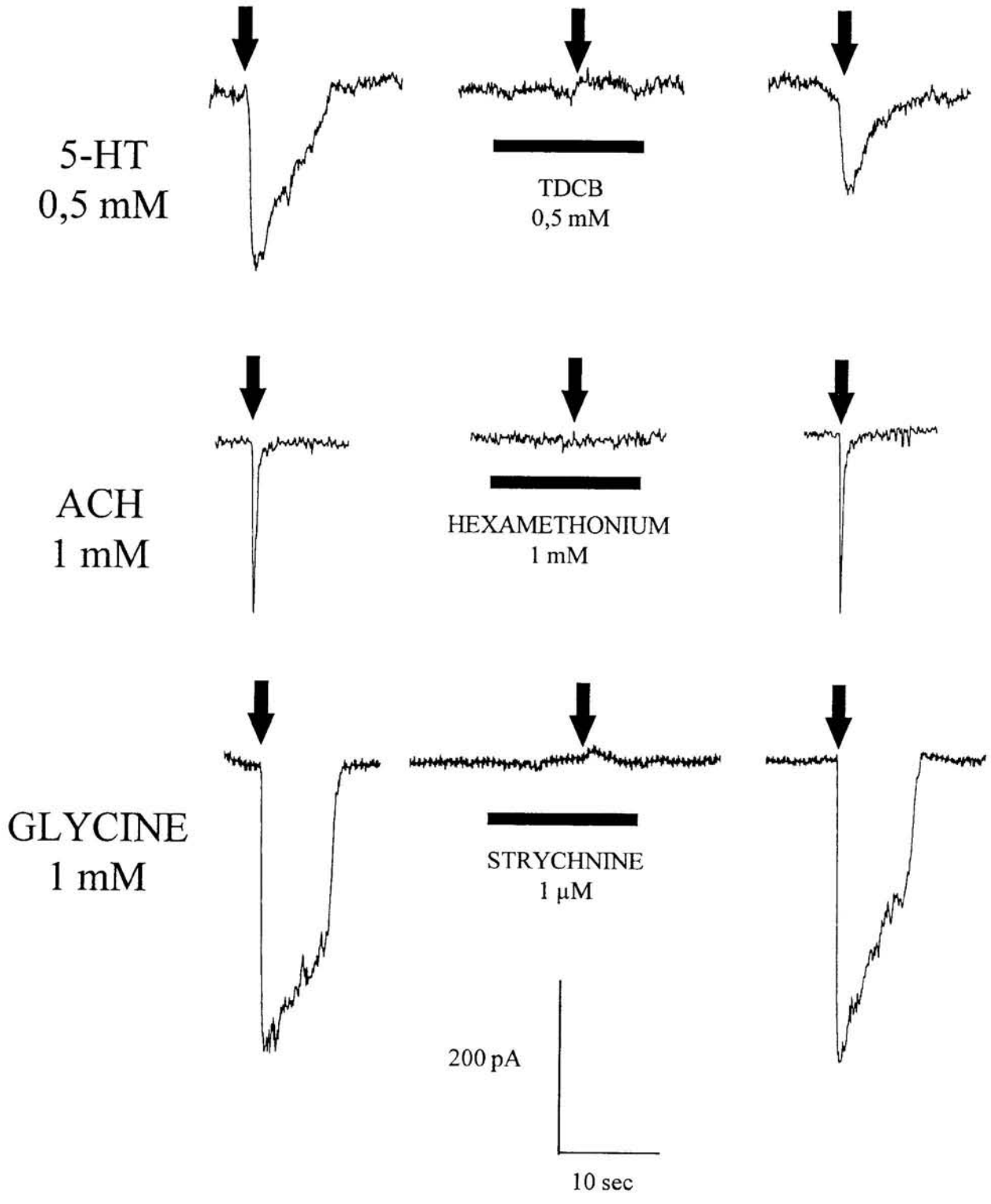

FIG. 2. Specific reversible inhibition of neurotransmitter responses. 5-HT-, ACh- and glycine-induced inward currents were inhibited by TDCB, hexamethonium and strychnine, which are respectively 5-HT_3, nicotinic and glycine receptor antagonists.

FIG. 1. Development characterization of neurotransmitter-induced currents during the oligodendrocyte maturation *in vitro*. (**A**) All the neurotransmitters were applied for 10 s by microperfusion at the same concentration (1 mM) and the resulting inward currents were recorded. The five traces were obtained from one individual OP cell and are separated by 60 s. (**B**) Histograms representing amplitudes of maximum currents (mean ± s.e.m.) for several neurotransmitters at three progressive stages of maturation in DMEM–N_1. These data were analyzed for significance using Student's *t*-test. The results are expressed relative to the day 3 population; $*p < 0.05$, $**p < 0.01$, $***p < 0.001$. (**C**) Responsiveness as the proportion of responsive cells as a function of time in culture. Responsive cells were defined as cells with neuroligand-induced currents of $\geqslant$ 10 pA.

Calcium imaging: For calcium studies, we imaged day 1 OP cells, day 3 intermediate differentiated cells, mature ODC (day 7 in DMEM–N_1) and type-2 astroglial cells (day 7 in DMEM–N_1–FCS). In this latter medium, 95% of the cells were GFAP+. Typical recordings are illustrated in Fig. 3. For the five neuroactive substances tested (Fig. 4), we observed a decrease in the proportion of responding cells when OP matured to ODC. After ODC differentiation, we also demonstrated a decrease of the percentage of calcium responding cells during a depolarizing stimulus induced by extracellular solutions containing high potassium concentration (50 mM). When OP differentiated into type-2 astrocytes, we observed an unchanged proportion of responding cells for substance P and glutamate stimulations, and a decreased proportion of responding type-2 astrocytes as compared to OP for 5-HT, TRH, met-enkephalin and high K^+ applications.

Discussion

$GABA_A$ and non-NMDA ionotropic receptors have already been demonstrated in cells of the ODC lineage and their development regulation has been described.[13] Glycine receptors had only been described on spinal cord ODC cells.[23] Here we extend these data to other ionotropic receptors studied on primary cortical ODC cultures. The reversible inhibition of glycine-, 5-HT- and acetylcholine-induced currents by selective antagonists demonstrates that the corresponding receptors are present in cultured cortical ODC. At the concentration used in the present study, the amplitude of the inward current measured at the same holding potential allows a comparison of receptor densities. As already reported for GABA and glutamate,[13] glycine and acetylcholine induced a decrease in I_{max} with progressive ODC differentiation, while the 5-HT I_{max}

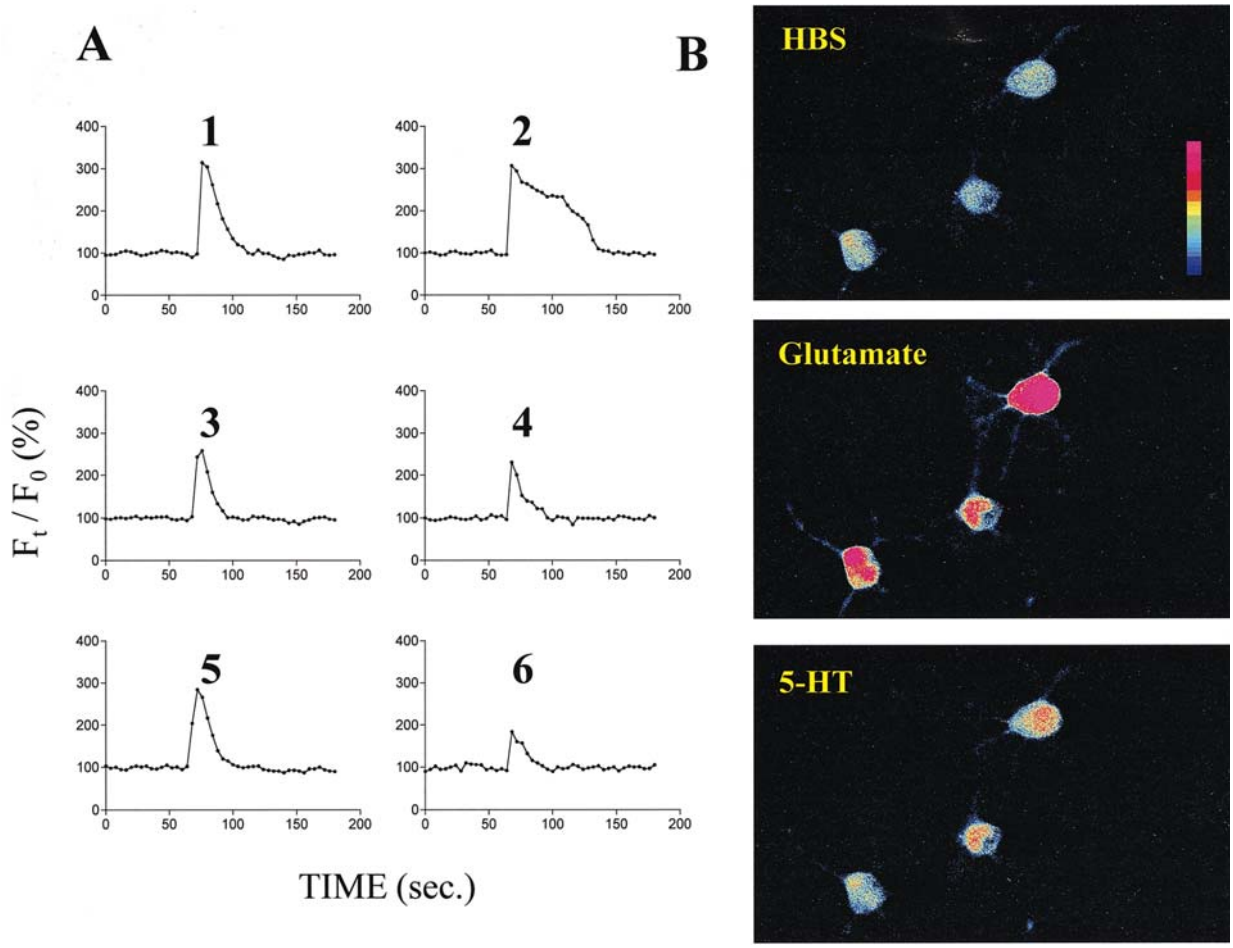

FIG. 3. Fluo-3 measurements of neuroligand-induced calcium mobilization. (**A**) Time-course of depolarization- and neuroligand-induced intracellular calcium increase in day 1 progenitor cells. High potassium concentration (50 mM) (1), glutamate (2), serotonin (3), TRH (4) substance P (5) and met-enkephalin (6) were applied by microperfusion for 30 s. (**B**) Example of three fluo-3 loaded OP cells in control condition, during application of glutamate and during application of 5-HT.

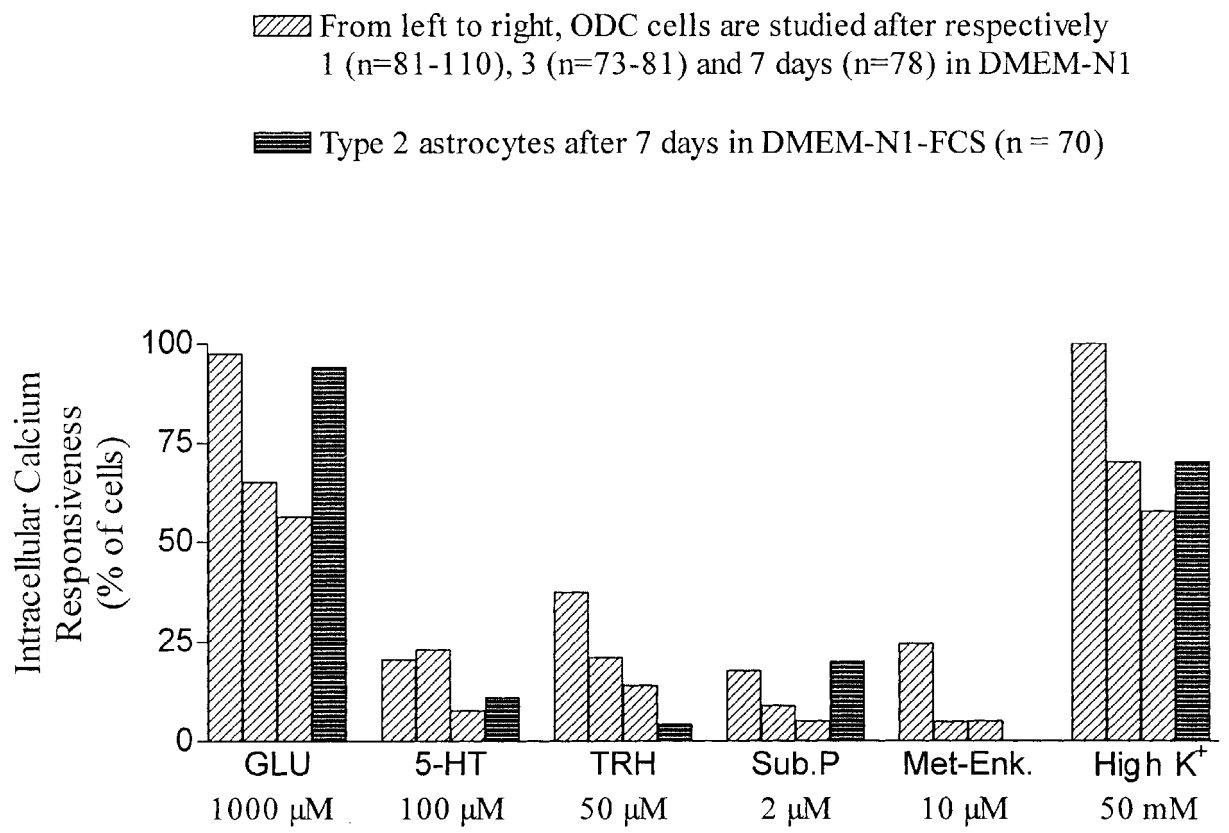

FIG. 4. Proportion of responsive cells as a function of cell type (OP, pre-oligodendrocyte, oligodendrocyte and type-2 astrocyte). Responsive cells were defined as cells with neuroligand-induced increase of F_t/F_0 of $\geqslant 10\%$ above the baseline within 30 s of drug application. Responsiveness is expressed as in Fig. 1C.

response increased, suggesting a parallel evolution of the corresponding receptors densities between days 3 and 7 in culture. Surprisingly, the values of I_{max} recorded in day 1 OP cells were much lower than those recorded at day 3. This could reflect a lower expression of neurotransmitters receptors at the early progenitor stage. Nevertheless, it has to be pointed out that the cells recorded at day 1 have just been switched from a medium containing 30% B104CM which might contain neurotransmitters. Therefore, the low I_{max} measured at day 1 could result from a down-regulation of the receptors.

Regarding intracellular calcium studies, type-2 astrocytes differed from ODC commitment by the maintenance of substance P and glutamate responsiveness. During ODC differentiation, we observed a decrease in cells responding to the five neuroactive substances tested. If we consider only the ODC cells which do not respond to high K^+ depolarization by increasing intracellular calcium (43%, $n = 78$), we never observed calcium responses to neuroligands in these cells except in the case of glutamate, and then only in a few cells (11%) (data not shown). This suggests that neuroligand-induced calcium responses in the oligodendroglial lineage depend on the presence of voltage-dependent calcium channels (VDCC). Therefore, the decrease of responsiveness during ODC differentiation could simply result from the decrease of VDCC expression. Further experiments are needed to demonstrate that this correlation between the absence of calcium response to neuroligands and depolarization results indeed from a decreased density of VDCC expression with ODC differentiation.

If on the contrary, we correlate the depolarizing effects of glycine, GABA[24] and acetylcholine in oligodendroglial cells with the well known high densities of VDCC especially at the progenitor stage,[13] it can be suggested that the neuroligands tested in the present study interfere through depolarization with intracellular calcium homeostasis of oligodendroglial cells. Calcium signals are known to be involved in the regulation of glial differentiation, protein synthesis, and gene expression through modulation of calcium-binding proteins, kinases and phospholipases.[25] However, the precise role of receptor-mediated calcium signalling in oligodendrocytes *in vivo* remains undefined. We speculate

that neuroligand-mediated communications between neurons and oligodendrocytes might influence the behavior of the cells within the ODC lineage. Furthermore, as it is established that developing oligodendrocytes are connected by functional gap junctions,[14] the neuroligand-induced effects might spread to adjacent myelinating cells.

Conclusion

We studied oligodendroglial neuroligand receptors densities using I_{max} measurements and the percentage of responding cells as a function of the differentiation stages. The results demonstrate that expression of neurotransmitters and neuropeptide receptors is regulated during differentiation and suggest a role for these ligands during the emergence of myelinating cells within the CNS.

References

1. Goldman JE, Geier SS and Hirano M. *J Neurosci* **6**, 52–60 (1986).
2. Raff MC. *Science* **243**, 1450–1455 (1989).
3. Young GM and Levison SW. *Dev Neurosci* **18**, 255–265 (1996).
4. Barres BA, Hart IK, Coles HS *et al. J Neurobiol* **23**, 1221–1230 (1992).
5. Lillien LE and Raff MC. *Neuron* **5**, 111–119 (1990).
6. McKinnon RD, Smith C, Behar T *et al. Glia* **7**, 245–254 (1993).
7. McMorris FA, Mozell RL, Carson MJ *et al. Ann NY Acad Sci* **692**, 321–334 (1993).
8. Barres BA, Raff MC, Gaese F *et al. Nature* **367**, 371–375 (1994).
9. Cohen RI and Almazan G. *Neuroreport* **4**, 1115–1118 (1993).
10. Vartanian T, Sprinkkle TJ, Dawson G *et al. Proc Natl Acad Sci USA* **85**, 939–943 (1988).
11. Karschin A, Wischmeyer E, Davidson N *et al. Eur J Neurosci* **6**, 1756–1764 (1994).
12. Barres BA, Koroshetz WJ, Swartz KJ *et al. Neuron* **4**, 507–524 (1990).
13. Kettenmann H, Blankenfeld GV and Trotter J. *Ann NY Acad Sci* **633**, 64–77 (1991).
14. Takeda M, Nelson DJ and Soliven B. *Glia* **14**, 225–236 (1995).
15. Liu H and Almazan G. *Eur J Neurosci* **7**, 2355–2363 (1995).
16. Almazan G and Cohen RI. *Trans Am Soc Neurochem* **24**, 176–176 (1993).
17. Avellana-Adalid V, Nait Oumesmar B, Lachapelle F *et al. J Neurosci Res* **45**, 558–570 (1996).
18. Cole R and de Vellis J. Preparation of astrocyte and oligodendrocyte cultures from rat glial cultures. In: Shahar A, de Vellis J, Vernadakis A and Haber B eds. *A Dissection and Tissue Culture Manual of the Nervous System*. New York: Alan R. Liss, 1989: 121–133.
19. Gensert JM and Goldman JE. *Neuron* **19**, 197–203 (1997).
20. Bottenstein JE and Sato G. *Proc Natl Acad Sci USA* **76**, 514–517 (1979).
21. Malgrange B, Delrée P, Rigo J-M *et al. J Neurosci Methods* **53**, 111–122 (1994).
22. Hamill OP, Marty A, Neher E *et al. Pflugers Arch* **391**, 85–100 (1981).
23. Pastor A, Chvatal A, Sykova A *et al. Eur J Neurosci* **7**, 1188–1198 (1995).
24. Gilbert P, Kettenmann H and Schachner M. *J Neurosci* **4**, 561–569 (1984).
25. Finkbeiner SM. *Glia* **9**, 83–104 (1993).

ACKNOWLEDGEMENTS: This work was supported by the Fonds National de la Pecherche Scientifique (FNRS), the Concerted Action of the French Community of Belgium and by the Fondation Médicale Reine Elisabeth (FMRE). We thank P. Ernst-Gengoux for her technical support and expertise. B. Rogister, S. Belachew and B. Malgrange are supported by the FNRS.

Received 17 December 1997; accepted 21 January 1998

7.10 Publication #10 (was part of our *PhD* thesis) : Belachew, S., Rogister, B., Rigo, J.-M., Malgrange, B., Mazy-Servais, C., Xhauflaire, G., Coucke, P., and Moonen, G. (1998). Cultured oligodendrocyte progenitors derived from cerebral cortex express a glycine receptor which is pharmacologically distinct from the neuronal isoform. *Eur. J. Neurosci.* 10:3556-3564.

European Journal of Neuroscience, Vol. 10, pp. 3556–3564, 1998

Cultured oligodendrocyte progenitors derived from cerebral cortex express a glycine receptor which is pharmacologically distinct from the neuronal isoform

Shibeshih Belachew,[1,2] Bernard Rogister,[1,2] Jean-Michel Rigo,[1] Brigitte Malgrange,[1] Cécile Mazy-Servais,[1] Gaël Xhauflaire,[1] Paul Coucke[1] and Gustave Moonen[1,2]
[1]Department of Human Physiology and Pathophysiology, University of Liège, 17 Place Delcour, B-4020 Liège, Belgium
[2]Department of Neurology, University of Liège, CHU (B35) Sart Tilman, B-4000 Liège, Belgium

Keywords: glycine receptor, oligodendroglia, patch-clamp, rat cerebral cortex

Abstract

Using the whole-cell patch-clamp technique, we demonstrate glycine-induced currents in oligosphere-derived oligodendrocyte progenitors cultured from newborn rats. Similar inward currents are also triggered by β-alanine and taurine, two established glycine receptor agonists. In our recording conditions, glycine-gated currents in oligodendrocyte progenitors reverse about 0 mV and are reversibly inhibited by the glycine competitive antagonist strychnine, the Cl^- channel blocker picrotoxinin and the non-competitive antagonist cyanotriphenylborate. The oligodendrocyte progenitors glycine receptor (GlyR) differs from the corresponding neuronal receptor: [^{3}H]strychnine binding data and the strychnine inhibition curve of glycine-induced currents in oligodendrocyte progenitor cultures suggest the existence of two strychnine binding sites on the oligodendroglial GlyR. Using total RNA isolated from oligodendrocyte progenitors cultures, reverse transcription–polymerase chain reaction analysis of glycine receptor subunit expression shows the presence of α_2 and β subunits and immunocytochemical stainings confirm that this GlyR contains an α subunit which is not α_1. The molecular structure of the oligodendroglial GlyR could be either homopentameric α_2 or heteromeric $\alpha_2\beta$ but in both cases, the sequence of the α_2 or β subunits have to be different from the known neuronal sequences in order to explain, respectively, the cyanotriphenylborate (α_2) and picrotoxinin (β) sensitivities. This work thus demonstrates that GlyR are expressed by oligodendrocytes obtained not only from spinal cord but also from supraspinal structures. The pharmacological properties and presumably the molecular structure of oligodendroglial GlyR are original. The physiological meaning of the presence of such receptors on developing and mature oligodendrocytes remains unknown.

Introduction

Fast synaptic inhibition in the central nervous system (CNS) is mostly mediated by γ-aminobutyric acid (GABA) and glycine. Binding of these amino acids to specific receptors on the postsynaptic membrane opens intrinsic chloride channels resulting in inhibition of neuronal firing (Curtis *et al*., 1968). The glycine receptor (GlyR) is an heteropentameric transmembrane protein composed of α (48 kDa) and β (58 kDa) subunits (Betz *et al*., 1994). This structure is characteristic of the ligand-gated ion channel superfamily (Betz, 1990). Developmentally and regionally regulated expression of the different subunit variants of the GlyR occurs and leads to their assembly into functionally and pharmacologically distinct receptors(Betz, 1991). To date, cDNAs of three different genes encoding GlyR α subunits (α_1–α_3) are known in rats and humans (Betz *et al*., 1994). In addition, a murine gene (α_4) and a cDNA encoding a rat α_2 subunit variant (α_2*) have been described (Kuhse *et al*., 1990; Matzenbach *et al*., 1994). Moreover, alternative splicing contributes to GlyR heterogeneity resulting in the formation of two isoforms for both the α_1 and α_2 subunits (Betz *et al*., 1994). The sequences of all α-subunits display a high degree of amino acid identity. The α_1 polypeptide is the originally described adult GlyR ligand-binding subunit whereas α_2 is mainly expressed at the perinatal period and α_3 during a transient postnatal period (Betz, 1991).

The α subunit variants carry the GlyR binding sites for the agonists glycine, β-alanine and taurine (Langosch *et al*., 1990; Vandenberg *et al*., 1992b), for the competitive antagonist strychnine, a convulsive alkaloid (Grenningloh *et al*., 1987) and for cyanotriphenylborate, a non-competitive use-dependent channel blocker (Rundström *et al*., 1994). In contrast, the β subunit is expressed in a single form throughout the CNS at all developmental stages. This subunit is not required for ligand binding (Grenningloh *et al*., 1990) but confers via one of its four hydrophobic segments (M2) the resistance to the alkaloid picrotoxinin (Schmieden *et al*., 1989; Pribilla *et al*., 1992).

Correspondence: G. Moonen, Department of Human Physiology and Pathophysiology, University of Liège, 17 Place Delcour, B-4020 Liège, Belgium. E-mail: sbelachew@ulg.ac.be

Received 12 February 1998, revised 10 June 1998, accepted 29 June 1998

TABLE 1. PCR primers sequences for the different GlyR subunits, and predicted sizes of PCR fragments

GlyR receptor subunits	Primer sequences (5′-3′)	Annealing temperature	Predicted product size (bp)
α_1	426-AGACAACCATGGACTACAGGGT-447 748-ACCAAAGCTTTCCAGTTGCATG-727 (Grenningloh *et al*., 1987)	57 °C	323
α_2	1058-AAGAAGAGAAGGAACTTGG-1076 1373-AACACAAACAGAAGGCAC-1356 (Grenningloh *et al*., 1990	52 °C	316
α_3	1191-CCTTCTGATTGTCATTCTGTCC-1212 1534-TCTCCCTCACCTCATCATCC-1515 (Kuhse *et al*., 1990)	56 °C	344
β	50-AAAGGGAAGGGGAAAAAG-67 468-TCCCGAAAGATAAACAACAG-449 (Mülhardt *et al*., 1994)	53 °C	419

Cells of the oligodendroglial lineage have been shown to express different developmentally regulated voltage- and ligand-gated ion channels (Kettenmann *et al*., 1991; Belachew *et al*., 1998). So far, little information about glial GlyR is available. Using patch-clamp techniques, glycine-induced currents have been demonstrated in astrocytes, oligodendrocytes and precursor cells from spinal cord slices derived from newborn rats (Pastor *et al*., 1995). Single-cell reverse transcription–polymerase chain reaction (RT–PCR) studies have provided evidence for two populations of spinal cord glial cells expressing the GlyR: one group expresses only α_1 transcripts while the second expresses both α_1 and β. The α_2 and α_3 subunits transcripts were not detected in newborn spinal cord glial cells and no correlation was found between the GlyR molecular structure and the differentiation stage (Kirchhoff *et al*., 1996).

The present study was undertaken in order to see if glycine receptors are also expressed on oligodendrocytes obtained from the cerebral cortex where the role of glycine as an inhibitory neurotransmitter is at best marginal. We characterized in detail the pharmacology of these receptors as compared with their neuronal counterparts. These details are important to elucidate the functional meaning of oligodendrocyte glycine receptor during both physiological and pathological processes.

Materials and methods

Cell culture

Preparation of B104-conditioned medium

The B104 is a rat CNS neuroblastoma cell line that is maintained in the logarithmic phase of growth in Dulbecco's modified minimum essential medium (DMEM, Gibco, Menelbke, Belgium) supplemented with 10% heat-inactivated fetal calf serum and 2 mM glutamine. Medium conditioning was made after 2 days of culture. The B104 cultures (seeding density: 100–150 cells/mm^2) are washed twice with phosphate-buffered saline (PBS) and then incubated in serum-free DMEM containing 2 mM glutamine and the N_1 supplement (insulin 5 µg/mL; transferrin 5 µg/mL; progesterone 20 nM; putrescine 100 µM, selenium 30 nM) (Bottenstein & Sato, 1979). After 3 days of incubation, the medium is collected, filtered (0.22 µm) and stored at –20 °C until use.

Primary oligodendrocyte progenitor cell cultures

They are prepared using a slight modification of the procedure described by Avellana-Adalid *et al*. (1996). The cerebral cortices of 1–3-day-old rat pups are dissected (in PBS supplemented with glucose at 4.5 g/L), carefully freed of meninges and vessels, and dissociated by sieving through successive 225 µm and 25 µm nylon meshes. Cells are collected in PBS containing 25 mM HEPES. The cell suspension is layered on top of a precentrifuged (30 min; 26 000 ***g***) Percoll density gradient (1.04 g/mL; Pharmacia, Roosendeal, the Netherlands) and centrifuged for 15 min at 26 000 ***g***. Cell debris remaining in the top aqueous phase are discarded and the interphase between the debris and the red blood cells is resuspended in PBS–HEPES. This suspension is centrifuged three times (10 min; 400 ***g***) in PBS–HEPES to eliminate Percoll. The final pellet is resuspended in DMEM supplemented with N_1, biotin (10 ng/mL) and 30% (v/v) of B104 conditioned medium (B104-CM). Five millilitres of the cell suspension are then seeded on an uncoated 25 cm^2 tissue culture flask (Falcon, Delta-Bio, Nivelles, Belgium) at a concentration of 4.10^6 cells/mL. After 24 and 48 h, the flask is smoothly shaken and the suspension transferred into a new flask allowing the elimination of adhering cells. After these platings, the progenitor cells make up spheroid aggregates termed 'oligospheres' (150–300 µm diameter). To obtain an oligodendrocyte commitment, oligospheres are switched to a DMEM-N_1 medium and 50 µL of that suspension are seeded on polyornithine (0.1 mg/mL in distilled water) -coated glass coverslips (10 mm diameter) in the centre of 35-mm plastic Petri dishes (NUNC, Life Technologies, Menelbeke, Belgium) at a concentration of 200–500 oligospheres per mL.

Embryonic rat spinal cord neurons culture

Spinal cord neurons in culture were obtained from 13-day-old rat embryos using an adaptation of a method fully described by Withers *et al.* (1997). Briefly, spinal cords are carefully dissected and freed of meninges and attached dorsal root ganglia. They are, then, incubated in trypsin (0.25%) and deoxyribonuclease (1%) in Ca^{2+}–Mg^{2+} free salt solution for 20 min at 37 °C. They are, then, washed in DMEM supplemented with the previously described N_1 supplement, bovine insulin (5 µg/mL; Sigma, St Louis, MO, USA), fetal calf serum (5% v/v; Gibco) and horse serum (5% v/v; Gibco). After mechanical dissociation using flame-narrowed Pasteur pipettes, the resulting cell suspension is filtered through a 40-µm-nylon sieve and diluted to a concentration of 1×10^6 cells/mL. Fifty microlitres of this final cell suspension is seeded on polyornithine coated glass coverslips as described above for OP. The medium is renewed twice weekly and cells are used for electrophysiological recordings after 10–12 days old *in vitro*.

Immunocytochemistry

Cultures on coverslips are fixed in 4% (v/v) paraformaldehyde for 10 min at room temperature. Non-specific binding is blocked by a 60-min incubation in PBS containing non-fat dry milk (15 mg/mL). This is followed by a 60-min incubation at 37 °C in the presence of a rabbit polyclonal anti-Gal-C antibody (Sigma) and of a mouse monoclonal anti-A2B5 antibody (Boehringer Mannheim, Brussels, Belgium) both of them at 1 : 100 dilution. As secondary antibodies, a rhodamine-conjugated antirabbit IgG (Jackson, Lucron, Brussels, Belgium) at 1 : 400 and a FITC-conjugated antimouse immunoglobulin (Boehringer Mannheim) at 1 : 30 dilution are used for a 60 min

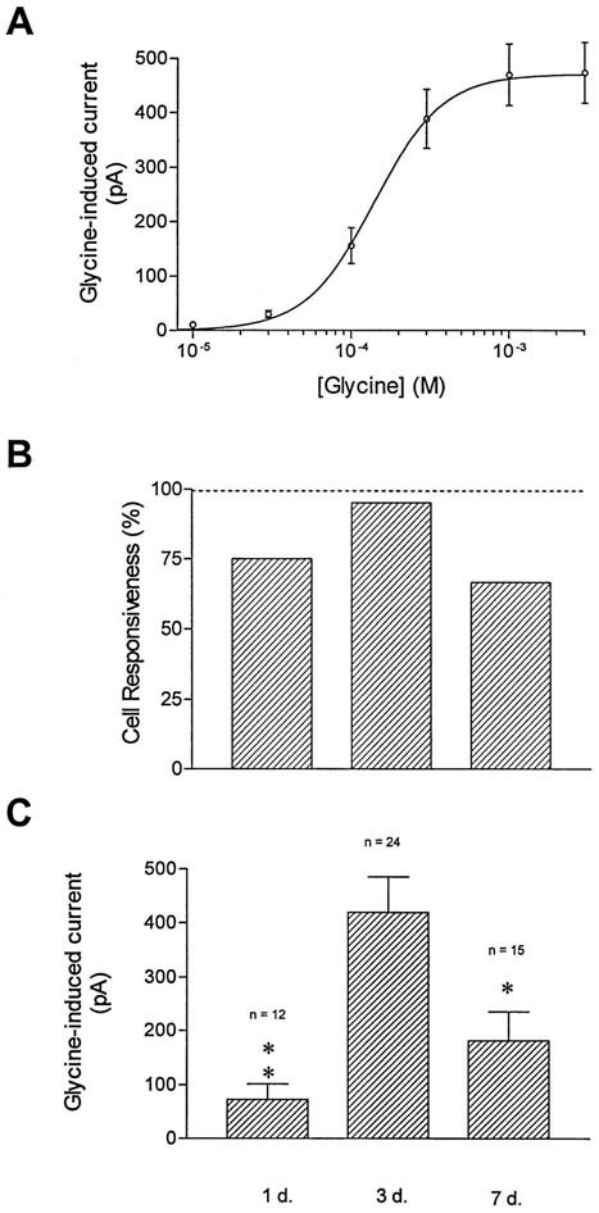

FIG. 1. Characterization of glycine-induced currents during oligodendrocyte maturation *in vitro*. (A) Currents evoked in day 3 OP cells by increasing glycine concentrations are expressed as mean ± SEM ($n = 15$). The EC50 and Hill coefficient derived from the curve fitting procedure are 140 ± 2.5 µM and 2.0 ± 0.1, respectively. (B,C) Histograms representing, respectively (B) the percentage of responding cells and (C) mean amplitudes of maximum peak currents induced by glycine (1 mM) at three progressive stages of maturation in DMEM-N_1 (1, 3 and 7 days). The statistical results are expressed as compared with the day 3 population; $*P < 0.05$ and $**P < 0.01$.

incubation at room temperature. For GFAP staining, the same fixation protocol is followed by a 30 min incubation in PBS containing non-fat dry milk and Tween 20 (1 : 2000). Monoclonal anti-GFAP (1 : 1000) is diluted in the same solution and is applied for 45 min at 37 °C. A 10-min Triton-X100 (0.1% in PBS) permeabilization precedes the 45 min incubation with a FITC-conjugated antimouse IgG (1 : 250) (Jackson). Triple PBS rinses are performed between the different steps. For antineurofilament staining, we used the mouse antibodies SMI 31 and SMI 32 (Sternberger-Meyer, Jarretsville, MD, USA) as described by Malgrange *et al. (*1994). For labelling with mAB 4a and 2b (Pfeiffer *et al*., 1984) (ConneX, Martinsried, Germany), we used the same procedure than for GFAP staining with primary antibodies diluted at 50 µg/mL and rhodamine-conjugated antimouse IgG (Jackson) at 1 : 500 as secondary antibody. Digitized images are acquired with a Bio-Rad MRC 1000 laser scanning confocal system coupled to Zeiss Axiovert 135 microscope with a plan-NEOFLUAR objective (40 ×, 1.3 n.a., oil immersion). For all the different immunostainings, negative control experiments were performed by using the same procedures without the primary antibodies.

Electrophysiology

For recording of membrane currents, the cells are transferred to the stage of an inverted Hoffman contrast microscope and maintained at room temperature (20–25 °C) in a recording chamber which is continuously perfused permitting application of drugs.

The extracellular perfusion solution contains (mM): NaCl, 116.0; D-glucose, 11.1; KCl, 5.4; $CaCl_2.2H_2O$, 1.8; $MgCl_2.6H_2O$, 2.0; HEPES, 10.0; pH 7.2. In Cs^+-containing solutions, KCl is replaced by equimolar amount of CsCl and $BaCl_2.2H_2O$ is added at 5 mM. In low Cl^- solutions 108 mM NaCl is replaced by equimolar amount of sodium gluconate. Glycine is purchased from UCB, cyanotriphenylborate (CTPB) from ABCR (Karlsruhe, Germany) and taurine, β-alanine, strychnine, bicucullin and picrotoxin are from Sigma. The reagents diluted in the external solution are applied by a rapid microperfusion system (SPS-8, List-Medical).

Recording electrodes are made from borosilicate capillaries (Hilgenberg) using a Flaming-Brown microelectrode puller (Model P97, Sutter Instruments Co). Recording pipettes (10–20 MΩ) are filled with a solution containing (mM): KCl, 130.0; $CaCl_2.2H_2O$, 1.0; D-glucose, 11.1; EGTA, 10.0; and Na- or Mg-ATP, 5.0; HEPES, 10.0; pH 7.4. In Cs^+-containing pipettes, KCl is equimolarly replaced by CsCl and $BaCl_2.2H_2O$ is added at 5 mM.

Voltage-clamp recordings are performed with a Bio-Logic RK-400 patch-clamp amplifier using the tight-seal whole-cell recording configuration (Hamill *et al*., 1981). Series resistances are in the range 10–20 MΩ and were electronically compensated (up to 85–90%). Current traces are digitized and stored on an AT-compatible computer system. Control of drug application, data acquisition and data analysis were achieved using an ITC-16 acquisition board (Instrutech Corporation) and the TIDA for Windows software (HEKA Elektronik, Lombrecht/Pfolz, Germany). Curve fitting is made using GraphPAD Prism software. Statistical significance of the data is derived from analysis of variance (ANOVA) and, when significance is reached, Dunnett's post-test are used for multiple comparisons (GraphPAD InStat software, San Diego, CA, USA).

[^{3}H]Strychnine binding assays

Day-3 oligodendrocyte progenitor (OP) cells are incubated with [^{3}H]strychnine (0.01–20 nM, 27 Ci/mM; DuPont NEN, Brussels, Belgium) diluted in PBS, using 100 µM cold strychnine to determine non-specific binding. After incubation to equilibrium at 4 °C for 20 min, 100 µL aliquots of the cells incubation medium are sampled to determine free ligand concentration. The cells are then washed four times with cold PBS to stop binding and digested for 10 min with NaOH 0.1 M at 37 °C. The digestion products are transferred into vials containing 7 mL scintillation fluid (Ecoscint-a, National diagnostics, Atlanta, GA, USA) and 10 µL of 12 M HCl. Protein determination was done according to Bradford (1976). Radioactivity is determined by conventional liquid scintillation counting using a Beckman LS3801 counter. All experimental points are done in

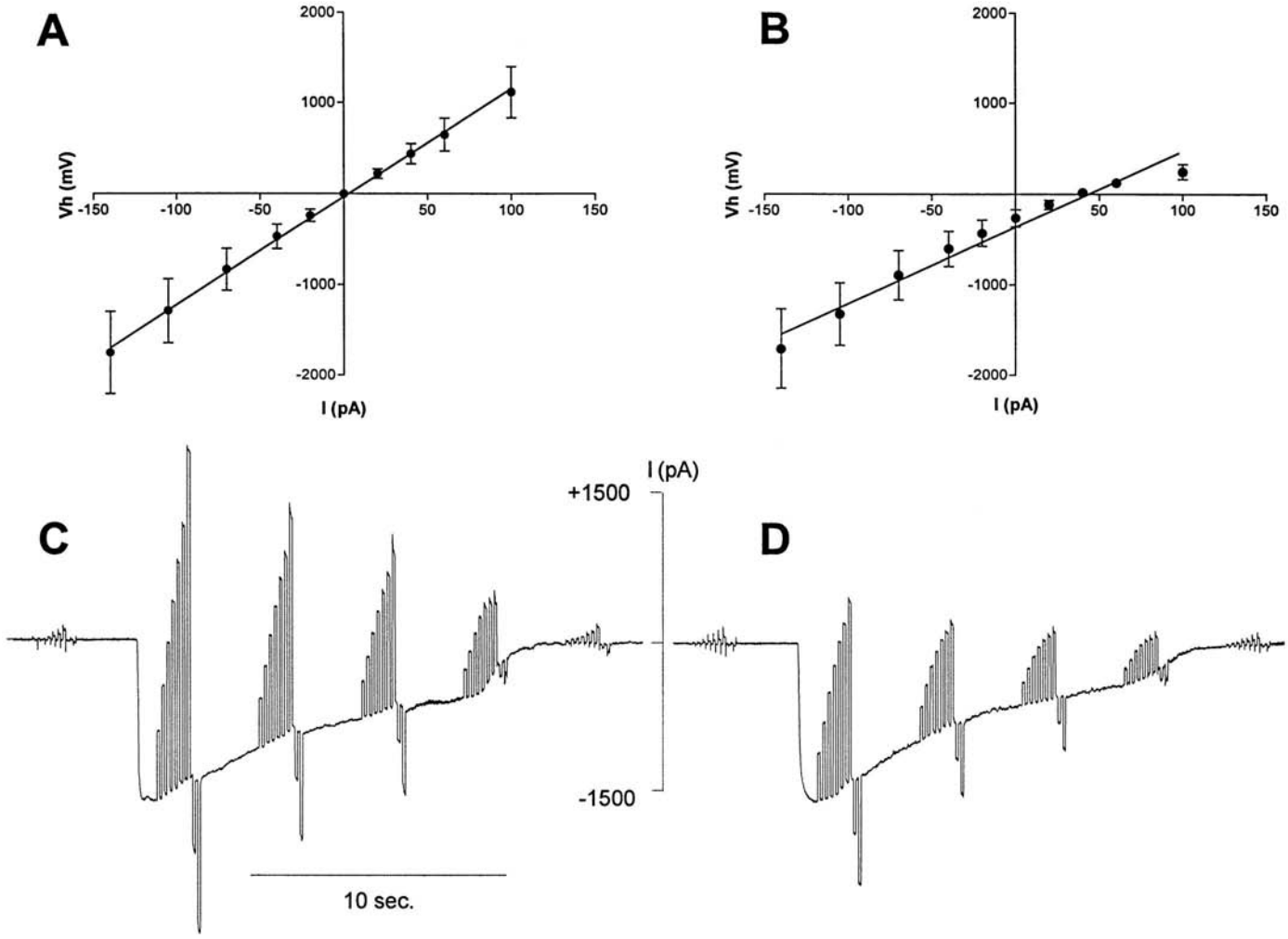

FIG. 2. Reversal potential of glycine-induced currents. The recordings were obtained from day 3 OP. A series of depolarizing (–40, –20, 0, 20, 40, 60, 100) and hyperpolarizing voltage steps (–105, –140) from a holding potential of – 70 mV was applied repeatedly. Glycine applied for 10 s in a Cs^+-containing solution supplemented with the K^+ channel blocker Ba^{2+} (5 mm) induced a significant conductance increase and an inward current at –70 mV. To characterize the glycine-induced conductance, currents prior to the application of glycine were subtracted from currents at the peak of the glycine response. The current–voltage relationship of glycine-induced currents is linear and the reversal potential was 2.0 ± 1.9 mV in control chloride gradient conditions (A–C) and 42.9 ± 4.1 mV when extracellular chloride concentration was decreased (B–D). The calculated slope of the linear regression curve display lower glycine-induced membrane conductance in the low external chloride condition (7.5 ± 0.4 nS in B vs. 11.9 ± 0.2 nS in A).

triplicate. The K_d and B_{max} values for [^{3}H]strychnine specific binding are estimated using the GraphPAD Prism software.

Isolation of total RNA, cDNA synthesis and polymerase chain reaction

Total RNAs from day 3 OP (100 mg of fresh weight) and from adult and neonatal rat cortex and spinal cord are extracted in guanidine thiocyanate buffer using the single step method of Chomczynski & Sacchi (1987). RNAs are quantified spectrophotometrically. The cDNA synthesis and PCR are performed using the TITAN One Tube RT–PCR system from Boehringer Mannheim. Briefly, a 50 µL RT–PCR tube containing 0.2 mM of each dNTP, 250 ng of each primer (forward and reverse), 300 ng of total RNA, 5 mM of dithiothreitol, 5 U of RNAse inhibitor (Promega, Leiden, the Netherlands), 1.5 mM of $MgCl_2$ and 1 µL of the Expend High Fidelity AMV Reverse Transcriptase enzyme mix is placed in a MJ Research PTC 200 engine. The programme is: 50 °C for 30 min, 94 °C for 2 min, 10 cycles of 94 °C for 30 s, appropriate annealing temperature for 30 s and 68 °C for 1 min, 25 cycles of 94 °C for 30 s, appropriate annealing temperature for 30 s and 68 °C for 1 min plus 5 s for each additional cycle. A final 68 °C extension time of 7 min is performed.

The PCR products are purified using Qiaex Extraction Kit from Qiagen, Westburg, Leusden, the Netherlands and analysed on a 1.5% Agarose TAE gel containing ethidium bromide. The products are cloned in a PCR 2.1. plasmid (In Vitrogen, Leek, the Netherlands) and sequenced using the dideoxy sequencing method (Sanger *et al*., 1977) according to the instructions from the manufacturer (Pharmacia). The oligonucleotide primers for PCR (obtained from Pharmacia) are listed in Table 1.

Results

In oligodendrocyte progenitor cells, glycine induces inward currents which are developmentally regulated

The cultured cells were studied in the outgrowth zone of expanded oligospheres at various differentiation stages, i.e. 1, 3 and 7 days

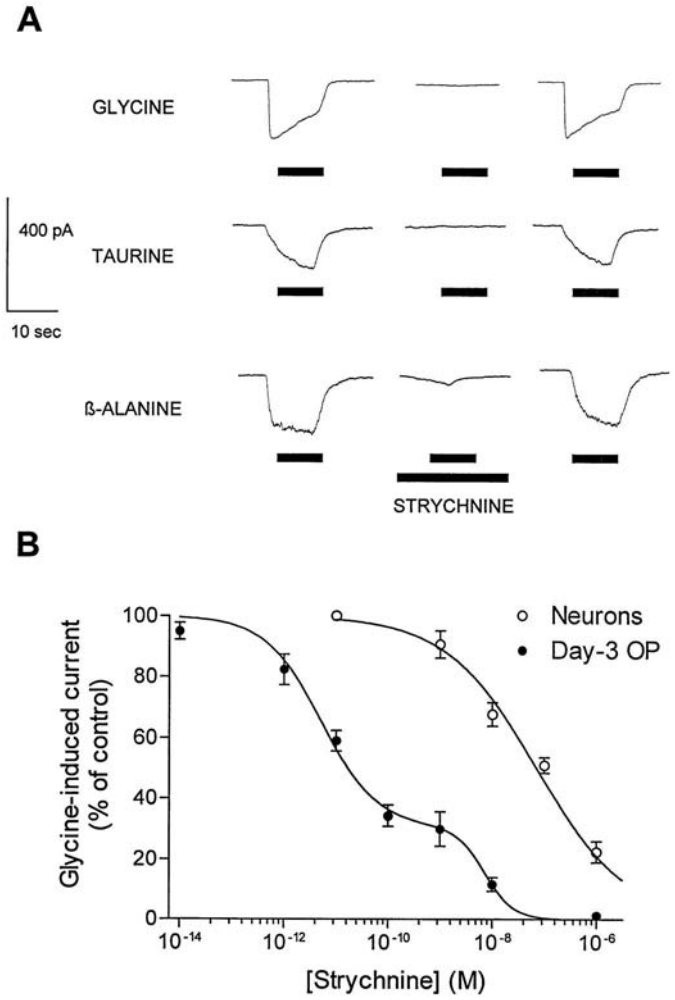

FIG. 3. Strychnine competitive inhibition of glycine-induced currents. (A) Day 3 OP cells were perfused for 10 s with glycine, taurine and β-alanine (1 mM) alone or in combination with strychnine (25 s, 1 μM). The three recordings for each agonist were obtained from a single cell and are separated by 60 s. Similar recordings were obtained in six different day 3 OP cells. (B) Currents evoked by 0.15 mM glycine for OP and 0.05 mM for neurons (concentrations which elicit a half-maximum response in both cell types) were recorded in the presence of increasing strychnine concentrations. Results are expressed as percentage of glycine-induced currents in the absence of strychnine (mean ± SEM, $n = 5$). The best fitting curve for strychnine inhibition of glycine-induced currents in day 3 OP is described by a two-site competition curve. As compared with cultured embryonic rat spinal cord neurons, strychnine sensitivity was much more important in OP cells. The curve fitting procedure yielded a IC50 of 71 ± 7 nM for neurons (Hill coefficient of 0.5) and two IC50 for OP cells, respectively, 7 ± 1 nM (Hill coefficient of 1.6) and 5 ± 1 pM (Hill coefficient of 0.8).

after switching to DMEM-N_1. In this growth factor-free medium, immunocytochemical staining demonstrated that after 7 days, 97% of the cells are multipolar, A2B5 negative and Gal-C positive while in 1 day cultures 95% of the cells are bipolar, A2B5 positive and Gal-C negative. Three-day-old cultures contained a mixed population with 60% A2B5 positive cells and 60% Gal-C positive cells, thus including many double-stained cells. After 7 days in DMEM-N_1 only 3% of the cells are GFAP-positive cells. In the areas where the electrophysiological recordings were made, no cells were positive after immunocytochemical staining using antiphosphorylated and anti-unphosphorylated neurofilament antibodies.

In our recording conditions, day 1 progenitor cells and day 7 oligodendrocytes had respective mean resting potentials of –70 ± 6 mV (SEM; $n = 14$) and –56 ± 5 mV (SEM; $n = 22$). In cells voltage-clamped at a holding potential of –70 mV, bath application of glycine (10 s) elicited inward currents. The plot of absolute current amplitudes as a function of glycine concentrations obtained from day 3 cultures (Fig. 1A) was best fitted by a sigmoidal curve yielding an EC50 of 140 ± 2.5 μM glycine (mean ± SEM; $n = 7$) and a Hill coefficient (n_H) of 2.0 ± 0.1. Maximum current amplitudes (elicited by 1 mM glycine) were measured at different stages of cell differentiation. Confirming previous data (Belachew *et al*., 1998), we observed significantly larger responses in the day 3 population and a similar trend for the evolution of the percentage of responding cells (Fig. 1B,C). As maximum current amplitudes is an indirect measure of receptor density, these data suggest a decreased expression of GlyR at the differentiated oligodendrocyte stage. To be noticed is the large range of current amplitudes observed during application of 1 mM glycine: 10–281 pA in day 1, 45–2179 pA in day 3 and 11–590 pA in day 7 cultures.

Glycine activates a chloride conductance

In order to define the ionic species carrying the glycine-induced currents, cells with large responses were selected. For this purpose, day 3 cells were particularly suitable. The resting K^+ conductance was blocked by adding Ba^{2+} (5 mM) in the external solution and replacing K^+ by equimolar concentrations of Cs^+ both in the pipette and the bathing solution. To study glycine-evoked currents at different membrane potentials, the membrane was clamped at a series of potentials ranging between + 100 and –140 mV. From a holding potential of –70 mV, each voltage step lasted for 100 ms and the series of voltage steps was applied every 4 s (Fig. 2C,D). Specific glycine-induced membrane currents were obtained by subtracting currents under control conditions from those measured at the peak of the glycine response. The resulting current–voltage curve was linear and reversed at +2.0 ± 1.9 mV (range –4.7 to +7.2 mV; $n = 5$) (Fig. 2A) which is close to the calculated Nernst chloride equilibrium potential (+0.5 mV). When the extracellular chloride concentration was decreased by substituting for the sodium chloride equimolar concentration of sodium gluconate, the reversal potential was shifted to +42.9 ± 4.1 mV (range +30.6 to +48.6 mV; $n = 4$) (Fig. 2B) which again is close to the calculated chloride equilibrium potential (+45.8 mV) in those conditions. These experiments thus demonstrate that glycine-induced currents in oligosphere-derived OP are mainly carried by Cl^- ions.

Pharmacological characterization of glycine-induced currents

The GlyR agonists β-alanine and taurine also triggered inward currents that were studied in day 3 cells. However, the relative amplitudes of β-alanine- and taurine-evoked currents were significantly different from those elicited by glycine at the same concentration in the same cell (respectively 130 ± 8 and 81 ± 5% of $I_{glycine}$, mean ± SEM). Moreover, currents induced by β-alanine and taurine at 1 mM did not show the typical biphasic pattern of an initial peak rapidly inactivating to a plateau (Fig. 3A) as seen with glycine. The glycine-, β-alanine- and taurine-induced responses were all reversibly blocked by the GlyR antagonist strychnine (1 μM) but the inhibition of β-alanine currents was not complete. The $GABA_A$ receptor antagonist bicuculline had no effect on glycine-induced currents (data not shown). The best fitting curve for strychnine inhibition of glycine-induced currents was given by a two sites competition model allowing calculation of two distinct IC50 (Fig. 3B). Thus, unlike rat spinal cord neuronal GlyR,

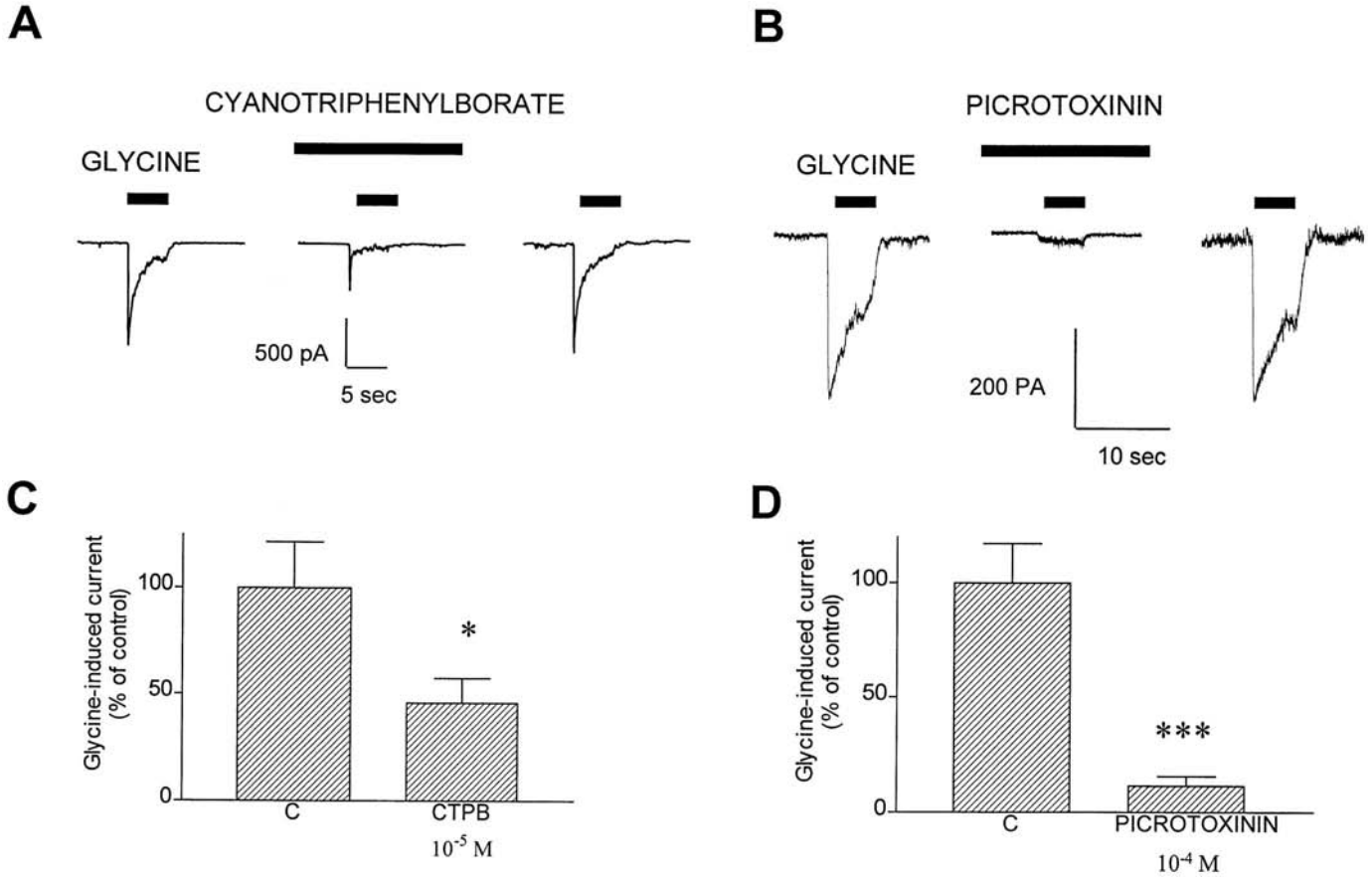

FIG. 4. Picrotoxinin and cyanotriphenylborate (CTPB) blockade of glycine response. (A,B) Representative recordings of day 3 OP cells superfused with glycine (1 mM) alone or together with cyanotriphenylborate (0.01 mM) or picrotoxinin (0.1 mM). (B–D) Results are expressed as in Fig. 3B. The statistical data are expressed as compared with glycine-induced currents; ***$P < 0.001$.

the OP GlyR seems to have two different strychnine binding sites. One hundred per cent of the glycine-responding cells ($n = 15$) were sensitive to the chloride channel blocker picrotoxinin (0.1 mM) which inhibited 90 ± 2% (mean ± SEM) of the glycine-induced currents (Fig. 4B–D). All the tested day 3 OP cells ($n = 10$) were also sensitive to cyanotriphenylborate (CTPB, 10 μM) which inhibited 55% ± 11% (mean ± SEM) of glycine currents (Fig. 4A–C).

[^{3}H]Strychnine binding assays with cultured oligodendrocyte progenitor cells

We next used [^{3}H]strychnine binding assays to further confirm the existence of two different strychnine binding sites on OP GlyR. After Scatchard transformation (Fig. 5), [^{3}H]strychnine binding data are best fitted with a two-sites ($K_{d1} = 0.46$ nM, $B_{max1} = 0.56$ pmol/mg protein, $r2_1 = 0.88$ and $K_{d2} = 16.23$ nM, $B_{max2} = 7.43$ pmol/mg protein, $r2_2 = 0.76$) than a one-site model ($K_d = 4.77$ nM, $B_{max} = 3.51$ pmol/mg protein, $r^2 = 0.46$). It has, however, to be pointed out that the binding assays, which were performed four times, showed important variations in the high affinity site calculated values (K_{d1} ranging from 0.13 to 0.85 nM and B_{max1} from 0.55 to 3.03 pmol/mg protein). These variations are likely to be a consequence of the relatively low specific activity of commercially available [^{3}H]strychnine, the low number of these high affinity strychnine binding sites and an uneven cell distribution inherent in the oligosphere culture model. Although these binding data are not conclusive, they strengthen

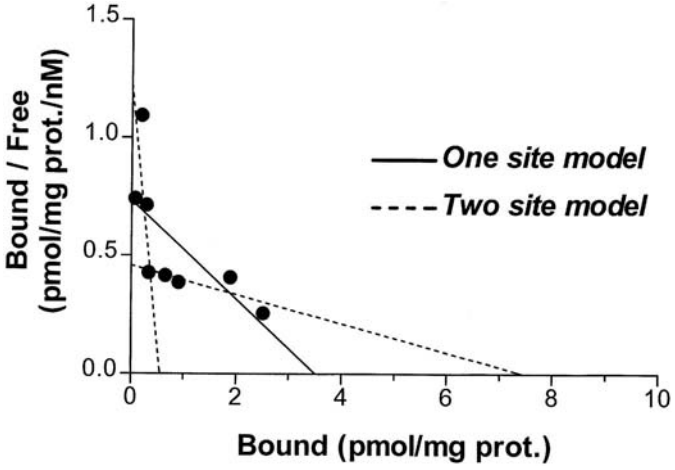

FIG. 5. [^{3}H]Strychnine binding assays with day 3 oligodendrocyte progenitor cells cultures. Scatchard transform analysis of the data showed a very bad fitting with the one-site model. It was also possible to get two different Scatchard plots with much better fitting (dashed lines) determining two distinct K_D (values in the text).

the conclusion drawn from electrophysiological experiments on the existence of a high affinity strychnine site on the oligodendroglial GlyR.

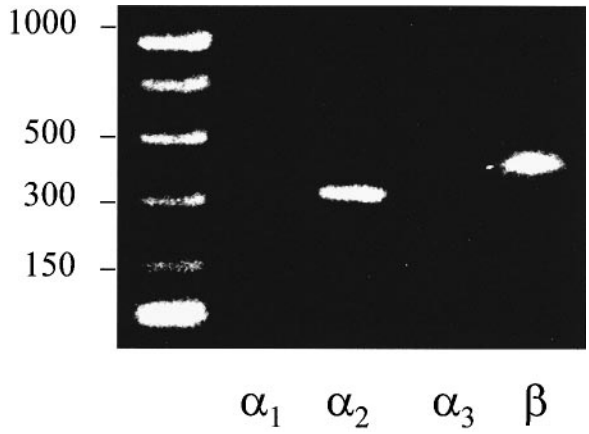

FIG. 6. RT–PCR amplification of GlyR subunit transcripts in neonatal rat cortical OP cultures. PCR with α_1-, α_2-, α_3- and β-specific oligonucleotide combinations were performed in parallel using equal amounts of cDNA reversely transcribed from RNA isolated from day 3 oligosphere-derived OP cultures. Left margin: migration of standard DNA markers with size indicated in base pairs.

Reverse transcription–polymerase chain reaction and immunocytochemical characterization of the GlyR subunits expressed in oligodendrocyte progenitor cultures

Total RNA extracted from pooled day 3 OP cultures were reverse transcribed and amplified with primers for either α_1, α_2, α_3 and β subunit transcripts. This procedure yielded bands for α_2 and β, the size of which corresponding to that predicted for each set of primers (Fig. 6). The amplified material was cloned, sequenced and found to be identical to the published sequence of each GlyR subunit. These experiments were repeated four times all yielding identical results. α_1- or α_3-amplified products were never detected whereas control experiments using adult and neonatal rat spinal cord total RNA gave positive signals with the four sets of primers. Moreover, using mAB 2b which is a monoclonal antibody that selectively labels the GlyR α_1 subunit and mAB 4a which has been mapped to an epitope (Schröder *et al*., 1991) common to all rat GlyR α subunits, we showed that oligodendroglial cells at various time in culture were never labelled by mAB 2b while they were positive for mAB 4a staining (Fig. 7) thus confirming that OP cells express GlyR that do not contain the α_1 subunit.

Discussion

The inhibitory GlyR has been characterized as a ligand-gated chloride-selective channel expressed by neurons throughout the CNS. In this study, we report that exogenously applied glycine induces inward

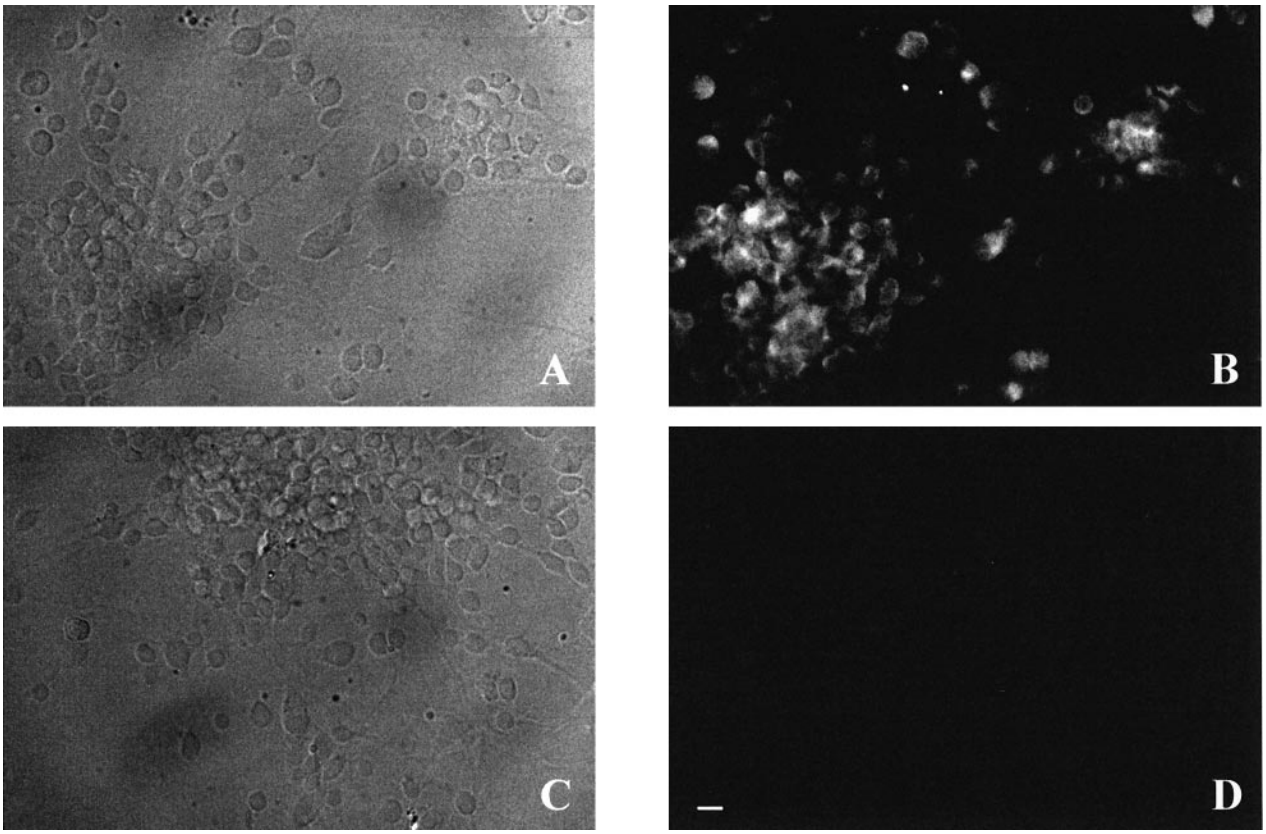

FIG. 7. Fluorescence microscopy of day 3 OP cells. (A–C) Digital interferential contrast view of OP cells after 3 days in culture. (B) Fluorescence view of the cells in field (A) labelled with mAB 4a. (D) Fluorescence view of the cells in field (C) labelled with mAB 2b. Bar = 10 µm.

currents in voltage-clamped oligosphere-derived cortical OP. We show that these glycine-evoked currents are the consequence of the activation of the GlyR, as: (i) they are also elicited by β-alanine and taurine; (ii) they are bicucullin-insensitive; (iii) they are blocked by strychnine, a GlyR competitive antagonist, and by picrotoxin and cyanotriphenylborate, two chloride channel blockers; and (iv) they reverse at a potential close to the Nernst chloride equilibrium potential. Glycine-induced currents were recorded all along the differentiation process from early progenitors (day 1) up to mature oligodendrocytes (day 7). The pattern of evolution of maximum current amplitudes suggests a transient increased GlyR expression during an intermediate period along the oligodendrocyte lineage. Immunocytochemical stainings and RT–PCR experiments confirm the presence of glycine receptor on cultured OP derived from cortex and further demonstrates that only the α_2 and β subunits are present.

As compared with *in vitro* studies of neuronal GlyR (EC50 ≈ 40–90 μM) (Tokutomi *et al*., 1989; Xu *et al*., 1996), or to α_2 and $\alpha_2\beta$ transfected cells (EC50, respectively, 60 and 85 μM) (Pribilla *et al*., 1992), OP GlyR has a glycine affinity (EC50 = 140 ± 2.5 μM) which although slightly lower is not significantly different. The Hill coefficient value (2.0 ± 0.1) suggests that several glycine molecules are required to activate one single oligodendroglial GlyR channel. The strychnine inhibition curve of OP glycine-induced currents demonstrates a higher antagonist affinity for OP as compared with typical neuronal GlyR (Tokutomi *et al*., 1989) including embryonic spinal cord neuronal GlyR that we have used for comparison. Moreover, unlike neuronal GlyR, our electrophysiological and ligand binding data suggest the existence of two strychnine binding sites on the oligodendrocyte progenitor glycine receptor with high (picomolar range) and low (nanomolar range) affinities. In the classical model of GlyR α subunit, two domains of the amino-terminal extracellular region (Tyr-161; Lys-200 and Tyr-202) are required for strychnine binding to the receptor (Vandenberg *et al*., 1992b). It is now demonstrated that the agonist binding site of this receptor is distinct from the strychnine binding site and located at the residue Thr-204 (Vandenberg *et al*., 1992a). The current hypothesis for the mechanism of strychnine antagonism is a steric blockade of the secondary structure motif of the glycine binding site. The existence of a second strychnine binding site has never been suggested by studies on neurons. Unexpectedly, our electrophysiological characterization of OP GlyR provides evidence for a double site model for strychnine interaction with glycine-induced currents. Unfortunately, the relatively low specific activity of the commercially available [^{3}H]strychnine preparations and the low number of high affinity strychnine binding sites in OP cultures prevents an accurate determination of its dissociation constant. Regarding the molecular basis of this new potential strychnine binding site, sequencing of the whole OP α_2 subunit that has been detected in our PCR experiments is needed before any suggestion is made. This work is currently in progress in our laboratory.

In spinal cord slices, Pastor *et al*. (1995) demonstrated that picrotoxinin reversibly blocked the glycine-induced currents in all precursor cells which have voltage-dependent sodium channels, whereas in astrocytes and fully mature oligodendrocytes, the effect of picrotoxinin is more heterogeneous. In the present study, we observed picrotoxinin blockade of the glycine response in 100% of the day 3 oligosphere-derived cortical OP. This result fits with the lack of β subunit in the OP GlyR complex as described by Pribilla *et al*. (1992) but is discordant with our detection by RT–PCR of β subunit in day 3 OP cultures. This discrepancy could be due to a minor contamination by fully mature oligodendrocytes which are known to be partially picrotoxin-insensitive (Pastor *et al*., 1995) as a consequence of the presence of a β subunit within the GlyR complex. However, since all the tested day 3 OP cells were also sensitive to cyanotriphenylborate which has no effect on α_2-subunit homo-oligomers (Rundström *et al*., 1994), we suggest that OP GlyR could either correspond to (i) a hetero-oligomeric $\alpha_2\beta$ structure in which the β subunit would be a yet undescribed variant with differences for instance in the M2 segment sequence which is known to confer picrotoxinin resistance (Pribilla *et al*., 1992), or (ii) a homo-oligomeric α_2 structure with a new α_2 sequence that would fit with both the CTPB sensitivity and the double site strychnine interaction hypothesis.

Considering now the physiological significance of the presence of GlyR in the oligodendroglial cells derived from subcortical white matter, it is interesting to point out that non-ketotic hyperglycinaemia is a heritable disorder of amino acid metabolism in which large amounts of glycine accumulate in plasma and cerebrospinal fluid (Nyhan, 1989). Pathological features of non-ketotic hyperglycinaemia include decreased or absent myelination of supratentorial white-matter tracts whereas myelination of the brainstem and cerebellum progresses normally (Press *et al*., 1989). It is tempting to speculate that pathological findings in hyperglycinaemic patients could, at least partially, be mediated by cortical oligodendroglial GlyR hyperactivation. As for the $GABA_A$ receptor, the functional role of GlyR in oligodendroglial cells could be associated with its depolarizing effect (Gilbert *et al*., 1984). Indeed, spinal cord oligodendrocytes possess a furosemide-sensitive $Na^+/K^+/Cl^-$-uptake system (Hoppe & Kettenmann, 1989) that keeps intracellular chloride concentration above the value expected from pure passive distribution. In these conditions, glycine-induced increase of chloride conductance would result in a depolarization of the cell as has already been established for GABA (Gilbert *et al*., 1984). Such a depolarization could be sufficient to open voltage-gated Ca^{2+} channels thus leading to an increase of intracellular calcium concentration. This intracellular Ca^{2+} concentration increase could trigger downstream events which are important for the generation of the mature CNS myelin-forming. Comparison of maximum current amplitude values, which are an indirect measure of receptor density, at the different stages of the O2A lineage shows that the expression of GlyR culminates at an intermediate stage of differentiation. This suggests that the functional consequences of GlyR activation are likely to concern the regulation of early events during cell progression along the oligodendrocyte lineage such as proliferation, motility or migration, the deficit of which could lead to defective myelination such as seen in non-ketotic hyperglycinaemia.

Acknowledgements

This work was supported by the Fonds National de la Recherche Scientifique (FNRS), the Fondation Médicale Reine Elisabeth (FMRE), the Concerted Action of the Government of the French Community of Belgium, the Ligue Belge de la Sclérose en Plaques and the Fondation Charcot. We thank P. Ernst-Gengoux for her technical support and expertise. Bernard Rogister, Brigitte Malgrange and Shibeshih Belachew are supported by the FNRS-Belgium.

Abbreviations

B104-CM	B104 cell line conditioned medium
CNS	central nervous system
CTPB	cyanotriphenylborate
DMEM	Dulbecco's modified Eagle's medium
GABA	γ-aminobutyric acid
Gal-C	galactocerebroside
GFAP	glial fibrillary acidic protein
GlyR	glycine receptor
HEPES	*N*-(2-hydroxyethyl)piperazine-*N*′-(2-ethanesulphonic acid)

OP	oligodendrocyte progenitor
PBS	phosphate-buffered saline
RT–PCR	reverse transcription–polymerase chain reaction

References

Avellana-Adalid, V., Nait Oumesmar, B., Lachapelle, F. & Baron-Van Evercooren, A. (1996) Expansion of rat oligodendrocyte progenitors into proliferative 'oligospheres' that retain differentiation potential. *J. Neurosci. Res.*, **45**, 558–570.

Belachew, S., Malgrange, B., Rigo, J.-M., Rogister, B., Coucke, P., Mazy-Servais, C. & Moonen, G. (1998) Developmental regulation of neuroligand-induced responses in cultured oligodendroglia. *Neuroreport*, **9**, 973–980.

Betz, H. (1990) Ligand-gated ion channels in the brain: the amino acid receptor family. *Neuron*, **5**, 383–392.

Betz, H. (1991) Glycine receptors: heterogeneous and widespread in the mammalian brain. *Trends Neurosci.*, **10**, 458–461.

Betz, H., Kuhse, J., Fischer, M., Schmieden, V., Laube, B., Kuryatov, A., Langosch, D., Meyer, G., Bormann, J. & Rundström, N. (1994) Structure, diversity and synaptic localization of inhibitory glycine receptors. *J. Physiol. (Paris)*, **88**, 243–248.

Bottenstein, J.E. & Sato, G. (1979) Growth of rat neuroblastoma cell line in serum-free supplemented medium. *Proc. Natl Acad. Sci. USA*, **76**, 514–517.

Bradford, M.M. (1976) A rapid and sensitive method for the quantification of microgram quantities of protein utilizing the principal of protein-dye binding. *Anal. Biochem..*, **72**, 248–255.

Chomczynski, P. & Sacchi, N. (1987) A rapid method of RNA isolation by acid guanidinium thiocyanate-phenol-chloroform extraction. *Anal. Biochem.*, **162**, 156–159.

Curtis, D.R., Hösli, L. & Johnston, G.A.R. (1968) A pharmacological study of the depression of spinal neurones by glycine and related amino acids. *Exp. Brain Res.*, **6**, 1–18.

Gilbert, P., Kettenmann, H. & Schachner, M. (1984) Gamma-aminobutyric acid directly depolarizes cultured oligodendrocytes. *J. Neurosci.*, **4**, 561–569.

Grenningloh, G., Rienitz, A., Schmitt, B., Methfessel, C., Zensen, M., Beyreuther, K., Gundelfinger, E.D. & Betz, H. (1987) The strychnine-binding subunit of the glycine receptor shows homology with nicotinic acetylcholine receptors. *Nature*, **328**, 215–220.

Grenningloh, G., Schmieden, V., Schofield, P.R., Seeburg, P.H., Siddique, T., Mohandas, T.K., Becker, C.-M. & Betz, H. (1990b) Alpha subunit variants of the human glycine receptor: primary structures, functional expression and chromosomal localization of the corresponding genes. *EMBO J.*, **3**, 771–776.

Hamill, O.P., Marty, A., Neher, E., Sakmann, B. & Sigworth, F.J. (1981) Improved patch-clamp techniques for high-resolution current recording from cells and cell-free membrane patches. *Pflugers Arch.*, **391**, 85–100.

Hoppe, D. & Kettenmann, H. (1989) GABA triggers a chloride efflux from cultured oligodendrocytes. *Neurosci. Lett.*, **97**, 334–339.

Kettenmann, H., Blankenfeld, G.V. & Trotter, J. (1991) Physiological properties of oligodendrocytes during development. *Ann. NY. Acad. Sci.*, **633**, 64–77.

Kirchhoff, F., Mulhardt, C., Pastor, A., Becker, C.-M. & Kettenmann, H. (1996) Expression of glycine receptor subunits in glial cells of the rat spinal cord. *J. Neurochem.*, **4**, 1383–1390.

Kuhse, J., Schmieden, V. & Betz, H. (1990) Identification and functional expression of a novel ligand binding subunit of the inhibitory glycine receptor. *J. Biol. Chem.*, **36**, 22317–22320.

Langosch, D., Becker, C.-M. & Betz, H. (1990) The inhibitory glycine receptor: a ligand-gated chloride channel of the central nervous system. *Eur. J. Biochem..*, **194**, 1–8.

Malgrange, B., Delrée, P., Rigo, J.-M., Baron, H. & Moonen, G. (1994) Image analysis of neuritic regeneration by adult rat dorsal root ganglion neurons in culture: Quantification of the neurotoxicity of anticancer agents and of its prevention by NGF or bFGF but not BDNF or NT-3. *J. Neurosci. Methods*, **53**, 111–122.

Matzenbach, B., Maulet, Y., Sefton, L., Courtier, B., Avner, P., Guénet, J.L. & Betz, H. (1994) Structural analysis of mouse glycine receptor alpha subunit genes. *J. Biol. Chem.*, **269**, 2607–2612.

Mülhardt, C., Fischer, M., Gass, P., Simon-Chazottes, D., Guénet, J.L., Kuhse, J., Betz, H. & Becker, C.-M. (1994) The spastic mouse: aberrant splicing of glycine receptor β subunit mRNA caused by intronic insertion of L1 element. *Neuron*, **13**, 1003–1015.

Nyhan, W.L. (1989) Nonketotic hyperglycinemia. In Scriver, C.R., Beaudet, A.L., Sly, W.S. & Valle, D. (eds), *The Metabolic Basis of Inherited Disease*. McGraw-Hill, New York,.

Pastor, A., Chvatal, A., Sykova, A. & Kettenmann, H. (1995) Glycine- and GABA-activated currents in identified glial cells of the developing rat spinal cord. *Eur. J. Neurosci.*, **7**, 1188–1198.

Pfeiffer, F., Simler, R., Grenningloh, G. & Betz, H. (1984) Monoclonal antibodies and peptide mapping reveal structural similarities between the subunits of the glycine receptor of rat spinal cord. *Proc. Natl Acad. Sci. USA*, **81**, 7224–7227.

Press, G.A., Barshop, B.A., Haas, R.H., Nyhan, W.L., Glass, R.F. & Hesselink, J.R. (1989) Abnormalities of the brain in nonketotic hyperglycinemia: MR manifestations. *AJNR*, **10**, 21.4

Pribilla, I., Takagi, T., Langosch, D., Bormann, J. & Betz, H. (1992) The atypical M2 segment of the β subunit confers picrotoxinin resistance to inhibitory glycine receptor channels. *EMBO J.*, **11**, 4305–4311.

Rundström, N., Schmieden, V., Betz, H., Bormann, J. & Langosch, D. (1994) Cyanotriphenylborate: subtype-specific blocker of glycine receptor chlorine channels. *Proc. Natl Acad. Sci. USA*, **91**, 8950–8954.

Sanger, F., Nicklen, S. & Coulson, A.R. (1977) DNA sequencing with chain-terminating inhibitors. *Proc. Natl Acad. Sci. USA*, **74**, 5463–5467.

Schmieden, V., Grenningloh, G., Schofield, P.R. & Betz, H. (1989) Functional expression in *Xenopus* oocytes of the strychnine binding 48 kD subunit of the glycine receptor. *EMBO J.*, **8**, 695–700.

Schröder, S., Hoch, H., Becker, C.-M., Grenningloh, G. & Betz, H. (1991) Mapping of antigenic epitopes on the alpha-1 subunit of the inhibitory glycine receptor. *Biochemistry*, **30**, 42–47.

Tokutomi, N., Kaneda, M. & Akaike, N. (1989) What confers specificity on glycine for its receptor site? *Br. J. Pharmacol.*, **97**, 353–360.

Vandenberg, R.J., French, C.R., Barry, P.H., Shine, J. & Schofield, P.R. (1992a) Antagonism of ligand-gated ion channel receptors: two domains of the glycine receptor alpha subunit form the strychnine binding site. *Proc. Natl Acad. Sci. USA*, **89**, 1765–1769.

Vandenberg, R.J., Handford, C.A. & Schofield, P.R. (1992b) Distinct agonist- and antagonist-binding sites on the glycine receptor. *Neuron*, **9**, 491–496.

Withers, M.D. & St John, P.A. (1997) Embryonic rat spinal cord neurons change expression of glycine receptor subtypes during development *in vitro*. *J. Neurobiol.*, **32**, 579–592.

Xu, T.-L., Nabekura, J. & Akaike, N. (1996) Protein kinase C-mediated enhancement of glycine response in rat sacral dorsal commissural neurones by serotonin. *J. Physiol.*, **2**, 491–501.

7.11 Publication #11 (was part of our *PhD* thesis) : Belachew, S., Malgrange, B., Rigo, J.-M., Rogister, B., Leprince, P., Hans, G., Nguyen, L., and Moonen G. (2000). Glycine triggers an intracellular calcium influx in oligodendrocyte progenitor cells which is mediated by the activation of both the ionotropic glycine receptor and Na^+- dependent transporters. *Eur. J. Neurosci.* 12:1924-1930.

European Journal of Neuroscience, Vol. 12, pp. 1924–1930, 2000

Glycine triggers an intracellular calcium influx in oligodendrocyte progenitor cells which is mediated by the activation of both the ionotropic glycine receptor and Na^+-dependent transporters

Shibeshih Belachew,[1,2] Brigitte Malgrange,[1] Jean-Michel Rigo,[1] Bernard Rogister,[1,2] Pierre Leprince,[1] Gregory Hans,[1] Laurent Nguyen,[1] and Gustave Moonen[1,2]
[1]Department of Human Physiology and Pathophysiology, University of Liège, 17 Place Delcour, B-4020 Liège, Belgium
[2]Department of Neurology, University of Liège, CHU (B35) Sart Tilman, B-4000 Liège, Belgium

Keywords: calcium imaging, Fluo-3, rat cerebral cortex

Abstract

Using fluo-3 calcium imaging, we demonstrate that glycine induces an increase in intracellular calcium concentration ($[Ca^{2+}]_i$) in cortical oligodendrocyte progenitor (OP) cells. This effect results from a calcium entry through voltage-gated calcium channels (VGCC), as it is observed only in OP cells expressing such channels, and it is abolished either by removal of calcium from the extracellular medium or by application of an L-type VGCC blocker. Glycine-triggered Ca^{2+} influx in OP cells actually results from an initial depolarization that is the consequence of the activation of both the ionotropic glycine receptor (GlyR) and Na^+-dependent transporters, most probably the glycine transporters 1 (GLYT1) and/or 2 (GLYT2) which are colocalized in these cells. Through this GlyR- and transporter-mediated effect on OP intrcellular calcium concentration $[Ca^{2+}]_i$, glycine released by neurons may, as well as other neurotransmitters, serve as a signal between neurons and OP during development.

Introduction

During recent years, evidence has emerged that oligodendroglial cells express a complex array of functional receptors to a variety of neuroligands previously known to affect mostly neurons. These include not only neurotransmitter but also neuropeptide and neurohormone receptors (Belachew *et al*., 1998a; Verkhratsky *et al*., 1998) which, via several pathways activate molecular cascades regulating intracellular calcium ($[Ca^{2+}]_i$). Actually, $[Ca^{2+}]_i$ increase is already known to be induced in oligodendroglial cells by stimulation of AMPA/kainate-3 type glutamate (Holtzclaw *et al*., 1995), ATP (P2y and/or P2u; Kirischuk *et al*., 1995a, b), adrenergic (Cohen & Almazan, 1993) and muscarinic (Cohen & Almazan, 1994) receptors. Interestingly, the expression by oligodendrocytes of carbachol and ATP receptors is controlled by oligodendrocyte–neuronal contacts (He *et al*., 1996). Taken together, these data suggest that oligodendroglial calcium signalling could be a target on which converge various signals involved in the neuronal regulation of the oligodendroglial growth and fate.

Regarding these signals, it is now established that glycine receptors (GlyR) are expressed in oligodendroglial lineage cells (Kirchhoff *et al*., 1996; Belachew *et al*., 1998a, b). The peak of glycine-induced chloride current is observed at the progenitor stage (OP), thus suggesting a maximum expression of the GlyR during a transient developmental period which takes place just before the O4-positive stage (Belachew *et al*., 1998b). The pharmacological properties and presumably the molecular structure of the oligodendroglial GlyR are specific (Belachew *et al*., 1998b) but the functional consequences of GlyR activation in OP cells still remain to be elucidated.

Spinal cord oligodendrocytes are known to possess a furosemide-sensitive $Na^+/K^+/2Cl^-$ uptake system that maintains an unusually high intracellular chloride concentration (Hoppe & Kettenmann, 1989). As a consequence of this chloride uptake, the calculated Nernst chloride equilibrium potential ($E_{Cl} = -35$ mV) is more positive in oligodendrocytes than neurons and therefore, as already demonstrated for $GABA_A$ (Gilbert *et al*., 1984), GlyR activation-induced increase of chloride conductance should result in a depolarization of oligodendrocytes. Moreover, in cultures derived from cortex, oligodendrocytes express both low-voltage- (T-type) and high-voltage (presumably L-type)-gated calcium channels (Von Blankenfeld *et al*., 1992). In cultured murine precursor cells of oligodendrocyte lineage, GABA-induced depolarization of the cells exceeds the opening threshold for voltage-gated calcium channels (VGCC) and thereby produces Ca^{2+} influx and a measurable $[Ca^{2+}]_i$ increase which exclusively result from a Ca^{2+} entry via VGCC as removal of extracellular calcium ($[Ca^{2+}]_o$) inhibits this $[Ca^{2+}]_i$ rise (Kirchhoff & Kettenmann, 1992). Here, we demonstrate that the activation of GlyR, the other major ligand-gated anion channel, also induces calcium influx in cultured OP cells derived from newborn rat cerebral cortex as is the case for developing cortical neurons (Flint *et al*., 1998). Furthermore, we also provide evidence that this depolarization-induced calcium increase could be in part the consequence of the

Correspondence: Dr S. Belachew, as above.
E-mail: sbelachew@ulg.ac.be

Received 26 April 1999, revised 14 December 1999, accepted 28 February 2000

activation of a Na^+-dependent electrogenic uptake, most probably the $2Na^+/Cl^-$/glycine uptake system (Aragon *et al*., 1987) through the glycine transporters 1 (GLYT1) and/or 2 (GLYT2) which are both expressed by cultured OP cells. To date, two different glycine transporter genes have been cloned: (i) three isoforms of GLYT1 (a, b and c) with different amino terminals can be produced by alternative splicing and/or alternative promoter usage and are thought to be exclusively present in astroglial processes surrounding *N*-methyl-D-aspartate and glycinergic synapses (Guastella *et al*., 1992; Liu *et al*., 1992; Smith *et al*., 1992; Borowsky *et al*., 1993; Kim *et al*., 1994; Adams *et al*., 1995; Zafra *et al*., 1995a); and (ii), GLYT2, expressed mainly in presynaptic nerve terminals but also in glial elements selectively in the brainstem and spinal cord where it could specifically modulate glycinergic neurotransmission (Liu *et al*., 1993; Zafra *et al*., 1995b; Morrow *et al*., 1998).

The demonstration of glycine transporter expression in OP cells allows us to hypothesize that GLYT1 and GLYT2 also regulate, together with GlyR, glycine-mediated neurono–oligodendroglial interactions.

Materials and methods

Cell culture

Preparation of B104 conditioned medium (B104-CM)

The B104 rat CNS neuroblastoma cell line was maintained in the logarithmic phase of growth in Dulbecco's modified Minimum Essential Medium (DMEM; GIBCO, Belgium) supplemented with 10% fetal calf serum and 2 mM glutamine. For the production of conditioned medium, confluent B104 cultures were washed twice with phosphate buffered saline (PBS) and incubated in serum-free DMEM containing 2 mM glutamine and the N_1 supplement (insulin 5 µg/mL, transferrin 5 µg/mL, progesterone 20 nM, putrescine 100 µM and selenium 30 nM). After 3 days, the medium was collected, filtered (0.22 µm) and stored at –20 °C until use. The same conditioning procedure was used with MEM instead of DMEM for the preparation of the MEM-B104-CM.

Primary oligodendrocyte progenitor cell cultures

Primary oligodendrocyte cultures were prepared using a slight modification of the isolation procedure described by Avellana-Adalid *et al*. (1996). The cerebral cortices of 1–3-day-old rat pups were dissected and collected in PBS supplemented with glucose at 4.5 g/L, carefully freed of meninges and vessels, and dissociated by sieving successively through a 225 µm and a 25 µm nylon mesh. Cells were collected in PBS containing 25 mM HEPES. The cell suspension was layered on top of a precentrifuged (30 min at 26 000 ***g***) Percoll density gradient (1.04 g/mL; Pharmacia, Sweden) and centrifuged for 15 min at 26 000 g. Cell debris which remained in the top aqueous phase were discarded and the interphase below the debris and just above the red blood cells was resuspended in PBS–HEPES. The suspension was centrifuged three times (10 min at 400 ***g***) in PBS–HEPES to eliminate Percoll. The final pellet was resuspended in DMEM supplemented with N_1, biotin (10 ng/mL) and 30% (v/v) of B104-CM. Five millilitres of the cell suspension were then seeded on an uncoated 25 cm^2 tissue culture flask (Falcon; Becton–Dickinson, USA) at a concentration of 4×10^6 cells/mL. After 24 and 48 h, the flask was smoothly shaken and the suspension transferred into a new flask, thus eliminating adherent cells. After these preplatings, the progenitor cells are present as spheroid aggregates termed 'oligospheres' (150–300 µm diameter). To obtain an oligodendrocyte commitment, oligospheres were switched to DMEM-N_1 medium and seeded on polyornithine-coated (0.1 mg/mL) glass coverslips in the centre of 35 mm plastic Petri dishes (NUNC, Denmark) at a density of 10–25 oligospheres per coverslip.

Calcium imaging

Cells were loaded with the calcium indicator dye fluo-3 AM (6 µM; Molecular Probes, USA) by bath application for 45 min at 37 °C. Fluo-3 AM is a nonratiometric indicator dye that increases cellular fluorescence intensity with increased intracellular calcium concentration. Loaded cells were then washed three times with Locke solution containing (in mM): NaCl, 154; KCl, 5.6; glucose, 5.6; HEPES, 10; $CaCl_2.2H_2O$, 2.3. The responses of the cells to experimental conditions were recorded as digitized images from a Bio-Rad MRC 1000 laser scanning confocal system coupled to Zeiss Axiovert 135 microscope with a plan-NEOFLUAR objective (40 ×, 1.3 n.a., oil immersion). The TCSM program (Bio-Rad, USA) was used to control the confocal microscope and obtain a series of images at intervals from 2–5 s. The different reagents diluted in Locke solution were applied by a fast microperfusion system (SPS-8, List-Medical, Germany). Strychnine, nifedipine and bicuculline were obtained from Sigma (USA), glycine from UCB (Belgium) and EGTA from ACROS (New Jersey, USA). In the sodium-free Locke solution, NaCl was substituted with an equimolar concentration of choline chloride. The series of digitized fluorescence images were analysed by a program which determined the average level of fluorescence above background level of each cell and for every time point sampled. The locations of cells were delimited by placing rectangular boxes around every cell in a field. A 'background' box was also defined in a noncellular area of the scanned image. The average intensity of the pixels within a boxed cellular region was calculated and the average intensity of the pixels within the 'background' box defined for the image was subtracted from this value. In order to compensate for variable dye loading between cells, these background-corrected values were normalized by conversion to percentage changes relative to a baseline measurement for each boxed cellular region at the start of a time series (F_t/F_0). Statistical analysis was performed using GraphPAD Prism and GraphPAD InStat software (USA).

Immunocytochemistry

The coverslip cultures were fixed in 4% (v/v) paraformaldehyde for 10 min at room temperature. Nonspecific binding was blocked by a 60-min treatment in a PBS solution containing non-fat dry milk (15 mg/mL). This was followed by an overnight incubation at 4 °C with goat polyclonal anti-GLYT1 or sheep polyclonal anti-GLYT2 antibodies (Chemicon Int., Temecula, USA) both at 1 : 5000 dilution. As secondary antibodies, a TRITC-conjugated antigoat IgG (Sigma, USA) at 1 : 400 dilution (60 min incubation at 37 °C) or a TRITC-conjugated antisheep IgG (Jackson ImmunoResearch, USA) at 1 : 250 dilution were used, respectively. For double stainings, the coverslips were then postfixed for another 10 min incubation in 4% (v/v) paraformaldehyde and the A2B5 and O4 stainings were performed as described by Belachew *et al*. (1998a) using primary antibodies obtained from Boehringer–Mannheim. Triple PBS rinses were performed between each step. For cell counting, all the stains were analysed in triplicate by counting at least 10 fields per coverslip. The control for antibody specificity omitted the primary antibody in the staining protocol. The immunofluorescence images were obtained by Z-series with a Bio-Rad MRC-1000 confocal microscope.

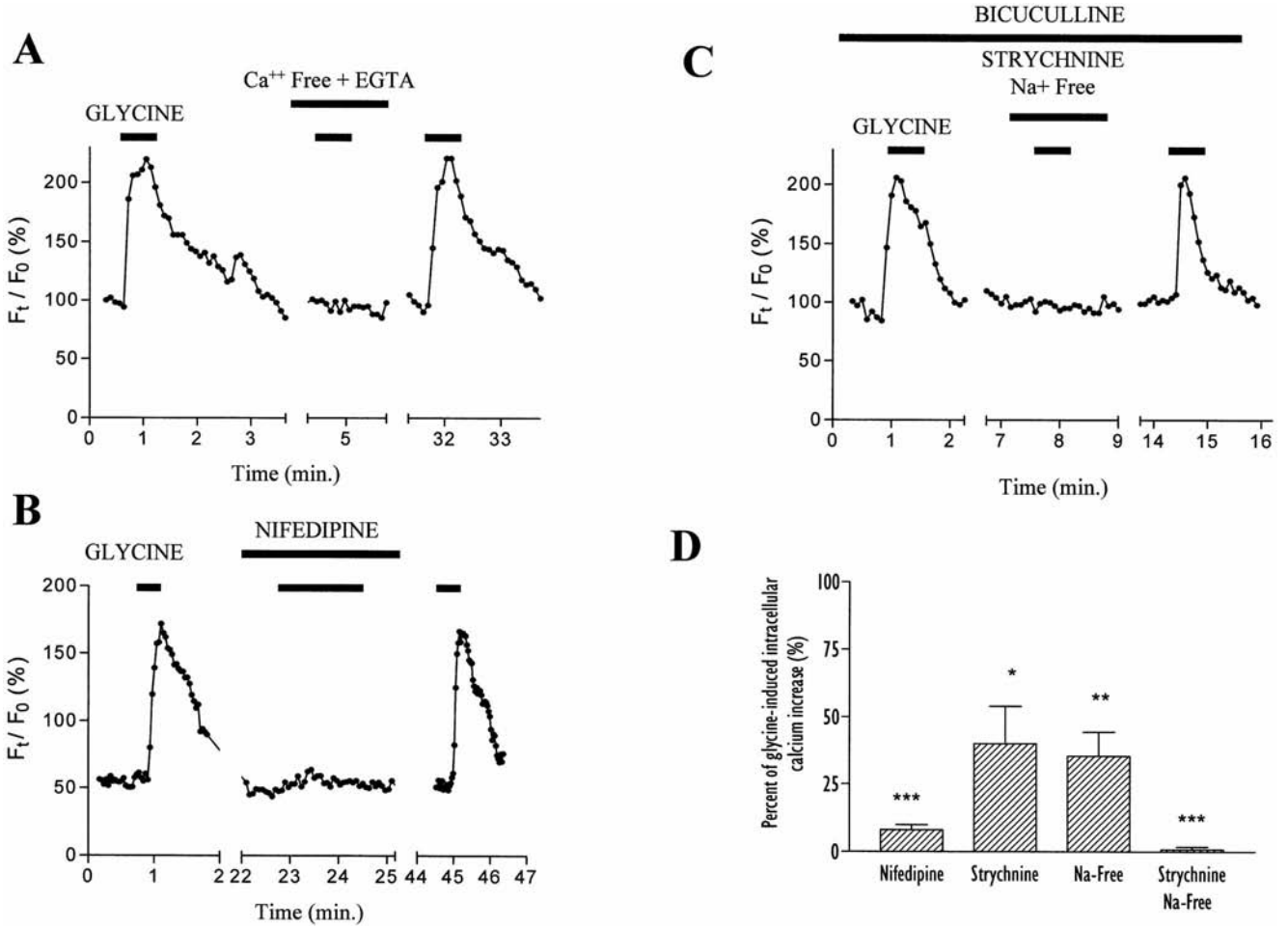

FIG. 1. Fluo-3 measurements of glycine-induced intracellular calcium increase in oligodendrocyte progenitor cells. (A) Time-course of glycine-evoked $[Ca^{2+}]_i$ rise in the presence of bicuculline (100 μM). The calcium response is abolished in calcium-free extracellular solution supplemented with EGTA (2 mM). Glycine was applied at 0.5 mM for 40 s. (B) Glycine-induced calcium increase is completely inhibited by simultaneous application of nifedipine (10 μM) in Locke solution. (C) Glycine-induced calcium increase is completely inhibited by simultaneous application of strychnine (30 μM) in a sodium-free Locke solution. (D) Mean amplitudes (± SEM) of relative glycine-evoked $[Ca^{2+}]_i$ rises elicited in the presence of nifedipine ($n = 41$), strychnine ($n = 8$), Na^+-free medium ($n = 7$) or in both conditions simultaneously ($n = 11$). Results are expressed as percentage of glycine-induced $[Ca^{2+}]_i$ responses and statistical data (using Student's *t*-test) are derived from comparison with these control responses. $^*P < 0.05$, $^{**}P < 0.01$, $^{***}P < 0.0001$.

Results

Glycine induces an increase of intracellular calcium concentration in OP cells through the opening of voltage-gated calcium channels

The cultured cells were studied in the outgrowth zone of expanded oligospheres 3 days after switching to DMEM-N_1. We have previously shown that, in this growth factor-free medium, the cultures contain mainly A2B5-positive cells with many of them already coexpressing a galactocerebroside immunophenotype (Belachew *et al.*, 1998a). We also demonstrated that there was virtually no neuronal or glial fibrillary acidic protein-positive cells (< 1%) in such cultures (Belachew *et al.*, 1998a).

To investigate whether GlyR activation could affect intracellular oligodendroglial calcium concentration, we used 3-day-old cultures because the peak density of GlyR expression occurs at this intermediate stage of differentiation (Belachew *et al.*, 1998b).

OP cells were imaged using confocal microscopy and the calcium indicator dye fluo-3 in Locke standard extracellular solution. All the recordings were made in the presence of bicuculline (100 μM) to avoid any nonspecific increase of intracellular calcium that would result from a glycine-induced cross-activation of $GABA_A$ receptors. In such conditions, the application of glycine (0.5 mM) results in a prolonged rise of $[Ca^{2+}]_i$ in around 50% of the cells (30 out of 61 tested cells). A glycine-evoked change in $[Ca^{2+}]_i$ was not observed in these OP cells (16 out of 61 tested cells) which do not exhibit an intracellular calcium response to depolarization induced by high extracellular K^+ concentration (50 mM). The glycine-elicited $[Ca^{2+}]_i$ increase in OP cells ($n = 7$; Fig. 1A) is completely abolished in a calcium-free extracellular solution supplemented with EGTA (2 mM). Moreover, nifedipine (10 μM) an L-type calcium channel blocker, reversibly inhibits the glycine-induced $[Ca^{2+}]_i$ rise in all the tested OP cells ($n = 41$; Fig. 1B). These data thus suggest that, in OP cells, glycine triggers a depolarization-induced calcium entry through VGCC.

Glycine-induced calcium influx in OP cells is mediated by both GlyR and Na^+-dependent transporters, most probably GLYTs

Strychnine (30 μM), a competitive antagonist of GlyR, produces a reversible but variable inhibition of glycine-induced calcium responses (Fig. 1D). In three of eight OP cells, the strychnine block of $[Ca^{2+}]_i$ increase was complete, whereas the inhibition was only

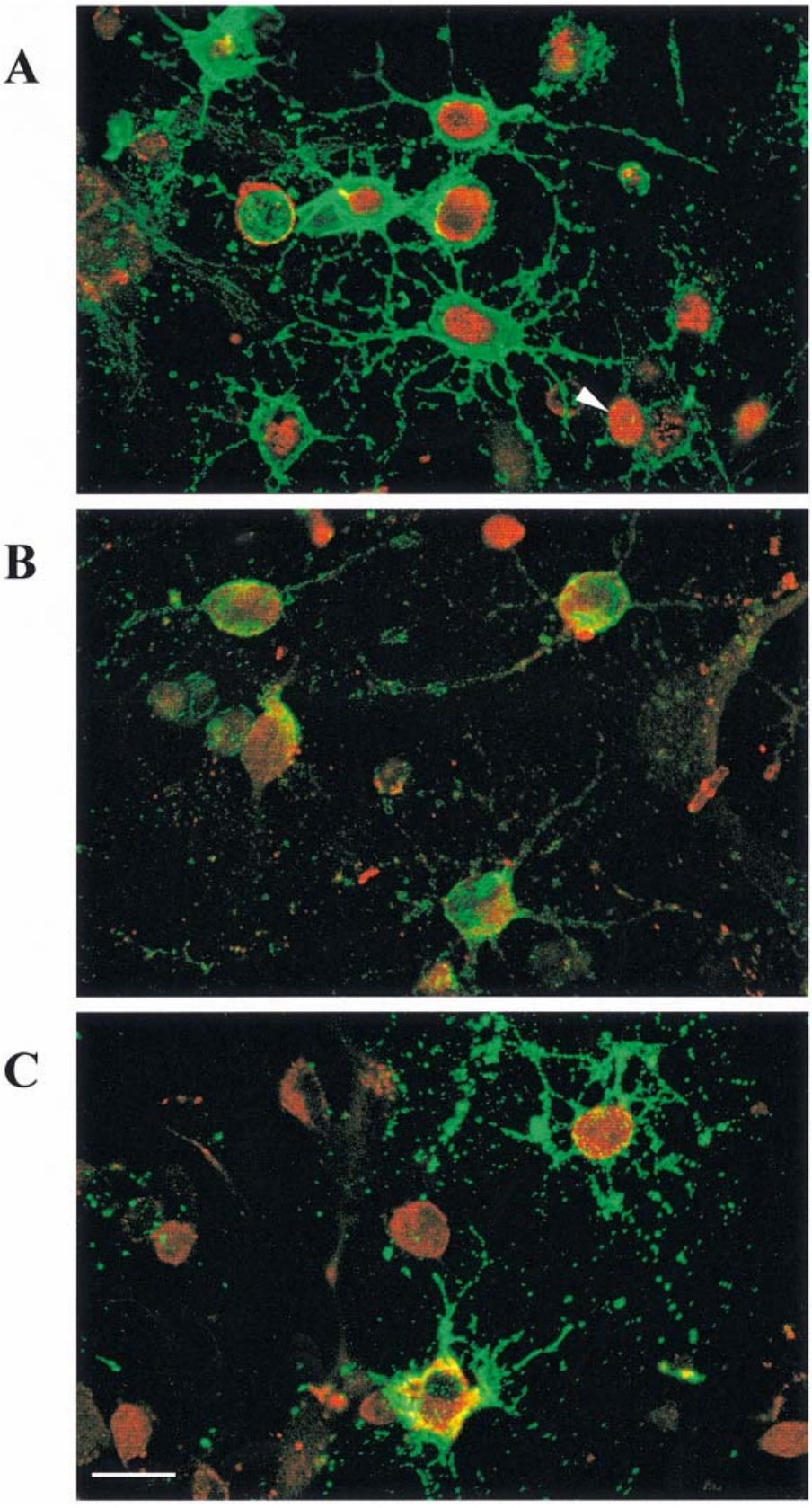

FIG. 2. Confocal microscopy images of GLYT1 and GLYT2 immunofluorescence stainings in oligodendroglial cells after 3 days of differentiation *in vitro*. (A) Double stained OP cells with A2B5 (green) and anti-GLYT1 (red) antibodies. The GLYT1 staining is only located on the cell body and not on oligodendroglial processes. GLYT1-positive A2B5 cells are probably already at the O4 stage (arrow). (B) A2B5-positive OP cells (green) are also stained by anti-GLYT2 (red) antibodies. (C) The GLYT1 staining (red) remains in O4-positive cells (green). Many GLYT1-positive O4-negative cells are probably still A2B5-positive OP cells. Scale bar, 10 µm

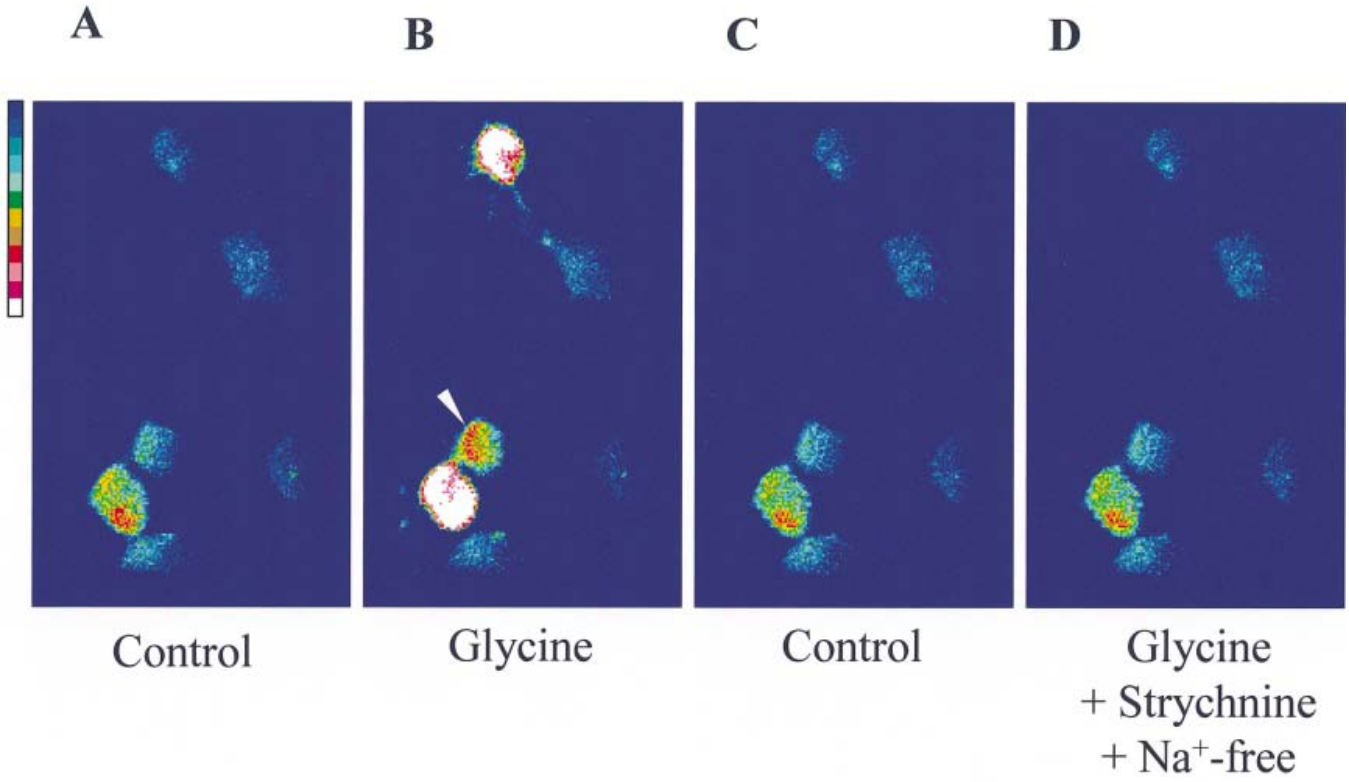

FIG. 3. Pseudocolored fluorescence images of OP cells loaded with fluo-3. Illustrated example of progenitor cells fluorescence that reflects $[Ca^{2+}]_i$ variations in response to external application of successively control medium (A and C), glycine (0.5 mM) in Locke solution (B), or glycine with strychnine in a Na^+-free Locke solution (D). Images are pseudocolored according to the scale, which represents a linear increase in fluo-3 fluorescence. This example was selected to underline that glycine-induced $[Ca^{2+}]_i$ increase was delayed in one of these OP (arrow) which suggests an intercellular calcium wave propagation through gap junctional contacts which are known to be present in OP cells (Takeda *et al*., 1995).

partial in the other tested OP cells, despite a virtually full blockade of OP GlyR at such strychnine concentrations (Belachew *et al*., 1998b). This suggested that the glycine-induced depolarization in OP cells and its subsequent calcium entry is only partly due to GlyR activation. As it was recently demonstrated that the glial glycine uptake transport systems mediated by GLYT1b and GLYT2 induce inward depolarizing uptake currents in HEK 293 cells transfected with these transporters (López-Corcuera *et al*., 1998), we suspected the presence of such transporters in oligodendroglial cells. Immunocytochemical stainings (Fig. 2) indeed show that all the A2B5-positive ($98 \pm 2\%$, mean $\pm$ SEM) and the majority of O4-positive OP cells ($76 \pm 5\%$, mean $\pm$ SEM) express GLYT1 *in vitro*. We also observed the expression of GLYT2 in most of the A2B5-positive OP cells ($90 \pm 3\%$, mean $\pm$ SEM). These two transporters are thus colocalized with GlyR because, as we previously shown, GlyR is expressed in more than 90% of the cells at this stage after 3 days of differentiation in DMEM-N_1 (Belachew *et al*., 1998b).

In order to investigate the role of the GLYTs and/or less specific electrogenic transporters in glycine-induced $[Ca^{2+}]_i$ increase in OP cells, we blocked these Na^+-dependent transporters by using Na^+-free Locke solution. In such conditions, a partial inhibition of glycine-evoked calcium responses was observed ($n = 7$; Fig. 1D). Finally, if strychnine (30 µM) and external Na^+ removal are combined, a full inhibition of the glycine response is obtained ($n = 11$; Figs 1C and D, and 3), thus demonstrating that a glycine-triggered $[Ca^{2+}]_i$ increase in OP cells is actually due to the activation of not only GlyRs but also Na^+-dependent transporters, most probably GLYTs.

It is noteworthy that the inhibition in Na^+-free solution is greater (65%) than that expected based on strychnine-resistant inhibition (40%). This discrepancy could arise from inhibition of Na^+-dependent chloride transporters affecting the chloride gradient and thus influencing GlyR signalling.

Discussion

Glial cells, obviously non-excitable according to the classical view of excitability (i.e. the ability to generate action potentials), express voltage-gated Ca^{2+} channels that constitute an important pathway for calcium entry in oligodendroglial cells (Kirischuk *et al*., 1995b). Such calcium influx through VGCCs and the resulting increase of $[Ca^{2+}]_i$ are likely to regulate various intracellular events in OP cells (including metabolic reactions, gene expression or ion transport systems) that could ultimately be linked to the myelinating function. In this study, we report that exogenously applied glycine induces an important elevation of $[Ca^{2+}]_i$ in cortical OP cells. We show that this effect is observed only in cells which express functional VGCCs, as demonstrated by $[Ca^{2+}]_i$ increase in response to depolarization. Glycine-evoked $[Ca^{2+}]_i$ rise results from a depolarization-induced calcium influx as it is completely suppressed by VGCC blockade or removal of extracellular calcium. However, we cannot exclude that plasmalemnal calcium entry could secondarily trigger a calcium release from intracellular stores but, so far, such a Ca^{2+}-induced Ca^{2+}-release mechanism has not been demonstrated in oligodendroglial cells (Kirischuk *et al*., 1995b).

We consider that glycine-induced depolarization and calcium influx in OP cells are mediated by the simultaneous activation of the ionotropic GlyR and the Na^+-dependent transporters, the best candidates being glycine transporters, since: (i) we demonstrate by immunostaining the presence of GLYT1 and GLYT2 in the majority of OP cells, and these transporters ($2Na^+/Cl^-$/glycine) are known to be electrogenic, and thus their activation produces an inward depolarizing uptake current (López-Corcuera *et al*., 1998); (ii) we have previously shown the presence of GlyR in OP cells (Belachew *et al*., 1998b), the activation of which should induce a depolarization as is the case after $GABA_A$ receptor activation; (iii) glycine-evoked $[Ca^{2+}]_i$ increase is significantly, but only partly, inhibited either by application of saturating concentrations of strychnine or by choline substitution of extracellular Na^+, which are conditions that block the GlyR and Na^+-dependent transporters, respectively; and, (iv) glycine-evoked $[Ca^{2+}]_i$ increase is totally abolished by the simultaneous blockade of oligodendroglial GlyR and Na^+-dependent transporters, therefore demonstrating that both types of membrane proteins transduce the effect of glycine leading to an increased OP $[Ca^{2+}]_i$. Due to the lack of availability of pharmacological agents that would specifically block both GLYT1 and GLYT2, we cannot provide conclusive, but only circumstantial, evidence demonstrating that GLYTs are the sole Na^+-dependent transporters implied.

The coexpression of glycine receptors and transporters and the consequences of their stimulation on calcium homeostasis has not been reported in oligodendroglial cells. This oligodendroglial colocalization of GLYT1 and GlyR is, however, not surprising considering the *in situ* hybridization data that show a temporal and spatial coincidence of GLYT1 and GlyR β-subunit mRNA expression (Zafra *et al*., 1995b). Contrary to GLYT1, GLYT2 expression is prominently neuronal and restricted to the brainstem, the spinal cord and the cerebellum, where it colocalizes with GlyR and glycine immunoreactivity (Jursky & Nelson, 1995; Luque *et al*., 1995; Poyatos *et al*., 1997). Such correlating distributions of GLYTs and GlyR suggest that GLYTs reuptake activity could regulate the glycinergic neurotransmission by modulating glycine concentrations locally bathing presynaptic elements of glycinergic synapses *in vivo*. It is also known that in cultured astroglial cells, the initiation and the maintenance of GLYT1 expression require the presence of neurons whereas we show that it is not the case for oligodendroglial GLYTs (Zafra *et al*., 1997). Consequently, we consider that glycine, via its receptors and transporters, could be involved in a bidirectional neuron–oligodendrocyte dialogue that could regulate oligodendroglial development through glycine-induced $[Ca^{2+}]_i$ increase. There is currently good evidence that neurons influence oligodendrogliogenesis through the release of growth factors (Calver *et al*., 1998) and electrical activity (Demerens *et al*., 1996). Neurotransmitters may also play a role in this neuronal regulation of oligodendrocyte behaviour. However, as oligodendroglial calcium signalling can be triggered by numerous membrane receptor systems (Verkhratsky *et al*., 1998), the question of the specificity of such effects arises. In other words do oligodendrocytes distinguish, for instance through spatiotemporal cell-specific pattern of $[Ca^{2+}]_i$ rise, between different stimulations that all increase $[Ca^{2+}]_i$? At present, the functional responses of oligodendroglial cells that are triggered by an elevation of $[Ca^{2+}]_i$ has still to be investigated. In cortical OP cells, calcium influx can induce the phosphorylation of the cAMP response element binding protein (CREB; Pende *et al*., 1997) that is known to be a crucial factor for Ca^{2+}-dependent gene expression. Very recent data support the idea that CREB phosphorylation, which is increased when $[Ca^{2+}]_i$ rises, could mediate neuronal signals that, coupled to specific transduction cascades, may play different regulatory roles at specific stages of oligodendrocyte differentiation (Sato-Bigbee *et al*., 1999). Interestingly, OP cells also express a G-protein-coupled $[Ca^{2+}]_o$-sensing receptor (CaR; Chattopadhyay *et al*., 1998). The stimulation of CaR by $[Ca^{2+}]_o$ elevation increases OP proliferation by triggering a $[Ca^{2+}]_i$ rise which is likely to activate an outward K^+ channel (Chattopadhyay *et al*., 1998) whose role is essential for the regulation of OP cell cycle (Knutson *et al*., 1997). Considering this emerging evidence for a central role of $[Ca^{2+}]_i$ in oligodendroglial development, we would expect that glycine-induced $[Ca^{2+}]_i$ elevation in OP cells could be one of several neuronal signals modulating proliferation, migration or differentiation of OP cells, and therefore ultimately myelination and possibly remyelination, thus opening therapeutic prospects.

Acknowledgements

We thank Dr Frank Kirchhoff (Max Delbrueck Center for Molecular Medicine, Berlin, Germany) for his helpful comments on the manuscript. This work was supported by the Fonds National de la Recherche Scientifique (FNRS), the Concerted Action of the Government of the French Community of Belgium, the Fondation Médicale Reine Elisabeth (FMRE) and the Ligue Belge de la Sclérose en Plaques. We thank P. Ernst-Gengoux for her technical support and expertise. B. Rogister and S. Belachew are, respectively, Research Associate and Research Assistant of the FNRS.

Abbreviations

AMPA, α-amino-3-hydroxy-5-methyl-4-isoxazolepropionate; B104-CM, B104 cell line conditioned medium; $[Ca^{2+}]_i$, intracellular calcium concentration; DMEM, Dulbecco's modified Eagle's medium; EGTA, ethylene glycol-bis(β-aminoethyl ether)-N-tetraacetic acid; GABA, γ-aminobutyric acid; GlyR, glycine receptor; GLYT, glycine transporter; HEK, human embryonic kidney (cell line); HEPES, *N*-(2-hydroxyethyl)piperazine-*N*′-2-ethanesulphonic acid; MEM, minimum essential medium; OP, oligodendrocyte progenitor; PBS, phosphate-buffered saline; VGCC, voltage-gated calcium channels.

References

Adams, R.H., Sato, K., Shimada, S., Tohyama, M., Pschel, A.W. & Betz, H. (1995) Gene structure and glial expression of the glycine transporter GlyT1 in embryonic and adult rodents. *J. Neurosci.*, **15**, 2524–2532.

Aragon, M.C., Gimenez, C. & Mayor, F. (1987) Stoichiometry of sodium- and chloride-coupled glycine transport in synaptic plasma membrane vesicles derived from rat brain. *FEBS Lett.*, **212**, 87–90.

Avellana-Adalid, V., Nait Oumesmar, B., Lachapelle, F. & Baron-Van Evercooren, A. (1996) Expansion of rat oligodendrocyte progenitors into proliferative 'oligospheres' that retain differentiation potential. *J. Neurosci. Res.*, **45**, 558–570.

Belachew, S., Malgrange, B., Rigo, J.-M., Rogister, B., Coucke, P., Mazy-Servais, C. & Moonen, G. (1998a) Developmental regulation of neuroligand-induced responses in cultured oligodendroglia. *Neuroreport*, **9**, 973–980.

Belachew, S., Rogister, B., Rigo, J.-M., Malgrange, B., Mazy-Servais, C., Xhauflaire, G., Coucke, P. & Moonen, G. (1998b) Cultured oligodendrocyte progenitors derived from cerebral cortex express a glycine receptor which is pharmacologically distinct from the neuronal isoform. *Eur. J. Neurosci.*, **10**, 3556–3564.

Borowsky, B., Mezey, E. & Hoffman, B.J. (1993) Two glycine transporter variants with distinct localization in the CNS and peripheral tissues are encoded by a common gene. *Neuron*, **10**, 851–863.

Calver, A.R., Hall, A.C., Yu, W.P., Walsh, F.S., Heath, J.K., Betsholtz, C. & Richardson, W.D. (1998) Oligodendrocyte population dynamics and the role of PDGF in vivo. *Neuron*, **20**, 869–882.

Chattopadhyay, N., Ye, C.P., Yamaguchi, T., Kifor, O., Vassilev, P.M., Nishimura, R. & Brown, E.M. (1998) Extracellular calcium-sensing receptor in rat oligodendrocytes: Expression and potential role in regulation of cellular proliferation and an outward K + channel. *Glia*, **24**, 449–458.

Cohen, R.I. & Almazan, G. (1993) Norepinephrine-stimulated PI hydrolysis in oligodendrocytes is mediated by alpha 1A-adrenoceptors. *Neuroreport*, **4**, 1115–1118.

Cohen, R.I. & Almazan, G. (1994) Rat oligodendrocytes express muscarinic receptors coupled to phosphoinositide hydrolysis and adenylyl cyclase. *Eur. J. Neurosci.*, **6**, 1213–1224.

Demerens, C., Stankoff, B., Logak, M., Anglade, P., Allinquant, B., Couraud, F., Zalc, B. & Lubetzki, C. (1996) Induction of myelination in the central nervous system by electrical activity. *Proc. Natl Acad. Sci. USA*, **93**, 9887–9892.

Flint, A.C., Liu, X.L. & Kriegstein, A.R. (1998) Nonsynaptic glycine receptor activation during early neocortical development. *Neuron*, **20**, 43–53.

Gilbert, P., Kettenmann, H. & Schachner, M. (1984) Gamma-aminobutyric acid directly depolarizes cultured oligodendrocytes. *J. Neurosci.*, **4**, 561–569.

Guastella, J., Brecha, N., Weigmann, C., Lester, H.A. & Davidson, N. (1992) Cloning, expression, and localization of a rat brain high-affinity glycine transporter. *Proc. Natl Acad. Sci. USA*, **89**, 7189–7193.

He, M.H., Howe, D.G. & McCarthy, K.D. (1996) Oligodendroglial signal transduction systems are regulated by neuronal contact. *J. Neurochem.*, **67**, 1491–1499.

Holtzclaw, L.A., Gallo, V. & Russell, J.T. (1995) AMPA receptors shape calcium responses in cortical oligodendrocyte progenitors and CG-4 cells. *J. Neurosci. Res.*, **42**, 124–130.

Hoppe, D. & Kettenmann, H. (1989) GABA triggers a chloride efflux from cultured oligodendrocytes. *Neurosci. Lett.*, **97**, 334–339.

Jursky, F. & Nelson, N. (1995) Localization of glycine neurotransmitter transporter (GLYT2) reveals correlation with the distribution of glycine receptor. *J. Neurochem.*, **64**, 1026–1033.

Kim, K.M., Kingsmore, S.F., Han, H., Yang-Feng, T.L., Godinot, N., Seldin, M.F., Caron, M.G. & Giros, B. (1994) Cloning of the human glycine transporter type 1: molecular and pharmacological characterization of novel isoform variants and chromosomal localization of the gene in the human and mouse genomes. *Mol. Pharmacol.*, **45**, 608–617.

Kirchhoff, F. & Kettenmann, H. (1992) GABA triggers a [Ca 2+]i increase in murine precursor cells of the oligodendrocyte lineage. *Eur. J. Neurosci.*, **4**, 1049–1058.

Kirchhoff, F., Mulhardt, C., Pastor, A., Becker, C.-M. & Kettenmann, H. (1996) Expression of glycine receptor subunits in glial cells of the rat spinal cord. *J. Neurochem.*, **4**, 1383–1390.

Kirischuk, S., Scherer, J., Kettenmann, H. & Verkhratsky, A. (1995a) Activation of P2 -purinoreceptors triggered Ca 2+ release from Ins*P*3 -sensitive internal stores in mammalian oligodendrocytes. *J. Physiol. (London)*, **483**, 41–57.

Kirischuk, S., Scherer, J., Möller, T., Verkhratsky, A. & Kettenmann, H. (1995b) Subcellular heterogeneity of voltage-gated Ca 2+ channels in cells of the oligodendrocyte lineage. *Glia*, **13**, 1–12.

Knutson, P., Ghiani, C.A., Zhou, J.M., Gallo, V. & McBain, C.J. (1997) K + channel expression and cell proliferation are regulated by intracellular sodium and membrane depolarization in oligodendrocyte progenitor cells. *J. Neurosci.*, **17**, 2669–2682.

Liu, Q.R., Löpez-Corcuera, B., Mandiyan, S., Nelson, H. & Nelson, N. (1993) Cloning and expression of a spinal cord- and brain-specific glycine transporter with novel structural features. *J. Biol. Chem*, **268**, 22802–22808.

Liu, Q.R., Nelson, H., Mandiyan, S., Löpez-Corcuera, B. & Nelson, N. (1992) Cloning and expression of a glycine transporter from mouse brain. *FEBS Lett.*, **305**, 110–114.

López-Corcuera, B., Martínez-Maza, R., Núnez, E., Roux, M., Supplisson, S. & Aragón, C. (1998) Differential properties of two stably expressed brain-specific glycine transporters. *J. Neurochem.*, **71**, 2211–2219.

Luque, J.M., Nelson, N. & Richards, J.G. (1995) Cellular expression of glycine transporter 2 messenger RNA exclusively in rat hindbrain and spinal cord. *Neuroscience*, **64**, 525–535.

Morrow, J.A., Collie, I.T., Dunbar, D.R., Walker, G.B., Shahid, M. & Hill, D.R. (1998) Molecular cloning and functional expression of the human glycine transporter GlyT2 and chromosomal localisation of the gene in the human genome. *FEBS Lett.*, **439**, 334–340.

Pende, M., Fisher, T.L., Simpson, P.B., Russell, J.T., Blenis, J. & Gallo, V. (1997) Neurotransmitter- and growth factor-induced cAMP response element binding protein phosphorylation in glial cell progenitors: role of calcium ions, protein kinase C, and mitogen-activated protein kinase/ribosomal S6 kinase pathway. *J. Neurosci.*, **17**, 1291–1301.

Poyatos, I., Ponce, J., Aragon, C., Gimenez, C. & Zafra, F. (1997) The glycine transporter GLYT2 is a reliable marker for glycine-immunoreactive neurons. *Brain Res. Mol. Brain Res.*, **49**, 63–70.

Sato-Bigbee, C., Pal, S. & Chu, A.K. (1999) Different neuroligands and signal transduction pathways stimulate CREB phosphorylation at specific developmental stages along oligodendrocyte differentiation. *J. Neurochem.*, **72**, 139–147.

Smith, K.E., Borden, L.A., Hartig, P.R., Branchek, T. & Weinshank, R.L. (1992) Cloning and expression of a glycine transporter reveal colocalization with NMDA receptors. *Neuron*, **8**, 927–935.

Takeda, M., Nelson, D.J. & Soliven, B. (1995) Calcium signaling in cultured rat oligodendrocytes. *Glia*, **14**, 225–236.

Verkhratsky, A., Orkand, R.K. & Kettenmann, H. (1998) Glial calcium: Homeostasis and signaling function. *Physiol. Rev.*, **78**, 99–141.

Von Blankenfeld, G., Verkhratsky, A. & Kettenmann, H. (1992) Calcium channel expression in the oligodendrocyte lineage. *Eur. J. Neurosci.*, **4**, 1035–1048.

Zafra, F., Aragon, C., Olivares, L., Danbolt, N.C., Gimenez, C. & Storm-Mathisen, J. (1995a) Glycine transporters are differentially expressed among CNS cells. *J. Neurosci.*, **15**, 3952–3969.

Zafra, F., Gomeza, J., Olivares, L., Aragon, C. & Gimenez, C. (1995b) Regional distribution and developmental variation of the glycine transporters GLYT1 and GLYT2 in the rat CNS. *Eur J. Neurosci.*, **7**, 1342–1352.

Zafra, F., Poyatos, I. & Gimenez, C. (1997) Neuronal dependency of the glycine transporter GLYT1 expression in glial cells. *Glia*, **20**, 155–162.

7.12 Publication #12: Nguyen, L., Malgrange, L., Breuskin, I., Lallemend, F., Hans, G., Moonen, G., Belachew, S., and Rigo, J.-M. (2004) Striatal PSA-NCAM$^+$ precursor cells from the newborn rat express functional glycine receptors. *Neuroreport* 15:583-587.

Striatal PSA-NCAM$^+$ precursor cells from the newborn rat express functional glycine receptors

Laurent Nguyen,[1,CA,†] Brigitte Malgrange,[1] Ingrid Breuskin,[1] François Lallemend,[1] Grégory Hans,[1,2] Gustave Moonen,[1,2] Shibeshih Belachew[1,2,*] and Jean-Michel Rigo[1,*]

[1]Center for Cellular and Molecular Neurobiology, University of Liège, 17 Place Delcour, B-4020 Liège; [2]Department of Neurology, University of Liège, C.H.U. (B35) Sart Tilman, B-4000 Liège, Belgium

[†]Present address: Division of Molecular Neurobiology, National Institute for Medical Research, The Ridgeway, Mill Hill, London, NW7 1AA

[CA] Corresponding Author: lnguyen@nimr.mrc.ac.uk

[*]S.B. and J.-M. R. contributed equally to this work

Received 19 February 2003; accepted 21 May 2003

DOI: 10.1097/01.wnr.0000094860.49817.dd

Immunocytochemical analysis showed that ionotropic glycine receptors are expressed in neurogenic progenitors purified from the newborn rat striatum and expressing the polysialylated form of the neural cell adhesion molecule, both *in vitro* and *in situ*. To ascertain whether glycine receptors were functional *in vitro*, whole-cell patch-clamp recordings demonstrated that glycine triggers inward strychnine-sensitive currents in the majority of these cells. Moreover, we found that glycine receptors expressed by these neurogenic progenitors display intermediate electrophysiological characteristics between those of glycine receptors expressed by neural stem cells and by mature interneurons from the rat striatum. Altogether, the present data show that functional strychnine-sensitive glycine receptors are expressed in neurogenic progenitors purified from the newborn rat striatum. *NeuroReport* 15:583–587 © 2004 Lippincott Williams & Wilkins.

Key words: Glycine receptors; Immunocytochemistry; Neuroblast; Newborn rat; PSA-NCAM; Strychnine; Whole-cell patch-clamp

INTRODUCTION

During CNS development, neural stem cells differentiate initially into progenitors that express the polysialylated form of the neural cell adhesion molecule (PSA-NCAM) [1], a molecule which plays important roles in developmental processes and in neuronal plasticity occurring throughout the adulthood [2,3]. Although already committed either to a glial [4] or a neuronal [5,6] preferential fate, PSA-NCAM$^+$ progenitors preserve a relative degree of pluripotentiality in culture [7]. Considering that PSA-NCAM$^+$ progenitors are well suited for brain repair purposes [3,7,8], there is much interest in studying signalling factors that regulate their development. In this respect, recent studies reported possible roles for neurotransmitter receptors in the regulation of neural stem/progenitor cell biology before the onset of synaptogenesis (see [9] for review). In the adult CNS, strychnine-sensitive glycine receptors (GlyR) are ligand-gated anion channels widely expressed within the spinal cord and brainstem, where they mediate inhibitory neurotransmission [10]. GlyRs are also found in the developing CNS in neural stem/progenitor cells [11], in oligodendrocyte progenitors [12] and in neuroblasts [13], where they have been suggested to mediate developmental signals. In the present study, we found evidence for the expression of functional GlyRs in neurogenic progenitors βIII-tubulin$^+$/PSA-NCAM$^+$ isolated from newborn rat striatum and cultured as proliferative spheres. Moreover, their electrophysiological and pharmacological characterization interestingly suggests an intermediate functional profile between neural stem cells and mature interneurons.

MATERIALS AND METHODS

Cell culture: Care and use of animals reported in this study were approved by the Belgian National Fund for Scientific Research in accordance with NIH guidelines. Newborn Wistar rats (0–3 days old) raised in our animal facility were sacrificed following National Institutes of Health animal welfare guidelines. They were first anaesthetized on ice and subsequently decapitated. Striata were dissected out and collected in phosphate buffer saline (PBS) solution supplemented with glucose at 4.5 g/l. Isolated striata, possibly including small parts of subventricular zones, were next triturated in PBS-HEPES (25 mM) before being filtered with a 15 μm nylon mesh. The cell suspension was then layered on top of a pre-centrifuged (15 min at 26 000 × *g*) Percoll density gradient (1.04 g/ml, Amersham Biosciences, Uppsala, Sweden) and further ultracentrifuged for 15 min at 26 000 × *g*. Proliferating PSA-NCAM$^+$ precursor cells were separated from differentiated post-mitotic neural cells and cell debris by collecting the interphase located between the bands at 1.052 and 1.102 g/ml, as determined using density marker beads (Amersham Biosciences) for the calibration of the Percoll gradient after centrifugation [14]. The resulting suspension was then

centrifuged three times (10 min at 400 *g*) in PBS-HEPES to eliminate Percoll. The final pellet was resuspended in DMEM/F12 (1:1, v:v, Invitrogen, Merelbeke, Belgium) medium supplemented with 1% (v:v) of N2 (25 μg/ml bovine insulin, 100 μg/ml transferrin, 20 nM progesterone, 60 μM putrescine, 30 nM sodium selenite), 1% (v:v) B27 (Invitrogen) and epidermal growth factor (EGF, 20 ng/ml; PeproTech, Rocky Hill, NJ, USA). Cells grown in uncoated conditions generated floating spheres (Fig. 1a,b). After 3 days in EGF-containing medium, growing spheres were allowed to attach for 1 h onto polyornithine-coated coverslips before being used for patch-clamp recordings or immunocytochemical studies.

Immunostaining: Cells were fixed with 4% (v:v) paraformaldehyde for 10 min at room temperature and permeabilized in 0.1% Triton X100 (v:v) for 15 min, when subsequent immunostaining was directed towards cytoplasmic epitopes. For all immunostaining, non-specific binding was blocked by a 30 min treatment in a PBS solution containing non-fat dry milk (15 mg/ml). Cells were then incubated overnight at 4°C with primary antibodies: mouse anti-PSA-NCAM at 1:500 (AbCys S.A., Paris, France), mouse anti-βIII tubulin at 1:1500 (clone Tuj1, BAbCO, USA), rabbit anti-$GlyR_{\alpha 1/2}$ at 1:100 (Chemicon, Temacula, CA), rabbit anti-glial fibrillary acidic protein (GFAP) at 1:1500 (Dako, Prosan, Belgium), and mouse monoclonal anti-O4 at 1:150 (Chemicon, Temacula, CA, USA). Secondary antibodies were diluted in PBS solution and applied for 45 min at room temperature. These included: FITC-, rhodamine-conjugated anti-mouse IgM (1:500), rhodamine-, Cy5-conjugated anti-mouse IgG, and FITC-conjugated anti-rabbit Ig antibodies (all purchased from Jackson Immunoresearch Laboratory, Inc., West Grove, USA). Three rinses in PBS were performed between all different steps. Preparations were mounted in Fluoprep (Biomerieux, France). Frozen 30 μm tissue sections were prepared as described previously [15]. Immunohistochemical stainings were processed following a procedure identical to that of cultured cells. In the control experiments, where primary antibodies were omitted, no detectable immunofluorescence was observed. Images were acquired using a laser scanning confocal microscope (MRC1024, BioRad, Hertfordshire, UK).

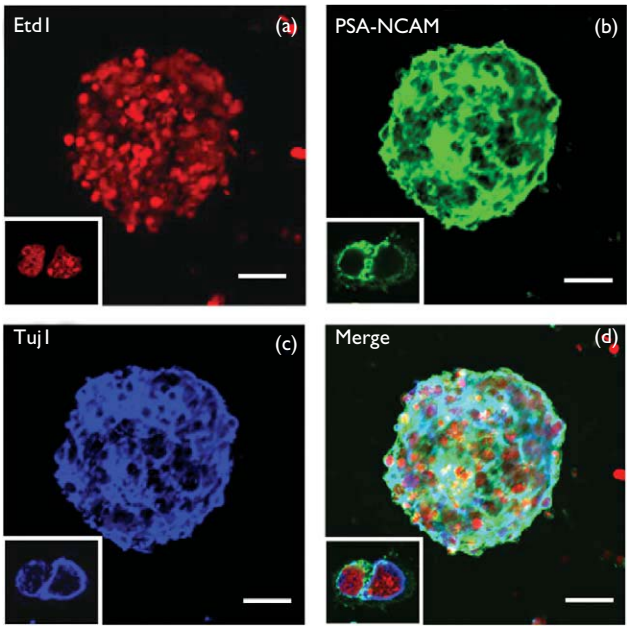

Fig. 1. Immunocytochemical analysis of neurogenic PSA-NCAM$^+$ progenitors from early postnatal striatum. Confocal images of a 3-DIV sphere showing respectively: nuclei stained by the nuclear dye ethidium-homodimere I (EtdI, **a**), the corresponding field where cells were immunostained for PSA-NCAM (**b**), immunostaining for βIII-tubulin (TujI, **c**), and the merge of (a–c) (**d**). Inserts display in each panel a higher magnification view (5 times) of two cells co-expressing PSA-NCAM and TujI (a–d). Bars = 15 μm.

BrdU incorporation assay: To label cells in S phase *in vitro*, BrdU (20 μM, Sigma, USA), which is incorporated into replicating DNA, was added to the cultures for 18 h prior to fixation and staining. The PSA-NCAM and Tuj1 labellings were performed as described in the preceding section. Coverslips were next post-fixed for another 10 min incubation in 4% (v/v) paraformaldehyde, incubated in NaOH 0.07 N for 10 min, post-fixed again for 10 min, permeabilized in Triton X100 (0.1%) and finally incubated for 45 min with an anti-BrdU FITC-conjugated antibody (1:3, Becton-Dickinson, USA).

Cell counting: For quantitative immunostainings, spheres were mechanically dissociated prior to immunocytochemical procedure and further plated onto polyornithine-coated coverslips. Cells were allowed to attach for 1 h before fixation. Cells were counterstained with the nuclear dye: ethidium homodimer-1 (Etd1, applied at 6×10^{-7} M for 7 min, Molecular Probes, Leiden, The Netherlands). Ten non-overlapping microscopic fields (~50 cells/field; Axiovert 135 fluorescence microscope, ×40 objective, Zeiss) were counted for each coverslip in a minimum of three separate experiments. Results are expressed as mean ± s.e.m.

Electrophysiological recordings: Cell-Tak (Becton Dickinson)-coated coverslips containing 1–3 h adhesive spheres were transferred to the stage of a Zeiss interferential contrast microscope equipped with fluorescence. Coverslips were maintained at 37°C in a recording chamber which was continuously perfused with a physiological saline solution containing (in mM): NaCl, 116; D-glucose, 11.1; KCl, 5.4; $CaCl_2.2H_2O$, 1.8; $MgCl_2.6H_2O$, 2.0; HEPES, 10.0; pH 7.2. Glycine was purchased from UCB (Brussels, Belgium) and strychnine and SR-95531 were obtained from Sigma. All the drugs were applied by means of a local microperfusion system (SPS-8, List Medical). Borosilicate recording electrodes (15–20 MΩ) were made using a Flaming-Brown microelectrode puller (P97, Sutter Instrument Co). Micropipettes were filled with an intracellular-like solution containing (in mM): KCl, 130.0; $CaCl_2.2H_2O$, 1.0; D-glucose, 11.1; EGTA, 10.0; Na_2-ATP, 2.5; Mg-ATP, 2.5; HEPES, 10.0, pH 7.4. Electrophysiological recordings were performed with a Bio-Logic RK400 patch-clamp amplifier using the whole-cell configuration of the patch-clamp technique [16]. Series resistances (10–20 Ω) were electronically compensated (80–85%) and current traces were filtered at 3 kHz, acquired and digitized at 0.5 kHz, and stored on a personal computer system. Control of drug application, data acquisition and data analysis was achieved using an ITC-16 acquisition board (Instrutech Corporation) and the TIDA for Windows software (HEKA Elektronik Lombrecht/Pfolz, Germany).

RESULTS

Using a procedure allowing the purification of neurogenic PSA-NCAM$^+$ progenitors from the newborn rat striatum [6], we isolated and cultured neurogenic PSA-NCAM$^+$ progenitors in suspension for 3 days (3 DIV) in EGF-containing medium where they proliferate and form spheres. As described previously [6], these spheres are mainly composed by neuronal precursors co-expressing PSA-NCAM (92.8 $\pm$ 3.2% of the total cells, $n = 6$ experiments) and βIII-tubulin (Tuj1$^+$; 52.3 $\pm$ 7.8% of the total cells, $n = 6$ experiments), with all Tuj1$^+$ cells expressing PSA-NCAM (Fig. 1). Markers of oligodendrocytes (O4) or astrocytes (glial fibrillary acidic protein, GFAP) were almost absent from the spheres (O4, 4.8 $\pm$ 1.0% of the total cells, $n = 8$ experiments; GFAP, 8.7 $\pm$ 1.3% of the total cells, $n = 4$ experiments). The cells proliferate since 18.5 $\pm$ 8.3% ($n = 4$ experiments) of striatal PSA-NCAM$^+$ cells within 3 DIV spheres incorporate BrdU (18 h treatment).

Given that previous works reported the expression of functional GlyRs before synaptogenesis in early progenitors from the newborn rat brain [11–13], we sought to investigate the presence of GlyRs in neurogenic PSA-NCAM$^+$ precursors from the postnatal rat striatum. The expression of GlyR proteins was firstly analyzed by immunocytochemistry in 3 DIV PSA-NCAM$^+$ spheres. For that purpose, we used polyclonal antibodies directed against the α_1 and α_2 subunits of GlyR. As illustrated in Fig. 2a–c staining (highest magnification in Fig. 2c) for GlyR proteins was found in 62.1 $\pm$ 2.6% of the total PSA-NCAM$^+$ cells ($n = 3$; Fig. 3a), probably corresponding to the Tuj1$^+$ PSA-NCAM$^+$ cell subpopulation that composes the spheres. Indeed, we observed that all Tuj1$^+$ cells co-expressed GlyRs (Fig. 2d–f). Finally, simultaneous immunostainings of striatal tissue sections from newborn rat with anti-PSA-NCAM (Fig. 2g) and anti-GlyR (Fig. 2h) antibodies also revealed a co-expression of PSA-NCAM and GlyRs *in situ* (Fig. 2i).

We next performed an electrophysiological characterization of GlyRs in PSA-NCAM$^+$ cells cultured in proliferative spheres by using the patch-clamp technique in the whole-cell configuration. The mean membrane potential of cells located at the periphery of 3-DIV spheres and recorded in current-clamp was -58.3 ± 20.8 mV ($n = 52$ cells). In voltage-clamp mode and at a holding potential of -70 mV, bath application of 1 mM glycine, a concentration that saturates

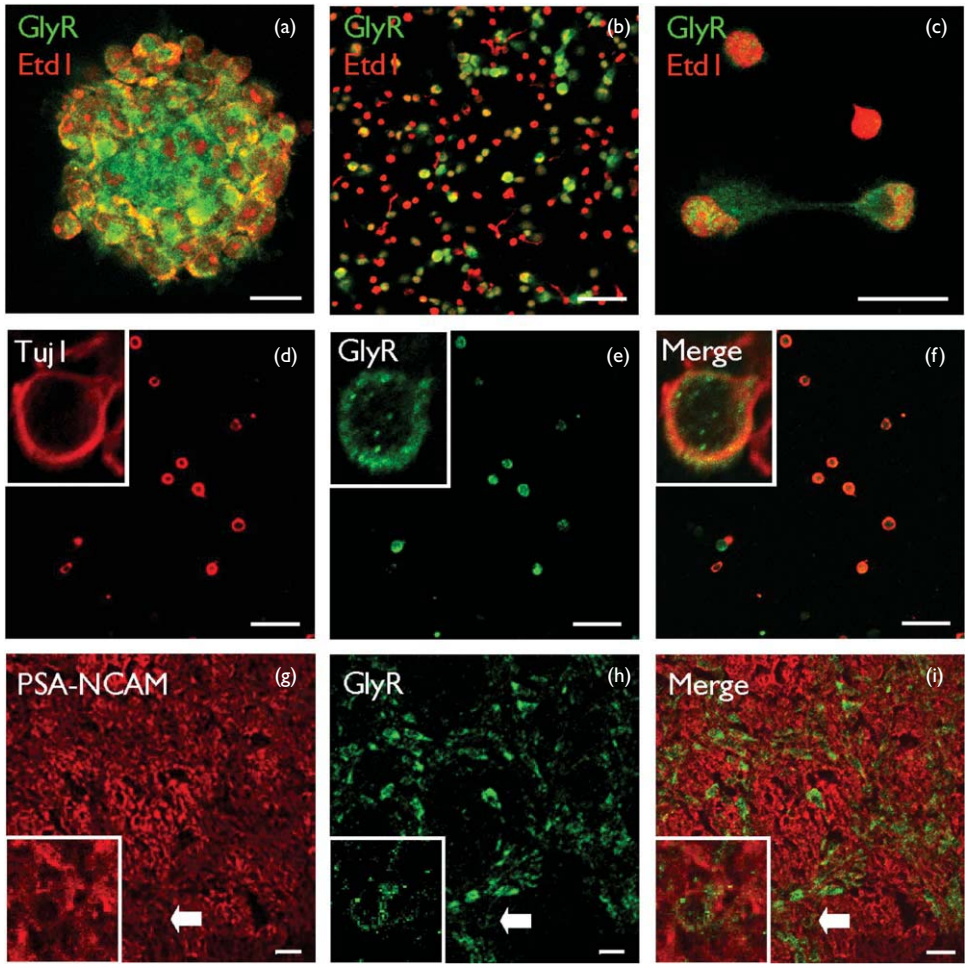

Fig. 2. GlyRs are expressed by PSA-NCAM$^+$ progenitors from early postnatal striatum. (**a**–**c**) Immunodetection of GlyRs in 3-DIV PSA-NCAM$^+$ progenitors. Confocal images of 3-DIV striatal cells showing GlyR immunostaining (green) and cell nuclei (EtdI, red) in an intact sphere (a) or after acute dissociation (b). (c) Higher magnification view showing the labelling of GlyRs (green) in acutely dissociated cells. (**d**–**f**) Immunodetection of GlyRs in TujI$^+$ cells dissociated from 3-DIV PSA-NCAM$^+$ spheres showing the co-expression of both TujI (d) and GlyR (e) in a majority of cells (see (f) for co-expression). (**g**–**i**) Immunostaining of striatal slices from newborn rat displaying immunoreactive cells for both PSA-NCAM (g) and GlyR (h). Bars = 25 μm for (b,d,e,f); 10 μm (a,c,g,h,i).

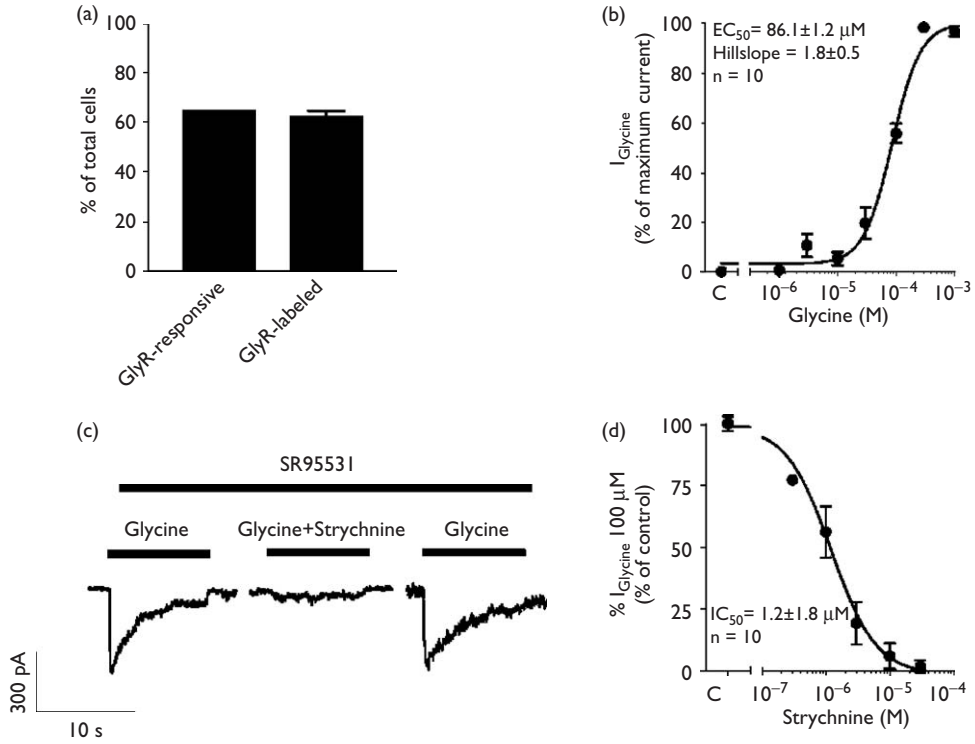

Fig. 3. GlyR activation triggers strychnine-sensitive inward currents in striatal PSA-NCAM$^+$ progenitor cells. (**a**) Histogram representing respectively, the percentage of cells responding to 1 mM glycine, and the percentage of total cells immunostained for GlyR in the population of 3-DIV PSA-NCAM$^+$ cells. All recordings were performed in the continuous presence of 100 µM SR-95531 (a specific antagonist of $GABA_AR$) to avoid the cross-activation of $GABA_AR$ by glycine. (**b**) Concentration–response curve obtained from glycine-responsive PSA-NCAM$^+$ progenitors. (**c**) Recording from a PSA-NCAM$^+$ cell illustrating an inward current elicited by 100 µM glycine (a concentration close to its EC_{50}, see (b)) and reversibly blocked by 10 µM strychnine (an antagonist of the GlyR). (**d**) In 3-DIV striatal PSA-NCAM$^+$ cells, glycine-induced currents were completely, reversibly and dose dependently inhibited by strychnine.

GlyRs (see Fig. 3b), elicited inward currents in 64.6% of the cells (Fig. 3a). Glycine-induced current amplitudes distribution ranged from 25 pA to 1042 pA, with a mean maximum amplitude of 231.3 ± 48.9 pA ($n = 31$ cells). In glycine-responsive PSA-NCAM$^+$ progenitors, the EC_{50} value calculated from the sigmoidal concentration–response curve was 86.1 ± 1.2 µM with a Hill coefficient (n_H) of 1.8 ± 0.5 ($n = 10$ cells, Fig. 3b). Confirming that glycine-elicited currents were specifically due to the activation of GlyRs, co-application of strychnine, a GlyR antagonist, completely and reversibly inhibited glycine responses (Fig. 3c). The effect of strychnine was concentration dependent with an IC_{50} value of 1.2 ± 1.8 µM ($n = 10$ cells; Fig. 3d). All the data were obtained in the presence of 10 µM SR-95531, precluding any cross-activation of $GABA_A$ receptors by glycine.

DISCUSSION

During CNS maturation, PSA-NCAM$^+$ progenitor cells differentiate into neurons [17,18] and glial cells [4] for which the spatial and temporal generation is orchestrated by a combination of intrinsic and extrinsic molecules, probably including neurotransmitters. It is now well established that specific neurotransmitters and their corresponding receptors are expressed by progenitor cells during CNS development and may play a role as growth regulatory signals [9]. Along this line, we had already demonstrated that some nestin$^+$ neural stem/progenitors cells derived from the newborn rat striatum express functional GlyRs [11]. Here we clearly demonstrate by combining immunocytochemical and electrophysiological techniques that functional GlyRs are also expressed at a later developmental stage, i.e. in neurogenic Tuj1$^+$ PSA-NCAM$^+$ progenitors isolated from the newborn rat striatum and cultured 3 DIV on a non-adhesive substrate as floating spheres. These *in vitro* data were corroborated by the demonstration that GlyRs are also expressed *in situ* in PSA-NCAM$^+$ cells of the newborn rat striatum.

The GlyRs of neurogenic Tuj1$^+$ PSA-NCAM$^+$ progenitors show intermediate elecrophysiological characteristics between those of the GlyRs expressed by nestin$^+$ neural stem/progenitors derived from the postnatal rat striatum [11] and by mature striatal neurons [21]. Glycine displayed a mean effective concentration (EC_{50}) of 86.1 ± 1.2 µM in neurogenic Tuj1$^+$ PSA-NCAM$^+$ progenitors that is intermediate between 68.2 ± 1.7 µM in nestin$^+$ neural stem/progenitors [11] and 106 ± 4 to 125 ± 7 µM in mature striatal neurons [20,21]. Differences in Hill coefficient for glycine have also been observed between neurogenic Tuj1$^+$ PSA-NCAM$^+$ progenitors ($n_H = 1.8$), nestin$^+$ neural stem/progenitors ($n_H = 1$) [11] and mature striatal neurons ($n_H = 1.7$–2.1) [20,21]. Moreover, the mean effective concentration (IC_{50}) of the antagonist strychnine to block glycine currents differed significantly between Tuj1$^+$ PSA-NCAM$^+$ progenitors (1.2 ± 1.8 µM), nestin$^+$ neural stem/progenitors (192.7 ± 1.2 nM) [11], and mature striatal neurons (70 ± 5 nM) [20]. As described for cortical neuroblasts [13], this could reflect the incorporation, at the Tuj1$^+$

PSA-NCAM$^+$ maturation stage, of GlyR α2*, an α2 isoform known for its weak sensitivity to strychnine [24]. Previous studies have indicated that neuronal development can induce several changes in the properties of GlyRs, e.g. the switch from an α2 homopentameric structure to α1/β heteromeres in spinal cord motoneurons [25]. Our observation of graded differences in terms of EC_{50}, n_H, and strychnine sensitivity with neuronal maturation suggests that a change in GlyR stoichiometry could also occur within the striatum.

In the adult striatum, GlyRs are expressed in medium spiny projection neurons and in cholinergic aspiny interneurons [19–21], where they do not seem to participate in inhibitory neurotransmission [19]. Our findings could suggest that GlyR-expressing Tuj1$^+$ PSA-NCAM$^+$ cells are direct precursors of these two subpopulations of striatal neurons [21]. Moreover, those GlyRs expressed before synaptogenesis could regulate some processes for the maturation of striatal Tuj1$^+$ PSA-NCAM$^+$ progenitors along the restriction pathway leading to functional striatal neurons. This hypothesis is consistent with previous studies that have indicated a role of GlyRs in the early development of cortical neuroblasts [13] and of progenitors of cerebellar Purkinje neurons [22], and in the neuronal maturation [23].

CONCLUSION

It is now well established that neurotransmitters and their corresponding ligand-gated ion channel receptors exert numerous roles during CNS development, prior to the emergence of their role in neurotransmission [9]. In the present study we demonstrate that functional GlyRs are expressed in neurogenic Tuj1$^+$ PSA-NCAM$^+$ progenitors from the postnatal rat striatum. The roles of those GlyRs remain to be elucidated, and our future studies will be dedicated to untangle their function(s) in the regulation of proliferation, and/or differentiation of neurogenic Tuj1$^+$ PSA-NCAM$^+$ progenitors within the developing striatum.

REFERENCES

1. Doetsch F, Caille I, Lim DA, Garcia-Verdugo JM and Alvarez-Buylla A. Subventricular zone astrocytes are neural stem cells in the adult mammalian brain. *Cell* **97**, 703–716 (1999).
2. Bruses JL and Rutishauser U. Roles, regulation, and mechanism of polysialic acid function during neural development. *Biochimie* **83**, 635–643 (2001).
3. Nguyen L, Rigo JM, Malgrange B, Moonen G and Belachew S. Untangling the functional potential of PSA-NCAM-expressing cells in CNS development and brain repair strategies. *Curr Med Chem* (2003). In press.
4. Ben Hur T, Rogister B, Murray K, Rougon G and Dubois-Dalcq M. Growth and fate of PSA-NCAM$^+$ precursors of the postnatal brain. *J Neurosci* **18**, 5777–5788 (1998).
5. Mayer-Proschel M, Kalyani AJ, Mujtaba T and Rao MS. Isolation of lineage-restricted neuronal precursors from multipotent neuroepithelial stem cells. *Neuron* **19**, 773–785 (1997).
6. Nguyen L, Malgrange B, Breuskin I, Bettendorff L, Moonen G, Belachew S *et al.* Autocrine/paracrine activation of the $GABA_A$ receptor inhibits the proliferation of neurogenic polysialylated neural cell adhesion molecule-positive (PSA-NCAM$^+$) precursor cells from postnatal striatum. *J Neurosci* **23**, 3278–3294 (2003).
7. Vitry S, Avellana-Adalid V, Lachapelle F and Evercooren AB. Migration and multipotentiality of PSA-NCAM$^+$ neural precursors transplanted in the developing brain. *Mol Cell Neurosci* **17**, 983–1000 (2001).
8. Keirstead HS, Ben Hur T, Rogister B, O'Leary MT, Dubois-Dalcq M and Blakemore WF. Polysialylated neural cell adhesion molecule-positive CNS precursors generate both oligodendrocytes and Schwann cells to remyelinate the CNS after transplantation. *J Neurosci* **19**, 7529–7536 (1999).
9. Nguyen L, Rigo JM, Rocher V, Belachew S, Malgrange B, Rogister B *et al.* Neurotransmitters as early signals for central nervous system development. *Cell Tissue Res* **305**, 187–202 (2001).
10. Legendre P. The glycinergic inhibitory synapse. *Cell Mol Life Sci* **58**, 760–793 (2001).
11. Nguyen L, Malgrange B, Belachew S, Rogister B, Rocher V, Moonen G *et al.* Functional glycine receptors are expressed by postnatal nestin positive neural stem/progenitor cell. *Eur J Neurosci* **15**, 1299–1305 (2002).
12. Belachew S, Rogister B, Rigo JM, Malgrange B, Mazy-Servais C, Xhauflaire G *et al.* Cultured oligodendrocyte progenitors derived from cerebral cortex express a glycine receptor which is pharmacologically distinct from the neuronal isoform. *Eur J Neurosci* **10**, 3556–3564 (1998).
13. Flint AC, Liu X and Kriegstein AR. Nonsynaptic glycine receptor activation during early neocortical development. *Neuron* **20**, 43–53 (1998).
14. Maric D, Maric I, Ma W, Lahojuji F, Somogyi R, Wen X *et al.* Anatomical gradients in proliferation and differentiation of embryonic rat CNS accessed by buoyant density fractionation: alpha 3, beta 3 and gamma 2 GABAA receptor subunit co-expression by post-mitotic neocortical neurons correlates directly with cell buoyancy. *Eur J Neurosci* **9**, 507–522 (1997).
15. Yuan X, Chittajallu R, Belachew S, Anderson S, McBain CJ and Gallo V. Expression of the green fluorescent protein in the oligodendrocyte lineage: a transgenic mouse for developmental and physiological studies. *J Neurosci Res* **70**, 529–545 (2002).
16. Hamill OP, Marty A, Neher E, Sakmann B and Sigworth FJ. Improved patch-clamp techniques for high-resolution current recording from cells and cell-free membrane patches. *Pflugers Arch* **391**, 85–100 (1981).
17. Doetsch F, Garcia-Verdugo JM and Alvarez-Buylla A. Cellular composition and three-dimensional organization of the subventricular germinal zone in the adult mammalian brain. *J Neurosci* **17**, 5046–5061 (1997).
18. Seki T and Arai Y. Highly polysialylated neural cell adhesion molecule (NCAM-H) is expressed by newly generated granule cells in the dentate gyrus of the adult rat. *J Neurosci* **13**, 2351–2358 (1993).
19. Darstein M, Landwehrmeyer GB, Kling C, Becker CM and Feuerstein TJ. Strychnine-sensitive glycine receptors in rat caudatoputamen are expressed by cholinergic interneurons. *Neuroscience* **96**, 33–39 (2000).
20. Sergeeva OA and Haas HL. Expression and function of glycine receptors in striatal cholinergic interneurons from rat and mouse. *Neuroscience* **104**, 1043–1055 (2002).
21. Sergeeva OA. Comparison of glycine- and GABA-evoked currents in two types of neurons isolated from the rat striatum. *Neurosci Lett* **243**, 9–12 (1998).
22. Furuya S, Tabata T, Mitoma J, Yamada K, Yamasaki M, Makino A *et al.* L-Serine and glycine serve as major astroglia-derived trophic factors for cerebellar Purkinje neurons. *Proc Natl Acad Sci USA* **97**, 11528–11533 (2000).
23. Tapia JC, Cardenas AM, Nualart F, Mentis GZ, Navarrete R and Aguayo LG. Neurite outgrowth in developing mouse spinal cord neurons is modulated by glycine receptors. *Neuroreport* **11**, 3007–3010 (2000).
24. Kuhse J, Schmieden V and Betz H. A single amino-acid exchange alters the pharmacology of neonatal rat glycine receptor subunit. *Neuron* **5**, 867–873 (1990).
25. Tapia JC and Aguayo LG. Changes in the properties of developing glycine receptors in cultured mouse spinal neurons. *Synapse* **28**, 185–194 (1998).

Acknowledgements: We thank P. Ernst-Gengoux and A. Brose for their technical support and expertise. B. Malgrange and S. Belachew are research associates of the FNRS (Belgium). This work was supported by the Fonds pour la Formation à la Recherche dans l'Industrie et dans l'Agriculture (FRIA), the Fonds National de la Recherche Scientifique (FNRS), the Fondation Médicale Reine Elisabeth (FMRE), the Fondation Charcot and the Ligue Belge de la Sclérose en Plaques.

7.13 Publication #13: Nguyen, L., Malgrange, B., Belachew, S., Rogister, B., Rocher, V., Moonen, G., and Rigo J.-M. (2002). Functional glycine receptors are expressed by postnatal nestin-positive neural stem/progenitor cells. *Eur. J. Neurosci.* 15:1299-1305.

European Journal of Neuroscience, Vol. 15, pp. 1299–1305, 2002

Functional glycine receptors are expressed by postnatal nestin-positive neural stem/progenitor cells

Laurent Nguyen,[1] Brigitte Malgrange,[1] Shibeshih Belachew,[1,2] Bernard Rogister,[1,2] Véronique Rocher,[1] Gustave Moonen,[1,2] and Jean-Michel Rigo[1]
[1]Center for Cellular and Molecular Neurobiology, University of Liège, 17 Place Delcour, B-4020 Liège, Belgium
[2]Department of Neurology, University of Liège, C.H.U. (B35) Sart Tilman, B-4000 Liège, Belgium

Keywords: glycine receptor, immunocytochemistry, neural stem/precursor cells, rat striatum, RT-PCR, whole-cell patch-clamp

Abstract

Multipotent neural stem and progenitor cells (NS/PCs) are well-established cell subpopulations occurring in the developing, and also in the mature mammalian nervous systems. Trophic and transcription factors are currently the main signals known to influence the development and the commitment of NS/PCs and their progeny. However, recent studies suggest that neurotransmitters could also contribute to neural development. In that respect, rodent-cultured embryonic NS/PCs have been reported to express functional neurotransmitter receptors. No similar investigation has, however, been made in postnatal and/or in adult rodent brain stem cells. In this study, using RT-PCR and immunocytochemical methods, we show that α_1-, α_2- and β-subunit mRNAs and α-subunit proteins of the glycine ionotropic receptor are expressed by 80.5 ± 0.9% of postnatal rat striatum-derived, nestin-positive cells within cultured neurospheres. Whole-cell patch-clamp experiments further demonstrated that glycine triggers in 33.5% of these cells currents that can be reversibly blocked by strychnine and picrotoxin. This demonstrates that NS/PCs express functional glycine receptors, the consequence(s) of their activation remaining unknown.

Introduction

Stem cell research is nowadays a widely addressed question, especially in the nervous system, due to the promise it has shown for repairing the damaged brain. Despite this growing interest, replacement strategies must cope with the fact that the transplantation of neural stem/progenitor cells (NS/PCs) and their differentiation into the appropriate neuronal and/or glial phenotype are strongly influenced by extracellular and intracellular regulatory signals (Edlund & Jessell, 1999). Hence much effort has been devoted to characterize those intrinsic and extrinsic factors that regulate NS/PC proliferation and differentiation both *in vitro* and *in vivo*.

Among these extracellular molecules, neurotransmitters — which belong to the chemical microenvironment of neural cells — are worthy candidates. Indeed, it has been known for many years that neurotransmitter receptors are present in the developing brain well before synaptogenesis occurs, suggesting that they could mediate signalling unrelated to classical neurotransmission (Lipton *et al*., 1988; Lipton & Kater, 1989; Lauder, 1993; LoTurco *et al*., 1995; Gallo *et al*., 1996; Antonopoulos *et al*., 1997; Gould & Cameron, 1997; Ikeda *et al*., 1997; Flint *et al*., 1998; Lauder *et al*., 1998; Ma *et al*., 1998, 2000; Fiszman *et al*., 1999; Gould, 1999; Haydar *et al*., 2000; Maric *et al*., 2000; Atluri *et al*., 2001). Accordingly, and more recently, several neurotransmitter receptors have also been found on neural stem cells and various progenitors including G-protein-coupled (Ma *et al*., 2000) but also ionotropic receptors (reviewed in Cameron *et al*., 1998; Nguyen *et al*., 2001). In that respect, much effort has been devoted to study the implication of glutamate-, acetylcholine-, serotonin-, γ-aminobutyric acid- (GABA-) and glycine-gated channels in the control of proliferation and differentiation of neural stem cells and committed progenitors (reviewed in Cameron *et al*., 1998; Nguyen *et al*., 2001). Here, we have searched for the presence of ligand-gated channels in NS/PCs within neurospheres derived from postnatal rat striata. In a preliminary report published in abstract form (Nguyen *et al*., 2000), we observed currents elicited by glutamate, GABA, glycine, and to a lesser extent, acetylcholine and serotonin. In this work, by means of molecular, immunocytochemical and electrophysiological techniques, we provide evidence for the expression of strychnine-sensitive glycine receptors (GlyRs) by *in vitro*-cultured, nestin-expressing cells derived from postnatal rat striata. We show that GlyRs are not only present but also functional before synaptogenesis in early progenitors, suggesting a possible developmental role for these receptors.

Correspondence: L. Nguyen, as above.
E-mail: laurent.nguyen@student.ulg.ac.be

Received 29 August 2001, revised 26 February 2002, accepted 4 March 2002

Materials and methods

Cell culture

NS/PCs were prepared using the procedure described by Ben-Hur *et al*. (1998). Newborn Wistar rats (0- to 3-day-old rat pups) obtained from our breeding rodent facility were killed following National Institute of Health animal welfare guidelines. Newborn Wistar rats (0- to 3-day-old rat pups) obtained from our breeding rodent facility were anaesthetized with CO_2 and decapitated. Striata (including the subventricular zone) were excised and collected in phosphate-buffered saline (PBS) supplemented with 4.5 g/L glucose. Isolated striata were then gently triturated in

PBS-HEPES (25 mM, pH 7.4) by passing through a fire-polished Pasteur pipette. The resulting cell suspension was filtered with a 15-μM nylon mesh. Dissociated cells were resuspended in serum-free medium containing: Dulbecco's modified Eagle's medium and F12 (1 : 1 v/v; Life Technologies, Belgium), the N2 supplement (25 μg/mL bovine insulin, 100 μg/mL transferrin, 20 nM progesterone, 60 μM putrescine, 30 nM sodium selenite), B27 (1% v/v, Gibco, Belgium) and 20 ng/mL epidermal growth factor (PeproTech, Rocky Hill, NJ, USA). Five millilitres of the cell suspension at a cell concentration of 10^5 cells/mL were next transferred into nonadherent T25 culture flasks (Life Technologies). Half of the medium was renewed every 4 days. This technique allows dissociated NS/PCs to proliferate in suspension as spheroid aggregates called neurospheres. After 4–10 days *in vitro*, growing neurospheres were attached either during 1 h on Cell-Tak-coated (Becton Dickinson, Erembodegem, Belgium) Cellocate microgrid coverslips (Eppendorf, Germany) or for 1 week *in vitro* in the same culture medium but without epidermal growth factor to allow cell differentiation.

Immunocytochemistry

The cultures were fixed with 4% (v/v) paraformaldehyde for 10 min at room temperature and permeabilized thereafter in 1% Triton X100 (v/v) during 15 min when subsequent immunostainings were directed towards cytoplasmic epitopes. Nonspecific binding was blocked by a 30-min treatment in a PBS solution containing nonfat dry milk (15 mg/mL). Cells were then incubated overnight at 4 °C with primary antibodies, i.e. a rabbit anti-nestin antibody (1 : 400, a generous gift from Professor J. Eriksson, University of Turku; Finland), a mouse anti-βIII tubulin antibody (1 : 1500) (clone Tuj1; Babco, Richmond, CA, USA), a mouse monoclonal (IgM) O4 1 : 5 (Boehringer, Mannheim, Germany), a rabbit anti-glial-fibrillary acidic protein (GFAP) antibody (1 : 1500) (Dako, Prosan, Belgium) or a mouse IgG1 anti-GlyR α-subunits antibody at 1 : 20 (clone mAb 4a, ConneX, Martinsried, Germany). Secondary antibodies, applied for 45 min at room temperature were: Cy5 or tetramethylrhodamine B isothiocyanate (TRITC) -conjugated antirabbit Ig antibody (1 : 500), TRITC or fluorescein isothiocyanate (FITC) -conjugated antimouse IgG (1 : 500) and FITC-conjugated antimouse IgM (all purchased from Jackson ImmunoResearch Laboratory, West Grove, PA, USA). After three rinses in PBS, the preparations were mounted in Fluoprep (Biomerieux, France). Images were acquired using a laser scanning confocal microscope (MRC1024; Bio-RAD, Herts, UK).

For cell counting, neurospheres were mechanically dissociated, counterstained with the nuclear dye ethidium homodimer-1 (Molecular Probes, Eugene, OR, USA) and 10 microscopic fields (± 50 cells per field) (Axiovert 135 fluorescence microscope, 40 × objective, Zeiss) were counted for each coverslip (n = 3).

Bromodeoxyuridine incorporation assay

To label cells in S phase *in vitro*, bromodeoxyuridine (BrdU, 10 μM, Sigma, St Louis, MO, USA), which is incorporated into replicating DNA, was added to the cultures for 18 h prior to staining. The nestin labelling was performed as described earlier. Coverslips were then postfixed for another 10 min incubation in 4% (v/v) paraformalde-

TABLE 1. Primers (upstream, up; downstream, lo) were synthesized by Eurogentec (Belgium)*

cDNA	Primer	Corresponding nucleotides	Size of product (base pairs)
GlyR α1	Up 5′-GTC CCA ACA ACA ACA ACA CC-3′ Lo 5′-TCC CAG AGC CTT CAC TTG TT-3′	1335–1595	211
GlyR α2	Up 5′-CTA CAC CTG CCA ACC CAC-3′ Lo 5′ CTT GTG GAC ATC TTC ATG CC-3′	1722–1904	182
GlyR β	Up 5′-GAA GAA CAC TGT GAA CGG CA-3′ Lo 5′-GGC TTC TTG TTC TTT GCC TG-3′	1155–1382	228

*Eurogentec (Liège, Belgium).

FIG. 1. Glycine receptors are expressed by postnatal rat nestin-positive multipotent NS/PCs in neurosphere cultures. (A) Confocal microscopy optical section through 1-week-old neurosphere cultured in the presence of BrdU for 18 h. Neurospheres were stained with rabbit antibodies directed against nestin and secondarily detected by TRITC-coupled antibodies (red) and with mouse monoclonal anti-BrdU antibodies directly coupled to FITC. These neurospheres contain 21.8 ± 3.9% (mean ± SEM, n = 4 different experiments) of BrdU-incorporating nestin-positive cells (counting was done using cells dissociated from neurospheres). Scale bar = 25 μM. (B) After 1 week of plating, NS/PCs can differentiate into the three main central nervous system lineages: neurons (red, mouse monoclonal anti-βIII tubulin antibodies secondarily detected by TRITC-coupled antibodies), oligodendrocytes (green, mouse monoclonal anti-O4 antibodies secondarily detected by FITC-coupled antibodies) and astrocytes (blue, rabbit polyclonal anti-GFAP antibodies detected by Cy5-coupled antibodies). Scale bar = 25 μM. (C) RT-PCR amplification of α_1-, α_2- and β-subunit transcripts using RNA extracted from postnatal rat neurospheres. Bands of a size corresponding to α_1-amplicon (211 pb), α_2-amplicon (182 pb) and β-amplicon (228 pb) were detected in samples (+, with RT; –, without RT). Left and right margins: migration of standard DNA markers with size indicated in base pairs. (D) Immunodetection of GlyRs using confocal microscopy, nestin is detected by TRITC-coupled antibodies (red) and GlyR α-subunits by FITC-coupled antibodies (green). Scale bar, 25 μM.

FIG. 2. Glycine triggers membrane currents in postnatal rat nestin-positive stem/progenitor cells in neurosphere cultures. (A) Brightfield picture showing the localization of the recorded cell inside the neurosphere. (B) The corresponding fluorescent field showing the lucifer yellow-injected cell during the recording. (C) Confocal microscopy optical section of the same neurosphere as in A and B stained with anti-nestin antibodies secondarily detected by TRITC-coupled antibodies (red). The recorded cell (arrow) filled with lucifer appeared in green but also displayed yellow areas underlying its nestin-positive status (scale bar = 25 μM). (D) Histogram showing, respectively, the total percentage of nestin-positive cells (93.4 ± 2.6% (mean ± SEM, n = 3 different experiments) and the percentage of glycine-responsive, nestin-positive cells (33.5%, n = 85).

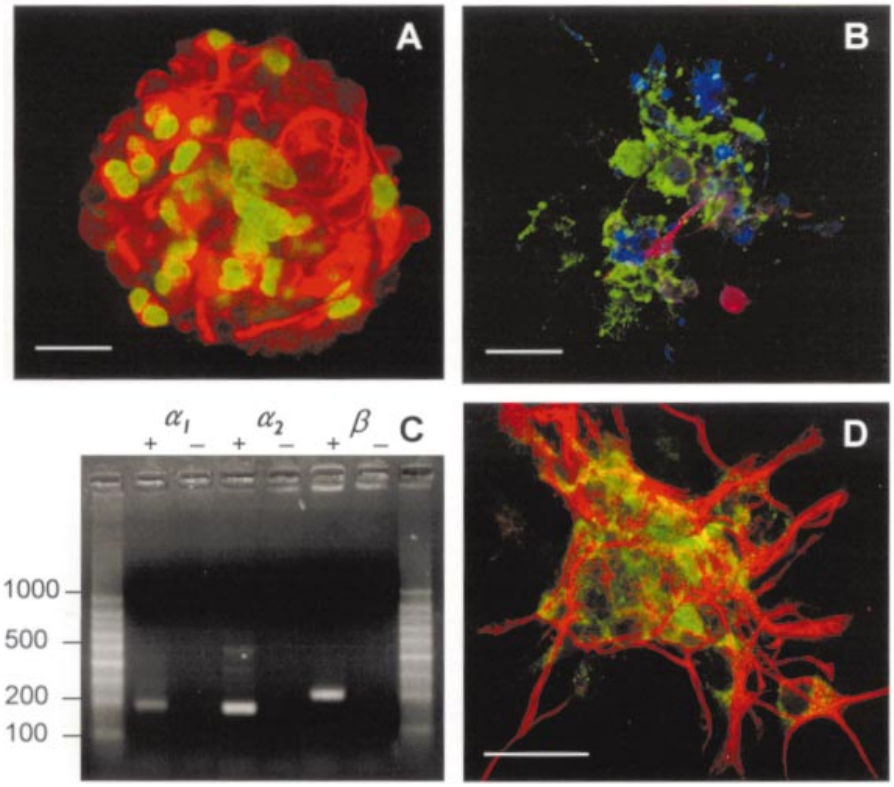

FIG. 1.

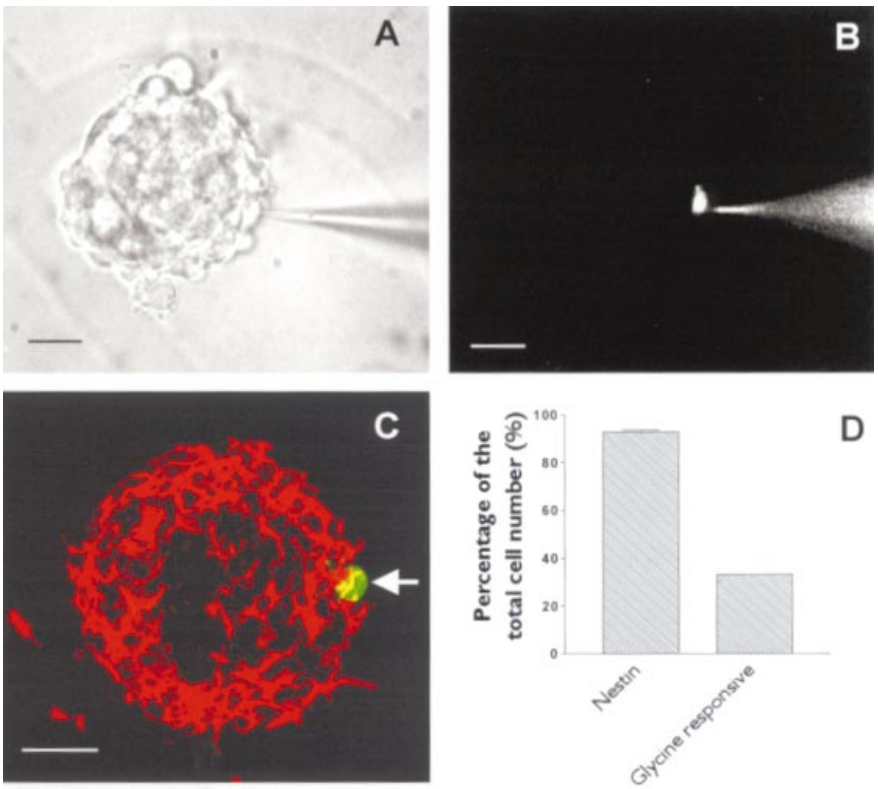

FIG. 2.

hyde, incubated in NaOH 0.07 M for 10 min, postfixed for another 10 min, permeabilized in Triton X100 (0.1%) and finally incubated for 45 min with an anti-BrdU FITC-conjugated antibody (1 : 3, Becton Dickinson).

Electrophysiology

For patch-clamp recordings, cellocate microgrid coverslips containing 1–3 h of adhesive neurospheres were transferred to the stage of a Zeiss interferential contrast microscope equipped with fluorescence. They were maintained at room temperature (20 °C) in a recording chamber which was perfused continuously with a physiological saline solution containing (in mM): NaCl, 116; D-glucose, 11.1; KCl, 5.4; $CaCl_2.2H_2O$, 1.8; $MgCl_2.6H_2O$, 2.0; HEPES, 10.0; pH 7.2. Glycine was purchased from UCB (Brussels, Belgium), whereas strychnine, picrotoxin and SR 95531 were obtained from Sigma. All the drugs were applied by a rapid microperfusion system (SPS-8; List Medical). Borosilicate recording electrodes (15–20 MΩ) were made using a Flaming-Brown microelectrode puller (P97; Sutter Instrument Co, Novato, CA, USA). Micropipettes were filled with an intracellular-like solution containing (in mM): KCl, 130.0; $CaCl_2.2H_2O$, 1.0; D-glucose, 11.1; EGTA, 10.0; Na_2-ATP, 2.5; Mg-ATP, 2.5; HEPES, 10.0, pH 7.4. For low chloride solution, KCl was replaced by an equimolar amount of potassium gluconate. For some experiments, lucifer yellow CH potassium salt was added at 1 mg/mL (Molecular Probes). Electrophysiological recordings were performed with a patch-clamp amplifier (RK400; Bio-Logic, Claix, France) using the whole-cell recording configuration of the patch-clamp technique (Hamill *et al.*, 1981). Current–voltage relationships for glycine-evoked currents were obtained using a series of voltage steps (ranging from –140 to +130 mV) during the agonist application. To allow the immunocytochemical characterization of the recorded cells inside neurospheres, they were injected with lucifer yellow (1 μg/mL of lucifer yellow solution added to the pipette) during voltage-clamp recordings. Photographs of recorded cells were taken on Kodak T-Max CN 400 films with a Minolta 9000 camera. Series resistances (10–20 MΩ) were electronically compensated and current traces were digitized and stored on a PC. Control of drug application, data acquisition and data analysis were achieved using an ITC-16 acquisition board (Instrutech Corporation, Great Neck, NY, USA) and the TIDA for Windows software (HEKA Elektronik Lombrecht/Pfolz, Germany).

RT-PCR

Total RNAs from spinal cord of Wistar rat embryos (after 14 days of gestation) and adult rats, and from striata-derived neurospheres from newborn rats were extracted and purified using a RNeasy kit (Qiagen, Westburg, The Netherlands). As determined by 260/280 OD readings, 1 μg of total RNA was reverse-transcribed using primers with oligodT and 200 U of reverse transcriptase (Superscript, Life Technologies, Belgium). A 2-μL aliquot of the resulting cDNA reaction, used as template, was added to a 50-μL PCR reaction mixture containing: 330 ng of primers (see Table 1), 0.2 mM of each dNTP, 1.5 mM of $MgCl_2$ and 5 U of Taq polymerase (Promega, The Netherlands). The PCR program was achieved in a PTC 200 instrument (MJ Research, Waltham, MA, USA). After a 3-min denaturation step at 94 °C, amplifications were carried out for 33 cycles (94 °C for 30 s, 50 °C for 15 s and 72 °C for 30 s), followed by a final extension at 72 °C for 9 min. Ten microlitres of the PCR reaction was analysed in a 2% agarose gel in tris-acetic acid-EDTA (TAE) buffer.

Results

Glycine receptors are expressed by postnatal rat nestin-positive stem/progenitor cells in neurosphere cultures

In our culture conditions, 93.4 ± 2.6% (mean ± SEM, $n = 3$ different experiments) of the cells in growing neurospheres expressed nestin, a cytoskeletal protein found mainly in stem and progenitor cells of the nervous system (Lendahl *et al.*, 1990), as assessed by immunofluorescence staining using rabbit anti-nestin antibodies (red cells in Fig. 1A). We operationally defined these nestin-positive cells as multipotent NS/PCs because (i) they seemed able to self-renew: 21.8 ± 3.9% (mean ± SEM, $n = 4$ different experiments) of the nestin-expressing cells were also stained with anti-BrdU antibodies after an 18-h BrdU treatment; see Fig. 1A, and (ii) they were able to give rise, after 1 week of plating on an adhesive substratum, to the three main central nervous system lineages: neurons, evidenced as βIII tubulin-expressing cells, oligodendrocytes (O4-positive cells) and astrocytes (GFAP-positive cells) (see Fig. 1B).

Total RNAs extracted from newborn rats' neurosphere cultures were subjected to RT-PCR using specific primers aimed at detecting the presence of α_1-, α_2- and β-subunit transcripts of the glycine receptor (GlyR). Such a procedure was repeated three times, each time yielding bands consistent with the amplicon expected sizes for: α_1 (211 pb), α_2 (182 pb) and β (228 pb), an example of which is given in Fig. 1C. RNAs extracted from embryonic and adult rat spinal cord were used as positive controls (data not shown).

The monoclonal antibody mAb 4a, which is directed against an epitope shared by all GlyRα-subunits (Schroder *et al.*, 1991), was used to detect the presence of GlyR proteins within cultured NS/PCs. Figure 1D shows that most of nestin-positive cells, actually 80.5 ± 0.9% (mean ± SEM, $n = 2$ different experiments), were also stained with the mAb 4a antibody.

Glycine triggers membrane currents in postnatal rat nestin-positive stem/progenitor cells in neurosphere cultures

We next addressed the question of whether GlyRs expressed by NS/PCs were functional. Therefore, electrophysiological recordings of cells within neurospheres were performed using the patch-clamp technique. To correlate glycine responsiveness with nestin expression, pipettes were loaded with lucifer yellow, which diffused into the recorded cells thanks to the whole-cell configuration that was used (see Fig. 2A and B). At the end of the experiment, cells were fixed and processed for nestin immunostaining (Fig. 2C). In what follows, only recordings obtained from nestin-positive cells were taken into account in order to restrict the data to the operationally defined multipotent NS/PCs. In our recording conditions and in current-clamp mode, cells located at the accessible periphery of adherent neurospheres had a mean membrane potential of –52.8 ± 2.0 mV (mean ± SEM, $n = 67$). Action potentials were never observed, neither spontaneous, nor elicited by depolarizing currents. All data that follow were acquired in the presence of 10 μM SR 95531 to avoid cross-activation of type A γ-aminobutyric acid ($GABA_A$) receptors. In voltage-clamp mode and at a holding potential of –70 mV, bath application of 1 mM glycine, a concentration that likely saturates glycine-gated channels, elicited inward currents characterized by a peak that rapidly declined to a plateau during glycine application (see Fig. 3A, C andD). Such currents were observed in 33.5% of the cells ($n = 85$, see Fig. 2D).

Glycine-elicited currents recorded in multipotent NS/PCs are mediated by strychnine-sensitive ionotropic glycine receptors

In whole-cell patch- and voltage-clamped NS/PCs, peak current amplitudes induced by glycine averaged 172.8 ± 37.9 pA ($n = 38$). The concentration–response curve obtained from glycine-responsive NS/PCs was best fitted with a Hill equation and yielded an EC_{50} of 68.2 ± 1.7 μM and a Hill coefficient (n_h) of 1.0 ± 0.2 ($n = 5$) (Fig. 3A).

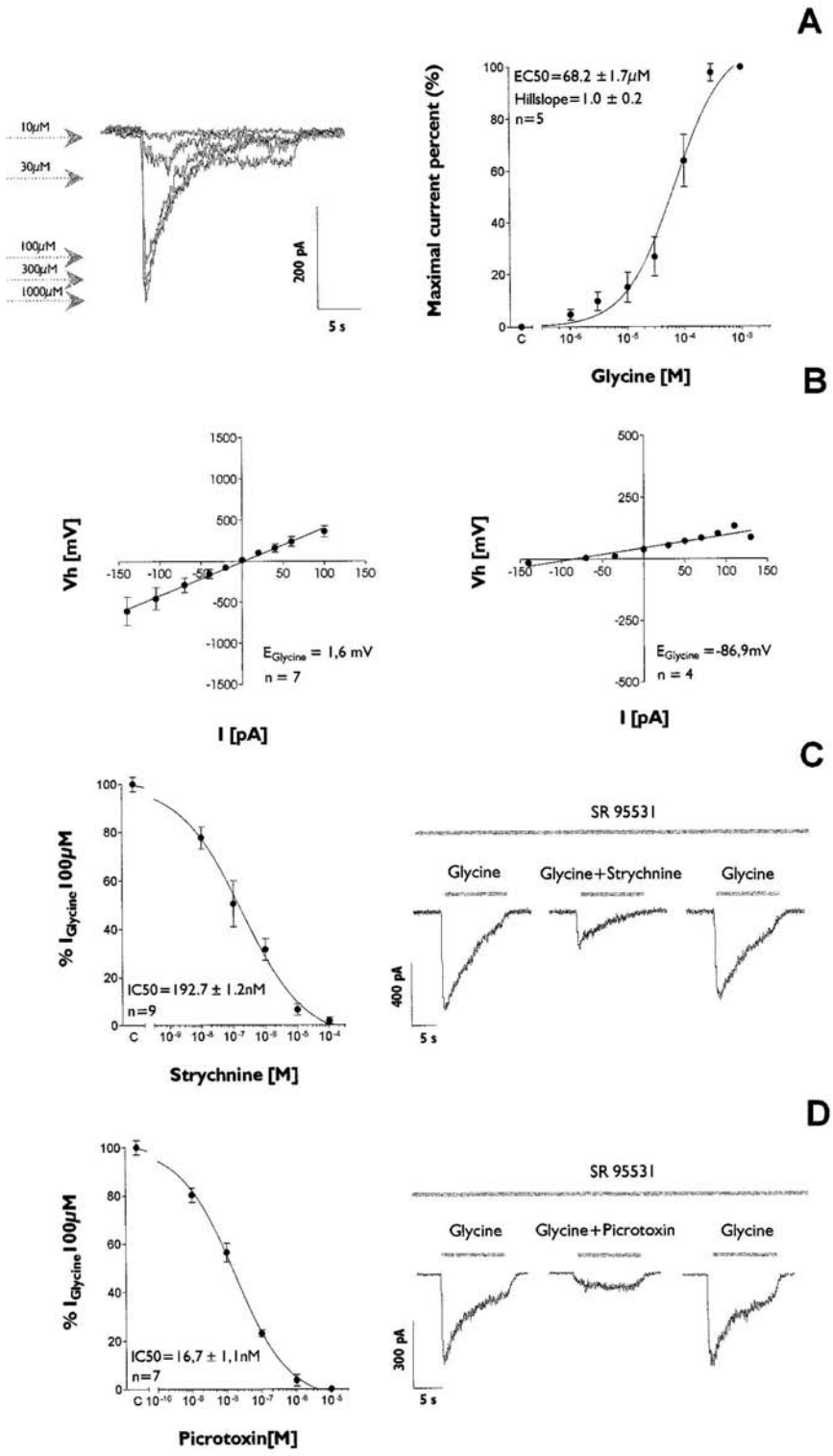

FIG. 3. Glycine-elicited currents recorded in multipotent NS/PCs are mediated by strychnine-sensitive ionotropic glycine receptors. (A) In the continuous presence of SR 95531 10 µM (a specific $GABA_A$ receptor antagonist), glycine was applied at increasing concentrations and the resulting whole-cell currents were recorded. The mean maximal current amplitude induced by 1 mM glycine was 172.8 ± 37.9 pA (mean ± SEM, n = 38) (left panel). Concentration–response curve obtained from glycine-responsive NS/PCs was fitted with a Hill equation and yielded an EC_{50} of 68.2 ± 1.7 µM and a Hill coefficient (n_h) of 1.0 ± 0.2 (n = 5) (right panel). (B) Reversal potential of glycine-induced currents ($E_{Glycine}$). Current–voltage relationship of glycine-evoked currents was obtained by applying voltage steps ranging from –130 to +140 mV during glycine application. The linear resulting current–voltage curve reverse at +1.6 mV (n = 7), which is close to the calculated Nernst chloride equilibrium potential (+0.6 mV) (left panel). When intracellular chloride concentration was decreased, the reversal potential was shifted to –86.9 mV (n = 4), which again is close to the expected chloride equilibrium potential in this condition (–104.2 mV) (right panel). (C) Sensitivity of NS/PCs glycine receptors to strychnine. The dose–response curve of the inhibition by strychnine of peak currents elicited by 100 µM glycine yielded an IC_{50} of 192.7 ± 1.2 nM (n = 9) (left panel). A typical recording obtained from one cell illustrates the inhibition by 1 µM strychnine of 100 µM glycine-evoked currents and its reversibility (right panel). (D) Sensitivity of NS/PCs glycine receptors to picrotoxin. The concentration–response curve to this alkaloid yields an IC_{50} of 16.8 ± 1.1 nM (n = 7) (left panel). Illustration of 0.1 µM picrotoxin reversible inhibition of 100 µM glycine evoked-current in one typical recorded cell (right panel).

Current–voltage relationship of glycine-evoked currents was obtained by applying voltage steps ranging from –140 to +130 mV during glycine application. As shown in Fig. 3B, the resulting current–voltage curve was linear and reversed at +1.6 mV (n = 7), which is close to the calculated Nernst chloride equilibrium potential (+0.6 mV) (Fig. 3B). When intracellular potassium chloride was replaced by an equimolar amount of potassium gluconate, the reversal potential shifted to a more negative value (–86.9 mV, n = 4; Fig. 3B) according to the predicted shift in Nernst chloride equilibrium potential (–104.2 mV). This demonstrates that glycine currents in NS/PCs are mainly carried by Cl^- ions.

Currents elicited by glycine at a concentration close to its EC_{50} were completely and reversibly inhibited by the competitive antagonist strychnine. The effect was dose-dependant with an IC_{50} of

192.7 ± 1.2 nM (n = 9) (Fig. 3C). Glycine-triggered currents were also fully and reversibly blocked by picrotoxin, a toxin described to block mostly α-homomeric GlyRs (Pribilla *et al*., 1992). The IC_{50} of picrotoxin blockade of the glycine response was unexpectedly low: 16.8 ± 1.1 nM (n = 7) (Fig. 3D).

Discussion

Considering that GlyRs have been described in neonatal glioblasts (Belachew *et al*., 1998) and neuroblasts (Flint *et al*., 1998; Ye, 2000) where they could be involved – as several other neurotransmitter receptors – in the regulation of cell development (reviewed in Cameron *et al*., 1998), we have investigated here the expression and the functionality of such receptors in postnatal nestin-expressing cells. As these cells retain an ability to divide and differentiate into neurons, astrocytes and oligodendrocytes, they are likely to include true stem cells and/or, at least, multipotent progenitors. Using the neurosphere culture model where almost all cells are nestin-positive, we demonstrated the presence of GlyR α_1-, α_2- and β-subunit mRNAs by RT-PCR techniques and GlyRα-subunit proteins by immunocytochemical means. Furthermore, using electrophysiological techniques, we provided evidence that these subunits were able to form functional chloride channels gated by glycine and sensitive to strychnine and picrotoxin. To our knowledge, this is the first demonstration of the expression of a functional neurotransmitter-gated channel in NS/PCs derived from postnatal animals.

Regarding GlyR expression, it is obvious from our data that the nestin-positive cells present in the neurospheres are not a homogenous population as only a subset of them express functional GlyRs. Glycine-evoked currents in NS/PCs are clearly caused by the activation of GlyRs because strychnine, the specific GlyR antagonist, totally and reversibly blocked these membrane currents. The discrepancy between the number of cells that express GlyR alpha proteins (80%) and those where glycine-induced currents were recorded (33%) could have several explanations, the most likely being cytoplasmic GlyRs. Indeed, it has already been shown that not all translated GlyR-subunits assemble within the membrane into functional channels, some of which remain cytoplasmic (Bechade *et al*., 1996). Our confocal immunodetection of cytoplasmic GlyR-subunits may be the reflection of such a fact (see Fig. 1D). This could also arise from a high endocytosis : exocytosis ratio, such as observed when GlyR-subunits proteins are ubiquitinated (Buttner *et al*., 2001).

Glycine-evoked currents in NS/PCs are clearly caused by the activation of GlyRs as: (i) they reverse at a potential close to the calculated Nernst chloride equilibrium potential, demonstrating its anion channel nature, and (ii) strychnine, the specific glycine antagonist at GlyRs, and picrotoxin, another GlyR inhibitor, totally and reversibly blocked these membrane currents. Both the glycine and strychnine half-maximum effects, and the picrotoxin sensitivity of glycine-induced currents support the idea of homomeric channels, perhaps the so-called neonatal α_2-homomeric phenotype if we consider our reported strychnine sensitivity in the hundred nanomolar range (Schmieden *et al*., 1999; Ye, 2000).

Unexpectedly, glycine-gated NS/PCs were blocked by very low concentrations of picrotoxin. This raises two questions, the first being that we expected to find picrotoxin-resistant glycine responses as GlyR β-subunit mRNAs were detected in neurospheres (Pribilla *et al*., 1992). No such picrotoxin sensitivity was ever observed in β-subunit-containing GlyRs, hence only speculations can be made to explain our results. It is known that β-subunit mRNAs are abundantly expressed throughout the entire mammalian brain, even in areas devoid of functional GlyRs (Malosio *et al*., 1991). As RT-PCR were performed using mRNAs from whole neurospheres, one could speculate that the β-subunit comes from cells that do not express GlyR α-proteins or functional GlyRs, as evidenced by patch-clamp recordings. Further experiments, certainly including single-cell RT-PCR techniques, are needed to fully address this question. The second question concerns the outstanding low picrotoxin concentration needed to achieve GlyR inhibition in NS/PCs. To our knowledge, a half-maximal picrotoxin inhibitory concentration of tens of nanomolar has never been described so far for GlyRs, they usually are at least two orders of magnitude higher, in the micromolar range (Pribilla *et al*., 1992; Shan *et al*., 2001). Kinetics and molecular studies are needed to address both issues of the mode of inhibition by low picrotoxin concentrations and of the subunit(s) and/or subunit variant(s) underlying such a high sensitivity.

The last, but not the least, important question to be answered relates to the specific properties of these subpopulations of nestin-positive cells, including their ability to differentiate into one or several mature neural cell types. The question to know whether functional GlyR expression in a subset of nestin-positive NS/PCs is a sign of precommitment to neurons or glia and/or plays roles in terms of proliferation, differentiation and survival, certainly deserves further studies which might include GlyR-expressing cell purification. As opposed to its major inhibitory role in the adult nervous system, glycine is known to depolarize immature neural progenitors, including oligodendroglial (Belachew *et al*., 2000) and neuronal progenitors (Flint *et al*., 1998; Tapia *et al*., 2000; Ye, 2000), resulting from a chloride equilibrium potential more positive than the resting potential in these progenitors (reviewed in Legendre, 2001). Glycine-induced depolarization may in turn trigger calcium entry via voltage-gated calcium channels, representing an important signalling mechanism for the promotion of neural progenitor maturation (LoTurco *et al*., 1995; Ikeda *et al*., 1997; Flint *et al*., 1998; Fiszman *et al*., 1999; Tapia *et al*., 2000; Maric *et al*., 2001). Hence, the study of glycine-elicited membrane depolarization, voltage-gated calcium channel openings and calcium entry, by means of perforated patch-clamp recordings and calcium imaging, will be the next step in our understanding of the physiological importance of GlyRs in postnatal NS/PCs.

Acknowledgements

This work was supported by the Fonds pour la Formation à la Recherche dans l'Industrie et dans l'Agriculture (FRIA), the Fonds National de la Recherche Scientifique (FNRS), the Fondation Médicale Reine Elisabeth (FMRE), the Fondation Charcot and the Ligue Belge de la Sclérose en Plaques. We thank J. Eriksson for his generous gift of the anti-nestin antibody. We thank P. Ernst-Gengoux for her technical support and expertise. B. Rogister is a senior research associate, B. Malgrange is a research associate and S. Belachew is a postdoctoral researcher of the FNRS.

Abbreviations

BrdU, bromodeoxyuridine; FITC, fluorescein isothiocyanate; GABA, γ-aminobutyric acid; GFAP, glial-fibrillary acidic protein; GlyR, glycine receptor; NS/PCs, neural stem/progenitor cells; PBS, phosphate-buffered saline; TRITC, tetramethylrhodamine B isothiocyanate.

References

Antonopoulos, J., Pappas, I.S. & Parnavelas, J.G. (1997) Activation of the GABAA receptor inhibits the proliferative effects of bFGF in cortical progenitor cells. *Eur. J. Neurosci.*, **9**, 291–298.

Atluri, P., Fleck, M.W., Shen, Q., Mah, S.J., Stadfelt, D., Barnes, W., Goderie, S.K., Temple, S. & Schneider, A.S. (2001) Functional nicotinic acetylcholine receptor expression in stem and progenitor cells of the early embryonic mouse cerebral cortex. *Dev. Biol.*, **240**, 143–156.

Bechade, C., Colin, I., Kirsch, J., Betz, H. & Triller, A. (1996) Expression of glycine receptor alpha subunits and gephyrin in cultured spinal neurons. *Eur. J. Neurosci.*, **8**, 429–435.

Belachew, S., Malgrange, B., Rigo, J.M., Rogister, B., Leprince, P., Hans, G., Nguyen, L. & Moonen, G. (2000) Glycine triggers an intracellular calcium influx in oligodendrocyte progenitor cells which is mediated by the activation of both the ionotropic glycine receptor and Na^+-dependent transporters. *Eur. J. Neurosci.*, **12**, 1924–1930.

Belachew, S., Rogister, B., Rigo, J.M., Malgrange, B., Mazy-Servais, C., Xhauflaire, G., Coucke, P. & Moonen, G. (1998) Cultured oligodendrocyte progenitors derived from cerebral cortex express a glycine receptor which is pharmacologically distinct from the neuronal isoform. *Eur. J. Neurosci.*, **10**, 3556–3564.

Ben-Hur, T., Rogister, B., Murray, K., Rougon, G. & Dubois-Dalcq, M. (1998) Growth and fate of PSA-NCAM+ precursors of the postnatal brain. *J. Neurosci.*, **18**, 5777–5788.

Buttner, C., Sadtler, S., Leyendecker, A., Laube, B., Griffon, N., Betz, H. & Schmalzing, G. (2001) Ubiquitination precedes internalization and proteolytic cleavage of plasma membrane-bound glycine receptors. *J. Biol. Chem.*, **276**, 42978–42985.

Cameron, H.A., Hazel, T.G. & McKay, R.D. (1998) Regulation of neurogenesis by growth factors and neurotransmitters. *J. Neurobiol.*, **36**, 287–306.

Edlund, T. & Jessell, T.M. (1999) Progression from extrinsic to intrinsic signaling in cell fate specification: a view from the nervous system. *Cell*, **96**, 211–224.

Fiszman, M.L., Borodinsky, L.N. & Neale, J.H. (1999) GABA induces proliferation of immature cerebellar granule cells grown *in vitro*. *Brain Res. Dev. Brain Res.*, **115**, 1–8.

Flint, A.C., Liu, X. & Kriegstein, A.R. (1998) Nonsynaptic glycine receptor activation during early neocortical development. *Neuron*, **20**, 43–53.

Gallo, V., Zhou, J.M., McBain, C.J., Wright, P., Knutson, P.L. & Armstrong, R.C. (1996) Oligodendrocyte progenitor cell proliferation and lineage progression are regulated by glutamate receptor-mediated K^+ channel block. *J. Neurosci.*, **16**, 2659–2670.

Gould, E. (1999) Serotonin and hippocampal neurogenesis. *Neuropsychopharmacology*, **21**, 46S–51S.

Gould, E. & Cameron, H.A. (1997) Early NMDA receptor blockade impairs defensive behavior and increases cell proliferation in the dentate gyrus of developing rats. *Behav. Neurosci.*, **111**, 49–56.

Hamill, O.P., Marty, A., Neher, E., Sakmann, B. & Sigworth, F.J. (1981) Improved patch-clamp techniques for high-resolution current recording from cells and cell-free membrane patches. *Pflugers Arch.*, **391**, 85–100.

Haydar, T.F., Wang, F., Schwartz, M.L. & Rakic, P. (2000) Differential modulation of proliferation in the neocortical ventricular and subventricular zones. *J. Neurosci.*, **20**, 5764–5774.

Ikeda, Y., Nishiyama, N., Saito, H. & Katsuki, H. (1997) GABAA receptor stimulation promotes survival of embryonic rat striatal neurons in culture. *Brain Res. Dev. Brain Res.*, **98**, 253–258.

Lauder, J.M. (1993) Neurotransmitters as growth regulatory signals: role of receptors and second messengers. *Trends Neurosci.*, **16**, 233–240.

Lauder, J.M., Liu, J., Devaud, L. & Morrow, A.L. (1998) GABA as a trophic factor for developing monoamine neurons. *Perspect. Dev. Neurobiol.*, **5**, 247–259.

Legendre, P. (2001) The glycinergic inhibitory synapse. *Cell Mol. Life Sci.*, **58**, 760–793.

Lendahl, U., Zimmerman, L.B. & McKay, R.D. (1990) CNS stem cells express a new class of intermediate filament protein. *Cell*, **60**, 585–595.

Lipton, S.A., Frosch, M.P., Phillips, M.D., Tauck, D.L. & Aizenman, E. (1988) Nicotinic antagonists enhance process outgrowth by rat retinal ganglion cells in culture. *Science*, **239**, 1293–1296.

Lipton, S.A. & Kater, S.B. (1989) Neurotransmitter regulation of neuronal outgrowth, plasticity and survival. *Trends Neurosci.*, **12**, 265–270.

LoTurco, J.J., Owens, D.F., Heath, M.J., Davis, M.B. & Kriegstein, A.R. (1995) GABA and glutamate depolarize cortical progenitor cells and inhibit DNA synthesis. *Neuron*, **15**, 1287–1298.

Ma, W., Liu, Q.Y., Maric, D., Sathanoori, R., Chang, Y.H. & Barker, J.L. (1998) Basic FGF-responsive telencephalic precursor cells express functional GABA (A) receptor/Cl-channels *in vitro*. *J. Neurobiol.*, **35**, 277–286.

Ma, W., Maric, D., Li, B.S., Hu, Q., Andreadis, J.D., Grant, G.M., Liu, Q.Y., Shaffer, K.M., Chang, Y.H., Zhang, L., Pancrazio, J.J., Pant, H.C., Stenger, D.A. & Barker, J.L. (2000) Acetylcholine stimulates cortical precursor cell proliferation *in vitro* via muscarinic receptor activation and MAP kinase phosphorylation. *Eur. J. Neurosci.*, **12**, 1227–1240.

Malosio, M.L., Marqueze-Pouey, B., Kuhse, J. & Betz, H. (1991) Widespread expression of glycine receptor subunit mRNAs in the adult and developing rat brain. *EMBO J.*, **10**, 2401–2409.

Maric, D., Liu, Q.Y., Grant, G.M., Andreadis, J.D., Hu, Q., Chang, Y.H., Barker, J.L., Joseph, J., Stenger, D.A. & Ma, W. (2000) Functional ionotropic glutamate receptors emerge during terminal cell division and early neuronal differentiation of rat neuroepithelial cells. *J. Neurosci. Res.*, **61**, 652–662.

Maric, D., Liu, Q.Y., Maric, I., Chaudry, S., Chang, Y.H., Smith, S.V., Sieghart, W., Fritschy, J.M. & Barker, J.L. (2001) GABA expression dominates neuronal lineage progression in the embryonic rat neocortex and facilitates neurite outgrowth via GABA (A) autoreceptor/Cl- channels. *J. Neurosci.*, **21**, 2343–2360.

Nguyen, L., Belachew, S., Malgrange, B., Rogister, B., Rocher, V., Hans, G., Moonen, G. & Rigo, J. (2000) M. Neurotransmitters trigger a diversity of ligand-gated ionic currents in neural progenitor cells. International Society of Developmental Neuroscience.

Nguyen, L., Rigo, J.M., Rocher, V., Belachew, S., Malgrange, B., Rogister, B., Leprince, P. & Moonen, G. (2001) Neurotransmitters as early signals for central nervous system development. *Cell Tissue Res.*, **305**, 187–202.

Pribilla, I., Takagi, T., Langosch, D., Bormann, J. & Betz, H. (1992) The atypical M2 segment of the beta subunit confers picrotoxinin resistance to inhibitory glycine receptor channels [published erratum appears in *EMBO J.* (1994), **13**, 1493]. *EMBO J.*, **11**, 4305–4311.

Schmieden, V., Kuhse, J. & Betz, H. (1999) A novel domain of the inhibitory glycine receptor determining antagonist efficacies: further evidence for partial agonism resulting from self-inhibition. *Mol. Pharmacol.*, **56**, 464–472.

Schroder, S., Hoch, W., Becker, C.M., Grenningloh, G. & Betz, H. (1991) Mapping of antigenic epitopes on the alpha 1 subunit of the inhibitory glycine receptor. *Biochemistry*, **30**, 42–47.

Shan, Q., Haddrill, J.L. & Lynch, J.W. (2001) A single beta subunit M2 domain residue controls the picrotoxin sensitivity of alphabeta heteromeric glycine receptor chloride channels. *J. Neurochem.*, **76**, 1109–1120.

Tapia, J.C., Cardenas, A.M., Nualart, F., Mentis, G.Z., Navarrete, R. & Aguayo, L.G. (2000) Neurite outgrowth in developing mouse spinal cord neurons is modulated by glycine receptors. *Neuroreport*, **11**, 3007–3010.

Ye, J. (2000) Physiology and pharmacology of native glycine receptors in developing rat ventral tegmental area neurons. *Brain Res.*, **862**, 74–82.

7.14 Publication #14: Vautier, F., Belachew, S., Chittajallu, R., and Gallo, V. (2004). *Shaker*-type potassium channel subunits Kv1.3-1.4 and Kv1.6 differentially control oligodendrocyte progenitor cell cycle progression. *Glia* 48:337-345.

GLIA 48:337–345 (2004)

Shaker-Type Potassium Channel Subunits Differentially Control Oligodendrocyte Progenitor Proliferation

FRANÇOIS VAUTIER,[1†] SHIBESHIH BELACHEW,[1,2,3†] RAMESH CHITTAJALLU,[1,2] AND VITTORIO GALLO[1,2*]

[1]*Laboratory of Cellular and Synaptic Neurophysiology, National Institute of Child Health and Human Development, National Institutes of Health, Bethesda, Maryland*

[2]*Center for Neuroscience Research, Children's Research Institute, Children's National Medical Center, Washington, DC*

[3]*Center for Cellular and Molecular Neurobiology, University of Liège, Liège, Belgium*

KEY WORDS oligodendrocyte precursor cells; K^+ channels; Kv1 subunits; mitogens

ABSTRACT Oligodendrocyte precursor (OP) cells are exposed to multiple extrinsic signals that control their proliferation and differentiation. Previous cell proliferation studies and electrophysiological analysis in cultured cells and in brain slices have suggested that outward potassium channels, particularly Kv1 subunits, may have a prominent role in OP cell proliferation. In the present study, we assessed to what extent overexpression of Kv1.3, Kv1.4, Kv1.5, and Kv1.6 can affect OP cell proliferation and differentiation in culture. We observed that overexpression of Kv1.3 or Kv1.4 increased OP cell proliferation in the absence of mitogens, whereas Kv1.6 overexpression inhibited mitogen-induced OP cell cycle progression. Interestingly, Kv1.3, Kv1.4, Kv1.5, and Kv1.6 overexpression did not interfere with the kinetics of oligodendrocyte differentiation. This study represents the first demonstration that the activity of potassium channels containing distinct Kv1 subunit proteins directly controls oligodendroglial proliferation in the presence of mitogens, as well as in growth factor-free conditions.

INTRODUCTION

During the development of the central nervous system (CNS), proliferation and differentiation of neural cells are regulated by extrinsic and intrinsic signals. Mature oligodendrocytes, the principal myelinating cells in the CNS, originate primarily from highly proliferative oligodendrocyte precursor (OP) cells (Levison et al., 1993; Levison and Goldman, 1993). The complex array of extrinsic signals required for OP cells to migrate, proliferate, and differentiate into oligodendrocytes is not yet completely defined.

It has been demonstrated that OP cell cycle progression in vitro and in situ (Gallo and Ghiani, 2000) can be controlled by extracellular cues such as glutamate, norepinephrine, and adenosine (Gallo and Ghiani, 2000; Ghiani et al., 1999a), but also by pharmacological K^+ channel blockade (Ghiani et al., 1999b; Chittajallu et al., 2002). Previous studies in cultured cells and in mutant mice have analyzed some of the intrinsic cell cycle regulatory mechanisms in OP cells, with a focus on proteins involved in G1/S progression (Durand et al., 1997, 1998; Casaccia-Bonnefil et al., 1997, 1999;

Grant sponsor: National Institute of Child Health and Human Development (NICHD); National Institutes of Health MRDDRC; Grant number: P30HD40677; Grant sponsor: Wadsworth Foundation; Grant sponsor: Fonds National de la Recherche Scientifique (Belgium); Grant sponsor: Wellcome Trust Fellowship.

[†]F.V. and S.B. contributed equally to this work.

*Correspondence to: Vittorio Gallo, Center for Neuroscience Research, Children's Research Institute, Room 5345, Children's National Medical Center, 111 Michigan Ave. NW, Washington, DC 20010. E-mail: vgallo@cnmcresearch.org

Received 8 April 2004; Accepted 12 May 2004

DOI 10.1002/glia.20088

Published online 6 July 2004 in Wiley InterScience (www.interscience.wiley.com).

Tang et al., 1998; Ghiani et al., 1999a,b; Ghiani and Gallo, 2001). One of the mechanisms that have received much attention involves the endogenous cdkis $p21^{Cip1}$ and $p27^{Kip1}$ and their binding to the cyclin E-cdk2 complex. The levels of these cdkis increase in OP cells either during permanent cell cycle withdrawal associated with differentiation (Durand et al., 1997, 1998; Casaccia-Bonnefil et al., 1997, 1999; Ghiani et al., 1999a) or during reversible cell cycle arrest in G1 caused by extracellular signals, such as K^+ channel blockade (Ghiani et al., 1999b), which inhibit cell cycle progression driven by the mitogen platelet-derived growth factor (PDGF). Finally, it was demonstrated that cdk2 overexpression prevented G1 cell cycle arrest induced by the K^+ channel blocker tretraethylammonium (TEA), providing evidence that a causal relationship exists between regulation of K^+ conductance, cyclin E-cdk2 activity, and OP cell proliferation (Belachew et al., 2002).

K^+ channels are formed by tetrameric protein complexes, which can be homomeric or heteromeric (Ruppersberg et al., 1990; Chandy and Gutman, 1993; Sheng et al., 1993). Pharmacological blockage of such potassium channels prevents cell proliferation in different cell types (DeCoursey et al., 1984; Dubois and Rouzaire-Dubois, 1993; Wonderlin and Strobl, 1996; Knutson et al., 1997; MacFarlane and Sontheimer, 1997; Sobko et al., 1998).

In OP cells, all six *Shaker*-type Kv1 (Kv1.1 to 1.6) potassium channel subunits can be detected with different RNA and protein levels (Attali et al., 1997; Chittajallu et al., 2002). Proliferative OP cells express large I_k, whereas nondividing and mature oligodendrocytes display much smaller outward currents (Knutson et al., 1997). We demonstrated previously that I_k currents are upregulated in G1 phase of the cell cycle, which is attributed to an RNA synthesis-dependent and selective increase of K^+ channel subunit proteins Kv1.3 and Kv1.5 (Gallo et al., 1996; Knutson et al., 1997; Ghiani et al., 1999b; Chittajallu et al., 2002). Furthermore, inhibition of outward K^+ channels by blocker tetraethylammonium or by cell membrane depolarization through Na^+ channel opener veratridine inhibits OP cell proliferation (Knutson et al., 1997; Ghiani et al., 1999b). Interestingly, selective pharmacological block of Kv1.3 closely mimics the inhibitory effect of TEA on OP cell proliferation, indicating a critical role of this subunit in OP cell cycle progression (Chittajallu et al., 2002).

In the present study, our goal was to determine whether a direct causal link exists between the expression of specific Kv1 subunits and OP proliferation and differentiation. Therefore, we took advantage of a previously characterized model system (Ghiani et al., 1999b; Belachew et al., 2002) to overexpress different Kv subunits in OP cells. We assessed proliferation and differentiation of purified OP cells after transfection with plasmid vectors bearing different Kv1 potassium channel subunits.

MATERIALS AND METHODS

DNA Constructs

The oligodendroglial promoter used (in Bluescript SK^+, Stratagene) was the 3.7-kb *Xba*I–*Hin*dIII sequence that contains the CNP1 and CNP2 promoter core elements of the mouse 2′,3′-cyclic nucleotide 3′-phosphodiesterase (CNP) gene (Gravel et al., 1998; Belachew et al., 2001; Yuan et al., 2002) (Genebank accesssion no. M31810). The first ATG (position 0, end of exon 0), located in the promoter region, was mutated by replacing the A with a C (pSK-CNP-Mut). The GFP reporter sequence was derived from the pIRES2-EGFP plasmid (Clontech Laboratories, Cat no. 6064-1). The unique *Not*I site (position 1977) was deleted to create the pIRES2-EGFPδ*Not* plasmid. Kv1.3–1.6 rat cDNAs (generous gift from Olaf Pongs, Institute for Neural Signal Transduction, Hamburg, Germany; Genebank accession no. Kv1.3: X16002, Kv1.4: X16002, Kv1.5: M27158, Kv1.6: X17621) were extracted from pAS18 (Kv1.3), pNKS2 (Kv1.5), and pAKS2 (Kv1.4 and Kv 1.6) plasmids.

The CNP-GFP control vector was obtained by subcloning the *Bam*HI-blunt/*Ssp*I 1.6-kb fragment from pIRES2-EGFPδ*Not* in the *Hin*dIII-blunt site of pSK-CNP-Mut.

Kv1.3 cDNA (*Bam*HI/*Hin*dIII 1.85-kb fragment from pAS18-Kv1.3) was first subcloned in pBluescript SK^+ (*Bam*HI/*Hin*dIII). The *Bam*HI-blunt/*Sal*I fragment from SK-Kv1.3 was then cloned downstream of the CNP promoter (in *Hin*dIII-blunt/*Sal*I sites of pSK-CNP-Mut). The *Not*I-blunt/*Sal*I fragment from this plasmid was cloned upstream of IRES-GFP (in pIRES2-EGFP *Sac*I-blunt/*Sal*I). In a final step, the pCMV promoter (from in pIRES2-EGFP) was discarded, to obtain the CNP-Kv1.3-GFP vector. Kv1.4 cDNA was extracted from pAKS2-Kv1.4 by enzymatic digestion *Hin*dIII/*Kpn*I (2.7 kb) and cloned downstream of the CNP promoter in pSK-CNP-Mut. The IRES-GFP sequence (*Ssp*I/*Bam*HI fragment from pIRES2-EGFP) was then cloned downstream of CNP-Kv1.4 (*Kpn*I-blunt/*Bam*HI) to obtain the CNP-Kv1.4-GFP vector. Kv1.5 cDNA (*Apa*I/*Apa*I double blunt fragment from pNKS2-Kv1.5, 2 kb) was first subcloned in pBluescript SK^+. The *Bam*HI-blunt/*Sal*I fragment from SK-Kv1.5 was then cloned downstream of the CNP promoter (in *Hin*dIII-blunt/SalI sites of pSK-CNP-Mut), and the IRES-GFP (*Ssp*I/*Sal*I fragment from pIRES2-EGFP) was cloned downstream of CNP-Kv1.5 (*Kpn*I-blunt/*Sal*I), to form the CNP-Kv1.5-GFP vector. Finally, Kv1.6 cDNA was extracted from pAKS2-Kv1.6 and cloned (1.8 kb) downstream of the CNP promoter between *Sal*I-blunt/*Hin*dIII sites of pSK-CNP-Mut. The IRES-GFP (*Not*I-blunt/*Sal*I fragment from pIRES2-EGFP) was then cloned downstream of CNP-Kv1.6 (*Bam*HI-blunt/*Sal*I) to obtain the CNP-Kv1.6-GFP vector.

Cell Cultures

All culture media were from Life Technologies (Gaithersburg, MD). Fetal bovine serum (FBS) was from Hy-

clone (Logan, UT). Platelet-derived growth factor (PDGF) was from Upstate Biotechnology (Lake Placid, NY). Purified cortical OP cell cultures were prepared as previously described from neonatal (P0) Sprague-Dawley rat pups, using a standard experimental protocol (McCarthy and de Vellis, 1980) with slight modifications (Ghiani et al., 1999b). OP cells were expanded for 2–3 weeks (3–4 passages) in poly-D-ornithine-treated 100-mm plastic Petri dishes in DME-N1 medium supplemented with B104-conditioned medium (30% v/v) (Louis et al., 1992). One day before transfection, OP cells were transferred onto poly-D-ornithine treated 12-mm glass coverslips at a density of 80,000 (differentiation experiments) or 100,000 (proliferation experiments) cells/coverslip in DME-N_1 medium supplemented with platelet-derived growth factor (PDGF, 10 ng/ml) (Upstate Biotechnology).

Transfection Procedure

All plasmid constructs were introduced into cultured OP cells by liposomal transfection in 24-well dishes, using 0.2 μg of DNA and 0.8 μl of lipofectamine in OPTI-MEM (Life Technologies) for each well (80,000–100,000 cells/coverslips). The duration of the transfection procedure was 6 h. After transfection, OP cells were cultured in DME-N1 supplemented with PDGF (10 ng/ml). The average efficiency of the transfection procedure for each plasmid (48 h post-transfection; GFP-expressing cells as percentage of total cells) was: 13% with CNP-GFP, 11% with CNP-Kv1.3-GFP, 15% with CNP-Kv1.4-GFP, 19% with CNP-Kv1.5-GFP, and 17% with CNP-Kv1.6-GFP. Transient transfection with any of the Kv subunits did not affect OP cell viability or number (data not shown; see also Belachew et al., 2002).

At 24 h after transfection, OP cells were switched to different experimental conditions: (1) PDGF withdrawal, culture in DME-N1 + 0.5% FBS; (2) DME-N1 + 0.5% FBS supplemented with r-margatoxin (50 nM, Alomone Laboratories) or with dendrotoxin (100 nM, Alomone Laboratories). Proliferation assays were performed by adding bromodeoxyuridine (BrdU, 20 μM, Sigma) 24 h after the end of the transfection for 24 h. Cells were then fixed as previously described (Belachew et al., 2002).

Differentiation into $O4^+$ postmitotic pre-oligodendrocytes and $O1^+$ mature oligodendrocytes was assessed by growing transfected OP cells for 4 days after the end of the transfection procedure.

Immunostaining

Immunohistochemical characterization of transfected OP cells (as assessed by the presence of GFP fluorescence) with O4, O1, and anti-BrdU staining was carried out as previously described (Yuan et al., 1998; Belachew et al., 2003). For BrdU immunostaining, since the necessary alkaline denaturation of cell DNA (NaOH 0.07 N) was partially quenching GFP fluorescence, GFP immunostaining (1:100, polyclonal anti-GFP, Santa Cruz Biotechnology, Santa Cruz, CA) was performed before BrdU staining, to permit more precise detection of transfected cells.

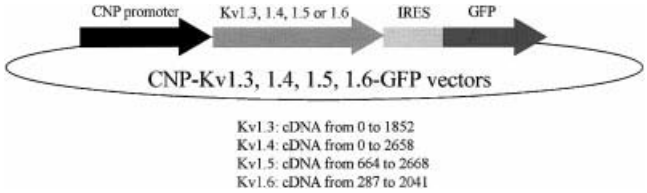

Fig. 1. Schematic diagrams of plasmid vectors. The different constructs used for cell transfections contained cDNAs encoding for the *shaker*-type potassium channel subunits Kv1.3, Kv1.4, Kv1.5, or Kv1.6 (1852, 2658, 2004, and 1,754 bp, respectively) under the control of the CNP gene promoter. GFP was used as reporter gene and was cloned downstream of an internal ribosomal entry site (IRES), allowing concomitant transcription of GFP and Kv1 subunits RNAs, but translation of GFP protein independent from that of potassium channels subunits. The control vector (CNP-GFP) contained only the IRES-GFP sequence driven by the CNP promoter.

RESULTS

To determine the functional role of potassium channels subunits in OP cell proliferation and differentiation, we overexpressed GFP-tagged Kv1.3, Kv1.4, Kv1.5, or Kv1.6 subunits in rat primary cultures of OP cells, using the CNP gene promoter (Fig. 1). A CNP-GFP empty vector was used as a control. Cell proliferation was assessed by using bromodeoxyuridine (BrdU) incorporation assays, to quantify GFP-expressing S-phase precursors, either in the presence of PDGF (for 24 h; OPs in cell cycle), or after PDGF withdrawal (24 h without PDGF; cell cycle-arrested OPs) (Ghiani and Gallo, 2001).

Overexpression of Kv1.3 and 1.4 Prevents OP Cell Cycle Arrest Induced by Mitogen Withdrawal, Whereas Kv1.6 Inhibits Mitogen-Induced OP Cell Proliferation

Overexpression of Kv1.3, Kv1.4, or Kv1.5 in the presence of PDGF did not modify OP proliferation (Fig. 2A). In contrast, Kv1.6 overexpression inhibited mitogen-induced proliferation. After PDGF withdrawal, overexpression of Kv1.3 or Kv1.4, but not of Kv1.5 or Kv1.6, increased the percentage of proliferating OP cells (Fig. 2B). Interestingly, Kv1.3 and Kv1.4 overexpression almost completely restored the level of cell proliferation to that of OP cells that were cultured in the presence of PDGF.

Effect of Kv1.3 Overexpression on OP Cell Proliferation Is Dependent of Kv1.3-Containing Channels

To establish that the pro-mitotic effect observed with Kv1.3 overexpression was mediated by an increase in

Kv1.3-containing functional channels, we performed pharmacological experiments using margatoxin (MgTx), a specific antagonist for Kv1.3-containing channels previously used in OP cells (Chittajallu et al., 2002). Margatoxin (50 nM) was added to transfected OP cultures at the time of PDGF withdrawal (Fig. 3).

We first confirmed that MgTx itself had no effect on the proliferation of mitogen-deprived CNP-GFP-transfected control cultures (Fig. 3). This is consistent with the low level of expression of Kv1.3 in OP cells maintained in the absence of PDGF (Chittajallu et al., 2002). In contrast, MgTx completely blocked the increase in OP proliferation observed in mitogen-deprived OP cells that overexpressed Kv1.3 (Fig. 3). This provides evidence that overexpression of the Kv1.3 subunit in OP cells results in the formation of MgTx-sensitive functional potassium channels, and that these newly formed channels are causally linked to the increase in cell proliferation observed in these OP cells. Consistent with its pharmacological profile,

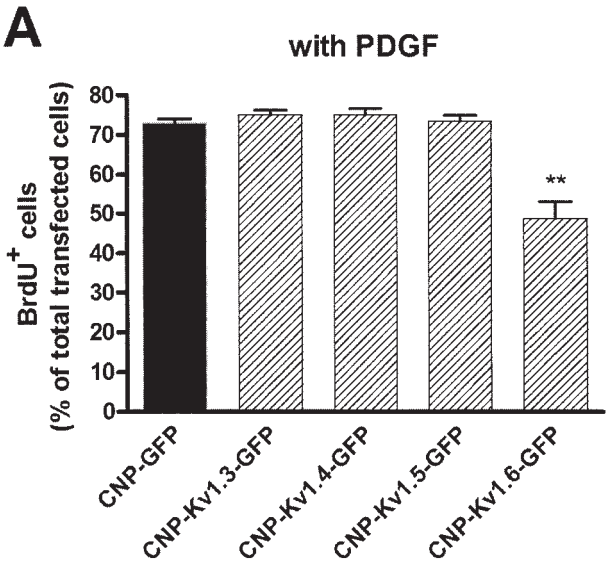

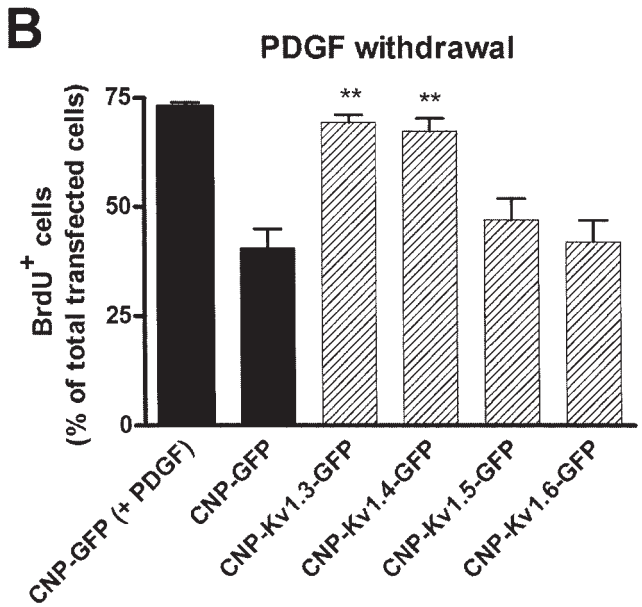

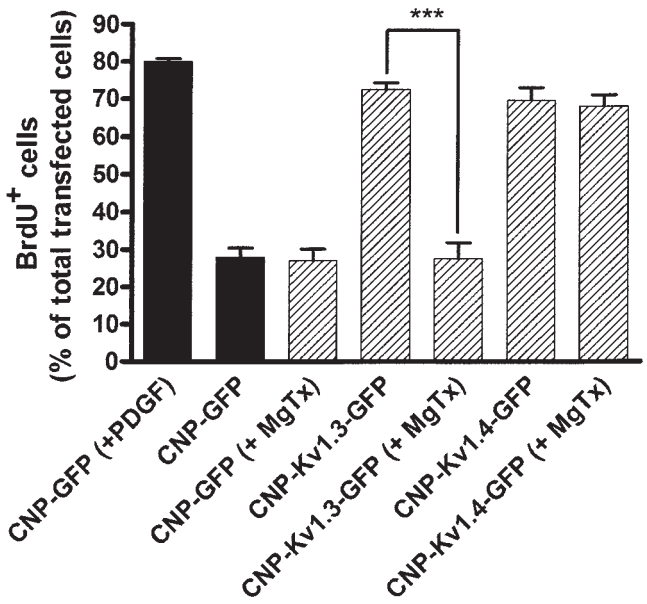

Fig. 3. Effect of Kv1.3 overexpression is inhibited by a blocker of Kv1.3-containing channels. Transfected oligodendrocyte precursor (OP) cells were treated with r-margatoxin (MgTx). R-margatoxin had no effect on cell proliferation of cultures transfected with the control vector (CNP-GFP). In contrast, MgTx abolished the Kv1.3-induced increase of OP cell proliferation observed after platelet-derived growth factor (PDGF) withdrawal (24 h without PDGF; $***P < 0.001$, Bonferroni's multiple comparison test). Consistently, MgTx did not inhibit the increase in OP proliferation induced by Kv1.4 overexpression in the absence of mitogen ($P > 0.05$, Bonferroni's multiple comparison test). Histograms represent mean ± SEM of counts from two separate experiments (> 200 GFP^+ cells counted for each condition, triplicate coverslips for each condition).

Fig. 2. Differential effects of Kv1 subunits overexpression on oligodendrocyte precursor (OP) cell proliferation. OP cells were transfected with plasmid constructs containing cDNAs encoding for Kv1.3, 1.4, 1.5, and 1.6 subunits (see methods). The BrdU incorporation index was calculated as number of $BrdU^+$ cells/number of total transfected GFP^+ cells × 100. In the presence of platelet-derived growth factor (PDGF) (for 24 h), Kv1.6 overexpression strongly inhibited OP cell proliferation (33% decrease, $**P < 0.01$, Dunnett's test). Overexpression of Kv1.3, 1.4, and 1.5 subunits had no effect on cell proliferation in the presence of the mitogen (DME-N1 + PDGF) ($P > 0.05$, Dunnett's test). After PDGF withdrawal (24 h without PDGF), the percentage of $BrdU^+$ OP cells dramatically decreased in the control cultures (compare the first two black bars). Overexpression of Kv1.3 and Kv1.4 prevented the cell cycle arrest induced by PDGF withdrawal ($**P < 0.01$ Dunnett's test). Kv1.5 and Kv1.6 overexpression did not affect OP cell proliferation after PDGF withdrawal. Histograms represent mean ± SEM of counts from four separate experiments (> 600 GFP^+ cells counted for each condition, triplicate coverslips for each condition).

MgTx did not interfere with the Kv1.4-mediated increase in OP cell proliferation (Fig. 3).

Kv1.6 Overexpression Inhibits Mitogen-, Kv1.3-, and Kv1.4-Driven OP Cell Proliferation

Kv1.6 overexpression prevented the effect of PDGF on OP cell proliferation, as no difference in cell proliferation was observed in Kv1.6-overexpressing OPs before or after PDGF withdrawal (Fig. 4A). In the absence of PDGF, overexpression of Kv1.6 partially inhibited Kv1.3-driven OP proliferation, and completely blocked the stimulating effects of Kv1.4 on OP proliferation (Fig. 4A,B). Interestingly, co-overexpression of Kv1.3 + Kv1.4, Kv1.3 + Kv1.5 or Kv1.4 + Kv1.5 did not yield any significant difference in OP cell proliferation rate ($P > 0.4$, Student's t-test), as compared to Kv1.3 or Kv1.4 alone (data not shown).

Effect of Kv1.6 Overexpression on OP Cell Proliferation Is Dependent on Kv1.6-Containing Channels

To define whether the effect of Kv1.6 overexpression was mediated by an increase in the activity of Kv1.6-containing channels, we used dendrotoxin (DTx, 100 nM), which is known to block Kv1.6-containing channels without affecting channels containing Kv1.3, 1.4, or 1.5 subunits. DTx did not influence control-transfected cells or did not modify the increase in cell proliferation observed in Kv1.3-overexpressing cells. In contrast, DTx totally reversed the inhibition of OP proliferation caused by Kv1.6 overexpression in the presence of PDGF (Fig. 5).

Overexpression of Kv1 Subunits Does Not Affect OP Cell Differentiation

At 3–4 days after PDGF withdrawal, only Kv1.3 overexpression slightly increased (by 15%) the percentage of pre-oligodendrocytes immunostained with the O_4 antibody (Fig. 6A). Overexpression of Kv1.4, 1.5, and 1.6 subunits did not modify the percentage of O_4^+ cells. None of the Kv1.3, 1.4, 1.5, and 1.6 subunits had any effect on OP differentiation to O_1^+ mature oligodendrocytes (Fig. 6B).

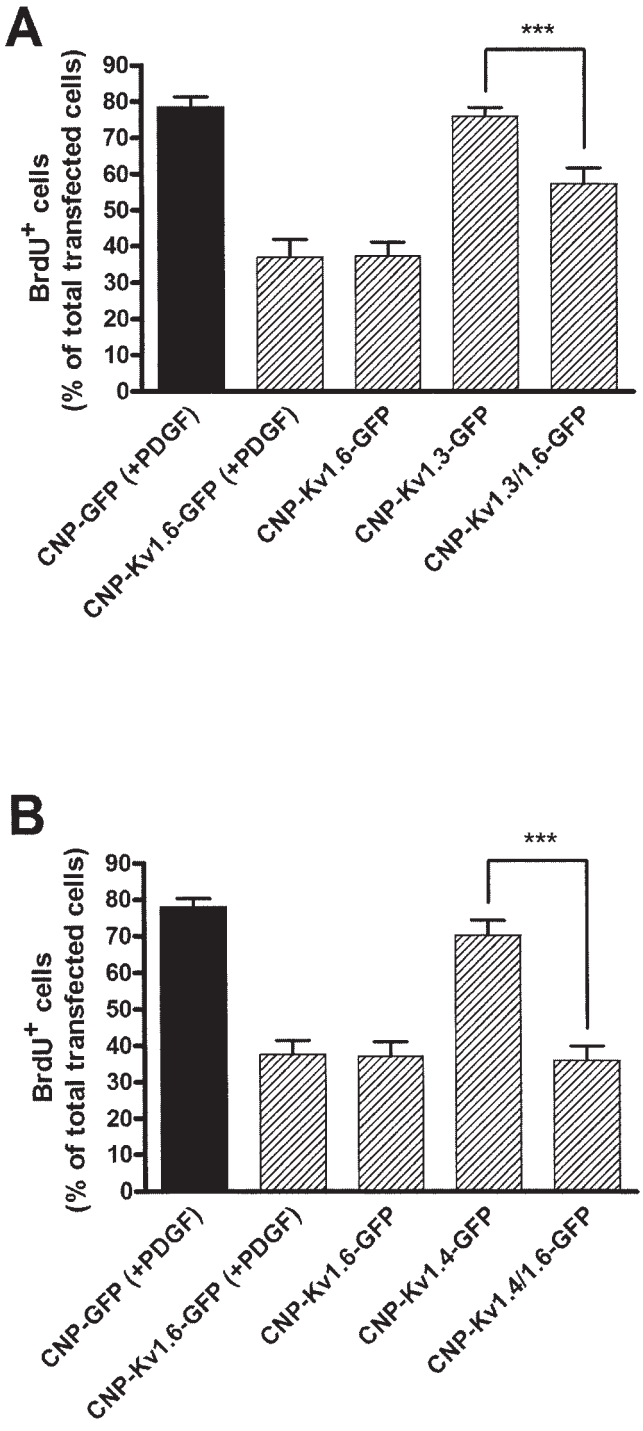

Fig. 4. Kv1.6 prevents the effects of Kv1.3–1.4 overexpression. Kv1.6 was co-transfected with Kv1.3 or Kv1.4. Oligodendrocyte precursor (OP) cells were transfected with either Kv1.6, or Kv1.3, or Kv1.3 + Kv1.6 (***$P < 0.001$, Bonferroni's multiple comparison test). OP cells were transfected with either Kv1.6 or Kv1.4, or Kv1.4 + Kv1.6 (***$P < 0.001$, Bonferroni's multiple comparison test). Histograms represent mean ± SEM of counts from two separate experiments (> 250 GFP^+ cells counted for each condition, triplicate coverslips for each condition).

DISCUSSION

In the present study, we provide the first experimental evidence that Kv1.3, Kv1.4, and Kv1.6 potassium channel subunits directly regulate proliferation of perinatal OP cells. Overexpression of Kv1.3 and Kv1.4 mimics the mitogenic effect of PDGF. OP cells maintained in culture without mitogens and with increased

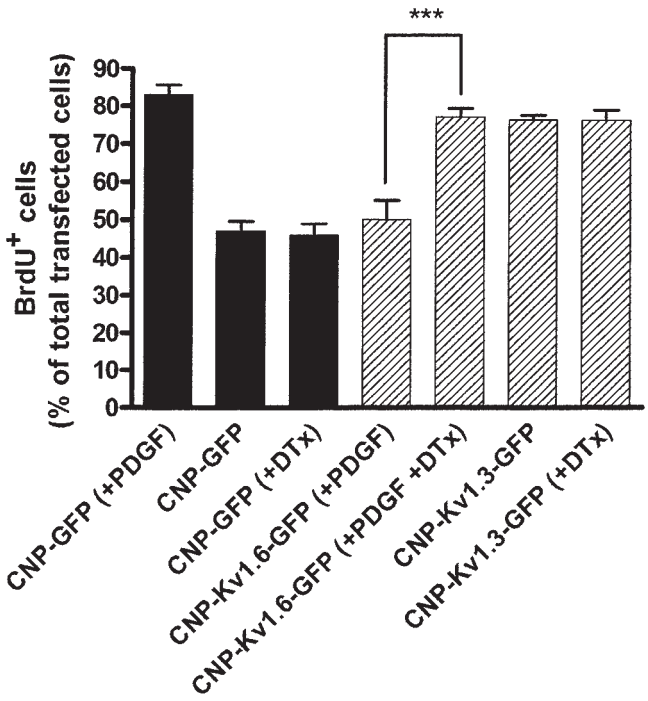

Fig. 5. Effect of Kv1.6 overexpression is inhibited by a blocker of Kv1.6-containing channels. Dendrotoxin (DTx, 100 nM) had no effect on the proliferation of oligodendrocyte precursor (OP) cells transfected with the control plasmid (CNP-GFP). DTx selectively prevented the antiproliferative effect of Kv1.6 overexpression in the presence of platelet-derived growth factor (PDGF) (for 24 h; $***P < 0.001$, Bonferroni's multiple comparison test), but did not modify the increase of OP proliferation induced by Kv1.3 overexpression in the absence of mitogen (24 h without PDGF; $P > 0.05$, Bonferroni's multiple comparison test). Histograms represent mean ± SEM of counts (> 200 GFP^+ cells counted for each condition, triplicate coverslips for each).

levels of Kv1.3 and Kv1.4 display a cell proliferation rate similar to that of cells cultured in the presence of the mitogen. Interestingly, the proliferative effects of Kv1.3 and Kv1.4 overexpression are not additive (data not shown), nor do they enhance the cell proliferation rate of dividing OP cells cultured in the presence of PDGF. Our data thus suggest that the maximum rate of OP cell proliferation (75–80% of total cells) is Kv1.3 or Kv1.4 dependent. These results are consistent with previous studies, which demonstrated that PDGF stimulates Kv1.3 expression in OP cells and that blockers of Kv1.3-containing channels inhibit OP cell proliferation (Chittajallu et al., 2002).

In the present study, we also show that the effect of Kv1.3 overexpression is indeed dependent on Kv1.3-containing channels, since is blocked by MgTx. In contrast, Kv1.4-induced proliferation is completely unaffected by MgTx, indicating that Kv1.4 overexpression leads to the formation of multimeric potassium channels that are MgTx-insensitive. Altogether, given that selective inhibition of Kv1.3 does not alter the effects of Kv1.4 overexpression, it is likely that Kv1.3 and Kv1.4 do not co-assemble in the same multimeric channels in OP cells, at least under the conditions of our experimental system. Further-

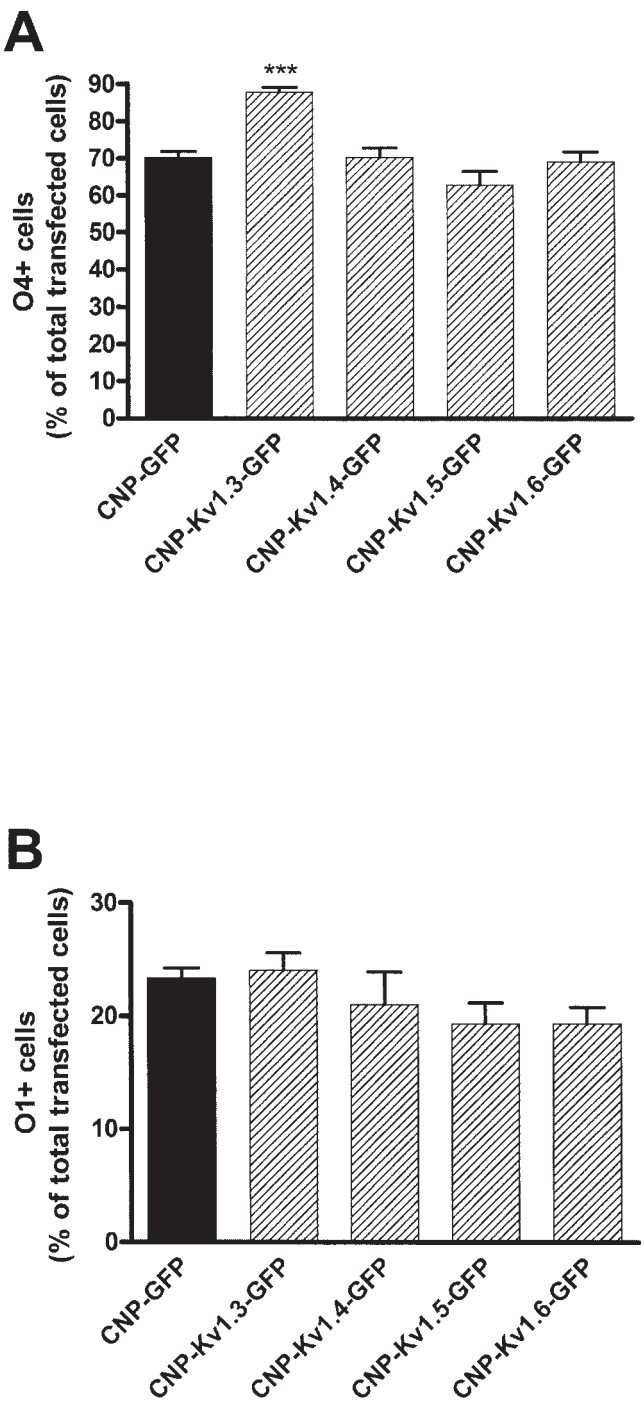

Fig. 6. Overexpression of Kv1.3, 1.4, 1.5, and 1.6 did not significantly influence with oligodendrocyte lineage progression. Transfected oligodendrocyte precursor (OP) cell cultures were allowed to undergo mitogen withdrawal-induced differentiation for 4 days after transfection. Immunostainings were then performed with markers of pre-oligodendrocytes (O_4 antibody) and mature oligodendrocytes (O_1 antibody). Only Kv1.3 overexpression caused a small (~15% increase), but significant change in the percentage of O_4^+ pre-oligodendrocytes ($P < 0.001$, Bonferroni's multiple comparison test). Overexpression of Kv1.4, 1.5, and 1.6 subunits did not have any effect. Overexpression of any of the Kv1.3, 1.4, 1.5, and 1.6 subunits did not affect the generation of O_1^+ oligodendrocytes ($P > 0.05$, Bonferroni's multiple comparison test).

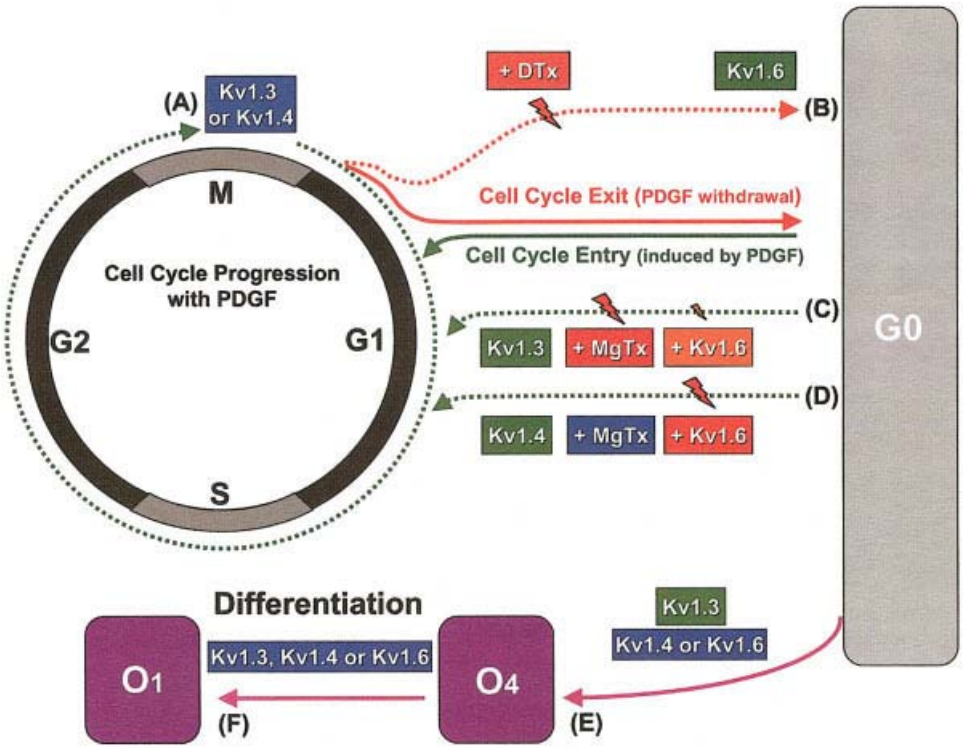

Fig. 7. Schematic illustration of the effects of Kv1 subunit overexpression on oligodendrocyte precursor (OP) cell proliferation and differentiation, summarizing the major findings of the current study. Green boxes denote a significant effect on cell cycle following overexpression of the corresponding Kv1 subunits. Red and orange boxes denote antagonism of these effects. Blue boxes denote no effect following overexpression of Kv1 subunits. Note that experiments in which Kv1.5 was overexpressed consistently resulted in no effect on cell cycle and so are omitted from the schematic for clarity. **A:** Overexpression of Kv1.3 and 1.4 had no effect on OPCs that were already within platelet-derived growth factor (PDGF)-induced cell cycle. **B:** In contrast, overexpression of Kv1.6 causes withdrawal from the cell cycle. This effect was completely antagonized by DTx. **C,D:** Kv1.3 and 1.4 overexpression in cell cycle arrested OPCs led to the induction of proliferation in a manner similar to PDGF. MgTx inhibited this cell cycle entry only in response to Kv1.3 overexpression. Co-expression of Kv1.6 partially inhibited the Kv1.3 induced cell cycle entry and completely abolished the Kv1.4 effect. **E,F:** Prolonged withdrawal of PDGF leads to differentiation of OPCs through O4 and O1 lineage stages. Kv1.4 and 1.6 overexpression does not affect this process. However, a small increase in $O4^+$ cell number (but not $O1^+$) is noted with Kv1.3 overexpression.

more, since PDGF is known to stimulate Kv1.3 expression in OP cells and not that of Kv1.4 (Chittajallu et al., 2002), it could be speculated that Kv1.3-containing channels are the essential mediator of PDGF-driven proliferation in the oligodendroglial lineage. Nevertheless, Kv1.4-containing channels can functionally replace the role of Kv1.3-containing channels in OP cell cycle progression. Kv1.4-containing channels may also be regulated by extracellular signals, other than PDGF, other than PDGF that are part of the complex network that controls OP cell proliferation during CNS development. Studies of chronic spinal cord injury showed that Kv1.4 is largely upregulated in OP cells after insult, and that cells exhibiting changes in Kv1.4 expression may represent proliferating oligodendroglia in the chronically injured spinal cord (Edwards et al., 2002). Therefore, we propose that, under pathological conditions, "reactive" OP cells might divide under the control of the Kv1.4 subunit, rather than through Kv1.3-dependent mechanisms.

Kv1.5 overexpression does not increase proliferation of OP cells in the absence of PDGF, and does not interfere with the proliferative effects of Kv1.3 and Kv1.4 overexpression. These results are consistent with previous demonstration that Kv1.5 antisense oligonucleotides do not cause OP cell cycle arrest, in spite of reducing the functional outward K^+ current (Attali et al., 1997). Thus, both gain-of-function and loss-of-function in vitro studies failed at yielding significant data to support a role of Kv1.5 in oligodendrocyte development, whereas Kv1.5 is known to regulate astrocyte development (MacFarlane and Sontheimer, 2000). Further investigation in vivo after genetic manipulation of this subunit in OP cells will unravel the potential role of Kv1.5 in the oligodendroglial lineage.

Surprisingly, Kv1.6 overexpression had a strong inhibitory effect on OP cell proliferation, i.e. it completely blocked the mitogenic effects of PDGF and antagonized Kv1.3- and Kv1.4-driven proliferation. This could be due to the formation of homomeric Kv1.6-containing channels that negatively modulate OP cell proliferation because of their distinct biophysical properties (Coetzee et al., 1999). Alternatively, overexpression of Kv1.6 by itself could act as

a dominant-negative subunit with formation of heteromeric Kv1.3/Kv1.4/Kv1.6-containing channels, whose pro-mitotic effects are reduced by the presence of Kv1.6. Finally, overexpression of Kv1.6 could indirectly or directly prevent the generation of Kv1.3- and Kv1.4-containing channels and reduce their density. Since DTx completely reversed the effects of Kv1.6 overexpression, Kv1.6-induced inhibition of OP cell proliferation is related to functional Kv1.6-containing channels.

Of all four subunits tested, only overexpression of Kv1.3 had a minor effect on OP cell differentiation, albeit restricted to the early stages of the oligodendrocyte lineage leading to the formation of O_4^+ pre-oligodendrocytes. None of the Kv1 subunits affected cell differentiation to the stage of mature $O1^+$ oligodendrocytes. These results are consistent with our previous findings that OP cell proliferation and differentiation are uncoupled (Belachew et al., 2002).

In conclusion, the present study indicates that specific *shaker*-type Kv1 potassium channel subunits may play differential roles during oligodendrocyte development (Fig. 7). Kv1.3 and Kv1.4 mimic the effects of a well characterized and potent mitogen (PDGF) to promote OP cell proliferation, because they are likely to be the mediators of such effects. In contrast, Kv1.6 prevents the mitogenic effects of PDGF, and of Kv1.3 and Kv1.4 overexpression (Fig. 7). The extent to which these functions of Kv1 channels can be regulated by spatial, temporal, and contextual cues in vivo remains to be explored. Another essential issue to be addressed in the near future will be to understand how early stages of oligodendroglial development can be influenced by distinct stoichiometry of potassium channel subunits, which elicit similar I_k currents with only subtle kinetic differences.

ACKNOWLEDGMENTS

The authors are particularly grateful to Professor O. Pongs for providing all Kv1 cDNAs. We thank Dr. Alexei Morozov for critically reading this manuscript.

REFERENCES

Attali B, Wang N, Kolot A, Sobko A, Cherepanov V, Soliven B. 1997. Characterization of delayed rectifier Kv channels in oligodendrocytes and progenitor cells. J Neurosci 17:8234–8245.

Belachew S, Yuan X, Gallo V. 2001. Unraveling oligodendrocyte origin and function by cell-specific transgenesis. Dev Neurosci 23:287–298.

Belachew S, Aguirre AA, Wang H, Vautier F, Yuan X, Anderson S, Kirby M, Gallo V. 2002. Cyclin-dependent kinase-2 controls oligodendrocyte progenitor cell cycle progression and is downregulated in adult oligodendrocyte progenitors. J Neurosci 22:8553–8562.

Belachew S, Chittajallu R, Aguirre AA, Yuan X, Kirby M, Anderson S, Gallo V. 2003. Postnatal NG2 proteoglycan-expressing progenitor cells are intrinsically multipotent and generate functional neurons. J Cell Biol 161:169–186.

Casaccia-Bonnefil P, Tikoo R, Kiyokawa H, Friedrich V Jr, Chao MV, Koff A. 1997. Oligodendrocyte precursor differentiation is perturbed in the absence of the cyclin-dependent kinase inhibitor p27Kip1. Genes Dev 11:2335–2346.

Casaccia-Bonnefil P, Hardy RJ, Teng KK, Levine JM, Koff A, Chao MV. 1999. Loss of p27Kip1 function results in increased proliferative capacity of oligodendrocyte progenitors but unaltered timing of differentiation. Development 126:4027–4037.

Chandy KG, Gutman GA. 1993. Nomenclature for mammalian potassium channel genes. Trends Pharmacol Sci 14:434.

Chittajallu R, Chen Y, Wang H, Yuan X, Ghiani CA, Heckman T, McBain CJ, Gallo V. 2002. Regulation of Kv1 subunit expression in oligodendrocyte progenitor cells and their role in G_1/S phase progression of the cell cycle. Proc Natl Acad Sci USA 99:2350–2355.

Coetzee WA, Amarillo Y, Chiu J, Chow A, Lau D, McCormack T, Moreno H, Nadal MS, Ozaita A, Pountney D, Saganich M, Vega-Saenz dM, Rudy B. 1999. Molecular diversity of K^+ channels. Ann NY Acad Sci 868:233–285.

DeCoursey TE, Chandy KG, Gupta S, Cahalan MD. 1984. Voltage-gated K^+ channels in human T lymphocytes: a role in mitogenesis? Nature 307:465–468.

Dubois JM, Rouzaire-Dubois B. 1993. Role of potassium channels in mitogenesis. Prog Biophys Mol Biol 59:1–21.

Durand B, Gao FB, Raff M. 1997. Accumulation of the cyclin-dependent kinase inhibitor p27/Kip1 and the timing of oligodendrocyte differentiation. EMBO J 16:306–317.

Durand B, Fero ML, Roberts JM, Raff MC. 1998. p27Kip1 alters the response of cells to mitogen and is part of a cell-intrinsic timer that arrests the cell cycle and initiates differentiation. Curr Biol 8:431–440.

Edwards L, Nashmi R, Jones O, Backx P, Ackerley C, Becker L, Fehlings MG. 2002. Upregulation of Kv 1.4 protein and gene expression after chronic spinal cord injury. J Comp Neurol 443:154–167.

Gallo V, Ghiani CA. 2000. Glutamate receptors in glia: new cells, new inputs and new functions. Trends in Pharmacological Sciences 21: 252–258.

Gallo V, Zhou JM, McBain CJ, Wright P, Knutson PL, Armstrong RC. 1996. Oligodendrocyte progenitor cell proliferation and lineage progression are regulated by glutamate receptor-mediated K^+ channel block. Journal of Neuroscience 16:2659–2670.

Ghiani CA, Eisen AM, Yuan XQ, DePinho RA, McBain CJ, Gallo V. 1999a. Neurotransmitter receptor activation triggers $p27^{Kip1}$ and $p21^{CIP1}$ accumulation and G_1 cell cycle arrest in oligodendrocyte progenitors. Development 126:1077–1090.

Ghiani CA, Gallo V. 2001. Inhibition of cyclin E-cyclin-dependent kinase 2 complex formation and activity is associated with cell cycle arrest and withdrawal in oligodendrocyte progenitor cells. Journal of Neuroscience 21:1274–1282.

Ghiani CA, Yuan XQ, Eisen AM, Knutson PL, DePinho RA, McBain CJ, Gallo V. 1999b. Voltage-activated K^+ channels and membrane depolarization regulate accumulation of the cyclin-dependent kinase inhibitors $p27^{Kip1}$ and $p21^{CIP1}$ in glial progenitor cells. J Neurosci 19:5380–5392.

Gravel M, Di Polo A, Valera PB, Braun PE. 1998. Four-kilobase sequence of the mouse CNP gene directs spatial and temporal expression of lacZ in transgenic mice. J Neurosci Res 53:393–404.

Knutson P, Ghiani CA, Zhou JM, Gallo V, McBain CJ. 1997. K^+ channel expression and cell proliferation are regulated by intracellular sodium and membrane depolarization in oligodendrocyte progenitor cells. J Neurosci 17:2669–2682.

Levison SW, Goldman JE. 1993. Both oligodendrocytes and astrocytes develop from progenitors in the subventricular zone of postnatal rat forebrain. Neuron 10:201–212.

Levison SW, Chuang C, Abramson BJ, Goldman JE. 1993. The migrational patterns and developmental fates of glial precursors in the rat subventricular zone are temporally regulated. Development 119:611–622.

Louis JC, Magal E, Muir D, Manthorpe M, Varon S. 1992. CG-4, a new bipotential glial cell line from rat brain, is capable of differentiating in vitro into either mature oligodendrocytes or type-2 astrocytes. J Neurosci Res 31:193–204.

MacFarlane SN, Sontheimer H. 1997. Electrophysiological changes that accompany reactive gliosis in vitro. J Neurosci 17:7316–7329.

MacFarlane SN, Sontheimer H. 2000. Modulation of Kv1.5 currents by Src tyrosine phosphorylation: potential role in the differentiation of astrocytes. J Neurosci 20:5245–5253.

McCarthy KD, de Vellis J. 1980. Preparation of separate astroglial and oligodendroglial cell cultures from rat cerebral tissue. J Cell Biol 85:890–902.

Ruppersberg JP, Schroter KH, Sakmann B, Stocker M, Sewing S, Pongs O. 1990. Heteromultimeric channels formed by rat brain potassium-channel proteins. Nature 345:535–537.

Sheng M, Liao YJ, Jan YN, Jan LY. 1993. Presynaptic A-current based on heteromultimeric K^+ channels detected in vivo. Nature 365:72–75.

Sobko A, Peretz A, Shirihai O, Etkin S, Cherepanova V, Dagan D, Attali B. 1998. Heteromultimeric delayed-rectifier K^+ channels in Schwann cells: developmental expression and role in cell proliferation. J Neurosci 18:10398–10408.

Tang XM, Strocchi P, Cambi F. 1998. Changes in the activity of cdk2 and cdk5 accompany differentiation of rat primary oligodendrocytes. J Cell Biochem 68:128–137.

Wonderlin WF, Strobl JS. 1996. Potassium channels, proliferation and G1 progression. J Membr Biol 154:91–107.

Yuan X, Eisen AM, McBain CJ, Gallo V. 1998. A role for glutamate and its receptors in the regulation of oligodendrocyte development in cerebellar tissue slices. Development 125:2901–2914.

Yuan X, Chittajallu R, Belachew S, Anderson S, McBain CJ, Gallo V. 2002. Expression of the green fluorescent protein in the oligodendrocyte lineage: a transgenic mouse for developmental and physiological studies. J Neurosci Res 70:529–545.

7.15 Publication #15: Nguyen, L., Malgrange, B., Breuskin, I., Bettendorff, L., Moonen, G., Belachew, S., and Rigo, J.-M. (2003). Autocrine/paracrine activation of the $GABA_A$ receptor inhibits the proliferation of neurogenic polysialylated neural cell adhesion molecule-positive ($PSA\text{-}NCAM^+$) precursor cells from postnatal striatum. *J. Neurosci.* 23:3278-3294.

3278 • The Journal of Neuroscience, April 15, 2003 • 23(8):3278–3294

Autocrine/Paracrine Activation of the $GABA_A$ Receptor Inhibits the Proliferation of Neurogenic Polysialylated Neural Cell Adhesion Molecule-Positive ($PSA\text{-}NCAM^+$) Precursor Cells from Postnatal Striatum

Laurent Nguyen,[1] Brigitte Malgrange,[1] Ingrid Breuskin,[1] Lucien Bettendorff,[1] Gustave Moonen,[1,2] Shibeshih Belachew,[1,2]* and Jean-Michel Rigo[1]*

[1]Center for Cellular and Molecular Neurobiology, University of Liège, B-4020 Liège, Belgium, and [2]Department of Neurology, University of Liège, C.H.U. Sart Tilman, B-4000 Liège, Belgium

GABA and its type A receptor ($GABA_AR$) are present in the immature CNS and may function as growth-regulatory signals during the development of embryonic neural precursor cells. In the present study, on the basis of their isopycnic properties in a buoyant density gradient, we developed an isolation procedure that allowed us to purify proliferative neural precursor cells from early postnatal rat striatum, which expressed the polysialylated form of the neural cell adhesion molecule (PSA-NCAM). These postnatal striatal $PSA\text{-}NCAM^+$ cells were shown to proliferate in the presence of epidermal growth factor (EGF) and formed spheres that preferentially generated neurons *in vitro*. We demonstrated that $PSA\text{-}NCAM^+$ neuronal precursors from postnatal striatum expressed $GABA_AR$ subunits *in vitro* and *in situ*. GABA elicited chloride currents in $PSA\text{-}NCAM^+$ cells by activation of functional $GABA_AR$ that displayed a typical pharmacological profile. $GABA_AR$ activation in $PSA\text{-}NCAM^+$ cells triggered a complex intracellular signaling combining a tonic inhibition of the mitogen-activated protein kinase cascade and an increase of intracellular calcium concentration by opening of voltage-gated calcium channels. We observed that the activation of $GABA_AR$ in $PSA\text{-}NCAM^+$ neuronal precursors from postnatal striatum inhibited cell cycle progression both in neurospheres and in organotypic slices. Furthermore, postnatal $PSA\text{-}NCAM^+$ striatal cells synthesized and released GABA, thus creating an autocrine/paracrine mechanism that controls their proliferation. We showed that EGF modulated this autocrine/paracrine loop by decreasing GABA production in $PSA\text{-}NCAM^+$ cells. This demonstration of GABA synthesis and $GABA_AR$ function in striatal $PSA\text{-}NCAM^+$ cells may shed new light on the understanding of key extrinsic cues that regulate the developmental potential of postnatal neuronal precursors in the CNS.

Key words: **$GABA_A$ receptors; newborn rat striata; proliferation; PSA-NCAM; whole-cell patch-clamp; RT-PCR; HPLC; immunocytochemistry**

Introduction

During CNS development, all types of neurons and glial cells are derived from primordial neural stem cells (NSCs) (Edlund and Jessell, 1999) and emerge, according to a precise time schedule, through a complex sequence of intermediate precursors. Although the conventional view of the adult CNS used to be a structurally constant organ, recent experimental evidence determined that cells are regularly added *de novo* to several CNS areas during adulthood (for review, see Gross, 2000). NSCs are defined by their ability to self-renew and to generate the main cell lineages of the CNS (McKay, 1997). NSCs have been isolated from embryonic and newborn CNS as well as from specific restricted regions of the adult mammalian CNS, including the subventricular zone [(SVZ) postnatally termed the subependymal zone] and the dentate gyrus of the hippocampus (for review, see Weissman et al., 2001). At early stages of CNS cell fate determination, NSCs give rise to progenitors that express the polysialylated form of the neural cell adhesion molecule (PSA-NCAM) (Doetsch et al., 1999). Many tissues expressing PSA-NCAM during development show a progressive loss of PSA carbohydrate residues, but $PSA\text{-}NCAM^+$ cells persist in several adult brain regions in which neuronal plasticity and sustained formation of new neurons occur (Bonfanti et al., 1992; Seki and Arai, 1993; Doetsch et al., 1997). PSA-NCAM has been shown to be involved in changes of cell morphology that are necessary for motility, axonal guidance, synapse formation, and functional plasticity in the CNS (for review, see Yoshida et al., 1999; Bruses and Rutishauser, 2001).

Although they are already restricted to either a glial (Trotter et

Received July 31, 2002; revised Jan. 27, 2003; accepted Jan. 29, 2003.

We are grateful to Dr. P. Legendre (Université Pierre et Marie Curie, Paris, France) for providing helpful comments on this manuscript. We thank B. Rogister (Université de Liège, Liège, Belgium), G. Rougon (Université de la Méditerranée, Marseille, France), and J. Eriksson (University of Turku, Turku, Finland) for their generous gifts of antibodies. We thank P. Ernst-Gengoux, A. Brose, and M. Louvet for their technical support and expertise. B. Malgrange and S. Belachew are research associate and postdoctoral researcher, respectively, of the Fonds National de la Recherche Scientifique (FNRS) (Belgium). This work was supported by the Fonds pour la Formation à la Recherche dans l'Industrie et dans l'Agriculture, the FNRS, the Fondation Médicale Reine Elisabeth, the Fondation Charcot, and the Ligue Belge de la Sclérose en Plaques.

*S.B. and J.-M.R. contributed equally to this work.

Correspondence should be addressed to L. Nguyen, Center for Cellular and Molecular Neurobiology, University of Liège, 17 Place Delcour, B-4020 Liège, Belgium. E-mail: laurent.nguyen@student.ulg.ac.be.

 0270-6474/03/233278-17$15.00/0

al., 1989; Grinspan and Franceschini, 1995; Ben Hur et al., 1998; Vitry et al., 1999) or a neuronal (Mayer-Proschel et al., 1997) preferential fate, cultured PSA-NCAM$^+$ progenitors preserve a relative degree of pluripotentiality (Marmur et al., 1998; Vitry et al., 2001). Considering that PSA-NCAM$^+$ cells can be neatly used for brain repair purposes (Keirstead et al., 1999; Vitry et al., 2001), there is much interest in studying signaling factors that regulate their development. In this regard, it has been known for many years that neurotransmitters, which belong to the microenvironment of neural cells *in vivo*, regulate morphogenetic events preceding synaptogenesis such as cell proliferation, migration, differentiation, and death (for review, see Nguyen et al., 2001). Along this line, previous reports have suggested that GABA, the major inhibitory neurotransmitter in the mammalian brain, exerts trophic roles during CNS embryonic and postnatal development (Barker et al., 1998).

To investigate whether GABA may control the proliferation of postnatal PSA-NCAM$^+$ neural precursors, we first established an isolation procedure that allows the purification of PSA-NCAM$^+$ precursors from newborn rat striata. Using this *in vitro* preparation together with postnatal striatal organotypic slices, we report the following: (1) epidermal growth factor (EGF)-responsive proliferative PSA-NCAM$^+$ precursors generate spheres committed mostly to a neuronal fate; (2) postnatal PSA-NCAM$^+$ precursors express functional type A GABA receptors ($GABA_A$Rs) and glutamate decarboxylase (GAD) 65 and GAD 67; (3) proliferation of PSA-NCAM$^+$ precursors is inhibited by an EGF-controlled endogenous production of GABA that activates $GABA_A$R in these cells; and (4) $GABA_A$R-dependent inhibition of PSA-NCAM$^+$ cell proliferation is mediated by a complex intracellular signaling involving notably the inhibition of the mitogen-activated protein kinase (MAPK) pathway and an increase of intracellular calcium concentration by opening of voltage-gated calcium channels.

Materials and Methods

Sequential purification of PSA-NCAM$^+$ progenitors. Newborn Wistar rats (0- to 3-d-old rat pups) were raised from our animal facility. They were killed following National Institutes of Health animal welfare guidelines. Briefly, rats were anesthetized and subsequently decapitated. Striata were dissected out and collected in PBS solution supplemented with glucose at 4.5 gm/l. Next, isolated striata, possibly including small parts of subventricular zones, were gently triturated in PBS-HEPES (25 mM) by passing through a fire-polished Pasteur pipette before being filtered with a 15 μm nylon mesh. The cell suspension was then layered on top of a precentrifuged (15 min at 26,000 × *g*) Percoll density gradient (1.04 gm/ml; Amersham Biosciences, Uppsala, Sweden) and further ultracentrifuged for 15 min at 26,000 × *g*. Proliferating PSA-NCAM$^+$ precursor cells were separated from differentiated postmitotic neural cells and cell debris by collecting the interphase located between the bands at 1.052 and 1.102 gm/ml as determined by using density marker beads (Amersham Biosciences) for the calibration of the Percoll gradient after centrifugation (Maric et al., 1997) (see Fig. 1*A*,*B*). The resulting suspension was then centrifuged three times (10 min at 400 × *g*) in PBS-HEPES to eliminate Percoll. The final pellet was resuspended in DMEM/F12 (1:1, v/v; Invitrogen, Merelbeke, Belgium) medium supplemented with 1% (v/v) N2 (25 μg/ml bovine insulin, 100 μg/ml transferrin, 20 nM progesterone, 60 μM putrescine, 30 nM sodium selenite), 1% (v/v) B27 (Invitrogen) with or without EGF (20 ng/ml) supplementation (PeproTech, Rocky Hill, NJ). We refer hereafter to these media as either EGF-containing or EGF-free medium. The final cell suspension was plated either in 50 μl droplets on poly-ornithine-coated (Becton Dickinson, Erembodegem, Belgium) coverslips at a density of 2.10^6 cells/ml for immunocytochemical studies or onto uncoated nonadherent T25 culture flasks in 5 ml of EGF-containing medium at a density of 2.10^5 cells/ml (Sarstedt, Newton, NC). Cells grown in uncoated conditions generated floating spheres (see Fig. 1*I*). After 3 d in EGF-containing medium, growing spheres were allowed to attach for 1 hr on poly-ornithine-coated coverslips before being used further for patch-clamp recordings or immunocytochemical studies.

Immunostainings. Cultures were fixed with 4% (v/v) paraformaldehyde for 10 min at room temperature and permeabilized in 0.1% Triton X-100 (v/v) for 15 min during which subsequent immunostainings were directed toward cytoplasmic epitopes. For anti-$GABA_A$ α subunit staining, cells were fixed with a methanol/acetic acid (95:5, v/v) mixture for 5 min. For all immunostainings, nonspecific binding was blocked by a 30 min treatment in a PBS solution containing nonfat dry milk (15 mg/ml). Cells were then incubated overnight at 4°C with primary antibodies, i.e., mouse anti-PSA-NCAM at 1:500 (anti-Men-B antibody; generous gift from G. Rougon, Université de la Méditerranée, Marseille, France), rabbit anti-nestin at 1:400 (generous gift from Prof. J. Eriksson, University of Turku, Turku, Finland), mouse anti-A2B5 at 1:100 (Boehringer Mannheim, Mannheim. Germany), mouse anti-βIII tubulin at 1:1500 (clone Tuj1, Babco, Richmond, CA), mouse anti-MAP2ab at 1:100 (clone AP20, Boehringer Mannheim), mouse monoclonal anti-O4 at 1:150 (Chemicon, Temecula, CA), rabbit anti-glial fibrillary acidic protein (GFAP) at 1:1500 (Dako, Prosan, Belgium), rabbit anti-NF-M at 1:350 (Chemicon), mouse anti-synaptophysin at 1:200 (Sigma-Aldrich, Bornem, Belgium), goat anti-$GABA_A$ α subunits (α_1–α_3, α_5) at 1:40 (clone C-20, Santa Cruz Biotechnology, Santa Cruz, CA), goat anti-$GABA_A$ $\beta_{1\text{-}3}$ subunits at 1:50 (clone N-19, Santa Cruz Biotechnology), goat anti-$GABA_A$ $\gamma_{1\text{-}4}$ subunits antibody at 1:50 (clone M-20, Santa Cruz Biotechnology), rabbit anti-GABA at 1:400 (Incstar, Stillwater, MN), rabbit anti-GAD (GAD 67) at 1:500 (Biogenesis, Poole, UK), and rabbit anti-GAD 65 at 1:50 (clone H-95, Santa Cruz Biotechnology). Secondary antibodies were diluted in PBS solution and applied for 45 min at room temperature. These included Cy5-, FITC-, or TRITC-conjugated anti-rabbit Ig antibodies (1:500), Cy5-, FITC-, or TRITC-conjugated anti-mouse IgG (1:500), and Cy5-, FITC-, or TRITC-conjugated anti-mouse IgM (all from Jackson ImmunoResearch Laboratory, West Grove, PA), or FITC- or TRITC-conjugated anti-mouse IgG_2a (ImTec Diagnostics, Antwerp, Belgium). Three rinses in PBS were performed between different steps. Preparations were mounted in Fluoprep (Biomerieux). Images were acquired using a laser scanning confocal microscope (MRC1024, Bio-Rad, Hertfordshire, UK).

For quantitative immunostainings, before immunocytochemical procedure, spheres were mechanically dissociated and further plated onto poly-ornithine-coated coverslips. Cells were allowed to attach for 1 hr before fixation. For counting, cells were counterstained with the nuclear dye ethidium homodimer-1 (Etd1) (applied at 6.10^{-7} M for 7 min; Molecular Probes, Leiden, The Netherlands) or Hoescht 33258 (0.4 μg/ml for 15 min). Ten nonoverlapping microscopic fields (±50 cells per field) (Axiovert 135 fluorescence microscope, 40× objective; Zeiss) were counted for each coverslip in a minimum of two or three separate experiments.

Frozen 30 μm tissue sections were prepared as described previously (Yuan et al., 2002). Immunohistochemical stainings were processed following a procedure identical to that of cultured cells.

Electrophysiological recordings. For patch-clamp recordings, Cell-Tak (Becton Dickinson)-coated coverslips containing 1–3 hr adhesive spheres were transferred to the stage of a Zeiss interferential contrast microscope equipped with fluorescence. Coverslips were maintained at 37°C in a recording chamber that was perfused continuously with a saline solution containing (in mM): 116.0 NaCl, 11.1 D-glucose, 5.4 KCl, 5.4, 1.8 $CaCl_2{\cdot}2H_2O$, 2.0 $MgCl_2{\cdot}6H_2O$, 10.0 HEPES, pH 7.2. Cs^+-containing solutions were composed as follows (in mM): 116.0 NaCl, 5.4 CsCl, 11.1 D-glucose, 1.8 $CaCl_2{\cdot}2H_2O$, 2.0 $MgCl_2{\cdot}6H_2O$, 9.0 HCl, 5.0 HEPES, 26.2 $NaHCO_3$, 5.0 $BaCl_2{\cdot}2H_2O$, pH 7.2. Low chloride solution contained (in mM): 8.0 NaCl, 108.0 Na-gluconate, 5.4 CsCl, 5.4, 11.1 D-glucose, 1.8 $CaCl_2{\cdot}2H_2O$, 2.0 $MgCl_2{\cdot}6H_2O$, 17.0 HCl, 5.0 HEPES, 26.2 $NaHCO_3$, 5.0 $BaCl_2{\cdot}2H_2O$, pH 7.4. All drugs were applied by a microperfusion system (SPS-8, List Medical). Borosilicate recording electrodes (15–20 MΩ) were made using a Flaming-Brown microelectrode puller (P97, Sutter Instruments Novato, CA). Micropipettes were filled with an

intracellular-like solution containing (in mM): 130.0 KCl, 1.0 $CaCl_2 \cdot 2H_2O$, 11.1 D-glucose, 10.0 EGTA, 2.5 Na_2-ATP, 2.5 Mg-ATP, 10.0 HEPES, pH 7.4. In Cs^+-containing pipettes, used for the establishment of the GABA-evoked current–voltage relationship, KCl was equimolarly replaced by CsCl and $BaCl_2 \cdot 2H_2O$ was added at 5 mM to block K^+ channels. Current–voltage relationships were obtained using a series of voltage steps (ranging from −140 to +100 mV) before, during, and after application of GABA. The current–voltage curve was established by fitting experimental data to the Goldman-Hodgkin and Katz equation:

$$I_S = P_S \cdot Z_S \cdot \frac{E \cdot F^2}{R \cdot T} \cdot \frac{[S]_i - [S]_o \cdot \exp\left(-Z_S \cdot \frac{F \cdot E}{R \cdot T}\right)}{1 - \exp\left(-Z_S \cdot \frac{F \cdot E}{R \cdot T}\right)},$$

where I_s corresponds to the current generated (ampere), P_s the membrane permeability, Z_s the valence, $[S]_i$ the intracellular concentration ($M \cdot l^{-1}$), and $[S]_o$ the extracellular concentration ($M \cdot l^{-1}$) of the ion *S*, respectively. *E* corresponds to the membrane potential, *F* is the Faraday's constant, *R* is the ideal gas constant, and *T* is the absolute temperature. Electrophysiological recordings were performed with a patch-clamp amplifier (RK400, Bio-Logic, Claix, France) using the whole-cell configuration of the patch-clamp recording technique (Hamill et al., 1981). Cells were injected with Lucifer yellow (Molecular Probes) (1 μg/ml Lucifer yellow solution in the recording pipette) during voltage-clamp recordings to allow their *post hoc* immunocytochemical characterization. Series resistances (10–20 Ω) were electronically compensated (80–85%), and current traces were filtered at 3 kHz, acquired and digitized at 0.5 kHz, and stored on an personal computer system. Control of drug application, data acquisition, and data analysis was achieved using an ITC-16 acquisition board (Instrutech Corporation, Great Neck, NY) and the TIDA for Windows software (HEKA Elektronik Lombrecht/Pfolz, Germany).

RT-PCR. Total RNAs from adult Wistar rat brains and from PSA-NCAM$^+$ spheres derived from postnatal day 0 (P0)–P3 Wistar rat striata were extracted and purified using the RNAgents Total RNA Isolation System kit (Promega, Leiden, The Netherlands). One microgram of total RNA was reverse transcribed using primers with oligo-dT and 200 U of reverse transcriptase (Kit Superscript 1, Life Technologies). Two microliters resulting from the RT reaction were used as template and added to 50 μl of PCR reaction mixture containing 0.2 μM of both forward and reverse primers synthesized by Eurogentec (Seraing, Belgium) (see Table 1), 0.2 mM of each dNTP, 1.5 mM of $MgCl_2$, and 5 U of *Taq* Polymerase (Promega). The PCR program was run with an MJ Research PTC 200 instrument. The thermal cycling protocol started with a 2 min preincubation at 94°C followed by 35 cycles made (1) 30 sec at 94°C, (2) 30 sec at 60°C, and (3) 30 sec at 72°C. The protocol was finally completed by an extension step at 72°C for 7 min. We used 64°C for the annealing of α_3 primers and 55°C for γ_3, GAD 65, and GAD 67 primers. Ten microliters of the PCR reaction were analyzed in a 1.4% agarose gel in Tris–acetic acid–EDTA (TAE) buffer.

Bromodeoxyuridine and [^{3}H]thymidine incorporation assays. After 2 d of growth in EGF-containing medium (as described previously), PSA-NCAM$^+$ spheres were harvested, centrifuged (10 min at 200 × *g*), and rinsed three times in the EGF-free medium before being transferred into uncoated nonadherent T25 culture flasks (Sarstedt) in mitogen-free medium. After 24 hr in this medium, bromodeoxyuridine (BrdU) (20 μM; Sigma), which is a S-phase marker, was added to the cultures for 18 hr before fixation and staining. All treatments were performed simultaneously with the addition of BrdU. PSA-NCAM, βIII tubulin, O4, and GFAP immunolabelings were performed as described above. Coverslips were then postfixed for 10 min in 4% (v/v) paraformaldehyde, permeabilized in 0.1% Triton X-100 for 10 min, incubated in 0.07N NaOH for 10 min, and finally postfixed again for 10 min before incubation with an anti-BrdU FITC-conjugated antibody for 45 min (1:3, v/v; Becton-Dickinson). The preparations were mounted in Fluoprep and imaged using a Bio-Rad MRC1024 laser scanning confocal microscope. The fraction of cells that incorporated BrdU was determined by counting 10 nonoverlapping microscopic fields (±50 cells per field) (Axiovert 135 fluorescence microscope, 40× objective, Zeiss) for each coverslip in at least three separate experiments.

In similar culture conditions, the proliferation of PSA-NCAM$^+$ spheres was also quantified by measuring the incorporation of [^{3}H]thymidine (Amersham Biosciences, Roosendaal, The Netherlands). All treatments were performed simultaneously with the addition of [^{3}H]thymidine (2 μCi/ml) to the medium for 18 hr. Cultures were washed three time with PBS and digested with NaOH (0.1N), and the radioactivity was counted in a liquid scintillation counter (Wallac WinSpectral 1414 liquid scintillation counter, Turku, Finland). The [^{3}H]thymidine incorporation was normalized for cellular protein concentration measured by the Bradford technique (Bradford, 1976) and expressed as disintegrations per minute of [^{3}H]thymidine incorporated per milligram of protein. Results from the treated conditions were then expressed as percentages of control values. We always performed three separate experiments in triplicate wells for each condition.

Terminal deoxynucleotidyl transferase-mediated dUTP nick end labeling assay. To assess apoptosis occurring in our cultures, spheres were gently dissociated after treatments, and cells were plated for 15–30 min on Cell-Tak (Becton Dickinson)-coated coverslips at a density of 2.10^6 cells/ml. Terminal deoxynucleotidyl transferase-mediated dUTP nick end labeling (TUNEL) staining was then performed according to the method of Gavrieli et al.(1992), using the ApopTag fluorescent detection kit (Oncor, Gaithersburg, MD). Cultures were fixed with 4% paraformaldehyde for 10 min at room temperature. Equilibration buffer was then applied for 30 min at 20°C. Cultures were incubated with working strength stop/wash buffer, washed, and further incubated with anti-digoxigenin–FITC. For cell counting, cultures were counterstained with ethidium homodimer-1 (Molecular Probes; applied at 6.10^{-7} M for 7 min). Ten nonoverlapping microscopic fields (±50 cells per field) (Axiovert 135 fluorescence microscope, 40× objective, Zeiss) were counted for each coverslip in a minimum of three separate experiments.

HPLC procedure. We used an adaptation of a procedure described previously (Bettendorff et al., 1996). Cultures of PSA-NCAM$^+$ spheres (25 mg) were homogenized in 1 ml of an 80% ethanol solution at 0°C in a glass–glass homogenizer (Potter-Elvehjem device). Homogenates were centrifuged (30 min at 5000 × *g*), and the supernatants were saved. The pellets were resuspended in 1 ml of a 60% ethanol solution, homogenized, and centrifuged as described above. The second supernatant was pooled with the first, and the liquids were evaporated under a stream of nitrogen. The residue was dissolved in 300 μl of water and centrifuged (30 min, 5000 × *g*). An aliquot of 100 μl from the supernatant was added to 100 μl of $LiCO_3$ (80 mM, pH 8.5) before dansylation by addition of 100 μl dansyl chloride (1.5 mg/ml in acetonitrile). The mixture was incubated in the dark for 35 min at 25°C, and the reaction was stopped with 10 μl of 2% ethylamine.

We used a Bio-SiL C18 HL column (5 μm, 150 × 4.6 mm; Bio-Rad Laboratories, Nazareth-Eke, Belgium) heated at 50°C. After injection of the dansylated solution (20 μl), GABA was eluted by means of a linear gradient at a flow rate of 1.5 ml/min. The column was equilibrated in 85% solvent A (3% tetrahydrofuran, 0.57% acetic acid, 0.088% triethylamine in water) and 15% solvent B (3% tetrahydrofuran, 0.57% acetic acid, 0.088% triethylamine, 70% methanol in water). After injection, the percentage of solvent B was increased linearly to reach 100% after 40 min. Initial conditions were restored within 2 min, and the next sample was injected after a reequilibration period of 5 min. A fluorescent spectrometer (LS-4, Perkin-Elmer, Norwalk, CT) was used with the wavelengths set at 334 nm for excitation and 522 nm for emission. A reference standard, composed of a GABA solution (0.1 mM) in water, was dansylated simultaneously with samples.

Calcium imaging. PSA-NCAM$^+$ cells were loaded with the calcium indicator dye fluo-3 AM (6 μM) (Molecular Probes) by bath application for 30 min at 37°C. Fluo-3 AM is a non-ratiometric indicator dye that triggers an increase of cell fluorescence intensity when the intracellular calcium concentration increases. After fluo-3 loading, cells were washed three times in Locke solution containing (in mM): 154 NaCl, 5.6 KCl, 5.6 glucose 5.6, 2.3 $CaCl_2 \cdot 2H_2O$, 10.0 HEPES, pH 7.2. Calcium responses were recorded as digitized images acquired with a Bio-Rad MRC 1000 laser scanning confocal system coupled to a Zeiss Axiovert 135 micro-

scope with a plan-NEOFLUAR objective (40×, 1.3 numerical aperture, oil immersion). The Time Course Software Module program (Bio-Rad) was used to control the confocal microscope to acquire a series of images at intervals from 2 to 5 sec. The different reagents diluted in Locke solution were applied by a microperfusion system (SPS-8, List-Medical). The series of digitized fluorescence images were analyzed by a program that determined the average level of fluorescence above the background level of each cell for every time point sampled. The recorded areas were delimited by placing rectangular boxes around every cell in a field. A "background" box was also defined in a noncellular area of each scanned image. The averaged intensity of the pixels within a boxed cellular region was calculated by the program, and the averaged intensity of the pixels within the "background" box defined for the image was subtracted from this value. To compensate for variable dye loading between cells, these background-corrected values were normalized by conversion to percentage changes relative to a baseline measurement for each boxed cellular region at the start of a time series (F_t/F_0).

Organotypic slice cultures. We used a technique adapted from Yuan et al. (1998). Briefly, whole brains were dissected from P1 Sprague Dawley rats and placed in oxygenated (carbogen, 95% O_2/5% CO_2) artificial CSF containing (in mM): 120 NaCl, 25 $NaHCO_3$, 3.3 KCl, 1.2 NaH_2PO_4, 1.8 $CaCl_2$, 2.4 $MgSO_4$, 10 glucose, pH 7.2. Brains were then sliced coronally (400 μm) using a vibratome. The SVZ and striatum (as depicted in Fig. 10*A1*) were separately microdissected to allow a distinct assessment of SVZ and striatal cells. SVZ and striatal slices were placed into sterile Millicell (Millipore, Bedford, MA) in six-well plates (Falcon) containing 1 ml of EGF-free medium (as described previously). Treatments with drugs began 4 hr after the slicing procedure. The medium was replaced by EGF-free medium containing simultaneously BrdU (20 μM; Sigma) and drugs for 18 hr. Cell viability was assessed in each experiment at the end of the BrdU incorporation time frame by using a LIVE/DEAD viability/cytotoxicity kit (L-3224, Molecular Probes). Slices were then gently mechanically dissociated, and cells were plated for 1 hr on poly-ornithine-coated coverslips before fixation and immunocytochemical analysis.

Drugs. GABA, muscimol, bicuculline, picrotoxin, pentobarbital, baclofen, saclofen, SR-95531, U0126, and nifedipine were obtained from Sigma-Aldrich, and clonazepam was purchased from Roche Diagnostics Belgium (Brussels, Belgium).

Data analysis. For electrophysiological recordings, *n* represented the number of recorded cells. Peak currents in the different experimental conditions were measured and subsequently normalized to the initial response (100%) in control conditions. Agonist concentration–response profiles were fitted to the following equation: $I/I_{max} = 1/(1+(EC_{50}/[\text{agonist}])^{nh})$, where I and I_{max}, respectively, represent the normalized agonist-induced current at a given concentration and the maximum current induced by a saturating concentration of the agonist. EC_{50} is the half-maximal effective agonist concentration, and *nh* is the Hill slope. The concentration–response of modulations was fitted by a similar procedure, except for clonazepam, where a polynomial curve was used.

The quantitative results of [^{3}H]thymidine incorporation assays and immunocytochemical experiments were expressed as mean ± SEM values arising from a minimum of three independent experiments (*n*).

For all experiments, a statistical analysis was performed either using unpaired two-tailed Student's *t* test between control and experimental conditions or using a one-way ANOVA (ANOVA-1) followed by a Dunnett's post-test for multiple comparisons (GraphPad Prism software, version 2.04 a, San Diego, CA). The level of significance was expressed as follows: $^*p < 0.05$, $^{**}p < 0.01$, and $^{***}p < 0.0001$.

Results

Purification and characterization of PSA-NCAM$^+$ progenitors acutely isolated from newborn rat striata

To obtain a highly enriched population of PSA-NCAM$^+$ progenitors, newborn rat (P0–P3) striata were first dissociated as described previously for neural stem cell cultures (Reynolds and Weiss, 1992). The cell suspension was then layered on top of a buoyant density Percoll gradient and further ultracentrifuged (Fig. 1*A*). This isopycnic centrifugation allowed cells to sediment in an equilibrium position equivalent to their own natural buoyant density. We demonstrated that viable, small (7 ± 1 μm in diameter), round cells were separated from more differentiated cells and cell debris by collecting the interphase located in the range of densities between 1.052 and 1.102 gm/ml (Fig. 1*B*). The final cell suspension harvested according to these density criteria was resuspended in EGF-containing medium.

To validate our protocol of purification, we assessed PSA-NCAM$^+$ cells before and after the Percoll centrifugation. The isopycnic centrifugation of cell suspension in a buoyant density gradient allowed us to increase the percentage of PSA-NCAM$^+$ cells from 62.5 ± 15.1% ($n = 3$) to 94 ± 1.0% of total cells ($n = 6$) (Fig. 1*C–E*). After purification by the Percoll centrifugation step, the phenotype of PSA-NCAM$^+$ cell suspension was characterized more extensively. Nestin was observed in 74.9 ± 8.3% ($n = 4$) of total cells, and all nestin$^+$ cells also expressed PSA-NCAM (Fig. 1*E*). We observed that 47.6 ± 4.5% of total cells ($n = 2$) were A2B5$^+$ (Fig. 1*E*). Neuronal phenotypes were investigated by studying the expression of neuron-specific antigens. We found that 74.6 ± 1.4% ($n = 4$) of total acutely purified cells expressed βIII-tubulin (i.e., Tuj1$^+$) (Fig. 1*E,F*), 4.5 ± 2.6% ($n = 2$) expressed type 2a,b microtubule-associated protein (i.e., MAP2ab$^+$) (Fig. 1*E,G*), and 2.6 ± 1.6% ($n = 2$) were neurofilament 145 kDa-positive (i.e., NF-M$^+$) (Fig. 1*E,H*). Importantly, we never found cells that were immunoreactive for synaptophysin, which is a marker of synapse formation (Fig. 1*E*). Finally, we found a low expression of oligodendrocyte (O4) or astrocyte (GFAP) specific markers. Respectively, 2.8 ± 1.2% ($n = 4$) of total cells were O4$^+$ and 4.4 ± 0.8% of total cells ($n = 4$) were GFAP$^+$ (Fig. 1*E*). These results provide evidence that purified PSA-NCAM$^+$ cells from early postnatal rat striatum mostly show antigenic features of neuron-committed progenitor cells.

Purified proliferative PSA-NCAM$^+$ cells form spheres that preferentially generate neurons

After 3 d *in vitro* (DIV) in EGF-containing medium, PSA-NCAM$^+$ progenitor cells proliferated and formed spheres with a mean diameter of 61.8 ± 7.3 μM ($n = 4$) (Fig. 1*I*). A vast majority of cells within 3-DIV-old spheres remained PSA-NCAM$^+$ (89.6 ± 4.7% of total cells; $n = 6$), and Tuj1$^+$ (57.3 ± 1.2% of total cells; $n = 4$) (Fig. 1*J,M*). Interestingly, we observed that all Tuj1$^+$ cells were still PSA-NCAM$^+$ in 3-DIV spheres (data not shown). To quantify cell proliferation within PSA-NCAM$^+$ spheres, we performed a BrdU incorporation assay (18 hr) at 3 DIV. The BrdU incorporation index (BrdU$^+$ cells per total cells) was 17.2 ± 4.0% in the presence of EGF (20 ng/ml) ($n = 2$) (Fig. 1*K,L*). By double immunostaining, we observed that proliferating cells were mostly PSA-NCAM$^+$ because 16.0 ± 4.1% of total cells ($n = 3$) were immunoreactive for both PSA-NCAM and BrdU (Fig. 1*K,L*, left panel). The other way around, we showed that 92.9 ± 4.1% of the total BrdU$^+$ cells were PSA-NCAM$^+$ (Fig. 1*L*, right panel). Conversely, cells expressing markers of lineage commitment were weakly involved in the overall BrdU incorporation index because only 3% of Tuj1$^+$ cells, 1% of O4$^+$ cells, and 2% of GFAP$^+$ cells were also BrdU$^+$ (Fig. 1*L*, left panel). Interestingly, cultured PSA-NCAM$^+$ cells generated predominantly neuron-committed cells after 3 DIV in EGF-containing medium (Fig. 1*E,M–O*). As compared with acutely purified cells, we observed a fourfold and a fivefold increase, respectively, of the relative percentages of MAP2ab$^+$ and NF-M$^+$ cells in 3-DIV spheres, whereas no change was observed for O4$^+$ or GFAP$^+$ cells. Furthermore, with respect to the calculated 1.8-fold increase of the total cell number during the 3-DIV

growth of PSA-NCAM$^+$ spheres (data not shown), the absolute number of cells expressing mature neuronal antigens MAP2ab and NF-M were increased by seven- and eightfold, respectively (Figs. 1*N*,*O*).

PSA-NCAM$^+$ spheres express type A GABA receptors

Given that previous works reported the expression of $GABA_AR$ in early postnatal neuronal progenitor cells, notably in the anterior subventricular zone, we sought to investigate the presence of these receptors in striatal PSA-NCAM$^+$ neuronal precursors (Stewart et al., 2002). To characterize $GABA_AR$ subunit transcripts expressed in PSA-NCAM$^+$ progenitors, total RNAs extracted from 3-DIV spheres were reverse transcribed, and the subsequent cDNAs were amplified by PCR using specific sets of primers aimed at detecting transcripts for α_{1-5}, β_{1-3}, γ_{1-3}, and $\delta GABA_AR$ subunit genes (Table 1). Experiments were replicated three times and consistently yielded bands with the appropriate amplicon size for α_2 (549 bp), α_4 (532 bp), α_5 (300 bp), β_1 (578 bp), β_3 (587 bp), γ_1 (296 bp), γ_2 (423 bp), and γ_3 (336 bp) transcripts, respectively (Fig. 2*A*,*B*). RNAs isolated from total adult rat brains were used as positive control.

The expression of $GABA_AR$ subunit proteins was analyzed by immunocytochemistry in PSA-NCAM$^+$ spheres. We used three polyclonal antibodies directed against $\alpha_{1-3,5}$, β_{1-3}, and γ_{1-4} subunits, respectively, of $GABA_AR$. As illustrated in Figure 2*C–E*, 70.6 ± 13.8% of total cells (counted after mechanical dissociation of spheres) were immunoreactive for $GABA_AR$ α subunit proteins (i.e., $\alpha_{1-3,5}$; $n = 2$) (Fig. 2*C*), 65.6 ± 4.3% of total cells were immunoreactive for $GABA_AR$ β subunits (i.e., β_{1-3}; $n = 2$) (Fig. 2*D*), and 66.6 ± 6.2% of total cells expressed $GABA_AR$ γ subunits (i.e., γ_{1-4}; $n = 3$) (Fig. 2*E*).

GABA triggers whole-cell currents in PSA-NCAM$^+$ spheres by $GABA_A$ receptor activation

We wanted to ascertain by electrophysiological recordings whether PSA-NCAM$^+$ cells expressed functional $GABA_A$ receptors. We therefore recorded cells within PSA-NCAM$^+$ spheres using the whole-cell patch-clamp technique. Occasionally, the Lucifer yellow fluorescent dye was added to the intracellular solution and allowed to diffuse in the recorded cell for *post hoc* immunostainings. All recorded cells filled with Lucifer yellow were PSA-

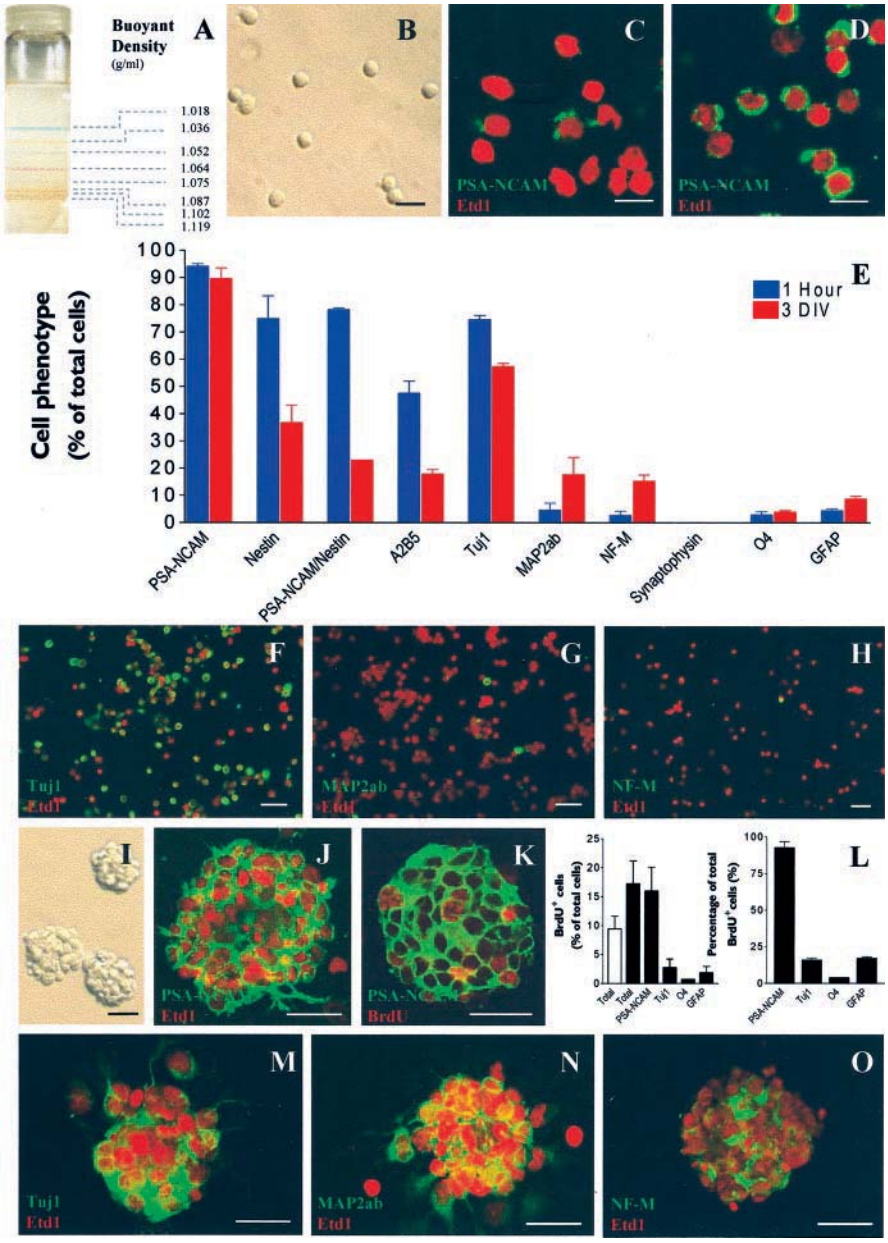

Figure 1. Purification and *in vitro* amplification of proliferative and neurogenic PSA-NCAM$^+$ progenitors from early postnatal striatum. *A*, Bands of color-coded density marker beads in ultracentrifuged Percoll gradient. According to their isopycnic buoyant densities, living PSA-NCAM$^+$ cells (*B*) were separated from differentiated neural cells and cell debris in a continuous Percoll gradient. Cells were collected in the interphase located between the ranges of density: 1052–1102 gm/ml as determined by a tube containing control density beads that was ultracentrifuged simultaneously. *C*, *D*, Confocal images of acutely dissociated cell suspension from newborn rat striatum before (*C*) and after (*D*) selection by centrifugation in a Percoll density gradient. Cells were immunostained for PSA-NCAM (green) and counterstained with the nuclear dye Etd1 (red). Cells acutely purified from early postnatal striatum (1 hr) or dissociated from 3-DIV-old spheres were allowed to adhere onto poly-ornithine-coated coverslips and were assessed by immunostaining. *E*, Histogram comparing the percentage of total cells expressing various markers 1 hr after purification (blue bars) and after 3 d of growth *in vitro* in EGF-containing medium (red bars). *F–H*, Confocal images of representative fields showing acutely purified cells immunostained for markers of neuronal commitment: *F*, Tuj1 (green); *G*, MAP2ab (green); *H*, NF-M (green), and *F–H*, counterstaining with Etd1 (red). Purified cells cultured in EGF-containing medium for 3 d in uncoated conditions formed spheres (*I*) that were composed almost exclusively of PSA-NCAM$^+$ cells. *J*, PSA-NCAM in green and Etd1 in red. *K*, Confocal optical section of a 3-DIV sphere immunostained for BrdU after 18 hr of BrdU incorporation assay in EGF-containing medium (PSA-NCAM in green and BrdU in red). *L*, Histograms representing the percentage of total cells that incorporated BrdU (20 μM) for each immunophenotype (left panel) and the percentage of total BrdU$^+$ cells that expressed a given immunophenotype (right panel), respectively, in the presence (black bars) or absence (open bar) of EGF (20 ng/ml). *M–O*, Confocal optical section of 3-DIV spheres expressing markers of neuron commitment: *M*, Tuj1 (green); *N*, MAP2ab (green); *O*, NF-M (green) and counterstaining with Etd1 (red). Scale bars: *B–D*, 10 μm; *F–K*, 25 μm; *M–O*, 20 μm.

Table 1. Sequences of primers (forward, reverse) used for PCR

cDNA	Primer	Size of product (base pairs)	Sources
$GABA_AR\ \alpha1$	For 5′-CAT TCT GAG CAC TCT CTC GGG AAG-3′ Rev 5′-GTG ATA CGC AGG AGT TTA TTG GGC-3′	396	(Khrestchatisky et al., 1989)
$GABA_AR\ \alpha2$	For 5′-AGG TTG GTG CTG GCT AAC ATCC-3′ Rev 5′-AAC AGA GTC AGA AGC ATT GTA AGT CC-3′	549	(Khrestchatisky et al., 1991)
$GABA_AR\ \alpha3$	For 5′-CAA CAT AGT GGG AAC ACC TAT CC-3′ Rev 5′-GGG AGC TCT GGG GTT TGG GAT TT-3′	350	(Criswell et al., 1997)
$GABA_AR\ \alpha4$	For 5′-CAA AAC CTC CTC CAG AAG TTC CA-3′ Rev 5′-ATG TTA AAT AAT GCC CCA AAT GTG ACT-3′	532	(Wisden et al., 1991)
$GABA_AR\ \alpha5$	For 5′-TGA CCA AAA CCC TCC TTG TCT TCT-3′ Rev 5′-ACC GCA GCC TTT CAT CTT TCC-3′	300	(Khrestchatisky et al., 1989)
$GABA_AR\ \beta1$	For 5′-GTT TGG GGC TTC TCT CTC TTT TCC T-3′ Rev 5′-AGT TAC TGC TCC CTC TCC TCC ATT-3′	578	(Ymer et al., 1989a)
$GABA_AR\ \beta2$	For 5′-CAG GTT CTT ATC CCA GAT TGT CCC-3′ Rev 5′-GGT CCA TCT TGT TGA CAT CCA GG-3′	408	(Ymer et al., 1989b)
$GABA_AR\ \beta3$	For 5′-CTT TTC GGC ATC TTC TCG GC-3′ Rev 5′-TCC ACG CCA GTA ACA GCC TTG-3′	587	(Ymer et al., 1989b)
$GABA_AR\ \gamma1$	For 5′-TAG TAA CAA TAA AGG AAA AAC CAC CAG A-3′ Rev 5′-CCA GAT TGA ACA AGG CAA AAG CT-3′	296	(Ymer et al., 1990)
$GABA_AR\ \gamma2$	For 5′-TGG TGA CTA TGT GGT TAT TGC CGT G-3′ Rev 5′-AGG TGG GTG GCA TTG TTC ATT T-3′	423	(Khrestchatisky et al., 1989)
$GABA_AR\ \gamma3$	For 5′-GAA ATC ATG GCG GCT CTA GTT-3′ Rev 5′-CTC CAT CAG TGC GGC AAA GAC AAA-3′	336	(Stewart et al., 2002)
$GABA_AR\delta$	For 5′-GAC TAC GTG GGC TCC AAC CTG GA-3′ Rev 5′-ACT GTG GAG GTG ATG CGG ATG CT-3′	398	(Zhao and Joho, 1990)
GAD 65	For 5′-CCA TTA CCC CAA TGA GCT TCT-3′ Rev 5′-CCC CAA GCA GCA TCC ACG T-3′	698	(Dkhissi et al., 2001)
GAD 67	For 5′-AAT TGC ACC CGT GTT TGT TCT TAT G-3′ Rev 5′-AGC GCA GCC CCA GCC TTC TTT A-3′	252	(Stewart et al., 2002)

For, Forward; Rev, reverse.

NCAM$^+$ in 3-DIV spheres (Fig. 3*A*). We selectively assessed cells that were located at the accessible periphery of the spheres. The mean membrane potential recorded in current-clamp configuration was -52.9 ± 1.9 mV ($n = 110$ cells). All recordings were performed in the presence of 1 μM strychnine to avoid cross-activation of ionotropic glycine receptors. In voltage-clamp mode (the holding potential was kept at -70 mV), bath application of 1 mM GABA, a concentration that saturates $GABA_A$Rs (Fig. 3*C*), elicited inward currents in 94.6% of total cells with a peak current displaying a mean maximum amplitude of 408.9 ± 46.8 pA ($n = 53$ cells) (Fig. 3*B*).

In GABA-responsive PSA-NCAM$^+$ progenitors, the EC_{50} value (i.e., the concentration that yielded an inward current of half-maximum amplitude) calculated from the sigmoidal concentration–response curve was 6.2 ± 1.1 μM, with a Hill coefficient (n_h) of 0.7 ± 0.2 ($n = 11$ cells) (Fig. 3*C*,*D*). To confirm that GABA-elicited currents were caused specifically by the activation of $GABA_A$Rs, we showed that the specific $GABA_A$R agonist muscimol also induced inward currents in PSA-NCAM$^+$ cells (Fig. 3*F*). For muscimol-induced currents, the concentration–response curve, fitted by the Hill equation, yielded an EC_{50} of 6.5 ± 1.1 μM, with a Hill coefficient (n_h) of 0.5 ± 0.2 ($n = 5$ cells) (Fig. 3*E*,*F*).

The current–voltage relationship of GABA-evoked currents was obtained by applying voltage steps ranging from -140 to $+100$ mV during GABA application. As shown in Figure 3, *G* and *I*, the resulting current–voltage curve could be fitted by the Goldman-Hodgkin-Katz relation (see Materials and Methods) and reversed at $+5.9$ mV ($n = 4$ cells), which is close to the calculated Nernst chloride equilibrium potential (-1.1 mV). When 108 mM of extracellular sodium chloride was replaced by sodium gluconate, the reversal potential shifted to a more positive value ($+27.9$ mV; $n = 5$ cells) (Fig. 3*H*,*J*), consistent with the predicted shift of the calculated Nernst chloride equilibrium potential ($+29.0$ mV).

Pharmacological characterization of functional $GABA_A$Rs expressed in striata-derived PSA-NCAM$^+$ progenitors

In 3-DIV PSA-NCAM$^+$ cells, GABA-induced currents were completely and reversibly inhibited in a dose-dependent manner by the competitive antagonists bicuculline ($IC_{50} = 1.54 \pm 1.12$ μM; $n = 5$ cells) (Fig. 4*A*,*B*) and SR95531 ($IC_{50} = 0.15 \pm 0.01$ μM; $n = 6$ cells) (Fig. 4*C*,*D*) and by the noncompetitive antagonist picrotoxin ($IC_{50} = 4.5 \pm 1.1$ μM; $n = 7$ cells) (Fig. 4*E*,*F*). We also assessed the effect of benzodiazepines and barbiturates, which are positive allosteric modulators of $GABA_A$R. The effects of clonazepam and pentobarbital were studied on currents elicited by a low concentration of GABA (1 μM = EC_{10} = GABA concentration inducing an inward current corresponding to 10% of the maximum GABA-evoked current) to sensitize the detection of a enhancing effect. Our results showed that clonazepam potentiated GABA currents at concentrations ranging from 10 nM to 100 μM, with a maximum effect at 1 μM (212% of I_{GABA} at EC_{10}) (Fig. 4*G*,*H*). Pentobarbital triggered a maximal 5.6-fold increase of the amplitude of GABA-evoked currents in a concentration-dependent manner ($EC_{50} = 2.1 \pm 0.3$ μM; $n = 11$ cells) (Fig. 5*I*,*J*).

$GABA_A$R activation inhibits the proliferation of PSA-NCAM$^+$ progenitors

Because the activation of ionotropic $GABA_A$R has been reported to affect the proliferation of neural progenitors in the ventricular and subventricular zones of the embryonic neocortex (LoTurco et al., 1995; Haydar et al., 2000), we decided to analyze the effect of GABA on proliferation kinetics in striatal early postnatal PSA-NCAM$^+$ progenitor cells. After 48 hr of growth in EGF-containing medium, spheres were transferred to the same medium but devoid of EGF for the next 24 hr. This procedure allowed us to obtain a synchronization of most cells in G_0 (Jones and Kazlauskas, 2001) before starting BrdU or [^{3}H]thymidine incorporation assays (18 hr). The removal of EGF from the medium did not affect the phenotype of cells within these 3-DIV spheres (data not shown).

To compare the proliferation rates of the different cell phenotypes present within 3-DIV spheres, cells were colabeled for BrdU and lineage markers (i.e., PSA-NCAM, Tuj1, O4, and GFAP) (Fig. 5*C*,*F*,*I*). Cytosine arabinoside (10 μM) was used as an internal control inhibiting proliferation in all phenotypes. Although agonists and antagonists of $GABA_A$R did not modify the percentages of O4$^+$/BrdU$^+$ and GFAP$^+$/BrdU$^+$ cells (data not shown), treatment with $GABA_A$R agonists (GABA at 100 μM and musci-

mol at 100 μM), but not with $GABA_BR$ agonist (baclofen 100 μM), significantly reduced the percentage of PSA-NCAM$^+$ cells that incorporated BrdU (Fig. 5*A*) at both the Tuj1$^-$ (Fig. 5*G*) and Tuj1$^+$ (Fig. 5*D*) stages. The addition of SR-95531 (10 μM) totally abolished the muscimol (100 μM)-induced decrease of proliferation in PSA-NCAM$^+$ cells (Fig. 5*A*) at Tuj1$^-$ (Fig. 5*G*) and Tuj1$^+$ stages (Fig. 5*D*).

EGF (20 ng/ml) increased the proliferation of PSA-NCAM$^+$ cells (Fig. 5*B*) similarly at Tuj1$^-$ (Fig. 5*H*) and Tuj1$^+$ stages (Fig. 5*E*) ($n = 4$; Student's t test; $^{**}p < 0.01$, $^{***}p < 0.0001$) but had no effect on O4$^+$ and GFAP$^+$ cells (data not shown). Interestingly, muscimol (100 μM) inhibited EGF-induced increase of proliferation ($n = 4$; Student's t test; $^{*}p < 0.05$) in PSA-NCAM$^+$ cells (Fig. 5*B*) at the Tuj1$^+$ stage only (Fig. 5*E*,*H*), whereas addition of SR-95531 (10 μM) totally abolished the effect of muscimol (Fig. 5*B*,*E*). This discrepancy may reflect developmental differences of $GABA_AR$ expression and/or function between potentially more immature Tuj1$^-$/PSA-NCAM$^+$ precursors and their Tuj1$^+$/PSA-NCAM$^+$ neuroblastic progeny.

The influence of $GABA_AR$ modulators assessed by BrdU incorporation was also analyzed on the whole-cell population using the [^{3}H]thymidine incorporation assay with similar results (data not shown, but see Fig. 8).

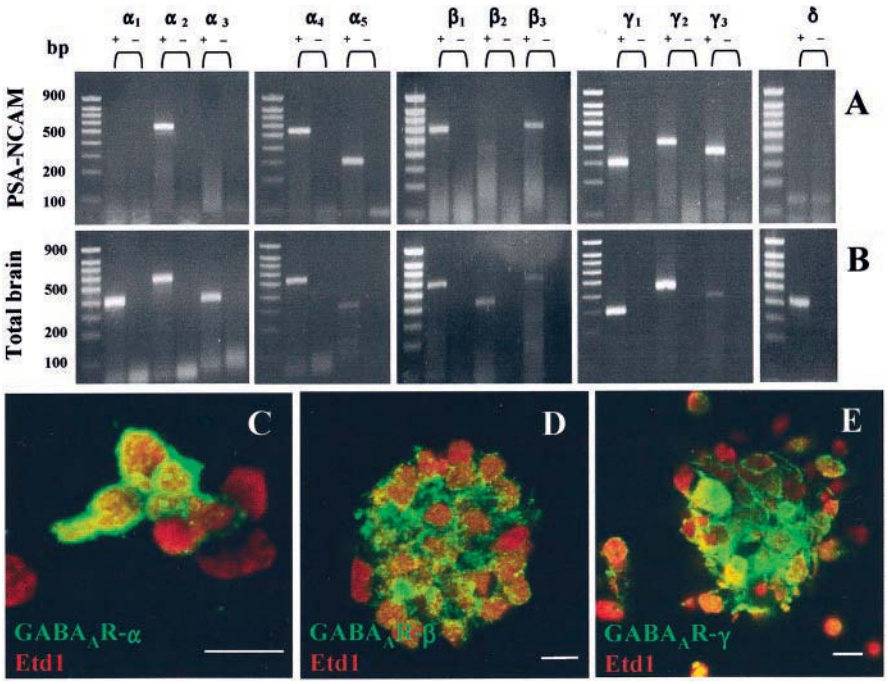

Figure 2. $GABA_A$ receptors are expressed by PSA-NCAM$^+$ progenitors from early postnatal striatum. *A*, *B*, RT-PCR amplification of $GABA_AR$ α_{1-5}, β_{1-3}, γ_{1-3}, and δ subunit transcripts using RNA extracted from 3-DIV PSA-NCAM$^+$ spheres (*A*) and adult rat brain tissue (*B*). Bands corresponding to α_2 (549 bp), α_4 (532 bp), α_5 (300 bp), β_1 (578 bp), β_3 (587 bp), γ_1 (296 bp), and γ_3 (336 bp) were detected (+, with RT; −, without RT). Left margins indicate migration of standard DNA markers with size indicated in base pairs. *C*, Z-series confocal image of 3-DIV PSA-NCAM$^+$ cells immunoreactive for $GABA_AR$ α subunits (green). *D*, *E*, Confocal images of 3-DIV PSA-NCAM$^+$ spheres showing $GABA_AR$ β^+ cells (*D*, green), and $GABA_AR$ γ^+ cells (*E*, green), respectively. All cultures were counterstained with Etd1 (red). Scale bars: *C*–*E*, 10 μm.

EGF-controlled GABA-mediated autocrine/paracrine inhibition of proliferation in cultured PSA-NCAM$^+$ cells and Tuj1$^+$ neuron-committed precursor cells from early postnatal striatum

To investigate whether PSA-NCAM$^+$ progenitors were able to synthesize GABA, we performed RT-PCR experiments with specific primers to detect the enzymes required for GABA synthesis by decarboxylation of glutamate,: i.e., the 65 kDa (GAD 65) and 67 kDa (GAD 67) glutamate decarboxylases (Table 1). During brain development, alternative splicing produces three transcript isoforms for the GAD 67 but not the GAD 65 gene (Szabo et al., 1994). With RNAs extracted both from 3-DIV PSA-NCAM$^+$ spheres and from control adult total brain, we detected an appropriate 698 bp band by using a specific set of primers for GAD 65 (Fig. 6*A*). For GAD 67 RT-PCR, we used a set of primers aimed at amplifying cDNAs for the three alternatively spliced isoforms. However, we detected only a 252 bp band corresponding to the full-length functional isoform of GAD 67 with RNAs extracted both from PSA-NCAM$^+$ spheres and control adult total brain (Fig. 6*A*). We next sought for the presence of GABAergic cells among PSA-NCAM$^+$ progenitors by immunocytochemical stainings using antibodies directed against GABA, GAD 65, and GAD 67. We found that GAD 65$^+$ cells represented 48.9 ± 5.2% ($n = 2$) (Fig. 6*B*) of total cells from 3-DIV PSA-NCAM$^+$ spheres, whereas 61.5 ± 4.1% ($n = 3$) (Fig. 6*C*) of the progenitors expressed GAD 67. GABA$^+$ cells represented 19.3 ± 9.8% ($n = 3$) (Fig. 6*D*) of total cells.

Given this demonstration of GABA synthesis in striatal PSA-NCAM$^+$ cells, we next investigated whether these cells were able to actively secrete GABA, which in turn could regulate their proliferation level by an autocrine or paracrine activation of $GABA_AR$. To test this hypothesis of an endogenous activation of $GABA_AR$ within PSA-NCAM$^+$ spheres, we studied the effects on proliferation of antagonists (SR-95531 at 10 μM, picrotoxin at 5 μM, and bicuculline at 100 μM) and positive allosteric modulators (clonazepam at 1 μM and pentobarbital at 10 μM) of $GABA_AR$ in the absence of exogenously added GABA in our proliferation assay. In the absence of EGF, $GABA_AR$ antagonists triggered an increase ($n = 3$; ANOVA-1 followed by a Dunnett's post-test; $^{*}p < 0.05$, $^{**}p < 0.01$), whereas positive allosteric modulators induced a decrease ($n = 3$; not significant) of proliferation in total PSA-NCAM$^+$ and Tuj1$^+$/PSA-NCAM$^+$ cells (Fig. 6*E*,*F*). The lower level of increase of BrdU labeling in total PSA-NCAM$^+$ cells in comparison with the Tuj1$^+$ subpopulation in the presence of $GABA_AR$ antagonists underlies the fact that Tuj1$^-$/PSA-NCAM$^+$ cells were less sensitive to this pharmacological effect (data not shown). Our data suggest the existence of an endogenous GABA-dependent inhibition of proliferation in PSA-NCAM$^+$ spheres.

Furthermore, in the presence of EGF (20 ng/ml), the GABA antagonist SR-95531 (10 μM) did not increase the proliferation of total PSA-NCAM$^+$ and Tuj1$^+$/PSA-NCAM$^+$ cells (Fig. 6*G*,*H*). Therefore, using the HPLC technique, we measured the GABA contents in spheres synchronized for 24 hr and subsequently grown for 18 hr in DMEM/F12/N2/B27 with or without EGF (20 ng/ml). We found that EGF-treated spheres contained a lower amount of GABA when compared with untreated cultures ($n = 3$; Student's t test; $^{*}p < 0.05$) (Fig. 6*I*). These results emphasize

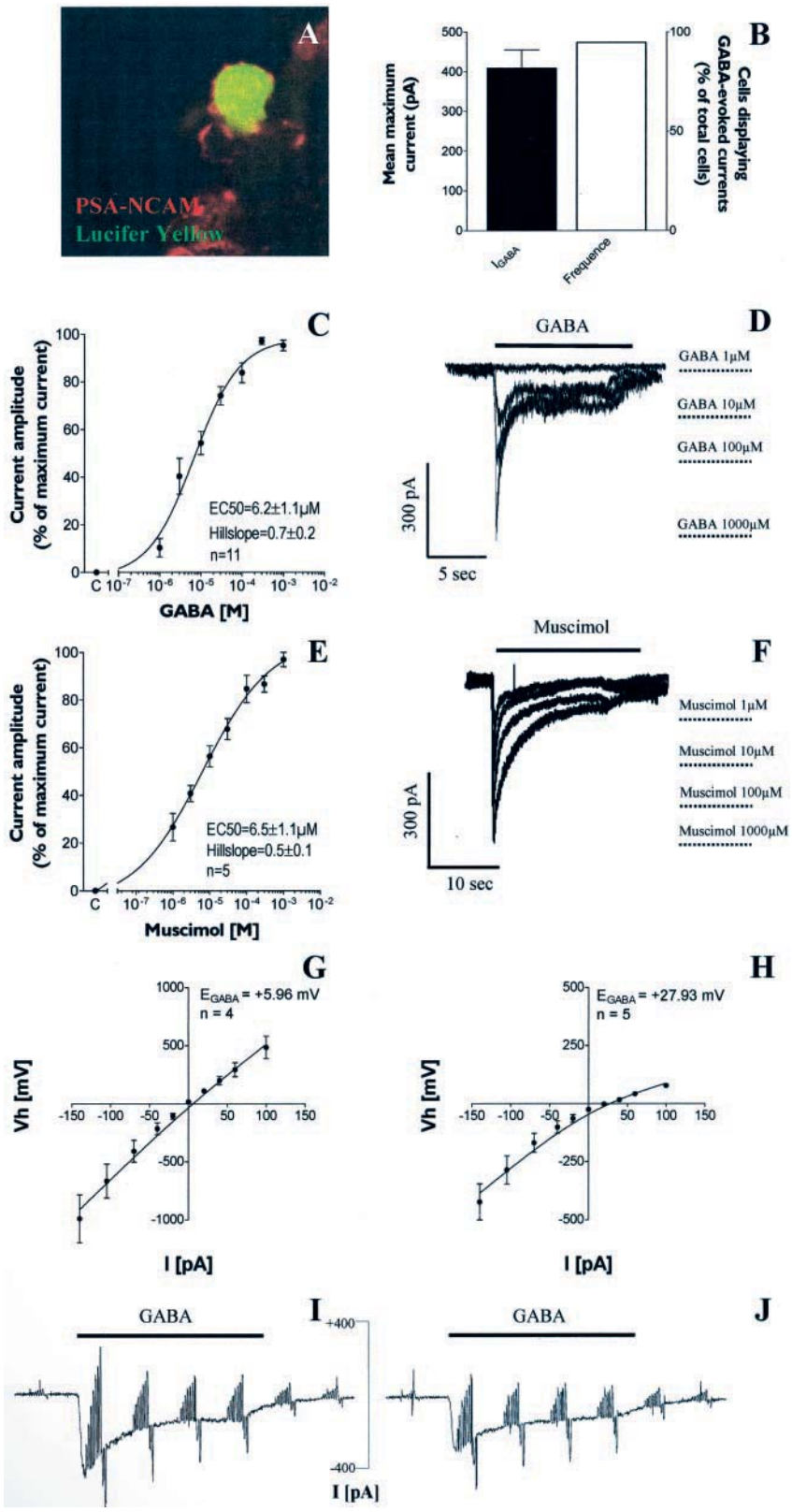

Figure 3. $GABA_A$ receptor activation triggers chloride-mediated inward currents in PSA-NCAM$^+$ progenitor cells. *A*, Confocal image showing a GABA-responsive cell injected with Lucifer yellow (green) and expressing PSA-NCAM (red). *B*, Histogram representing the mean maximum current induced by GABA 1 mM and the percentage of responding cells in the total recorded population of 3 DIV PSA-NCAM$^+$ cells, respectively. *C*, Concentration–response curve obtained from GABA-responsive PSA-NCAM$^+$ progenitors. *E*, The specific $GABA_AR$ agonist muscimol also induced concentration-dependent currents in PSA-NCAM$^+$ cells. *D*, *F*, Traces illustrating inward currents elicited by different concentrations of GABA (*D*) and muscimol (*D*). *G–J*, Reversal potential of GABA-induced currents (E_{GABA}). *I*, *J*, Current–voltage relationship of GABA-evoked currents was studied by applying voltage steps ranging from −140 to +100 mV repetitively every 5 sec before, during, and after GABA (100 µM) application. Mean control currents (before and after GABA application) were subtracted from the currents recorded at the peak of the GABA response. *G–I*, Using the currents obtained in *I*, we constructed a current–voltage curve reversing at +5.89 mV ($n = 4$ cells), which is close to the calculated Nernst chloride equilibrium potential (−1.1 mV) (left panel). *H–J*, When extracellular chloride concentration was lowered (*J*), the reversal potential shifted to +30.63 mV ($n = 5$ cells), which again is close to the expected chloride equilibrium potential in this condition (+29.00 mV).

that GABA production in PSA-NCAM$^+$ cells may be controlled by EGF signaling.

GABA$_A$R activation does not interfere with the survival of PSA-NCAM$^+$ cells

We performed TUNEL bioassays to ascertain that GABA$_A$R agonists, antagonists, and positive allosteric modulators did not modify the percentage of BrdU-incorporating PSA-NCAM$^+$ cells by interfering with apoptotic cell death. As shown in Figure 7*A*, GABA$_A$R agonist (muscimol 100 μM), antagonist (SR-95531 10 μM), or positive allosteric modulators (pentobarbital and clonazepam) did not influence the apoptotic events in PSA-NCAM$^+$ cells. Roscovitine at a high concentration (40 μM) (Ljungman and Paulsen, 2001) was used as positive control ($n = 3$; ANOVA-1 followed by a Dunnett's post-test; $^{**}p < 0.01$) (Fig. 7*A*,*B*).

Intracellular signaling pathways mediating the effects of GABA$_A$R activation on cell cycle progression in PSA-NCAM$^+$ progenitors

Because the mitogen-activated protein kinase (MAPK) signaling pathway has been shown to be involved in the regulation of cell cycle progression in neuronal progenitor cells (Li et al., 2001), we studied the effect of a chemical inhibition of this cascade on GABA$_A$R-mediated modulation of PSA-NCAM$^+$ cell proliferation. We used U0126, a specific inhibitor of the mitogen-activated kinase kinases MEK1 and MEK2 (Duncia et al., 1998). U0126 (10 μM) had no effect on basal proliferation or on muscimol-induced arrest of proliferation (Fig. 8). Conversely, we found that U0126 totally abolished the increase of proliferation induced by SR-95531 or EGF ($n = 5$; Student's t test; $^{*}p < 0.05$, $^{**}p < 0.01$) (Fig. 8).

As described (Belachew et al., 2000), to assess GABA-induced calcium responses, PSA-NCAM$^+$ cells have been imaged using confocal microscopy and the calcium indicator dye fluo-3 in Locke standard extracellular solution. In such conditions, we first tested the presence of voltage-gated calcium channels (VGCCs) in PSA-NCAM$^+$ cells by studying the effects of depolarization. The application of a depolarizing solution containing a high K^+ concentration (50 mM) resulted in a prolonged rise of intracellular calcium concentration ($[Ca^{2+}]_i$) in 28.3% of the cells (28 of 99 cells tested) (Fig. 9*A*,*B*). A cell was considered to be a responding cell if it displayed a sustained increase of its fluorescence intensity that was significantly (at least 20%) above the average baseline flu-

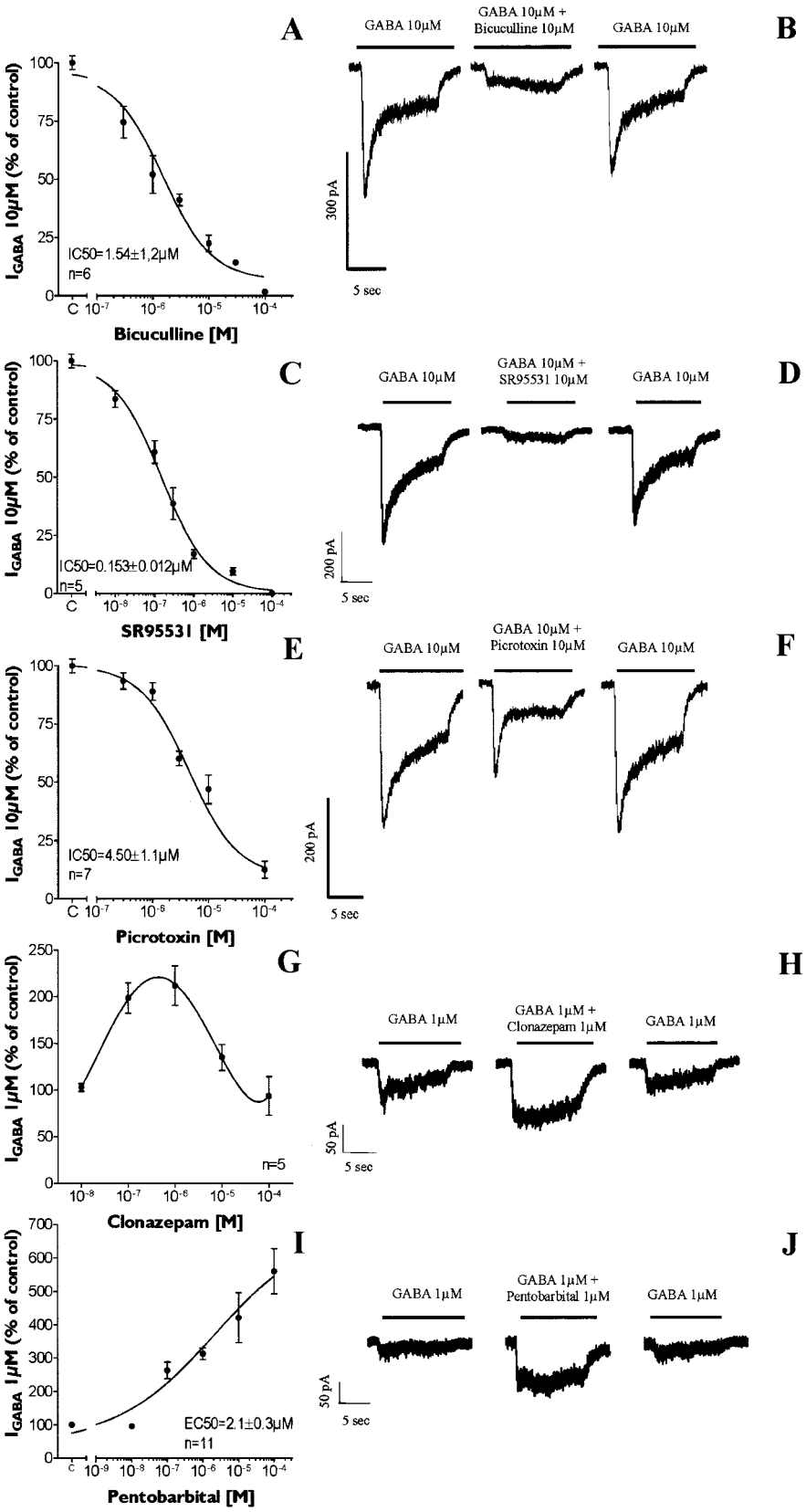

Figure 4. Pharmacological characterization of GABA$_A$R expressed by PSA-NCAM$^+$ progenitors. *A–F*, GABA was applied at 10 μM (I_{GABA} 10 μM), a concentration close to its EC_{50}. GABA-evoked currents were reversibly inhibited by bicuculline (*A*, *B*), SR-95531 (*C*, *D*), and picrotoxin (*E*, *F*). *G–J*, We also tested positive allosteric modulators of GABA$_A$R. Clonazepam potentiated GABA-induced currents (GABA at 1 μM, EC_{10}) in a range of concentrations between 10 nM and 100 μM, with a maximal effect at 1 μM (*G*, *H*). *I–J*, Pentobarbital also enhanced GABA-evoked currents in a concentration-dependent manner.

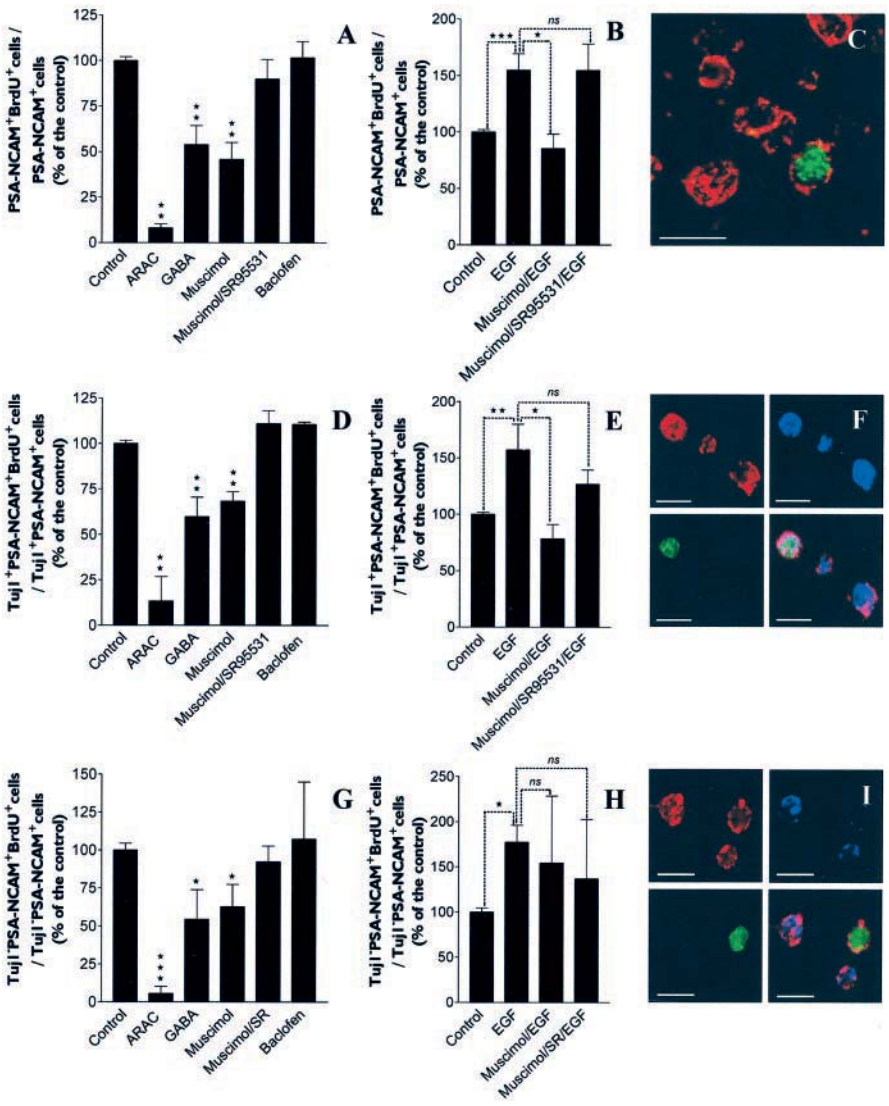

Figure 5. $GABA_AR$ activation inhibits the proliferation of PSA-NAM$^+$ cells at both Tuj1$^-$ and Tuj1$^+$ stages. Cells were incubated simultaneously with drugs and BrdU (20 μM) for 18 hr in EGF-free medium. The anti-mitotic agent cytosine arabinoside (AraC, 10 μM) was used as an internal control condition. (*A, D, G*). $GABA_AR$ agonists (100 μM GABA and 100 μM muscimol) inhibited the incorporation of BrdU ($n = 6$; ANOVA-1 followed by a Dunnett's post-test; $^*p < 0.05$, $^{**}p < 0.01$, $^{***}p < 0.0001$) in total PSA-NCAM$^+$ cells (*A*), in Tuj1$^+$/PSA-NCAM$^+$ cells (*D*), and in Tuj1$^-$/PSA-NCAM$^+$ cells (*G*). The effect of muscimol was totally abolished by SR-95531 (100 μM). Baclofen (100 μM), a $GABA_BR$ agonist, had no effect on BrdU incorporation. (*A, D, G*). Muscimol (100 μM) significantly inhibited ($n = 4$; Student's *t* test; $^*p < 0.05$) the mitogenic effect of EGF (20 ng/ml) ($n = 4$, Student's *t* test; $^{**}p < 0.01$, $^{***}p < 0.0001$) in total PSA-NCAM$^+$ cells (*B*) and in Tuj1$^+$/PSA-NCAM$^+$ cells (*E*), but not in Tuj1$^-$/PSA-NCAM$^+$ cells (*H*). *C, F, I*, Confocal images of double-immunostaining for PSA-NCAM (red) and BrdU (green) (*C*), triple-immunostaining for PSA-NCAM (red), Tuj1 (blue), and BrdU (green) (*F, I*), respectively, showing that both Tuj1$^+$/PSA-NCAM$^+$ and Tuj1$^-$/PSA-NCAM$^+$ cells are proliferative. Because a vast majority of cells constituting 3-DIV spheres expressed PSA-NCAM, we found similar results on the whole-cell population, and these results were confirmed in [^{3}H]thymidine incorporation assay (data not shown, but see Fig. 8). Scale bars: *C, F, I*, 10 μm.

orescence. A muscimol-evoked $[Ca^{2+}]_i$ increase was observed in 20.2% of PSA-NCAM$^+$ cells (20 of 99 cells tested), and all muscimol-responsive cells exhibited intracellular calcium responses to depolarization induced by high extracellular K^+ (Fig. 9*A,B*). Muscimol-induced calcium responses in PSA-NCAM$^+$ cells were consistently inhibited by the VGCC blocker nifedipine (10 μM; $n = 20$ cells) (Fig. 9*A,B*). These data suggest that GABA interferes with $[Ca^{2+}]_i$ homeostasis in a subpopulation (20%) of postnatal PSA-NCAM$^+$ cells from striatum by inducing a sufficient depolarization to open VGCCs.

We have also investigated the effect of the VGCC blocker nifedipine on $GABA_AR$-mediated regulation of cell cycle progression in PSA-NCAM$^+$ cells. Therefore, we provided evidence that a $GABA_AR$-mediated increase of $[Ca^{2+}]_i$ in striatal PSA-NCAM$^+$ cells was involved in $GABA_AR$-mediated inhibition of proliferation in neuron-committed Tuj1$^+$/PSA-NCAM$^+$ progenitor cells but not in Tuj1$^-$/PSA-NCAM$^+$ cells (Fig. 9*C,D*).

$GABA_AR$ is expressed in PSA-NCAM$^+$ cells *in situ* and autocrine/paracrine $GABA_AR$ activation regulates proliferation of postnatal striatal PSA-NCAM$^+$ cells in organotypic slices

We performed immunostaining in coronal frozen tissue sections (30 μm) from postnatal (P1) rat brains. We were able to demonstrate that PSA-NCAM$^+$ cells from striatum as well as from the adjacent SVZ were immunoreactive for $GABA_AR$ α subunits (Fig. 10*A–C*). GABA- expressing cells were also detectable in the postnatal striatum and adjacent SVZ regions (Fig. 10*E,F*). Finally, we wanted to assess cell proliferation, as described previously (Yuan et al., 1998), in organotypic slice (P1, 400 μm thick) cultures to gain more insights from a cytoarchitecturally intact postnatal striatum (Fig. 10*G*), closer to the *in vivo* situation. To restrict our analysis to the postnatal striatum, SVZ regions (as defined in Fig. 10*A1*) were microdissected out and assessed similarly but separately. BrdU incorporation was performed during the first 24 hr of culture, i.e., between +4 and +22 hr after dissection. Slices next were mechanically dissociated and plated onto poly-ornithine-coated coverslips to attach for 1 hr before fixation and immunostaining (Fig. 10*H*). We ascertained the viability of our slice culture system by running LIVE/DEAD cytotoxicity assays just before fixation after each experiment, yielding to values of 88.6 ± 0.6 living cells and 11.4 ± 0.6 dead cells (percentage of total cells; mean ± SEM; $n = 3$ independent experiments).

In EGF-free conditions, consistent with our data from cultured cells, we observed *in situ* that the $GABA_AR$ agonist muscimol (100 μM) inhibited proliferation of striatal PSA-NCAM$^+$ cells both at the Tuj1$^-$ stage (Fig. 10*I*) and in neuron-committed Tuj1$^+$ cells (Fig. 10*J*). Likewise, the addition of SR95531 (10 μM) totally abolished muscimol-induced inhibition of proliferation in striatal PSA-NCAM$^+$ cells at both the Tuj1$^-$ (Fig. 10*I*) and Tuj1$^+$ stages (Fig. 10*J*). Furthermore, in the absence of exogenously applied $GABA_AR$ agonists, SR95531 stimulated the proliferation of Tuj1$^-$ (Fig. 10*I*) and Tuj1$^+$ (Fig. 10*J*) cells within the PSA-NCAM$^+$ population, just as was shown in spheres.

We also confirmed with this *ex vivo* paradigm that EGF (20 ng/ml) stimulated proliferation of striatal PSA-NCAM$^+$ cells

at both the Tuj1$^-$ (Fig. 10*I*) and Tuj1$^+$ stages (Fig. 10*J*). In contrast to data from cultured cells, muscimol (100 μM) inhibited EGF-induced increase of proliferation in striatal PSA-NCAM$^+$ cells not only at the Tuj1$^-$ (Fig. 10*I*) but also at the Tuj1$^+$ stage, although without statistical significance. Finally, in the presence of EGF, SR95531 (10 μM) did not increase proliferation of PSA-NCAM$^+$ cells at either the Tuj1$^-$ (Fig. 10*I*) or Tuj1$^+$ stage (Fig. 10*J*), thus suggesting that EGF may also interact with GABA synthesis *in situ* in such organotypic striatal slices. Altogether, such findings emphasize that an autocrine/paracrine $GABA_AR$ activation may be an essential mechanism for cell cycle control in PSA-NCAM$^+$ cells from the postnatal striatum *in vivo*.

Interestingly, using this organotypic slice culture technique, we observed that the regulation of proliferative kinetics of Tuj1$^-$/PSA-NCAM$^+$ and Tuj1$^+$/PSA-NCAM$^+$ cells in response to EGF application and $GABA_AR$ activation appears to be qualitatively identical in the SVZ (microdissected as defined in Fig. 10*A1*) (Fig. 10*K*,*L*) as compared with that of the striatum area (microdissected as defined in Fig. 10*A1*) (Fig. 10*I*,*J*).

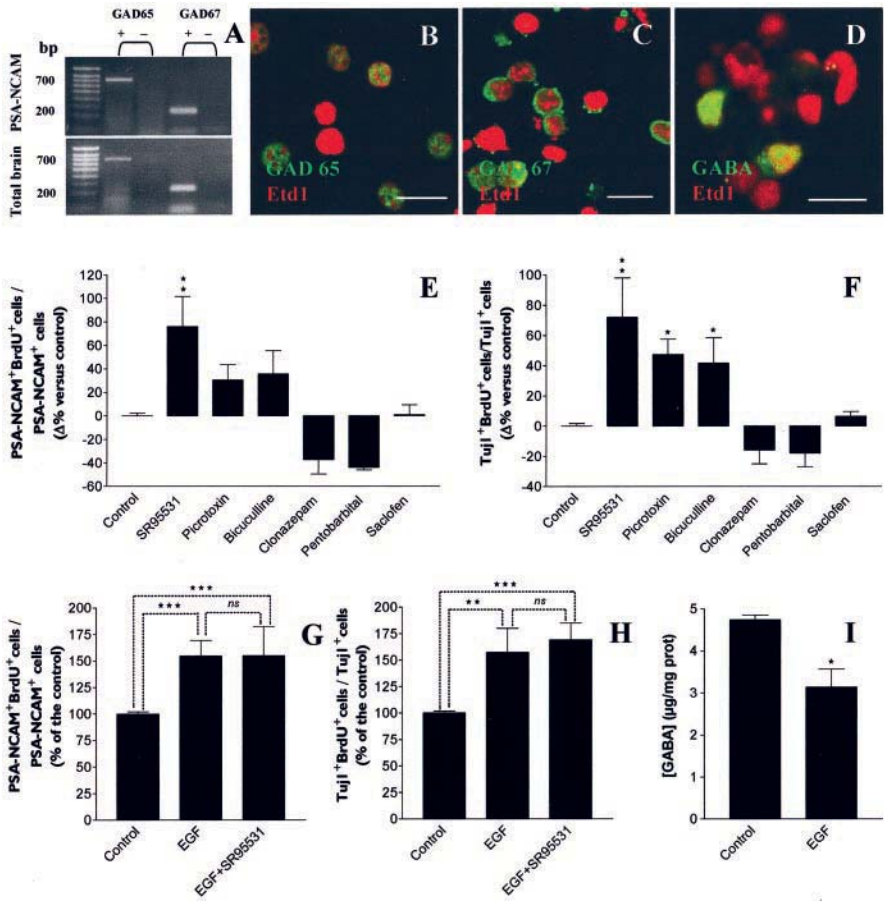

Figure 6. EGF-dependent production of endogenous GABA intrinsically inhibits the proliferation of PSA-NCAM$^+$ precursor cells. *A*, RT-PCR amplification of both GAD 65 and GAD 67 transcripts from 3-DIV PSA-NCAM$^+$ spheres and from control adult rat brain using specific sets of primers. RT-PCR analysis yielded bands with the appropriate amplicon size for GAD 65 (698 bp) and for the full-length functional GAD 67 (252 bp). Left margin indicates migration of standard DNA markers with size indicated in base pairs. *B*, *C*, Three-DIV-old dissociated PSA-NCAM$^+$ spheres labeled for GAD 65 (*B*, green) or GAD 67 (*C*, green) and counterstained by Etd1 (red). *D*, Dissociated 3-DIV progenitors immunostained for GABA (green) and counterstained with Etd1 (red). Scale bars: *B–D*, 10 μm. *E*, *F*, Histograms representing the differences of BrdU incorporation index (BrdU$^+$ cells/total cells, %) between treated and untreated conditions, respectively, in total PSA-NCAM$^+$ (*E*) and Tuj1$^+$/PSA-NCAM$^+$ cells (*F*). Antagonists and positive allosteric modulators of $GABA_AR$ were applied on 3-DIV-old synchronized cells for 18 hr of BrdU incorporation assay. $GABA_AR$ antagonists (10 μM SR-95531, 5 μM picrotoxin, and 100 μM bicuculline) significantly increased the percentage of PSA-NCAM$^+$/BrdU$^+$ cells ($n = 3$; ANOVA-1 followed by a Dunnett's post-test, ns; $^*p < 0.05$) (*E*) and Tuj1$^+$/PSA-NCAM$^+$/BrdU$^+$ cells ($n = 3$; ANOVA-1 followed by a Dunnett's post-test; $^*p < 0.05$, $^{**}p < 0.01$) (*F*). Conversely, $GABA_AR$-positive allosteric modulators decreased the percentage of PSA-NCAM$^+$/BrdU$^+$ cells (*E*) and Tuj1$^+$/PSA-NCAM$^+$/BrdU$^+$ cells (*F*) as compared with control. Saclofen (10 μM), a $GABA_BR$ antagonist, had no effect (*E*, *F*). *G*, *H*, In the presence of EGF (20 ng/ml) ($n = 4$; Student's *t* test; $^{***}p < 0.0001$), SR-95531 (10 μM) ($n = 4$; Student's *t* test; $^{**}p < 0.01$, $^{***}p < 0.0001$) had no effect on proliferation of total PSA-NCAM$^+$ cells (*G*) and of Tuj1$^+$/PSA-NCAM$^+$ cells (*H*). *I*, Histogram showing the concentration of GABA measured by HPLC in synchronized 3-DIV-old PSA-NCAM$^+$ spheres treated or not with EGF for 18 hr. EGF-treated spheres contained a lower amount of GABA than that of untreated cultures ($n = 3$; Student's *t* test; $^*p < 0.05$).

Discussion

The generation of cell diversity from mammalian NSCs is likely to be controlled by the interaction between both extrinsic and intrinsic cues. In addition to growth factors, hormones, integrins, and extracellular matrix components, neurotransmitters are present in the developing brain well before the onset of synaptic activity and have been shown to be part of the extrinsic control of CNS neurogenesis involving progenitor cell proliferation, migration, and differentiation as well as cell death (for review see Lauder, 1993; Cameron et al., 1998; Herlenius and Lagercrantz, 2001; Nguyen et al., 2001). Recent studies reported that functional neurotransmitter receptors are expressed by a wide variety of neuronal progenitors during embryonic development, thus pointing to a possible role in the transduction of important developmental cues (LoTurco et al., 1995; Flint et al., 1998; Haydar et al., 2000; Maric et al., 2000). In the present work, we show that (1) proliferative PSA-NCAM$^+$ neuronal precursors from early postnatal rat striata synthesize and release GABA and express functional $GABA_AR$ *in vitro* and *in situ*, (2) an EGF-dependent GABA-mediated autocrine/paracrine loop regulates neuronal precursor cell division in the postnatal striatum, and, (3) the levels of GABA synthesized by PSA-NCAM$^+$ cells *in vitro* were found to be in the same range of concentration as that of GABAergic brain areas *in vivo* (Miranda-Contreras et al., 1999). This work emphasizes that GABA may serve as a physiological signal that could regulate proliferation of neuronal progenitors and likely neurogenesis in the postnatal striatum.

Functional $GABA_A$ receptors are expressed in postnatal PSA-NCAM$^+$ cells

GABA, the principal inhibitory neurotransmitter of the adult CNS, may act as a trophic factor during CNS development long before the onset of inhibitory synaptogenesis (Barker et al., 1998). We wanted to determine whether functional $GABA_ARs$ were expressed in neurogenic PSA-NCAM$^+$ progenitors isolated from rat striatum at the early postnatal period, when spontaneous and growth factor-stimulated proliferation is established to persist at

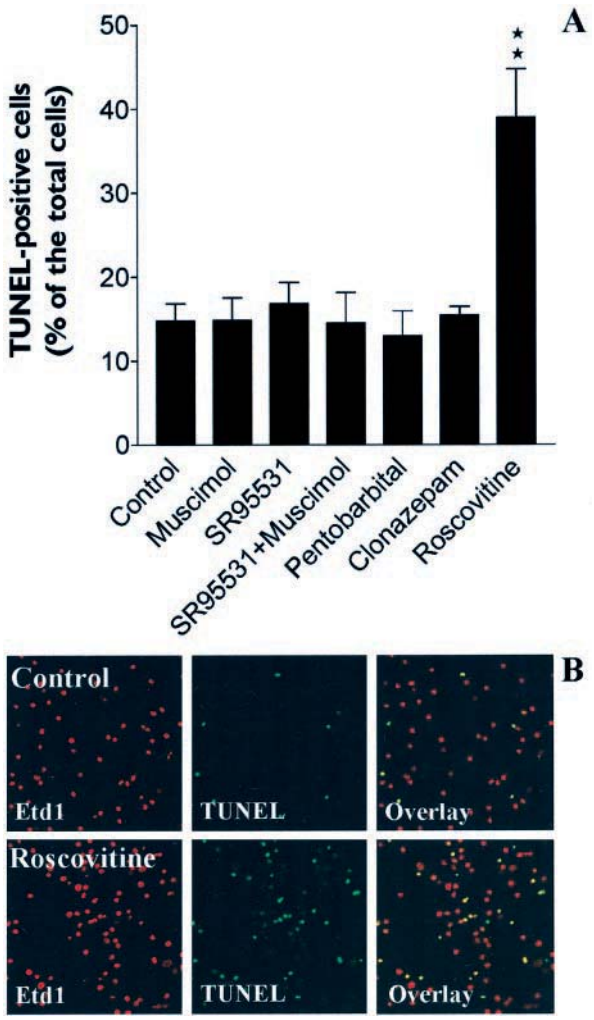

Figure 7. $GABA_AR$ modulators do not interfere with PSA-NCAM$^+$ cell survival. *A*, Histogram showing a TUNEL bioassay that demonstrated the absence of effect of $GABA_AR$ modulators on apoptotic events in PSA-NCAM$^+$ cell cultures (3-DIV, 18 hr of treatment in the different conditions. Roscovitine (40 μM) was used as a positive control ($n = 3$; ANOVA-1 followed by a Dunnett's post-test; $^{**}p < 0.01$). *B*, Confocal images displaying representative fields comparing the percentage of TUNEL$^+$ cells (green) in control (top row) versus roscovitine-treated (bottom row) conditions.

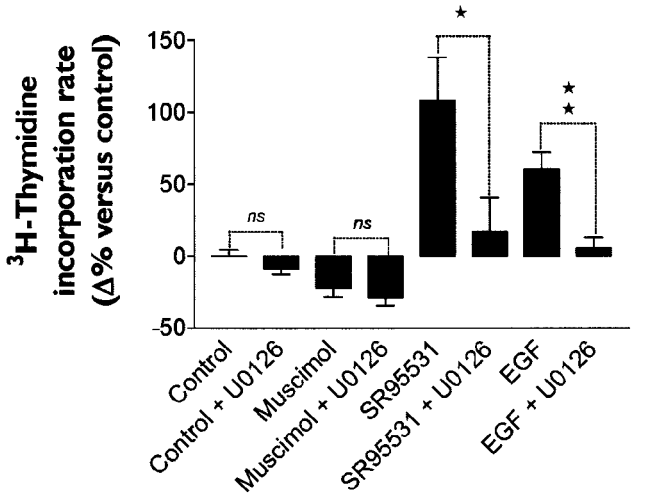

Figure 8. $GABA_AR$ activation inhibits proliferation of PSA-NCAM$^+$ progenitors by blocking MAPK signaling pathways. Histogram shows that the increase of [^{3}H]-thymidine incorporation induced by the $GABA_AR$ antagonist SR95531 (10 μM) and by EGF (20 ng/ml) was significantly blocked by U0126 (10 μM), a specific inhibitor of the mitogen-activated protein kinase kinases MEK1 and MEK2 ($n = 5$; Student's *t* test; $^*p < 0.05$, $^{**}p < 0.01$).

a significant rate (Reynolds and Weiss, 1992; Craig et al., 1996; Pencea et al., 2001). Because immature proliferative cells are characterized by lower buoyancy or higher specific buoyant densities (Maric et al., 1997), we used these isopycnic properties to develop a selection procedure that allowed us to obtain highly pure PSA-NCAM striatal cell suspensions that were enriched in proliferative progenitors.

After 3 d of growth in uncoated conditions, PSA-NCAM$^+$ cells generated spheres and were shown to express multiple $GABA_AR$ subunit genes (i.e., $\alpha_{2,4,5}$, $\beta_{1,3}$, and γ_{1-3}) that are known to be necessary for forming heteromeric functional receptors (Levitan et al., 1988; Malherbe et al., 1990; Sigel et al., 1990; Verdoorn et al., 1990). It is acknowledged that at least α_4, β_1, and γ_1, which are detected in rodent progenitors from the neocortical proliferative zone (Ma and Barker, 1995, 1998; Ma et al., 1998), may compose $GABA_ARs$ that have an extrasynaptic function in neural development. The absence of transcript coding for α_1, α_3, β_2, and δ subunits in PSA-NCAM$^+$ spheres was expected because these $GABA_AR$ subunits have been reported mostly in differentiating postmitotic neurons (Maric et al., 1997; Serafini et al., 1998; Stewart et al., 2002). At the protein level, we observed that PSA-NCAM$^+$ cells were intensely (~70%) immunoreactive for α-, β-, and γ-$GABA_AR$ subunits. Our electrophysiological recordings confirmed that GABA and muscimol elicited chloride currents in PSA-NCAM$^+$ cells. Finally, we provided evidence that GABA-evoked currents in PSA-NCAM$^+$ progenitors displayed a typical pharmacological profile with reversible inhibition by established antagonists and potentiation by positive allosteric modulators of $GABA_AR$. Altogether, our findings indicate that fully functional $GABA_ARs$ are expressed by striatal PSA-NCAM$^+$ precursor cells from early postnatal brain.

Autocrine/paracrine activation of $GABA_A$ receptor blocks cell cycle progression in PSA-NCAM$^+$ neuronal progenitor cells from postnatal striatum

In the present study, we provided evidence *in vitro* and *in situ* that EGF increased the proliferation of postnatal striatal PSA-NCAM$^+$ progenitors at both the Tuj1$^-$ and neuron-committed Tuj1$^+$ stages. Furthermore, we showed that the activation of $GABA_AR$ had no effect on apoptotic events but inhibited the proliferation of postnatal striatal PSA-NCAM$^+$ progenitors and of their Tuj1$^+$ neuroblastic progeny *in vitro* and *in situ*, either in the presence or in the absence of EGF mitogenic stimulation. Conversely, $GABA_AR$ activation had no effect on the proliferation of O4$^+$ oligodendroglial cells and GFAP$^+$ astrocytes that were only sparsely present in cultured PSA-NCAM$^+$ spheres. In our culture conditions, a large majority of striatal PSA-NCAM$^+$ cells were Tuj1$^+$ and underwent preferentially a neuronal differentiation as depicted by the expression of antigenic features of mature neurons. These results suggest that, in the postnatal striatum, $GABA_AR$-mediated signaling may be involved in the regulation of cell cycle progression specifically in PSA-NCAM$^+$ precursor cells that are directed toward a neuronal fate.

GABA-, GAD 65-, and GAD 67-expressing cells have been detected in embryonic and early postnatal rat striatum (Lauder et al., 1986; Greif et al., 1992), and extrasynaptically released GABA was found to be necessary for the establishment and patterning of functional neuronal networks by promoting the survival and po-

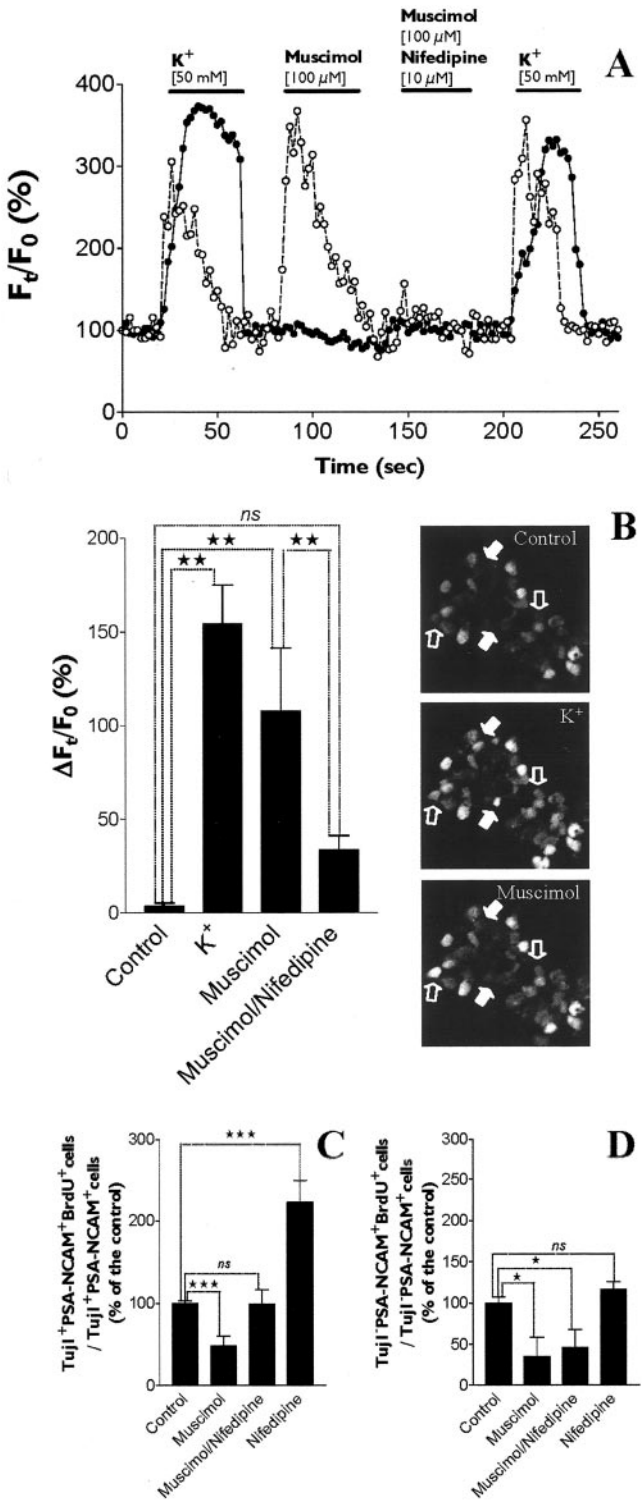

Figure 9. $GABA_AR$ activation inhibits the proliferation of Tuj1$^+$/PSA-NCAM$^+$ progenitors by inducing a rise of intracellular calcium concentration. *A*, Time course (F_t/F_0) of intracellular calcium concentration $[Ca]_i$ assessed in cultured (3 DIV) fluo-3 AM-loaded PSA-NCAM$^+$ cells. We displayed fluorescence data recordings and fluo-3 AM on the basis of confocal images from two different cells (i.e., depolarization and muscimol responsive, open circles in the dot plot; depolarization responsive and muscimol nonresponsive, black circles in the dot plot) during successive treatments with solutions containing a high extracellular K^+ concentration (50 mM), muscimol (100 μM), or muscimol (100 μM) + nifedipine (10 μM). The $[Ca]_i$ increase mediated by muscimol (100 μM) was abolished by the L-type voltage-gated calcium channel-blocker nifedipine (10 μM) (open circle-containing curve). *B*, Histogram representing the increase of $[Ca]_i$ ($\Delta F_t/F_0$, %) triggered by a high extracellular K^+ concentration (50 mM; $n = 28$) and muscimol (100 μM; $n = 20$) (ANOVA-1 followed by a Dunnett's post-test; $^{**}p < 0.01$). Moreover, the $[Ca]_i$ increase induced by muscimol (100 μM) was significantly reduced by nifedipine (10 μM; $n = 20$) (ANOVA-1 followed by a Dunnett's post-test; $^{**}p < 0.01$). Examples of responsive cells are represented on the right in the image series. Cells that were both depolarization responsive and muscimol responsive are indicated by open arrows, and cells that were depolarization responsive but muscimol nonresponsive are indicated by white arrows. *C*, Histograms showing that the inhibition of proliferation induced by muscimol (100 μM) in Tuj1$^+$/PSA-NCAM$^+$ cells was completely blocked by nifedipine (10 μM). When applied alone, nifedipine significantly increased the proliferation of Tuj1$^+$/PSA-NCAM$^+$ cells ($n = 4–5$; Student's *t* test; $^{***}p < 0.0001$). *D*, In contrast, nifedipine (10 μM) did not block the inhibition of proliferation mediated by muscimol (100 μM) in Tuj1$^-$/PSA-NCAM$^+$ cells and did not increase the proliferation of these cells when applied alone ($n = 4–5$; Student's *t* test; $^*p < 0.05$).

sitioning of newly generated neurons in the striatum (Ikeda et al., 1997; Luk and Sadikot, 2001). With respect to hypotheses about the potential source of GABA that could activate $GABA_AR$ in PSA-NCAM$^+$ cells *in vivo*, it is noteworthy that these cells appeared to produce GABA and express consistently GABA-synthesizing enzymes *in vitro*. In the absence of extrinsic addition of GABA or $GABA_AR$ agonist, we also showed that the proliferation of both PSA-NCAM$^+$ and Tuj1$^+$ neuronal precursors was increased by $GABA_AR$ antagonists and decreased by positive allosteric modulators of $GABA_AR$. Without extrinsic addition of GABA but in the presence of the EGF mitogenic effect, we observed that the application of $GABA_AR$ antagonists did not further stimulate cell cycle progression in PSA-NCAM$^+$ and Tuj1$^+$ neuronal precursors from early postnatal striatum. However, this discrepancy might be attributable to the fact that EGF decreased endogenous GABA synthesis in PSA-NCAM$^+$ spheres. In conclusion, these findings demonstrate convincingly that cultured postnatal PSA-NCAM$^+$ cells from striatum not only express $GABA_ARs$ that regulate their cell cycle but also produce and release GABA.

Furthermore, in organotypic slice preparations from early postnatal striatum, we were able to detect GABA and $GABA_AR$ subunits in PSA-NCAM$^+$ cells, and we provided evidence that an endogenous GABA production also inhibited proliferation of PSA-NCAM$^+$ cells *in situ*, both at the Tuj1$^-$ stage and in neuron-committed Tuj1$^+$ precursor cells. These data suggest that this autocrine/paracrine mode of regulation of cell cycle progression through $GABA_AR$ activation in postnatal PSA-NCAM$^+$ neuronal precursors may likely exist *in vivo* and could regulate postnatal striatal neurogenesis. By using a similar experimental approach, we confirmed that the same mechanism appears to occur in the SVZ area, as shown previously by other work suggesting that endogenous $GABA_AR$ activation does exist in the proliferative ventricular zone (VZ) and SVZ during late embryonic stages of murine cortical development (LoTurco et al., 1995; Haydar et al., 2000). Studies in organotypic slices have already demonstrated that $GABA_AR$ agonists may have contrasting effects on neuronal progenitors; i.e., they were found to be mitogenic in the embryonic VZ and anti-proliferative in the SVZ, but these works failed to ascertain whether it could be caused by an indirect receptor activation on other cells that in turn would regulate proliferation in VZ and SVZ cells (Haydar et al., 2000). We show here that a direct autocrine/paracrine GABA-mediated feedback can regulate proliferation of PSA-NCAM$^+$ cells both in the striatum and SVZ *in situ*.

The finding *in vitro* and *in situ* that EGF stimulates the proliferation of early postnatal PSA-NCAM$^+$ cells and particularly Tuj1$^+$/PSA-NCAM$^+$ neuronal progenitors must be put in perspective with the effect of EGF on GABA synthesis in these cells. It has not yet been determined to what extent the EGF mitogenic

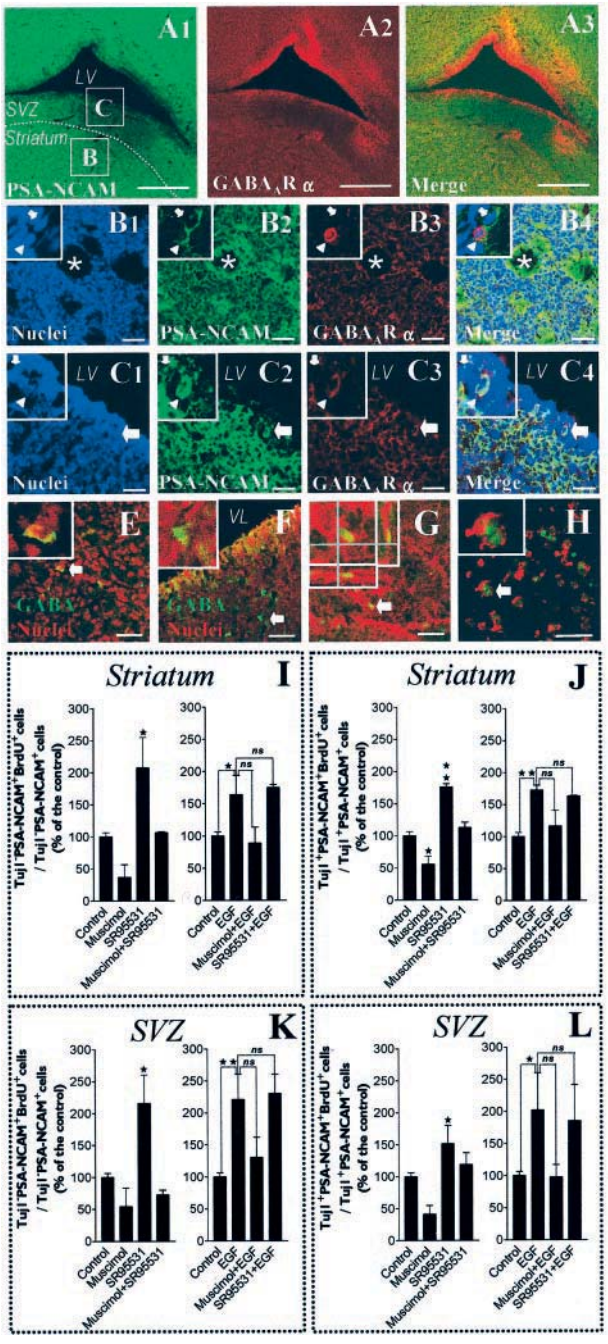

Figure 10. GABA$_A$R expression and activation in brain slices: the activation of GABA$_A$R inhibits the proliferation of PSA-NCAM$^+$ cells in the postnatal striatum and adjacent SVZ. *A1–3*, Confocal single plane images of immunohistochemical stainings (30-μm-thick tissue sections) showing a field containing the striatum separated from the subventricular zone (SVZ) by a white dotted line and bordered by the lateral ventricle (LV). PSA-NCAM staining appears in green (*A1*), GABA$_A$R α appears in red (*A2*), and merge of *A1* and *A2* appears in *A3*. *B1–4*, High-magnification views of the field delimited by the boxed area *B* of *A1*, which is a representative field of the striatum, with nuclei in blue (*B1*), PSA-NCAM in green (*B2*), GABA$_A$R α in red (*B3*), and merge of *B1*, *B2*, and *B3* in *B4*. Insets display two PSA-NCAM$^+$ cells (high magnification) that are immunoreactive (arrowhead) or not immunoreactive (arrow), respectively, for GABA$_A$R α. *C1–4*, High-magnification views of the field delimited by the boxed area *C* of *A1*, which is a representative field of the SVZ, with nuclei in blue (*C1*), PSA-NCAM in green (*C2*), GABA$_A$R α in red (*C3*), and merge of *C1*, *C2*, and *C3* in *C4*. Insets show two PSA-NCAM$^+$ cells (high magnification) immunoreactive (arrowhead) or not immunoreactive (arrow), respectively, for GABA$_A$R α. *E*, *F*, Confocal images showing immunostaining of a striatal area (*E*) and an SVZ area (*F*) with nuclei in red and GABA staining in green. Insets display a GABA$^+$ cell (arrow in full image) at higher magnification. *G*, Proliferation assay in acutely dissected organotypic tissue slices from postnatal striatum (Z-series confocal image) treated with EGF. We show BrdU (green) immunostaining in a PSA-NCAM (red)-expressing cell of a striatal slice after 18 hr of BrdU incorporation. Inset displays one cell (corresponding to the arrow in the full image) viewed as stacked Z-dimension images, comprising 0.5 μm optical sections taken 3 μm apart. The Z-dimension reconstruction was also observed orthogonally in both X–Z and Y–Z planes that are shown under and to the right of each Z-dimension composite, respectively. *H*, Confocal image of acutely isolated cells derived from mechanical dissociation of the striatal part of 400-μm-thick tissue slices at the end of the BrdU incorporation assay. These cells were immunostained for PSA-NCAM (red) and BrdU (green). Scale bars: *C1–4*, 30 μm; *B1–4*, *E–H*, 40 μm; *A1–3*, 500 μm. *I–L*, Histograms showing BrdU labeling indexes in Tuj1$^-$/PSA-NCAM$^+$ (*I*, *K*) and Tuj1$^+$/PSA-NCAM$^+$ (*J*, *L*) cells from the striatum (*I*, *J*) and the SVZ (*K*, *L*), as defined in *A1*. Striatal and SVZ areas were separated by microdissection of organotypic slices, placed in the same well, and then incubated with drugs and BrdU (20 μM) for 18 hr. In EGF-free medium, 100 μM muscimol inhibited the incorporation of BrdU in Tuj1$^-$/PSA-NCAM$^+$ and Tuj1$^+$/PSA-NCAM$^+$ cells from the striatum (*I*, *J*) and from the SVZ (*K*, *L*). These effects were totally abolished by SR-95531 (10 μM). Moreover, when applied alone, SR-95531 significantly increased the incorporation of BrdU in Tuj1$^-$/PSA-NCAM$^+$ cells and in Tuj1$^+$/PSA-NCAM$^+$ cells from the striatum (*I*, *J*) and from the SVZ (*K*, *L*) ($n = 2–4$; ANOVA-1 followed by a Dunnett's post-test; $^*p < 0.05$, $^{**}p < 0.01$). EGF (20 ng/ml) significantly increased the incorporation of BrdU in Tuj1$^-$/PSA-NCAM$^+$ and Tuj1$^+$/PSA-NCAM$^+$ cells from the striatum (*I*, *J*) and from the SVZ (*K*, *L*). In EGF-containing medium, muscimol exerted similar but less significant effects than in EGF-free conditions, and SR95531 had no effect when applied alone ($n = 2–5$; Student's *t* test; $^*p < 0.05$, $^{**}p < 0.01$).

effect on PSA-NCAM$^+$ cells may be caused in part by an EGF-mediated decrease of endogenous GABA production by PSA-NCAM$^+$ cells. Previous works have shown *in vivo* that intracerebroventricular administration of EGF induced newly formed cells in the adult mouse brain (Craig et al., 1996; Kuhn et al., 1997). However, although EGF promoted an increase of newborn cells in the adult SVZ and striatum, most of these cells were glial cells (Kuhn et al., 1997). There is an apparent discrepancy between our data showing that EGF is a potent mitogen for PSA-NCAM$^+$ neuronal precursors from the early postnatal striatum and the demonstration that EGF signaling has no effect on adult striatal neurogenesis and is preferentially a glial inducer in the adult SVZ and striatum (Craig et al., 1996; Kuhn et al., 1997), which contain PSA-NCAM$^+$ cells (Butler et al., 1997; Doetsch et al., 1997). We propose the following: (1) there may be a developmental regulation of the phenotypic potential of adult versus neonatal EGF-responsive PSA-NCAM$^+$ precursors from a given germinative postnatal region of the CNS, and (2) the effect of EGF on GABA synthesis, or the expression and function of GABA$_A$R, might differ in adult PSA-NCAM$^+$ precursors. To address this issue, adult PSA-NCAM$^+$ cells obtained from the SVZ and tightly adjacent areas will need to be investigated further with the experimental paradigm used in the present study.

MAPK signaling pathways and intracellular calcium are involved in GABA$_A$ receptor-mediated inhibition of proliferation in PSA-NCAM$^+$ neuronal progenitor cells from postnatal striatum

We also wanted to determine whether the proliferation of postnatal PSA-NCAM$^+$ precursors could be dependent on the MAPK pathway (Grewal et al., 1999), which is activated in the EGF receptor-signal transduction cascade (Grant et al., 2002) and appears to play a crucial ubiquitous role in the regulation of cell cycle progression in many cell types (Wilkinson and Millar, 2000; Li et al., 2001). Hence, to investigate the function of MAPK in the signal transduction of EGF- and GABA$_A$R-mediated regulation of cell cycle progression in PSA-NCAM$^+$ cells, we used U0126, a specific inhibitor of the MAPK kinases MEK1 and MEK2. As in other cell types (Grant et al., 2002), our results confirmed that EGF-dependent stimulation of PSA-NCAM$^+$ cell proliferation is

mediated by the activation of the MAPK cascade because U0126 totally abolished the increase of proliferation induced by EGF. Furthermore, U0126 had no effect on the low level of PSA-NCAM$^+$ cell proliferation in basal conditions in which endogenous GABA was shown to inhibit cell cycle progression. Conversely, U0126 inhibited the higher level of proliferation of PSA-NCAM$^+$ cells observed in the presence of pharmacological blockers that antagonized $GABA_AR$ activation by endogenous GABA and thereby repressed the potential intracellular pathways of $GABA_AR$-mediated signaling. Thus, these data consistently suggest that the autocrine/paracrine activation of $GABA_AR$ interacts with cell cycle progression in PSA-NCAM$^+$ cells, leading directly or indirectly to a tonic inhibition of MAPK activity.

Despite its role as a major inhibitory neurotransmitter in the adult brain, GABA is known to exert excitatory depolarizing inputs during the period of embryonic neurogenesis and until the first postnatal week (Owens and Kriegstein, 2002). Membrane depolarization evoked by GABA in immature neural cells results from a high intracellular chloride concentration maintained by specific regulations of chloride transport mechanisms (Kakazu et al., 1999; Rivera et al., 1999; Bettendorff et al., 2002). Depolarization-induced Ca^{2+} entry through VGCCs (LoTurco et al., 1995) is known to be a major mechanism by which GABA-mediated changes in membrane potential used to regulate gene expression (Ganguly et al., 2001). We showed here that $GABA_AR$ activation induced an increase of $[Ca^{2+}]_i$ in a subset of postnatal PSA-NCAM$^+$ neuronal precursor cells. However, as a matter of fact, because only 28% of striatal PSA-NCAM$^+$ cells expressed VGCCs, only 20% of the total cells responded to $GABA_AR$ agonists with an increase of $[Ca^{2+}]_i$, all by a mechanism involving VGCC opening. We also demonstrated that VGCC blockade by nifedipine reversed $GABA_AR$-mediated inhibition of proliferation in Tuj1$^+$/PSA-NCAM$^+$ striatal neuronal precursors but had no effect on uncommitted Tuj1$^-$/PSA-NCAM$^+$ cells. To explain this difference, one could assume that in comparison with Tuj1$^+$/PSA-NCAM$^+$ striatal precursors, more immature Tuj1$^-$/PSA-NCAM$^+$ cells either have specific calcium-insensitive cell cycle signaling pathways or may not elicit a $[Ca^{2+}]_i$ rise in response to $GABA_AR$ agonists because of lower levels of VGCC expression or specific regulations of chloride transport mechanisms or express nifedipine-insensitive VGCC. It remains to be elucidated to what extent and by which mechanism $GABA_AR$-induced depolarization and elevation of $[Ca^{2+}]_i$ might account for the tonic inhibition of the MAPK pathway that actively decreases proliferation in PSA-NCAM$^+$ neuronal precursors.

In conclusion, altogether our findings show that GABA acting via $GABA_AR$ activation is a growth regulatory signal that controls proliferation of PSA-NCAM$^+$ neuronal progenitors isolated from early postnatal striatum. Because cell cycle arrest and neuronal differentiation are tightly linked biological events (Perez-Juste and Aranda, 1999), $GABA_AR$ activation could influence not only the maintenance but also the fate specification and the rate of neuronal differentiation of PSA-NCAM$^+$ precursor cells in the postnatal brain.

References

Barker JL, Behar T, Li YX, Liu QY, Ma W, Maric D, Maric I, Schaffner AE, Serafini R, Smith SV, Somogyi R, Vautrin JY, Wen XL, Xian H (1998) GABAergic cells and signals in CNS development. Perspect Dev Neurobiol 5:305–322.

Belachew S, Malgrange B, Rigo JM, Rogister B, Leprince P, Hans G, Nguyen L, Moonen G (2000) Glycine triggers an intracellular calcium influx in oligodendrocyte progenitor cells which is mediated by the activation of both the ionotropic glycine receptor and Na+-dependent transporters. Eur J Neurosci 12:1924–1930.

Ben Hur T, Rogister B, Murray K, Rougon G, Dubois-Dalcq M (1998) Growth and fate of PSA-NCAM+ precursors of the postnatal brain. J Neurosci 18:5777–5788.

Bettendorff L, Sallanon-Moulin M, Touret M, Wins P, Margineanu I, Schoffeniels E (1996) Paradoxical sleep deprivation increases the content of glutamate and glutamine in rat cerebral cortex. Sleep 19:65–71.

Bettendorff L, Lakaye B, Margineanu I, Grisar T, Wins P (2002) ATP-driven, NA+-independent inward Cl- pumping in neuroblastoma cells. J Neurochem 81:792–801.

Bonfanti L, Olive S, Poulain DA, Theodosis DT (1992) Mapping of the distribution of polysialylated neural cell adhesion molecule throughout the central nervous system of the adult rat: an immunohistochemical study. Neuroscience 49:419–436.

Bradford MM (1976) A rapid and sensitive method for the quantitation of microgram quantities of protein utilizing the principle of protein-dye binding. Anal Biochem 72:248–254.

Bruses JL, Rutishauser U (2001) Roles, regulation, and mechanism of polysialic acid function during neural development. Biochimie 83:635–643.

Butler AK, Uryu K, Morehouse V, Rougon G, Chesselet MF (1997) Regulation of the polysialylated form of the neural cell adhesion molecule in the developing striatum: effects of cortical lesions. J Comp Neurol 389:289–308.

Cameron HA, Hazel TG, McKay RD (1998) Regulation of neurogenesis by growth factors and neurotransmitters. J Neurobiol 36:287–306.

Craig CG, Tropepe V, Morshead CM, Reynolds BA, Weiss S, van der KD (1996) In vivo growth factor expansion of endogenous subependymal neural precursor cell populations in the adult mouse brain. J Neurosci 16:2649–2658.

Criswell HE, McCown TJ, Moy SS, Oxford GS, Mueller RA, Morrow AL, Breese GR (1997) Action of zolpidem on responses to GABA in relation to mRNAs for GABA(A) receptor alpha subunits within single cells: evidence for multiple functional GABA(A) isoreceptors on individual neurons. Neuropharmacology 36:1641–1652.

Dkhissi O, Julien JF, Wasowicz M, Dalil-Thiney N, Nguyen-Legros J, Versaux-Botteri C (2001) Differential expression of GAD(65) and GAD(67) during the development of the rat retina. Brain Res 919:242–249.

Doetsch F, Garcia-Verdugo JM, Alvarez-Buylla A (1997) Cellular composition and three-dimensional organization of the subventricular germinal zone in the adult mammalian brain. J Neurosci 17:5046–5061.

Doetsch F, Caille I, Lim DA, Garcia-Verdugo JM, Alvarez-Buylla A (1999) Subventricular zone astrocytes are neural stem cells in the adult mammalian brain. Cell 97:703–716.

Duncia JV, Santella III JB, Higley CA, Pitts WJ, Wityak J, Frietze WE, Rankin FW, Sun JH, Earl RA, Tabaka AC, Teleha CA, Blom KF, Favata MF, Manos EJ, Daulerio AJ, Stradley DA, Horiuchi K, Copeland RA, Scherle PA, Trzaskos JM, et al. (1998) MEK inhibitors: the chemistry and biological activity of U0126, its analogs, and cyclization products. Bioorg Med Chem Lett 8:2839–2844.

Edlund T, Jessell TM (1999) Progression from extrinsic to intrinsic signaling in cell fate specification: a view from the nervous system. Cell 96:211–224.

Flint AC, Liu X, Kriegstein AR (1998) Nonsynaptic glycine receptor activation during early neocortical development. Neuron 20:43–53.

Ganguly K, Schinder AF, Wong ST, Poo M (2001) GABA itself promotes the developmental switch of neuronal GABAergic responses from excitation to inhibition. Cell 105:521–532.

Gavrieli Y, Sherman Y, Ben Sasson SA (1992) Identification of programmed cell death in situ via specific labeling of nuclear DNA fragmentation. J Cell Biol 119:493–501.

Grant S, Qiao L, Dent P (2002) Roles of ERBB family receptor tyrosine kinases, and downstream signaling pathways, in the control of cell growth and survival. Front Biosci 7:d376–d389.

Greif KF, Tillakaratne NJ, Erlander MG, Feldblum S, Tobin AJ (1992) Transient increase in expression of a glutamate decarboxylase (GAD) mRNA during the postnatal development of the rat striatum. Dev Biol 153:158–164.

Grewal SS, York RD, Stork PJ (1999) Extracellular-signal-regulated kinase signalling in neurons. Curr Opin Neurobiol 9:544–553.

Grinspan JB, Franceschini B (1995) Platelet-derived growth factor is a sur-

vival factor for PSA-NCAM+ oligodendrocyte pre-progenitor cells. J Neurosci Res 41:540–551.

Gross CG (2000) Neurogenesis in the adult brain: death of a dogma. Nat Neurosci Rev 1:67–72.

Hamill OP, Marty A, Neher E, Sakmann B, Sigworth FJ (1981) Improved patch-clamp techniques for high-resolution current recording from cells and cell-free membrane patches. Pflügers Arch 391:85–100.

Haydar TF, Wang F, Schwartz ML, Rakic P (2000) Differential modulation of proliferation in the neocortical ventricular and subventricular zones. J Neurosci 20:5764–5774.

Herlenius E, Lagercrantz H (2001) Neurotransmitters and neuromodulators during early human development. Early Hum Dev 65:21–37.

Ikeda Y, Nishiyama N, Saito H, Katsuki H (1997) GABAA receptor stimulation promotes survival of embryonic rat striatal neurons in culture. Brain Res Dev Brain Res 98:253–258.

Jones SM, Kazlauskas A (2001) Growth factor-dependent signaling and cell cycle progression. Chem Rev 101:2413–2424.

Kakazu Y, Akaike N, Komiyama S, Nabekura J (1999) Regulation of intracellular chloride by cotransporters in developing lateral superior olive neurons. J Neurosci 19:2843–2851.

Keirstead HS, Ben Hur T, Rogister B, O'Leary MT, Dubois-Dalcq M, Blakemore WF (1999) Polysialylated neural cell adhesion molecule-positive CNS precursors generate both oligodendrocytes and Schwann cells to remyelinate the CNS after transplantation. J Neurosci 19:7529–7536.

Khrestchatisky M, MacLennan AJ, Chiang MY, Xu WT, Jackson MB, Brecha N, Sternini C, Olsen RW, Tobin AJ (1989) A novel alpha subunit in rat brain GABAA receptors. Neuron 3:745–753.

Khrestchatisky M, MacLennan AJ, Tillakaratne NJ, Chiang MY, Tobin AJ (1991) Sequence and regional distribution of the mRNA encoding the alpha 2 polypeptide of rat gamma-aminobutyric acid A receptors. J Neurochem 56:1717–1722.

Kuhn HG, Winkler J, Kempermann G, Thal LJ, Gage FH (1997) Epidermal growth factor and fibroblast growth factor-2 have different effects on neural progenitors in the adult rat brain. J Neurosci 17:5820–5829.

Lauder JM (1993) Neurotransmitters as growth regulatory signals: role of receptors and second messengers. Trends Neurosci 16:233–240.

Lauder JM, Han VK, Henderson P, Verdoorn T, Towle AC (1986) Prenatal ontogeny of the GABAergic system in the rat brain: an immunocytochemical study. Neuroscience 19:465–493.

Levitan ES, Schofield PR, Burt DR, Rhee LM, Wisden W, Kohler M, Fujita N, Rodriguez HF, Stephenson A, Darlison MG (1988) Structural and functional basis for GABAA receptor heterogeneity. Nature 335:76–79.

Li BS, Ma W, Zhang L, Barker JL, Stenger DA, Pant HC (2001) Activation of phosphatidylinositol-3 kinase (PI-3K) and extracellular regulated kinases (Erk1/2) is involved in muscarinic receptor-mediated DNA synthesis in neural progenitor cells. J Neurosci 21:1569–1579.

Ljungman M, Paulsen MT (2001) The cyclin-dependent kinase inhibitor roscovitine inhibits RNA synthesis and triggers nuclear accumulation of p53 that is unmodified at Ser15 and Lys382. Mol Pharmacol 60:785–789.

LoTurco JJ, Owens DF, Heath MJ, Davis MB, Kriegstein AR (1995) GABA and glutamate depolarize cortical progenitor cells and inhibit DNA synthesis. Neuron 15:1287–1298.

Luk KC, Sadikot AF (2001) GABA promotes survival but not proliferation of parvalbumin-immunoreactive interneurons in rodent neostriatum: an in vivo study with stereology. Neuroscience 104:93–103.

Ma W, Barker JL (1995) Complementary expressions of transcripts encoding GAD67 and GABAA receptor alpha 4, beta 1, and gamma 1 subunits in the proliferative zone of the embryonic rat central nervous system. J Neurosci 15:2547–2560.

Ma W, Barker JL (1998) GABA, GAD, and GABA(A) receptor alpha4, beta1, and gamma1 subunits are expressed in the late embryonic and early postnatal neocortical germinal matrix and coincide with gliogenesis. Microsc Res Tech 40:398–407.

Ma W, Liu QY, Maric D, Sathanoori R, Chang YH, Barker JL (1998) Basic FGF-responsive telencephalic precursor cells express functional GABA(A) receptor/Cl-channels in vitro. J Neurobiol 35:277–286.

Malherbe P, Sigel E, Baur R, Persohn E, Richards JG, Mohler H (1990) Functional characteristics and sites of gene expression of the α1, β1, γ2-isoform of the rat $GABA_A$ receptor. J Neurosci 10:2330–2337.

Maric D, Maric I, Ma W, Lahojuji F, Somogyi R, Wen X, Sieghart W, Fritschy JM, Barker JL (1997) Anatomical gradients in proliferation and differentiation of embryonic rat CNS accessed by buoyant density fractionation: alpha 3, beta 3 and gamma 2 GABAA receptor subunit coexpression by post-mitotic neocortical neurons correlates directly with cell buoyancy. Eur J Neurosci 9:507–522.

Maric D, Liu QY, Grant GM, Andreadis JD, Hu Q, Chang YH, Barker JL, Joseph J, Stenger DA, Ma W (2000) Functional ionotropic glutamate receptors emerge during terminal cell division and early neuronal differentiation of rat neuroepithelial cells. J Neurosci Res 61:652–662.

Marmur R, Mabie PC, Gokhan S, Song Q, Kessler JA, Mehler MF (1998) Isolation and developmental characterization of cerebral cortical multipotent progenitors. Dev Biol 204:577–591.

Mayer-Proschel M, Kalyani AJ, Mujtaba T, Rao MS (1997) Isolation of lineage-restricted neuronal precursors from multipotent neuroepithelial stem cells. Neuron 19:773–785.

McKay R (1997) Stem cells in the central nervous system. Science 276:66–71.

Miranda-Contreras L, Benitez-Diaz PR, Mendoza-Briceno RV, Delgado-Saez MC, Palacios-Pru EL (1999) Levels of amino acid neurotransmitters during mouse cerebellar neurogenesis and in histotypic cerebellar cultures. Dev Neurosci 21:147–158.

Nguyen L, Rigo JM, Rocher V, Belachew S, Malgrange B, Rogister B, Leprince P, Moonen G (2001) Neurotransmitters as early signals for central nervous system development. Cell Tissue Res 305:187–202.

Owens DF, Kriegstein AR (2002) Is there more to GABA than synaptic inhibition? Nat Rev Neurosci 3:715–727.

Pencea V, Bingaman KD, Wiegand SJ, Luskin MB (2001) Infusion of brain-derived neurotrophic factor into the lateral ventricle of the adult rat leads to new neurons in the parenchyma of the striatum, septum, thalamus, and hypothalamus. J Neurosci 21:6706–6717.

Perez-Juste G, Aranda A (1999) The cyclin-dependent kinase inhibitor p27(Kip1) is involved in thyroid hormone-mediated neuronal differentiation. J Biol Chem 274:5026–5031.

Reynolds BA, Weiss S (1992) Generation of neurons and astrocytes from isolated cells of the adult mammalian central nervous system. Science 255:1707–1710.

Rivera C, Voipio J, Payne JA, Ruusuvuori E, Lahtinen H, Lamsa K, Pirvola U, Saarma M, Kaila K (1999) The K^+/Cl^- co-transporter KCC2 renders GABA hyperpolarizing during neuronal maturation. Nature 397:251–255.

Seki T, Arai Y (1993) Distribution and possible roles of the highly polysialylated neural cell adhesion molecule (NCAM-H) in the developing and adult central nervous system. Neurosci Res 17:265–290.

Serafini R, Ma W, Maric D, Maric I, Lahjouji F, Sieghart W, Barker JL (1998) Initially expressed early rat embryonic GABA(A) receptor Cl^- ion channels exhibit heterogeneous channel properties. Eur J Neurosci 10:1771–1783.

Sigel E, Baur R, Trube G, Mohler H, Malherbe P (1990) The effect of subunit composition of rat brain GABAA receptors on channel function. Neuron 5:703–711.

Stewart RR, Hoge GJ, Zigova T, Luskin MB (2002) Neural progenitor cells of the neonatal rat anterior subventricular zone express functional GABA(A) receptors. J Neurobiol 50:305–322.

Szabo G, Katarova Z, Greenspan R (1994) Distinct protein forms are produced from alternatively spliced bicistronic glutamic acid decarboxylase mRNAs during development. Mol Cell Biol 14:7535–7545.

Trotter J, Bitter-Suermann D, Schachner M (1989) Differentiation-regulated loss of the polysialylated embryonic form and expression of the different polypeptides of the neural cell adhesion molecule by cultured oligodendrocytes and myelin. J Neurosci Res 22:369–383.

Verdoorn TA, Draguhn A, Ymer S, Seeburg PH, Sakmann B (1990) Functional properties of recombinant rat GABAA receptors depend upon subunit composition. Neuron 4:919–928.

Vitry S, Avellana-Adalid V, Hardy R, Lachapelle F, Baron-Van Evercooren A (1999) Mouse oligospheres: from pre-progenitors to functional oligodendrocytes. J Neurosci Res 58:735–751.

Vitry S, Avellana-Adalid V, Lachapelle F, Evercooren AB (2001) Migration and multipotentiality of PSA-NCAM+ neural precursors transplanted in the developing brain. Mol Cell Neurosci 17:983–1000.

Weissman IL, Anderson DJ, Gage FH (2001) Stem and progenitor cells: origins, phenotypes, lineage commitments, and transdifferentiations. Annu Rev Cell Dev Biol 17:387–403.

Wilkinson MG, Millar JB (2000) Control of the eukaryotic cell cycle by MAP kinase signaling pathways. FASEB J 14:2147–2157.

Wisden W, Herb A, Wieland H, Keinanen K, Luddens H, Seeburg PH (1991) Cloning, pharmacological characteristics and expression pattern of the rat GABAA receptor alpha 4 subunit. FEBS Lett 289:227–230.

Ymer S, Draguhn A, Kohler M, Schofield PR, Seeburg PH (1989a) Sequence and expression of a novel GABAA receptor alpha subunit. FEBS Lett 258:119–122.

Ymer S, Schofield PR, Draguhn A, Werner P, Kohler M, Seeburg PH (1989b) GABAA receptor beta subunit heterogeneity: functional expression of cloned cDNAs. EMBO J 8:1665–1670.

Ymer S, Draguhn A, Wisden W, Werner P, Keinanen K, Schofield PR, Sprengel R, Pritchett DB, Seeburg PH (1990) Structural and functional characterization of the gamma 1 subunit of GABAA/benzodiazepine receptors. EMBO J 9:3261–3267.

Yoshida K, Rutishauser U, Crandall JE, Schwarting GA (1999) Polysialic acid facilitates migration of luteinizing hormone-releasing hormone neurons on vomeronasal axons. J Neurosci 19:794–801.

Yuan X, Eisen AM, McBain CJ, Gallo V (1998) A role for glutamate and its receptors in the regulation of oligodendrocyte development in cerebellar tissue slices. Development 125:2901–2914.

Yuan X, Chittajallu R, Belachew S, Anderson S, McBain CJ, Gallo V (2002) Expression of the green fluorescent protein in the oligodendrocyte lineage: a transgenic mouse for developmental and physiological studies. J Neurosci Res 70:529–545.

Zhao ZY, Joho RH (1990) Isolation of distantly related members in a multigene family using the polymerase chain reaction technique. Biochem Biophys Res Commun 167:174–182. .0